Design of Precatalysts and Phosphine Ligands for Pd-Catalyzed Transformations

by

Bryan Taylor Ingoglia

B.A., Chemistry
University of Kentucky, 2014

Submitted to the Department of Chemistry in Partial Fulfillment of the Requirements for the Degree of

DOCTOR OF PHILOSOPHY IN CHEMISTRY

at the

Massachusetts Institute of Technology

June 2019

Signature of the author ... Signature redacted .....
Department of Chemistry
May 10, 2019

Certified by ..... Signature redacted .....
Stephen L. Buchwald
Camille Dreyfus Professor of Chemistry
Thesis Supervisor

Accepted by ..... Signature redacted .....
Robert W. Field
Haslam and Dewey Professor of Chemistry
Chairman, Departmental Committee on Graduate Students

This doctoral thesis has been examined by a committee of the Department of Chemistry as follows:

Signature redacted

Professor Timothy F. Jamison: _____
Thesis Committee Chair

Signature redacted

Professor Stephen L. Buchwald: _____
Thesis Supervisor

Signature redacted

Professor Timothy M. Swager: _____
Thesis Committee

Design of Precatalysts and Phosphine Ligands for Pd-Catalyzed Transformations

by

Bryan Taylor Ingoglia

Submitted to the Department of Chemistry on May 10, 2019 in Partial Fulfillment of the Requirements for the Degree of Doctor of Philosophy in Chemistry

Abstract

The work described in this thesis pertains to the formation of carbon–heteroatom bonds facilitated by palladium catalysts supported by bulky phosphine ligands. The first chapter is a summary of how biaryl monophosphine ligands have been used for carbon–heteroatom bond formations, including a ligand selection guide. The second chapter demonstrates how phosphine-supported Pd(II) oxidative addition complexes can be used as precatalysts in a variety of cross-coupling reactions. The third chapter presents a systematic study of the ligand architecture in an effort to rationally design new ligands capable of facilitating the challenging C–F reductive elimination from Pd(II). The fourth chapter highlights a structurally interesting side-product that resulted during ligand synthesis.

Chapter 1: Biaryl Monophosphine Ligands in Palladium-Catalyzed C–N Coupling: An Updated User's Guide

Over the past three decades, Pd-catalyzed cross-coupling reactions have become a mainstay of organic synthesis. In particular, catalysts derived from biaryl monophosphines have shown wide utility in forming C–N bonds under mild reaction conditions. This work summarizes a variety of C–N cross-coupling reactions using biaryl monophosphines as supporting ligands, with the goal of directing synthetic chemists toward the ligands and conditions best suited for a particular coupling.

Chapter 2. Oxidative Addition Complexes as Precatalysts for Cross-Coupling Reactions Requiring Extremely Bulky Biarylphosphine Ligands.

Palladium-based oxidative addition complexes were found to be effective precatalysts for C–N, C–O, and C–F cross-coupling reactions with a variety of aromatic electrophiles. These Pd(II) complexes are easily prepared and offer a convenient alternative to previously developed classes of precatalysts as they can be formed even with extremely large phosphine ligands, for which palladacycle-based precatalysts do not readily form. The complexes were found to be stable to long-term storage under ambient conditions.

Chapter 3. Structure-Activity Relationship of Phosphine Ligands for the Fluorination of Five-membered Heteroaromatic Compounds

Palladium catalysts supported by bulky dialkyl triaryl monophosphine ligands have been shown to promote the coupling of metal fluorides with (hetero)aryl bromides and triflates in good yield. A limitation of this methodology is the use of five-membered heteroaryl bromides, as the reductive elimination is more challenging due to the smaller size and electron-rich nature of the aryl electrophiles. In order to understand which structural features of the ancillary ligand are critical to facilitating the desired transformation, the ligand backbone was systematically varied and the initial rate of fluorination was monitored. These studies revealed that substitution at the 2″ and 6″ positions of the ligand scaffold has a dramatic impact on the reaction rate. As a result of these studies, new ligands were proposed which may be better able to accelerate the fluorination reaction.

Chapter 4: Discovery of a Sterically Encumbered Hexasubstituted Arene through the Pd-mediated Dearomative Rearrangement of Biaryl Monophosphine Ligands

A key feature of the Pd-catalyzed aromatic fluorination reaction is the presence of the aryl group at the 3′ position of the ligand backbone. It has been shown that supporting ligands lacking substitution at this position can be modified through a dearomative rearrangement, which incorporates one catalytic equivalent of the aryl electrophile into the ligand backbone when very bulky biarylphosphines are used. In Chapter 3, it was demonstrated that this rearrangement reaction is useful for rapidly accessing a variety of dialkyl triaryl monophosphine derivatives. During these studies, it was noted that for electron-rich aryl groups, this arylation occurred twice to form an unusual sterically congested hexasubstituted arene. X-ray crystallographic data indicates that the fully substituted aromatic ring is not planar.

Thesis Supervisor: Stephen L. Buchwald
Title: Camille Dreyfus Professor of Chemistry

ACKNOWLEDGMENTS

First and foremost I would like to thank my advisor, Steve, for his support over the past five years, not only financially, but also as a scientific mentor. You taught me about identifying important problems that people care about and constantly challenged me. I thank you for allowing me to work on interesting problems and for believing in my abilities, even when I did not.

Thank you to my thesis committee members, Professors Tim Jamison and Tim Swager. It has been a pleasure to work with you both, and I have always found my discussions with you informative and refreshing.

Though I lacked confidence at the beginning of graduate school, I feel that my time in the Buchwald group has not only shaped me into a better scientist, but a better person. There are so many people to thank for this and I hope I do not forget anyone. Dr. Sandra King, Dr. John Nguyen, and Dr. Kurt Armbrust were extraordinarily helpful to me when I first started in the group, and I don't think I would be the synthetic chemist I am today without their help. Dr. Aaron Sather and Dr. Stig Friis were instrumental in teaching me how to run the glovebox. Dr. Mycah Uehling always had a positive attitude, which I'd like to think I adopted as I grew older. A special thanks Dr. Phill Milner (now Professor Milner!) for guiding me as an uninitiated first-year, even in the midst of compiling his thesis. I'd also like to sincerely thank Dr. Paula Ruiz-Castillo: you helped me get through some really difficult times as a young graduate student, and I think I would have been miserable if it weren't for you.

The current post-docs and graduate students in the group are some of the best people with which I have had the privilege to work. These include my bay-mates in 18-323: Dr. Zhaohong Lu, Dr. Alex Schuppe, Joey Dennis, Saki Ichikawa, Ryan King and Frieda Zhang. To all the current post-docs in the group: Dr. Andy Thomas, Dr. Ivan Buslov, Dr. Xi-Jie Dai, Dr. Heemal Dhanjee, Dr. Jason Tao, Dr. Sheng Guo, Dr. Chengxi Li, Dr. Achim Link, and Dr. Kwangmin Shin, you all have been magnificent coworkers and I have enjoyed working with each and every one of you. I'd like to specifically give a shout-out to Dr. Scott McCann, Dr. Liela Bayeh (Romero), and my desk neighbor Dr. Klaus Speck–you all have taught me so much about how to present scientific research and have been instrumental in my growth as a scientist.

I wish the very best to each of the graduate students in the group: you are all the most hard-working people I know. To Yujing Zhou and Elaine Reichert: the gloveboxes are now in your capable hands and I hope you are able to keep your sanity despite its never-ending demands. Mike Gribble and Richard Liu, I hope to someday possess even an iota of your knowledge; it has been a privilege to learn from both of you. To Team Bioconjugation: Aaron Mallek, Spencer Shinabery, Azin Saebi, and Jacob Rodriguez, I envy your ability to split your brainpower between two disciplines and your ability to explain it even to people like me. Erica Tsai, Sheng Feng, and Levi Knippel of Team Copper Hydride: may all your future yields and ee's (or is it er now?) always be high. Finally, to the graduate students on Team Palladium: Jess Xu, Joey Dennis and Frieda Zhang, you are, in a sense, the last of generation. It is up to you to pass on the secrets of palladium chemistry!

It has been my distinct pleasure to work with my UROP student, Corin Wagen, over the past year or so. I can't even begin to articulate how impressed I am with not only the depth of your knowledge, but your willpower and dedication to organic chemistry. I have no doubt that you will be successful in whatever you endeavor to do, and that whichever group you join will be exceptionally lucky to count you as a colleague. I wish you nothing but success and happiness in your future career, and look forward to seeing how your Ph.D. shapes up!

There are two people without which I would never have been able to get through graduate school. The first is Christine Nguyen, who might be the sole reason the group runs as smoothly as it does. You have my eternal thanks for managing the group as you have, because I know we all would be lost without you. The second individual is Jennifer Weisman, who has made every part of the graduate student experience here better. Thank you for keeping the administrative side of things working smoothly–I am not sure how you manage to do it year after year.

To my fellow graduate students in other groups: Jessica Weber, Liam Kelly, Tho Tran, Chase Olsson, we made it! It has been a long journey, but we all came out (relatively) unscathed on the other side! I am proud of each and every one of you, and I am glad to have worked alongside you during our time at MIT. To my fellow Organic Retreat 2018 committee members in other groups–Julian Cooper, Krysta Dummit, and Julia Zhao–I hope you'll join me for snickety snacks and drinky drinks, even after my time at MIT is over.

A special thank you to Professor Susan A. Odom (University of Kentucky) for recognizing my potential early. If not for your constant support, I would never have pursued chemistry, let alone my Ph.D. at MIT. I enjoyed not only the time I spent in the group as an undergraduate, but also our conversations over the years during my time in grad school.

Thank you to Mom, Dad, Jay, and Steve for all your support throughout these years: from before even college up until now. I would not be the person I am today without all your support. I know I am neurotic and that can be difficult to handle, but you have all embraced me with love and understanding. I would never have been able to make it through my dissertation without your constant support.

A most heartfelt thank you to my fiancée, Kelley Danahy, who has made these past few years bearable. We made it through everything together! I don't think I ever expected to fall in love in what is probably the most stressful time period of my life. I am so lucky to have met you here, and can't wait to see what our futures–both chemical and otherwise–hold.

PREFACE

Parts of this thesis have been adapted from the following articles co-written by the author.

"Biaryl Monophosphine Ligands in Palladium-Catalyzed C–N Coupling: An Updated User's Guide" Ingoglia, B.T.; Wagen, C.C.; Buchwald, S.L. *Manuscript submitted.*

"Oxidative Addition Complexes as Precatalysts for Cross-Coupling Reactions Requiring Extremely Bulky Biarylphosphine Ligands" Ingoglia, B.T.; Buchwald, S.L. *Organic Letters*, **2017**, *19*, 2853–2856.

"An Unexpected Route to Hexasubstituted Arenes Via Double Dearomative Ligand Rearrangement." Wagen, C.C.; Ingoglia, B.T.; Tsay, C.; Müller, P.; Buchwald, S.L. *Manuscript in preparation.*

RESPECTIVE CONTRIBUTIONS

This thesis contains work that is the result of collaborative efforts between the author and other colleagues at MIT. The specific contributions are detailed below.

The work discussed in Chapter 1 resulted from a collaborative effort between Corin Wagen and the author. Corin is credited with writing the substrate scope section of the review and the initial draft of the flowchart document. The author is responsible for writing the introduction, precatalyst section, and conclusion sections, as well as developing the flowchart document.

The work discussed in Chapter 3 resulted from a collaborative effort between Corin Wagen and the author. Corin and the author collaborated on synthesizing each ligand in this chapter. Additionally, Joey Dennis is credited with supplying **L2** and **L7**, for which the author is grateful. Dr. Aaron Sather developed the first half of the synthetic route towards **L4.**

The work discussed in Chapter 4 resulted from a collaborative effort between Corin Wagen and the author. Corin is credited with the initial discovery that a second dearomative rearrangement occurs from electron-rich aryl groups.

ABBREVIATIONS

The following abbreviations will be used throughout this thesis.

Ac	acetate
AcOH	acetic acid
Ad	1-adamantyl
Am	amyl
Ar	aryl
ArF	aryl fluoride
COD	1,5-cyclooctadiene
CPME	Cyclopentyl methyl ether
Cy	cyclohexyl
CyH	cyclohexane
DBU	1,8-diazabicyclo[5.4.0]undec-7-ene
DCM	dichloromethane
DMF	*N,N*-dimethylformamide
DMSO	dimethyl sulfoxide
Et_2O	diethyl ether
EtOAc	ethyl acetate
GC	gas chromatography
HPLC	high performance liquid chromatography
HRMS	high-resolution mass spectrum (spectrometry)
i-Pr	isopropyl
LC	liquid chromatography
MS	mass spectrometry
MTBE	methyl *tert*-butyl ether
n-Bu	*n*-butyl
NIS	*N*-iodosuccinimide
NMP	*N*-methylpyrrolidone
NMR	nuclear magnetic resonance (spectroscopy)
OA	oxidative addition
PhMe	toluene
rds	rate-determining step
t-Bu	*tert*-butyl
Tf	Trifluoromethanesulfonyl, triflyl
TFA	Trifluoroacetic acid
THF	tetrahydrofuran
2-MeTHF	2-methyltetrahydrofuran
TIPS	triisopropylsilyl
TLC	thin layer chromatography
TMS	trimethylsilyl
Trt	trityl

TABLE OF CONTENTS

Chapter 4. Discovery of a Sterically Encumbered Hexasubstituted Arene through the Pd-mediated Dearomative Rearrangement of Biaryl Monophosphine Ligands

INTRODUCTION

Palladium catalysis has become an indispensable strategy employed by synthetic chemists. The most prominent use of this methodology has been in the construction of C–C bonds to form structures that would otherwise be difficult to access. Indeed, this reaction is so important that Professors Richard F. Heck, Ei-ichi Negishi, and Akira Suzuki won the Nobel Prize in 2010 for their respective contributions towards Pd catalysis. In the past thirty years, the scope of this cross-coupling process was expanded to include heteroatom nucleophiles, namely those based on nitrogen. This has largely been accomplished by designing new supporting ligands that modify the catalyst properties, although many variables (e.g., Pd source, choice of base, solvent, temperature) also impact the outcome of a particular cross-coupling reaction.

Scattered throughout the development of C–N cross-coupling reactions were efforts made toward forming C–P, C–O, C–S, and C–F bonds. The last of these is particularly important, because aromatic fluorination is generally difficult to accomplish despite the prevalence of organofluorine compounds in agrochemicals[1] and pharmaceuticals.[2,3] Indeed, fluorine incorporation has been shown to increase the lipophilic character of medicinally relevant compounds, which increase their bioavailability.[4] The tendency of fluorine to form strong bonds to carbon (i.e., 125 kcal/mol for C_{sp^2}–F)[5] results in its use in blocking sites of metabolism, which also increases drug bioavailability.[6] The combination of these effects, in addition to its small van der Waal's radius (147 pm),[7] makes fluorine a good bioisotere for hydrogen.[8] Fluorine also possesses a high Pauling electronegativity (3.98),[8] rendering it a potent electron-withdrawing group. Consequently, fluorine substitutions have been used to modulate the pK_a of proximal functional groups, such as carboxylic acids[9] and amines.[9,10]

Traditionally, fluorine is installed on aromatic rings either through the **Hal**ogen **Ex**change (HalEx) process or the Balz–Schiemann reaction. The HalEx process is essentially a nucleophilic aromatic substitution reaction on an electron-poor arene (Figure 1a). Though this method has industrial relevance,[11] it requires exceedingly high temperatures (>150 °C)[12] and is limited in scope to compounds that can stabilize Meisenheimer complexes. The Balz–Schiemann reaction is the thermal- or light-mediated decomposition of aryl diazonium tetrafluoroborate salts (Figure 1b).[13] Aryl diazonium salts pose a significant safety hazard, as they are potential explosives,[14] and additionally their synthesis requires harsh conditions.[15,16] Moreover, this reaction is plagued by direct reduction of the diazonium salt to form a C–H bond upon loss of

nitrogen; this ArH side-product is generally quite difficult to separate from the desired aryl fluoride.[17] In addition to these traditional methods, electrophilic fluorination with "F^+ reagents" has become popular, though these reagents are often strongly oxidizing and expensive.[18–21]

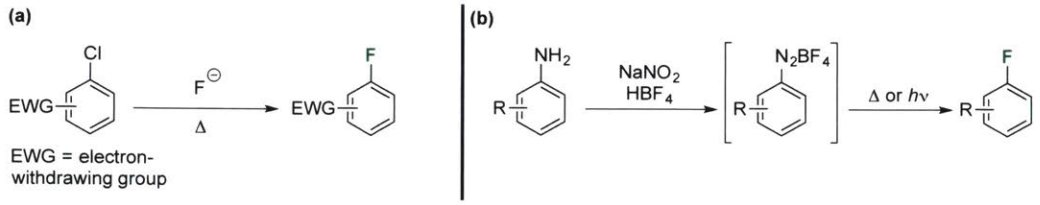

Figure 1. (a) The HalEx process (b) The Balz–Schiemann Reaction.

The conversion of an aryl halide or pseudohalide to the corresponding aryl fluoride using an abundant fluoride source mediated by a Pd catalyst (Figure 2) provides a useful alternative to traditional methods, since Pd catalysts often operate under mild conditions and tolerate a wide range of functional groups.[22] Indeed, this process has been studied as early as the 1990s, which established that C–F bond-forming reductive elimination is quite a challenging process.[23] Several other competing reactions predominate, such as the formation of stable μ_2-bridging fluoride dimers,[24,25] P–F reductive elimination, and P–C reductive elimination.[26] In the past decade, our group has demonstrated that sterically demanding dialkyl biaryl monophosphine ligands are competent ancillary ligands for this transformation, although five-membered heteroaryl electrophiles remain challenging coupling partners.[27]

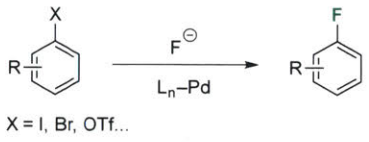

Figure 2. Pd-catalyzed fluorination of aryl (pseudo)halides.

This dissertation begins with a review on the use of biaryl monophosphine ligands in the context of C–N cross-coupling in Chapter 1. This chapter highlights the role of the supporting ligand, though the impact of Pd source, base, solvent, and temperature are also discussed. Chapter 2 discusses the role of palladium source at length in the context of precatalysts for challenging C–N, C–O, and C–F coupling reactions that use very large phosphine ligands.

Chapter 3 focuses on the role of the ancillary ligand in the Pd-catalyzed fluorination of five-membered heterocycles. A systematic ligand study is presented which identifies key structural features critical to the success of the transformation, as well as efforts in designing an improved catalyst system. Chapter 4 describes a serendipitous discovery made while synthesizing ligands, namely the formation of a heavily substituted aromatic ring during a Pd-mediated dearomative rearrangement reaction.

References

1. Jeschke, P. The Unique Role of Fluorine in the Design of Active Ingredients for Modern Crop Protection. *ChemBioChem* **2004**, *5*, 570–589.
2. Campbell, M. G.; Ritter, T. Late-Stage Fluorination: From Fundamentals to Application. *Org. Process Res. Dev.* **2014**, *18*, 474–480.
3. Zhou, Y.; Wang, J.; Gu, Z.; Wang, S.; Zhu, W.; Acenã, J. L.; Soloshonok, V. A.; Izawa, K.; Liu, H. Next Generation of Fluorine-Containing Pharmaceuticals, Compounds Currently in Phase II-III Clinical Trials of Major Pharmaceutical Companies: New Structural Trends and Therapeutic Areas. *Chem. Rev.* **2016**, *116*, 422–518.
4. Müller, K.; Faeh, C.; Diederich, F. Fluorine in Pharmaceuticals: Looking beyond Intuition. *Science* **2007**, *317*, 1881–1886.
5. Blanksby, S.J.; Ellison, G.B. Bond Dissociation Energies of Organic Molecules. *Acc. Chem. Res.* **2003**, *36*, 255–263.
6. Park, B. K.; Kitteringham, N. R.; O'Neill, P. M. Metabolism of Fluorine-Containing Drugs. *Annu. Rev. Pharmacol. Toxicol.* **2001**, *41*, 443–470.
7. Bondi, A. Van Der Waals Volumes and Radii. *J. Phys. Chem.* **1964**, *68*, 441–451.
8. O'Hagan, D. Understanding Organofluorine Chemistry. An Introduction to the C–F Bond. *Chem. Soc. Rev.* **2008**, *37*, 308–319.
9. Gillis, E. P.; Eastman, K. J.; Hill, M. D.; Donnelly, D. J.; Meanwell, N. A. Applications of Fluorine in Medicinal Chemistry. *J. Med. Chem.* **2015**, *58*, 8315–8359.
10. Percy, J.M. β-Fluoroamines. *Sci. Synth.* **2005**, *34*, 379–385.
11. Adams, D. J.; Clark, J. H. Nucleophilic Routes to Selectively Fluorinated Aromatics. *Chem. Soc. Rev.* **1999**, *28*, 225–231.
12. Finger, G. C.; Kruse, C. W. Aromatic Fluorine Compounds. VII. Replacement of Aromatic -Cl and -NO_2 Groups by -F[1,2]. *J. Am. Chem. Soc.* **1956**, *78*, 6034–6037.

13. Balz, G.; Schiemann, G. Aromatic Fluorine Compounds, I.: A new Method for Their Preparation. *Ber. Dtsch. Chem. Ges. B* **1927**, *60*, 1186–1190.

14. Ullrich, R.; Grewer, T. Decomposition of Aromatic Diazonium Compounds. *Thermochim. Acta* **1993**, *225*, 201–211.

15. Roe, A.; Hawkins, G. F. The Preparation of Heterocyclic Fluorine Compounds by the Schiemann Reaction. I. The Monofluoropyridines. *J. Am. Chem. Soc.* **1947**, *69*, 2443–2444.

16. Myhre, P. C.; Edmonds, J. W.; Kruger, J. D. Long-Range Spin-Spin Coupling in Alkylfluorobenzenes. The Stereochemical Requirements for Coupling of Fluorine and Hydrogen Separated by Five Bonds[1]. *J. Am. Chem. Soc.* **1966**, *88*, 2459–2466.

17. Park, N. H.; Senter, T. J.; Buchwald, S. L. Rapid Synthesis of Aryl Fluorides in Continuous Flow through the Balz-Schiemann Reaction. *Angew. Chemie Int. Ed.* **2016**, *55*, 11907–11911.

18. Mazzotti, A. R.; Campbell, M. G.; Tang, P.; Murphy, J. M.; Ritter, T. Palladium(III)-Catalyzed Fluorination of Arylboronic Acid Derivatives. *J. Am. Chem. Soc.* **2013**, *135*, 14012–14015.

19. Chan, K. S. L.; Wasa, M.; Wang, X.; Yu, J.-Q. Palladium(II)-Catalyzed Selective Monofluorination of Benzoic Acids Using a Practical Auxiliary: A Weak-Coordination Approach. *Angew. Chemie Int. Ed.* **2011**, *50*, 9081–9084.

20. Tang, P.; Wang, W.; Ritter, T. Deoxyfluorination of Phenols. *J. Am. Chem. Soc.* **2011**, *133*, 11482–11484.

21. Anbarasan, P.; Neumann, H.; Beller, M. Efficient Synthesis of Aryl Fluorides. *Angew. Chemie Int. Ed.* **2010**, *49*, 2219–2222.

22. *Metal-Catalyzed Cross-Coupling Reactions,* 2nd ed.; de Meijere, A., Diederich, F., Eds.; Wiley-VCH: Weinheim, Germany, 2004.

23. Grushin, V. V. The Organometallic Fluorine Chemistry of Palladium and Rhodium: Studies toward Aromatic Fluorination. *Acc. Chem. Res.* **2010**, *43*, 160–171.

24. Yandulov, D. V; Tran, N. T. Aryl-Fluoride Reductive Elimination from Pd(II): Feasibility Assessment from Theory and Experiment. *J. Am. Chem. Soc.* **2007**, *129*, 1342–1358.

25. Grushin, V. V.; Marshall, W. J. Is Fluoride Bonded to Two Pd Acceptors Still Basic? Three CH_2Cl_2 Molecules Encapsulating a $Pd_2(\mu\text{-}F)_2$ Square and New Implications for Catalysis. *Angew. Chemie Int. Ed.* **2002**, *41*, 4476–4479.

26. Grushin, V. V. Thermal Stability, Decomposition Paths, and Ph/Ph Exchange Reactions of $[(Ph_3P)_2Pd(Ph)X]$ (X = I, Br, Cl, F, and HF_2). *Organometallics*, **2000**, *19*, 1888–1900.

27. Sather, A. C.; Buchwald, S. L. The Evolution of Pd^{0}/Pd^{II}-Catalyzed Aromatic Fluorination. *Acc. Chem. Res.* **2016**, *49*, 2146–2157.

Chapter 1. Biaryl Monophosphine Ligands in Palladium-Catalyzed C–N Coupling: An Updated User's Guide

1.1. Introduction and General Principles

Transition metal catalysis enables mild and general access to molecular structures that would otherwise be challenging to prepare. In particular, palladium catalysts have become dependable tools in the rapid and modular construction of substituted aromatic compounds. The efficacy of such catalysts stems largely from the ability to tune their reactivity through modification of the ancillary ligand(s). To this end, biaryl monophosphines have emerged as a class of privileged ligands for a number of mechanistically related transformations. While we have focused this review on one class of ligands developed at MIT, many other groups have made important contributions, most notably, of course, the Hartwig laboratory.[1,2] Outstanding examples have also emerged from the laboratories of Beller,[3] Guram,[4] Nolan,[5] Organ,[6] Singer,[7] Stradiotto,[8] and many others.[9,10]

Herein, we aim to summarize Pd-catalyzed carbon–nitrogen cross-coupling reactions that are enabled by biaryl monophosphine ligands (Figure 1). The purpose of this paper is to aid synthetic chemists in choosing the most appropriate ligand for a desired transformation. In addition to ligand selection, we discuss the impact of palladium source and reaction conditions (e.g., base, temperature, solvent) on the reaction outcome. We emphasize that this review is not designed to be comprehensive or to replace information in the primary chemical literature, but rather to serve as a complement to existing publications.

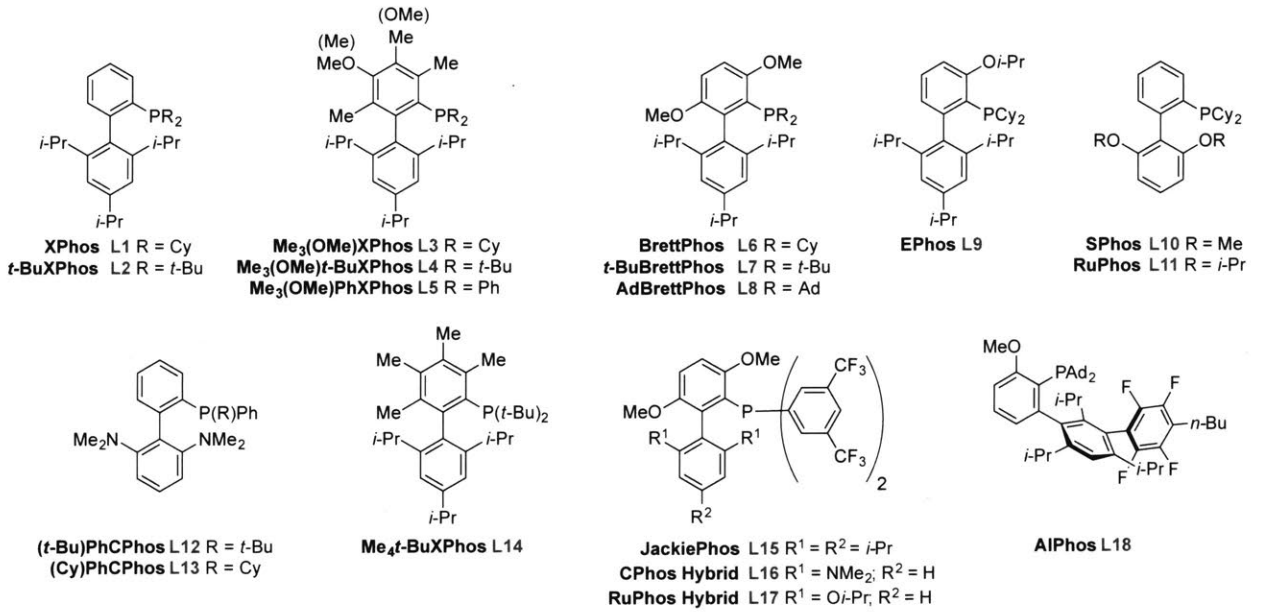

Figure 1. Examples of biaryl monophosphine ligands.

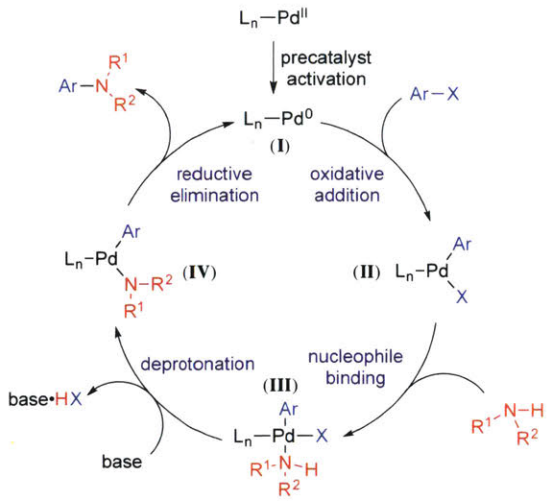

Scheme 1. General catalytic cycle for C–N cross-coupling reactions.

A generic mechanism for Pd-catalyzed C–N cross-coupling reactions is presented in Scheme 1. The catalytic cycle begins when a phosphine-ligated palladium(0) complex **(I)** undergoes oxidative addition to an aryl (pseudo)halide to give an aryl palladium(II) complex **(II)**. The net substitution of the amine for the (pseudo)halide resembles a "transmetalation" event and is thought to comprise a two-step sequence: nucleophile (amine) binding, followed by deprotonation. In the first step, the Pd(II) center acts as a Lewis acid to bind the amine, forming amine-bound complex **III**, thereby acidifying the proton on the nitrogen atom. In the second step, base-mediated elimination of HX forms an amido complex (**IV**), which regenerates $L_nPd(0)$ upon reductive elimination with concomitant release of amine product. The rate-limiting step varies depending on the type of coupling reaction, and each of these elementary steps can be modulated by the ancillary ligand.

1.1.a. General Features of the Catalyst

Dialkyl biaryl monophosphine ligands were first reported in 1998, and they have since shown broad applicability to a diverse array of cross-coupling reactions.[11–15] The reactivity of catalysts supported by these ligands is influenced in complex ways by the ligand architecture, as summarized in Figure 2.

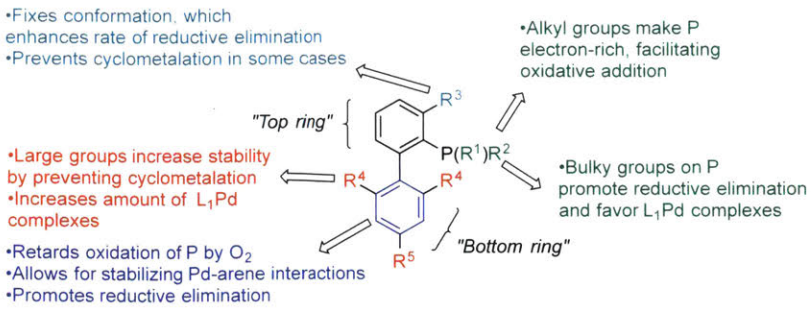

Figure 2. Features of dialkyl biaryl monophosphines.

The large substituents on phosphorus lend stability to the ligands by slowing the rate of oxidation of the phosphorus atom. This feature makes these ligands of even greater practical use in synthetic chemistry, as they can be stored under ambient conditions.[16] The bulkiness of the ligands also facilitates the formation and enhances the relative stability of L_1Pd complexes.[17]

Biaryl monophosphines have been shown to be pseudobidentate ligands for Pd, which also promotes the formation of monoligated Pd complexes.[18] The lower aromatic ring can serve as a ligand for the Pd center through C1′ (Figure 3). An alternative binding mode is operative for ligands bearing 2-methoxy substituents on the top ring (e.g., Figure 3, BrettPhos, **L6**); however, this binding mode is not observed for ligands that have large groups (e.g., 1-adamantyl or *t*-Bu) on phosphorus,[19] or larger alkoxy groups at C2.[20] Substituents R^3 and R^4 enhances catalyst stability by suppressing cyclometalative pathways for deactivation.[21] The presence of R^3 also serves to favor the conformation in which the Pd sits over the bottom ring. This both facilitates the rate of reductive elimination and enhances the stability of catalytically important intermediates.

Figure 3. Binding modes of BrettPhos (**L6**).

We will next discuss how specific structural features affect each elementary step (as summarized in Figure 2).

1.1.b. Oxidative Addition

In general, oxidative addition is fast for catalysts derived from dialkyl biaryl monophosphines even for less reactive electrophiles (e.g., aryl chlorides).[22] This is due to two main features: a) compared to $L_2Pd(0)$ complexes, the L_1Pd complexes formed with these ligands are more stable in the Pd(0) oxidation state, yet allow the aryl electrophile to approach more closely; and b) the alkyl groups on the phosphorus atom increase electron density on the Pd center (relative to triaryl phosphine-supported catalysts) which enhances the rate of oxidative addition. In terms of the aryl electrophile, the general order of reactivity is ArI > ArBr ~ ArOTf > ArCl ~ ArOMs. Using this hierarchy of reactivity exhibited by aryl (pseudo)halides, it is often possible to chemoselectively couple one electrophilic site, leaving another available for subsequent functionalization.

1.1.c. Transmetalation

Transmetalation refers to the process by which the nucleophilic coupling partner displaces the (pseudo)halide from the palladium center. Although this is the least well-understood step of the catalytic cycle, it is known to be generally sensitive to steric hindrance around the metal. Biaryl phosphines facilitate this step of the catalytic cycle by favoring low-coordinate L_1Pd complexes, which allows approach of the nucleophile to the metal center.[23]

The identity of the electrophile can have a significant impact on transmetalation. For example, when aryl triflates are employed as substrates, the triflate ion is dissociated from the metal center, rendering the complex formally cationic and opening a coordination site for the nucleophile; accordingly, transmetalation is usually faster in reactions employing aryl triflate electrophiles than analogous reactions employing aryl halide electrophiles.[19,24]

In many cases the rate of transmetalation is fastest for aryl chlorides (within the halide series), due to the increased polarity of the Pd–Cl bond, and smaller size of Cl relative to Br and I.[25] Indeed, aryl iodides can be challenging substrates, as the NaI formed during the reaction has been shown to have an inhibitory effect, although this issue can be circumvented by using a solvent that does not solubilize NaI (e.g., toluene).[26] In general, however, contrary to conventional wisdom from the early days of Pd coupling chemistry, the use of aryl iodide substrates should be avoided if possible.

1.1.d. Reductive Elimination

Reductive elimination is the last step of the catalytic cycle, which delivers the product and regenerates $L_nPd(0)$. The identity of the nucleophile plays a significant role in this elementary step: reductive elimination is more challenging for less nucleophilic coupling partners, such as diarylamines. There are three main ways that the structure of the ligand affects the rate of reductive elimination.

First, reductive elimination can be facilitated by withdrawing electron density from the metal center through the use of electron-poor phosphines (e.g., **L15**). The second strategy is to employ ligands bearing large alkyl substituents on the phosphorus atom (e.g., 1-adamantyl, *tert*-butyl), which force the aryl and amino ligands together, thereby shifting the ground state geometry closer to that of the reductive elimination transition state. Finally, it has been established that reductive elimination is faster from three-coordinate Pd(II) complexes than four-coordinate complexes.[27,28] Accordingly, the hemilabile character of the bottom ring of biaryl monophosphine ligands allows L–Pd(Ar)NR_2 complexes to adopt the preferred T-shaped geometry for reductive elimination. Thus, in general, reductive elimination is a rapid process in most C–N cross-coupling reactions. However, it can be rate-limiting in reactions that form triarylamines.[29] Furthermore, the role of reductive elimination in coupling reactions of *N*-heterocycles or amides has not been studied in detail.

1.2. Precatalyst Selection

It is clear that selection of an appropriate ligand can determine the success or failure of a cross-coupling reaction, but the palladium source can have a dramatic impact as well. The most commonly employed sources of Pd are complexes such as $Pd(OAc)_2$, $PdCl_2$, $PdCl_2(MeCN)_2$, $[PdCl(allyl)]_2$, and Pd_2dba_3. These metal sources are advantageous because they are bench-stable and commercially available. However, the metal must associate with the ligand, and with the exception of Pd_2dba_3, it must be reduced from Pd(II) to Pd(0) under the reaction conditions prior to entering the catalytic cycle.

The efficiency of the Pd(II) reduction step is dependent on the ligand used, the type of Pd source, and the reductant employed. The optimal reducing agent varies depending on the reaction conditions. Amines,[30–33] tertiary phosphines,[34] boronic acids,[35] and organometallic reagents (e.g.,

organozincs) have all been used.[36] With amines, β-hydride elimination from a Pd(II) amido complex is a major pathway; accordingly, nucleophiles that do not possess β-hydrogens, such as amides and anilines, are poor reductants. Tertiary phosphines, including bulky biaryl monophosphines, have been shown to reduce $Pd(OAc)_2$ in the presence of water to produce L–Pd(0) as well as an equivalent of phosphine oxide.[37] Organometallic reagents and boronic acids are used as sacrificial nucleophiles and successive transmetalation of two equivalents of the nucleophile onto Pd(II) followed by reductive elimination generates L–Pd(0), with concomitant formation of a C–C homocoupling product.

Some Pd(0) sources may also be used as precatalysts, such as Pd_2dba_3 and $Pd(PPh_3)_4$. However, in situ catalyst formation must still occur with both Pd(0) sources, which requires the displacement of already bound ligands such as dba or PPh_3. Generally, Pd(0) sources are air-sensitive and must be stored under inert atmosphere. Pd_2dba_3 is an exception to this, as the metal center is stabilized through π-backbonding with the dba ligand. However, the strength of this interaction may actually hamper catalyst reactivity.[38,39] Furthermore, commercial sources of Pd_2dba_3 are often contaminated with unreactive Pd(0) nanoparticles, which results in the formation of a less active catalyst.[40]

Over the past two decades, several types of pre-ligated Pd precatalysts have been developed to eliminate the need for in situ catalyst formation. These include π-allyl-,[41] indenyl-,[42] and palladacycle precatalysts[43–45] for phosphine ligands (Figure 4), as well as pyridine-based complexes for NHC ligands.[46] Of the palladacycle precatalysts, complexes **G3–G5** (where **G** denotes the generation of precatalyst) are most commonly used,[15] as they accommodate a wide range of bulky phosphine ligands, are bench-stable, and provide a reliable means of rapidly generating L–Pd(0). Upon exposure to base, the nitrogen atom is deprotonated, forming an intermediate amido complex. This complex undergoes a subsequent intramolecular C–N reductive elimination to form the corresponding carbazole and L–Pd(0) (Figure 4b). The parent carbazole byproduct (generated from **G3**-type palladacycles) can on occasion be deleterious at room temperature[41] and in certain couplings (e.g., C–F cross-coupling).[47] Palladacycles **G4** and **G5** circumvent this issue by generating *N*-substituted carbazoles, but ligands bearing large adamantyl or *tert*-butyl groups on phosphorus (e.g., **L7**, **L8**, **L18**) do not readily form these types of precatalysts.[48] These potential issues can be avoided by using the corresponding oxidative

addition complexes (**G6**) or π-allyl complexes, which are easily formed with a wide range of ligands and work well in a variety of cross-coupling reactions.[49]

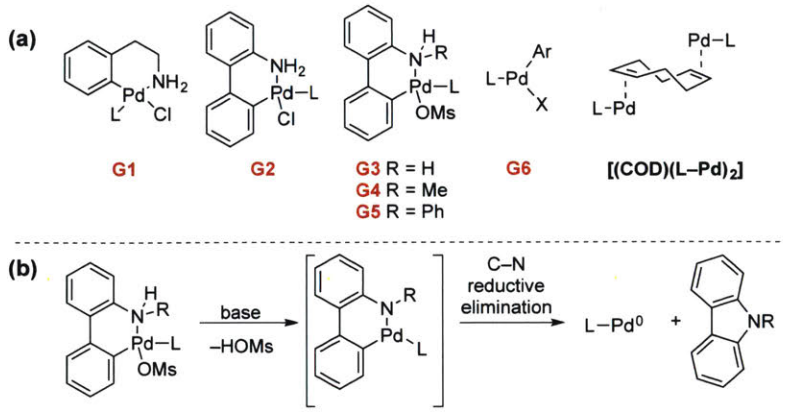

Figure 4. (a) Pre-ligated palladium precatalysts.[45,48–50] (b) Base-mediated activation of palladacycle precatalysts.

Complexes with formula [(1,5-cyclooctadiene)(L–Pd)$_2$] have also been developed. These precatalysts are a pre-ligated form of Pd(0) that rapidly react with aryl (pseudo)halides. However, they are often air-sensitive, exhibit poor solubility in organic solvents, and not all biaryl monophosphine ligands form precatalysts of this type.[50]

1.3. C–N Cross-Coupling Reactions

Nitrogen-based nucleophiles display wide variability in basicity, nucleophilicity, and steric hindrance, and thus, a diverse set of catalysts is required to facilitate optimum cross-coupling for all types of nucleophiles. Although the choice of ligand generally has the most pronounced effect on reaction outcome, the selection of base, reaction solvent, and temperature can also be critical. Our discussion of the effect of these four variables will be organized based on the subclass of nucleophile.

1.3.a. Secondary Amines

Both aliphatic and aromatic secondary amines are most often coupled with aryl halides using RuPhos (**L11**)-supported catalysts. Cyclic amines (pyrrolidines, piperidines) are better substrates than acyclic amines, due to their decreased steric hindrance.[51] The most common

conditions use NaO*t*-Bu in THF (Figures 5, 6), but base-sensitive substrates can be more effectively coupled using Cs_2CO_3 in *t*-BuOH (Figures 5, 6).[52] Protic substrates can be coupled using excess LiHMDS in THF, as the protic functional group is protected in situ by deprotonation (Figures 7, 8).[52,53] While RuPhos (**L11**) is typically the preferred ligand for secondary amine couplings, SPhos (**L10**) and XPhos (**L1**) have also been reported to be useful (Figures 8, 9).[15,53–55]

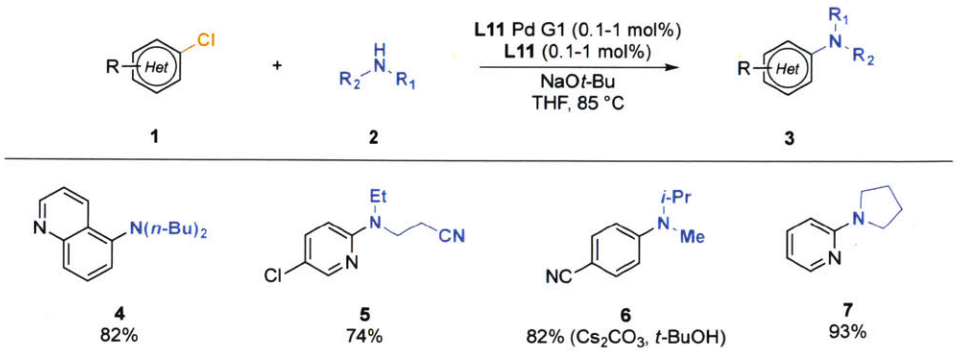

Figure 5. RuPhos-supported catalysts can couple cyclic and acyclic secondary amines to aryl chlorides.[52]

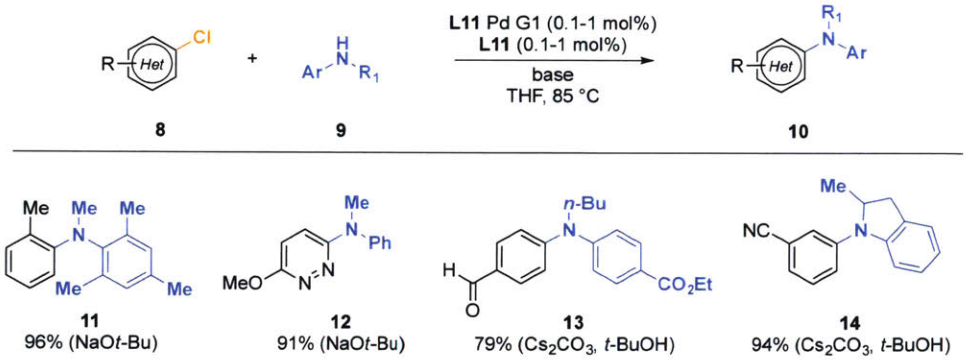

Figure 6. Coupling of aryl alkyl amines with RuPhos-supported catalysts.[52]

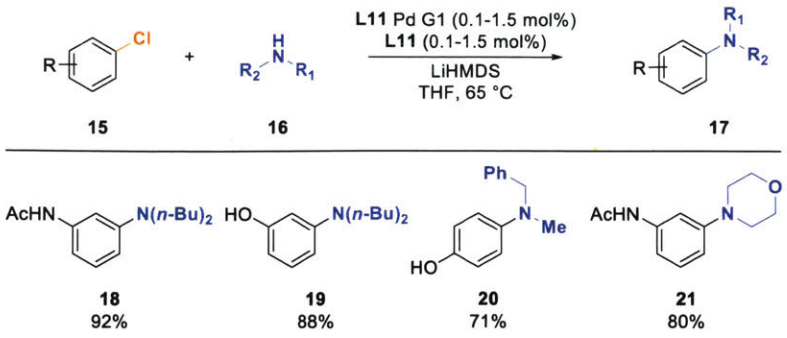

Figure 7. LiHMDS allows protic functional groups to be tolerated in the coupling of secondary aliphatic amines.[52]

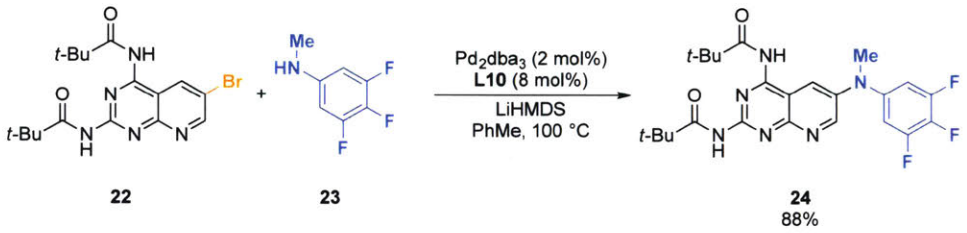

Figure 8. LiHMDS enables the coupling of a complex aryl bromide.[53]

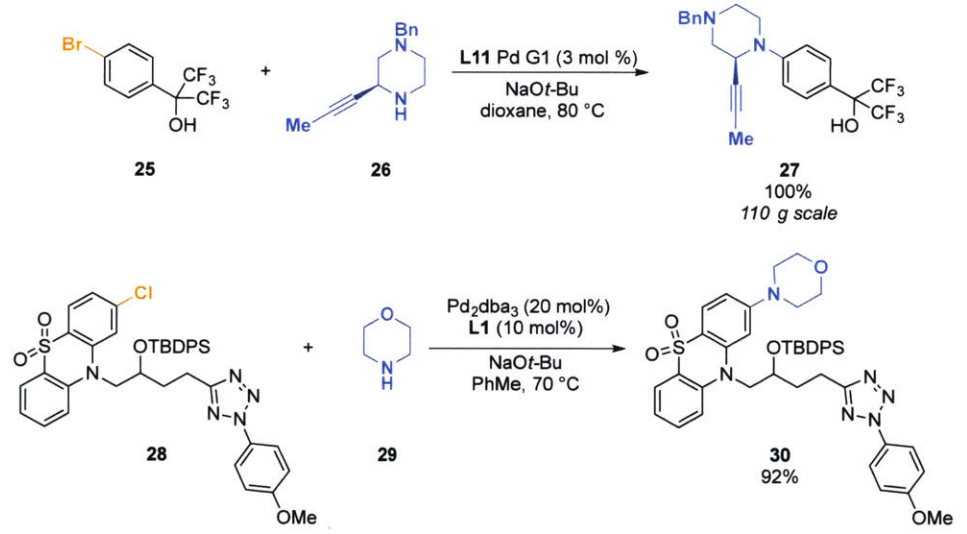

Figure 9. C–N coupling of secondary aliphatic amines with complex electrophiles.[54,55]

1.3.a.i. Hindered Secondary Amines

The coupling of secondary amines displaying α-branching is especially challenging, likely due to the difficulty of amine binding as a result of steric hindrance around the nitrogen

atom. The difficulty of this binding can result in competitive C–O coupling with NaO*t*-Bu when it is used as the base. To address this problem, **L16** and **L17** were designed; these compounds bear electron-deficient aryl groups on phosphorus which produces a more Lewis-acidic catalyst that facilitates amine binding. The use of **L16** Pd G4 and **L17** Pd G4 allowed for (hetero)aryl bromides and chlorides to be coupled with these hindered amines in good yields (Figure 10).[56]

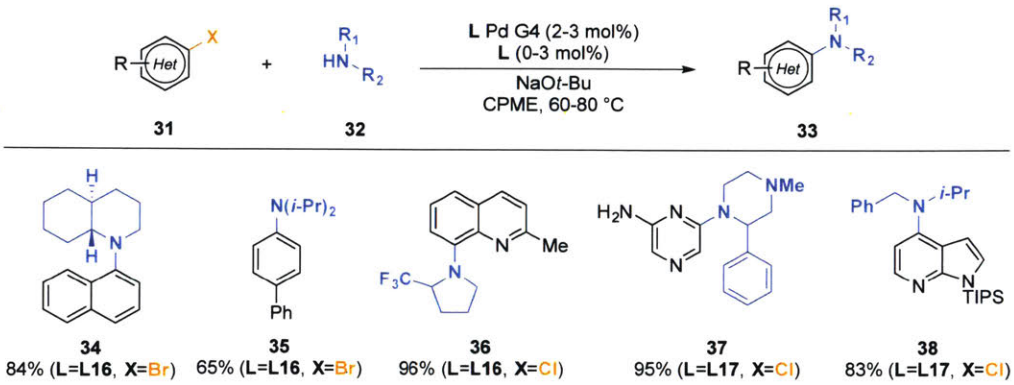

Figure 10. Coupling of α-branched secondary amines.[56]

1.3.a.ii. Diarylamines

Diarylamines are relatively challenging substrates for C–N coupling due to, at least in part, their low nucleophilicity and the difficulty of reductive elimination to form triaryl amines. Indeed, mechanistic studies indicate that reductive elimination is the rate-determining step for the arylation of diarylamines with RuPhos (**L11**)-supported catalysts.[29] Nevertheless, under optimized conditions, diarylamines can be coupled with (hetero)aryl chlorides using a RuPhos (**L11**)-supported catalyst (Figure 11).[52] Similar conditions are effective for coupling weakly nucleophilic iminostilbenes and iminodibenzyls (**44**).[57] For the latter reactions, the **G4** precatalyst is superior to the **G3** precatalyst, likely because **G3** precatalysts generate carbazole, which may compete with iminostilbenes and iminodibenzyls in binding to Pd.

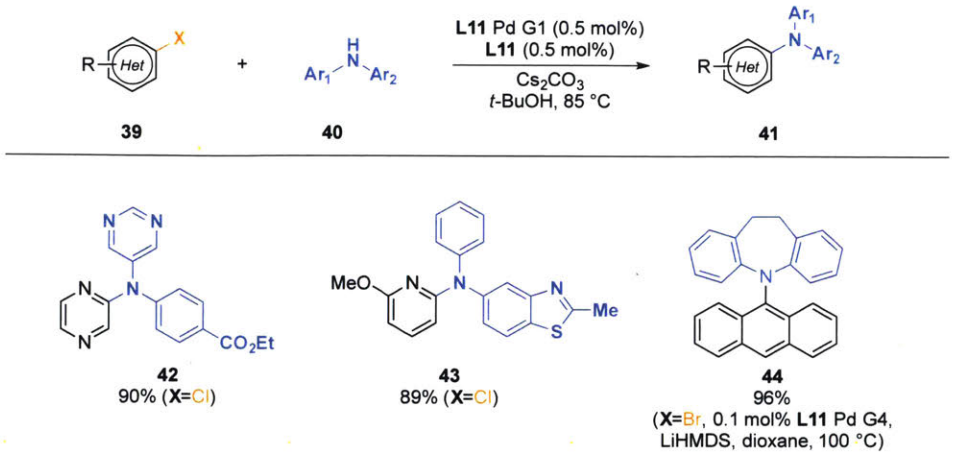

Figure 11. RuPhos-supported catalysts allow the arylation of diarylamines.[52,57]

1.3.b. Primary Amines

A major challenge of primary amine couplings is preventing further arylation of the product (a secondary amine). For primary alkyl and aryl amines, BrettPhos (**L6**)-supported catalysts are generally effective and give excellent selectivity for monoarylated product. The use of NaO*t*-Bu in ethereal solvents (e.g., dioxane, n-Bu_2O) is common. Weaker bases, such as Cs_2CO_3 and K_3PO_4, are also frequently employed in combination with a variety of solvents (e.g., *t*-BuOH, PhMe, dioxane).

1.3.b.i. Primary Aliphatic Amines

Primary aliphatic amines can be coupled in the presence of unprotected secondary amines. Even methylamine, the smallest primary amine substrate, can be selectively monoarylated by a variety of aryl chlorides (Figure 12).[19] As in the case of secondary amines, the use of LiHMDS allows for protic functional groups to be tolerated (Figure 13).[52]

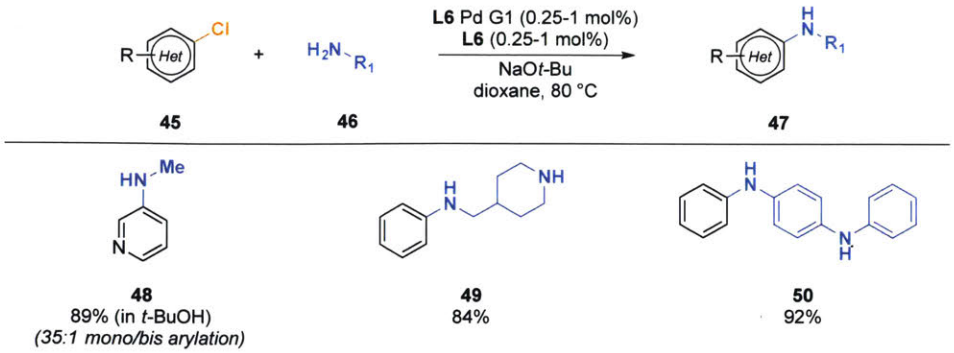

Figure 12. BrettPhos enables selective coupling of primary amines in the presence of secondary amines.[19]

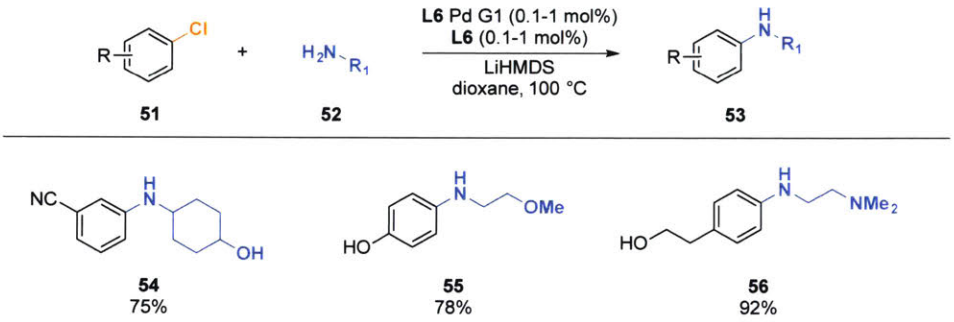

Figure 13. LiHMDS enables C–N coupling of primary amines in the presence of alcohols.[52]

Primary amines can also be coupled to (hetero)aryl bromides, chlorides, and triflates using a weaker base, DBU, and AlPhos (**L18**)-supported catalysts in MTBE (Figure 14). This method tolerates unprotected protic functional groups and allows highly base-sensitive substrates to be coupled, including primary alkyl halides (**64**).[58]

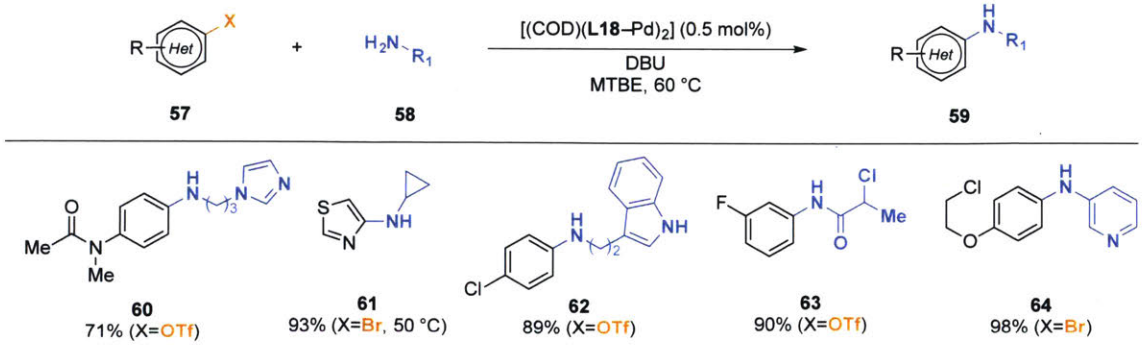

Figure 14. Coupling primary amines and base-sensitive substrates using DBU and an AlPhos-supported catalyst.[58]

When the primary amine is sterically encumbered (e.g., 1-adamantylamine, tritylamine), BrettPhos-based catalysts are not efficacious. Instead, *t*-BuPhCPhos (**L12**) and CyPhCPhos (**L13**) are superior ancillary ligands. Specifically, *t*-BuPhCPhos (**L12**) is an effective ligand for unhindered aryl bromides and chlorides, whereas CyPhCPhos (**L13**) promotes couplings of *ortho*-substituted aryl bromides and chlorides (Figure 15).[59]

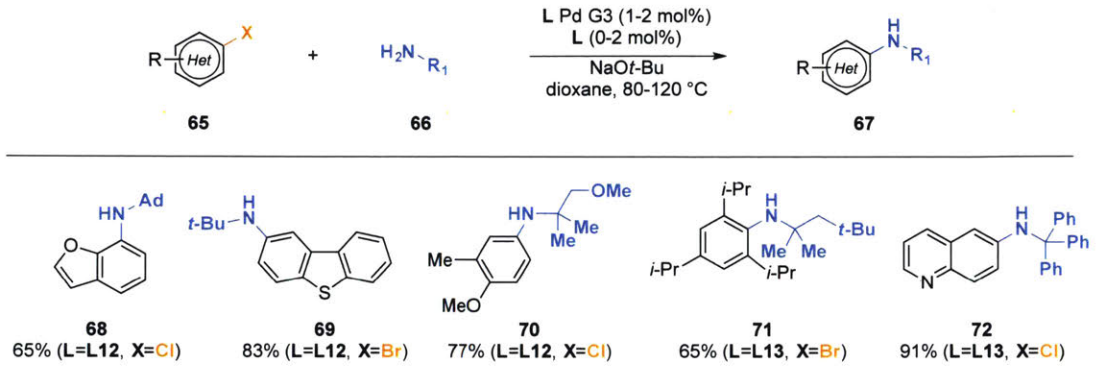

Figure 15. *t*-BuPhCPhos and CyPhCPhos enable coupling of highly hindered primary aliphatic amines.[59]

1.3.b.ii. Primary Anilines

In general, aryl amines derived from six-membered-ring (hetero)arenes couple to aryl (pseudo)halides smoothly with low catalyst loadings (Figures 16–18).[19,51,60] The use of *t*-BuBrettPhos (**L7**) as a supporting ligand and LiHMDS as the base allows unprotected five-membered heteroaryl halides to be suitable electrophiles in this type of process (Figure 19).[61]

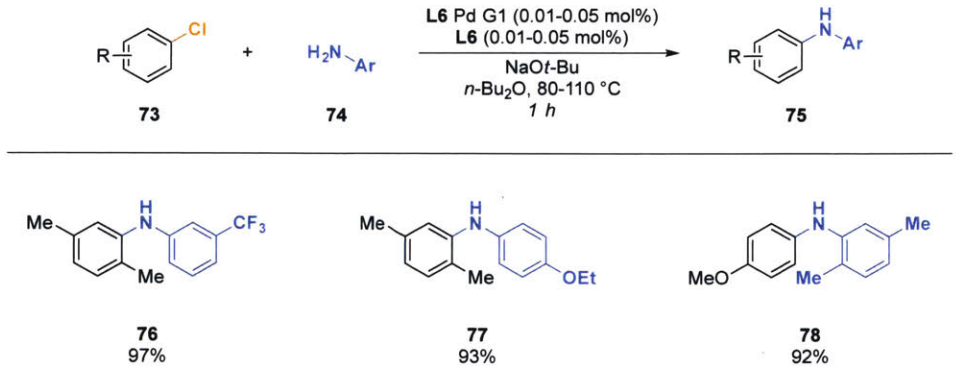

Figure 16. BrettPhos-supported catalysts couple primary anilines to aryl chlorides with low catalyst loadings.[19]

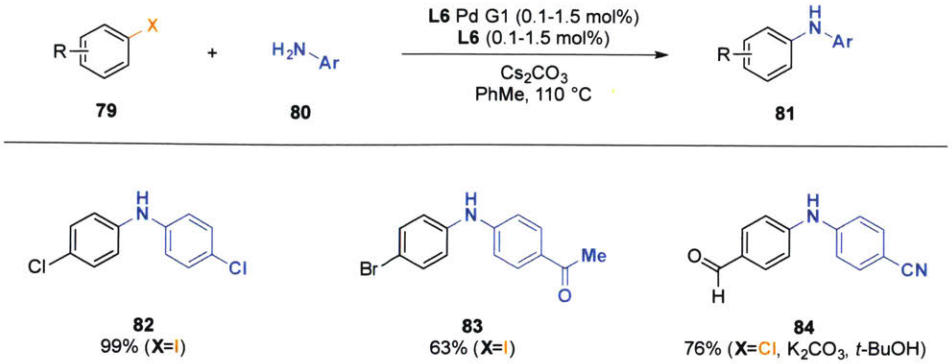

Figure 17. BrettPhos-supported catalysts couple functionalized aryl halides and aryl amines using Cs_2CO_3.[51]

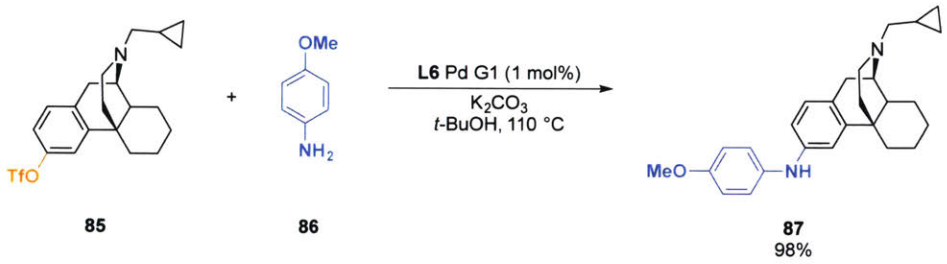

Figure 18. A BrettPhos-derived precatalyst enables the efficient amination of an aryl triflate.[60]

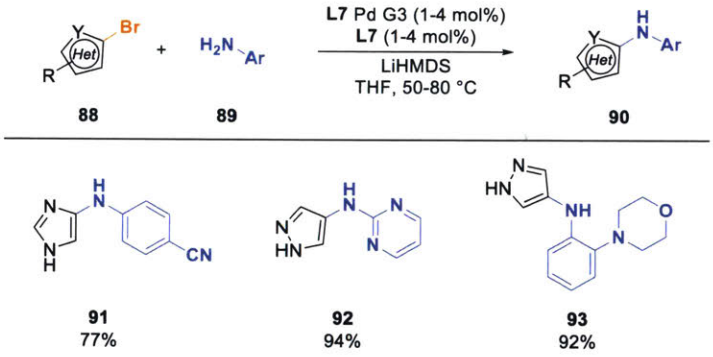

Figure 19. With LiHMDS, *t*-BuBrettPhos-supported catalysts couple primary amines to unprotected five-membered imidazole and pyrazole bromides.[61]

Five-membered-ring heteroaryl amines are challenging substrates.[62] In general, AlPhos (**L18**)-supported catalysts display the most general scope (Figure 20).[58] However, other less expensive ligands are effective in certain cases. For example, *t*-BuBrettPhos (**L7**) can be used

with 2-aminobenzimidazoles (Figure 21) or 2-aminothiazoles (Figure 22), but gives low yields for some amines (e.g., 2-aminooxazoles).[20,61-64] EPhos (**L9**)-supported catalysts give good yields for aminoazoles, which is attributed to suppression of off-cycle *O*-bound complexes (Figure 23).[20]

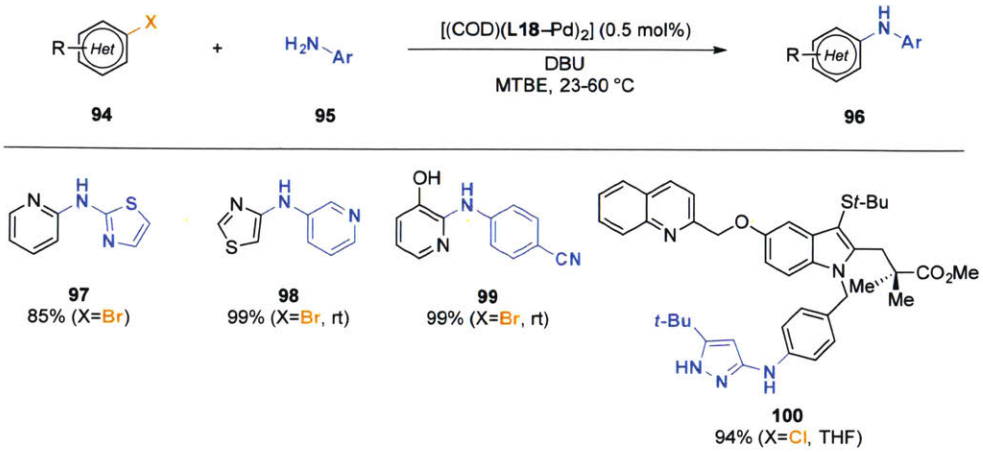

Figure 20. AlPhos-supported catalysts can couple a diverse range of heteroaryl halides and amines.[58]

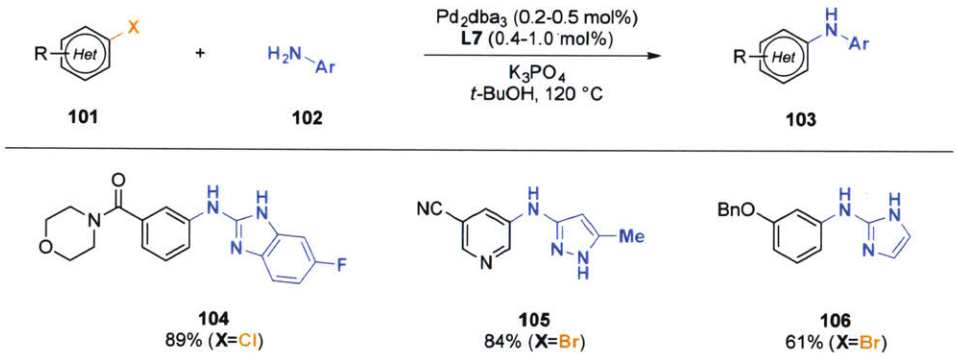

Figure 21. *t*-BuBrettPhos-supported catalysts can couple 2-aminoimidazoles and benzimidazoles to aryl halides.[63]

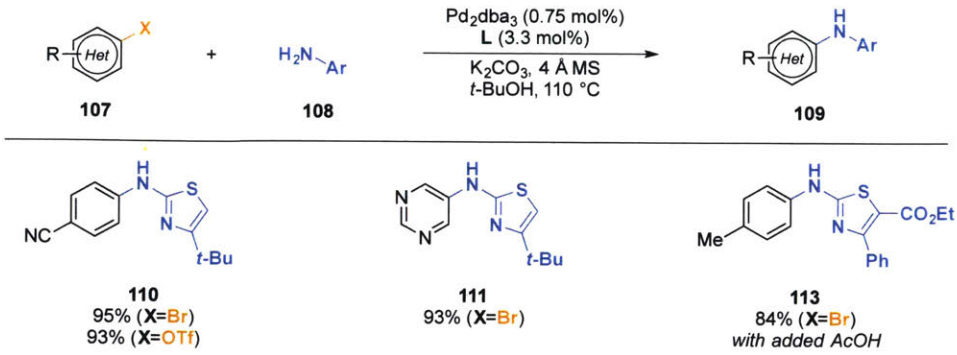

Figure 22. *t*-BuBrettPhos-supported catalysts can arylate 2-aminothiazoles.[64]

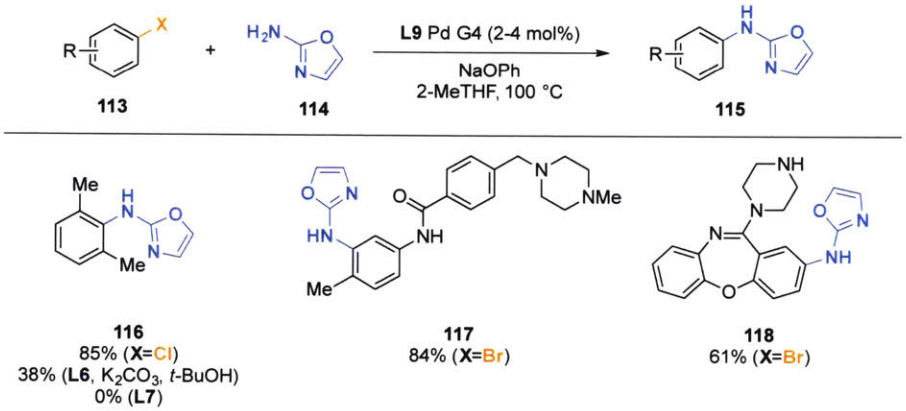

Figure 23. EPhos enables arylation of 2-aminooxazole, a challenging nucleophile.[20]

1.3.c. Ammonia and Hydrazine

Monoarylation of ammonia is challenging because the products, primary (hetero)aryl amines, are competent nucleophiles which can competitively undergo a second arylation to form diarylamines. Many methods have circumvented this problem by using an ammonia surrogate like benzophenone imine or LiHMDS, producing a protected product that is transformed into the desired primary (hetero)aryl amine after the coupling reaction is complete.[51]

However, recent advances in ligand design from our group[65] and others[8,66] have enabled the direct monoarylation of ammonia. In the case of dialkyl biaryl monophosphines, ligands with larger alkyl groups on phosphorus, like AdBrettPhos (**L8**) and Me_3(OMe)XPhos (**L3**), are effective at suppressing diarylation (Figure 24). In particular, Me_3(OMe)XPhos (**L3**) is superior for six-membered (hetero)arenes, whereas AdBrettPhos (**L8**) is best for five-membered heteroarene couplings. A third ligand, Me_3(OMe)PhXPhos (**L5**), works well for *ortho*-

substituted substrates. A typical reaction employs NaO*t*-Bu as the base and dioxane as the solvent. Commercially available solutions of ammonia in dioxane were found to be suitable for this reaction.[65]

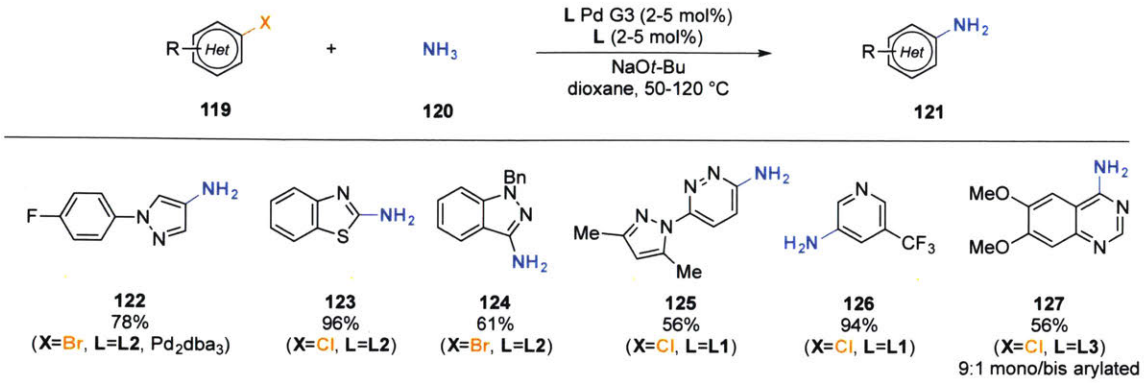

Figure 24. Ammonia can be monoarylated by five- and six-membered arenes and heteroarenes.[65]

Hydrazine presents similar challenges, as the product arylhydrazine can undergo a subsequent arylation at either nitrogen atom. Furthermore, hydrazine is a potential explosive, particularly in the presence of transition metals.[67] Although benzophenone hydrazone can in some cases be employed as a stable hydrazine surrogate, access to unprotected arylhydrazines permits facile synthesis of a wider variety of heterocycles and hydrazones.[68]

As in the case of ammonia, the use of large alkyl groups on phosphorus is needed to suppress diarylation. In order to perform this reaction more safely, the cross-coupling was conducted using continuous flow technology. The combination of *t*-BuBrettPhos (**L7**) Pd G1 and NaO*t*-Bu in THF selectively and rapidly couples hydrazine (as a solution in THF) with aryl chlorides. The resulting arylhydrazines were directly used in a condensation reaction to form the corresponding hydrazone, pyrazole, or indole (Figure 25).[67]

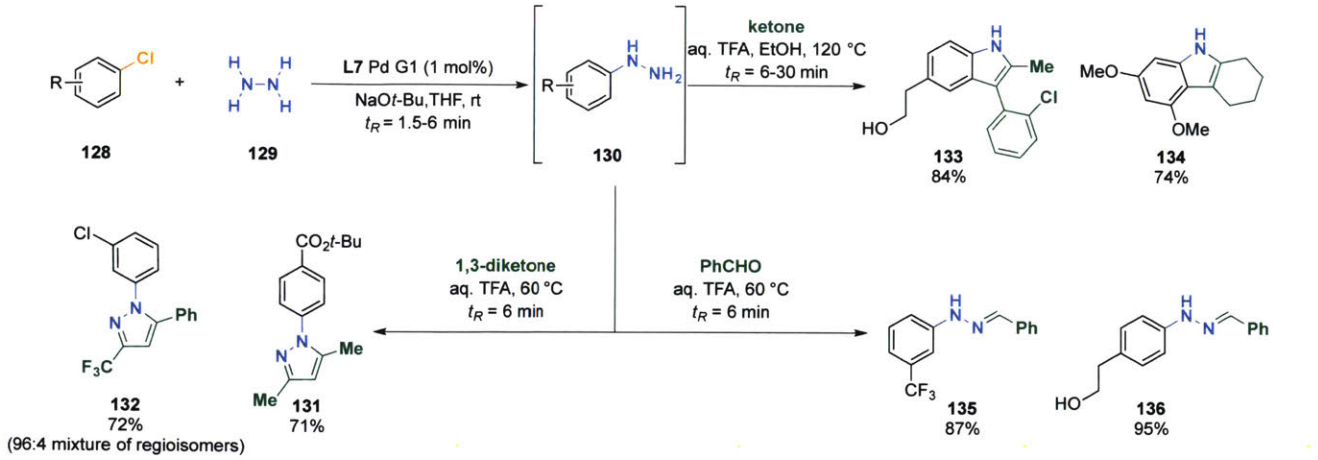

Figure 25. Coupling of hydrazine to aryl chlorides, and subsequent formation of azoles and hydrazones under continuous flow conditions.[67]

1.3.d. Amides, Ureas, Carbamates, and Sulfonamides

The coupling of amides, ureas, carbamates and sulfonamides can generally be achieved with phosphine ligands bearing larger groups (i.e., 1-adamantyl or *t*-Bu) on phosphorus. The combination of weak inorganic bases (e.g., Cs_2CO_3, K_3PO_4) in *t*-BuOH is most commonly employed.

1.3.d.i. Primary Amides

t-BuBrettPhos (**L7**)- and Me$_4$*t*-BuXPhos (**L14**)-supported catalysts can couple primary amides with aryl (pseudo)halides (Figures 26, 27).[69–71] Amides are inherently weak nucleophiles, and consequently aryl chlorides, triflates, and mesylates are superior to bromides and iodides for this reaction, since the Pd(II) complexes formed by oxidative addition are more electrophilic.[69] Catalysts based on **L7** and **L14** also prevent the formation of κ^2-amidate complexes, which are known to cause catalyst decomposition.[69–71] In cases where both catalysts give product, the use of *t*-BuBrettPhos (**L7**) is recommended, since reactions tend to be substantially faster than with Me$_4$*t*-BuXPhos (**L14**).[71]

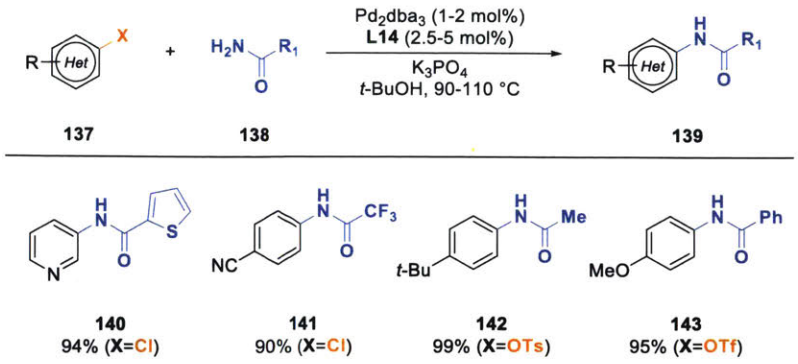

Figure 26: Me4*t*-BuXPhos-supported catalysts couple aryl (pseudo)halides with primary amides.[69]

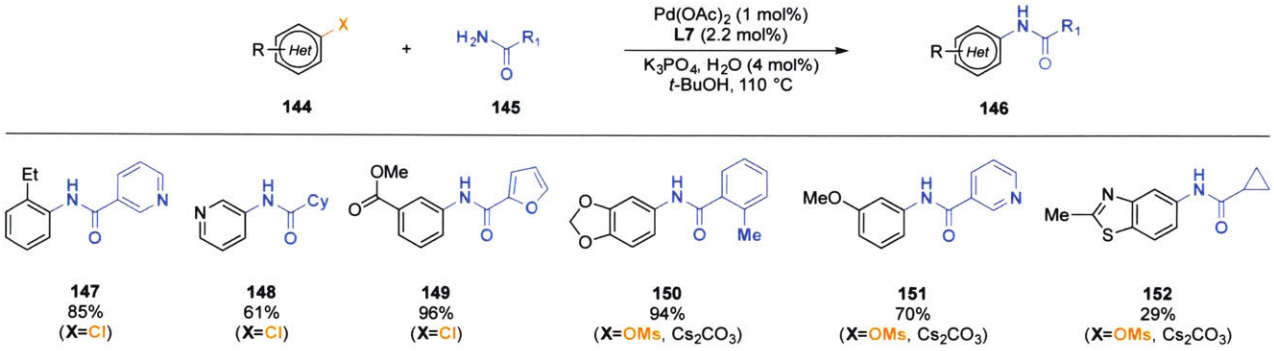

Figure 27. *t*-BuBrettPhos-supported catalysts couple aryl chlorides and mesylates with primary amides.[70–71]

t-BuBrettPhos (**L7**)- and Me4*t*-BuXPhos (**L14**)-supported catalysts are unable to couple primary amides to five-membered heteroaryl bromides. However, this transformation can be realized by using an AdBrettPhos (**L8**)-supported catalyst system (Figure 28). The increase in reactivity is attributed to the bulkier alkyl groups on phosphorus, which promote the challenging reductive elimination of small electron-rich heterocycles.[72] As is the case for primary anilines, AlPhos (**L18**)-supported catalysts (with DBU in MTBE) are effective for the amidation of a range of aryl electrophiles, including five-membered-ring heterocycles (Figure 29).[58]

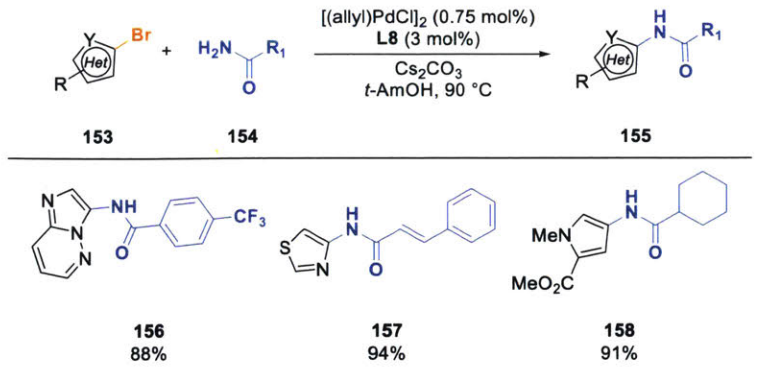

Figure 28. AdBrettPhos-supported catalysts can couple primary amides to five-membered-ring heteroaryl bromides.[72]

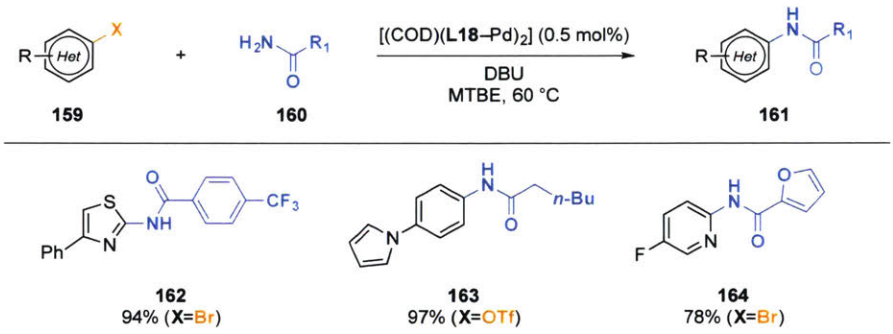

Figure 29. AlPhos enables coupling of primary amides with diverse heteroaryl (pseudo)halides.[58]

The Pd-catalyzed amidation reaction can be applied to a one-pot synthesis of substituted *N*-aryl benzimidazoles. Anilines and primary amides are coupled to 1,2-dihaloarenes using *t*-BuBrettPhos (**L7**)-derived catalysts, Cs_2CO_3, and *t*-BuOH. The *bis*-coupled product condenses intramolecularly to give benzimidazoles in good yield (Figure 30). When different halides are used (e.g., 1-bromo-2-chlorobenzene), the weakest carbon–halogen bond undergoes coupling first, and since the more nucleophilic aniline couples before the less nucleophilic primary amide, the final product is formed with complete regiocontrol.[73]

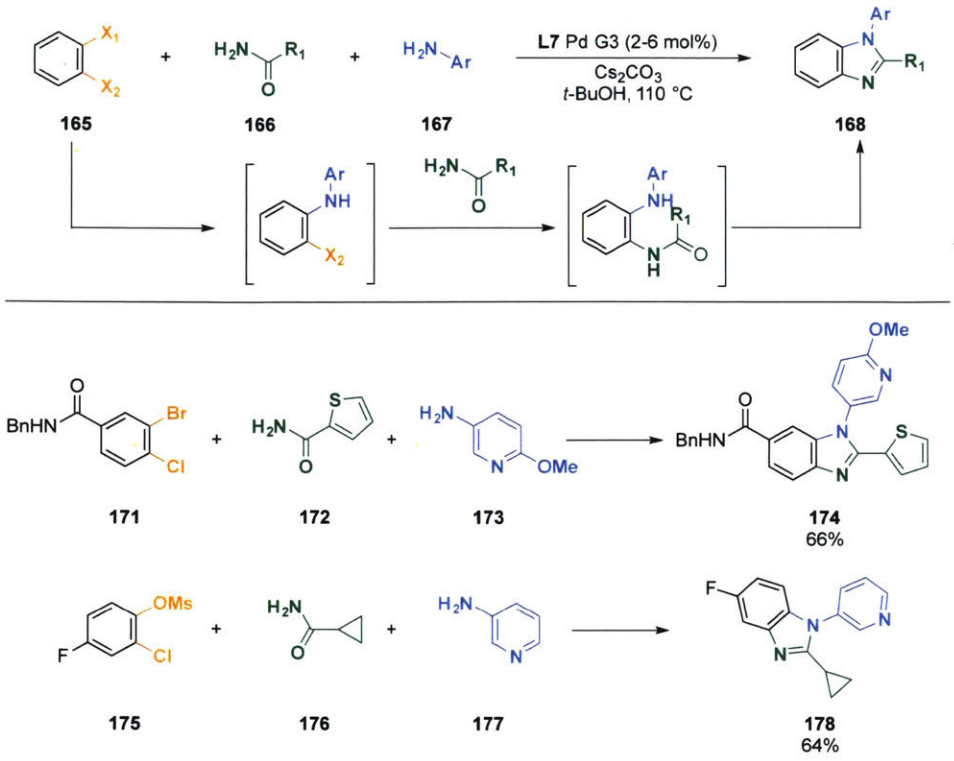

Figure 30. *t*-BuBrettPhos enables the synthesis of *N*-aryl benzimidazoles.[73]

1.3.d.ii. Secondary Amides

Cyclic secondary amides (i.e., lactams) and *N*-methyl amides can be coupled to aryl chlorides and triflates with catalysts derived from AlPhos (**L18**) or Me$_4$*t*-BuXPhos (**L14**) (Figure 31). As with cyclic secondary amines, the cyclic nature of lactams is thought to "tie back" the *N*-alkyl substituent, allowing for a more facile transmetalation.[58,69]

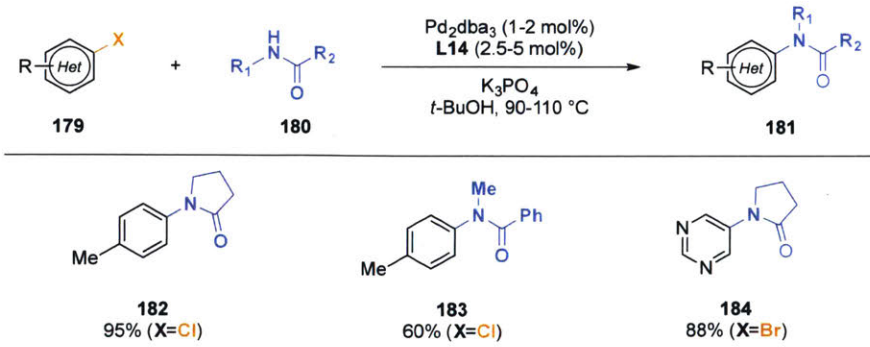

Figure 31. Lactams and *N*-methyl amides can be coupled under the same conditions as primary amides.[69]

Me4*t*-BuXPhos (**L14**), *t*-BuBrettPhos (**L7**), and AlPhos (**L18**) are unable to couple most acyclic secondary amides (namely, amides larger than *N*-methyl amides). Instead, a JackiePhos (**L15**)-supported catalyst can be employed, along with K_2CO_3 or Cs_2CO_3 and 3 Å molecular sieves in toluene (Figure 32). The electron-deficient phosphine is thought to promote binding of nitrogen and thereby accelerate transmetalation. Under these conditions, aryl nonaflates, triflates, and chlorides can be coupled; however, the use of aryl bromides and iodides appear to inhibit transmetalation and thus, these electrophiles are unsuitable reaction partners.[74]

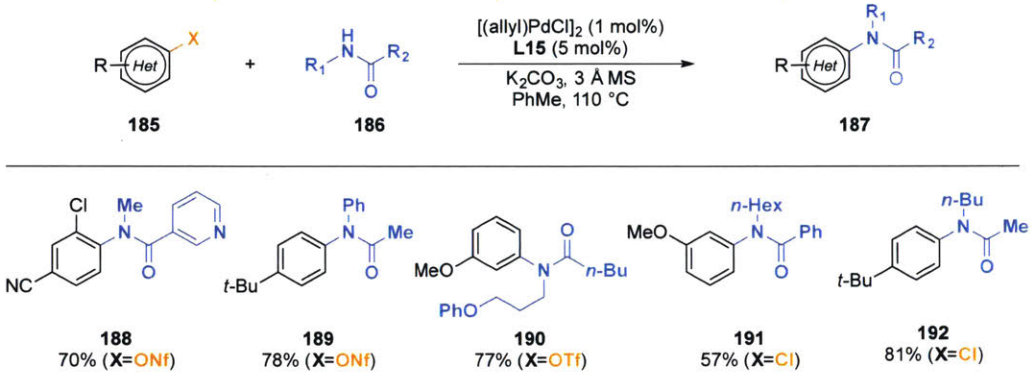

Figure 32. JackiePhos-mediated coupling of secondary amides with aryl chlorides, triflates, and nonaflates.[74]

1.3.d.iii. Ureas, Carbamates, and Sulfonamides

Ureas, carbamates, and sulfonamides react similarly to amides. Primary ureas and carbamates can be coupled when AlPhos (**L18**)[58] or *t*-BuBrettPhos (**L7**)[75] are used as supporting ligands (Figures 33, 34). Primary sulfonamides are suitable nucleophiles when *t*-BuBrettPhos (**L7**) is employed (Figure 35),[76] although *t*-BuXPhos (**L2**) has also shown promise as an ancillary ligand.[77]

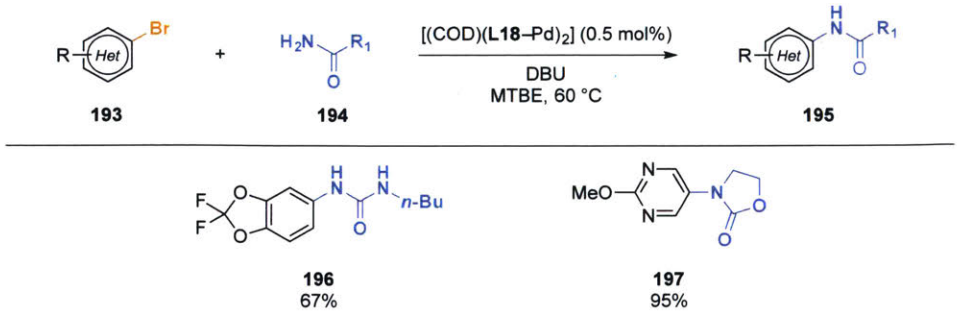

Figure 33. AlPhos-supported catalysts can couple ureas and carbamates to aryl bromides.[58]

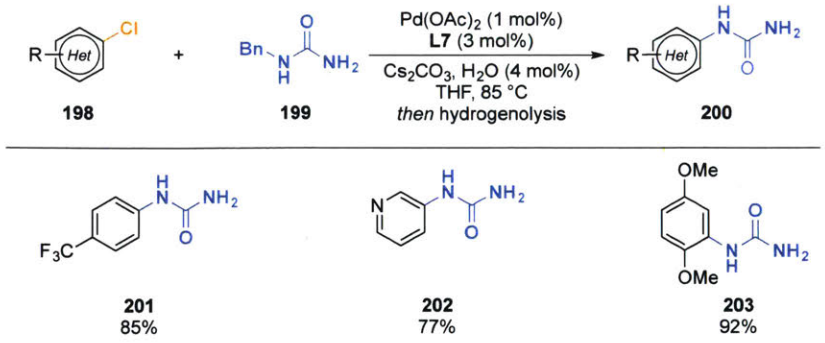

Figure 34. *t*-BuBrettPhos enables coupling of benzyl-protected urea to aryl chlorides.[75]

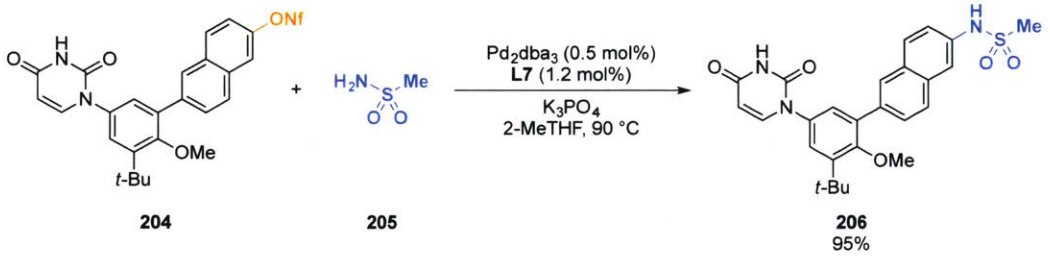

Figure 35. *t*-BuBrettPhos-supported catalysts can couple an aryl nonaflate with a primary sulfonamide.[76]

Secondary acyclic ureas, carbamates, and sulfonamides can be coupled to aryl triflates, chlorides, and nonaflates using a JackiePhos (**L15**)-supported catalyst (Figure 36).[74] As in the case of secondary amides, the effectiveness of **L15** can be attributed to the electron-withdrawing aryl groups on phosphorus, which enhance the Lewis acidity of palladium and thereby promote the binding of these weak nucleophiles.

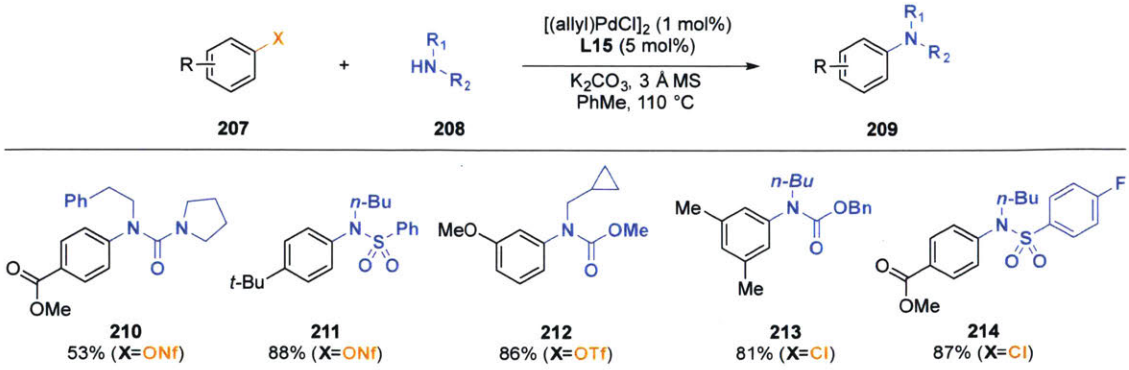

Figure 36. JackiePhos couples secondary ureas, carbamates, and sulfonamides to aryl (pseudo)halides.[74]

1.3.e. Imidazoles and Triazoles

Using catalysts derived from Me$_4$*t*-BuXPhos (**L14**) or Me$_3$(OMe)*t*-BuXPhos (**L4**), substituted imidazoles and benzimidazoles can be regioselectively arylated at the less hindered position with aryl bromides, chlorides, and triflates (Figure 37). Imidazoles are potent catalyst poisons, and therefore, pre-complexation of ligand and palladium (by preheating ligand and Pd_2dba_3, or by using a precatalyst) is necessary for high and reproducible yields.[78,79] These conditions are suitable for the *N*2-arylation of 1,2,3-triazoles, although benzotriazoles give a nearly 1:1 mixture of *N*1 and *N*2 isomers (Figure 38).[80]

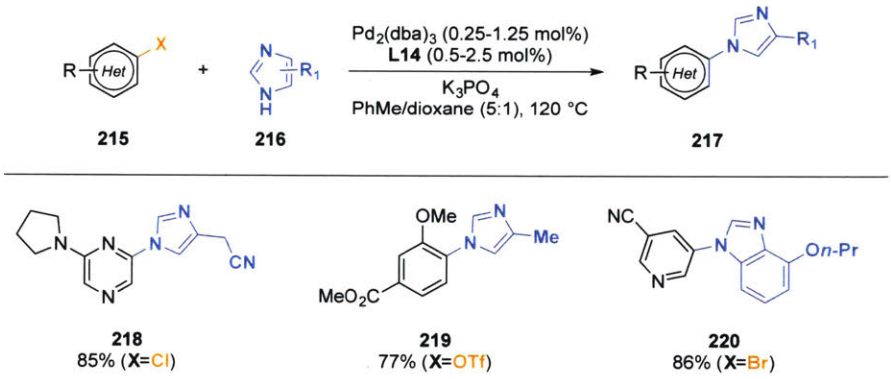

Figure 37. Regioselective arylation of imidazoles and benzimidazoles.[78]

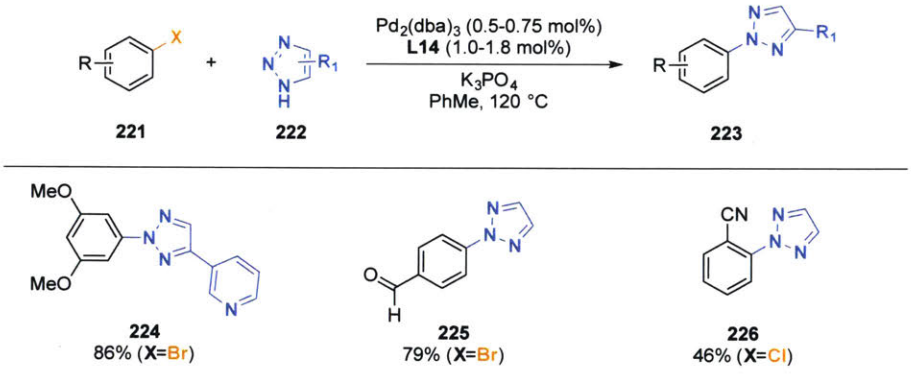

Figure 38. Regioselective arylations of triazoles.[80]

1.4. Conclusion

Palladium catalysis is a versatile tool for constructing carbon–nitrogen bonds under mild conditions. The palladium source, supporting ligand, base, temperature, and solvent all have an effect on the reaction outcome. Furthermore, these variables often strongly influence each other:

for instance, the choice of ligand may affect the optimal base for a particular process. A summary of each of the effects of these variables in the context of C–N coupling reactions is presented below.

Palladium source:

The use of precatalysts is recommended when possible in order to reliably and rapidly generate L–Pd(0). With precatalysts, many nitrogen nucleophiles can be coupled under mild conditions with low catalyst loadings.[51] In cases where a precatalyst is not available, it is recommended to use a known procedure to ensure that Pd(0) is formed, such as the water-mediated reduction of $Pd(OAc)_2$.[37]

Base:

The most widely used base for C–N coupling is NaO*t*-Bu, which typically allows for fast reactions and low catalyst loadings. Occasionally, other strong bases are used, such as LiHMDS. This can be advantageous when protic functional groups (e.g., carboxylic acids, amides, alcohols, indoles, etc.) are present, as initial deprotonation "protects" the functional group, allowing for subsequent C–N coupling.[81–83]

However, the use of a strong base can cause undesired side reactions or, in combination with amines, the decomposition of certain substrates.[84] In these cases, weak inorganic bases (e.g., Cs_2CO_3, K_3PO_4, K_2CO_3) allow for broader functional group tolerance. Cs_2CO_3 gives the fastest reaction rate of the weak inorganic bases, likely owing to the greater solubility of cesium salts in organic solvents compared to smaller alkali metals, but it is also more expensive and hygroscopic. These bases are typically mostly insoluble in the reaction mixture, and catalyst turnover can therefore be dependent on particle size. On large scales, this can lead to reproducibility challenges. Furthermore, reactions using weak bases are generally slower and require higher catalyst loadings.[51]

Catalysts supported by AlPhos (**L18**) are able to couple a broad range of primary amines and amides to a wide variety of (hetero)aryl electrophiles using DBU as the base. This reaction exhibits excellent functional group tolerance due to the low basicity of DBU.[58]

Temperature:

Most C–N coupling reactions with moderately complex substrates proceed at or above 60 °C. Although in many cases the on-cycle elementary steps are likely fast at room temperature, higher temperatures allow the palladium catalyst to be active in the presence of coordinating functional groups (e.g., pyridines, nitriles). Typical reaction temperatures used for the coupling of aliphatic or aromatic amines are around 80 °C, but there are instances where the temperature can be decreased if necessary. For instance, if the starting materials are thermally unstable, lower temperatures in combination with higher catalyst loadings will often give a better result. In contrast, challenging couplings involving a weak inorganic base or hindered nucleophiles require high temperatures (>100 °C) for catalytic turnover.

Solvent:

Palladium-catalyzed C–N coupling has been reported in a variety of solvents, including alcohol solvents (e.g., *t*-BuOH, *t*-AmOH), ethereal solvents (e.g., THF, 1,4-dioxane, 2-MeTHF, *tert*-butyl methyl ether), and aromatic solvents (e.g., toluene).[15,51] However, there are some notable exceptions. Chlorinated solvents (e.g., chloroform) have been reported to react with certain Pd(0) sources to form off-cycle oxidative addition complexes, and they are therefore undesirable.[50] Strongly coordinating solvents, like acetonitrile or pyridine, inhibit amine coordination by competitively binding palladium. Finally, the solubility of the reactants can be low in nonpolar solvents (e.g. pentane, hexane), hindering reaction progress. The importance of the latter consideration cannot be overstated. *It is essential that the substrates be soluble in the reaction mixture. Insolubility is one of the most common reasons that reactions fail to give good yields of products.*

Ligand:

Ligand choice tends to have the most pronounced effect on reaction outcome since changing the ancillary ligand modifies the catalyst structure. The appropriate ligand for a given reaction is determined largely by the class of nucleophile. For the coupling of primary amines, BrettPhos (**L6**) is most often employed, although AlPhos (**L18**) works well for challenging electrophiles (e.g., five-membered heterocycles).[51,58] RuPhos (**L11**)-based catalysts efficiently couple a variety of secondary amine nucleophiles.[51] For less nucleophilic compounds, such as

amides, larger ligands like *t*-BuBrettPhos (**L7**), AdBrettPhos (**L8**) or AlPhos (**L18**) are used.[51,58,61] Ultimately, the choice of ligand will also depend on the intended application: while the AlPhos (**L18**)-supported catalyst displays excellent functional group tolerance in many C–N coupling reactions, it is employed in higher loading, and the ligand is more expensive than BrettPhos (**L6**), *t*-BuBrettPhos (**L7**), or AdBrettPhos (**L8**).[58]

To summarize this work and to aid in selecting an appropriate ligand for a given reaction, we have developed a flowchart organized based on nucleophile (Figure 39). The ligands listed in each box are listed in order of (i) most effective ligand for the transformation and (ii) commercial availability. Listed beneath each box are the corresponding references. We hope the community finds this organizational flowchart useful, although we note that this updated user's guide cannot replace the vast wealth of chemical literature on Pd-catalyzed C–N cross-coupling.

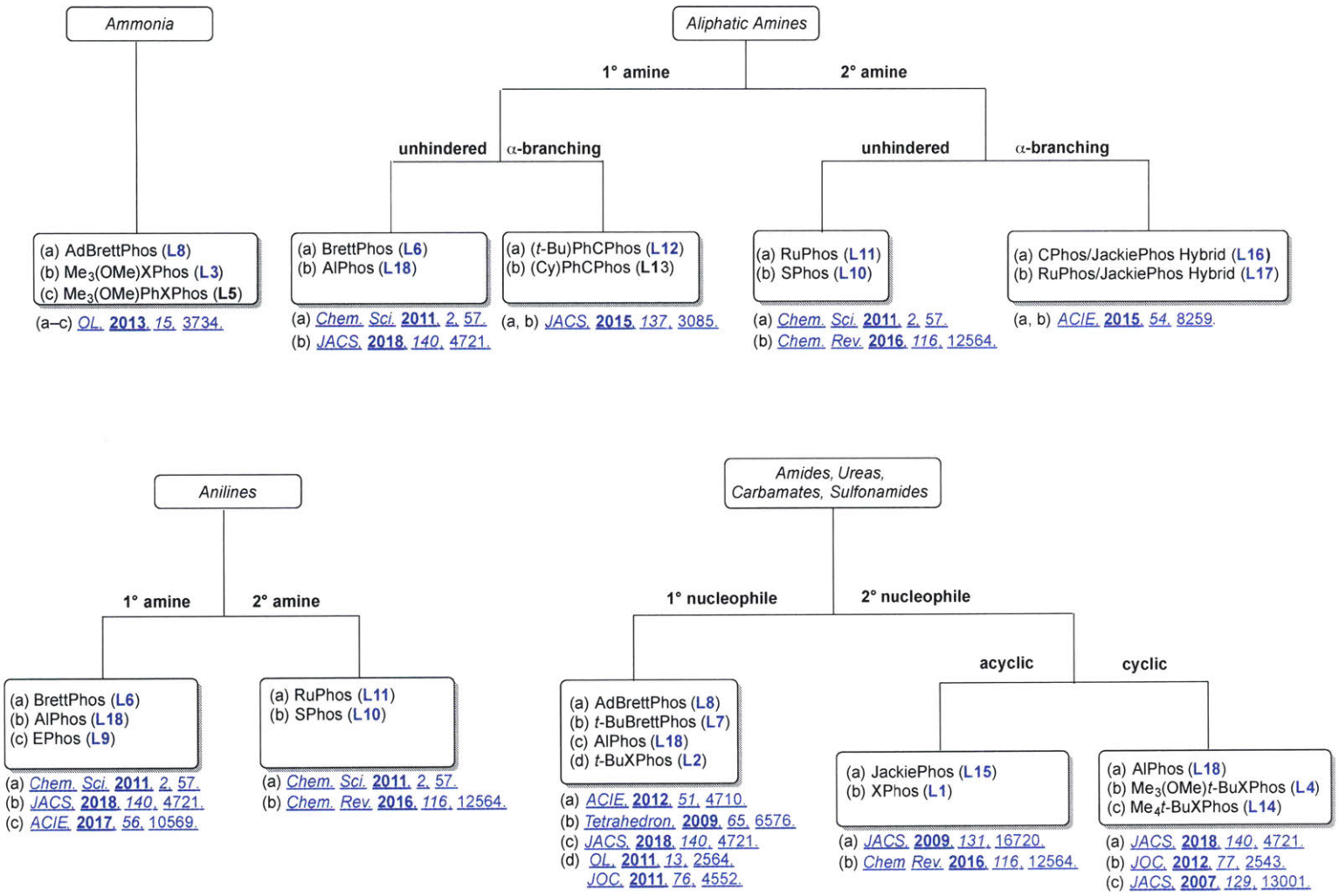

Figure 39. Ligand selection flowchart based on nucleophile. Blue text indicates ligands that are commercially available.

1.5. References

1. Hartwig, J. F. Carbon–heteroatom bond formation catalysed by organometallic complexes. *Nature*, **2008**, *455*, 314–322.
2. Hartwig, J. F. Evolution of a Fourth Generation Catalyst for the Amination and Thioetherification of Aryl Halides. *Acc. Chem. Res.* **2008**, *41*, 1534–1544.
3. Beller, M. Applying Homogenous Catalysis for the Synthesis of Pharmaceuticals. *Ernst Schering Found. Symp. Proc.* **2006**, *3*, 99–116.
4. Guram, A. S. Enabling Palladium/Phosphine-Catalyzed Cross-Coupling Reactions for Practical Applications. *Org. Proc. Res. Dev.* **2016**, *20*, 1754–1764.
5. Marian, N.; Nolan, S. P. Well-Defined N-Heterocyclic Carbenes—Palladium(II) Precatalysts for Cross-Coupling Reactions. *Acc. Chem. Res.* **2008**, *41*, 1440–1449.
6. Valente, C.; Pompeo, M.; Sayah, M.; Organ, M. G. Carbon–Heteroatom Coupling Using Pd-PEPPSI Complexes. *Org. Proc. Res. Dev.* **2014**, *18*, 180–190.
7. Singer, R. A.; Doré, M.; Sieser, J. E.; Berliner, M. A. Development of nonproprietary phosphine ligands for the Pd-catalyzed amination reaction. *Tet. Lett.* **2006**, *47*, 3727–3731.
8. Crawford, S. M.; Lavery, C. B.; Stradiotto, M. BippyPhos: A Single Ligand With Unprecedented Scope in the Buchwald–Hartwig Amination of (Hetero)aryl Chlorides. *Chem. - A Eur. J.* **2013**, *19*, 16760–16771.
9. Gildner, P. J.; Colacot, T. J. Reactions of the 21st Century: Two Decades of Innovative Catalyst Design for Palladium-Catalyzed Cross-Couplings. *Organometallics*, **2015**, *34*, 5497–5508.
10. Bariwal, J.; Van der Eycken, E. C–N bond forming cross-coupling reactions: an overview. *Chem. Soc. Rev.* **2013**, *42*, 9238–9303.
11. Old, D. W.; Wolfe, J. P.; Buchwald, S. L. A Highly Active Catalyst for Palladium-Catalyzed Cross-Coupling Reactions: Room-Temperature Suzuki Couplings and Amination of Unactivated Aryl Chlorides. *J. Am. Chem. Soc.* **1998**, *120*, 9722–9723.
12. Martin, R.; Buchwald, S. L. Palladium-Catalyzed Suzuki–Miyaura Cross-Coupling Reactions Employing Dialkylbiaryl Phosphine Ligands. *Acc. Chem. Res.* **2008**, *41*, 1461–1473.
13. Zhang, H.; Ruiz-Castillo, P.; Buchwald, S. L. Palladium-Catalyzed C–O Cross-Coupling of Primary Alcohols. *Org. Lett.* **2018**, *20*, 1580–1583.
14. Sather, A. C.; Buchwald, S. L. The Evolution of Pd^{0}/Pd^{II}-Catalyzed Aromatic Fluorination. *Acc. Chem. Res.* **2016**, *49*, 2146–2157.
15. Ruiz-Castillo, P.; Buchwald, S. L. Applications of Palladium-Catalyzed C–N Cross-Coupling Reactions. *Chem. Rev.* **2016**, *116*, 12564–12649.

16. Barder, T. E.; Buchwald, S. L. Rationale behind the Resistance of Dialkylbiaryl Phosphines toward Oxidation by Molecular Oxygen. *J. Am. Chem. Soc.* **2007**, *129*, 5096–5101.

17. Christmann, U.; Vilar, R. Monoligated Palladium Species as Catalysts in Cross-Coupling Reactions. *Angew. Chem. Int. Ed.* **2005**, *44*, 366–374.

18. Barder, T. E.; Biscoe, M. R.; Buchwald, S. L. Structural Insights into Active Catalyst Structures and Oxidative Addition to (Biaryl)Phosphine-Palladium Complexes via Density Functional Theory and Experimental Studies. *Organometallics,* **2007**, *26*, 2183–2192.

19. Fors, B. P.; Watson, D. A.; Biscoe, M. R.; Buchwald, S. L. A Highly Active Catalyst for Pd-Catalyzed Amination Reactions: Cross-Coupling Reactions Using Aryl Mesylates and the Highly Selective Monoarylation of Primary Amines Using Aryl Chlorides. *J. Am. Chem. Soc.* **2008**, *130*, 13552–13554.

20. Olsen, E. P. K.; Arrechea, P. L.; Buchwald, S. L. Mechanistic Insight Leads to a Ligand Which Facilitates the Palladium-Catalyzed Formation of 2-(Hetero)Arylaminooxazoles and 4-(Hetero)Arylaminothiazoles. *Angew. Chem. Int. Ed.* **2017**, *56*, 10569–10572.

21. Allgeier, A. M.; Shaw, B. J.; Hwang, T. L.; Milne, J. E.; Tedrow, J. S.; Wilde, C. N. Characterization of Two Stable Degradants of Palladium ^{t}BuXPhos Catalyst and a Unique Dearomatization Reaction. *Organometallics,* **2012**, *31*, 519–522.

22. Biscoe, M. R.; Fors, B. P.; Buchwald, S. L. A New Class of Easily Activated Palladium Precatalysts for Facile C–N Cross-Coupling Reactions and the Low Temperature Oxidative Addition of Aryl Chlorides. *J. Am. Chem. Soc.* **2008**, *130*, 6686–6687.

23. Echavarren, A. M.; Homs, A. Mechanistic Aspects of Metal-Catalyzed C,C- and C,X-Bond Forming Reactions. In *Metal-Catalyzed Cross-Coupling Reactions and More, 1, 2, and 3*; de Mejiere, A., Bräse, S., Oestreich, M., Eds.; Wiley-VCH, 2013; 18.

24. Jutand, A.; Mosleh, A. Rate and Mechanism of Oxidative Addition of Aryl Triflates to Zerovalent Palladium Complexes. Evidence for the Formation of Cationic (σ-Aryl)Palladium Complexes. *Organometallics,* **1995**, *14*, 1810–1817.

25. Kinzel, T.; Zhang, Y.; Buchwald, S. L. A New Palladium Precatalyst Allows for the Fast Suzuki-Miyaura Coupling Reactions of Unstable Polyfluorophenyl and 2-Heteroaryl Boronic Acids. *J. Am. Chem. Soc.* **2010**, *132*, 14073–14075.

26. Fors, B. P.; Davis, N. R.; Buchwald, S. L. An Efficient Process for Pd-Catalyzed C–N Cross Coupling Reactions of Aryl Iodides: Insight into Controlling Factors. *J. Am. Chem. Soc.* **2009**, *131*, 5766–5768.

27. Yamashita, M.; Hartwig, J. F. Synthesis, Structure, and Reductive Elimination Chemistry of Three-Coordinate Arylpalladium Amido Complexes. *J. Am. Chem. Soc.* **2004**, *126*, 5344–5345.

28. Hoffmann, R. Reductive Elimination. In *Frontiers of Chemistry*; Laidler, K. J., Ed.; Pergamon Press: Oxford, 1982; pp 247–263.

29. Arrechea, P. L.; Buchwald, S. L. Biaryl Phosphine Based Pd(II) Amido Complexes: The Effect of Ligand Structure on Reductive Elimination. *J. Am. Chem. Soc.* **2016**, *138*, 12486–12493.

30. Schlummer, B.; Scholz, U. Palladium-Catalyzed C–N and C–O Coupling - A Practical Guide from an Industrial Vantage Point. *Advanced Synthesis and Catalysis*. John Wiley & Sons, Ltd December 1, 2004, pp 1599–1626.

31. Trzeciak, A. M.; Ziółkowski, J. J. Synthesis of Palladium Benzyl Complexes from the Reaction of $PdCl_2[P(OPh)_3]_2$ with Benzyl Bromide and Triethylamine: Important Intermediates in Catalytic Carbonylation. *Organometallics,* **2002**, *21*, 132–137.

32. Louie, J.; Hartwig, J. F. A Route to Pd^0 from Pd^{II} Metallacycles in Animation and Cross-Coupling Chemistry. *Angew. Chem. Int. Ed.* **1996**, *35*, 2359–2361.

33. Strieter, E. R.; Blackmond, D. G.; Buchwald, S. L. Insights into the Origin of High Activity and Stability of Catalysts Derived from Bulky, Electron-Rich Monophosphinobiaryl Ligands in the Pd-Catalyzed C–N Bond Formation. *J. Am. Chem. Soc.* **2003**, *125*, 13978–13980.

34. Amatore, C.; Jutand, A.; M'Barki, M. A. Evidence of the Formation of Zerovalent Palladium from $Pd(OAc)_2$ and Triphenylphosphine. *Organometallics,* **1992**, *11*, 3009–3013.

35. Huang, X.; Anderson, K. W.; Zim, D.; Jiang, L.; Klapars, A.; Buchwald, S. L. Expanding Pd-Catalyzed C–N Bond-Forming Processes: The First Amidation of Aryl Sulfonates, Aqueous Amination, and Complementarity with Cu-Catalyzed Reactions. *J. Am. Chem. Soc.* **2003**, *125*, 6653–6655.

36. Achonduh, G.; Organ, M. G.; Hadei, N.; Lough, A.; Nasielski, J.; O'Brien, C. J.; Kantchev, E. A. B. Structure-Activity Relationship Analysis of Pd-PEPPSI Complexes in Cross-Couplings: A Close Inspection of the Catalytic Cycle and the Precatalyst Activation Model. *Chem. - A Eur. J.* **2010**, *16*, 10844–10853.

37. Fors, B. P.; Krattiger, P.; Strieter, E.; Buchwald, S. L. Water-Mediated Catalyst Preactivation: An Efficient Protocol for C–N Cross-Coupling Reactions. *Org. Lett.* **2008**, *10*, 3505–3508.

38. Fairlamb, I. J. S.; Kapdi, A. R.; Lee, A. F.; McGlacken, G. P.; Weissburger, F.; de Vries, A. H. M.; Schmieder-van de Vondervoort, L. Exploiting Noninnocent (E,E)-Dibenzylideneacetone (dba) Effects in Palladium(0)-Mediated Cross-Coupling Reactions: Modulation of the Electronic Properties of dba Affects Catalyst Activity and Stability in Ligand and Ligand-Free Reaction Systems. *Chem. - A Eur. J.* **2006**, *12*, 8750–8761.

39. Macé, Y.; Kapdi, A. R.; Fairlamb, I. J. S.; Jutand, A. Influence of the dba Substitution on the Reactivity of Palladium(0) Complexes Generated from Pd^0_2(dba-*n*,*n*′-Z)$_3$ or Pd^0(dba-*n*,*n*′-Z)$_2$ and PPh_3 in Oxidative Addition with Iodobenzene. *Organometallics,* **2006**, *25*, 1795–1800.

40. Zalesskiy, S.S.; Ananikov, V.P. $Pd_2(dba)_3$ as a Precursor of Soluble Metal Complexes and Nanoparticles: Determination of Palladium Active Species for Catalysis and Synthesis. *Organometallics,* **2012**, *31*, 2302–2309.

41. DeAngelis, A. J.; Gildner, P. G.; Chow, R.; Colacot, T. J. Generating Active "L-Pd(0)" via Neutral or Cationic π-Allylpalladium Complexes Featuring Biaryl/Bipyrazolylphosphines: Synthetic, Mechanistic, and Structure–Activity Studies in Challenging Cross-Coupling Reactions. *J. Org. Chem.* **2015**, *80*, 6794–6813.

42. Melvin, P. R.; Nova, A.; Balcells, D.; Dai, W.; Hazari, N.; Hruszkewycz, D. P.; Shah, H. P.; Tudge, M. T. Design of a Versatile and Improved Precatalyst Scaffold for Palladium-Catalyzed Cross-Coupling: $(\eta^3\text{-}1\text{-}^t\text{Bu-Indenyl})_2(\mu\text{-Cl})_2Pd_2$. *ACS Catal.* **2015**, *5*, 3680–3688.

43. Chartoire, A.; Lesieur, M.; Slawin, A. M. Z.; Nolan, S. P.; Cazin, C. S. J. Highly Active Well-Defined Palladium Precatalysts for the Efficient Amination of Aryl Chlorides. *Organometallics,* **2011**, *30*, 4432–4436.

44. Hursthouse, M. B.; Coles, S. J.; Light, M. E.; Horton, P. N.; Gelbrich, T.; Cazin, C. S. J.; Bedford, R. B. High-Activity Catalysts for Suzuki Coupling and Amination Reactions with Deactivated Aryl Chloride Substrates: Importance of the Palladium Source. *Organometallics,* **2003**, *22*, 2810–2810.

45. Bruno, N. C.; Tudge, M. T.; Buchwald, S. L. Design and Preparation of New Palladium Precatalysts for C–C and C–N Cross-Coupling Reactions. *Chem. Sci.* **2013**, *4*, 916–920.

46. O'Brien, C. J.; Kantchev, E. A. B.; Valente, C.; Hadei, N.; Chass, G. A.; Lough, A.; Hopkinson, A. C.; Organ, M. G. Easily Prepared Air- and Moisture-Stable Pd-NHC (NHC = N-Heterocyclic Carbene) Complexes: A Reliable, User-Friendly, Highly Active Palladium Precatalyst for the Suzuki-Miyaura Reaction. *Chem. - A Eur. J.* **2006**, *12*, 4743–4748.

47. Lee, H. G.; Milner, P. J.; Buchwald, S. L. An Improved Catalyst System for the Pd-Catalyzed Fluorination of (Hetero)Aryl Triflates. *Org. Lett.* **2013**, *15*, 5602–5605.

48. Bruno, N. C.; Niljianskul, N.; Buchwald, S. L. *N*-Substituted 2-Aminobiphenylpalladium Methanesulfonate Precatalysts and Their Use in C–C and C–N Cross-Couplings. *J. Org. Chem.* **2014**, *79*, 4161–4166.

49. Ingoglia, B. T.; Buchwald, S. L. Oxidative Addition Complexes as Precatalysts for Cross-Coupling Reactions Requiring Extremely Bulky Biarylphosphine Ligands. *Org. Lett.* **2017**, *19*, 2853–2856.

50. Lee, H. G.; Milner, P. J.; Colvin, M. T.; Andreas, L.; Buchwald, S. L. Structure and Reactivity of $[(L{\cdot}Pd)_n{\cdot}(1,5\text{-Cyclooctadiene})]$ (n = 1–2) Complexes Bearing Biaryl Phosphine Ligands. *Inorg. Chim. Acta,* **2014**, *422*, 188–192.

51. Surry, D. S.; Buchwald, S. L. Dialkylbiaryl Phosphines in Pd-Catalyzed Amination: A User's Guide. *Chem. Sci.* **2011**, *2*, 27–50.

52. Maiti, D.; Fors, B. P.; Henderson, J. L.; Nakamura, Y.; Buchwald, S. L. Palladium-Catalyzed Coupling of Functionalized Primary and Secondary Amines with Aryl and Heteroaryl Halides: Two Ligands Suffice in Most Cases. *Chem. Sci.* **2011**, *2*, 57–68.

53. Gangjee, A.; Namjoshi, O. A.; Raghavan, S.; Queener, S. F.; Kisliuk, R. L.; Cody, V. Design, Synthesis, and Molecular Modeling of Novel Pyrido[2,3- *d*]Pyrimidine Analogues As Antifolates; Application of Buchwald–Hartwig Aminations of Heterocycles. *J. Med. Chem.* **2013**, *56*, 4422–4441.

54. Takács, D.; Egyed, O.; Drahos, L.; Szabó, P.; Jemnitz, K.; Szabó, M.; Veres, Z.; Visy, J.; Molnár, J.; Riedl, Z.; et al. Synthesis and Pharmacological Investigation of New N-Hydroxyalkyl-2-Aminophenothiazines Exhibiting Marked MDR Inhibitory Effect. *Bioorg. Med. Chem.* **2013**, *21*, 3760–3779.

55. Bourbeau, M. P.; Ashton, K. S.; Yan, J.; St. Jean, D. J. Nonracemic Synthesis of GK–GKRP Disruptor AMG-3969. *J. Org. Chem.* **2014**, *79*, 3684–3687.

56. Park, N. H.; Vinogradova, E. V.; Surry, D. S.; Buchwald, S. L. Design of New Ligands for the Palladium-Catalyzed Arylation of α-Branched Secondary Amines. *Angew. Chem. Int. Ed.* **2015**, *54*, 8259–8262.

57. Huang, W.; Buchwald, S. L. Palladium-Catalyzed *N*-Arylation of Iminodibenzyls and Iminostilbenes with Aryl- and Heteroaryl Halides. *Chem. - A Eur. J.* **2016**, *22*, 14186–14189.

58. Dennis, J. M.; White, N. A.; Liu, R. Y.; Buchwald, S. L. Breaking the Base Barrier: An Electron-Deficient Palladium Catalyst Enables the Use of a Common Soluble Base in C–N Coupling. *J. Am. Chem. Soc.* **2018**, *140*, 4721–4725.

59. Ruiz-Castillo, P.; Blackmond, D. G.; Buchwald, S. L. Rational Ligand Design for the Arylation of Hindered Primary Amines Guided by Reaction Progress Kinetic Analysis. *J. Am. Chem. Soc.* **2015**, *137*, 3085–3092.

60. Sromek, A. W.; Provencher, B. A.; Russell, S.; Chartoff, E.; Knapp, B. I.; Bidlack, J. M.; Neumeyer, J. L. Preliminary Pharmacological Evaluation of Enantiomeric Morphinans. *ACS Chem. Neurosci.* **2014**, *5*, 93–99.

61. Su, M.; Hoshiya, N.; Buchwald, S. L. Palladium-Catalyzed Amination of Unprotected Five-Membered Heterocyclic Bromides. *Org. Lett.* **2014**, *16*, 832–835.

62. Noonan, G. M.; Dishington, A. P.; Pink, J.; Campbell, A. D. Studies on the coupling of substituted 2-amino-1,3-oxazoles with chloro-heterocycles. *Tet. Lett.* **2012**, *53*, 3038–3043.

63. Ueda, S.; Buchwald, S. L. Catalyst-Controlled Chemoselective Arylation of 2-Aminobenzimidazoles. *Angew. Chem. Int. Ed.* **2012**, *51*, 10364–10367.

64. McGowan, M. A.; Henderson, J. L.; Buchwald, S. L. Palladium-Catalyzed N-Arylation of 2-Aminothiazoles. *Org. Lett.* **2012**, *14*, 1432–1435.

65. Cheung, C. W.; Surry, D. S.; Buchwald, S. L. Mild and Highly Selective Palladium-Catalyzed Monoarylation of Ammonia Enabled by the Use of Bulky Biarylphosphine Ligands and Palladacycle Precatalysts. *Org. Lett.* **2013**, *15*, 3734–3737.

66. Schranck, J.; Tili, A. Transition-Metal-Catalyzed Monoarylation of Ammonia. *ACS Catal.* **2018**, *8*, 405–418.

67. DeAngelis, A.; Wang, D.-H.; Buchwald, S. L. Mild and Rapid Pd-Catalyzed Cross-Coupling with Hydrazine in Continuous Flow: Application to the Synthesis of Functionalized Heterocycles. *Angew. Chem. Int. Ed.* **2013**, *52*, 3434–3437.

68. Wagaw, S.; Yang, B.H.; Buchwald, S.L. A Palladium-Catalyzed Method for the Preparation of Indoles via the Fischer Indole Synthesis. *J. Am. Chem. Soc.* **1999**, *121*, 10251–10263.

69. Ikawa, T.; Barder, T. E.; Biscoe, M. R.; Buchwald, S. L. Pd-Catalyzed Amidations of Aryl Chlorides Using Monodentate Biaryl Phosphine Ligands: A Kinetic, Computational, and Synthetic Investigation. *J. Am. Chem. Soc.* **2007**, *129*, 13001–13007.

70. Dooleweerdt, K.; Fors, B. P.; Buchwald, S. L. Pd-Catalyzed Cross-Coupling Reactions of Amides and Aryl Mesylates. *Org. Lett.* **2010**, *12*, 2350–2353.

71. Fors, B. P.; Dooleweerdt, K.; Zeng, Q.; Buchwald, S. L. An Efficient System for the Pd-Catalyzed Cross-Coupling of Amides and Aryl Chlorides. *Tetrahedron* **2009**, *65*, 6576–6583.

72. Su, M.; Buchwald, S. L. A Bulky Biaryl Phosphine Ligand Allows for Palladium-Catalyzed Amidation of Five-Membered Heterocycles as Electrophiles. *Angew. Chem., Int. Ed.* **2012**, *51*, 4710–4713.

73. Jui, N. T.; Buchwald, S. L. Cascade Palladium Catalysis: A Predictable and Selectable Regiocontrolled Synthesis of *N* -Arylbenzimidazoles. *Angew. Chem. Int. Ed.* **2013**, *52*, 11624–11627.

74. Hicks, J. D.; Hyde, A. M.; Cuezva, A. M.; Buchwald, S. L. Pd-Catalyzed *N*-Arylation of Secondary Acyclic Amides: Catalyst Development, Scope, and Computational Study. *J. Am. Chem. Soc.* **2009**, *131*, 16720–16734.

75. Breitler, S.; Oldenhuis, N. J.; Fors, B. P.; Buchwald, S. L. Synthesis of Unsymmetrical Diarylureas via Pd-Catalyzed C–N Cross-Coupling Reactions. *Org. Lett.* **2012**, *13*, 3262–3265.

76. Shekhar, S.; Franczyk, T. S.; Barnes, D. M.; Dunn, T. B.; Haight, A. R.; Chan, V. S. Process for Preparing Antiviral Compounds. US Patent 20130224149, 2013.

77. Shekhar, S.; Dunn, T. B.; Koteki, B. J.; Montavon, D. K.; Cullen, S. C. A General Method for Palladium-Catalyzed Reactions of Primary Sulfonamides with Aryl Nonaflates. *J. Org. Chem.* **2011**, *76*, 4552–4563.

78. Ueda, S.; Su, M.; Buchwald, S. L. Completely *N*1-Selective Palladium-Catalyzed Arylation of Unsymmetric Imidazoles: Application to the Synthesis of Nilotinib. *J. Am. Chem. Soc.* **2012**, *134*, 700–706.

79. Ueda, S.; Ali, S.; Fors, B. P.; Buchwald, S. L. $Me_3(OMe)$*t*BuXPhos: A Surrogate Ligand for Me_4*t*BuXPhos in Palladium-Catalyzed C–N and C–O Bond-Forming Reactions. *J. Org. Chem.* **2012**, *77*, 2543–2547.

80. Ueda, S.; Su, M.; Buchwald, S. L. Highly *N*2-Selective Palladium-Catalyzed Arylation of 1,2,3-Triazoles. *Angew. Chem. Int. Ed.* **2011**, *50*, 8944–8947.

81. Henderson, J. L.; McDermott, S. M.; Buchwald, S. L. Palladium-Catalyzed Amination of Unprotected Halo-7-Azaindoles. *Org. Lett.* **2010**, *12*, 4438–4441.

82. Henderson, J. L.; Buchwald, S. L. Efficient Pd-Catalyzed Amination Reactions for Heterocycle Functionalization. *Org. Lett.* **2010**, *12*, 4442–4445.

83. Charles, M. D.; Schultz, P.; Buchwald, S. L. Efficient Pd-Catalyzed Amination of Heteroaryl Halides. *Org. Lett.* **2005**, *7*, 3965–3968.

84. Santanilla, A. B.; Christensen, M.; Campeau, L.-C.; Davies, I. W.; Dreher, S. D. P_2Et Phosphazene: A Mild, Functional Group Tolerant Base for Soluble, Room Temperature Pd-Catalyzed C–N, C–O, and C–C Cross-Coupling Reactions. *Org. Lett.* **2015**, *17*, 3370–3373.

Chapter 2. Oxidative Addition Complexes as Precatalysts for Cross-Coupling Reactions Requiring Extremely Bulky Biarylphosphine Ligands

2.1. Introduction

The use of biaryl phosphines as supporting ligands in palladium catalysis has played an important role in the development of synthetic methods that can be used to form C–C,[1] C–N,[2] C–O,[3] and C–F[4] bonds in a wide variety of settings. To facilitate the use of these ligands, we have developed several generations of palladacycle precatalysts (**G1**–**G5**, Figure 1), which are able to accommodate a range of phosphine-based ligands.[5,6] These precatalysts can be used to promote cross-coupling reactions with high efficiency. This is due, in part, to the pre-association of the ligand with the Pd center and to the rapid formation of a L–Pd(0) species under the reaction conditions. In addition, these Pd(II) precatalysts are easily handled and stable to long-term storage without the need to carefully exclude air or water.

Biaryl phosphine ligands bearing bis(*tert*-butyl) and bis(1-adamantyl) phosphino groups (e.g., **L1**–**L4**) are useful supporting ligands for catalysts that promote C–O and C–F cross-coupling reactions.[7] Among other things, these ligands are believed to facilitate the challenging reductive elimination steps of these processes.[3c,4] Methods to prepare palladacycle precatalysts based on these particularly bulky ligands are less successful than with other ligands. While **G3** precatalysts containing these ligands are readily isolated, they form carbazole upon catalyst activation, which occasionally can cause inhibition of the catalyst based on kinetic and mechanistic studies.[5c,6a,8] Precatalysts of type **G4** and **G5** were prepared to address this, among other issues. However, **G4** and **G5**-based precatalysts based on **L1**–**L4** are only formed with difficulty.[5d]

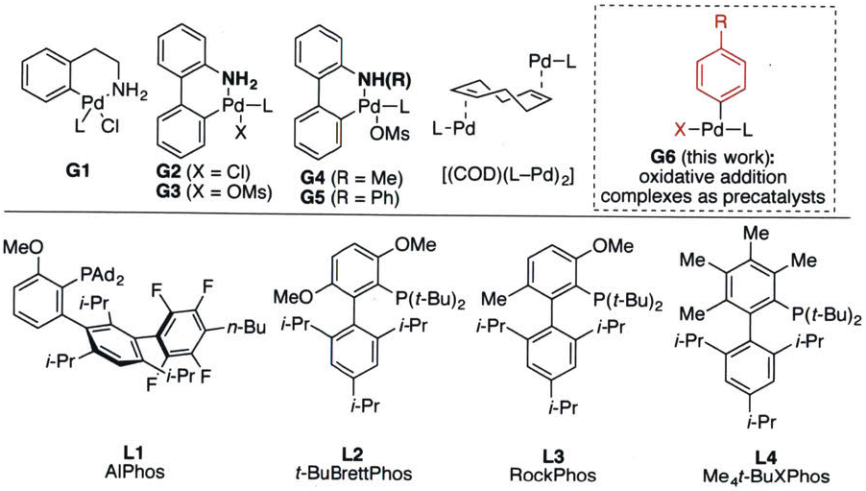

Figure 1. Evolution of precatalysts developed by the Buchwald group and selected bulky supporting ligands.

As an alternative, our group has developed [(COD)(L–Pd)$_2$] precatalysts (Figure 1) which are suitable for **L1**–**L4**.[9] However, not all biaryl phosphine ligands form precatalysts of this type. Furthermore, these complexes are generally air sensitive and exhibit poor solubility in organic solvents, making them less convenient to handle.[4a,9,10] Thus we set out to find alternative Pd(II) precatalysts that would overcome these issues.

We hypothesized that a potential solution would be to use oxidative addition complexes (OACs) of general formula L–Pd(Ar)X as precatalysts. These are readily obtained by oxidative addition of aryl (pseudo)halides to an *in situ* generated L–Pd(0) species. Moreover, since they serve as presumptive intermediates on the catalytic cycle for cross-coupling processes, these OACs should be competent palladium sources for a variety of C–X bond-forming reactions.[11,12]

We were particularly interested in the use of OACs for the development of a simplified and improved protocol for the palladium-catalyzed fluorination of aryl (pseudo)halides. Previously, **L1** (AlPhos) was found to be an effective supporting ligand for the palladium-catalyzed fluorination of a broad range of aryl bromides and triflates.[4] However, preliminary investigation into the use of palladacycle precatalysts yielded poor outcomes, likely due to the formation of inhibiting byproducts (e.g., HF or carbazole) during catalyst activation, as well as the inefficiency of catalyst activation itself in the absence of a suitable exogenous base.[4c] We expected OACs to address both of these issues as no base is needed for activation, while the only byproduct is simply another aryl fluoride, which is presumably innocuous.

2.2. Results and Discussion

To test this hypothesis, precatalysts **P1**–**P3** were prepared by combining the biaryl phosphine ligand, aryl bromide or triflate, and (COD)Pd(CH_2TMS)$_2$[4] in pentane, from which the desired complex precipitated. Filtering and washing the precipitate afforded the pure complexes in moderate to good isolated yield, while remaining free ligand could be recovered from the filtrate (Scheme I, see Supporting Information (SI) for details). 4-Trifluoromethylphenyl was selected as the aryl group for **P1** and **P2**, since catalyst activation via the formation of 4-fluorobenzotrifluoride under the reaction conditions was expected to be facile. Moreover, this byproduct was expected to be inert under the reaction conditions and readily removed due to its volatility. The structures of **P1** and **P2** were confirmed by NMR spectroscopy as well as by X-ray crystallography in the case of **P2**, providing the first crystal structure of a complex derived

from an aryl triflate with **L1** as the supporting ligand (Scheme 1). The complexes are stable under air in a bench-top desiccator in the solid state for at least 10 months, as judged by ^{31}P NMR spectroscopy.[13]

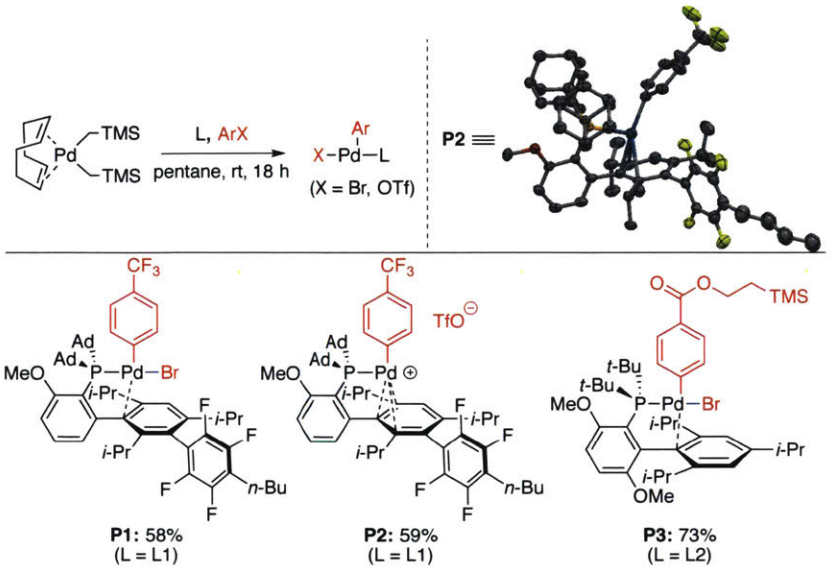

Scheme 1. Synthesis of Oxidative Addition Complexes and Structures of OACs used as precatalysts. Crystallographically determined X-ray structure of **P2** shown (thermal ellipsoid plot at 50% probability, triflate anion and hydrogen atoms are omitted).

Our reported conditions for the palladium-catalyzed fluorination of aryl bromides and triflates call for [(COD)(L–Pd)$_2$] as the source of ligand and palladium.[4a] We initially employed **P1** alone in place of the cyclooctadiene complex for the fluorination of 1-bromo-4-*n*-butylbenzene and found that it performed poorly compared to the previously developed conditions (Table 1, entries 1 vs. 2). However, when exogenous cyclooctadiene was added, the yield increased substantially (Table 1, entry 3). We postulate this additive may improve the yield by stabilizing any off-cycle Pd(0) species and averting irreversible catalyst deactivation.

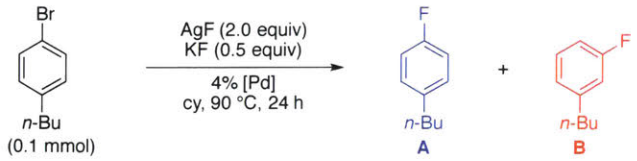

entry	[Pd]	additive	yield A (B)
1	[(COD)(**L1**–Pd)$_2$]	–	87% (5%)
2	P1	–	22% (1%)
3	P1	2% COD	91% (6%)

Table 1. Additive effects on the fluorination of 1-bromo-4-*n*-butylbenzene with **P1** as precatalyst. Yields reported as ^{19}F NMR yields using 1-fluoronaphthalene as an internal standard.

Encouraged by this result, we examined the generality of these conditions toward the fluorination of aryl triflates. Indeed, **P1** also served as a competent precatalyst for the fluorination of aryl triflates, although small amounts of the corresponding aryl bromides were also formed, complicating isolation of the desired products. To address this issue, we prepared triflate analogue **P2**. For aryl triflate substrates, this precatalyst exhibits the same catalytic activity as **P1**, while avoiding the formation of aryl bromide side products. However, **P2** does not efficiently transform aryl bromides into aryl fluorides, perhaps due to inefficient activation of the precatalyst by the fluoride sources present under the reaction conditions. Thus, we employed **P1** and **P2** for the fluorination of aryl bromides and triflates, respectively. To gain a sense of the generality of these new protocols, a small collection of substrates were examined under these conditions. Substrates containing potentially sensitive functional groups, including an internal alkyne (**2a**), an aldehyde (**2c**), and an azo (**2f**) were fluorinated in good to excellent yield, with a regioisomeric side product observed only in the case of **2e** (Scheme 2).[14]

After investigating OAC precatalysts in the context of C–F bond-forming reactions, we explored the applicability of this method to other bond-forming processes. To facilitate purification of the cross-coupling product, we considered precatalysts which would produce easily removed byproducts upon activation. In particular, we designed an OAC bearing a trimethylsilyl ethyl (TMSE) ester, which can be selectively cleaved with fluoride to liberate the corresponding carboxylate, which is easier to separate from the desired product. Based on previously reported C–O and C–N cross-coupling processes,[3,15] **L2** (*t*-BuBrettPhos) was selected as the ligand for the precatalyst.

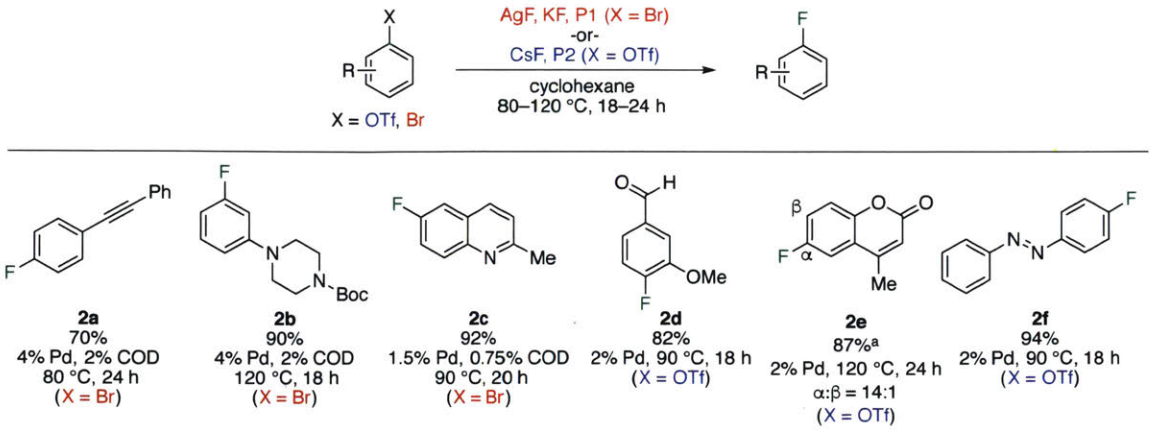

Scheme 2. Fluorination of aryl bromides and triflates with P1 and P2. [a]Toluene was used as the solvent. Isolated yields are reported as an average of two runs. See experimental section 2.4 for details.

Complex **P3** was therefore prepared as a precatalyst for these types of coupling reactions. The new precatalyst was first employed for the *N*-arylation of amino acid esters under mild and stereoretentive conditions. By employing **P3**, the desired arylation products were formed in moderate to good yields with high levels of enantioretention (Scheme 3). Treatment with TBAF, if necessary, was mild enough to cleave the aminated TMSE ester present in the byproduct selectively, simplifying purification of the desired product (**3b, 3d**) without eroding the enantiomeric excess and with merely one percent or less of the byproduct as judged by the ^{1}H NMR spectrum after chromatographic purification (see SI for details). Other compounds (**3a, 3c**) could be purified without the addition of fluoride.

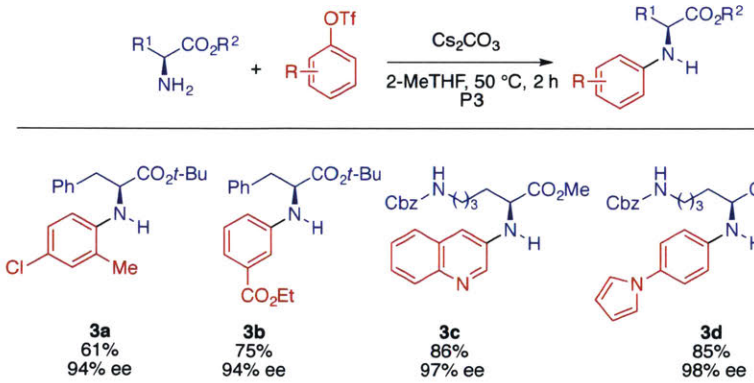

Scheme 3. Amino Acid Ester Arylation with P3. Isolated yields are reported as an average of two runs. Enantiomeric excess (ee, average of two runs) was determined by HPLC analysis using chiral stationary phases. See experimental section 2.4 for details.

Precatalyst **P3** was also found to be suitable for the cross-coupling of oxygen nucleophiles (Scheme 4). Heterocyclic aryl halides, including a quinoxaline (**4a**), an indazole (**4b**), and an isoquinoline (**4d**), were hydroxylated or methoxylated in good yield. An *N*-benzyl dibromophenothiazine (**4c**) readily underwent coupling to afford the bis(methoxylation) product in excellent yield.

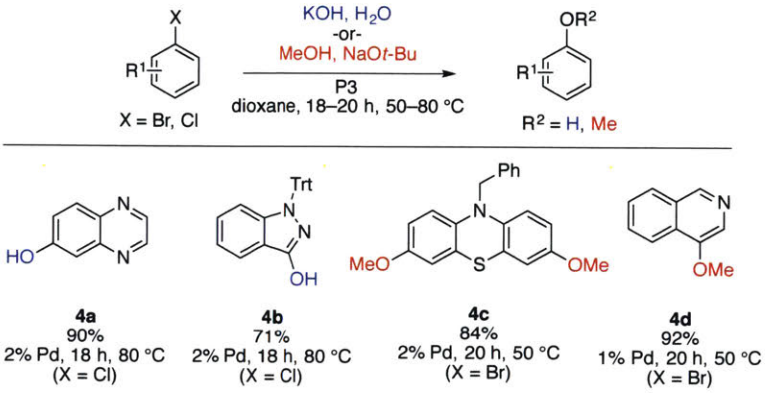

Scheme 4. Alcohol and Hydroxide Coupling with P3. Isolated yields are reported as an average of two runs. See experimental section 2.4 for details.

2.3. Conclusion

In summary, we have demonstrated that oxidative addition complexes based on palladium, supported by extremely bulky dialkyl biaryl phosphine ligands, can serve as active precatalysts for a wide variety of challenging, synthetically useful carbon–heteroatom bond-forming reactions. The complexes are well-characterized, easily handled outside of a glovebox, and provide a means of introducing L–Pd(0) into a reaction without the formation of potentially inhibitory byproducts.

2.4. Experimental

I. General Information

A) Procedures: All reactions were performed in oven-dried Fisher Scientific 25 mL, 20 x 150 mm screw-cap tubes (Cat. No. 14-959-37C) using Thermo Scientific PTFE/silicon septa (Cat. No. B7995-18) fit into screw-caps (Kimble-Chase, Open Top S/T Closure, Part No. 73804-18400), unless otherwise noted. Compounds were purified using a Biotage® Isolera system, employing polypropylene cartridges preloaded with silica gel (Silicycle SilaFlash® F60 silica gel) or with new Biotage® SNAP cartridges, unless otherwise noted. Samples were eluted using a flow rate of 50–100 mL/min, with detection by UV (254 nm). Analytical thin-layered chromatography (TLC) was performed using glass plates pre-coated with silica gel (0.25 mm, 60 Å pore size) impregnated with a fluorescent indicator (254 nm). TLC plates were visualized by exposure to ultraviolet light (UV).

B) Materials: Commercial solvents and reagents were purchased from Aldrich Chemical Company, Strem Chemicals, Acros Organics, Alfa Aesar, Combi Blocks, Oakwood Chemical, and Chem-Impex and used as received, with the following exceptions. *t*-BuBrettPhos (**L2**) was a gift from Aldrich, for which we are grateful. Anhydrous cyclohexane, 1,4-dioxane and 2-methyltetrahydrofuran (2-MeTHF) were purchased from Aldrich Chemical Company in Sure-Seal™ bottles and used as received. Toluene, tetrahydrofuran (THF) and CH_2Cl_2 were purchased from J.T. Baker in CYCLE-TAINER® solvent-delivery kegs and vigorously purged with argon for 2 h, followed by passing it under argon pressure through two packed columns of neutral alumina. Cesium carbonate, sodium *tert*-butoxide, and silver(I) fluoride were stored in a nitrogen-filled glovebox. Cesium fluoride (CsF) and potassium fluoride (KF) were ground in a nitrogen-filled glovebox using an oven-dried mortar and pestle. The finely ground CsF (or KF) was then filtered through a 45 μm stainless-steel size sieve (Cole Parmer) to obtain CsF (or KF) with particle size of <45 μm.[1] Unless otherwise noted, amino acid ester free bases were prepared from the corresponding hydrochloride salt by washing with 10% aqueous sodium carbonate. Degassed deionized water was prepared by filling a 20 mL scintillation vial with 10 mL of deionized water, sealing it with a septum, submerging it in a sonication bath, and evacuating it while sonicating for 5 min (or until the evolution of gas bubbles stopped); this process was

repeated a total of three times. Stock solutions of 1,5-cyclooctadiene were prepared in a nitrogen-filled glovebox. Tetrabutylammonium fluoride (1.0 M in tetrahydrofuran, ~5% H_2O) and 1,5-cyclooctadiene (≥99%) were purchased from Sigma-Aldrich.

Table of Starting Materials

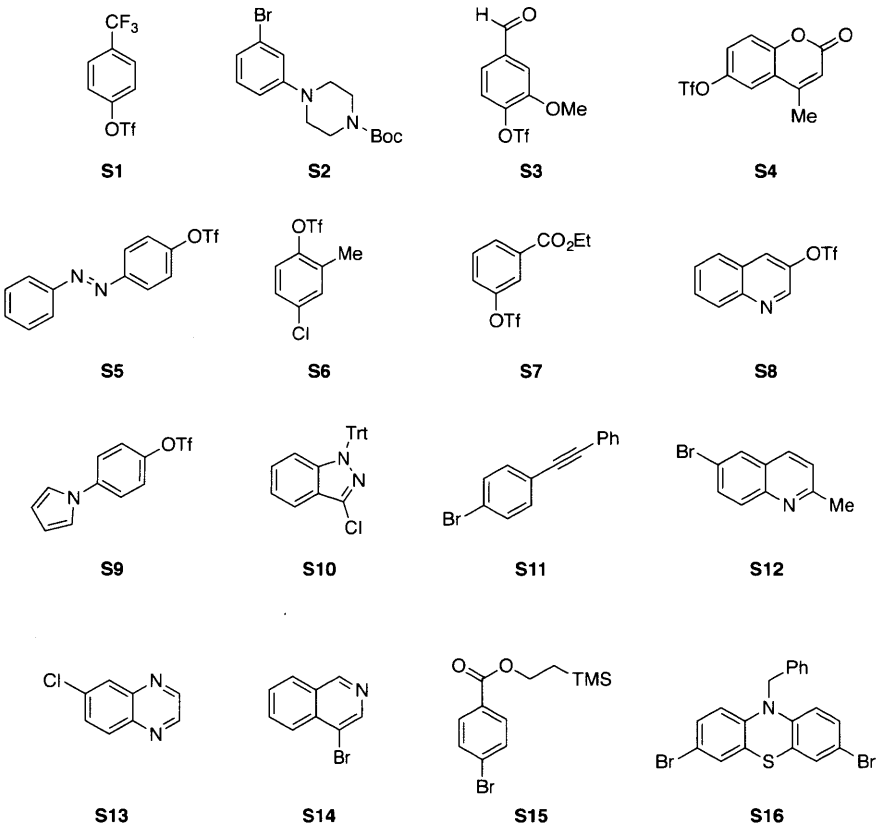

S1 S2 S3 S4

S5 S6 S7 S8

S9 S10 S11 S12

S13 S14 S15 S16

L1,[4a] (COD)Pd($CH_2TMS)_2$,[4a] [(COD)(L–Pd)$_2$],[4a] 4-(trifluoromethyl)phenyl trifluoromethanesulfonate (**S1**),[15] *tert*-butyl 4-(3-bromophenyl)piperazine-1-carboxylate (**S2**),[16] 4-formyl-2-methoxyphenyl trifluoromethanesulfonate (**S3**),[17] 4-methyl-2-oxo-2*H*-chromen-6-yl trifluoromethanesulfonate (**S4**),[18] (*E*)-4-(phenyldiazenyl)phenyl trifluoromethanesulfonate (**S5**),[19] 4-chloro-2-methylphenyl trifluoromethanesulfonate (**S6**),[15] ethyl 3-trifluoromethanesulfonyloxy-benzoate (**S7**),[20] 3-quinolinyl trifluoromethanesulfonate (**S8**),[15] 4-(1H-pyrrol-1-yl)phenyl trifluoromethanesulfonate (**S9**),[2] and 3-chloro-1-trityl-1*H*-indazole (**S10**)[3b] have been previously described. 1-bromo-4-(phenylethynyl)benzene (**S11**), 6-bromo-2-methylquinoline (**S12**), 6-chloroquinoxaline (**S13**), and 4-bromoisoquinoline (**S14**) are commercially available and used as

received. The syntheses of 2-(trimethylsilyl)ethyl 4-bromobenzoate (**S15**) and 10-benzyl-3,7-dibromo-10*H*-phenothiazine (**S16**) are reported in section II–I.

C) Instrumentation: Compounds were analyzed by ^{1}H, ^{13}C, ^{19}F, and ^{31}P nuclear magnetic resonance (NMR) spectroscopy where appropriate. ^{1}H, ^{13}C, and ^{19}F NMR spectra were recorded on a Varian Inova-500 MHz spectrometer, a Bruker Avance-400 MHz spectrometer, and a Varian Mercury-300 MHZ spectrometer. ^{1}H and ^{13}C spectra were calibrated using residual solvent as an internal reference ($CDCl_3$: δ 7.26 ppm and δ 77.2 ppm, respectively; C_6D_6: δ 7.16 ppm and δ 128.1 ppm, respectively; CD_2Cl_2: δ 5.32 ppm and δ 54.0 ppm, respectively; acetone-d_6: δ 2.05 ppm and δ 29.8 ppm, respectively; MeOD-d_4: δ 3.31 ppm and δ 49.0 ppm, respectively; THF-d_8: δ 1.72 ppm and δ 25.31 ppm, respectively). ^{19}F NMR spectra were calibrated to an external standard of trifluorotoluene in C_6D_6 (δ -63.7 ppm). ^{31}P NMR spectra were calibrated to an external standard of 85% aq. H_3PO_4 (δ 0.0 ppm). Elemental analyses were performed by Atlantic Microlabs Inc., Norcross, GA, USA. HRMS was recorded on a Bruker Daltonics APEXIV 4.7 Tesla Fourier transform ion cyclotron resonance mass spectrometer (FT-ICR-MS). The following abbreviations were used to explain multiplicities: s = singlet, bs = broad singlet, d = doublet, t = triplet, q = quartet, p = pentet, h = heptet, m = multiplet. Melting points were obtained using a Stanford Research Systems EZ-Melt melting point apparatus. Attenuated total reflectance Fourier transform infrared spectra (ATR-FTIR) were obtained using a Thermo Scientific iD5 ATR Nicolet iS5 FT-IR spectrometer referenced to a polystyrene standard and data reported as frequency of absorption (cm^{-1}). High-pressure liquid chromatography (HPLC) was performed on Agilent 1200 Series chromatographs using chiral columns (25 cm) as noted for each compound. Optical rotations were measured on a Jasco P-1010 polarimeter equipped with a sodium (589 nm, D) lamp. Optical rotation data are represented as follows: specific rotation ($[\alpha]_D^T$), concentration (g/100 mL), and solvent.

II. Experimental Procedures and Characterization Data

A) Synthesis of Oxidative Addition Complexes

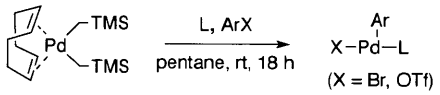

General Procedure A: In a nitrogen-filled glovebox, an oven-dried 25 mL screw-cap tube equipped with a stir bar and capped with a Teflon septum was charged with ligand (1.00 equiv) and aryl (pseudo)halide (1.50–2.20 equiv), if a solid. Pentane was added and the solution vigorously stirred until homogenous. The aryl (pseudo)halide, if a liquid, was added at this time followed by (COD)Pd($CH_2TMS)_2$ (1.00–1.15 equiv). Additional pentane (2 mL) was used to wash the sides of the tube, and the mixture allowed to stir vigorously for 16 h at room temperature. The resulting precipitate was filtered through a fine sintered glass filter inside the glovebox. The filter cake was washed with pentane (3 mL x 3) and dried under high vacuum to give the complex. The complexes are stable and can be stored outside the glovebox under air in a bench-top desiccator for at least 10 months as judged by ^{31}P NMR spectroscopy.

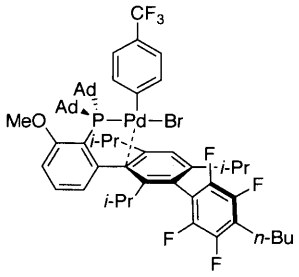

P1

P1 was prepared following general procedure A. A mixture of **L1** (510 mg, 0.625 mmol, 1.00 equiv) and 4-bromobenzotrifluoride (314 mg, 1.40 mmol, 2.20 equiv) was dissolved in pentane (25 mL) in an oven-dried 50 mL round-bottomed flask equipped with a stir bar and stirred until the mixture was colorless and homogenous. At this time, (COD)Pd($CH_2TMS)_2$ (280 mg, 0.716 mmol, 1.15 equiv) was added, and the sides of the reaction vessel washed with an additional 1 mL of pentane. The reaction mixture was sealed with a septum and stirred vigorously for 16 h. Then, the precipitate was filtered to give **P1** as a yellow solid (383 mg, 54%), which was stored in a bench-top desiccator under air. Note: this compound will slowly react with oxygen *in solution* to form a complex of formula **L1**–PdO_2. **^{1}H NMR** (500 MHz, C_6D_6) δ 7.67 – 7.58 (m,

3H), 7.19 (s, 1H), 6.98 (d, J = 8.6 Hz, 1H), 6.86 – 6.79 (m, 1H), 6.27 (dd, J = 7.8, 2.8 Hz, 1H), 6.19 (d, J = 8.2 Hz, 1H), 3.57 – 3.42 (m, 1H), 3.09 (s, 3H), 2.78 (h, J = 6.9 Hz, 1H), 2.59 (t, J = 7.7 Hz, 2H), 2.53 – 2.36 (m, 7H), 2.14 (d, J = 12.5 Hz, 3H), 1.99 – 1.88 (m, 6H), 1.83 (d, J = 12.2 Hz, 3H), 1.76 – 1.59 (m, 15H), 1.55 – 1.38 (m, 8H), 1.28 (d, J = 6.7 Hz, 3H), 1.20 (q, J = 7.5 Hz, 2H), 1.12 (dd, J = 7.1, 1.9 Hz, 3H), 0.85 (d, J = 6.7 Hz, 3H), 0.77 (t, J = 7.3 Hz, 3H). **^{13}C NMR** (151 MHz, THF-d_8) δ 161.2, 156.1, 151.9, 150.0, 149.6 (d, J = 19.0 Hz), 142.0, 141.0, 138.3, 131.7, 128.1 (d, J = 10.5 Hz), 126.6, 125.5, 124.2, 122.9, 121.0, 120.5, 109.8, 66.9, 53.4, 47.2 (d, J = 10.4 Hz), 46.2 (d, J = 9.4 Hz), 42.5, 40.1, 36.4, 36.0, 33.0, 31.4, 31.1 (d, J = 11.6 Hz), 29.7 (d, J = 9.5 Hz), 29.5 (d, J = 9.5 Hz), 25.8, 24.8, 24.7, 24.6, 24.5, 23.6, 23.3, 22.4, 22.2, 21.6, 13.1. **^{31}P NMR** (203 MHz, C_6D_6): 65.5 ppm. **^{19}F NMR** (471 MHz, C_6D_6) δ –62.5, –130.7, –138.3, –145.4, –147.3 ppm. IR (thin film, cm^{-1}): 2906, 2851, 2236, 2083, 1584, 1566, 1476, 1324, 1303, 1116, 1099, 1067, 1047, 1005, 972, 815. **HRMS** (ESI) m/z calcd for $C_{59}H_{71}BrF_7OPPd^+$ [M–Br]$^+$: 1065.4166; 1065.3877 found.

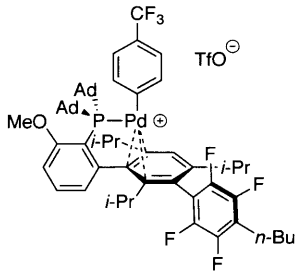

P2

P2 was prepared following general procedure A. A mixture of **L1** (105 mg, 0.129 mmol, 1.00 equiv) and 4-(trifluoromethyl)phenyltrifluoromethanesulfonate (**S1**, 83.5 mg, 0.284 mmol, 2.20 equiv) was dissolved in pentane (8 mL) until mixture was colorless and homogenous. At this time, (COD)Pd(CH_2TMS)$_2$ (52.5 mg, 0.134 mmol, 1.04 equiv) was added, and the sides of the reaction vessel washed with an addition 1 mL of pentane. The reaction mixture was stirred vigorously for 16 h. Then, the precipitate was filtered to give **P2** as an orange solid (89 mg, 55%), which was stored in a bench-top desiccator under air. X-ray quality crystals were grown by dissolving approximately 15 mg of the complex in benzene and then allowing crystallization to occur by slow-vapor diffusion from pentane over 3–5 days at rt. **^{1}H NMR** (500 MHz, C_6D_6) δ 7.68 (bs, 3H), 7.61 (t, J = 7.7 Hz, 1H), 7.11 (d, J = 8.3 Hz, 2H), 6.99 (d, J = 7.9 Hz, 2H), 3.56 (s, 3H), 3.00 (m, 1H), 2.62 (dt, J = 13.1, 6.7 Hz, 1H), 2.56 (t, J = 7.6 Hz, 2H), 2.30 (p, J = 7.7, 7.3

Hz, 1H), 2.26 – 2.13 (m, 6H), 2.14 – 2.04 (m, 3H), 2.01 – 1.89 (m, 6H), 1.86 (d, J = 6.7 Hz, 3H), 1.77 (bs, 3H), 1.67 (m, 3H), 1.61 – 1.49 (m, 6H), 1.45 (m, 5H), 1.17 (dt, J = 14.9, 7.4 Hz, 2H), 1.10 (d, J = 6.8 Hz, 3H), 1.06 (t, J = 6.8 Hz, 6H), 0.99 (d, J = 6.7 Hz, 3H), 0.76 (t, J = 7.3 Hz, 3H), 0.55 (d, J = 6.7 Hz, 3H). **^{13}C NMR** (126 MHz, C_6D_6) δ 161.0, 156.1, 153.5, 139.3, 134.6, 128.5, 126.1, 124.0, 122.8, 122.2, 122.0, 112.3, 54.6, 48.6 (d, J = 12.6 Hz), 47.3 (d, J = 12.4 Hz), 42.3, 41.0, 36.2 (d, J = 17.8 Hz), 33.3, 32.3, 31.6, 29.7 (d, J = 10.1 Hz), 29.3 (d, J = 9.9 Hz), 26.1, 23.7 (d, J = 14.3 Hz), 23.0, 22.8, 22.5, 13.8. **^{31}P NMR** (203 MHz, C_6D_6): 112.5 ppm. **^{19}F NMR** (471 MHz, C_6D_6) δ –62.3, –77.9, –136.2, –137.0, –143.3, –143.9 ppm. **IR** (neat, cm^{-1}): 2910, 1586, 1566, 1478, 1326, 1262, 1147, 1123, 1101, 1072, 1030, 1005, 972, 817, 638. **HRMS** (ESI) m/z calcd for $C_{60}H_{71}F_{10}O_4PPdS^+$ [M–OTf]$^+$: 1065.4166; 1065.3659 found.

For the recovery of **L1**[4a]

The filtrate that was collected from the isolation of **P1** (or **P2**) on a 0.64 mmol scale was concentrated *in vacuo*. The residue was dissolved in THF (50 mL) and 1,2-diaminopropane (1.10 mL, 12.90 mmol, 20.0 equiv) was added, and the reaction mixture stirred for 16 h at room temperature. The solution was diluted with EtOAc (50 mL) and transferred to a separatory funnel. The organic phase was washed with NH_4OH:brine (1:1, 50 mL x 3), brine (50 mL x 1), dried over $MgSO_4$, filtered, and concentrated *in vacuo*. The resulting oil was suspended in MeOH and sonicated in a water bath. A white precipitate formed, which was filtered through a fritted funnel and washed with MeOH (5 mL x 3) to give **L1** as a white solid (192 mg, 65% recovery after accounting for the amount of **L1** that reacted). The total efficiency is 80%: [(recovered **L1** + reacted **L1**)] / [Total **L1** used].

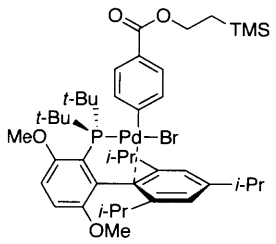

P3

P3 was prepared following general procedure A. A mixture of **L2** (295 mg, 0.609 mmol, 1.01 equiv) and 2-(trimethylsilyl)ethyl 4-bromobenzoate (**S15**, 261 mg, 0.866 mmol, 1.50 equiv) was

dissolved in pentane (8 mL) until mixture was colorless and homogenous. At this time, (COD)Pd($CH_2TMS)_2$ (236 mg, 0.604 mmol, 1.00 equiv) was added, and the sides of the reaction vessel washed with an addition 1 mL of pentane. The reaction mixture was stirred vigorously for 16 h. Then, the reaction tube was removed from the glovebox and the precipitate was filtered to give **P3** as a yellow solid (400 mg, 74%), which was stored in a bench-top desiccator under air. **^{1}H NMR** (500 MHz, CD_2Cl_2) δ 7.37 (d, J = 8.2 Hz, 2H), 7.26 – 7.21 (m, 2H), 7.05 (s, 2H), 6.93 (dd, J = 8.9, 2.6 Hz, 1H), 6.87 (d, J = 8.9 Hz, 1H), 4.33 – 4.26 (m, 2H), 3.79 (s, 3H), 3.32 (s, 3H), 3.03 (hept, J = 6.5 Hz, 1H), 2.59 (hept, J = 6.7 Hz, 2H), 1.59 (d, J = 6.8 Hz, 6H), 1.42 – 1.32 (m, 24H), 1.09 – 1.04 (m, 2H), 0.82 (d, J = 6.7 Hz, 6H), 0.06 (s, 9H). **^{13}C NMR** (126 MHz, CD_2Cl_2) δ 167.9, 154.9, 154.5, 152.4, 152.3, 146.5 (d, J = 7.8 Hz), 140.6 (d, J = 2.4 Hz), 127.9, 127.8, 125.6, 125.3, 125.1, 116.7, 113.9, 111.0, 62.9, 54.9, 54.3, 41.7, 41.6, 35.0, 32.9 (d, J = 5.8 Hz), 31.9, 30.7 (d, J = 5.5 Hz), 26.0, 25.0, 24.8, 17.8, –1.2 ppm. **^{31}P NMR** (203 MHz, CD_2Cl_2) δ 82.8 (rearranged), 72.0 ppm. **IR** (neat, cm^{-1}): 2958, 2864, 1695, 1574, 1456, 1421, 1263, 1253, 1176, 1163, 1107, 1095, 1086, 1052, 1010, 865, 839, 815, 756, 718. **HRMS** (ESI) m/z calcd for $C_{43}H_{66}BrO_4PPdSi^+$ $[M–Br]^+$: 811.3503; 811.3449 found.

B) X-Ray Structure Details

Low-temperature diffraction data (Φ-and ω-scans) were collected on a Bruker-AXS X8 Kappa Duo diffractometer coupled to a Smart APEX2 CCD detector with Mo Kα radiation (λ = 0.71073 Å) from an IμS micro-source for the structure of compound **P2**. Absorption and other corrections were applied using SADABS.[21] All structures were solved by direct methods using SHELXT[22] and refined against F^2 on all data by full-matrix least squares with SHELXL-2014[23] using established refinement approaches.[24] All hydrogen atoms were included into the model at geometrically calculated positions and refined using a riding model. The isotropic displacement parameters of all hydrogen atoms were fixed to 1.2 times the U_{eq} value of the atoms they are linked to (1.5 times for methyl groups). Details about crystal properties, diffraction data, and crystal structures can be found in the tables below.

Compound **P2** crystallizes in the triclinic centrosymmetric space group *P*-1 with one molecule of **P2** and one molecule of benzene per asymmetric unit. SQUEEZE[25] as implemented in PLATON[26] was used to account for highly disordered solvent.

Crystal data structure refinement for **P2**

Identification code	X8_16160	
Empirical formula	$C_{63}H_{74}F_{10}O_4PPdS$	
Formula weight	1254.722	
Temperature	−173.0 °C	
Wavelength	0.71073 Å	
Crystal system	Triclinic	
Space group	*P*-1	
Unit cell dimensions	*a* = 16.199(3) Å *b* = 18.065(3) Å *c* = 23.596(4) Å	α = 102.700(4)° β = 107.741(4)° γ = 106.042(4)°
Volume	5961.80 Å^3	
Z	4	
Density (calculated)	1.398 g/cm^3	
Absorption coefficient	0.451 mm^{-1}	
F(000)	2604	
Crystal size	0.120 x 0.075 x 0.045 mm^3	
Theta range for data collection	1.294 to 28.282°	
Index ranges	-21 ≤h ≤21, -24≤ k ≤24, -31≤ l ≤31	
Reflections collected	244620	

Independent reflections	29591	
Completeness to theta = 25.242 °	1.00	
Absorption correction	T_{max} = 0.7461; T_{min} = 0.6329	
Refinement method	Full-matrix least-squares on F^2	
Data / restraints / parameters	29591 / 4158 / 1613	
Goodness-of-fit on F^2	1.044	
Final R indices [$I>2\sigma(I)$]	$R1$ = 0.0777, $wR2$ = 0.2037	
R indices (all data)	$R1$ = 0.1272, $wR2$ = 0.2399	
Largest diff. peak and hole	5.663 and -14	

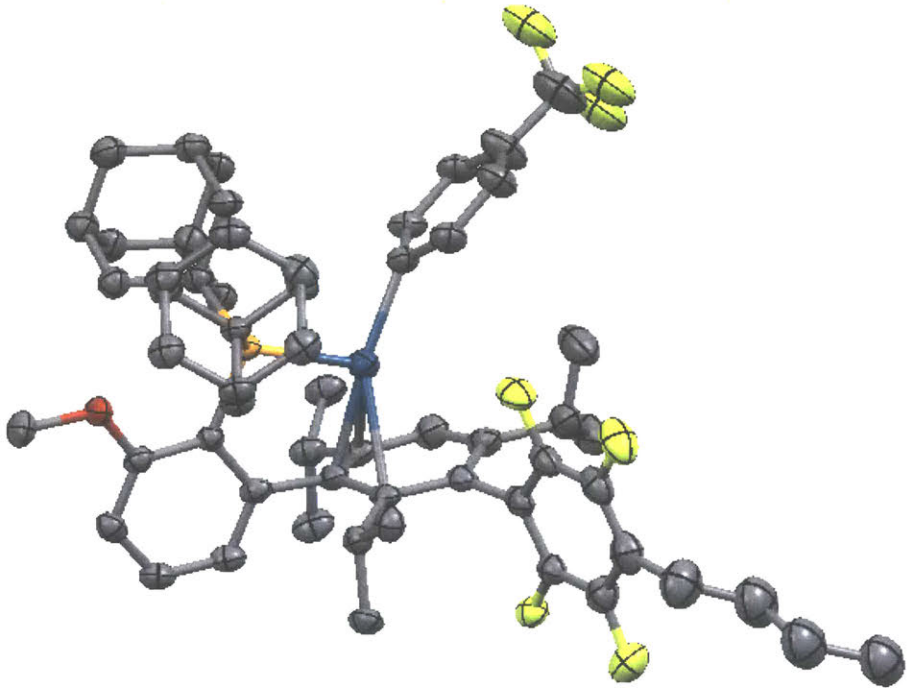

X-ray crystal structure of **P2**. Thermal ellipsoids shown at 50% probability. Triflate anion and hydrogen atoms are omitted.

C) General procedure for additive analysis (Table 1)

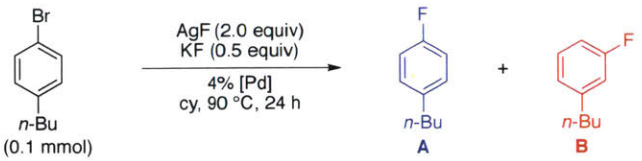

entry	[Pd]	additive	yield A (B)
1	[(COD)(L1–Pd)$_2$]	–	87% (5%)
2	P1	–	22% (1%)
3	P1	2% COD	91% (6%)

Procedure for fluorination of 1-bromo-4-*n*-butylbenzene: In a nitrogen-filled glovebox, an oven-dried 16 mL screw-cap tube (Fisher Scientific, 16 x 125 mm, Cat. No. 1495935A) equipped with a stir bar was charged sequentially with Pd source (4.0 mol %), AgF (25.4 mg, 0.200 mmol, 2.00 equiv), KF (2.90 mg, 0.05 mmol, 0.50 equiv), and cyclohexane (0.50 mL). 1-bromo-4-*n*-butylbenzene (21.3 mg, 0.100 mmol, 1.00 equiv) was added, followed by a stock solution of 1,5-cyclooctadiene in cyclohexane (0.498 M, 2 mol %), if appropriate, and then the remaining 0.50 mL of cyclohexane was used to rinse the sides of the reaction tube. The reaction tube was sealed with a screw cap (Kimble-Chase, Open Top S/T Closure, Part No. 73804-15425) containing a Teflon septum (Thermo Scientific, Cat. No. B7995-15), removed from the glovebox, and the reaction mixture vigorously stirred in a preheated oil bath at 90 °C for the 24 h. Then, the reaction mixture was allowed to cool to rt, the reaction tube was uncapped, and 1-fluoronaphthalene (15 μL, 0.116 mmol, 1.16 equiv.) was added by syringe. The reaction mixture was capped, shaken, and then transferred into an NMR tube, and analyzed by ^{19}F NMR spectroscopy.

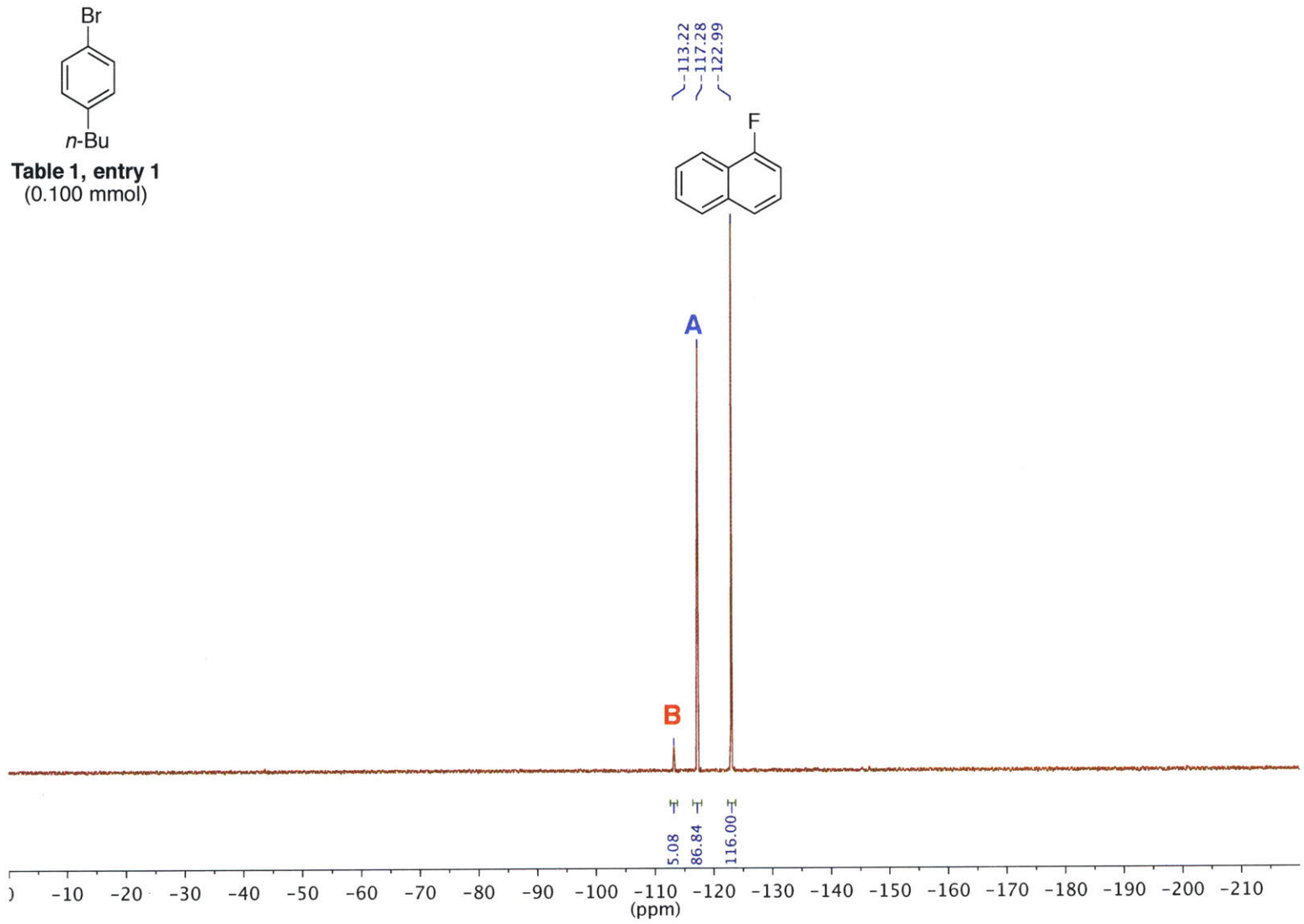
Br
n-Bu
Table 1, entry 1
(0.100 mmol)
-113.22
-117.28
-122.99
F
A
B
5.08
86.84
116.00
-10 -20 -30 -40 -50 -60 -70 -80 -90 -100 -110 -120 -130 -140 -150 -160 -170 -180 -190 -200 -210
(ppm)

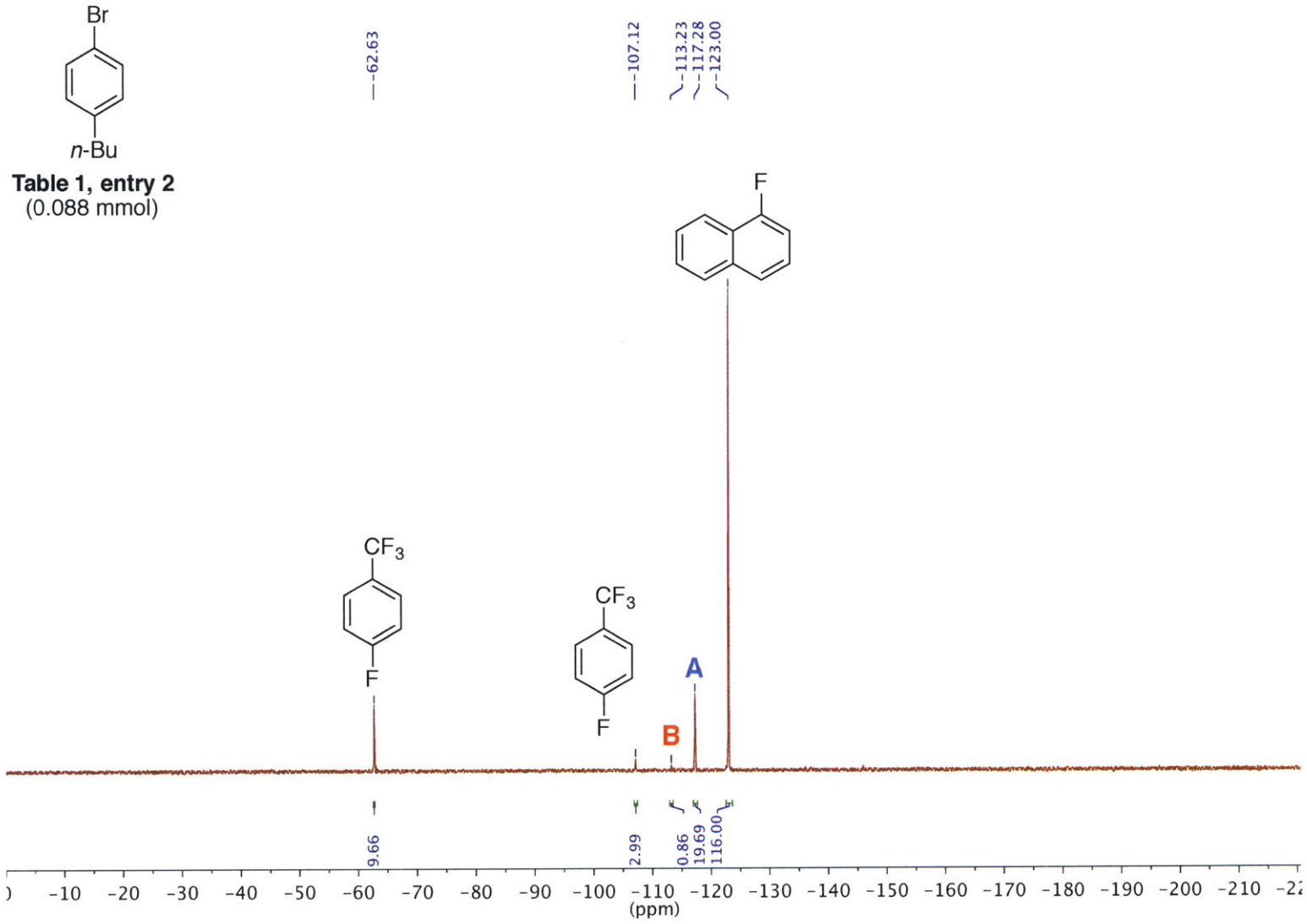
Br
n-Bu
Table 1, entry 2
(0.088 mmol)
-62.63
-107.12
-113.23
-117.28
-123.00
F
CF3
F
CF3
F
A
B
9.66
2.99
0.86
19.69
116.00
-10 -20 -30 -40 -50 -60 -70 -80 -90 -100 -110 -120 -130 -140 -150 -160 -170 -180 -190 -200 -210
(ppm)

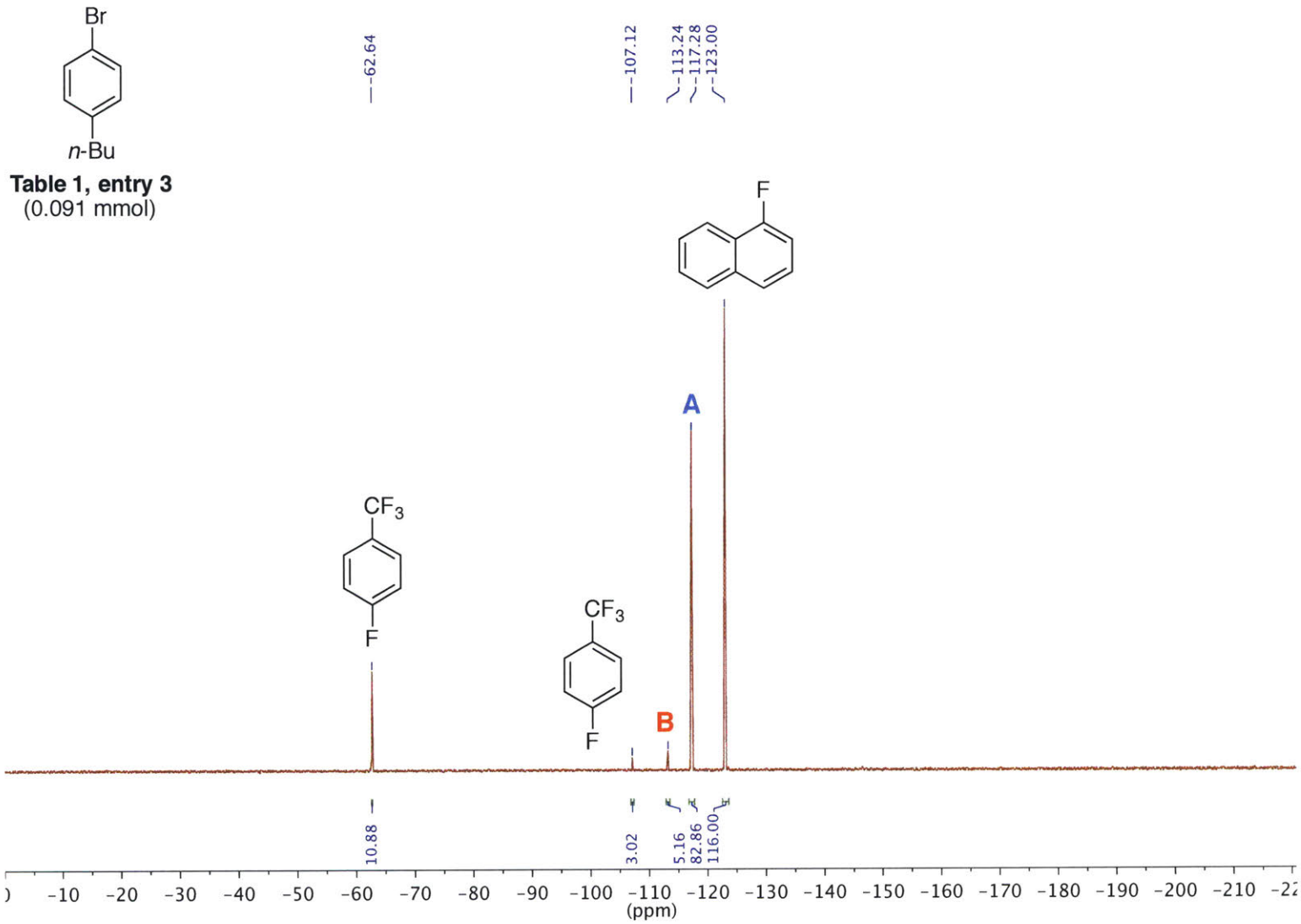
Br
n-Bu
Table 1, entry 3
(0.091 mmol)
-62.64
-107.12
-113.24
-117.28
-123.00
F
A
CF3
F
CF3
F
B
10.88
3.02
5.16
82.86
116.00
-10 -20 -30 -40 -50 -60 -70 -80 -90 -100 -110 -120 -130 -140 -150 -160 -170 -180 -190 -200 -210
(ppm)

D) Fluorination of aryl bromides

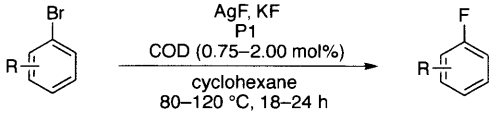

General procedure B for fluorination of aryl bromides: In a nitrogen-filled glovebox, an oven-dried 25 mL screw-cap tube equipped with a stir bar was charged sequentially with **P1** (1.50–4.00 mol %), AgF (254 mg, 2.00 mmol, 2.00 equiv), KF (29.0 mg, 0.50 mmol, 0.50 equiv), aryl bromide (1.00 mmol, 1.00 equiv) if a solid, and cyclohexane (5 mL). If the aryl bromide was a liquid, it was added at this time, followed by a stock solution of 1,5-cyclooctadiene in cyclohexane (0.154 M, 0.75–2.00 mol %), and then the remaining 5 mL of cyclohexane was used to rinse the sides of the reaction tube. The reaction tube was sealed with a screw cap containing a Teflon septum, removed from the glovebox, and the reaction mixture was vigorously stirred in a preheated oil bath for the time and temperature as indicated for each substrate. After the reaction was complete, the reaction mixture was allowed to cool to rt, the reaction tube was uncapped, and then the reaction mixture was filtered through a pad of celite, eluting with EtOAc (or Et_2O for **2c**), and concentrated *in vacuo*. The crude material was purified by silica gel chromatography. The yields reported are the average of two experiments. Compounds **2a,**[27] **2b,**[28] and **2c**[4a] have been previously described.

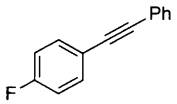

2a

1-fluoro-4-(phenylethynyl)benzene (2a)[27] was prepared following general procedure B. A mixture of 1-bromo-4-(phenylethynyl)benzene (**S11**, 256 mg, 1.00 mmol, 1.00 equiv), KF (29.0 mg, 0.50 mmol, 0.50 equiv), AgF (254 mg, 2.00 mmol, 2.00 equiv), **P1** (46.0 mg, 40.0 μmol, 4 mol%), and 1,5-cyclooctadiene (40.0 μL of stock solution, 2 mol%) was stirred in cyclohexane at 80 °C for 24 h. The reaction mixture was allowed to cool to rt before work-up and purification. The crude product was purified by automated flash-column chromatography (gradient elution 0% EtOAc/hexanes to 5% EtOAc/hexanes) to afford **2a** as a white solid (1st run: 135 mg, 68%; 2nd run: 143 mg, 72%). mp = 110–111 °C. **^{1}H NMR** (400 MHz, $CDCl_3$): δ 7.54–7.50 (m, 4 H), 7.37–7.34 (m, 3H), 7.07–7.03 (m, 2H) ppm. **^{13}C NMR** (100 MHz, $CDCl_3$) δ 162.6 (d, J = 249.5 Hz), 133.6 (d, J = 8.3 Hz), 131.7, 128.51, 128.47 123.2, 119.5 (d, J = 3.5 Hz), 115.8 (d, J = 22.1

Hz), 89.2, 88.4 ppm. **^{19}F NMR** (471 MHz, $CDCl_3$): δ –122.2 ppm. **IR** (neat, cm^{-1}): 3044, 1594, 1506, 1443, 1215, 1152, 1099, 843, 837, 792, 754, 686.

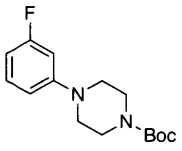

2b

***tert*-butyl 4-(3-fluorophenyl)piperazine-1-carboxylate (2b)**[28] was prepared following general procedure B. A mixture of *tert*-butyl 4-(3-bromophenyl)piperazine-1-carboxylate (**S2**, 341 mg, 1.00 mmol, 1.00 equiv), KF (29.0 mg, 0.50 mmol, 0.50 equiv), AgF (254 mg, 2.00 mmol, 2.00 equiv), **P1** (46.0 mg, 40.0 μmol, 4 mol%), and 1,5-cyclooctadiene (40.0 μL of stock solution, 2 mol%) was stirred in cyclohexane at 80 °C for 18 h. The reaction mixture was allowed to cool to rt before work-up and purification. The crude product was purified by automated flash-column chromatography (gradient elution 0% EtOAc/hexanes to 10% EtOAc/hexanes) to afford **2b** as a yellow-brown solid (1st run: 248 mg, 89%; 2nd run: 252 mg, 90%). mp = 52–53 °C. **^{1}H NMR** (400 MHz, $CDCl_3$): δ 7.19 (td, J = 8.2, 7.0 Hz, 1H), 6.67 (ddd, J = 8.4, 2.4, 0.9 Hz, 1H), 6.62 – 6.47 (m, 2H), 3.57 (t, J = 5.3 Hz, 4H), 3.14 (t, J = 5.2 Hz, 4H), 1.48 (s, 9H) ppm. **^{13}C NMR** (100 MHz, $CDCl_3$) δ 163.9 (d, J = 243.6 Hz), 154.8, 153.0 (d, J = 9.7 Hz), 130.3 (d, J = 9.9 Hz), 111.7, 106.5 (d, J = 21.5 Hz), 103.3 (d, J = 24.9 Hz), 80.1, 49.0, 43.6 (broad), 28.6 ppm. **^{19}F NMR** (471 MHz, $CDCl_3$): δ –113.3 ppm. **IR** (neat, cm^{-1}): 2977, 2931, 2825, 1674, 1611, 1582, 1494, 1415, 1364, 1241, 1173, 1158, 1121, 997, 967, 842, 774, 764, 685.

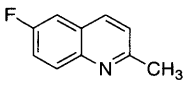

2c

6-fluoro-2-methylquinoline (2c)[4a] was prepared following general procedure B. A mixture of 6-bromo-2-methylquinoline (**S12**, 221 mg, 1.00 mmol, 1.00 equiv), KF (29.0 mg, 0.50 mmol, 0.50 equiv), AgF (254 mg, 2.00 mmol, 2.00 equiv), **P1** (17.0 mg, 15.0 μmol, 1.5 mol%), and 1,5-cyclooctadiene (7.7 μL of stock solution, 0.75 mol%) was stirred in cyclohexane at 90 °C for 20 h. The reaction mixture was allowed to cool to rt before work-up and purification. The crude product was purified by automated flash-column chromatography (gradient elution 30% Et_2O/pentane to 50% Et_2O /pentane) to afford **2c** as a yellow solid (1st run: 150 mg, 92%; 2nd run: 148 mg, 91%). mp = 51–53 °C **^{1}H NMR** (400 MHz, $CDCl_3$): δ 7.96 (ddt, J = 11.8, 8.5, 4.0

Hz, 2H), 7.45 – 7.38 (m, 1H), 7.34 (dd, J = 8.7, 2.4 Hz, 1H), 7.28 – 7.23 (m, 1H), 2.70 (s, 3H) ppm. **^{13}C NMR** (100 MHz, $CDCl_3$) δ 160.0 (d, J = 246.6 Hz), 158.4, 145.0, 135.6 (d, J = 5.1 Hz), 131.1 (d, J = 9.0 Hz), 127.0 (d, J = 9.9 Hz), 122.8, 119.5 (d, J = 25.5 Hz), 110.6 (d, J = 21.6 Hz), 25.3. **^{19}F NMR** (471 MHz, $CDCl_3$): δ –116.2 ppm. **IR** (neat, cm^{-1}): 3050, 2924, 1608, 1564, 1510, 1498, 1481, 1371, 1344, 1302, 1222, 1209, 1137, 1107, 964, 927, 896, 837, 822, 765, 755, 669, 654, 585.

E) Fluorination of aryl triflates

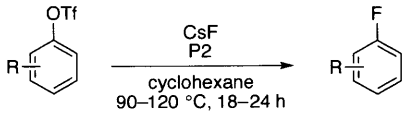

General procedure C for fluorination of aryl triflates: In a nitrogen-filled glovebox, an oven-dried 25 mL screw-cap tube equipped with a stir bar was charged sequentially with **P2** (2.00–4.00 mol %), CsF (456 mg, 3.00 mmol, 3.00 equiv), aryl triflate (1.00 mmol, 1.00 equiv) if a solid, and 5 mL of solvent. If the aryl triflate was a liquid, it was added at this time, and then the remaining 5 mL of solvent was used to rinse the sides of the reaction tube. The reaction tube was sealed with a screw cap containing a Teflon septum, removed from the glovebox, and the reaction mixture vigorously stirred in a preheated oil bath for the time and temperature as indicated for each substrate. After the reaction was complete, the reaction mixture was allowed to cool to rt, the reaction tube was uncapped, and then the reaction mixture was filtered through a pad of celite, eluting with EtOAc (or Et_2O for **2d**), and concentrated in vacuo. The crude material was purified by silica gel chromatography. The yields reported are the average of two experiments. Compound **2d** is commercially available. Compound **2e**[29] has been previously described.

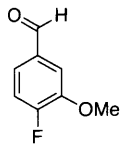

2d

4-fluoro-3-methoxybenzaldehyde (2d) was prepared following general procedure C. A mixture of 4-formyl-2-methoxyphenyl trifluoromethanesulfonate (**S3**, 284 mg, 1.00 mmol, 1.00 equiv), CsF (456 mg, 3.00 mmol, 3.00 equiv), and **P2** (17.0 mg, 15.0 μmol, 1.5 mol%) was stirred in

cyclohexane at 90 °C for 18 h. The reaction mixture was allowed to cool to rt before work-up and purification. The crude product was purified by automated flash-column chromatography (gradient elution 0% Et_2O/pentane to 10% Et_2O/pentane) to afford **2d** as a white solid (1st run: 129 mg, 83%; 2nd run: 126 mg, 81%). mp = 60–61 °C. **^{1}H NMR** (400 MHz, $CDCl_3$): δ 9.92 (s, 1H), 7.51 (dd, J = 8.2, 1.9 Hz, 1H), 7.45 (ddd, J = 8.2, 4.4, 1.9 Hz, 1H), 7.27 – 7.20 (m, 1H), 3.96 (s, 3H) ppm. **^{13}C NMR** (100 MHz, $CDCl_3$) δ 190.8, 156.6 (d, J = 257.5 Hz), 148.8 (d, J = 11.3 Hz), 133.4 (d, J = 3.2 Hz), 125.5 (d, J = 8.3 Hz), 116.6 (d, J = 19.5 Hz), 111.9 (d, J = 3.6 Hz), 56.4 ppm. **^{19}F NMR** (471 MHz, $CDCl_3$): δ –125.1 ppm. **IR** (neat, cm^{-1}): 3062, 2953, 2857, 1698, 1681, 1505, 1470, 1426, 1396, 1277, 1216, 1148, 1116, 1021, 855, 810, 731, 623.

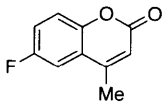

2e

6-fluoro-4-methyl-2*H*-chromen-2-one (2e)[29] was prepared following general procedure C. A mixture of 4-methyl-2-oxo-2H-chromen-6-yl trifluoromethanesulfonate (**S4**, 308 mg, 1.00 mmol, 1.00 equiv), CsF (456 mg, 3.00 mmol, 3.00 equiv), and **P2** (49.0 mg, 40.0 μmol, 4.0 mol%) was stirred in toluene (10 mL) at 120 °C for 24 h. The reaction mixture was allowed to cool to rt before work-up and purification. The crude product was purified by automated flash-column chromatography (gradient elution 10% EtOAc/hexanes to 30% EtOAc/hexanes) to afford **2e** as an off-white solid (1st run: 155 mg, 86%; 2nd run: 157 mg, 88%) as a 14:1 mixture of regioisomers as determined by ^{19}F NMR and ^{1}H NMR. An asterisk (*) in the characterization data indicates a signal attributed to the minor regioisomer. mp = 158–161 °C. **^{1}H NMR** (400 MHz, $CDCl_3$): δ 7.52* (m, 1H) 7.29 – 7.10 (m, 3H), 6.96* (m, 2H) 6.27 (s, 1H), 6.17* (s, 1H), 2.36* (s, 3H), 2.35 (s, 3H) ppm. **^{13}C NMR** (100 MHz, $CDCl_3$) δ 160.4, 158.9 (d, J = 243.8 Hz), 151.5 (d, J = 2.8 Hz), 149.8 (d, J = 2.0 Hz), 121.0 (d, J = 8.4 Hz), 119.2 (d, J = 24.3 Hz), 118.7 (d, J = 8.4 Hz), 116.2, 110.4 (d, J = 24.4 Hz), 18.7. **^{19}F NMR** (471 MHz, $CDCl_3$): δ –107.1*, –118.5 ppm. **IR** (neat, cm^{-1}): 3069, 2923, 1716, 1699, 1573, 1492, 1429, 1385, 1263, 1207, 1157, 922, 875, 867, 859, 838, 825, 810, 748, 716, 630.

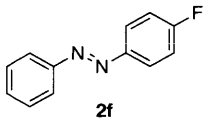

2f

(*E*)-1-(4-fluorophenyl)-2-phenyldiazene (2f) was prepared following general procedure C. A mixture of (*E*)-4-(phenyldiazenyl)phenyl trifluoromethanesulfonate (**S5**, 330 mg, 1.00 mmol, 1.00 equiv), CsF (456 mg, 3.00 mmol, 3.00 equiv), and **P2** (24.5 mg, 20.0 μmol, 2.0 mol%) was stirred in cyclohexane at 90 °C for 18 h. The reaction mixture was allowed to cool to rt before work-up and purification. The crude product was purified by automated flash-column chromatography (gradient elution 0% EtOAc/hexanes to 5% EtOAc/hexanes) to afford **2f** as a bright orange solid (1st run: 189 mg, 94%; 2nd run: 189 mg, 94%). mp = 73–74 °C. **^{1}H NMR** (400 MHz, $CDCl_3$): δ 8.21 – 7.79 (m, 4H), 7.69 – 7.37 (m, 3H), 7.24 – 7.14 (m, 2H) ppm. **^{13}C NMR** (100 MHz, $CDCl_3$) δ 164.5 (d, J = 251.9 Hz), 152.6, 149.3, 131.2, 129.3 , 125.0 (d, J = 8.9 Hz), 123.0, 116.2 (d, J = 22.9 Hz). **^{19}F NMR** (471 MHz, $CDCl_3$): δ –110.6 ppm. **IR** (neat, cm^{-1}): 3046, 1583, 1493, 1482, 1225, 1137, 1091, 843, 779, 766, 713, 685. **Anal. Calcd. for $C_{12}H_9FN_2$**: C, 71.99; H, 4.53, Found: C, 71.84; H, 4.54.

F) *N*-arylation of amino acid esters

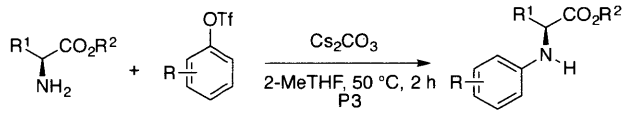

General procedure D for the *N*-arylation of amino acid esters: An oven-dried 25 mL screw-cap tube equipped with a stir bar was charged sequentially with the amino acid ester, if solid (1.10 mmol, 1.10 equiv), aryl triflate (1.00 mmol, 1.00 equiv), if solid, **P3** (45.0 mg, 50.0 μmol, 5.0 mol %), and cesium carbonate (977 mg, 3.00 mmol, 3.00 equiv). The reaction tube was sealed with a screw cap containing a Teflon septum. The septum was punctured with a needle attached to a Schlenk line, and the tube was evacuated and backfilled with argon (this process was repeated a total of two times). If the amino acid ester or triflate was a liquid, it was added at this time, followed by 2-MeTHF (2.00 mL). The Schlenk needle was removed and then the reaction tube was placed into a preheated oil bath at 50 °C and vigorously stirred for 2 h. Then, the reaction mixture was allowed to cool to rt, the reaction tube uncapped, and the reaction mixture was diluted with CH_2Cl_2 and filtered through a pad of celite. The filtrate was

concentrated *in vacuo*. If the substrates and byproducts coeluted on TLC, the crude reaction mixture was treated with TBAF (see below) before the residue was purified by silica gel chromatography. Otherwise it was directly purified by silica gel chromatography. The yields reported are the average of two experiments. The enantiomeric excesses (% ee) were determined by HPLC analysis using chiral stationary phases. Compound **3a**[15] has been previously described.

Fluoride-Assisted Work-up

For substrates where the byproduct of catalyst activation and the desired product coeluted on silica gel, the crude reaction mixture was dissolved in 0.20 mL of a freshly-prepared 0.498 M AcOH solution in THF (10 mol% AcOH, 0.100 equiv), followed by the addition of a freshly opened, Sure-Seal™ TBAF solution (0.50 mL, 0.50 mmol, 50 mol %, 0.50 equiv, 1.0 M in THF). The solution was stirred at 50 °C for 1.5 h. At this time, the reaction mixture was allowed to cool to rt, diluted with EtOAc (15 mL) and transferred to a separatory funnel. The organic phase was washed with deionized water (2 x 5 mL), followed by brine (10 mL). The organic fraction was dried over $MgSO_4$, filtered, and concentrated in vacuo. The resulting residue was purified by silica gel chromatography.

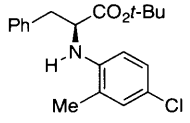

3a

***tert*-butyl (4-chloro-2-methylphenyl)-*L*-phenylalaninate (3a)**[15] was prepared following general procedure D. A mixture of L-phenylalanine *tert*-butyl ester (243 mg, 1.10 mmol, 1.10 equiv), 4-chloro-2-methylphenyl trifluoromethanesulfonate (**S6**, 275 mg, 1.00 mmol, 1.00 equiv), Cs_2CO_3 (977 mg, 3.00 mmol, 3.00 equiv), and **P3** (45.0 mg, 50.0 μmol, 5.0 mol %) was stirred in 2-MeTHF at 50 °C for 2 h. The reaction mixture was allowed to cool to rt before work-up and purification. The crude product was purified by automated flash chromatography (gradient elution 0% Et_2O/hexanes to 10% Et_2O/hexane) to afford **3a** as a colorless oil (1st run: 213 mg, 60%; 2nd run: 217 mg, 62%). **^{1}H NMR** (400 MHz, $CDCl_3$): δ 7.32 – 7.22 (m, 2H), 7.20 – 7.15 (m, 2H), 7.03 (d, J = 6.9 Hz, 2H), 6.48 – 6.43 (m, 1H), 4.23 (dt, J = 8.5, 6.2 Hz, 1H), 4.02 (d, J = 8.4 Hz, 1H), 3.17 – 3.07 (m, 2H), 2.07 (s, 3H), 1.36 (s, 9H) ppm. **^{13}C NMR** (100 MHz, $CDCl_3$) δ 172.2, 143.4, 136.5, 130.2, 129.6, 128.5, 127.1, 126.7, 124.6, 122.3, 111.6, 82.1, 58.1, 38.5, 28.1,

17.4 ppm. **IR** (neat, cm^{-1}): 3422, 3028, 2978, 2931, 1726, 1505, 1479, 1454, 1367, 1314, 1281, 1257, 1222, 1147, 847, 871, 801, 736, 699, 665. **HPLC analysis** (OJ-H, 2% IPA–hexanes, 0.8 mL/min, 254 nm) indicated 95% ee: tR (minor) = 12.3 min, tR (major) = 17.6 min.

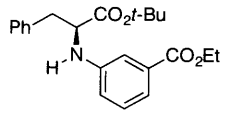

3b

ethyl (*S*)-3-((1-(*tert*-butoxy)-1-oxo-3-phenylpropan-2-yl)amino)benzoate (3b) was prepared following general procedure D. A mixture of L-phenylalanine *tert*-butyl ester (243 mg, 1.10 mmol, 1.10 equiv), ethyl 3-(((trifluoromethyl)sulfonyl)oxy)benzoate (**S7**, 298 mg, 1.00 mmol, 1.00 equiv), Cs_2CO_3 (977 mg, 3.00 mmol, 3.00 equiv), and **P3** (45.0 mg, 50.0 μmol, 5.0 mol %) was stirred in 2-MeTHF at 50 °C for 2 h. The reaction mixture was allowed to cool to rt before work-up and purification. The crude product was treated with TBAF (*vide supra*) and then purified by automated flash chromatography (gradient elution 0% EtOAc/hexanes to 15% EtOAc/hexanes) to afford **3b** as a yellow oil (1st run: 278 mg, 74%; 2nd run: 280 mg, 76%). **^{1}H NMR** (400 MHz, $CDCl_3$): δ 7.44 – 7.38 (m, 1H), 7.33 – 7.13 (m, 7H), 6.77 (ddd, J = 8.1, 2.6, 1.0 Hz, 1H), 4.35 (q, J = 7.1 Hz, 2H), 4.30 – 4.27 (m, 2H), 3.18 – 3.04 (m, 2H), 1.37 (overlapping t and s, J = 9.0 Hz, 12H) ppm. **^{13}C NMR** (100 MHz, $CDCl_3$) δ 172.1, 167.0, 146.8, 136.6, 131.6, 129.6, 129.3, 128.6, 127.1, 119.5, 118.2, 114.1, 82.1, 61.0, 58.1, 38.7, 28.1, 14.5 ppm. **IR** (neat, cm^{-1}): 3374, 2979, 1715, 1505, 1478, 1367, 1236, 1209, 1149, 1104, 1026, 848, 752, 739, 697, 683. **Specific rotation** $[\alpha]_D^{23}$ +6.0 (*c*, 1.0, $CHCl_3$). **HPLC analysis** (OJ-H, 2% IPA-hexanes, 0.8 mL/min, 230 nm) indicated 94% ee: tR (major) = 26.8 min, tR (minor) = 38.2 min. The product contained approximately 0.5% of the byproduct of catalyst activation as judged by ^{1}H NMR. **Anal. Calcd. for $C_{22}H_{27}NO_4$**: C, 71.52; H, 7.37, Found: C, 71.73; H, 7.40.

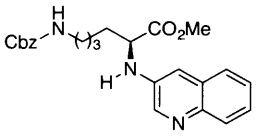

3c

methyl N^6-((benzyloxy)carbonyl)-N^2-(quinolin-3-yl)-*L*-lysinate (3c) was prepared following general procedure D. A mixture of L-Lysine-(Cbz)-OMe (324 mg, 1.10 mmol, 1.10 equiv),

quinolin-3-yl trifluoromethanesulfonate (**S8**, 277 mg, 1.00 mmol, 1.00 equiv), Cs_2CO_3 (977 mg, 3.00 mmol, 3.00 equiv), and **P3** (45.0 mg, 50.0 μmol, 5.0 mol %) was stirred in 2-MeTHF at 50 °C for 2 h. The reaction mixture was allowed to cool to rt before work-up and purification. The crude product was purified by automated flash chromatography (gradient elution 40% EtOAc/hexanes to 75% EtOAc/hexanes) to afford **3c** as a brown oil (1st run: 353 mg, 86%; 2nd run: 373 mg, 91%). **^{1}H NMR** (400 MHz, $CDCl_3$): δ 8.49 (d, J = 2.8 Hz, 1H), 7.94 (dd, J = 6.1, 3.5 Hz, 1H), 7.60 (dd, J = 6.2, 3.4 Hz, 1H), 7.42 (dd, J = 6.3, 3.3 Hz, 2H), 7.37 – 7.28 (m, 5H), 6.98 (d, J = 2.8 Hz, 1H), 5.09 (s, 2H), 4.81 (s, 1H), 4.59 (d, J = 8.5 Hz, 1H), 4.20 – 4.09 (m, 1H), 3.74 (s, 3H), 3.26 – 3.10 (m, 2H), 1.91 (ddd, J = 28.2, 14.0, 7.2 Hz, 2H), 1.63 – 1.40 (m, 4H) ppm. **^{13}C NMR** (100 MHz, $CDCl_3$) δ 173.9, 156.7, 143.5, 142.6, 140.3, 136.6, 129.3, 129.1, 128.7, 128.3, 127.2, 126.2, 125.5, 111.2, 66.9, 56.3, 52.6, 40.6, 32.2, 29.9, 22.7 ppm. **IR** (neat, cm^{-1}): 3032, 2948, 2862, 1699, 1609, 1521, 1222, 1173, 1136, 1017, 984, 780, 747, 696, 613. **Specific rotation** $[\alpha]_D^{23}$ –33.5 (*c*, 1.0, $CHCl_3$). **HPLC analysis** (OD-H, 30% IPA-hexanes, 0.8 mL/min, 254 nm) indicated 96% ee: tR (minor) = 15.9 min, tR (major) = 67.8 min. **HRMS** (DART) m/z calcd for $C_{24}H_{27}N_3O_4$ $[M+H]^+$: 422.2074; 422.2067 found.

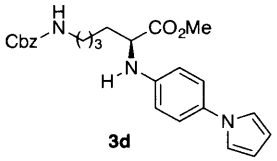

3d

methyl N^2-(4-(1*H*-pyrrol-1-yl)phenyl)-N^6-((benzyloxy)carbonyl)-*L*-lysinate (3d) was prepared following general procedure D. A mixture of L-Lysine-(Cbz)-OMe (324 mg, 1.10 mmol, 1.10 equiv), 4-(1*H*-pyrrol-1-yl)phenyl trifluoromethanesulfonate (**S9**, 291 mg, 1.00 mmol, 1.00 equiv), Cs_2CO_3 (977 mg, 3.00 mmol, 3.00 equiv), and **P3** (45.0 mg, 50.0 μmol, 5.0 mol %) was stirred in 2-MeTHF at 50 °C for 2 h. The reaction mixture was allowed to cool to rt before work-up and purification. The crude product was treated with TBAF (*vide supra*) and then purified by automated flash chromatography (gradient elution 40% EtOAc/hexanes to 80% EtOAc/hexanes) to afford **3d** as a thick yellow-orange oil (1st: 396 mg, 93%; 2nd: 372 mg, 89%). **^{1}H NMR** (500 MHz, $CDCl_3$): δ 7.39 – 7.29 (m, 5H), 7.20 (d, J = 8.7 Hz, 2H), 6.96 (t, J = 2.1 Hz, 2H), 6.64 (d, J = 8.7 Hz, 2H), 6.30 (t, J = 2.2 Hz, 2H), 5.10 (s, 2H), 4.80 (t, J = 6.0 Hz, 1H), 4.22 (d, J = 8.8 Hz, 1H), 4.06 (q, J = 7.0 Hz, 1H), 3.73 (s, 3H), 3.21 (qd, J = 6.8, 2.2 Hz, 2H), 1.83 (dq, J = 39.1, 7.1 Hz, 2H), 1.61 – 1.37 (m, 4H) ppm. **^{13}C NMR** (100 MHz, $CDCl_3$) δ 174.5,

156.6, 145.1, 136.7, 132.8, 128.7, 128.3, 122.6, 119.8, 114.1, 109.6, 66.8, 56.8, 52.4, 40.8, 32.6, 29.8, 22.8 (one signal missing due to overlap) ppm. **IR** (neat, cm^{-1}): 3366, 2948, 1704, 1521, 1314, 1242, 1173, 1134, 1071, 1021, 907, 821, 724, 696, 647, 632, 613, 573, 571. **Specific rotation** $[\alpha]_D^{23}$ –20.4 (*c*, 1.0, $CHCl_3$). **HPLC analysis** (OD-H, 20% IPA-hexanes, 0.8 mL/min, 254 nm) indicated 98% ee: tR (minor) = 28.3 min, tR (major) = 36.9 min. The product contained approximately 1% of the byproduct of catalyst activation as judged by ^1H NMR. **HRMS** (DART) m/z calcd for $C_{25}H_{29}N_3O_4$ $[M+H]^+$: 436.2231; 436.2219 found.

G) Hydroxylation of aryl halides

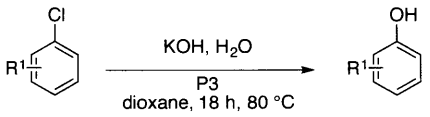

General procedure E for the hydroxylation of aryl halides: An oven-dried 25 mL screw-cap tube equipped with a stir bar was charged sequentially with the aryl halide, if solid (1.00 mmol, 1.00 equiv), KOH (3.00 mmol, 3.00 equiv), and **P3** (18.0 mg, 2.0 μmol, 2.0 mol %). The reaction tube was sealed with a screw cap containing a Teflon septum. The septum was punctured with a needle attached to a Schlenk line, and the tube was evacuated and backfilled with argon (this process was repeated a total of three times). If the aryl halide was a liquid, it was added at this time, followed by degassed deionized water (0.36 mL, 20 mmol, 20 equiv.) and 1,4-dioxane (2.00 mL). The Schlenk needle was removed and then the reaction tube was placed into a preheated oil bath at 80 °C and stirred for 18 h. Then, the reaction mixture was allowed to cool to rt, the reaction tube was uncapped, and the reaction mixture was diluted with EtOAc and 1.0 M HCl (5 mL). The reaction mixture was capped, then shaken until all the solids dissolved. The mixture was transferred to a separatory funnel and the aqueous layer neutralized with an aqueous saturated sodium bicarbonate solution (5 mL). The aqueous layer was extracted with EtOAc (2 x 5 mL) and the organic fractions were combined, dried over $MgSO_4$, filtered, and concentrated *in vacuo*. The crude material was purified by silica gel chromatography. The yields reported are the average of two experiments. Compounds **4a** and **4b** have been previously described.[3b]

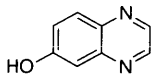

4a

quinoxaline-6-ol (4a)[3b] was prepared following general procedure E. A mixture of 4-chloroquinoxaline (**S13**, 165 mg, 1.00 mmol, 1.00 equiv), KOH (168 mg, 3.00 mmol, 3.00 equiv), water (0.36 mL, 20.00 mmol, 20.00 equiv), and **P3** (18.0 mg, 20.0 μmol, 2.0 mol %) was stirred in 1,4-dioxane for 18 h. The reaction mixture was allowed to cool to rt before work-up and purification. The crude product was purified by automated flash chromatography (gradient elution 0% MeOH/EtOAc to 10% MeOH/EtOAc) to afford **4a** as a yellow-brown solid (1st run: 130 mg, 87%; 2nd run: 137 mg, 93%). mp: 250–251 °C. **^{1}H NMR** (400 MHz, acetone-d_6): δ 9.42 (br s, 1H), 8.76 (d, J = 1.7 Hz, 1H), 8.68 (d, J = 1.8 Hz, 1H), 7.95 (d, J = 9.1 Hz, 1H), 7.47 (dd, J = 9.1, 2.7 Hz, 1H), 7.36 (d, J = 2.7 Hz, 1H) ppm. **^{13}C NMR** (100 MHz, MeOD-d_4) δ 161.0, 146.1, 145.6, 143.0, 139.3, 131.1, 124.6, 110.1. **IR** (neat, cm^{-1}): 2614, 2237, 2046, 1956, 1611, 1505, 1479, 1314, 1307, 1231, 1203, 1124, 1117, 1034, 959, 94, 851, 825, 775, 658.

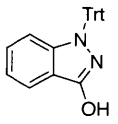

4b

1-trityl-1*H*-indazol-3-ol (4b)[3b] was prepared following general procedure E. A mixture of 3-chloro-1-trityl-1*H*-indazole (**S10**, 395 mg, 1.00 mmol, 1.00 equiv), KOH (168 mg, 3.00 mmol, 3.00 equiv), water (0.36 mL, 20.00 mmol, 20.00 equiv), and **P3** (18.0 mg, 20.0 μmol, 2.0 mol %) was stirred in 1,4-dioxane for 18 h. The reaction mixture was allowed to cool to rt before work-up and purification. The crude product was purified by automated flash chromatography (gradient elution 10% EtOAc/hexanes to 30% EtOAc/hexanes) to afford **4b** as a yellow solid (1st run: 262 mg, 69%; 2nd run: 274 mg, 71%). mp: 178–180 °C (decomposes). **^{1}H NMR** (500 MHz, CD_2Cl_2): δ 8.89 (bs, 1H), 7.53 (dt, J = 6.2, 1.6 Hz, 7H), 7.37 – 7.21 (m, 9H), 7.17 (ddd, J = 8.7, 7.0, 1.5 Hz, 1H), 7.01 (t, J = 7.5 Hz, 1H), 6.79 (d, J = 8.6 Hz, 1H) ppm. **^{13}C NMR** (100 MHz, CD_2Cl_2) δ 162.0, 148.1, 141.8, 130.4, 129.5, 128.5, 127.9, 123.1, 122.1, 112.0, 116.5, 79.6 ppm. **IR** (neat, cm^{-1}): 3023, 1670, 1609, 1458, 1450, 1339, 1218, 1067, 1000, 906, 759, 746, 705, 697.

H) Methoxylation of aryl halides

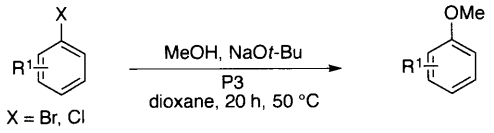

General procedure F for the methoxylation of aryl halides: An oven-dried 25 mL screw-cap tube equipped with a stir bar was charged sequentially with the aryl halide, if solid (1.00 mmol, 1.00 equiv), NaO*t*-Bu (1.40 mmol, 1.10 equiv), and **P3** (1.0–2.0 mol %). The reaction tube was sealed with a screw cap containing a Teflon septum. The septum was punctured with a needle attached to a Schlenk line, and the tube was evacuated and backfilled with argon (this process was repeated a total of three times). If the aryl halide was a liquid, it was added at this time, followed by anhydrous MeOH (0.21 mL, 5.00 mmol, 5.00 equiv) and 1,4-dioxane (2.00 mL). The Schlenk needle was removed and then the reaction tube was then placed into a preheated oil bath at 50 °C and stirred for 20 h. Then, the reaction mixture was allowed to cool to room temperature, the reaction tube was uncapped, and the reaction mixture was diluted with EtOAc and filtered through a pad of celite. The filtrate was concentrated *in vacuo*. The crude material was purified by silica gel chromatography. The yields reported are the average of two experiments. Compound **4d** has been previously described.[3a]

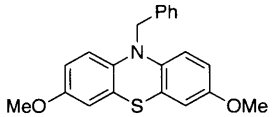

4c

10-benzyl-3,7-dimethoxy-10*H*-phenothiazine (4c) was prepared following general procedure F. A mixture of *N*-benzyl-3,7-dimethoxy-10*H*-phenothiazine (349 mg, 1.00 mmol, 1.00 equiv), NaO*t*-Bu (269 mg, 2.80 mmol, 2.80 equiv), MeOH (0.21 mL, 5.00 mmol, 5.00 equiv), and **P3** (18.0 mg, 20.0 μmol, 2.0 mol %) was stirred in 1,4-dioxane (4.00 mL) for 20 h. The reaction mixture was allowed to cool to rt before work-up and purification. The crude product was purified by automated flash chromatography (gradient elution 0% EtOAc/hexanes to 20% EtOAc/hexanes) to afford **4c** as an off-white solid (1st run: 292 mg, 84%; 2nd run: 293 mg, 83%). mp: 95–97 °C. **^{1}H NMR** (400 MHz, $CDCl_3$): δ 7.35 – 7.28 (m, 4H), 7.24 (m, 1H), 6.70 (dd, J = 2.3, 0.9 Hz, 2H), 6.54 (m, 4H), 5.01 (s, 2H), 3.72 (s, 6H) ppm. **^{13}C NMR** (100 MHz, $CDCl_3$) δ

155.2, 138.7, 137.2, 128.8, 127.0, 126.8, 124.3, 115.9, 112.6, 112.6, 55.8, 52.9 ppm. **IR** (neat, cm^{-1}): 3010, 2903, 2833, 1596, 1478, 1464, 1446, 1431, 1262, 1235, 1207, 1057, 1040, 1030, 853, 847, 844, 815, 794, 731, 726, 696, 611. **Anal. Calcd. for $C_{25}H_{29}N_3O_4$**: C, 72.18; H, 5.48, Found: C, 72.45; H, 5.42.

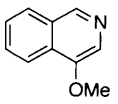

4d

4-methoxyisoquinoline (4d)[3a] was prepared following general procedure F. A mixture of 4-bromoisoquinoline (**S14**, 208 mg, 1.00 mmol, 1.00 equiv), NaO*t*-Bu (134 mg, 1.40 mmol, 1.40 equiv), MeOH (0.21 mL, 5.00 mmol, 5.00 equiv), and **P3** (9.0 mg, 10.0 μmol, 1.0 mol %) was stirred in 1,4-dioxane for 20 h. The reaction mixture was allowed to cool to rt before work-up and purification. The crude product was purified by automated flash chromatography (gradient elution 50% EtOAc/hexanes to 100% EtOAc/hexanes) to afford **4d** as a light brown solid (1st run: 149 mg, 93%; 2nd run: 146 mg, 90%). mp: 72–73 °C. **^{1}H NMR** (400 MHz, $CDCl_3$): δ 8.90 (s, 1H), 8.19 (dd, J = 8.4, 1.0 Hz, 1H), 8.08 (s, 1H), 7.92 (dt, J = 8.1, 1.0 Hz, 1H), 7.68 (ddd, J = 8.3, 6.9, 1.3 Hz, 1H), 7.61 (ddd, J = 8.1, 6.9, 1.3 Hz, 1H), 4.06 (s, 3H) ppm. **^{13}C NMR** (100 MHz, $CDCl_3$) δ 150.6, 145.4, 129.6, 129.2, 128.3, 127.7, 127.0, 123.2, 121.2, 56.1 ppm. **IR** (neat, cm^{-1}): 3063, 3010, 2967, 2938, 2842, 1578, 1461, 1455, 1393, 1286, 1241, 1275, 1125, 1154, 1093, 1015, 861, 852, 794, 782, 765.

I) Preparation of starting materials

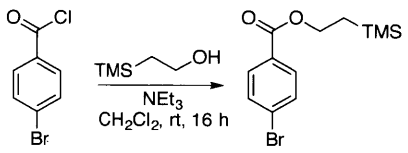

S15

An oven-dried 100 mL round-bottomed flask equipped with a stir bar was charged with 4-bromobenzoyl chloride (1.04 g, 4.74 mmol, 1.00 equiv). The flask was capped with a septum, evacuated and backfilled with argon (this process was repeated a total three times). Anhydrous CH_2Cl_2 (50 mL) was added, followed by triethylamine (0.75 mL, 5.38 mmol, 1.10 equiv) via syringe, and then the reaction mixture was stirred continuously. Then, 2-(trimethylsilyl)ethan-1-

ol (0.59 g, 4.99 mmol, 1.05 equiv) was added dropwise and the solution was stirred for 16 h at rt. Then, the reaction mixture was transferred to a separatory funnel. The reaction vessel was rinsed with CH_2Cl_2 (50 mL) and transferred into the separatory funnel. The organic layer was washed with deionized water (25 mL), followed by brine (2 x 25 mL). The organic fractions were combined, dried over $MgSO_4$, filtered, and concentrated *in vacuo*. The residue was purified by silica gel chromatography, eluting with 10% EtOAc/hexanes, to give the desired product as an off-white, greasy solid (1.20 g, 84%). mp: 33–34 °C. **^{1}H NMR** (400 MHz, $CDCl_3$): δ 7.89 (d, J = 8.5 Hz, 2H), 7.56 (d, J = 8.5 Hz, 2H), 4.47 – 4.31 (m, 2H), 1.25 – 1.04 (m, 2H), 0.08 (s, 9H) ppm. **^{13}C NMR** (100 MHz, $CDCl_3$) δ 166.1, 131.8, 131.2, 129.7, 127.9, 63.7, 17.5, –1.3 ppm. **IR** (neat, cm^{-1}): 2954, 2899, 1709, 1589, 1484, 1399, 1275, 1247, 1175, 1116, 1103, 1010, 935, 861, 851, 829, 755, 692, 681, 626, 608. **Anal. Calcd. for $C_{12}H_{17}BrO_2Si$**: C, 47.84; H, 5.69, Found: C, 48.06; H, 5.68.

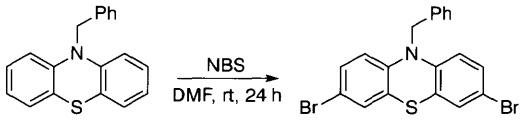

S16

An oven-dried 100 mL round-bottomed flask equipped with a stir bar was charged with 10-benzyl-10H-phenothiazine[30] (1.61 g, 5.57 mmol, 1.00 equiv). The flask was capped with a septum, evacuated and backfilled with argon (this process was repeated a total of three times). Anhydrous DMF (50 mL) was added via syringe and the reaction mixture was stirred. NBS (2.18 g, 12.3 mmol, 2.20 equiv) was added in three portions, twenty min apart, at rt by quickly removing the septum under a flow of argon. The reaction mixture was stirred at rt for 24 h. Then, the reaction mixture was transferred to a separatory funnel and diluted with Et_2O (150 mL). The reaction vessel was rinsed with Et_2O (150 mL) and transferred into the separatory funnel. The organic phase was washed with saturated sodium thiosulfate (1 x 10 mL), deionized water (3 x 100 mL), and brine (1 x 100 mL). The organic fractions were combined, dried over $MgSO_4$, and concentrated *in vacuo*. The residue was purified by silica gel chromatography (eluting with 0% Et_2O/pentane to 8% Et_2O/pentane). The fractions containing the product were combined, concentrated in vacuo, and the product further purified by recrystallization induced by adding boiling EtOAc/MeOH and storing the solution overnight at 0 °C. The yellow crystals that had formed were collected by vacuum filtration to yield the desired product (1.48 g, 60%). mp: 141–

142 °C. **^{1}H NMR** (500 MHz, $CDCl_3$): δ 7.39 – 7.32 (m, 2H), 7.31 – 7.22 (m, 3H), 7.18 (d, J = 2.3 Hz, 2H), 7.07 (dd, J = 8.7, 2.3 Hz, 2H), 6.47 (d, J = 8.7 Hz, 2H), 5.01 (s, 2H) ppm. **^{13}C NMR** (100 MHz, $CDCl_3$) δ 143.5, 135.7, 130.3, 129.3, 129.1, 127.5, 126.6, 124.8, 116.8, 115.1, 52.9 ppm. **IR** (neat, cm^{-1}): 3033, 2928, 2878, 1582, 1456, 1389, 1345, 1252, 1210, 1115, 863, 802, 793, 751, 723, 693, 662. **Anal. Calcd. for $C_{19}H_{13}Br_2NS$**: C, 51.03; H, 2.93, Found: C, 51.09; H, 3.01.

J) Control experiments without Pd for substrates **4b** and **4d**

Procedure for control experiment of 4b: General procedure E was followed with the following modification: no Pd source was added. A mixture of 3-chloro-1-trityl-1*H*-indazole (**S10**, 396 mg, 1.00 mmol, 1.00 equiv), KOH (196 mg, 3.49 mmol, 3.49 equiv), and water (0.36 mL, 20.00 mmol, 20.00 equiv) was stirred in 1,4-dioxane for 18 h. After cooling the reaction mixture to rt, the reaction tube was uncapped, 1,3,5-trimethoxybezene (174.5 mg, 1.04 mmol, 1 equiv) was added as an internal standard, and the mixture diluted with EtOAc and 1.0 M HCl (5 mL). The reaction mixture was capped, then shaken until all the solids dissolved. The mixture was transferred to a separatory funnel and the aqueous layer neutralized with an aqueous saturated sodium bicarbonate solution (5 mL). The aqueous layer was extracted with EtOAc (2 x 5 mL) and the organic fractions were combined, dried over $MgSO_4$, filtered, and concentrated *in vacuo*. The crude material was dissolved in CD_2Cl_2, transferred to an NMR tube, and analyzed by ^{1}H NMR spectroscopy. Analysis indicates 0% yield to **4b** and 0% conversion of the starting material. This result was confirmed by LC/MS.

Procedure for control experiments of 4d: General procedure F was followed with the following modification: no Pd source was added. A mixture of 4-bromoisoquinoline (**S14**, 204 mg, 0.980 mmol, 1.00 equiv), NaO*t*-Bu (107 mg, 1.11 mmol, 1.10 equiv), and MeOH (0.20 mL, 4.94 mmol, 4.94 equiv) was stirred in 1,4-dioxane for 18 h. After cooling the reaction mixture to rt, the reaction tube was uncapped, 1,3,5-trimethoxybezene (170.1 mg, 1.01 mmol, 1 equiv) was added as an internal standard, and the mixture diluted with EtOAc and filtered through a pad of celite. The filtrate was concentrated *in vacuo*. The crude material was dissolved in DMSO-d_6, transferred into an NMR tube, and analyzed by ^{1}H NMR spectroscopy. Analysis indicates 0% yield to **4d** and <15% conversion of the starting material. This result was confirmed by LC/MS.

Trt
N
N
Cl
S10
7.65
7.63
7.28
7.12
7.05
6.52
6.50
6.07
5.32
3.75
OMe
MeO
OMe
OMe
MeO
OMe
0.92
13.37
1.05
0.94
0.97
3.00
9.70
.0 10.5 10.0 9.5 9.0 8.5 8.0 7.5 7.0 6.5 6.0 5.5 5.0 4.5 4.0 3.5 3.0 2.5 2.0 1.5 1.0 0.5 0.0 -0.5 -1
(ppm)

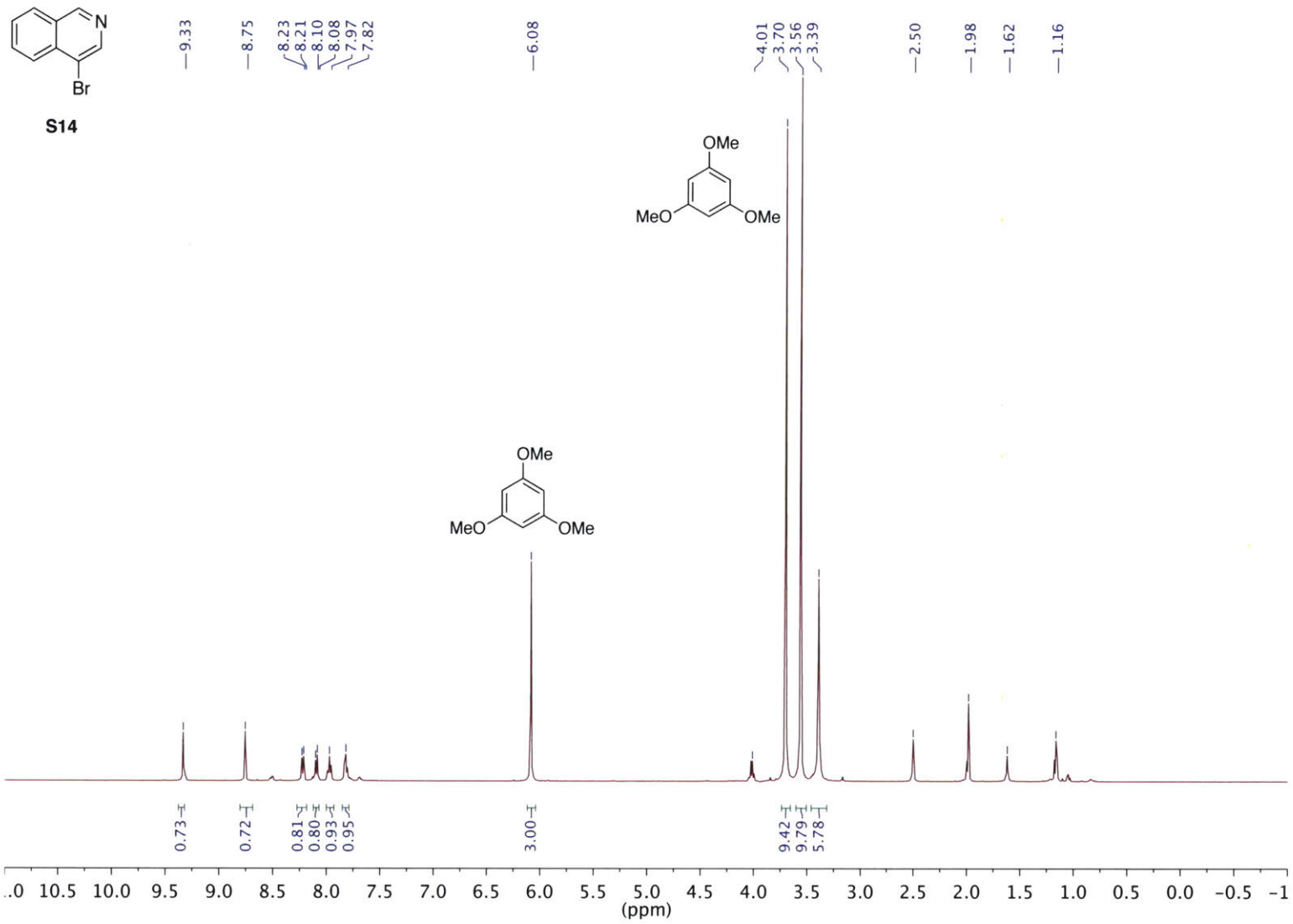
N
Br
S14
9.33
8.75
8.23
8.21
8.10
8.08
7.97
7.82
6.08
4.01
3.70
3.56
3.39
2.50
1.98
1.62
1.16
OMe
MeO
OMe
OMe
MeO
OMe
0.73
0.72
0.81
0.80
0.93
0.95
3.00
9.42
9.79
5.78
(ppm)

2.5. References and Notes

1. Han, C.; Buchwald, S.L. Negishi Coupling of Secondary Alkylzinc Halides with Aryl Bromides and Chlorides. *J. Am. Chem. Soc.* **2009**, *131*, 7532–7533. (b) Yang, Y.; Oldenhuis, N.J.; Buchwald, S.L. Mild and General Conditions for Negishi Cross-Coupling Enabled by the Use of Palladacycle Precatalysts. *Angew. Chem. Int. Ed.* **2013**, *52*, 615–619. (c) Martin, R.; Buchwald, S.L. Palladium-Catalyzed Suzuki–Miyaura Cross-Coupling Reactions Employing Dialkylbiaryl Phosphine Ligands. *Acc. Chem. Res.* **2008**, *41*, 1461–1473.

2. Ruiz-Castillo, P.; Buchwald, S.L. Applications of Palladium-Catalyzed C–N Cross-Coupling Reactions. *Chem. Rev.* **2016**, *116*, 12564–12649.

3. (a) Cheung, C.W.; Buchwald, S.L. Mild and General Palladium-Catalyzed Synthesis of Methyl Aryl Ethers Enabled by the Use of a Palladacycle Precatalyst. *Org. Lett.* **2013**, *15*, 3998–4001. (b) Cheung, C.W.; Buchwald, S.L. Palladium-Catalyzed Hydroxylation of Aryl and Heteroaryl Halides Enabled by the Use of a Palladacycle Precatalyst. *J. Org. Chem.* **2014**, *79*, 5351–5358. (c) Wu, X.; Fors, B.P.; Buchwald, S.L. A Single Phosphine Ligand Allows Palladium-Catalyzed Intermolecular C–O Bond Formation with Secondary and Primary Alcohols. *Angew. Chem. Int. Ed.* **2011**, *50*, 9943–9947.

4. (a) Sather, A.C.; Lee, H.G.; De La Rosa, V.Y.; Yang, Y.; Müller, P.; Buchwald, S.L. A Fluorinated Ligand Enables Room-Temperature and Regioselective Pd-Catalyzed Fluorination of Aryl Triflates and Bromides. *J. Am. Chem. Soc.* **2015**, *137*, 13433–13438. (b) Sather, A.C.; Buchwald, S.L. The Evolution of Pd^{0}/Pd^{II}-Catalyzed Aromatic Fluorination. *Acc. Chem. Res.* **2016**, *49*, 2146–2157. (c) Watson, D.A.; Su, M.; Teverovskiy, G.; Zhang, Y.; García-Fortanet, J.; Kinzel, T.; Buchwald, S.L. Formation of ArF from LPdAr(F): Catalytic Conversion of Aryl Triflates to Aryl Fluorides. *Science*, **2009**, *325*, 1661–1664. (d) Milner, P.J.; Kinzel, T.; Zhang, Y.; Buchwald, S.L. Studying Regioisomer Formation in the Pd-Catalyzed Fluorination of Aryl Triflates by Deuterium Labeling. *J. Am. Chem. Soc.* **2014**, *136*, 15757–15766.

5. (a) Biscoe, M.R.; Fors, B.P.; Buchwald, S. L. A New Class of Easily Activated Palladium Precatalysts for Facile C–N Cross-Coupling Reactions and the Low Temperature Oxidative Addition of Aryl Chlorides. *J. Am. Chem. Soc.* **2008**, *130*, 6686–6687. (b) Bruno, N.C.; Tudge, M.C.; Buchwald, S.L. Design and preparation of new palladium precatalysts for C–C and C–N cross-coupling reactions. *Chem. Sci.* **2013**, *4*, 916–920. (c) Bruno, N.C.; Buchwald, S.L. Synthesis and Application of Palladium Precatalysts that Accommodate Extremely Bulky Di-*tert*-butylphosphino Biaryl Ligands. *Org. Lett.* **2013**, *15*, 2876–2879. (d) Bruno, N.C.; Niljianskul, N.; Buchwald, S.L. *N*-Substituted 2-Aminobiphenylpalladium Methanesulfonate Precatalysts and Their Use in C–C and C–N Cross-Couplings. *J. Org. Chem.* **2014**, *79*, 4161–4166.

6. For a class of precatalysts based on π-allyl and indenyl complexes, which have been shown to accommodate very bulky biarylphosphines, see: (a) DeAngelis, A.J.; Gildner, P.G.; Chow, R.; Colacot, T.J. Generating Active "L-Pd(0)" via Neutral or Cationic π-Allylpalladium Complexes Featuring Biaryl/Bipyrazolylphosphines: Synthetic, Mechanistic, and Structure–Activity Studies in Challenging Cross-Coupling Reactions. *J.*

Org. Chem. **2015**, *80*, 6794–6813. (b) Melvin, P.R.; Nova, A.; Balcells, D.; Dai, W.; Hazari, N; Hruszkewycz, D.P.; Shah, H.P.; Tudge, M.T. Design of a Versatile and Improved Precatalyst Scaffold for Palladium-Catalyzed Cross-Coupling: (η^3-1-^{t}Bu-indenyl)$_2$(μ-Cl)$_2$Pd$_2$. *ACS Catal.* **2015**, *5*, 3680–3668.

7. (a) Lundgren, R.J.; Stradiotto, M. Addressing Challenges in Palladium-Catalyzed Cross-Coupling Reactions Through Ligand Design. *Chem. Eur. J.* **2012**, *18*, 9758–9759. (b) Bariwal, J.; Van der Eycken, E.V. C–N bond forming cross-coupling reactions: an overview. *Chem. Soc. Rev.* **2013**, *42*, 9283–9303. (c) DeAngelis, A.; Colacot, T.J. In *New Trends in Cross-Coupling: Theory and Applications;* Colacot, T.J., Ed.; RSC: Cambridge, U.K., 2015, pp. 20–90. (d) Seechurn, C. C. C.; Li, H.; Colacot, T.J. In *New Trends in Cross-coupling: Theory and Applications;* Colacot, T.J., Ed.; RSC: Cambridge, U.K., 2015, pp. 91–138.

8. Park, N.H.; Vinogradova, E.V.; Surry, D.S.; Buchwald, S.L. Design of New Ligands for the Palladium-Catalyzed Arylation of α-Branched Secondary Amines. *Angew. Chem. Int. Ed.* **2015**, *54*, 8259–8262.

9. Lee, H.G.; Milner, P.J.; Colvin, M.T.; Andreas, L.; Buchwald, S.L. Structure and reactivity of [(L·Pd)$_n$·(1,5-cyclooctadiene)] (n = 1–2) complexes bearing biaryl phosphine ligands. *Inorg. Chim. Acta* **2014**, *422*, 188–192.

10. For a capsule-based strategy to enable convenient handling of [L–Pd]$_2$(COD) complexes in combination with hygroscopic bases, see: Sather, A.C.; Lee, H.G.; Colombe, J.R.; Zhang, A.; Buchwald, S.L. Dosage delivery of sensitive reagents enables glove-box-free synthesis. *Nature* **2015**, *524*, 208–211.

11. In fact, OACs have found use in the context of mechanistic experiments, see: (a) Moser, W.R.; Wang, A.W.; Kildahl, N.K. Mechanistic studies of the palladium-catalyzed reaction of methanol with bromobenzene and carbon monoxide to produce methyl benzoate. 1. Stoichiometric study. *J. Am. Chem. Soc.* **1988**, *110*, 2816–2820. (b) Wallow, T.I.; Goodson, F.E.; Novak, B.M. New Methods for the Synthesis of ArPdL$_2$I (L = Tertiary Phosphine) Complexes. *Organometallics*, **1996,** *15*, 3708–3716. (c) Verbeeck, S.; Meyers, C.; Franck, P.; Jutand, A.; Maes, B.U.W. Dual Effect of Halides in the Stille Reaction: In Situ Halide Metathesis and Catalyst Stabilization. *Chem. Eur. J.* **2010**, *16*, 12831–12837.

12. For examples of a complex with formula (Ph$_3$P)$_2$Pd(Ph)I catalyzing a C–C coupling, see: (a) Fauvarque, J.F.; Jutand, A. Catalysis of the arylation of the reformatsky reagent by palladium or nickel complexes. Synthesis of aryl acid esters. *J. Organomet. Chem.* **1979**, *177*, 273–281. (b) Sekiya, A.; Ishikawa, N. The cross-coupling of aryl halides with grignard reagents catalyzed by iodo(phenyl)bis(triphenylphosphine)palladium(II). *J. Organomet. Chem.* ***1976***, *118*, 349–354.

13. Complex **P1** slowly reacts in solution with oxygen, but is stable in the solid state.

14. Formation of regioisomeric products occurs with certain types of substrates in the Pd-catalyzed fluorination reaction.[4d]

15. King, S.M.; Buchwald, S.L. Development of a Method for the *N*-Arylation of Amino Acid Esters with Aryl Triflates. *Org. Lett.* **2016**, *18*, 4128–4131.

16. Nara, H.; Sato, K.; Kaieda, A.; Oki, H.; Kuno, H.; Santou, T.; Kanzaki, N.; Terauchi, J.; Uchikawa, O.; Kori, M. Design, synthesis, and biological activity of novel, potent, and highly selective fused pyrimidine-2-carboxamide-4-one-based matrix metalloproteinase (MMP)-13 zinc-binding inhibitors. *Bioorg. Med. Chem.* **2016**, *24*, 6149–6165.

17. Dowd, C.S.; Davis-Herrick, K.; Egan, C.; DuPre, A.; Smith, C.; Teitler, M.; Glennon, R.A. 1-[4-(3-Phenylalkyl)phenyl]-2-aminopropanes as 5-HT2A Partial Agonists. *J. Med. Chem.* **2000**, *43*, 3074–3084.

18. Rao, Y. J.; Goud, Y.E.; Hemasri, Y.; Jain, N.; Gabriella, S. Synthesis and antiproliferative activity of 6,7-aryl/hetaryl coumarins. *Russ. J. Gen. Chem.* **2016**, *86*, 184–189.

19. Quandt, G.; Höfner, G.; Pabel, J.; Dine, J.; Eder, M; Wanner, K.T. First Photoswitchable Neurotransmitter Transporter Inhibitor: Light-Induced Control of γ-Aminobutyric Acid Transporter 1 (GAT1) Activity in Mouse Brain. *J. Med. Chem.* **2014**, *57*, 6809–6821.

20. Goossen, L. J.; Linder, C.; Rodríguez, N.; Lange, P. Biaryl and Aryl Ketone Synthesis via Pd-Catalyzed Decarboxylative Coupling of Carboxylate Salts with Aryl Triflates. *Chem. Eur. J.* **2009**, *15*, 9336–9349.

21. Krause, L.; Herbst-Irmer, R.; Sheldrick, G.M.; Stalke, D.J. Comparison of silver and molybdenum microfocus X-ray sources for single-crystal structure determination. *J. Appl. Cryst.* **2015**, *48*, 3–10.

22. Sheldrick, G.M. *SHELXT* – Integrated space–group and crystal–structure determination. *Acta Cryst.* **2015**, *A71*, 3–8.

23. Sheldrick, G.M. Crystal structure refinement with *SHELXL*. *Acta Cryst.* **2015**, *C71*, 3–8.

24. Müller, P. Practical suggestions for better crystal structures. *Crystallography Reviews*, **2009**, *15*, 57–83.

25. van der Sluis, P.; Spek, A.L. BYPASS: an effective method for the refinement of crystal structures containing disordered solvent regions. *Acta Cryst.* **1990**, *A46*, 194–201.

26. Spek, A.L. Structure validation in chemical crystallography. *Acta Cryst.* **2009**, *D65*, 148–155.

27. Li, P.; Wang, L.; Wang, M.; You, F. Gold(I) Iodide Catalyzed Sonogashira Reactions. *Eur. J. Org. Chem.* **2008**, *35*, 5946–5951.

28. Brindis, M.; Butini, S.; Franceschini, S.; Brogi, S.; Trotta, F.; Ros, S.; Cagnotto, A.; Salmona, M.; Casagni, A.; Andreassi, M.; Saponara, S.; Gorelli, B.; Weikop, P.; Mikkelsen, J.D.; Scheel-Kruger, J.; Sandager-Nielsen, K.; Novellino, E.; Campiani, G.; Gemma, S. Targeting Dopamine D_3 and Serotonin 5-HT_{1A} and 5-HT_{2A} Receptors for Developing Effective Antipsychotics: Synthesis, Biological Characterization, and Behavioral Studies. *J. Med. Chem.* **2014**, *57*, 9578–9597.

29. Liu, X.-G.; Zhang, S.-S.; Jiang, C.-Y.; Wu, J.-Q.; Li, Q.; Wang, H. Cp*Co(III)-Catalyzed Annulations of 2-Alkenylphenols with CO: Mild Access to Coumarin Derivatives. *Org. Lett.* **2015**, *17*, 5404–5407.

30. Zhao, S.; Kang, J.; Du, Y.; Kang, J.; Zhao, X.; Xu, Y.; Chen, R.; Wang, Q.; Shi, X. An Efficient Ultrasound-Assisted Synthesis of *N*-Alkyl Derivatives of Carbazole, Indole, and Phenothiazine. *J. Heterocyclic Chem.* **2014**, *51*, 683–689.

2.6. NMR Spectra

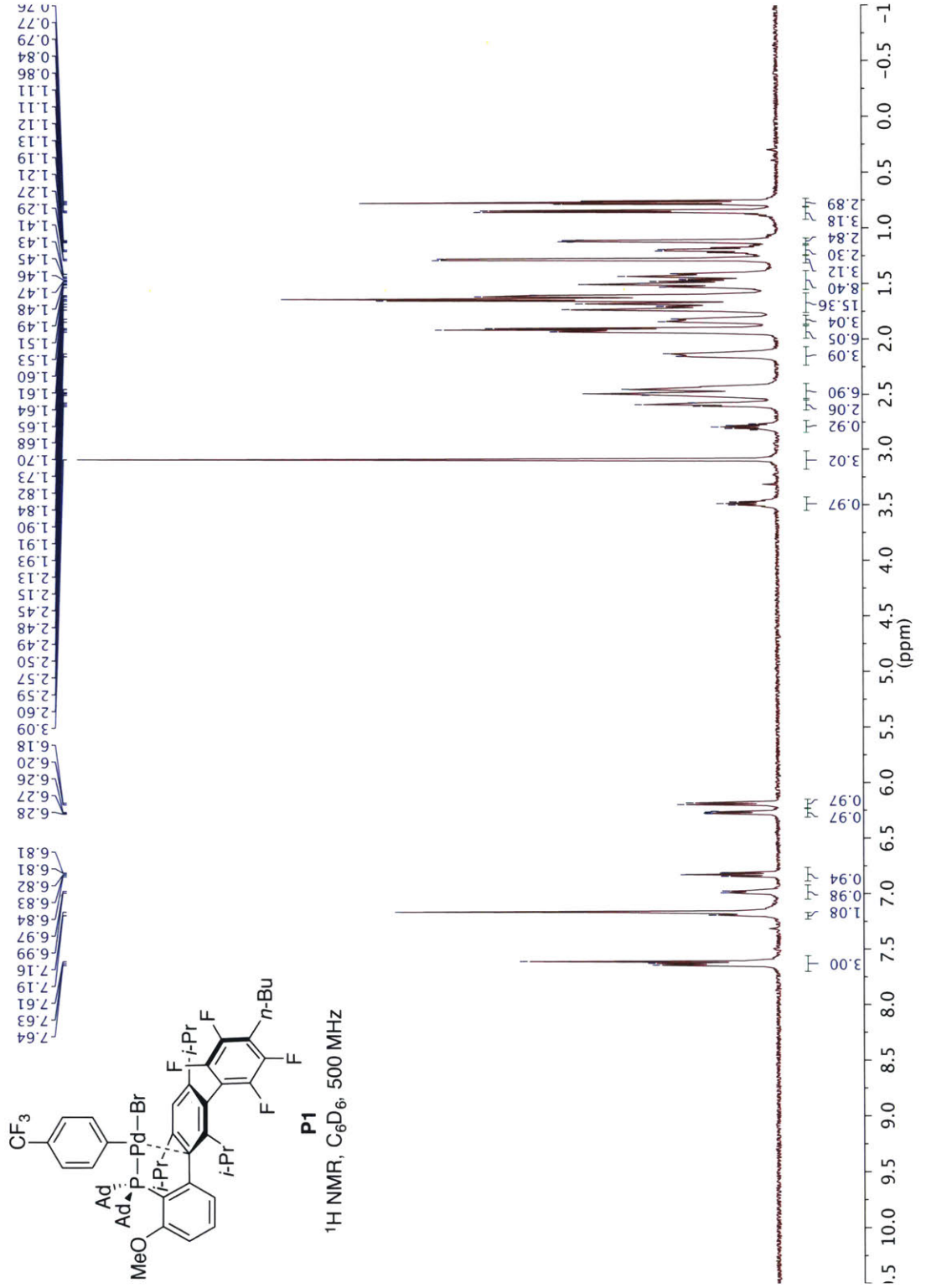

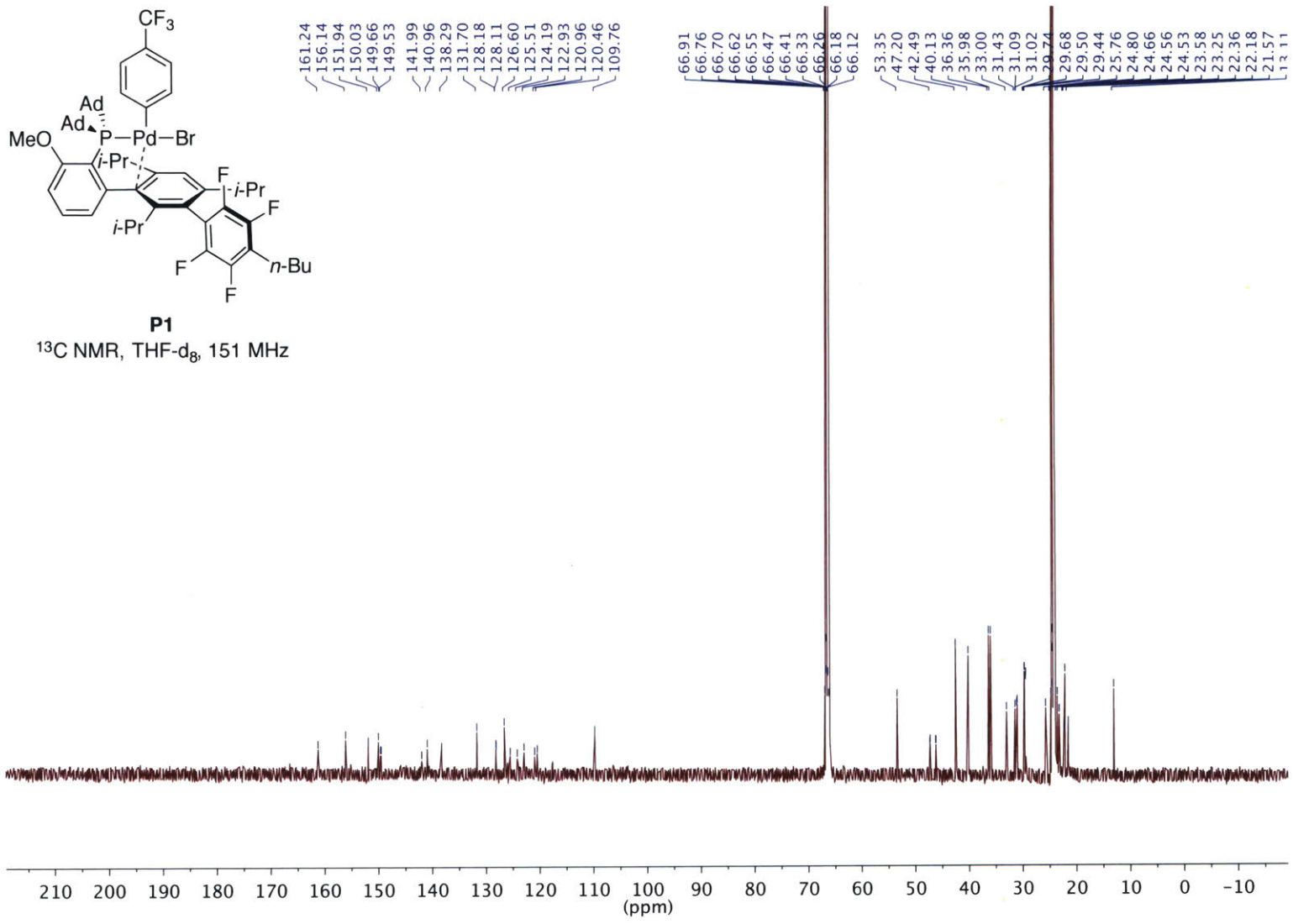

P1

^{13}C NMR, THF-d_8, 151 MHz

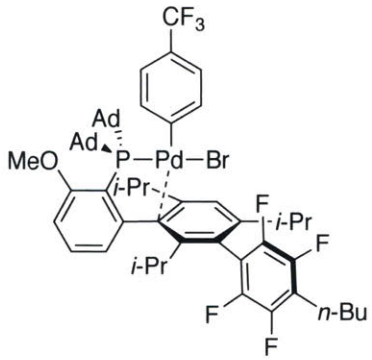

P1

^{31}P NMR, C_6D_6, 203 MHz

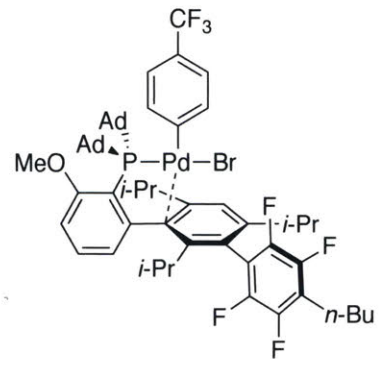

P1

^{19}F NMR, C_6D_6, 471 MHz

CF3
Ad
Ad
P—Pd ⊕
TfO⊖
MeO
i-Pr
i-Pr
F
i-Pr
F
F
F
n-Bu
P2
1H NMR, C6D6, 500 MHz
7.68
7.63
7.61
7.60
7.16
7.11
7.10
7.00
6.99
3.56
3.02
3.00
2.64
2.62
2.61
2.58
2.56
2.55
2.32
2.30
2.29
2.20
2.09
1.96
1.92
1.86
1.85
1.77
1.68
1.66
1.59
1.56
1.54
1.52
1.46
1.44
1.42
1.41
1.18
1.17
1.15
1.14
1.11
1.09
1.08
1.06
1.05
1.00
0.98
0.78
0.76
0.75
0.55
0.54
2.97
1.00
2.24
2.00
3.01
0.97
3.06
1.04
6.04
3.10
6.33
3.00
2.97
3.00
6.02
5.01
2.13
8.89
2.96
2.88
2.84
10.0
9.5
9.0
8.5
8.0
7.5
7.0
6.5
6.0
5.5
5.0
4.5
4.0
3.5
3.0
2.5
2.0
1.5
1.0
0.5
0.0
-0.5
-1
(ppm)

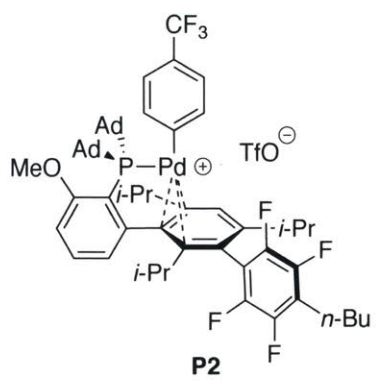

P2

^{13}C NMR, C_6D_6, 126 MHz

P2

^{31}P NMR, C_6D_6, 203 MHz

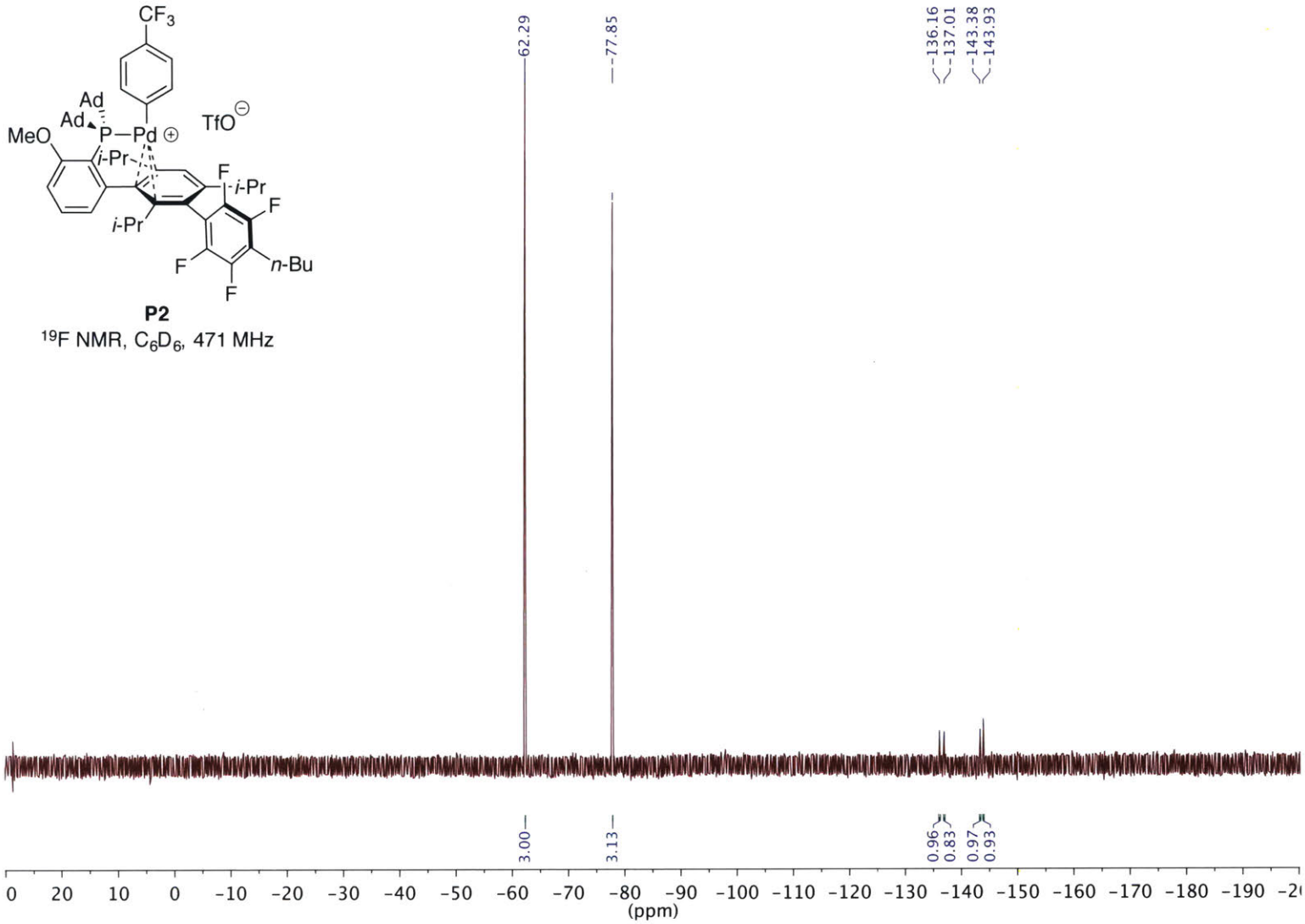

P2

^{19}F NMR, C_6D_6, 471 MHz

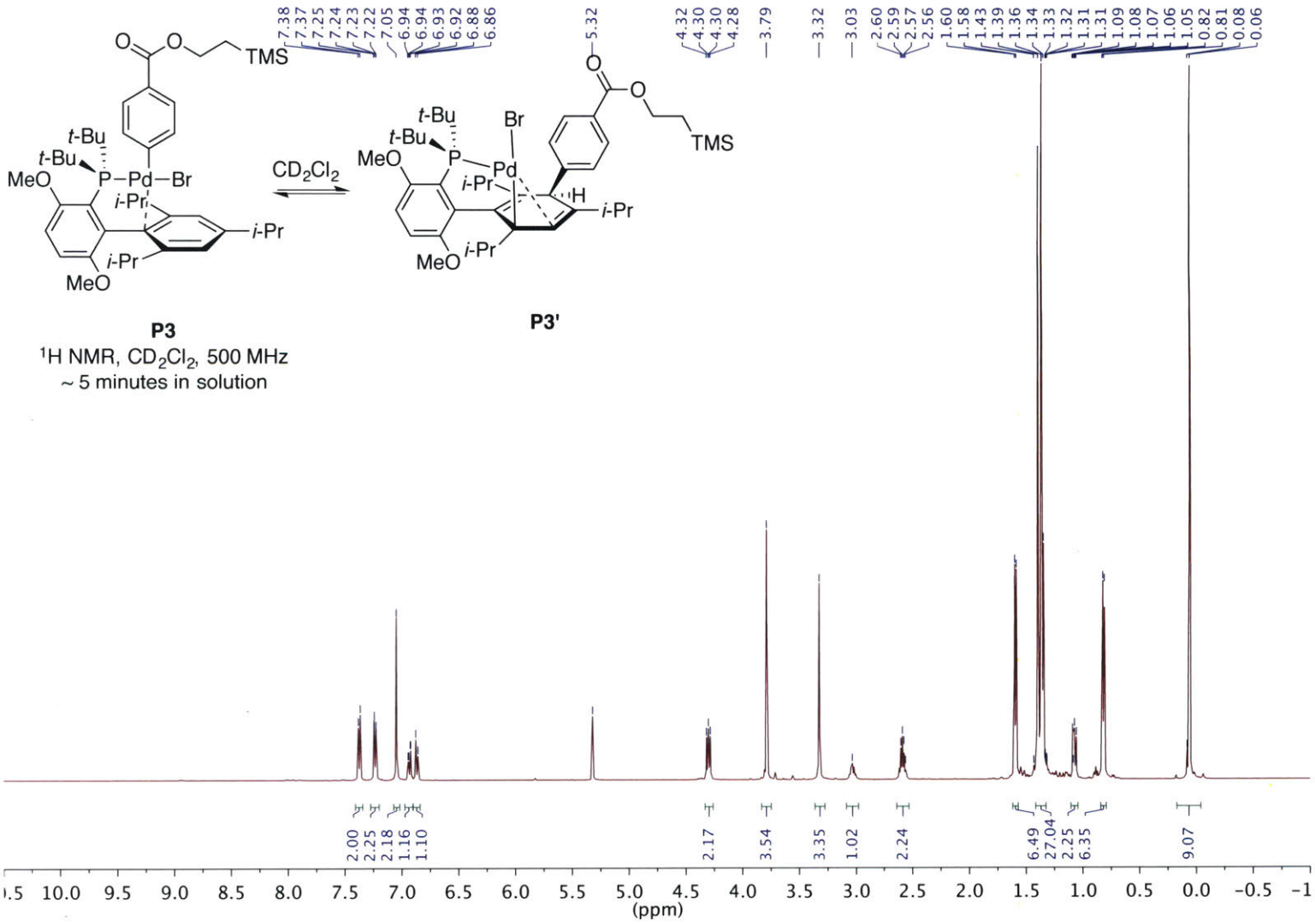
P3
P3'
^{1}H NMR, CD_2Cl_2, 500 MHz
~ 5 minutes in solution
CD_2Cl_2
(ppm)

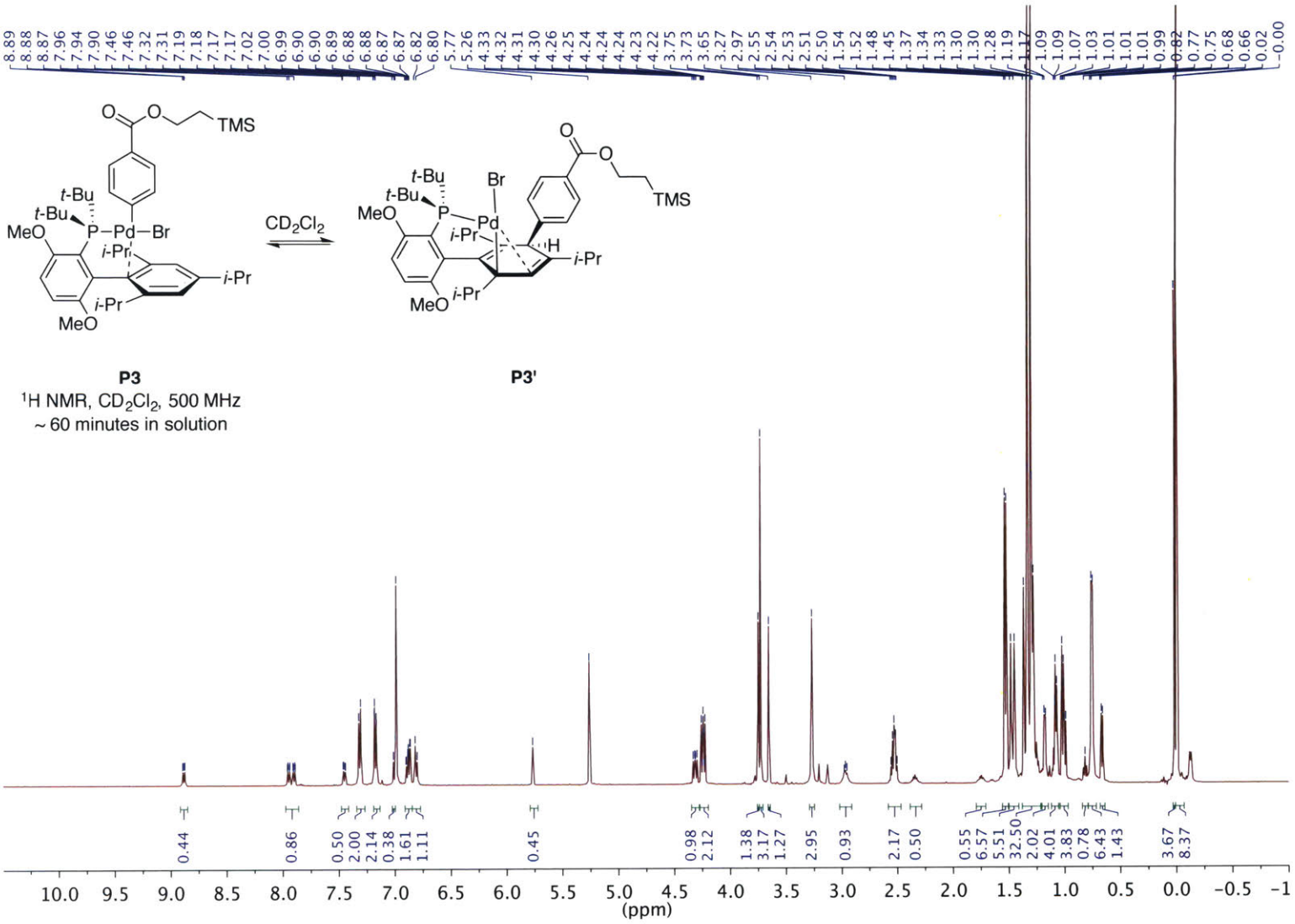
TMS
t-Bu
t-Bu
MeO
P–Pd–Br
i-Pr
i-Pr
i-Pr
i-Pr
MeO
CD2Cl2
Br
Pd
H
P3
P3'
1H NMR, CD2Cl2, 500 MHz
~ 60 minutes in solution
(ppm)

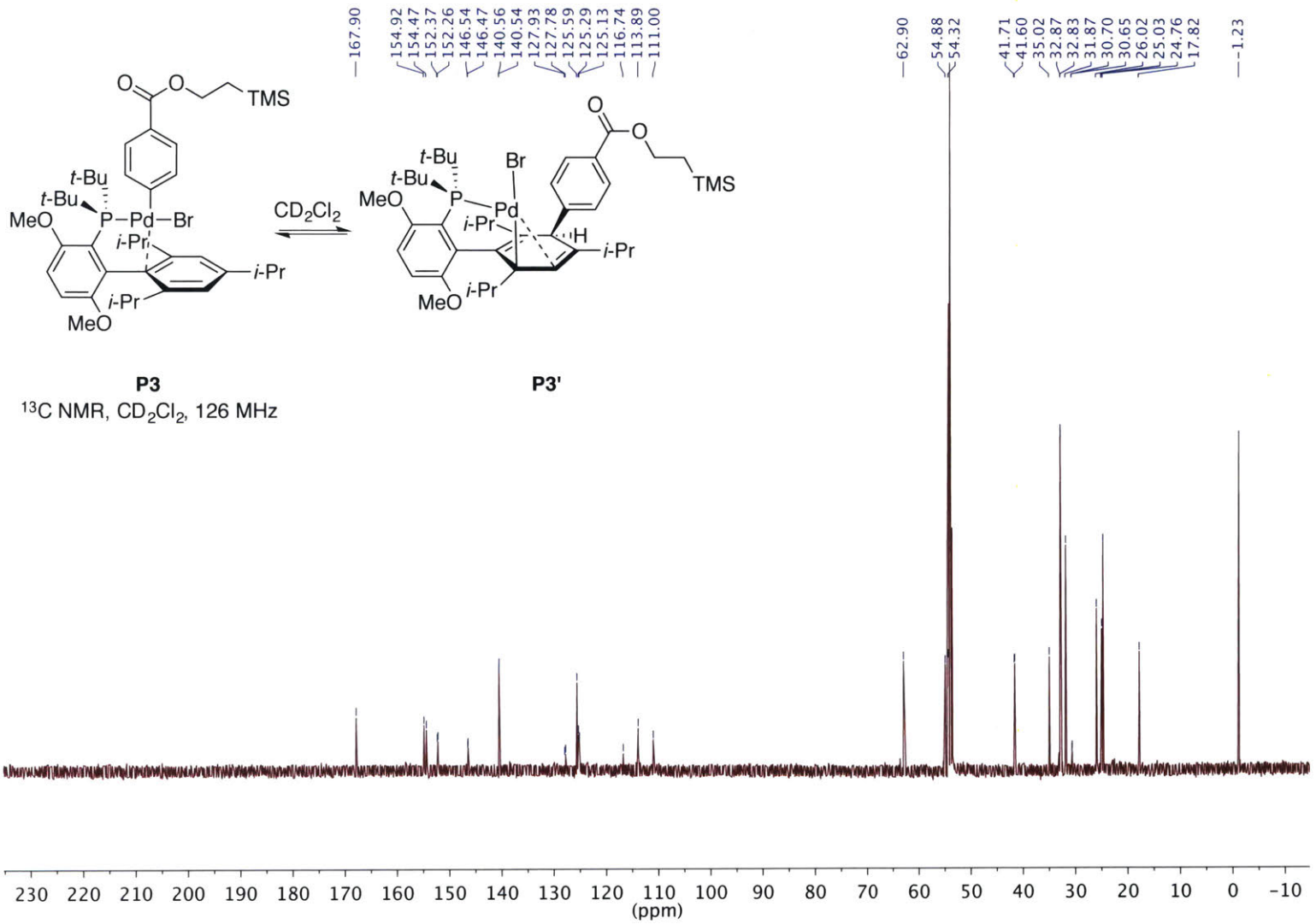

P3 **P3'**

^{13}C NMR, CD_2Cl_2, 126 MHz

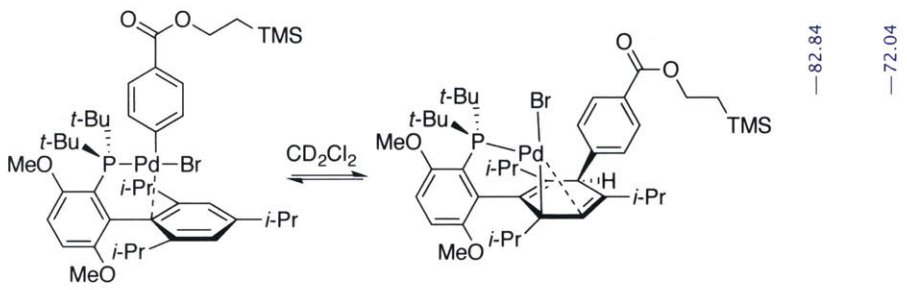

P3 **P3'**

^{31}P NMR, CD_2Cl_2, 203 MHz

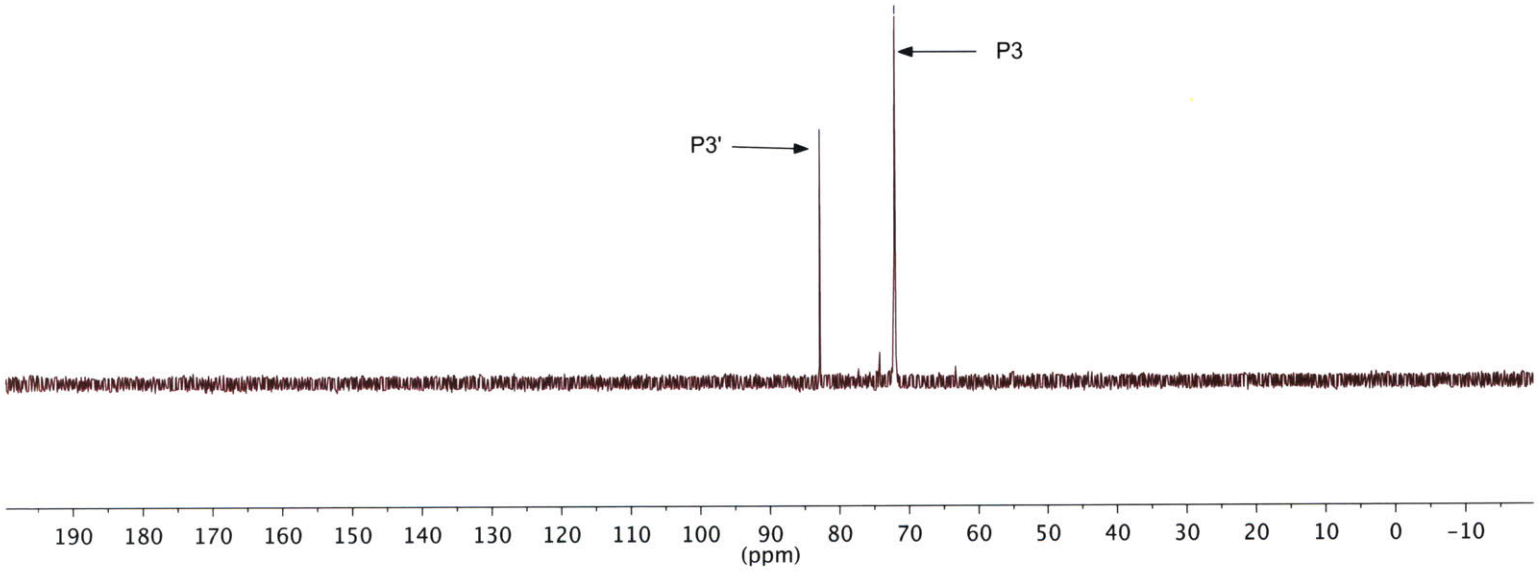

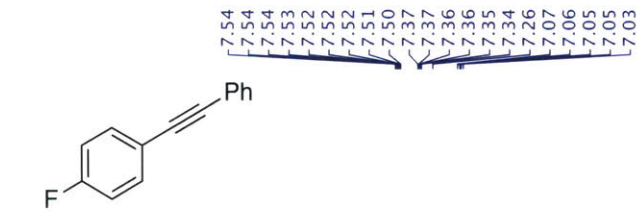

2a

^{1}H NMR, $CDCl_3$, 400 MHz

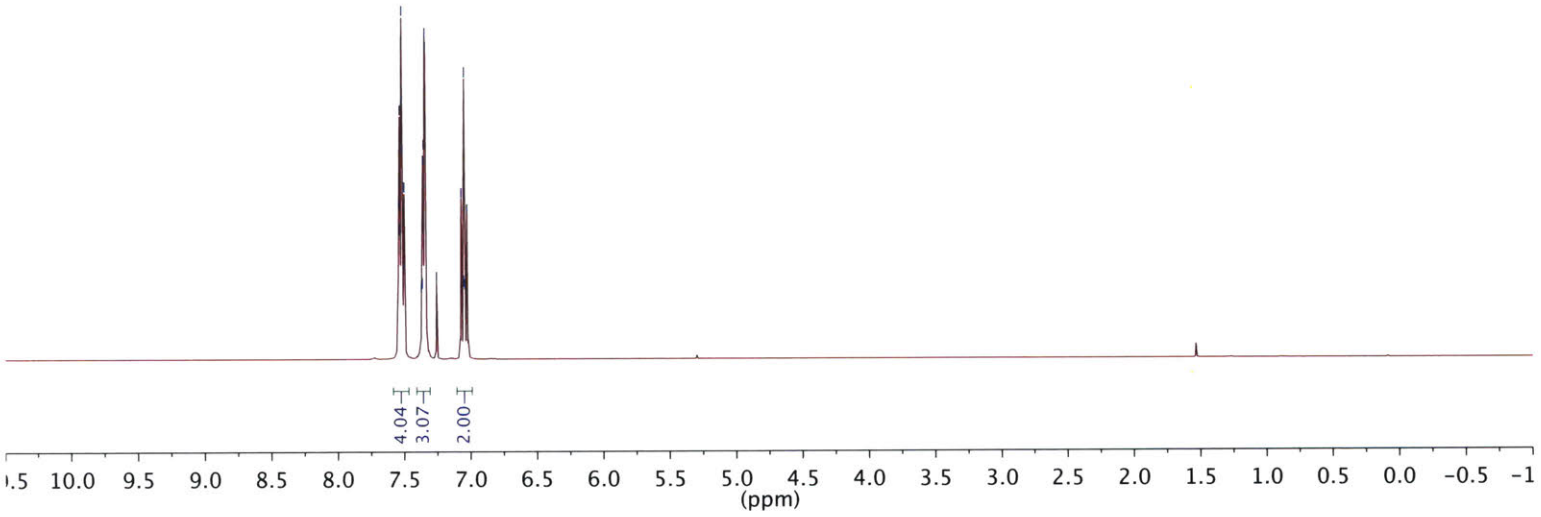

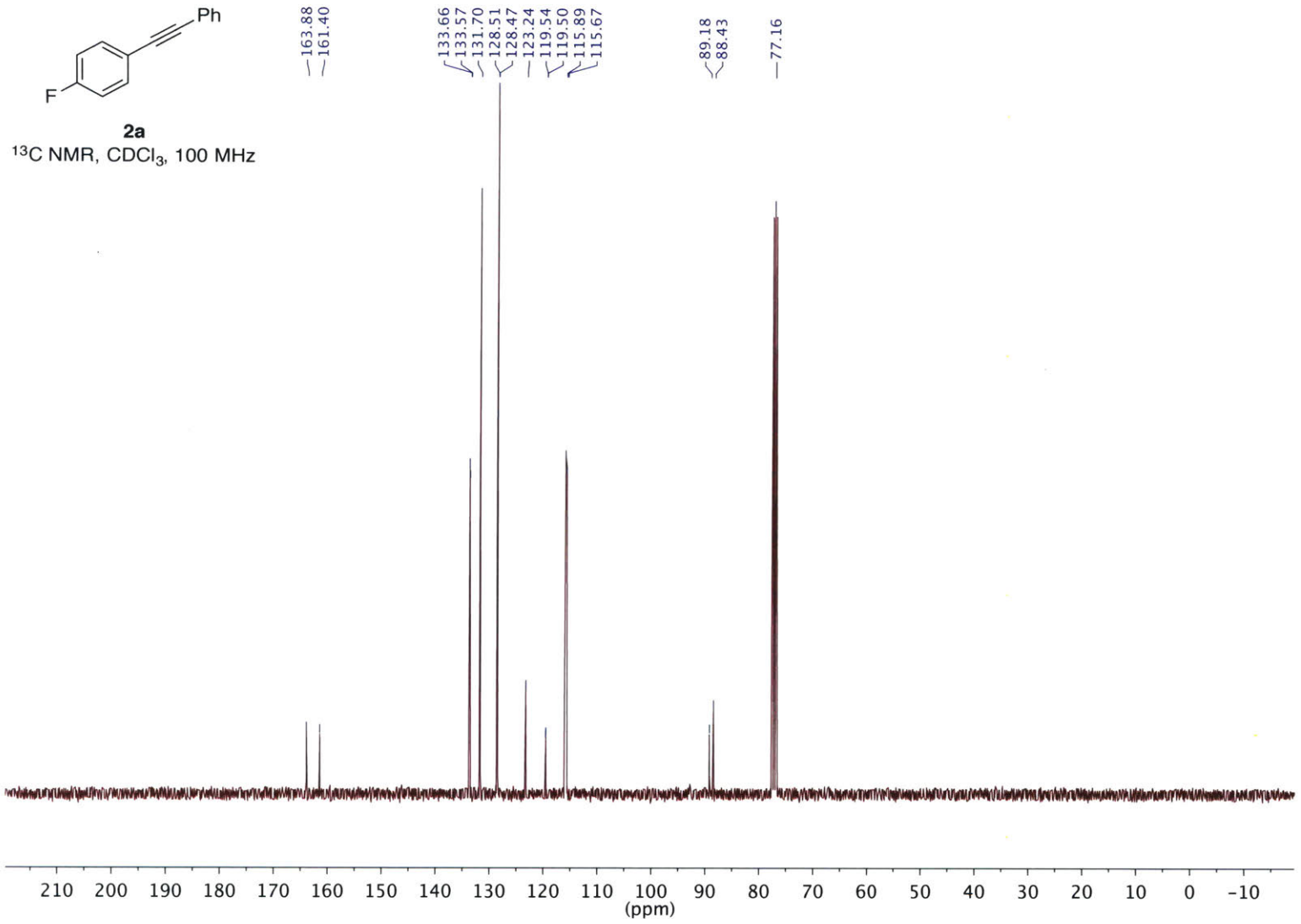
Ph
F
2a
13C NMR, CDCl3, 100 MHz
163.88
161.40
133.66
133.57
131.70
128.51
128.47
123.24
119.54
119.50
115.89
115.67
89.18
88.43
77.16
210 200 190 180 170 160 150 140 130 120 110 100 90 80 70 60 50 40 30 20 10 0 -10
(ppm)

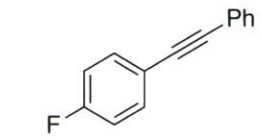

2a

^{19}F NMR, $CDCl_3$, 471 MHz

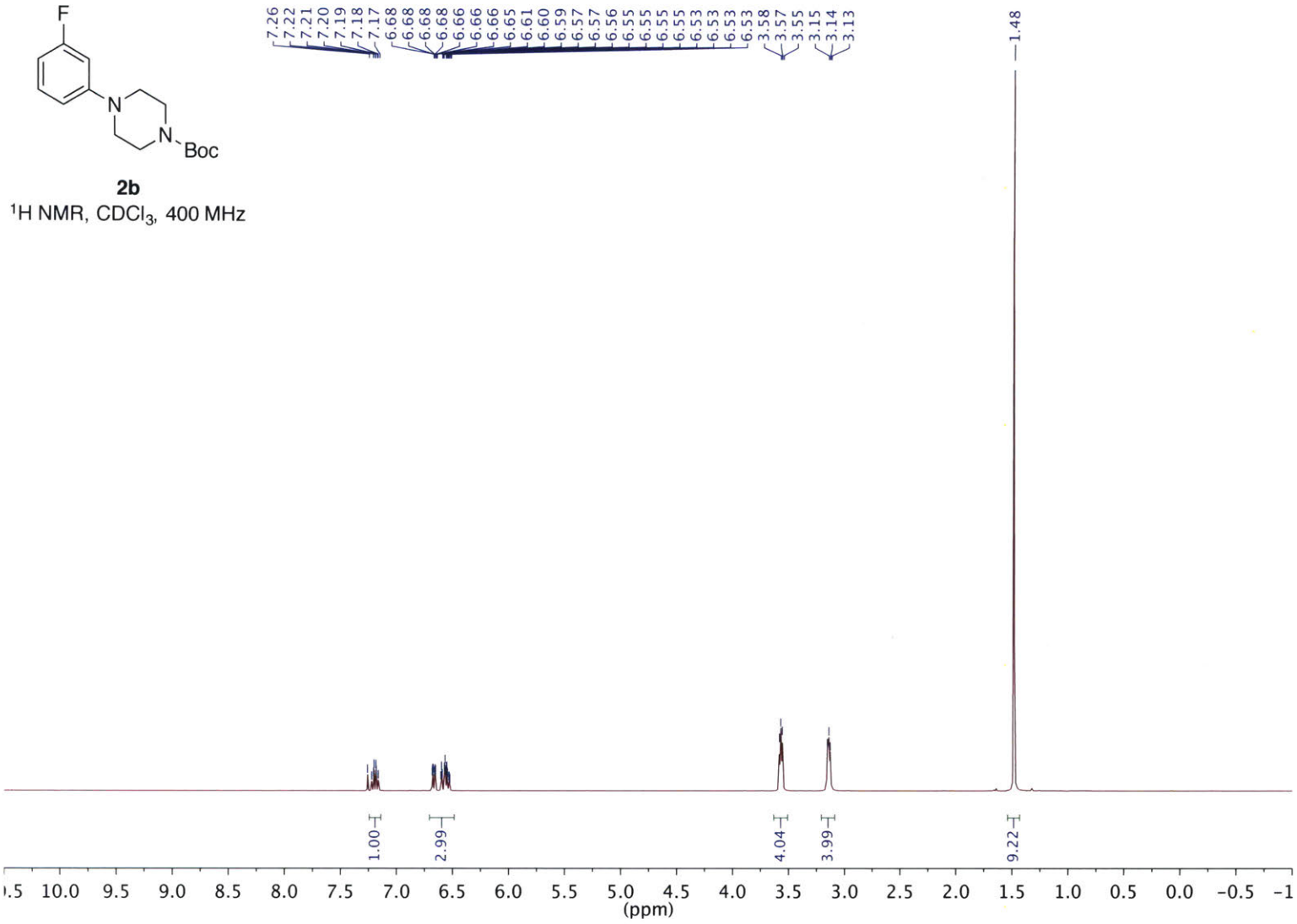
F
N
N
Boc
2b
1H NMR, CDCl3, 400 MHz
7.26
7.22
7.21
7.20
7.19
7.18
7.17
6.68
6.68
6.68
6.66
6.66
6.66
6.65
6.61
6.60
6.59
6.57
6.57
6.56
6.55
6.55
6.55
6.55
6.53
6.53
6.53
3.58
3.57
3.55
3.15
3.14
3.13
1.48
1.00
2.99
4.04
3.99
9.22
(ppm)

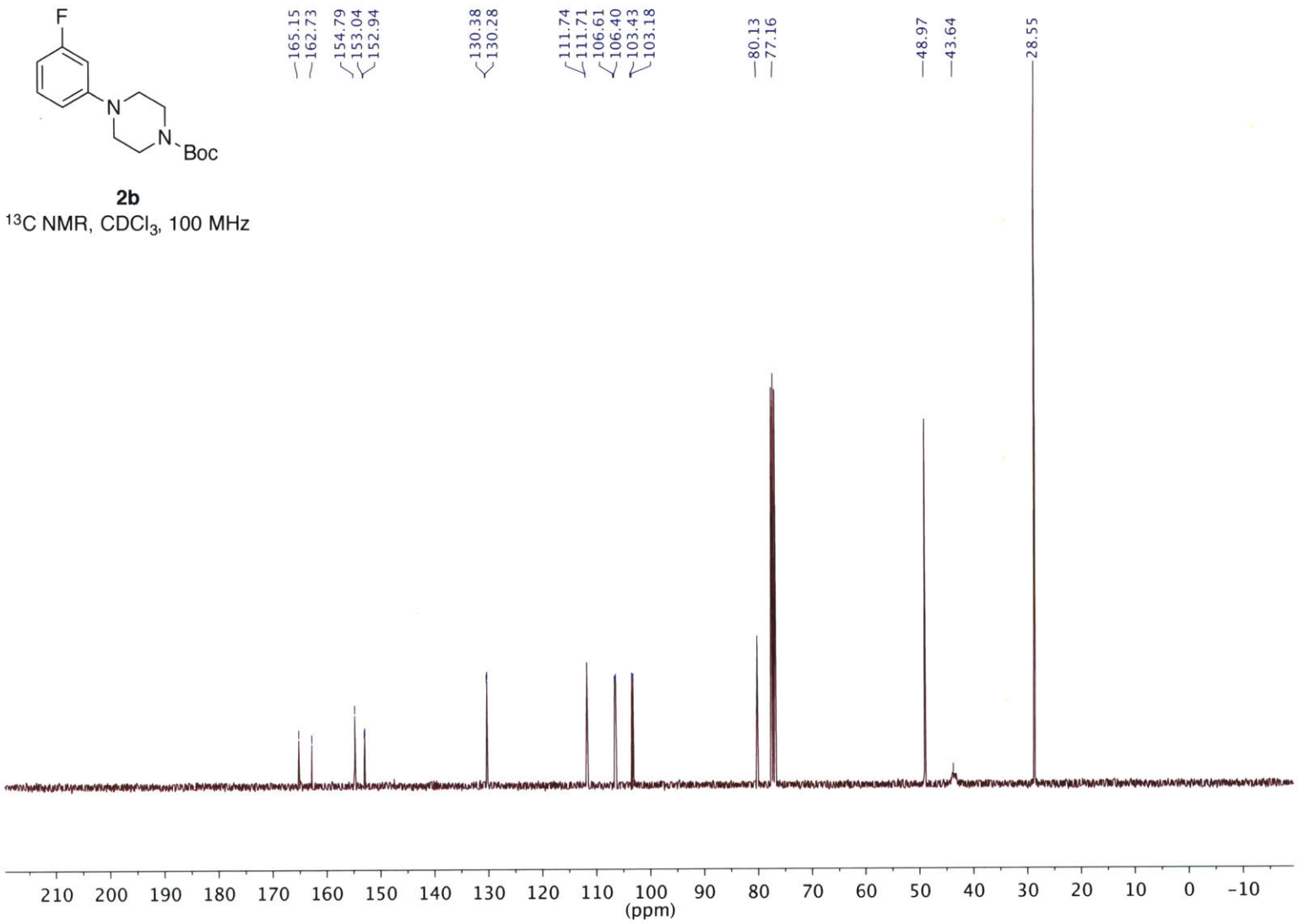

2b

^{13}C NMR, $CDCl_3$, 100 MHz

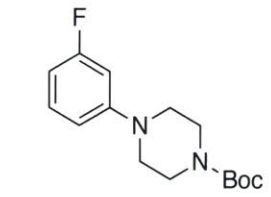

2b

^{19}F NMR, $CDCl_3$, 471 MHz

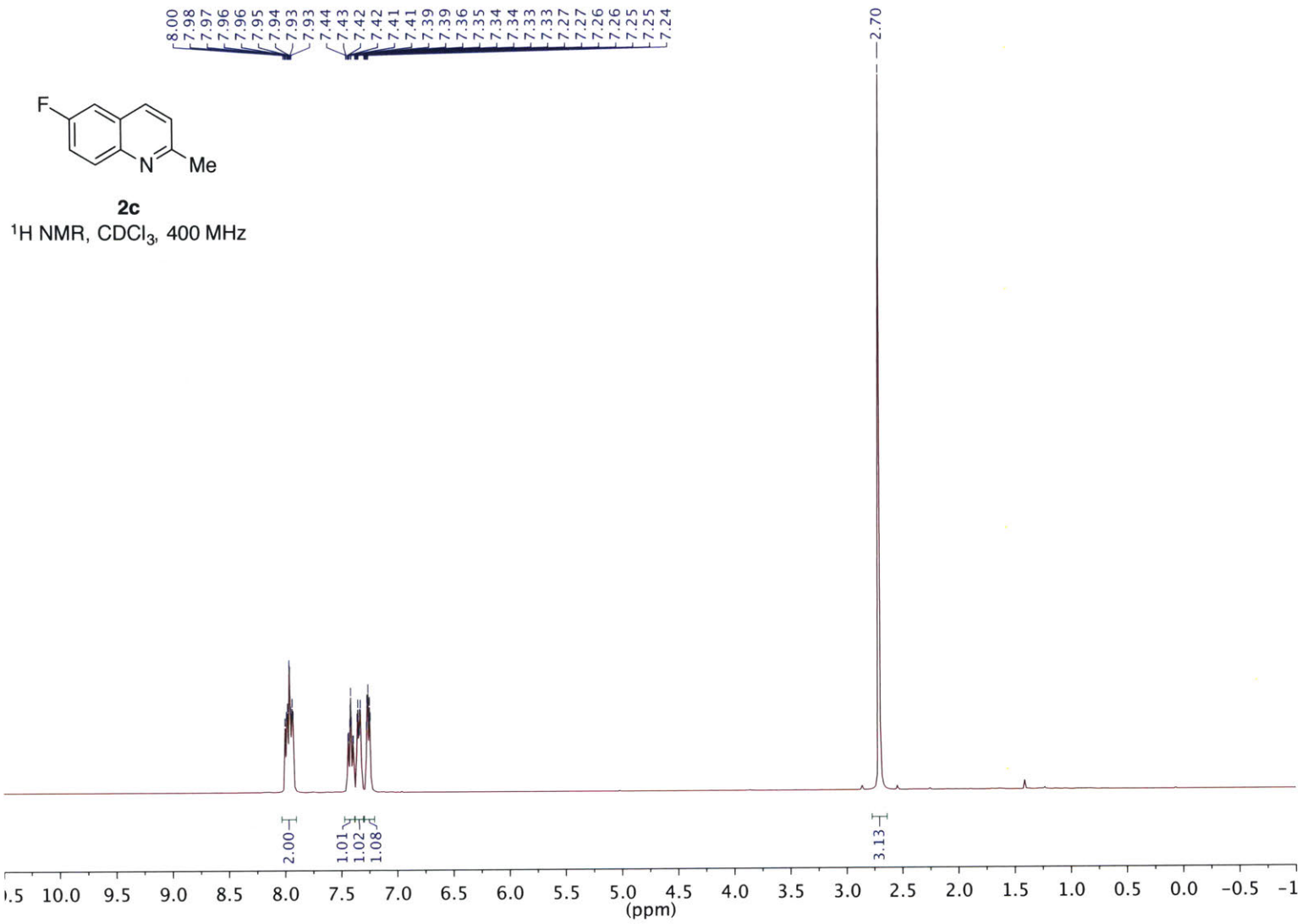
8.00
7.98
7.97
7.96
7.96
7.95
7.94
7.93
7.93
7.44
7.43
7.42
7.42
7.41
7.41
7.39
7.39
7.36
7.35
7.34
7.34
7.33
7.33
7.27
7.27
7.26
7.26
7.25
7.25
7.24
2.70
F
N
Me
2c
1H NMR, CDCl3, 400 MHz
2.00
1.01
1.02
1.08
3.13
10.0
9.5
9.0
8.5
8.0
7.5
7.0
6.5
6.0
5.5
5.0
4.5
4.0
3.5
3.0
2.5
2.0
1.5
1.0
0.5
0.0
-0.5
-1
(ppm)

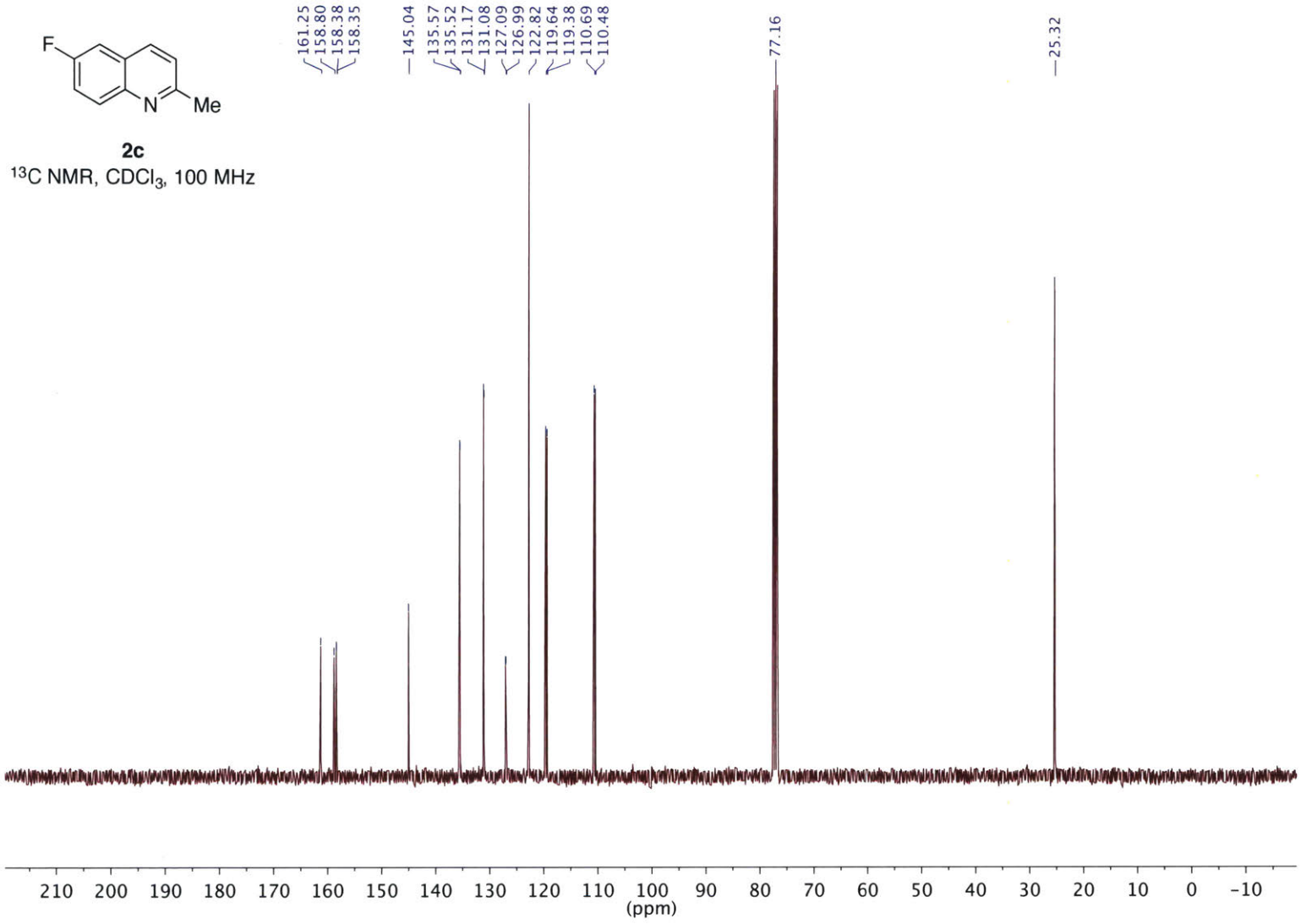
F
N
Me
2c
^{13}C NMR, $CDCl_3$, 100 MHz
161.25
158.80
158.38
158.35
145.04
135.57
135.52
131.17
131.08
127.09
126.99
122.82
119.64
119.38
110.69
110.48
77.16
25.32
210 200 190 180 170 160 150 140 130 120 110 100 90 80 70 60 50 40 30 20 10 0 -10
(ppm)

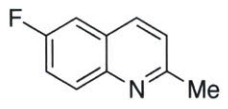

2c

^{19}F NMR, $CDCl_3$, 471 MHz

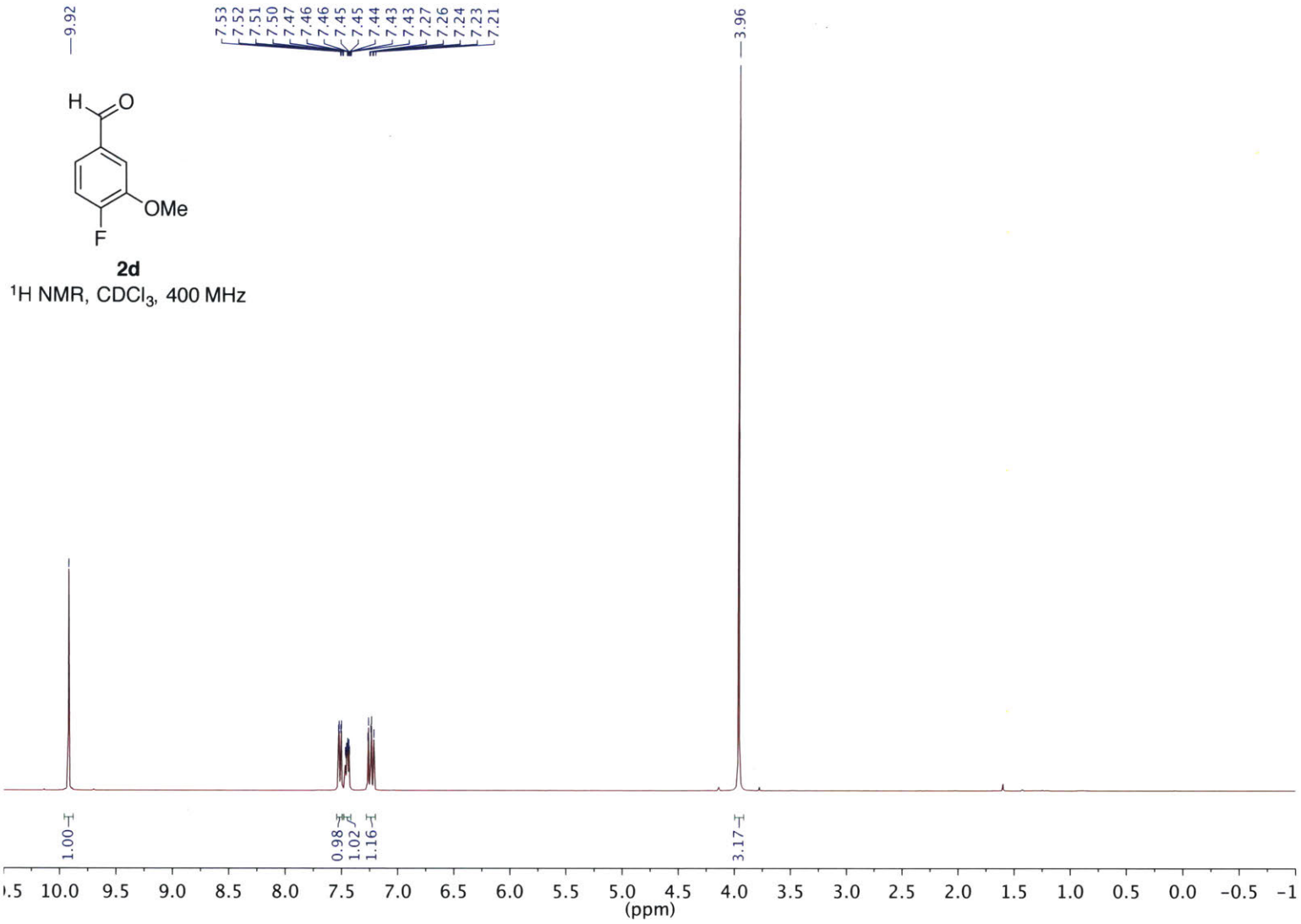
9.92
7.53
7.52
7.51
7.50
7.47
7.46
7.46
7.45
7.45
7.44
7.43
7.43
7.27
7.26
7.24
7.23
7.21
3.96
H
O
OMe
F
2d
1H NMR, CDCl3, 400 MHz
1.00
0.98
1.02
1.16
3.17
10.0 9.5 9.0 8.5 8.0 7.5 7.0 6.5 6.0 5.5 5.0 4.5 4.0 3.5 3.0 2.5 2.0 1.5 1.0 0.5 0.0 -0.5 -1
(ppm)

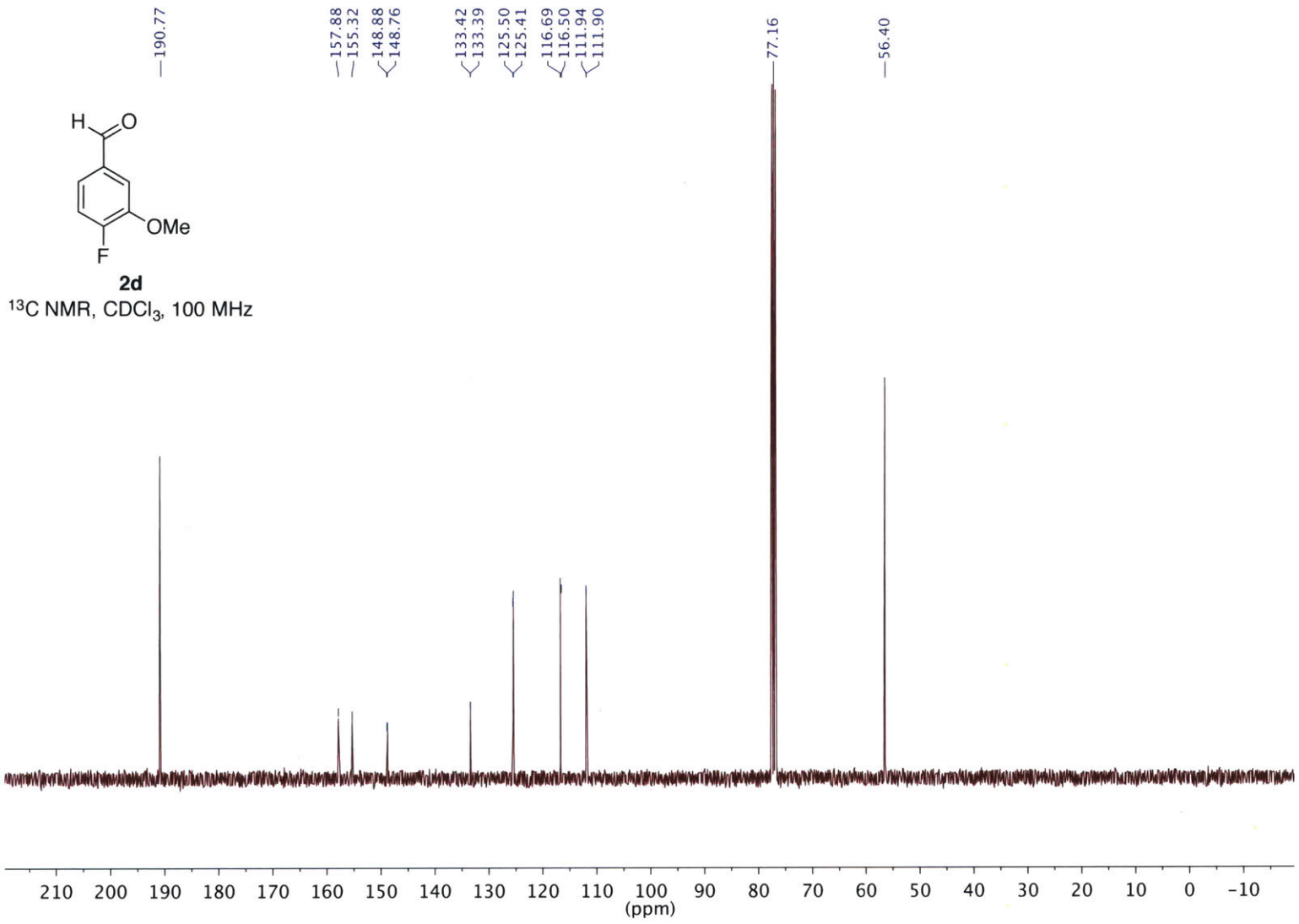
190.77
157.88
155.32
148.88
148.76
133.42
133.39
125.50
125.41
116.69
116.50
111.94
111.90
77.16
56.40
H
O
OMe
F
2d
13C NMR, CDCl3, 100 MHz
210 200 190 180 170 160 150 140 130 120 110 100 90 80 70 60 50 40 30 20 10 0 -10
(ppm)

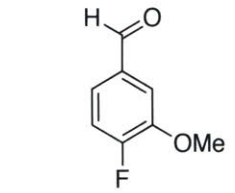

2d

^{19}F NMR, $CDCl_3$, 471 MHz

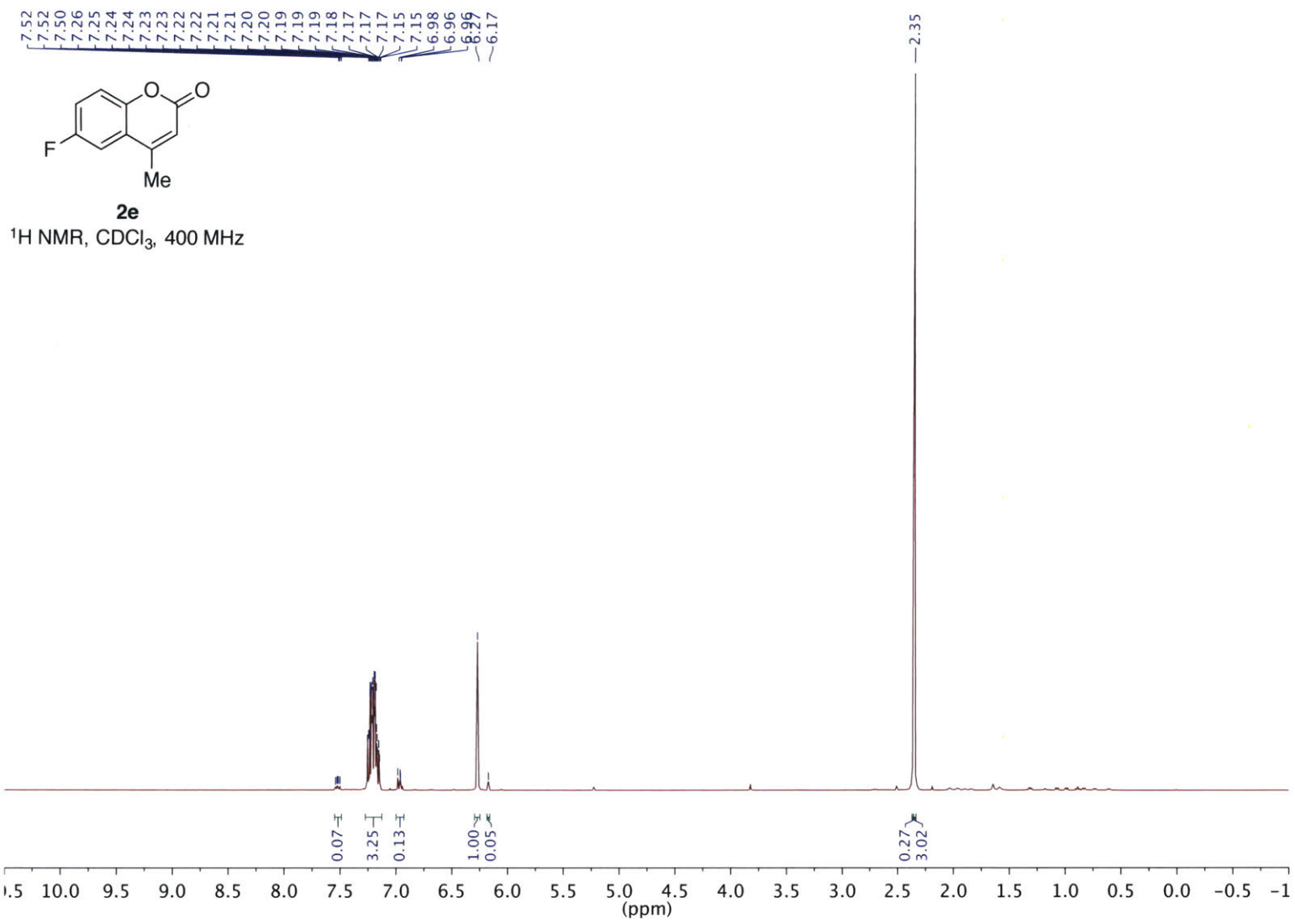

2e

^{1}H NMR, $CDCl_3$, 400 MHz

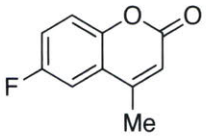

2e

^{13}C NMR, $CDCl_3$, 100 MHz

160.44
160.09
157.67
151.53
151.50
149.77
149.75
121.04
120.96
119.28
119.04
118.70
118.62
116.18
110.55
110.30
77.16
18.74

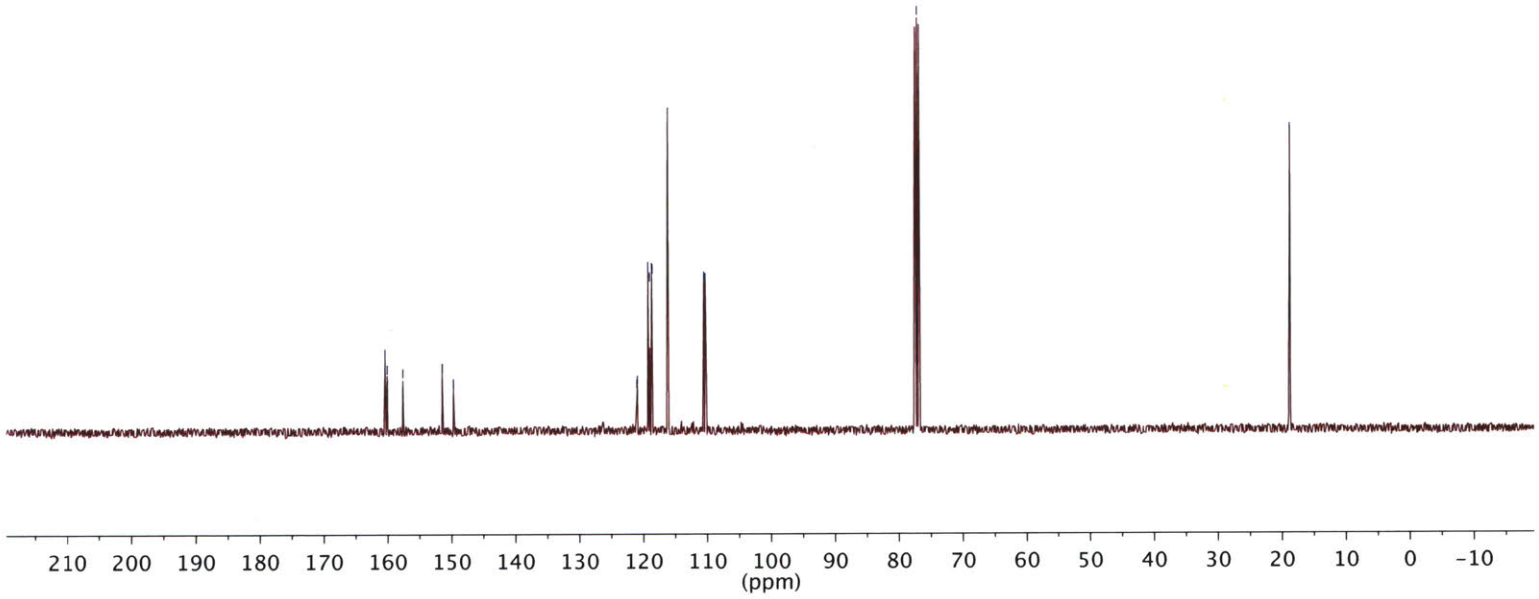

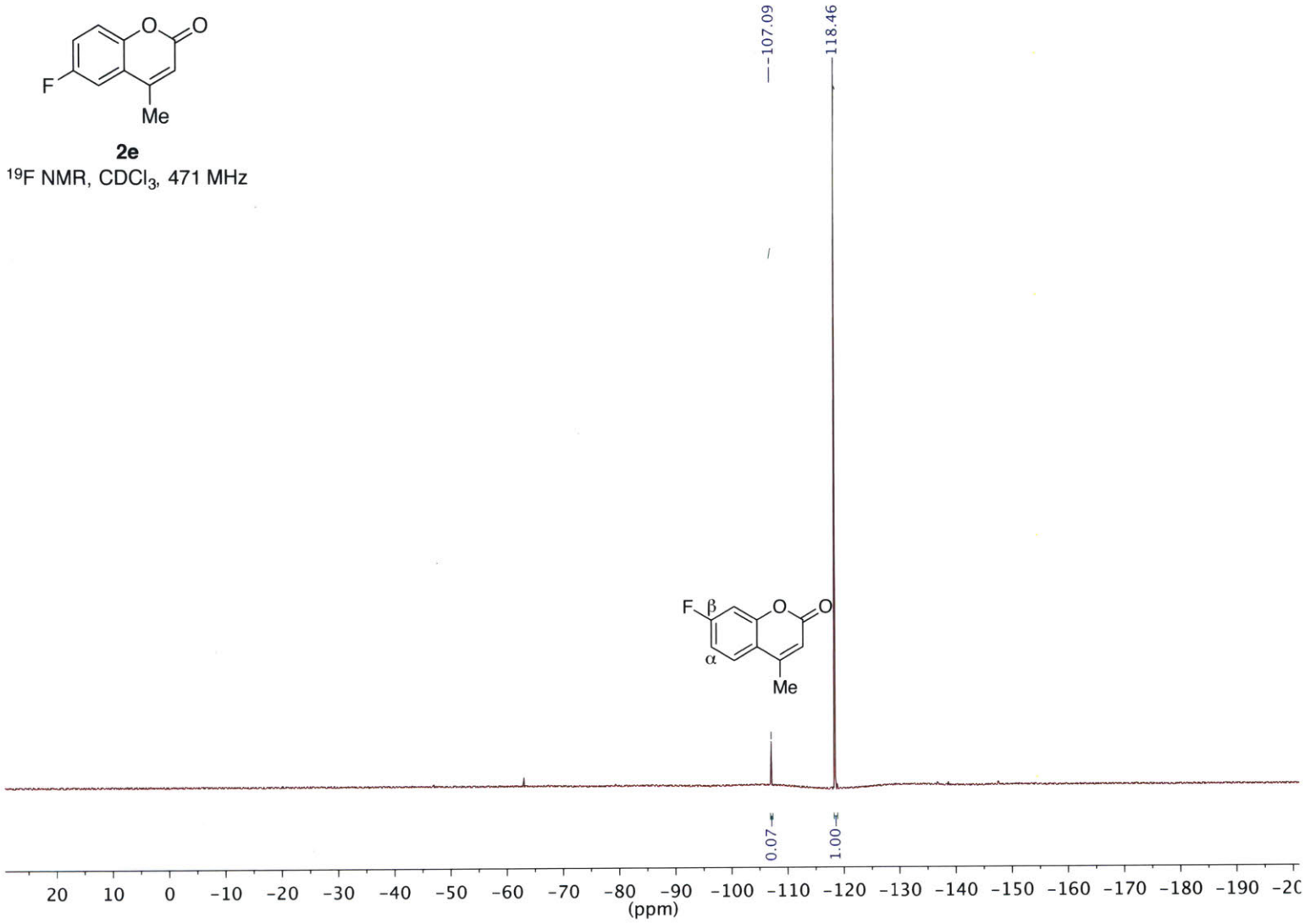
F
O
O
Me
2e
19F NMR, CDCl3, 471 MHz
107.09
118.46
F
β
O
O
α
Me
0.07
1.00
20 10 0 -10 -20 -30 -40 -50 -60 -70 -80 -90 -100 -110 -120 -130 -140 -150 -160 -170 -180 -190 -20
(ppm)

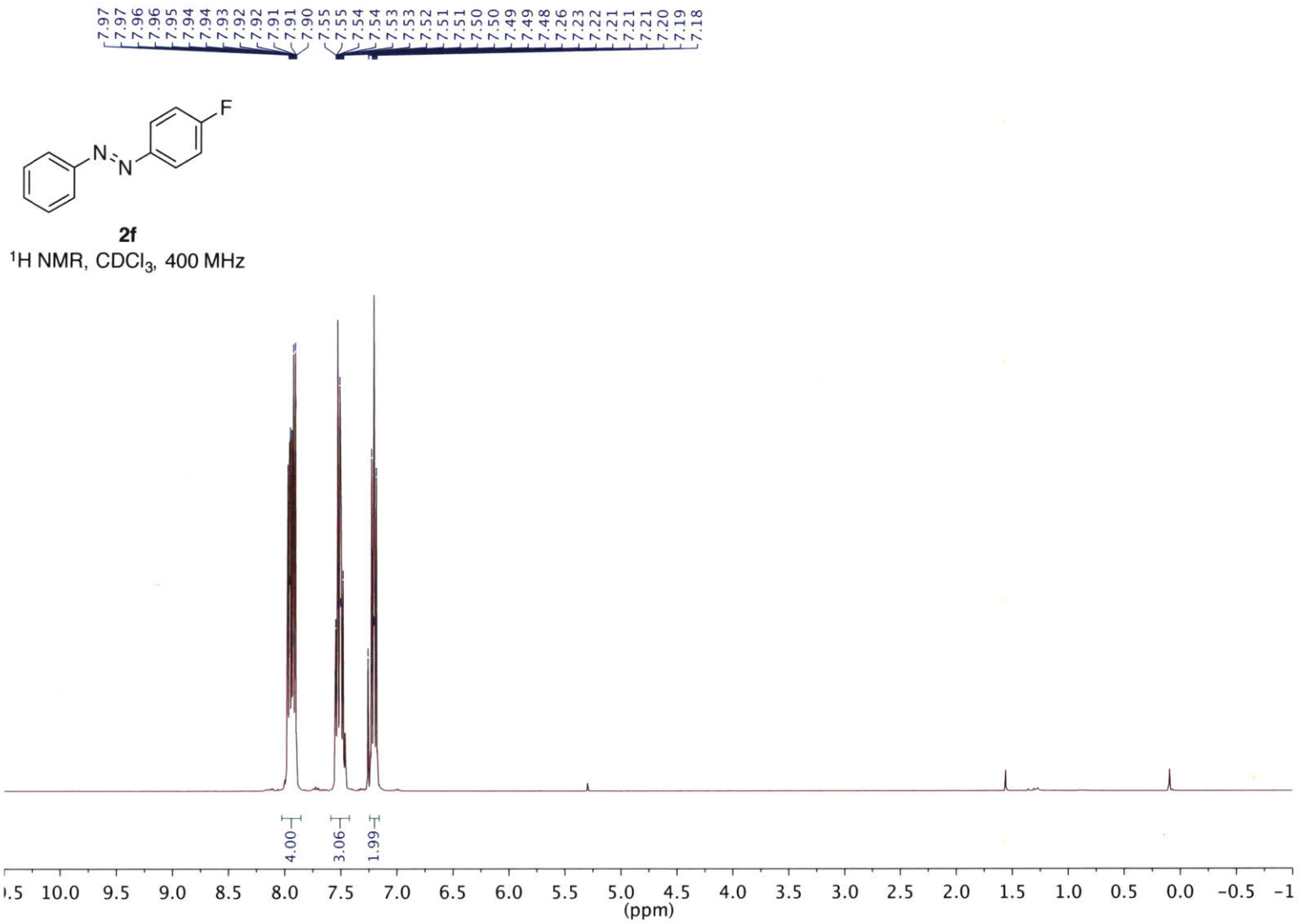
7.97
7.97
7.96
7.96
7.95
7.94
7.94
7.93
7.92
7.92
7.91
7.91
7.90
7.55
7.55
7.54
7.54
7.53
7.53
7.52
7.51
7.51
7.50
7.50
7.49
7.49
7.48
7.26
7.23
7.22
7.21
7.21
7.21
7.20
7.19
7.18
F
N
N
2f
1H NMR, CDCl3, 400 MHz
4.00
3.06
1.99
10.5
10.0
9.5
9.0
8.5
8.0
7.5
7.0
6.5
6.0
5.5
5.0
4.5
4.0
3.5
3.0
2.5
2.0
1.5
1.0
0.5
0.0
-0.5
-1
(ppm)

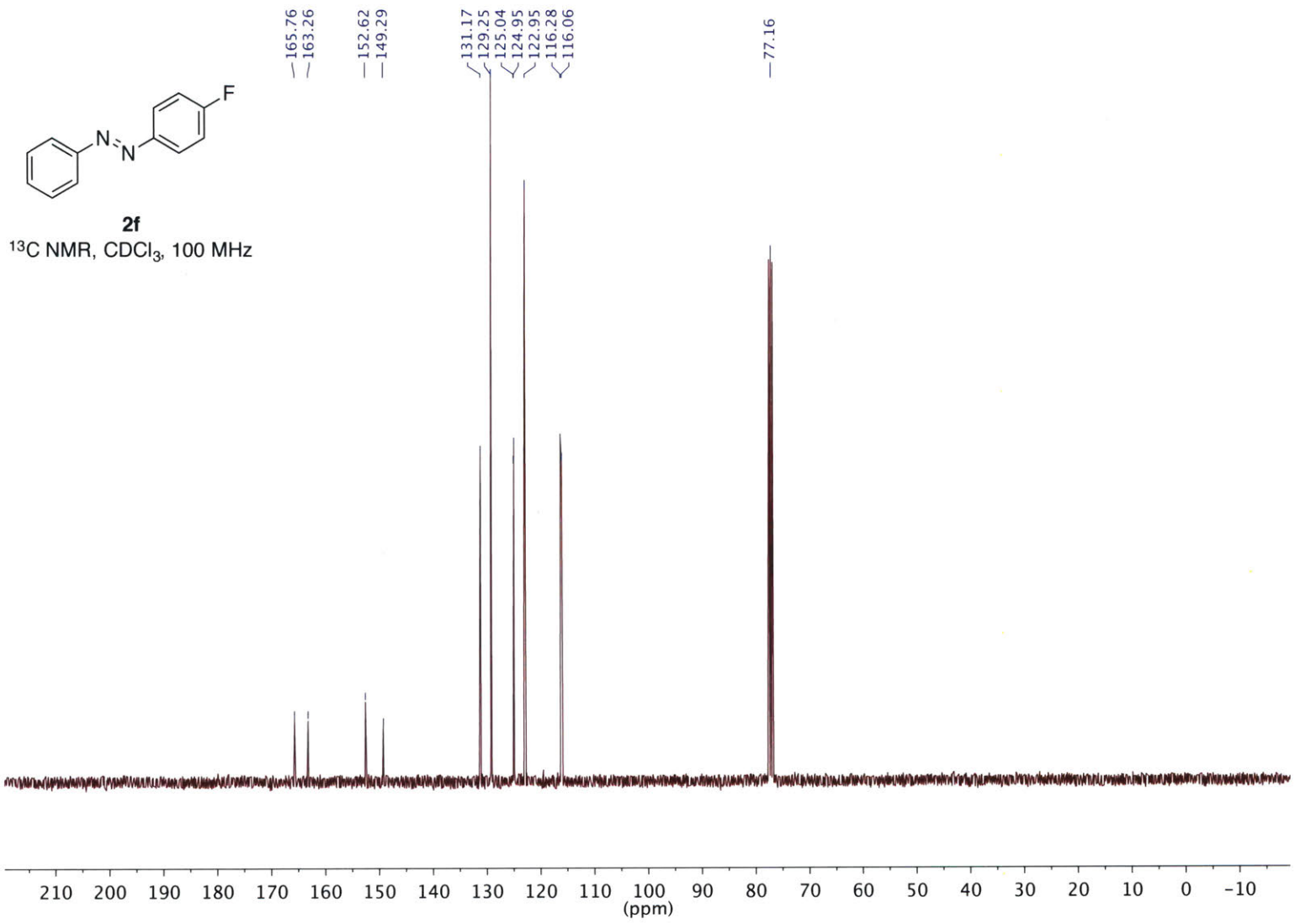
165.76
163.26
152.62
149.29
131.17
129.25
125.04
124.95
122.95
116.28
116.06
77.16
F
N
N
2f
13C NMR, CDCl3, 100 MHz
210 200 190 180 170 160 150 140 130 120 110 100 90 80 70 60 50 40 30 20 10 0 -10
(ppm)

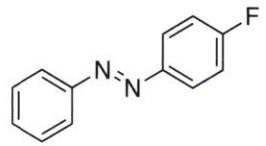

2f

^{19}F NMR, $CDCl_3$, 471 MHz

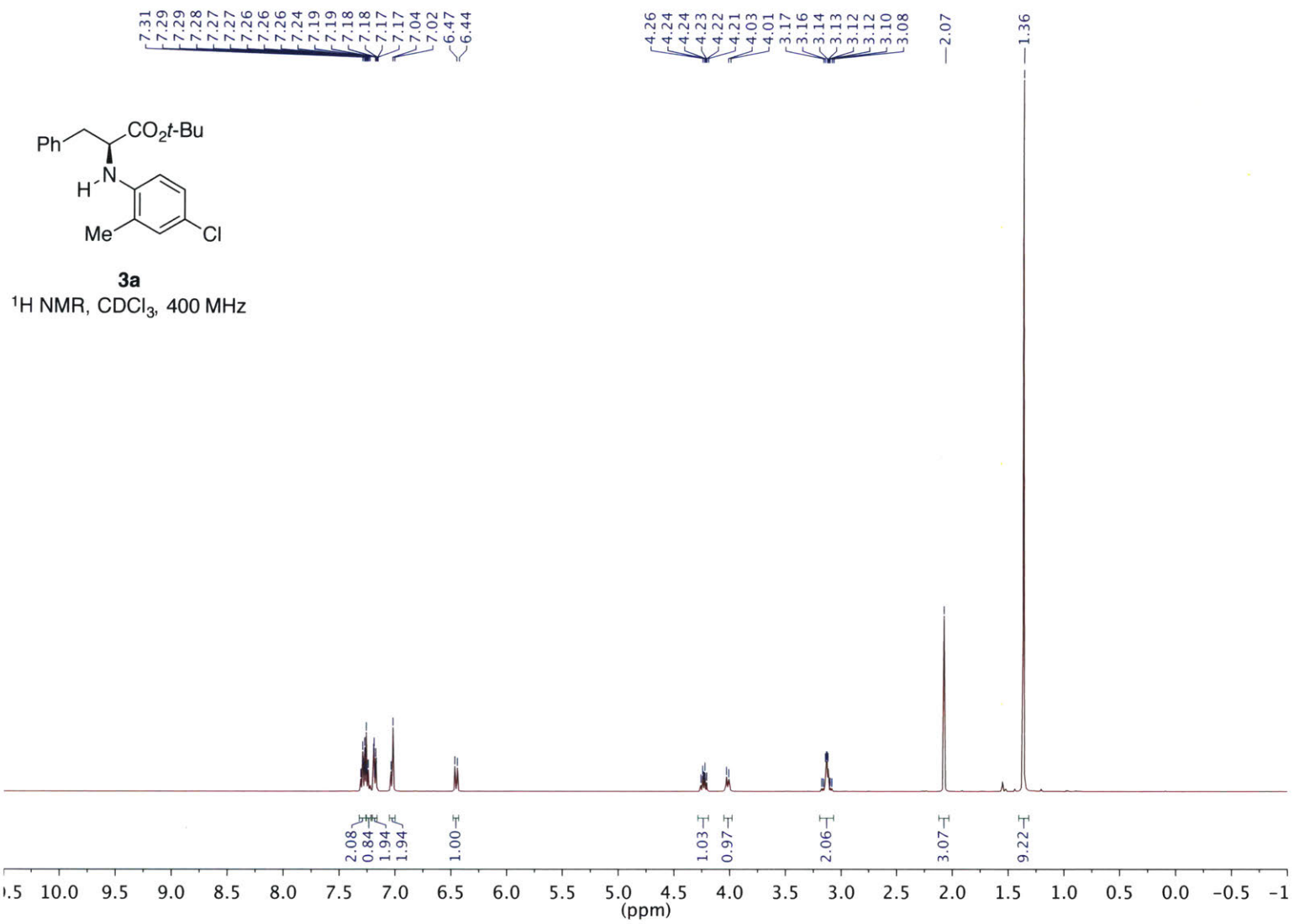

3a

^{1}H NMR, $CDCl_3$, 400 MHz

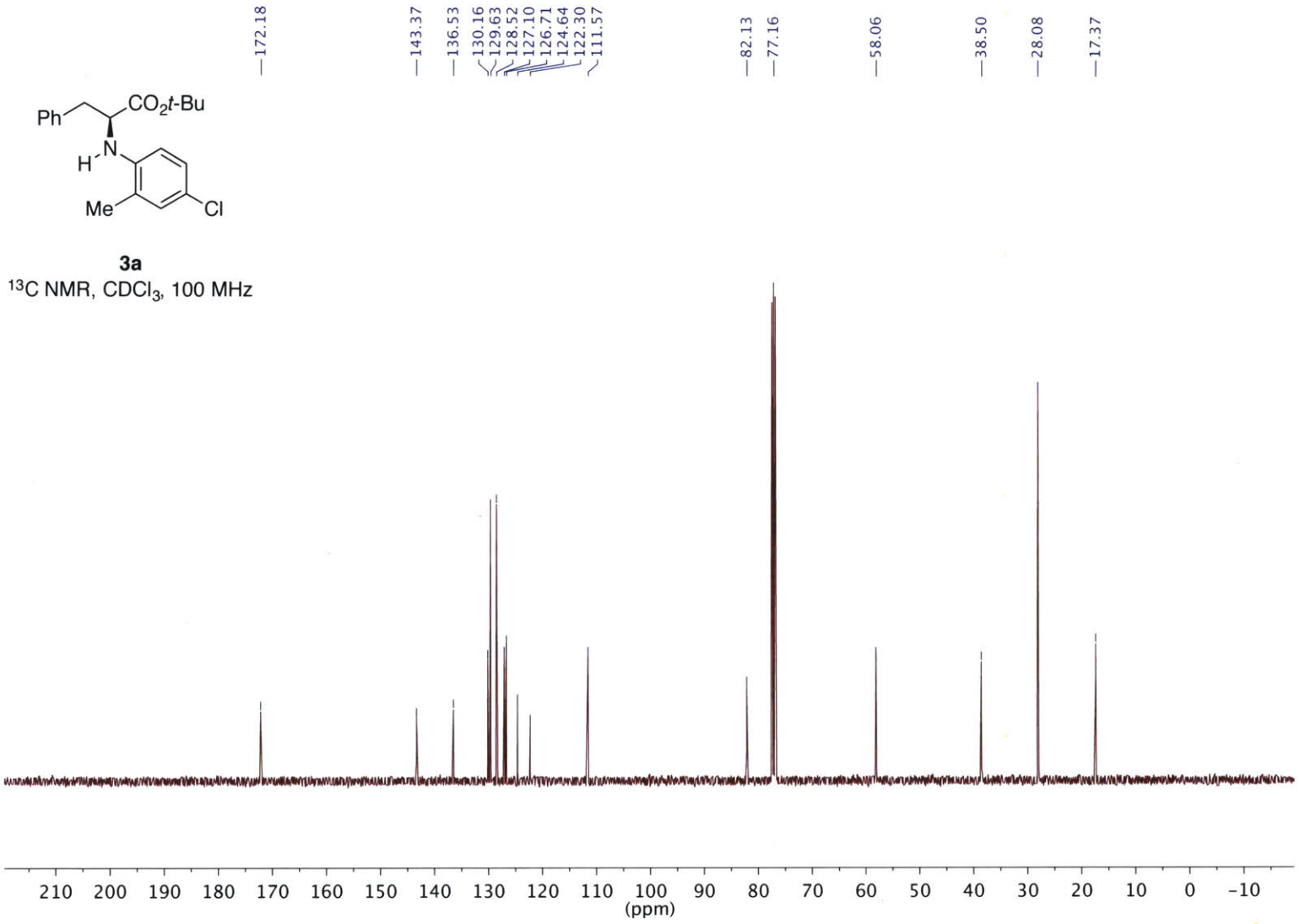
172.18
143.37
136.53
130.16
129.63
128.52
127.10
126.71
124.64
122.30
111.57
82.13
77.16
58.06
38.50
28.08
17.37
Ph
CO2t-Bu
H
N
Me
Cl
3a
13C NMR, CDCl3, 100 MHz
210 200 190 180 170 160 150 140 130 120 110 100 90 80 70 60 50 40 30 20 10 0 -10
(ppm)

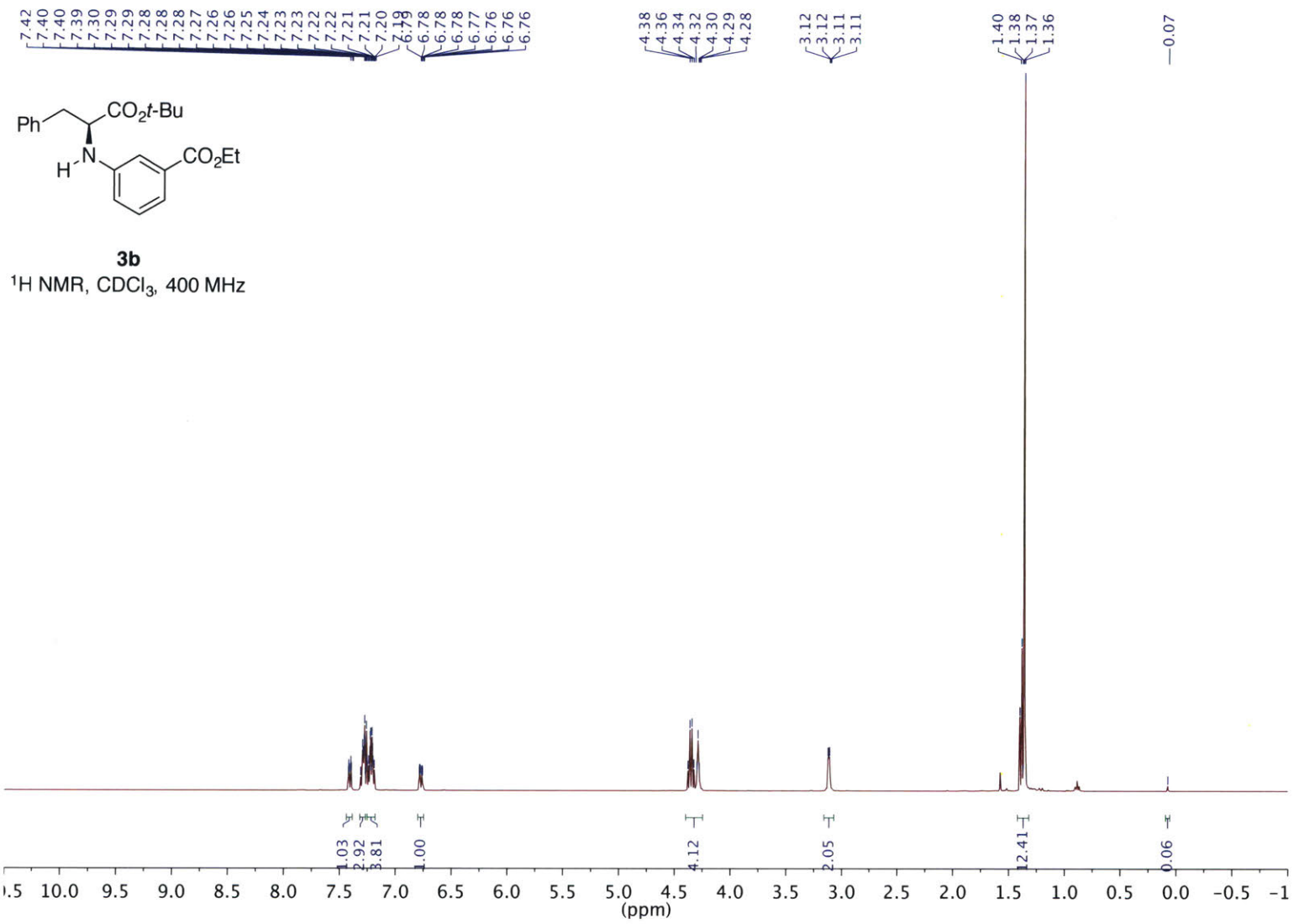

3b

^{1}H NMR, $CDCl_3$, 400 MHz

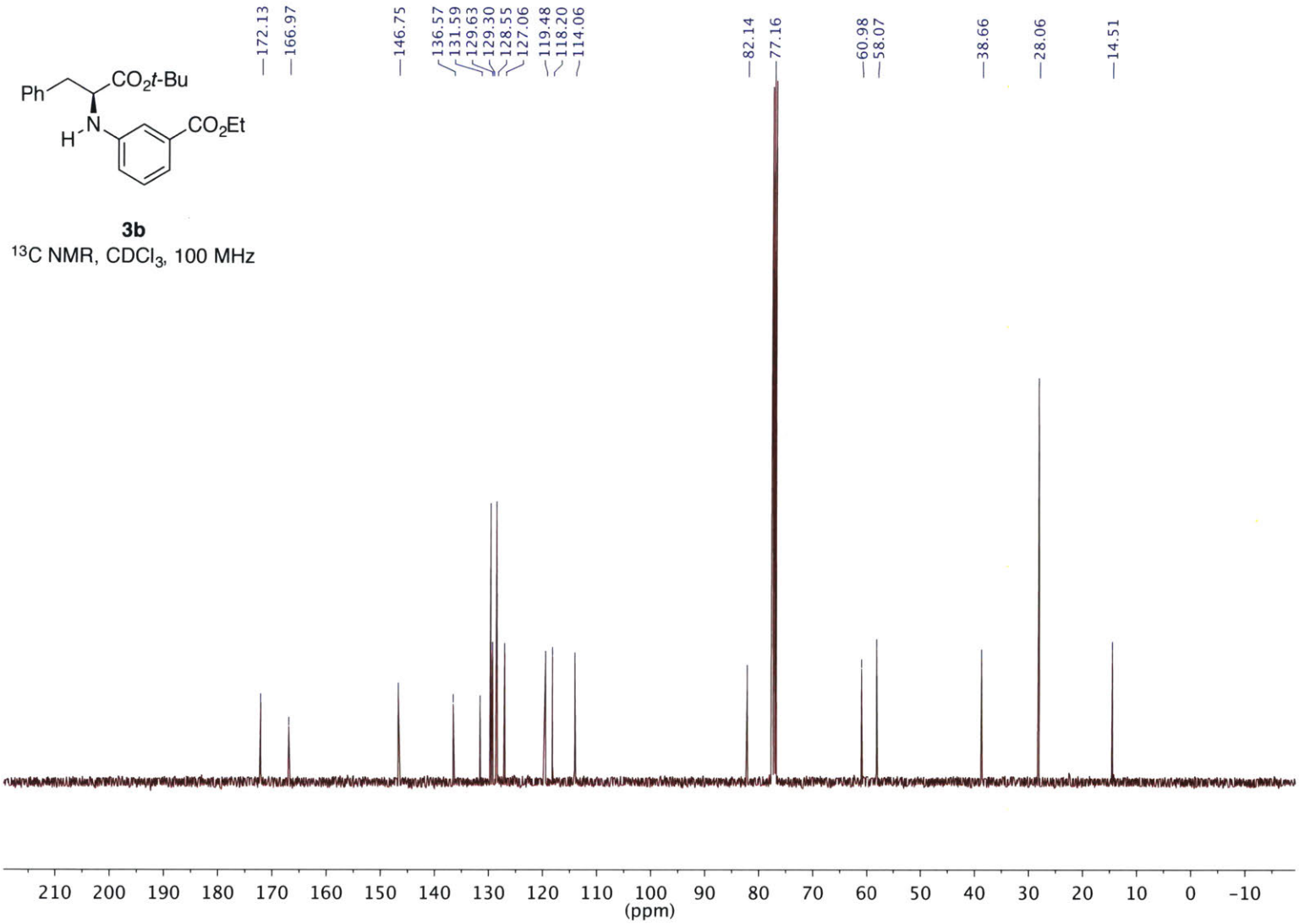

3b

^{13}C NMR, $CDCl_3$, 100 MHz

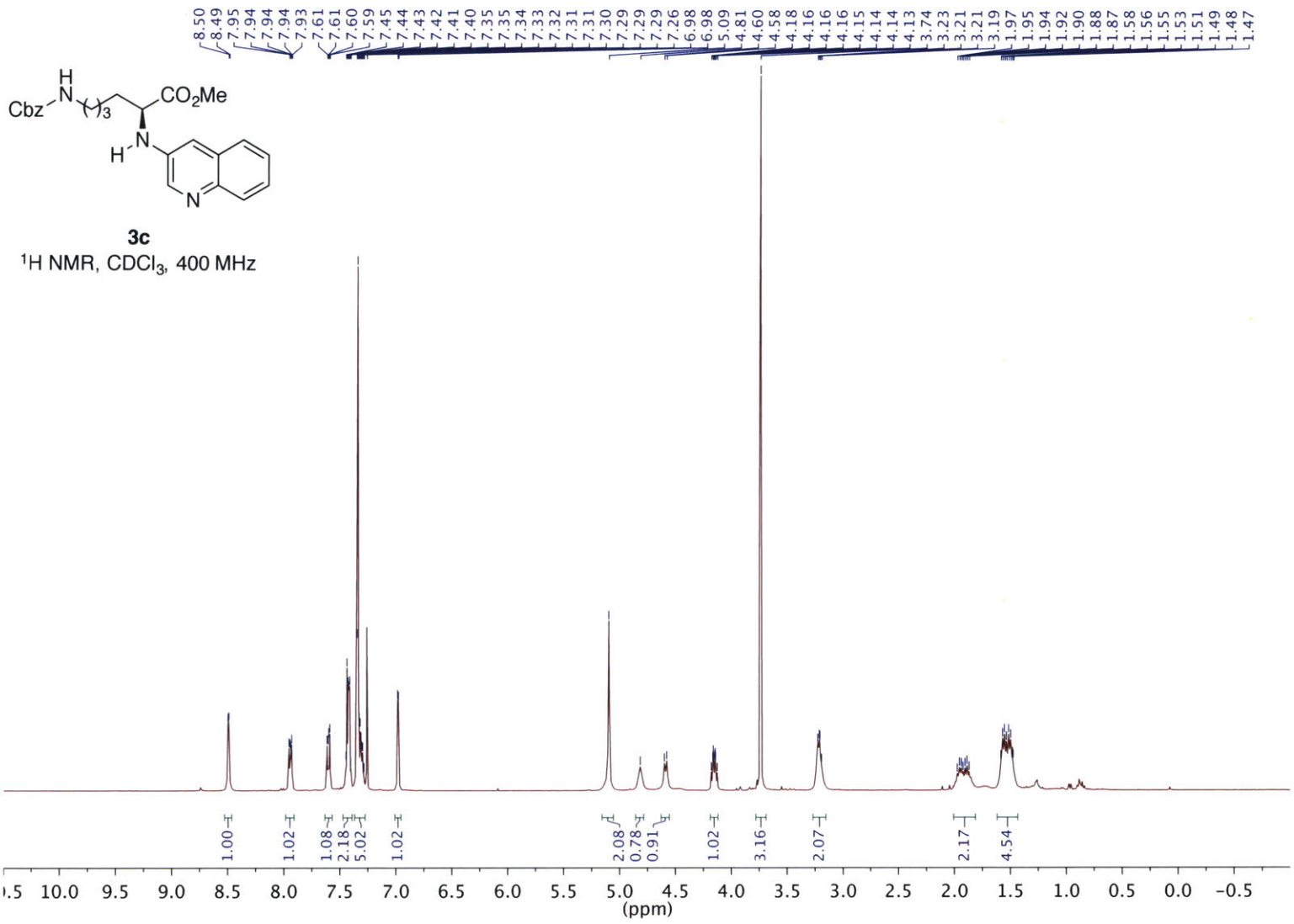
Cbz
H
N
CO2Me
H
N
N
3c
1H NMR, CDCl3, 400 MHz
8.50
8.49
7.95
7.94
7.94
7.94
7.93
7.61
7.60
7.59
7.45
7.44
7.43
7.42
7.41
7.40
7.35
7.35
7.34
7.33
7.32
7.31
7.31
7.30
7.29
7.29
7.29
7.26
6.98
5.09
4.81
4.60
4.58
4.18
4.16
4.16
4.16
4.15
4.14
4.14
4.13
3.74
3.23
3.21
3.21
3.19
1.97
1.95
1.94
1.92
1.90
1.88
1.87
1.58
1.56
1.55
1.53
1.51
1.49
1.48
1.47
1.00
1.02
1.08
2.18
5.02
1.02
2.08
0.78
0.91
1.02
3.16
2.07
2.17
4.54
10.0
9.5
9.0
8.5
8.0
7.5
7.0
6.5
6.0
5.5
5.0
4.5
4.0
3.5
3.0
2.5
2.0
1.5
1.0
0.5
0.0
-0.5
(ppm)

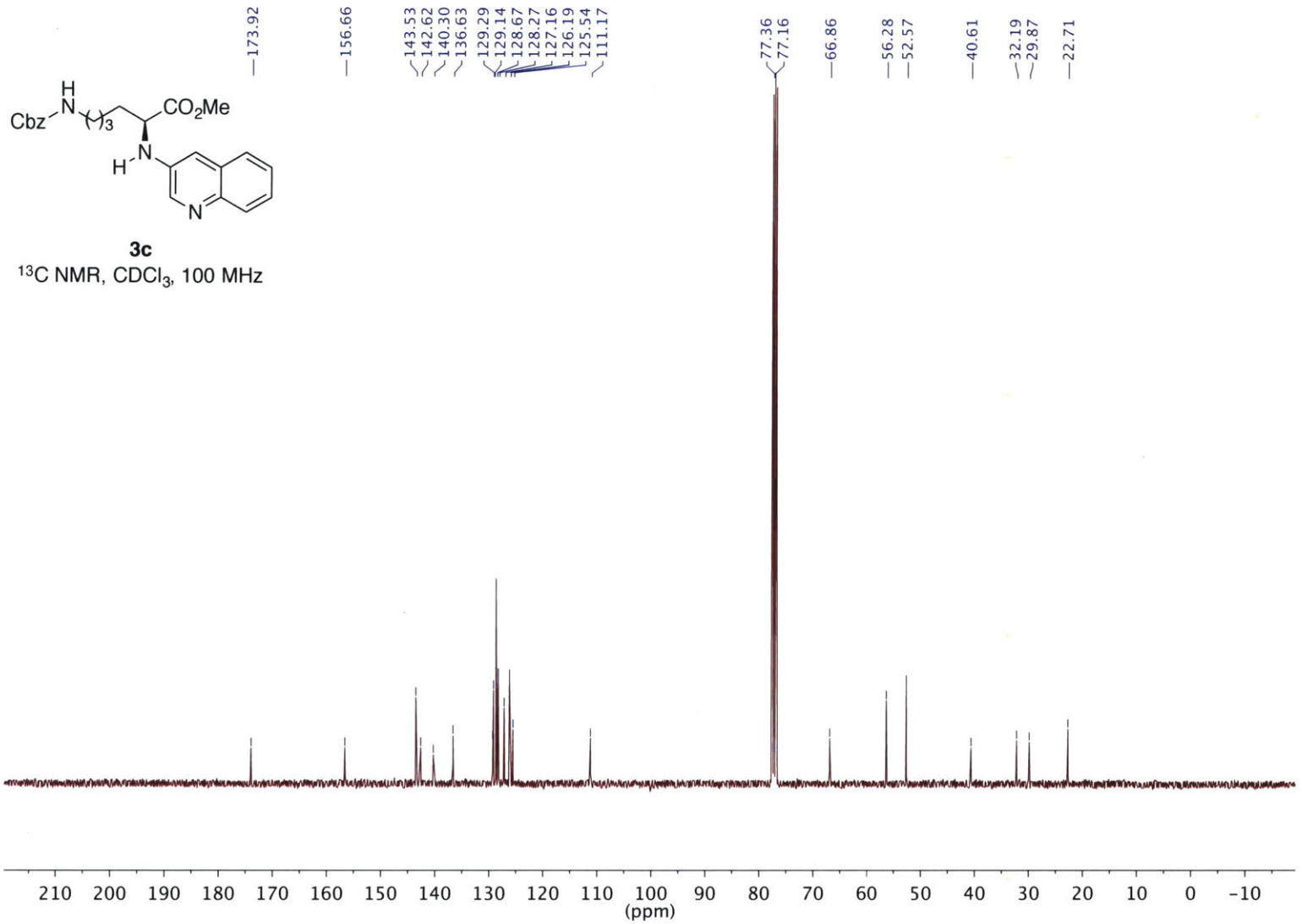

3c

^{13}C NMR, $CDCl_3$, 100 MHz

7.37
7.36
7.35
7.35
7.34
7.33
7.33
7.32
7.31
7.26
7.21
7.19
6.97
6.96
6.96
6.65
6.63
6.31
6.30
6.30
5.10
4.80
4.23
4.21
4.08
4.06
4.05
4.04
3.73
3.23
3.22
3.22
3.21
3.20
3.19
3.19
1.88
1.88
1.87
1.82
1.80
1.79
1.57
1.56
1.54
1.53
1.50
1.49
1.49
1.48
1.47
1.46
1.45
0.08
Cbz
H
N
CO2Me
H
N
N
3d
1H NMR, CDCl3, 500 MHz
4.84
2.22
2.06
2.29
2.00
2.25
0.87
0.99
1.20
3.43
2.40
2.47
4.98
0.11
10.0
9.5
9.0
8.5
8.0
7.5
7.0
6.5
6.0
5.5
5.0
4.5
4.0
3.5
3.0
2.5
2.0
1.5
1.0
0.5
0.0
-0.5
-1
(ppm)

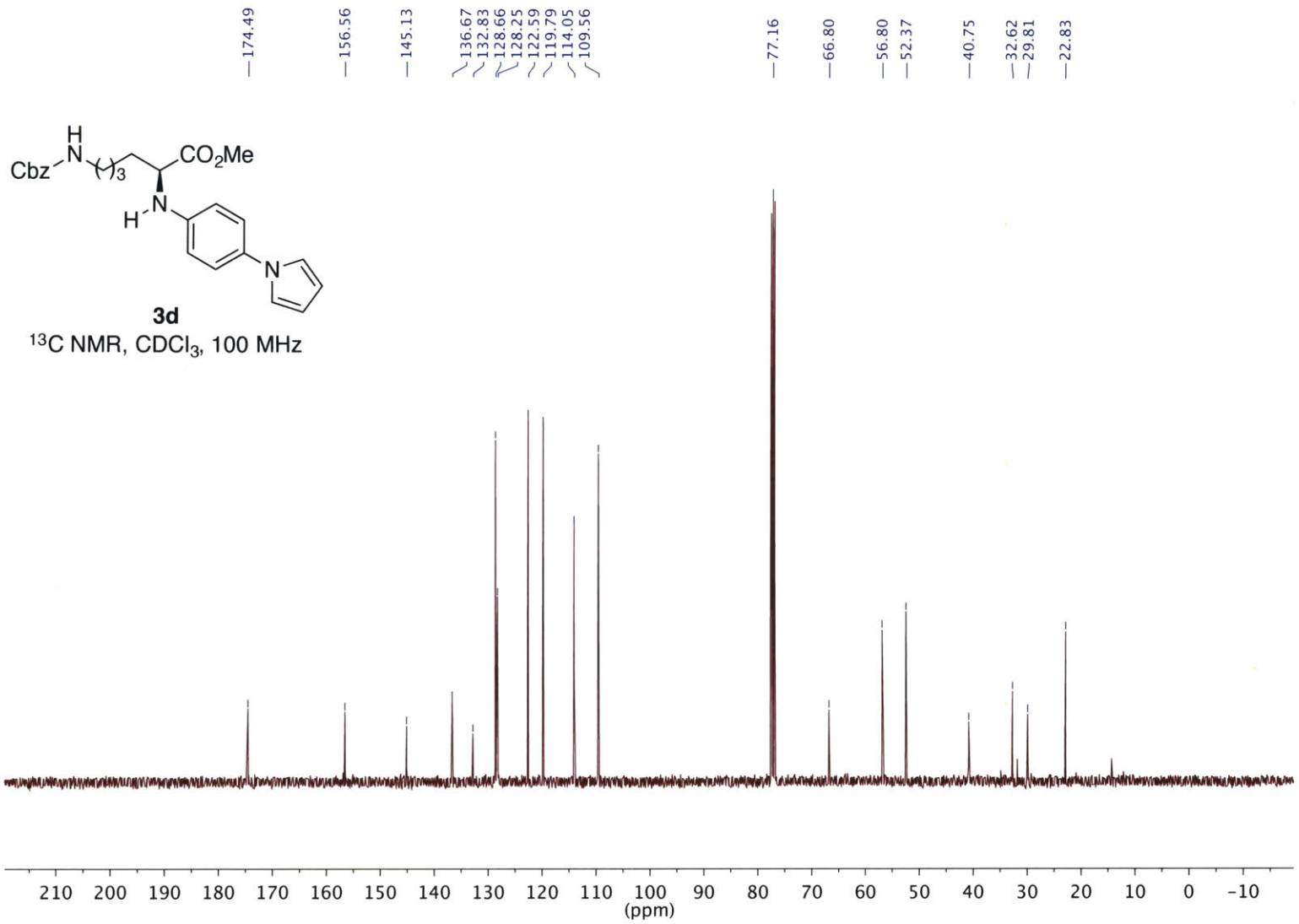
174.49
156.56
145.13
136.67
132.83
128.66
128.25
122.59
119.79
114.05
109.56
77.16
66.80
56.80
52.37
40.75
32.62
29.81
22.83
Cbz
CO2Me
3d
13C NMR, CDCl3, 100 MHz
210 200 190 180 170 160 150 140 130 120 110 100 90 80 70 60 50 40 30 20 10 0 -10
(ppm)

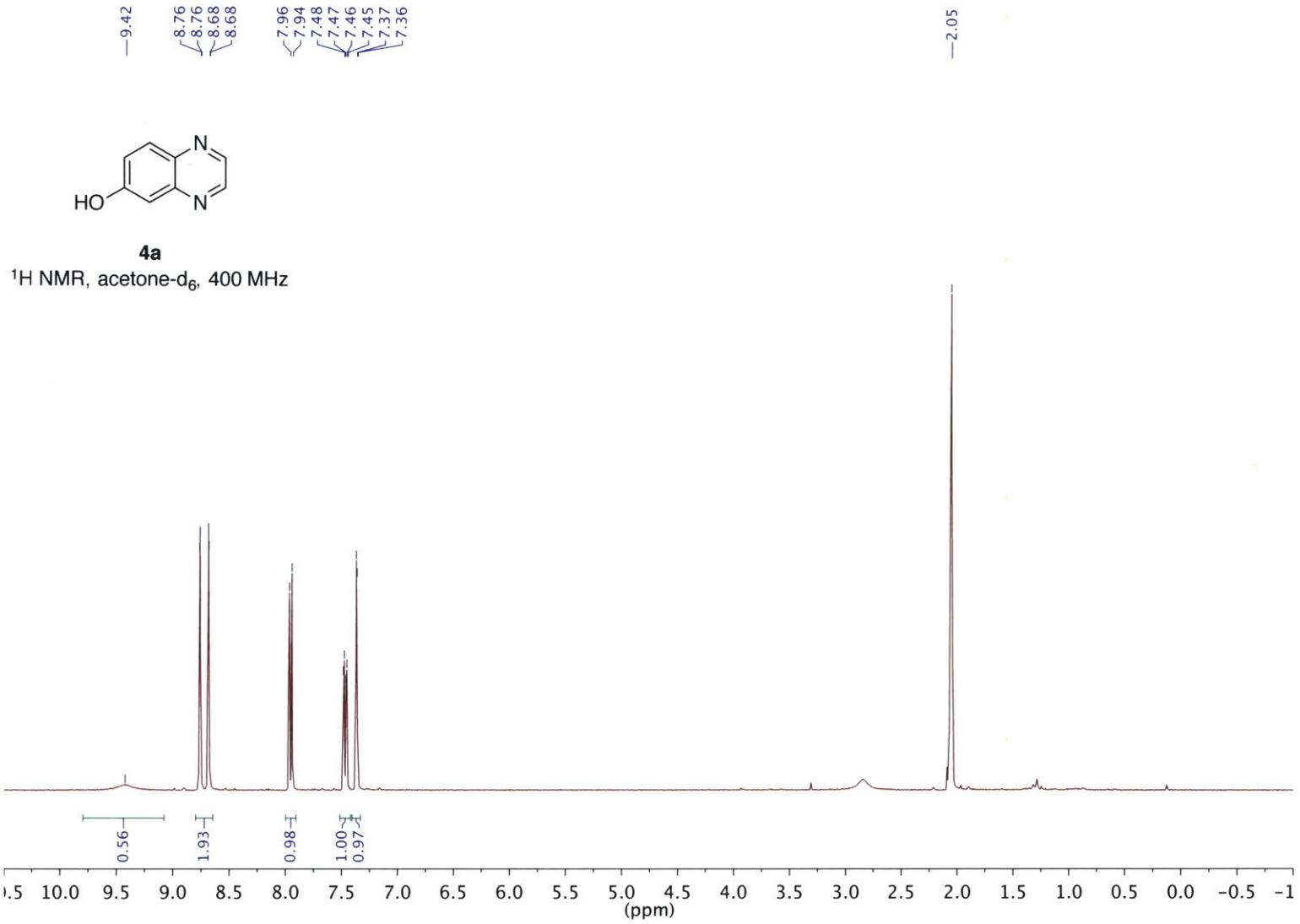

4a

^{1}H NMR, acetone-d_6, 400 MHz

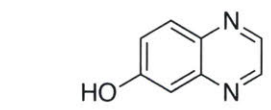

4a

^{13}C NMR, MeOD-d_4, 100 MHz

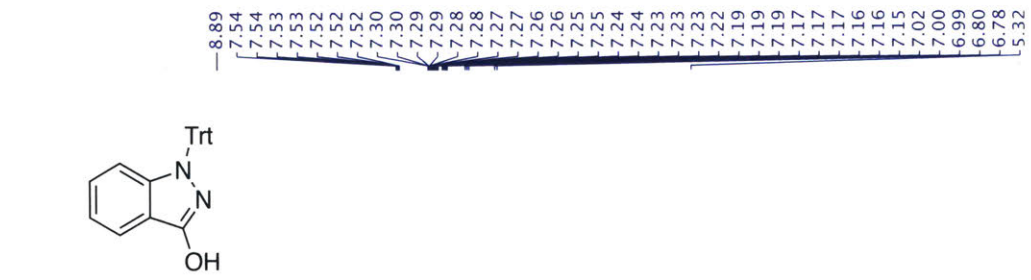

4b

^{1}H NMR, CD_2Cl_2, 500 MHz

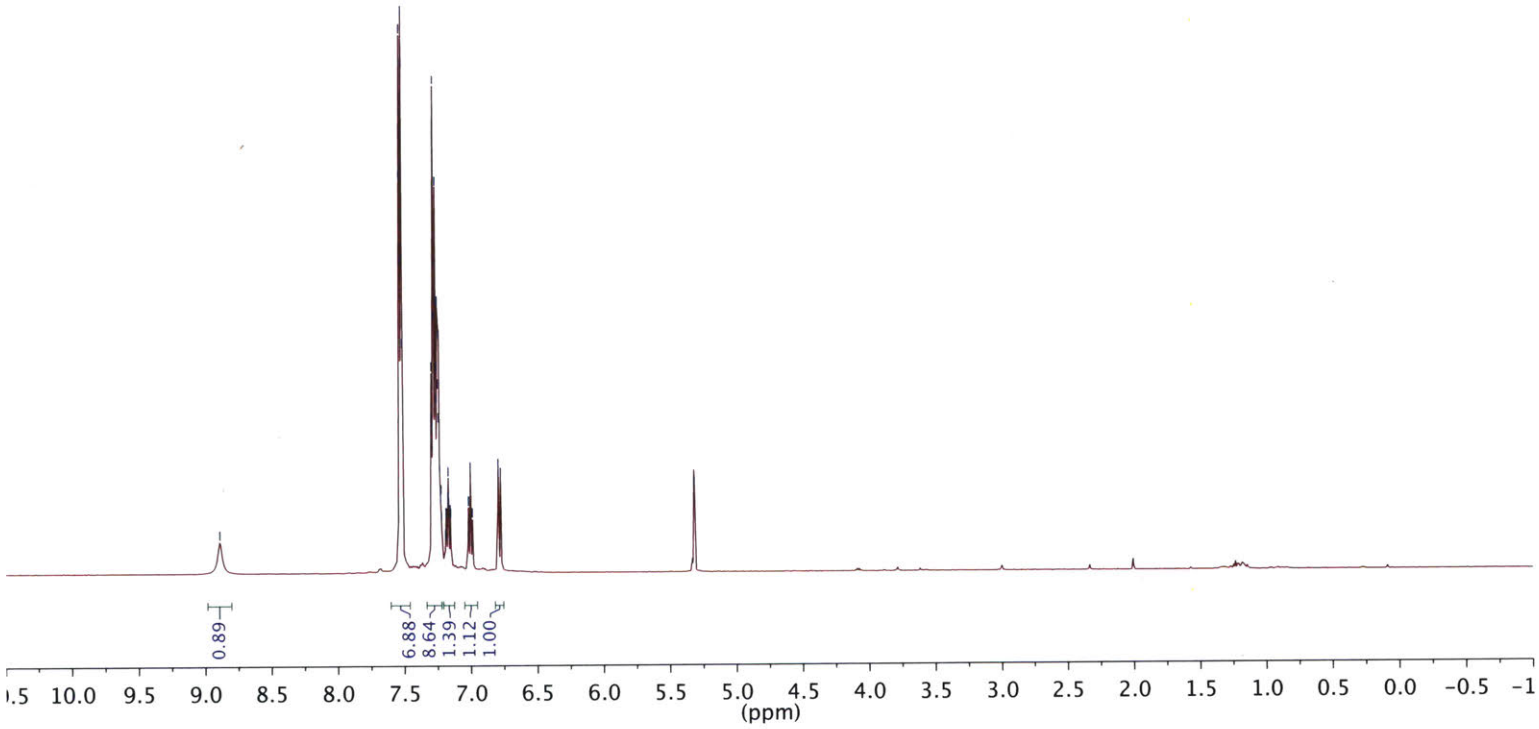

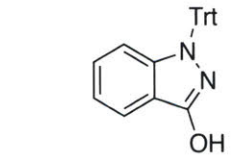

4b

^{13}C NMR, CD_2Cl_2, 100 MHz

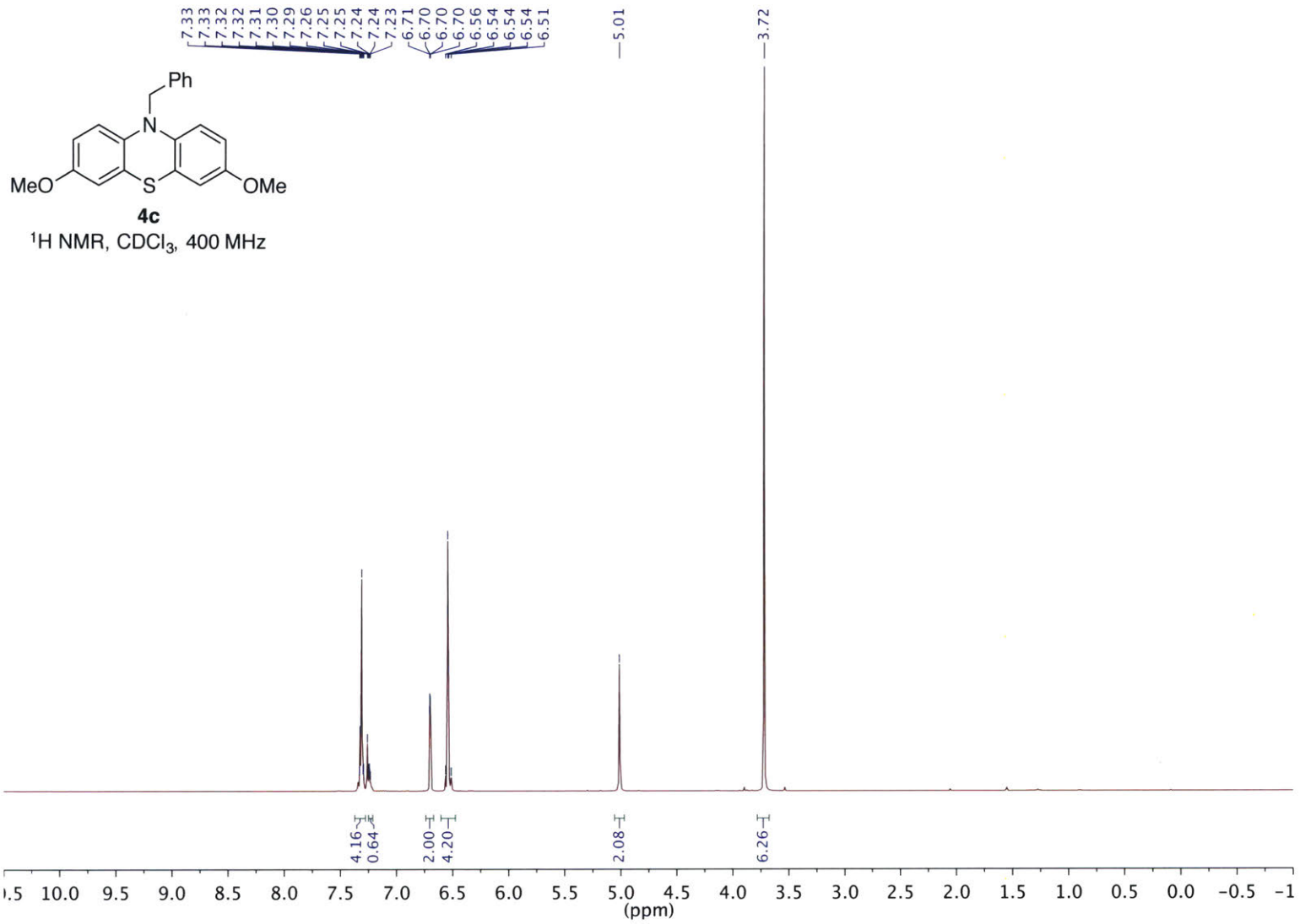
7.33
7.33
7.32
7.32
7.31
7.30
7.29
7.26
7.25
7.25
7.24
7.24
7.23
6.71
6.70
6.70
6.70
6.56
6.54
6.54
6.54
6.51
5.01
3.72
Ph
N
S
MeO
OMe
4c
¹H NMR, CDCl₃, 400 MHz
4.16
0.64
2.00
4.20
2.08
6.26
(ppm)

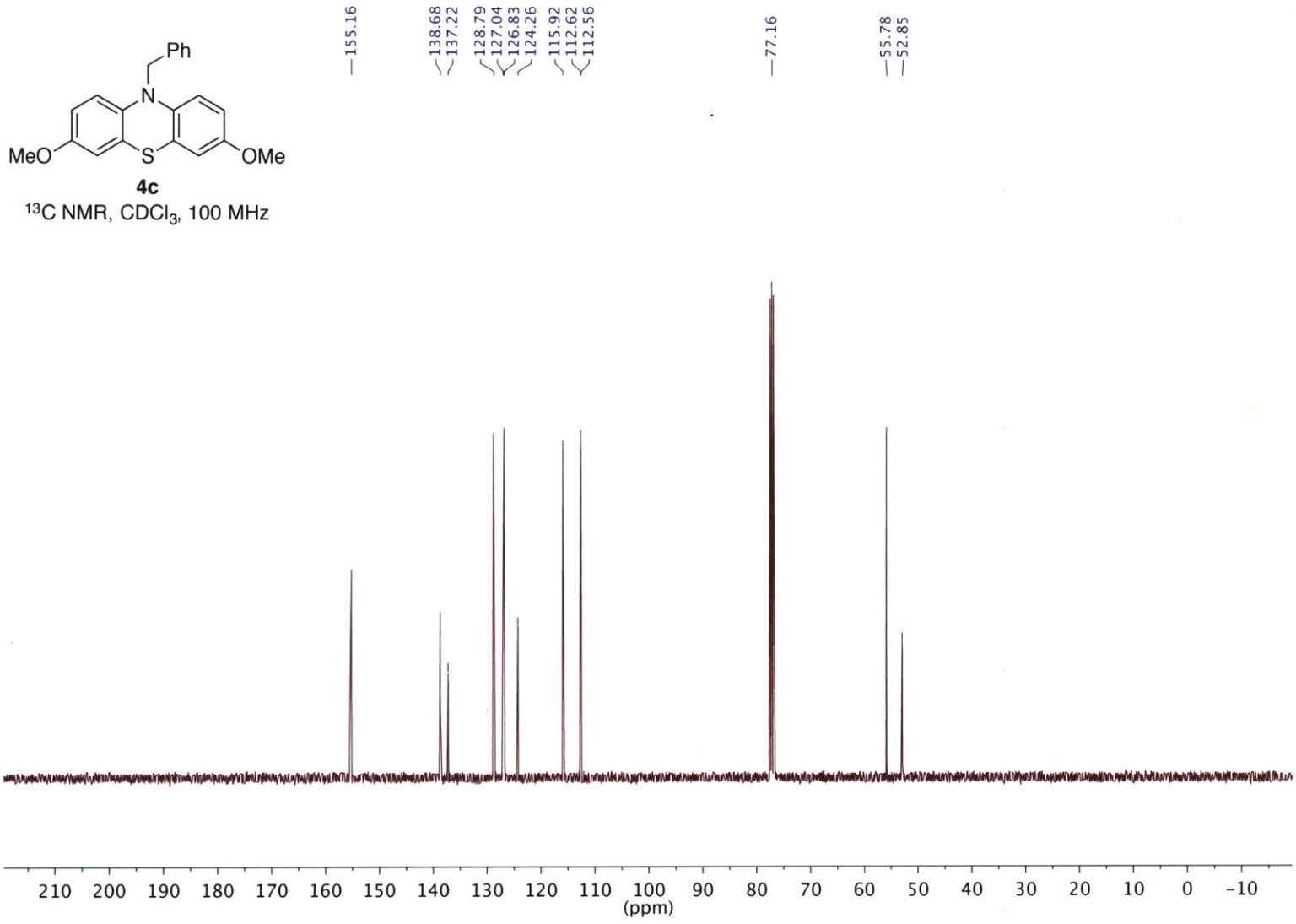
Ph
N
MeO
S
OMe
4c
^{13}C NMR, $CDCl_3$, 100 MHz
155.16
138.68
137.22
128.79
127.04
126.83
124.26
115.92
112.62
112.56
77.16
55.78
52.85
210 200 190 180 170 160 150 140 130 120 110 100 90 80 70 60 50 40 30 20 10 0 -10
(ppm)

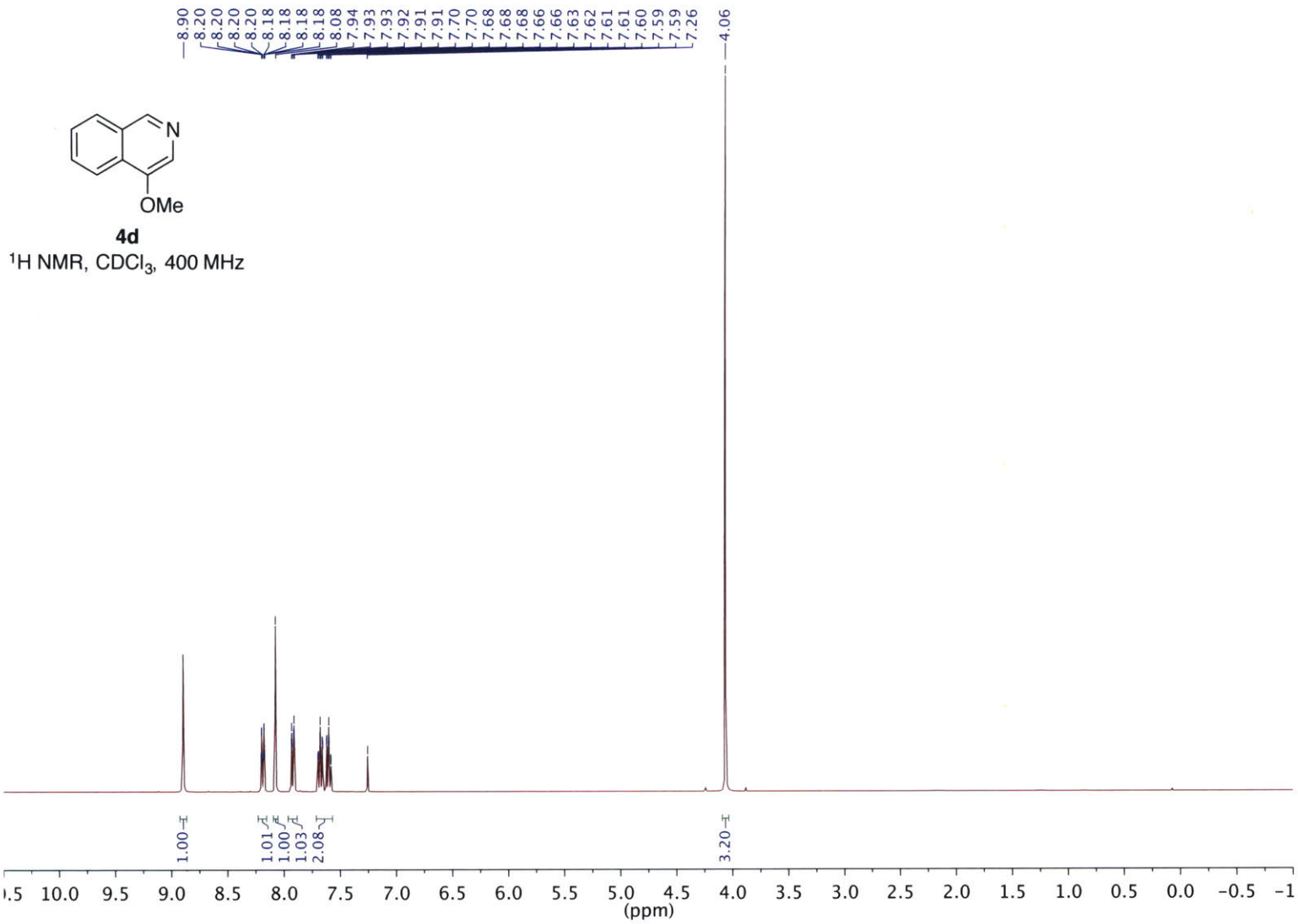
8.90
8.20
8.20
8.20
8.20
8.18
8.18
8.18
8.18
8.08
7.94
7.93
7.93
7.92
7.91
7.91
7.70
7.70
7.68
7.68
7.68
7.66
7.66
7.63
7.62
7.61
7.61
7.60
7.59
7.59
7.26
4.06
N
OMe
4d
1H NMR, CDCl3, 400 MHz
1.00
1.01
1.00
1.03
2.08
3.20
(ppm)

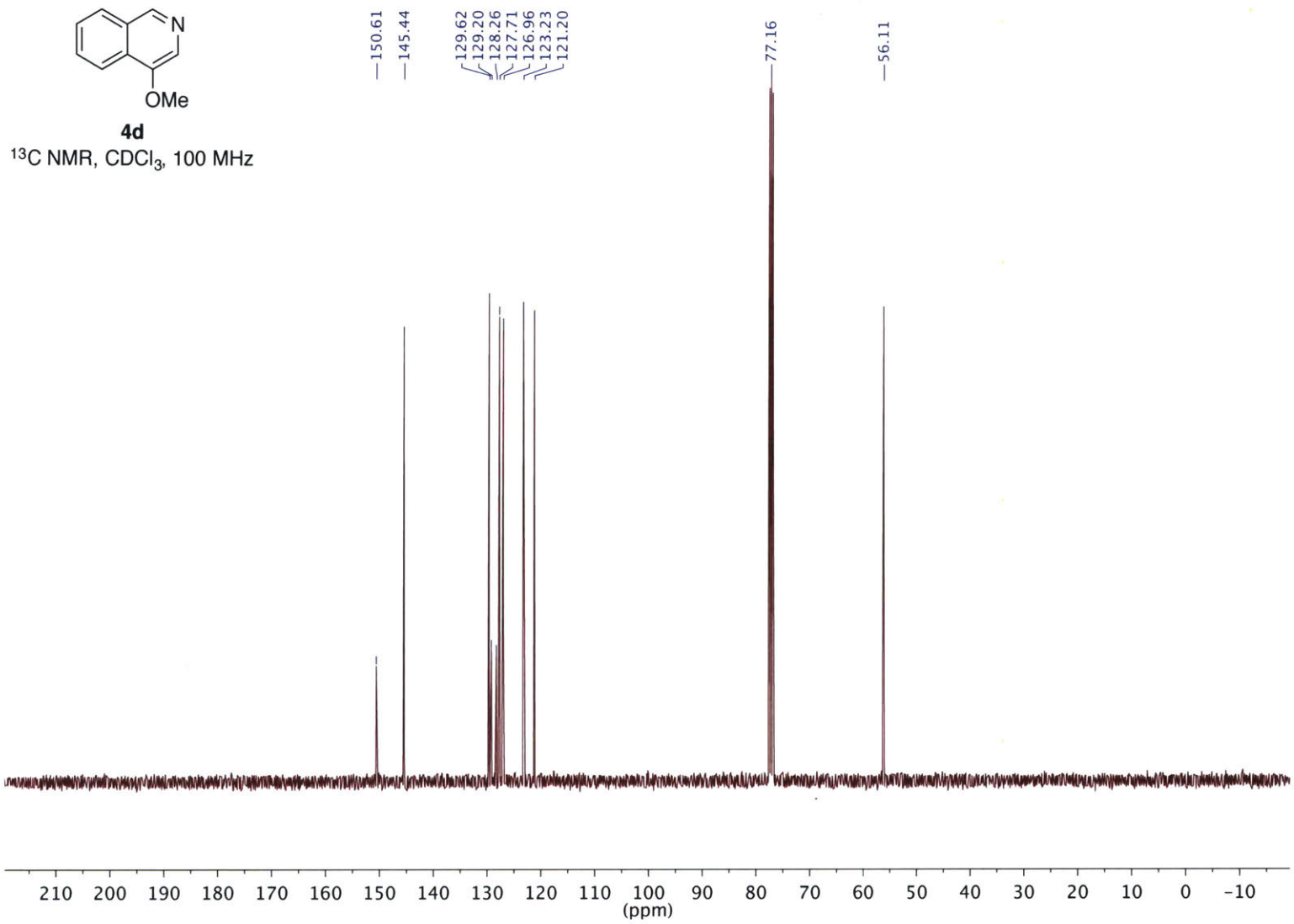
N
OMe
4d
^{13}C NMR, $CDCl_3$, 100 MHz
150.61
145.44
129.62
129.20
128.26
127.71
126.96
123.23
121.20
77.16
56.11
210 200 190 180 170 160 150 140 130 120 110 100 90 80 70 60 50 40 30 20 10 0 -10
(ppm)

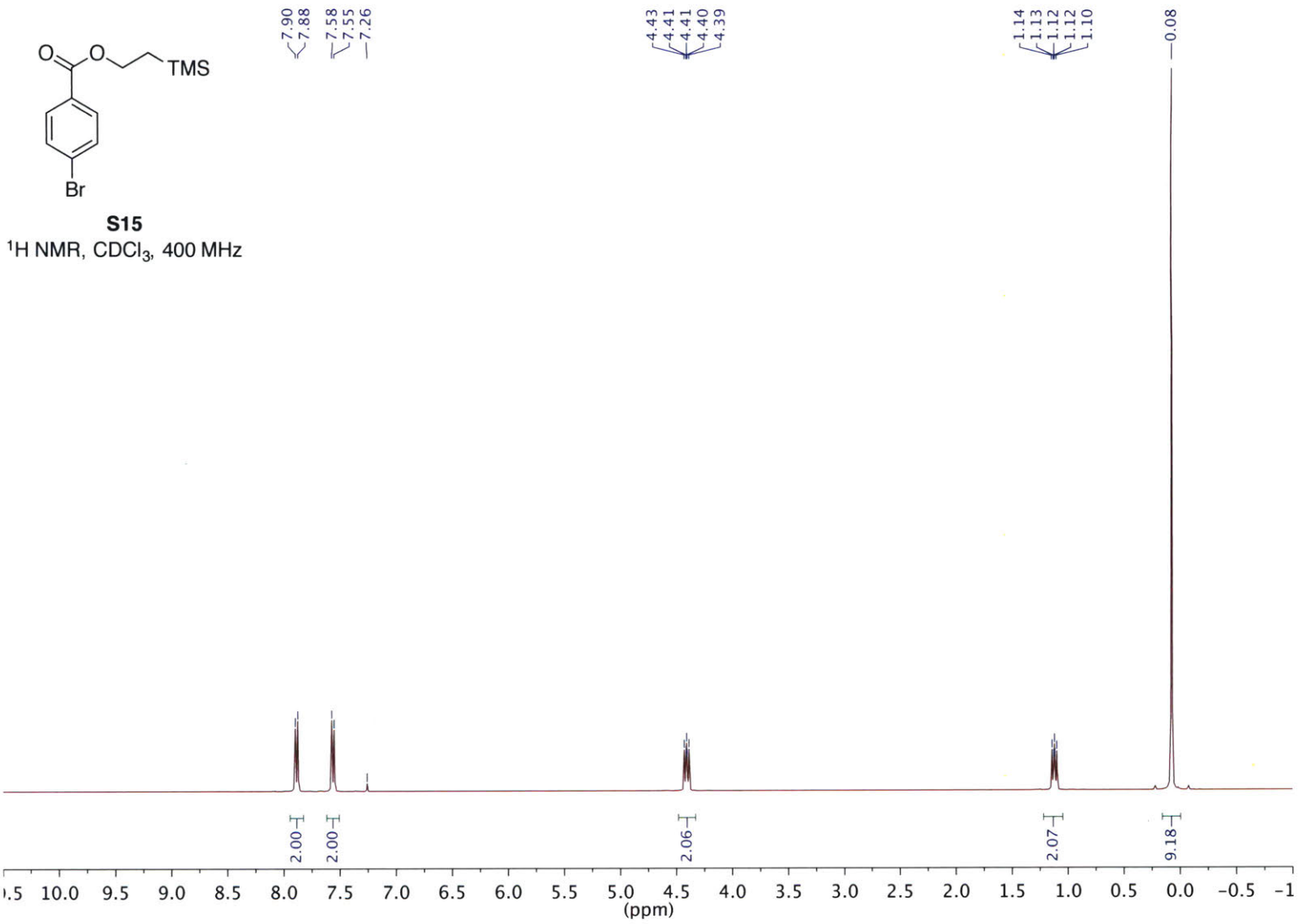

S15

^{1}H NMR, $CDCl_3$, 400 MHz

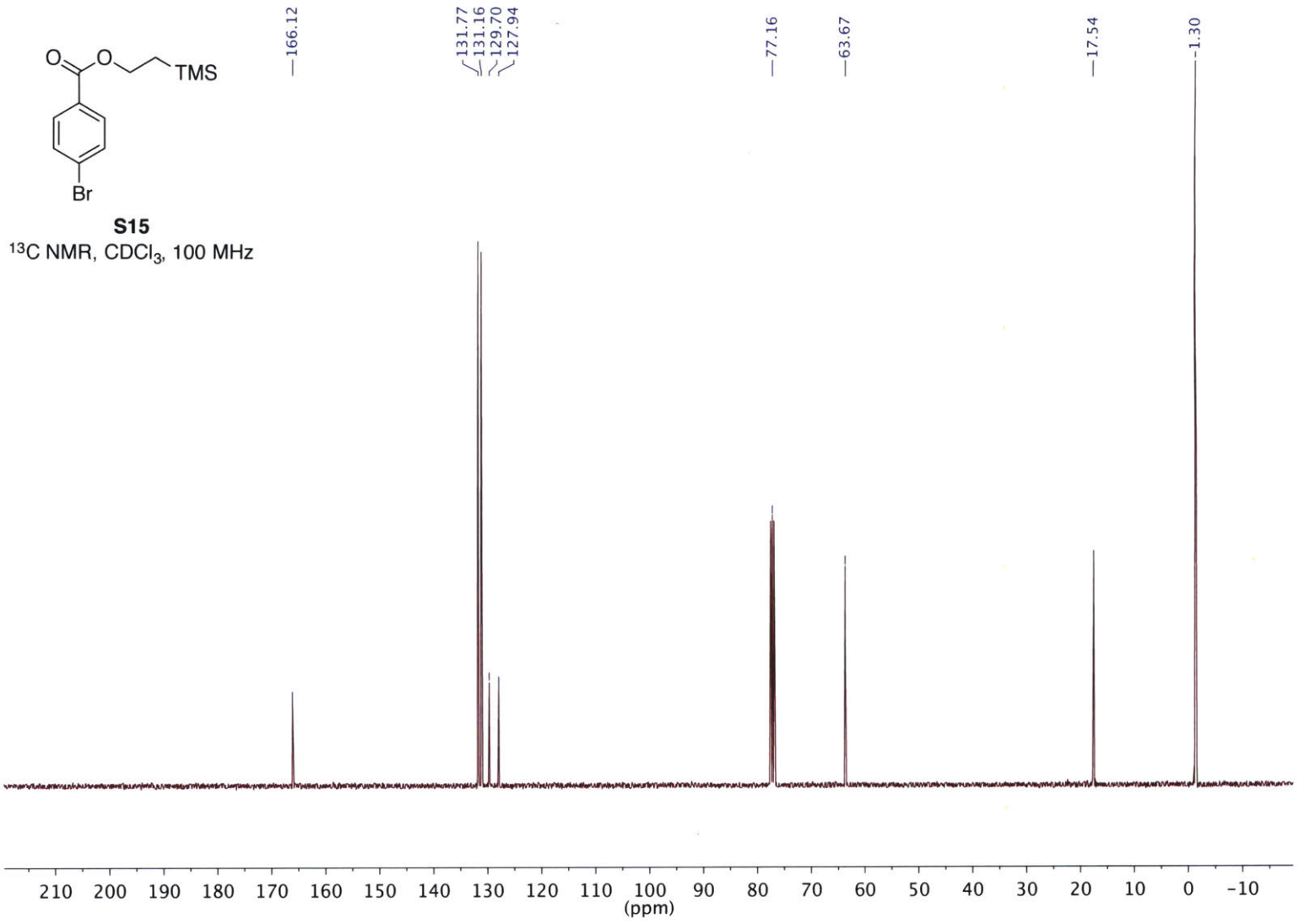

S15

^{13}C NMR, $CDCl_3$, 100 MHz

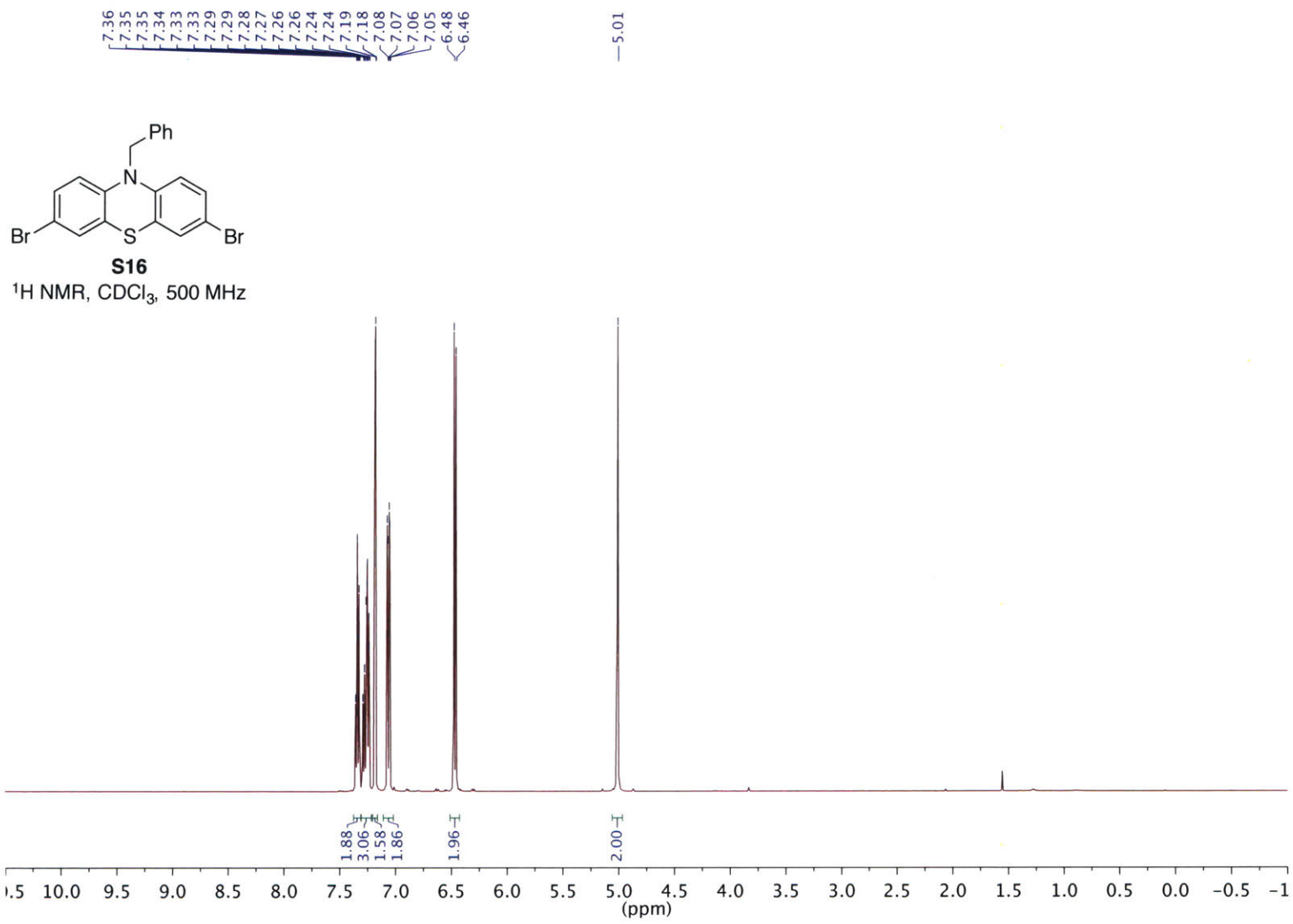
7.36
7.35
7.35
7.34
7.33
7.33
7.29
7.29
7.28
7.27
7.26
7.26
7.24
7.24
7.19
7.18
7.08
7.07
7.06
7.05
6.48
6.46
5.01
Ph
N
Br
S
Br
S16
1H NMR, CDCl3, 500 MHz
1.88
3.06
1.58
1.86
1.96
2.00
10.0
9.5
9.0
8.5
8.0
7.5
7.0
6.5
6.0
5.5
5.0
4.5
4.0
3.5
3.0
2.5
2.0
1.5
1.0
0.5
0.0
-0.5
-1
(ppm)

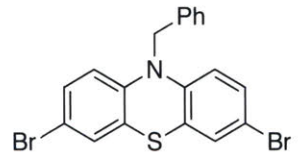

S16

^{13}C NMR, $CDCl_3$, 100 MHz

2.7. Chiral HPLC Spectra

NOTE: Since average ee values were reported, the displayed chromatograms may differ by 1% ee.

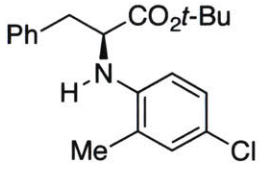

3a

HPLC analysis (OJ-H, 2% IPA–hexanes, 0.8 mL/min, 254 nm) indicated 95% ee: tR (minor) = 12.3 min, tR (major) = 17.6 min.

DL–3a

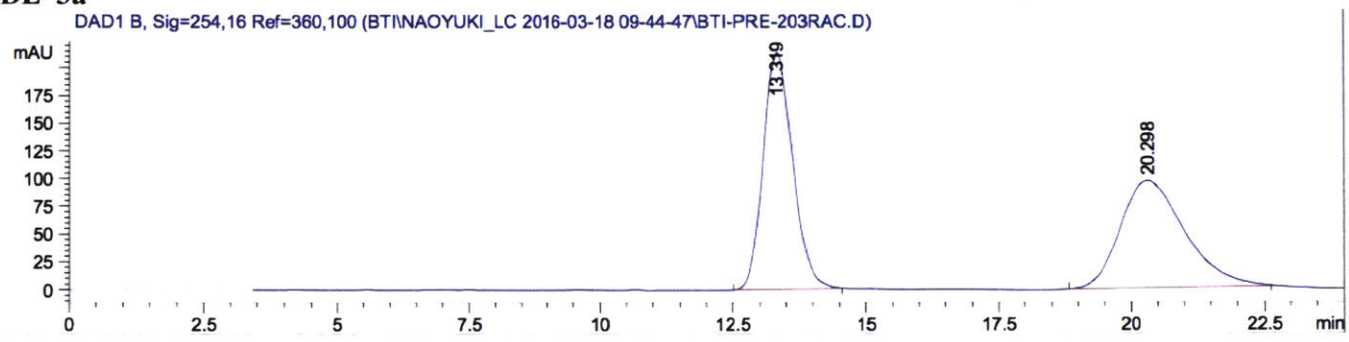

Peak #	RetTime [min]	Type	Width [min]	Area [mAU*s]	Height [mAU]	Area %
1	13.319	BB	0.6006	8279.04102	213.43217	50.3695
2	20.298	BB	1.2737	8157.56689	96.55048	49.6305

L–3a: 95% ee

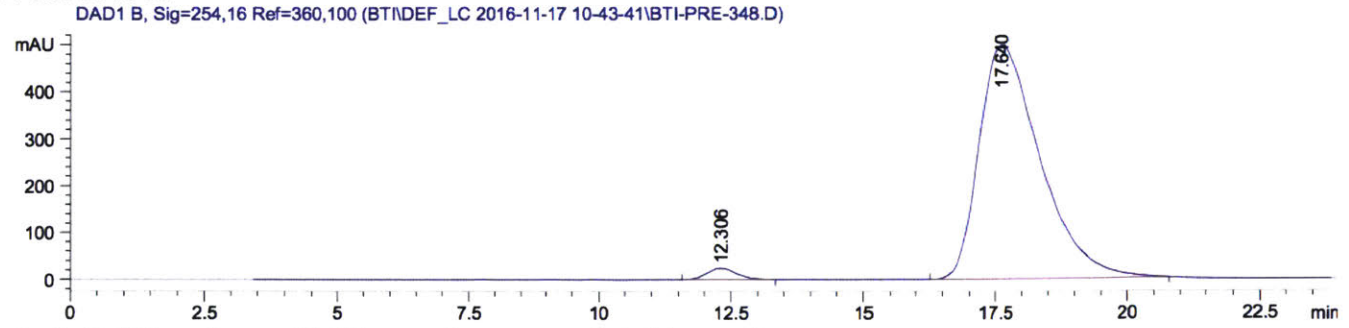

Peak #	RetTime [min]	Type	Width [min]	Area [mAU*s]	Height [mAU]	Area %
1	12.306	BB	0.6064	948.80786	24.15026	2.3094
2	17.640	BB	1.2277	4.01360e4	497.26773	97.6906

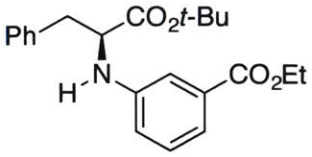

3b

HPLC analysis (OJ-H, 2% IPA-hexanes, 0.8 mL/min, 230 nm) indicated 94% ee: tR (major) = 26.8 min, tR (minor) = 38.2 min.

DL–3b

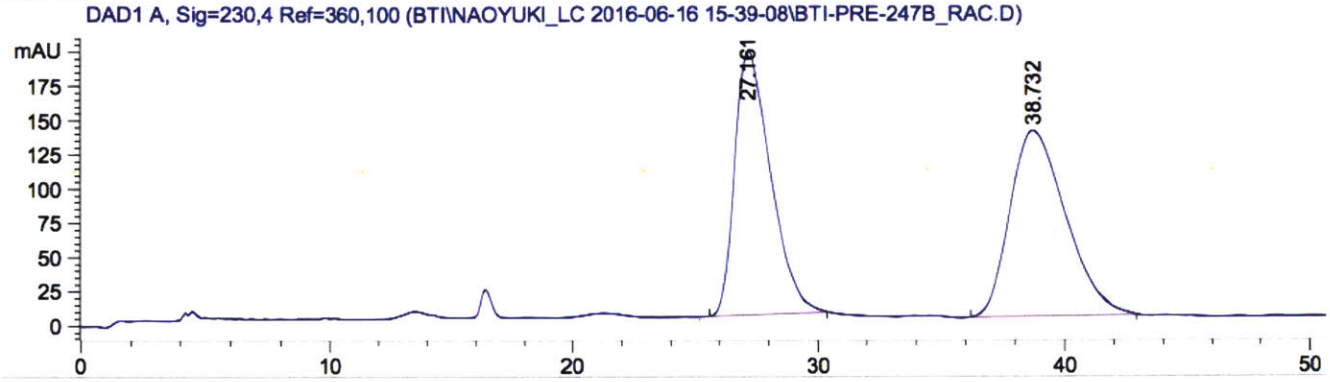

Peak #	RetTime [min]	Type	Width [min]	Area [mAU*s]	Height [mAU]	Area %
1	27.161	BB	1.4781	1.96700e4	192.83383	48.0204
2	38.732	BB	2.2410	2.12917e4	135.66818	51.9796

L–3b: 94% ee

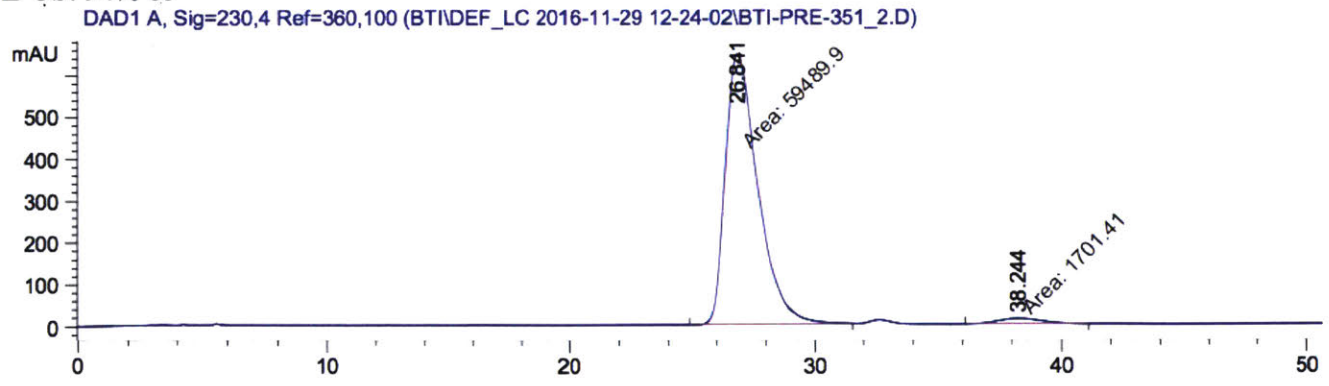

Peak #	RetTime [min]	Type	Width [min]	Area [mAU*s]	Height [mAU]	Area %
1	26.841	MM	1.5359	5.94899e4	645.56183	97.2195
2	38.244	MM	2.1205	1701.41028	13.37261	2.7805

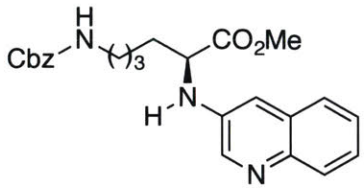

3c

HPLC analysis (OD-H, 30% IPA-hexanes, 0.8 mL/min, 254 nm) indicated 96% ee: tR (minor) = 15.9 min, tR (major) = 67.8 min.

DL–3c

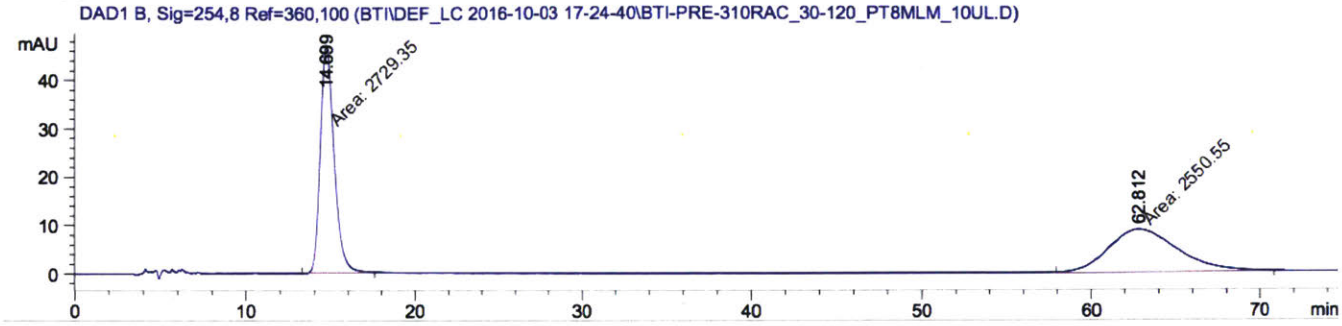

Peak #	RetTime [min]	Type	Width [min]	Area [mAU*s]	Height [mAU]	Area %
1	14.699	MM	0.9643	2729.34766	47.17174	51.6932
2	62.812	MM	4.7923	2550.54956	8.87030	48.3068

L–3c: 96% ee

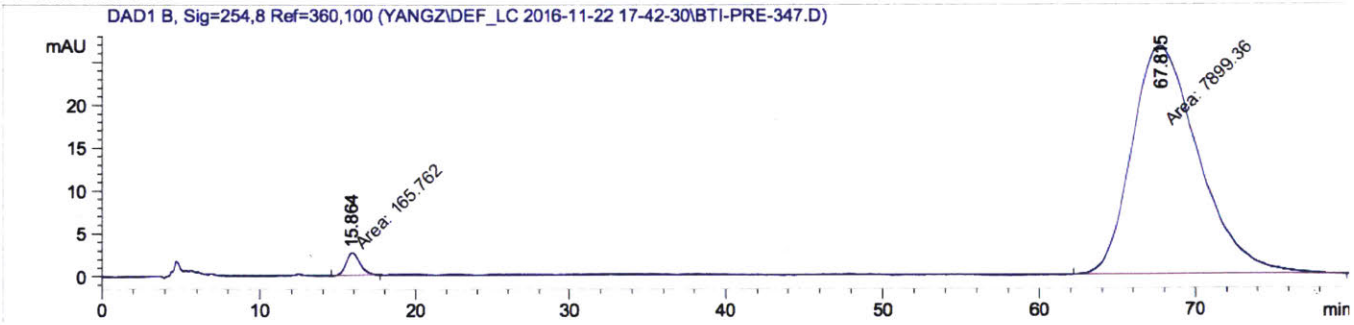

Peak #	RetTime [min]	Type	Width [min]	Area [mAU*s]	Height [mAU]	Area %
1	15.864	MM	1.0490	165.76157	2.63365	2.0553
2	67.815	MM	4.9541	7899.35938	26.57516	97.9447

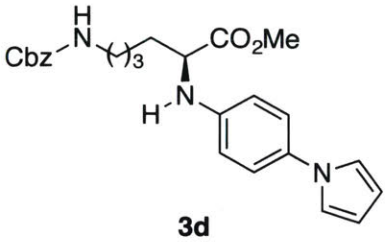

3d

HPLC analysis (OD-H, 20% IPA-hexanes, 0.8 mL/min, 254 nm) indicated 98% ee: tR (minor) = 28.3 min, tR (major) = 36.9 min.

DL–3d

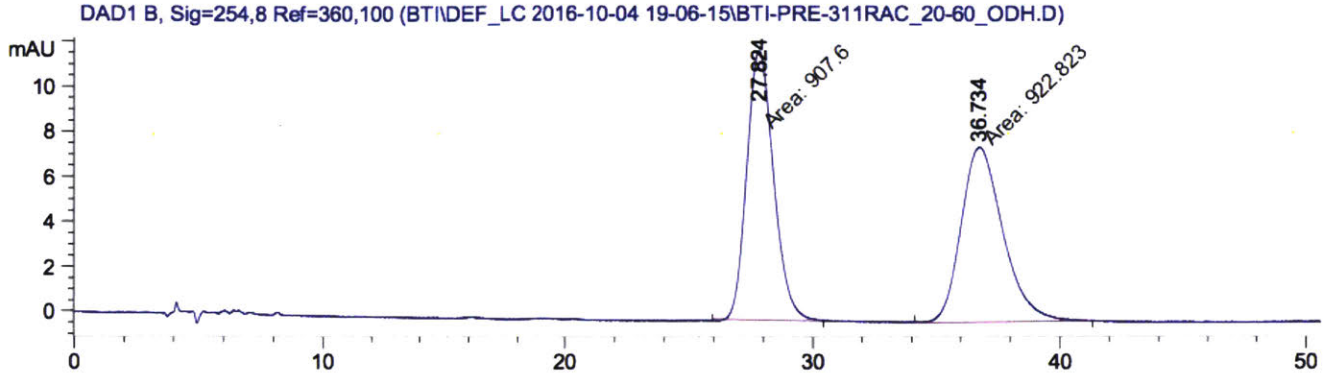

Peak #	RetTime [min]	Type	Width [min]	Area [mAU*s]	Height [mAU]	Area %
1	27.824	MM	1.2634	907.60040	11.97257	49.5842
2	36.734	MM	1.9675	922.82269	7.81737	50.4158

L–3d: 98% ee

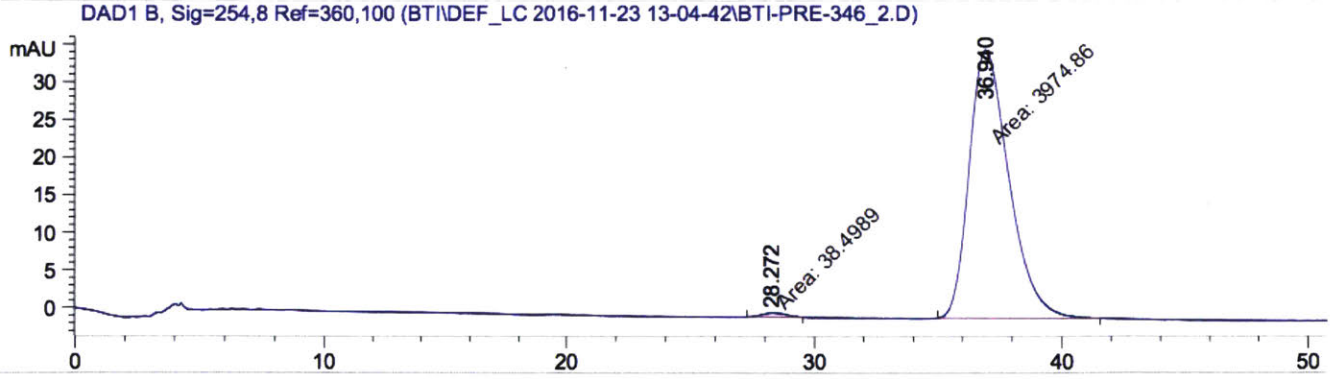

Peak #	RetTime [min]	Type	Width [min]	Area [mAU*s]	Height [mAU]	Area %
1	28.272	MF	1.1664	38.49888	5.50127e-1	0.9593
2	36.940	FM	1.8631	3974.85791	35.55776	99.0407

Chapter 3. Structure-Activity Relationship of Phosphine Ligands for the Fluorination of Five-membered Heteroaromatic Compounds

3.1. Introduction

Five-membered-ring heterocycles are prevalent structures in pharmaceuticals.[1] Despite the abundance of these structures and C–F bonds in medicinally relevant targets, there is a deficiency of such heterocycles possessing a C–F bond on the heteroaromatic ring.[2] As is the case for the six-membered-ring analogues, this is largely due to the synthetic challenges associated with installing the fluorine atom. In addition to the Balz–Schiemann and HalEx reactions (*vide supra;* Introduction, page 12), common methods for aromatic fluorination include reaction of organometallic intermediates with electrophilic fluorine sources[3] as well as direct fluorination with fluorine gas.[4,5] These methods have limited functional group compatibility, and in the case of fluorine gas, require special equipment.

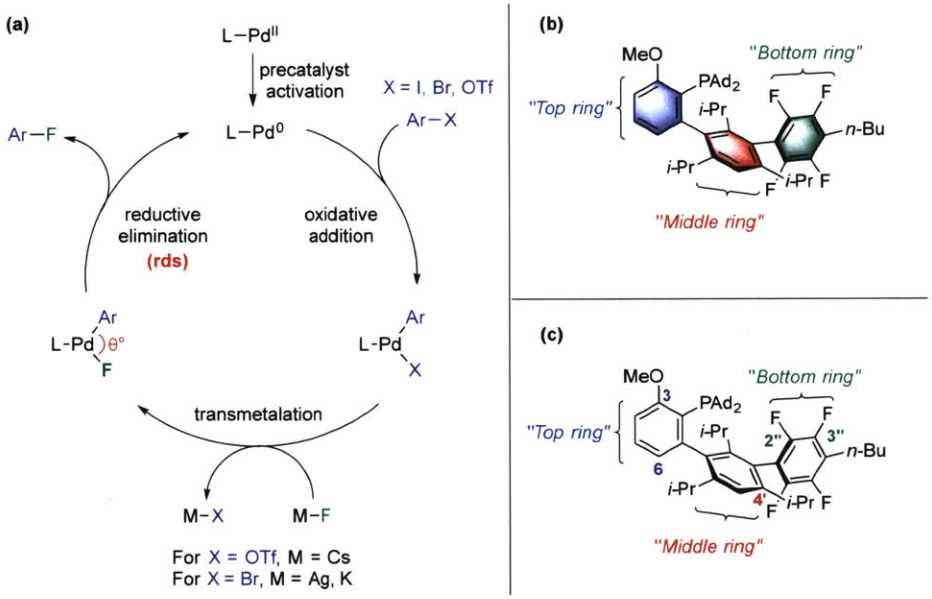

Figure 1. (a) Proposed catalytic cycle for Pd-catalyzed aromatic fluorination. (b) Structure of AlPhos and designation of ring systems (c) Numbering system of AlPhos.

In contrast, the Pd-catalyzed fluorination of aryl (pseudo)halides with metal fluorides takes place under mild conditions (Figure 1a). However, five-membered-ring heteroaryl electrophiles are particularly challenging substrates in this reaction despite recent advances in catalyst design. One major challenge arises from the Lewis basic nature of these heterocycles, as they are potential catalyst poisons.[6] In addition, the C–F reductive elimination is more challenging compared to the six-membered-ring arenes,[7] predominantly due to two effects. First,

the smaller size of the electrophile increases the angle between the aryl group and fluoride undergoing reductive elimination (θ in Figure 1a),[8] which is geometrically further away from the transition state for reductive elimination. The second effect is the electron-rich nature of the heteroarene, which is known to retard reductive elimination.[7,9] Indeed, it has been computed that the barrier for C–F reductive elimination is approximately 7.0 kcal/mol higher for five-membered ring electrophiles (i.e., 2-thienyl) compared to six-membered ring analogues (i.e., phenyl).[2]

We hypothesized that a change in catalyst structure might be able to facilitate the challenging reductive elimination of smaller electrophiles. Given that **L1** (AlPhos, Figure 1b) has been shown to be an excellent ancillary ligand in Pd-catalyzed C–F coupling,[10] we decided to undertake a systematic study of the ligand framework in order to understand which structural features are responsible for the higher reactivity of catalysts derived from **L1**. We subsequently examined nine phosphine ligands, generally modifying a single structural element at a time. Specifically, we iteratively modified the substituents on the top ring, middle ring, and the bottom ring (Figure 2).

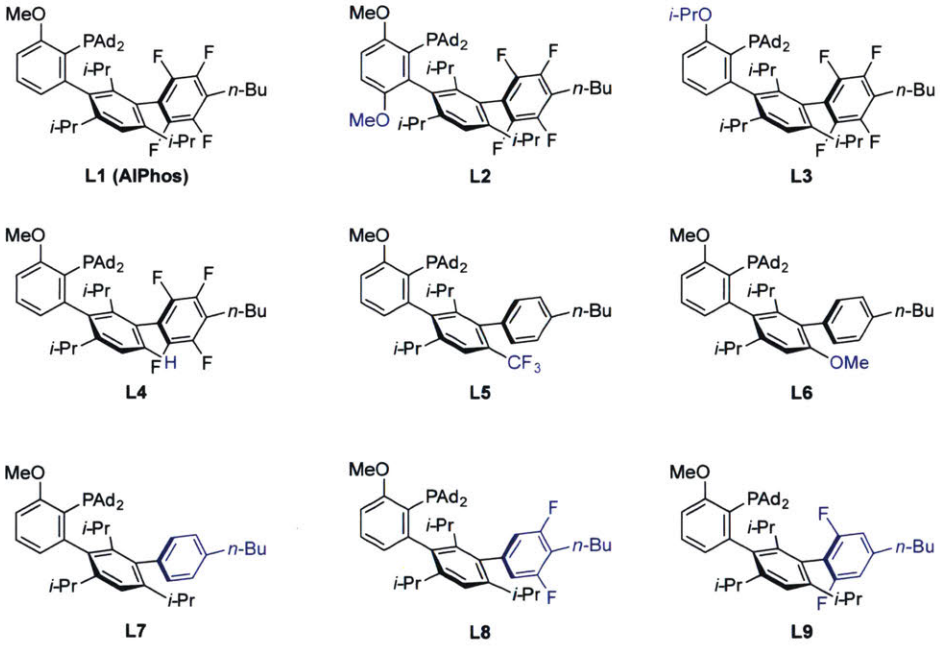

Figure 2. Ligand structures used to systematically study the Pd-catalyzed fluorination reaction.

3.2. Results and Discussion

The proposed ligands were synthesized and evaluated by forming the corresponding L–Pd(4-trifluoromethylphenyl)Br complexes, which were previously shown in Chapter 2 to be competent precatalysts. These complexes were thus used as the palladium and ligand source for the fluorination of model thiophene derivative **1** (Figure 3), since this substrate is known to give product under the reaction conditions. By analyzing the initial rate of fluorination, we could compare the reactivity of each catalyst system and rationally design new ones based on our assessment of which structural features were significant. Initial rate measurements were performed by setting up runs in parallel and monitoring the yield of **2** by ^{19}F NMR spectroscopy after 1, 3, and 5 hours.

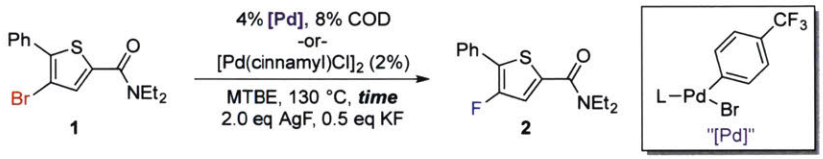

Figure 3. Fluorination of a model thiophene derivative.

We commenced our studies by examining changes to the top ring of the ligand. We hypothesized that increasing the steric hindrance near phosphorus would result in a faster C–F reductive elimination, and so **L3** was synthesized. Additionally, previous catalyst systems utilized ligands with substitution at the 6 position, so **L2** was prepared in order to make a direct comparison to **L1**. The initial rate of reactions employing catalysts derived from **L1** and **L3** were found to be comparable,[11] suggesting that **L3** does not provide a significant steric effect (Chart 1). On the other hand, the catalyst system derived from **L2** was notably slower, indicating that the "BrettPhos" family of top rings are not optimal for the fluorination reaction.

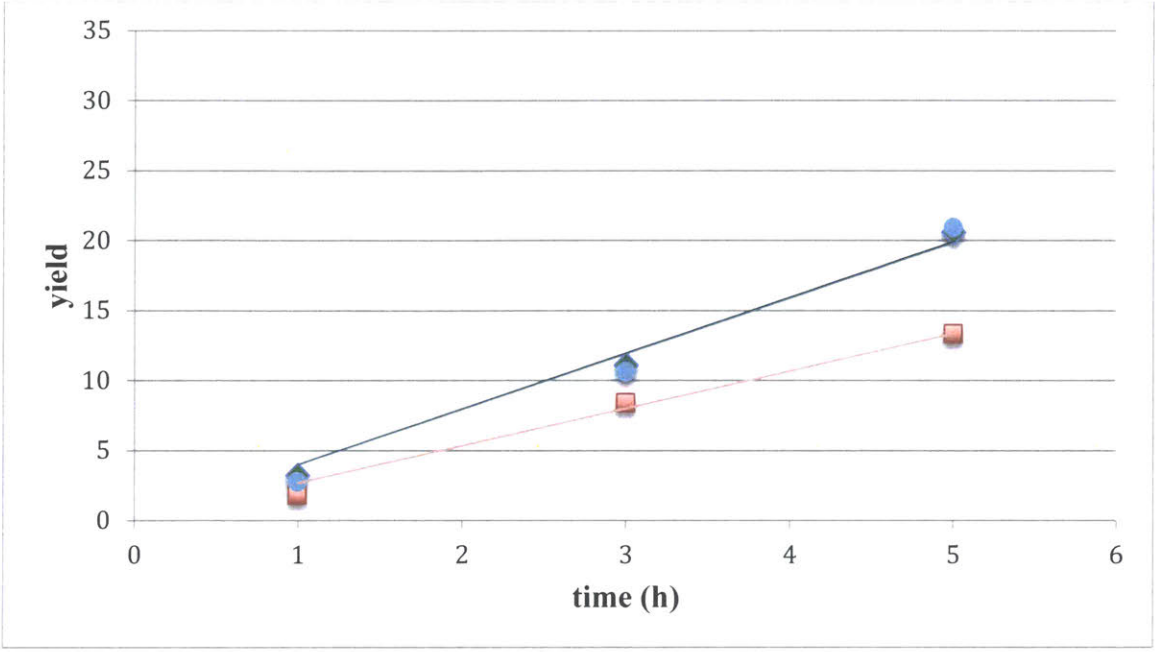

Chart 1. Initial rate data for catalysts derived from ligands with three different top rings. Data displayed as yield versus time for catalysts derived from **L1** (◆), **L2** (■), and **L3** (•). Note: data for **L1** and **L3** overlap.

Next, we sought to make changes to the middle ring, namely the 4′ position, which we thought might electronically perturb the C1′ *ipso* interaction with the palladium center. We first set out to synthesize **L4**, which differs from **L1** in that the 4′ *i*-Pr group is replaced by a hydrogen atom. Though eventually this ligand was obtained, the synthetic route was tedious (see experimental section 3.4.IV.), so we modified the study to incorporate ligands with more synthetically accessible *bottom* rings (i.e., **L5, L6**). Though **L5** and **L6** change both the 4′ substituent and the third aryl group, they can be directly compared to **L7** in order to ascertain their relative efficacy. As summarized in Chart 2, the rate of fluorination exhibited by the **L4**-based catalyst was significantly slower than those derived from either **L1** or **L7**. When the 4′ group was replaced with a trifluoromethyl group, as in **L5**, the reaction rate profile is similar to that of **L7**-based catalysts. Finally, substitution of a methoxy group at the 4′ position (i.e., **L6**) results in a totally ineffective catalyst system that fails to deliver any product. Taken together, these results suggest that an isopropyl, or possibly a trifluoromethyl, group is a superior 4′ substituent.

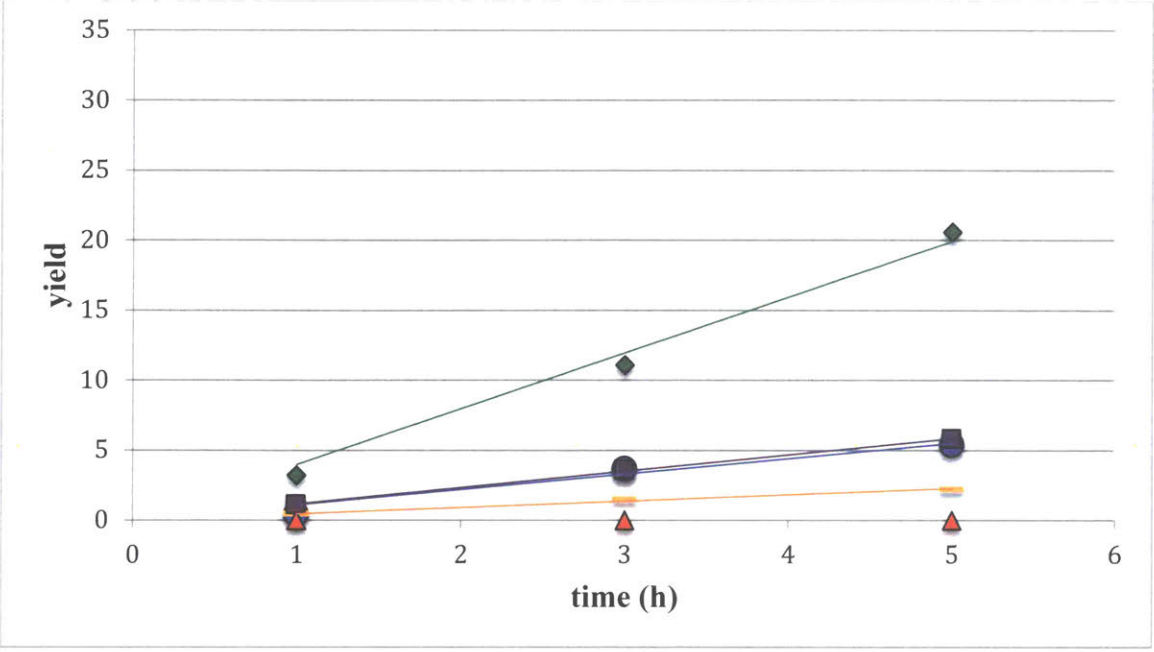

Chart 2. Initial rate data for catalysts derived from ligands with four different middle rings and **L1**. Data displayed as yield versus time for catalysts derived from **L1** (◆), **L4** (–), **L5** (■), **L6** (Δ), and **L7** (●). Note: data for **L5** and **L7** overlap.

The last three ligands analyzed possess changes to the bottom aryl group. We were particularly interested in assessing the role of fluorine substitution on this ring, so we designed ligands with no fluorine substitution (**L7**), substitution at the 3″ and 5″ positions (**L8**) and substitution at the 2″ and 6″ positions (**L9**). As noted previously, the catalyst derived from **L7** gives a rate of fluorination that is approximately one-third that of the corresponding **L1**-based catalyst. However, a striking difference was observed when examining **L8** and **L9** as supporting ligands: while the former gives comparable to reactivity to **L7**, the latter provides a rate of fluorination that rivals that of **L1** (Chart 3).

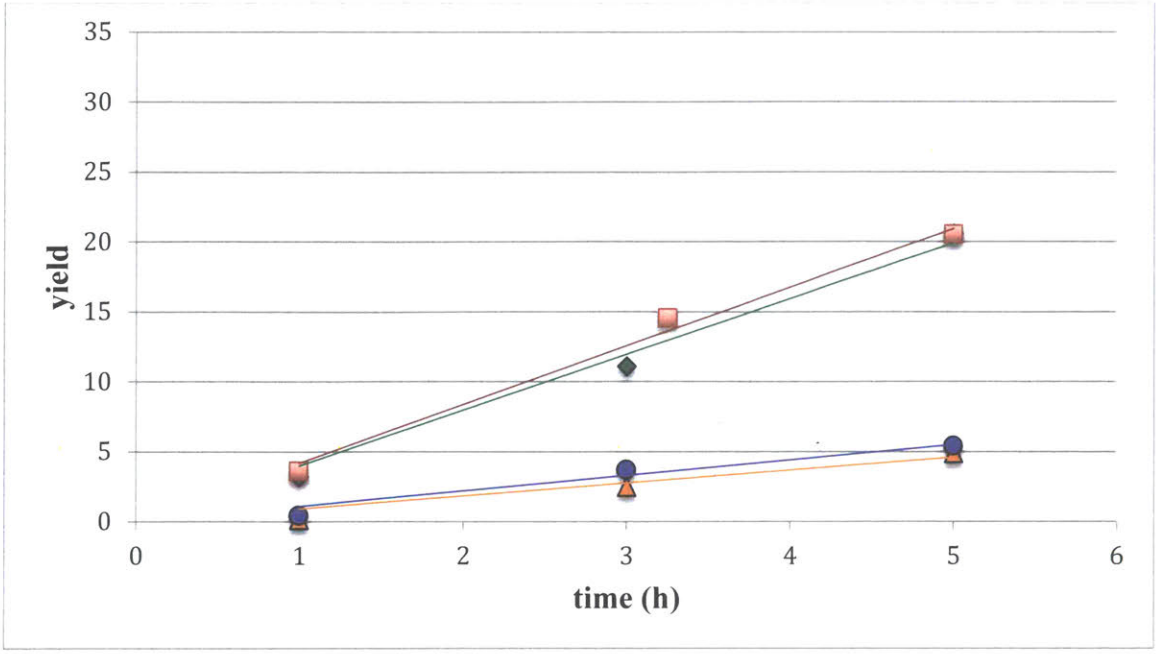

Chart 3. Initial rate data for catalysts derived from ligands with three different bottom rings and **L1**. Data displayed as yield versus time for catalysts derived from **L1** (◆), **L7** (●), **L8** (△), and **L9** (■).

We therefore concluded that substitution at C2″ and C6″ are critical for the fluorination reaction. Moreover, in light of these results, we suggest that the inclusion of some pairs of structural features provide cooperative effects: namely, substitution at the 4′ and the 2″/6″ positions of the ligand framework, since **L4** is a poor ancillary ligand but both **L1** and **L9** are competent supporting ligands. We hypothesize that having substitution at the 4′ position forces the bottom ring to be perpendicular to the middle ring, resulting in the 2″- and 6″-fluorine substituents pointing towards the presumptive Pd–F intermediate; the result is a repulsive interaction which destabilizes the ground state of the complex, causing an effective lowering of the barrier to reductive elimination (Figure 4a).[10] Furthermore, the group at C4′ must be large enough to enforce this geometry, which may explain why catalysts derived from **L5** and **L7** give improved rates compared to **L4** and **L6**: the trifluoromethyl group and isopropyl group are similar in size (A-values are 2.1 and 2.15, respectively), and significantly larger than H (A-value = 0) and OMe (A-value = 0.6).[12]

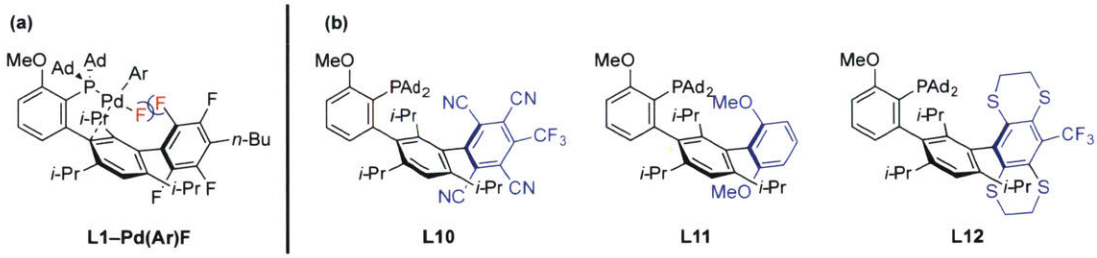

Figure 4. (a) Electronic repulsion between Pd–F and 2″–F of the ligand backbone. (b) New ligands proposed based on initial rate data.

These results suggested three new ligands (**L10, L11, L12**; Figure 4b) to us that retain the 4′ isopropyl substituent of the middle ring, but in which the 2″ and 6″ positions are modified, since this substitution pattern appeared to have the most profound impact on the rate of the fluorination reaction. Though **L10** could be prepared, we could not form a L–Pd(4-trifluoromethylphenyl)Br complex from it and no yield of **2** was realized employing conditions that utilized $[Pd(cinnamyl)Cl]_2$ as the Pd source. Presumably **L10** does not ligate to the metal center, and so the reactivity of the relevant catalyst could not be ascertained.

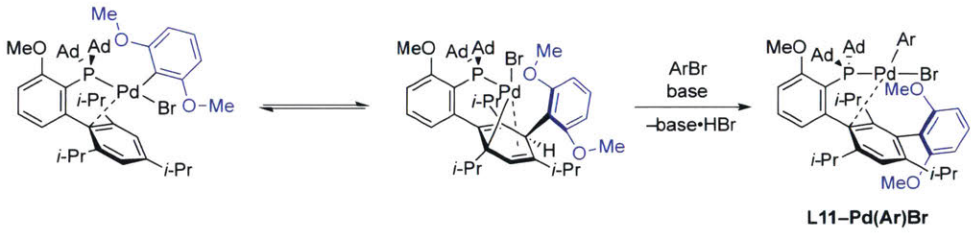

Figure 5. Synthesis of **L11** through a Pd-mediated dearomative rearrangement.

L11 could be readily synthesized through a Pd-mediated dearomative rearrangement (Figure 5),[13] and while its L–Pd(4-trifluoromethylphenyl)Br complex could be prepared, the complex was not soluble in organic solvents compatible with the fluorination reaction, making it difficult to obtain reliable initial rate data. The kinetic data was therefore obtained by using $[Pd(cinnamyl)Cl]_2$ as the Pd source.[14] The reaction performed in this way manifested an initial rate comparable to that seen using **L1** under the same conditions. This is consistent with the hypothesis that substitution at C2″ and C6″ exerts significant control over the reaction rate

(Chart 4). The last proposed ligand, **L12,** is currently being prepared. A summary of all the initial rate data is presented in Figure 6 as relative rates with **L1** set to $k_{rel} = 1.00$.

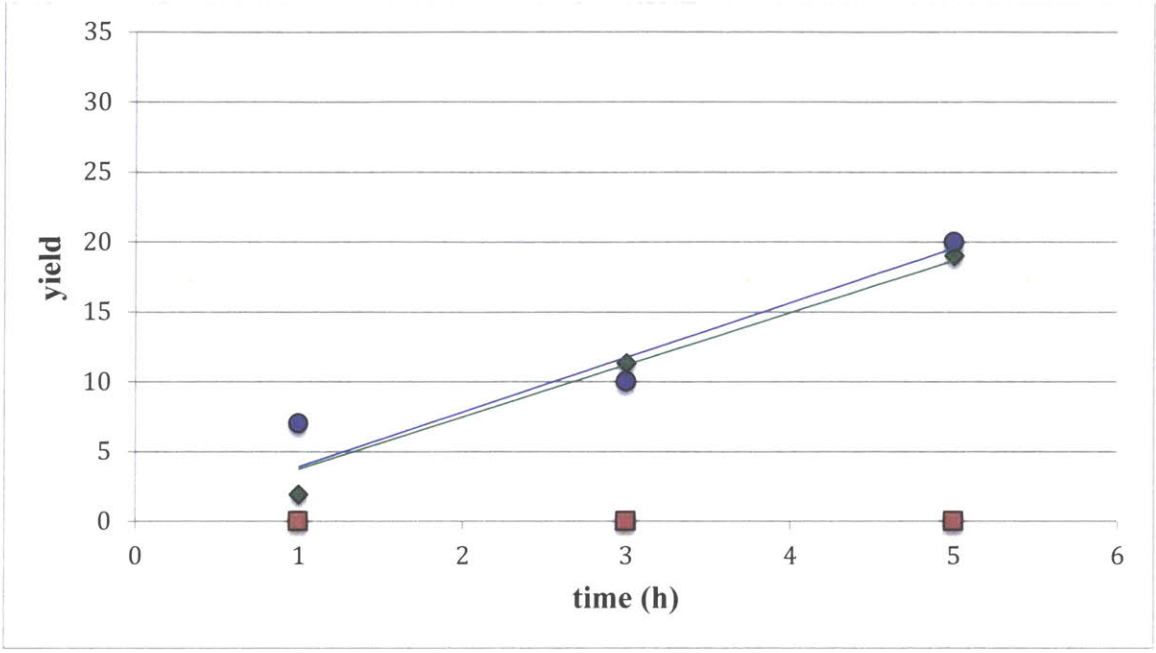

Chart 4. Initial rate data for catalysts derived from new proposed ligands and **L1** using $[Pd(cinnamyl)Cl]_2$ as Pd source. Data displayed as yield versus time for catalysts derived from **L1** (◆), **L10** (■), **L11** (●).

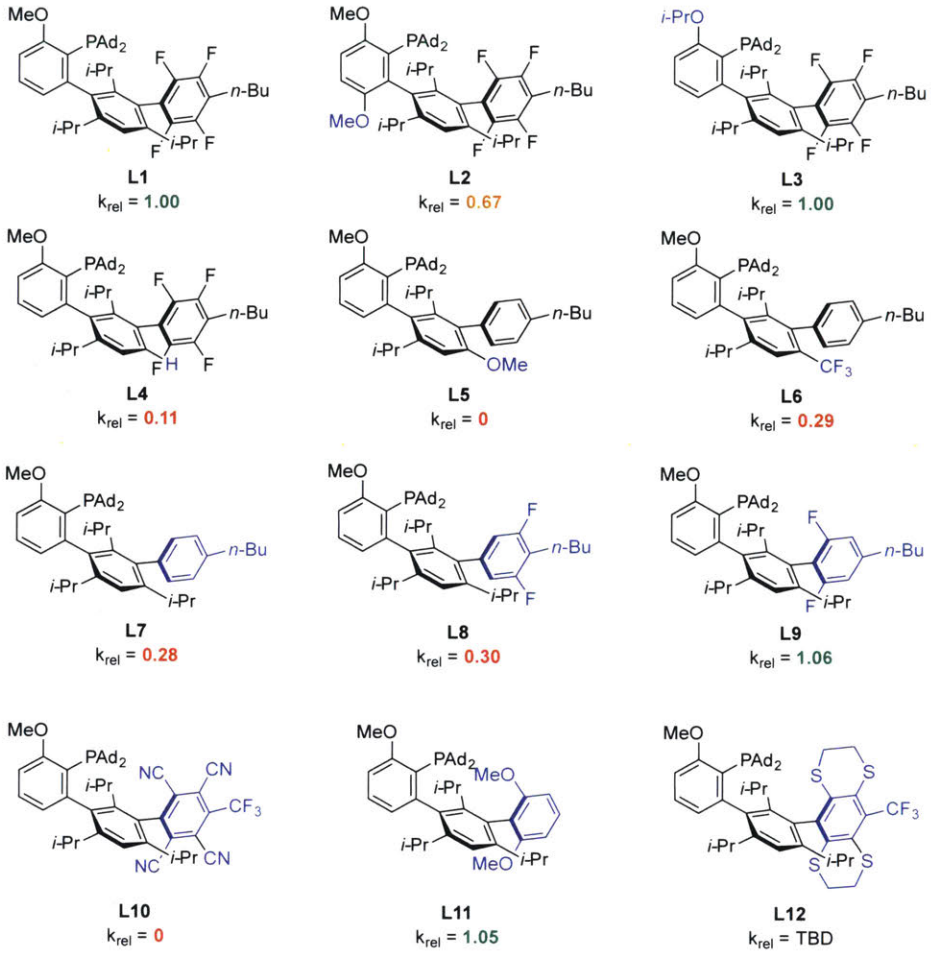

Figure 6. Relative rate data of **L1**–**L12** with **L1** set to k =1.00

3.3. Conclusion

In conclusion, we have systematically studied the ligand architecture of a dialkyl biaryl monophosphine that finds use in Pd-catalyzed aromatic fluorination. Initial rate studies revealed a significant rate dependence on the substitution pattern of C2″/C6″ as well as C4′ of the ligand framework. This analysis has enabled the rational design of new ligand scaffolds which may be able to more effectively promote the challenging C–F reductive elimination from Pd(II) with small, five-membered-ring heteroaryl electrophiles. The development of phosphine ligands for this transformation is an area of active research in the Buchwald laboratory.

3.4. Experimental

I. General Information

A) General Reagent Information: Commercial solvents and reagents were purchased from Aldrich Chemical Company, Strem Chemicals, Acros Organics, Alfa Aesar, Combi Blocks, Oakwood Chemical, and Chem-Impex and used as received, with the following exceptions. Phosphines **L2** and **L7** were prepared by Joey Dennis, for which the author is grateful. RuPhos was a gift from Sigma-Aldrich, for which the author is grateful. Anhydrous MTBE was purchased from Aldrich Chemical Company in Sure-Seal™ bottles, sparged with argon for one hour, and stored in a nitrogen-filled glovebox. Toluene, tetrahydrofuran (THF) and CH_2Cl_2 were purchased from J.T. Baker in CYCLE-TAINER® solvent-delivery kegs and vigorously purged with argon for 2 h, followed by passing it under argon pressure through two packed columns of neutral alumina. Silver(I) fluoride was stored in a nitrogen-filled glovebox. Potassium fluoride (KF) was ground in a nitrogen-filled glovebox using an oven-dried mortar and pestle. The finely ground KF was then filtered through a 45 μm stainless-steel size sieve (Cole Parmer) to obtain KF with particle size of <45 μm.[1] 1,5-cyclooctadiene (≥99%) were purchased from Sigma-Aldrich and stock solutions were prepared in a nitrogen-filled glovebox. Potassium carbonate, copper(I) chloride, and copper(I) bromide were stored in a nitrogen-filled glovebox. Large reaction tubes (36 mL capacity; 20 x 150 mm, Part No. 14-959-37C), medium reaction tubes (25 mL capacity, 20 x 125 mm, Part No. 14-959-37A), small reaction tubes (8 mL capacity, 13 x 100 mm, Part No. 14-959-35C), large/medium screw-caps (Kimble-Chase, Open Top S/T Closure, Part No. 73804-18400), small screw caps (Thermo Scientific, Part No. C401566), large/medium septa (Thermo Scientific PTFE/silicone, Cat No. B7995-18), and small septa (Thermo Scientific PTFE/Silicone, Cat No. C4015-60) were purchased from Fischer Scientific. Compounds were purified using a Biotage® Isolera system, employing polypropylene cartridges preloaded with silica gel (Silicycle SilaFlash® F60 silica gel) or with new Biotage® SNAP cartridges, unless otherwise noted. Samples were eluted using a flow rate of 50–100 mL/min, with detection by UV (254 nm). Analytical thin-layered chromatography (TLC) was performed using glass plates pre-coated with silica gel (0.25 mm, 60 Å pore size) impregnated with a fluorescent indicator (254 nm). TLC plates were visualized by exposure to ultraviolet light (UV). **L1**,[10] **S1**,[10] di(1-adamantyl)chlorophosphine,[15] (COD)Pd($CH_2TMS)_2$,[16] **1**,[9] **S4–S7**,[17] RuPhos Pd G3,[18] XantPhos

Pd G3[18] and **S17**[19] were prepared according to literature procedures. **L1–Pd(Ar)Br** was prepared as described in Chapter 2.

B) General Analytical Information: Compounds were analyzed by ^{1}H, ^{13}C, ^{19}F, and ^{31}P nuclear magnetic resonance (NMR) spectroscopy where appropriate. NMR spectra were recorded on a Bruker Avance Neo-400 MHz spectrometer, a Bruker Avance Neo-500 MHz spectrometer, and a Bruker Avance Neo-600 MHZ spectrometer. ^{1}H and ^{13}C spectra were calibrated using residual solvent as an internal reference ($CDCl_3$: δ 7.26 ppm and δ 77.16 ppm, respectively; C_6D_6: δ 7.16 ppm and δ 128.1 ppm, respectively). Elemental analyses were performed by Atlantic Microlabs Inc., Norcross, GA, USA. High-resolution mass spectra were recorded on an Agilent Technologies 6545 Q-TOF LC/MS system. The following abbreviations were used to explain multiplicities: s = singlet, bs = broad singlet, d = doublet, t = triplet, q = quartet, p = pentet, sx = sextet, h = heptet, m = multiplet. Melting points were obtained using a Stanford Research Systems EZ-Melt melting point apparatus. Attenuated total reflectance Fourier transform infrared spectra (ATR-FTIR) were obtained using a Thermo Scientific Nicolet iS5 FT-IR spectrometer (iD5 ATR, diamond) referenced to a polystyrene standard and data reported as frequency of absorption (cm^{-1}).

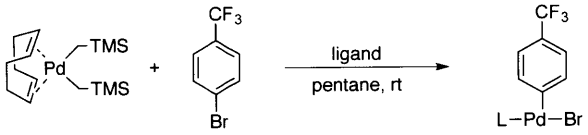

General Procedure A for the Synthesis of Oxidative Addition Complexes: In a nitrogen-filled glovebox, an oven-dried 36 mL screw-cap tube (or 50–100 mL round-bottomed flask) equipped with a magnetic stir bar was charged with ligand (1.00 equiv). Solvent (anhydrous pentane and/or Et_2O) was added and the reaction mixture was stirred until all of the ligand had dissolved. Then, 4-bromobenzotrifluoride (1.50–2.00 equiv) was added via microliter pipette, followed by (COD)Pd($CH_2TMS)_2$ (1.00–1.10 equiv). The reaction vessel was sealed with a screw-cap that had been fitted with a Teflon septum (or a rubber septum if a round-bottomed flask), removed from the glovebox, and the reaction mixture vigorously stirred at rt for 17–48 h. At this time, the reaction vessel was opened to the air and the resulting precipitate was isolated by filtration using a sintered glass funnel. The filter cake was washed with pentane and then dried under high vacuum to afford the oxidative addition complex.

General Procedure B: C–P Bond Formation

An oven-dried Schlenk tube bearing a sidearm and equipped with a magnetic stir bar was charged with aryl halide (1.00 equiv). The tube was sealed with a rubber septum and the side arm connected to a Schlenk line. The tube was evacuated and then backfilled with argon. This sequence was repeated two additional times. Then, anhydrous THF was added via syringe to bring the concentration of the aryl halide to 0.30 M. The tube was then cooled to –78 °C using a dry ice/acetone bath. Then, *t*-BuLi (1.70 M in pentane, 2.10 equiv) was added dropwise and the reaction mixture was allowed to stir at –78 °C for 1 h. At this time, the rubber septum was exchanged for a Teflon stopcock under a counterflow of argon, and the *n*-pentane from the *t*-BuLi solution was removed under vacuum with stirring at –78 °C using an in-line vacuum trap cooled with liquid nitrogen. Once the solvent had reached approximately two-thirds of its initial level, the vessel was backfilled with argon, and CuCl (1.10 equiv) was added in one solid portion under a counterflow of argon. The tube was sealed with a rubber septum and the reaction mixture was allowed to stir at rt for 0.5 h. Then, the rubber septum was removed and Ad_2PCl (1.10 equiv) was added as a solid in one portion under a counterflow of argon. Anhydrous toluene (approximately 1.4 times the volume of THF used) was then added via syringe, and the tube was sealed with a Teflon stopcock. The reaction mixture was allowed to stir in a pre-heated oil bath at 140 °C **behind a blast shield** for 16–24 h. At this time, the reaction mixture was allowed to cool to rt, the tube was unsealed, and the reaction mixture was diluted with EtOAc and transferred to a separatory funnel. The organic phase was washed with ammonium hydroxide (28–30% NH_3 basis)/brine solution (2:1) until the aqueous washings were no longer blue. Then, the organic phase was washed with brine, dried over magnesium sulfate, filtered, and concentrated with the aid of a rotary evaporator. The residue was purified via trituration from MeOH, by silica gel chromatography, or by crystallization as indicated for each ligand.

II. Experimental Procedure and Characterization of **L2**–Pd(Ar)Br

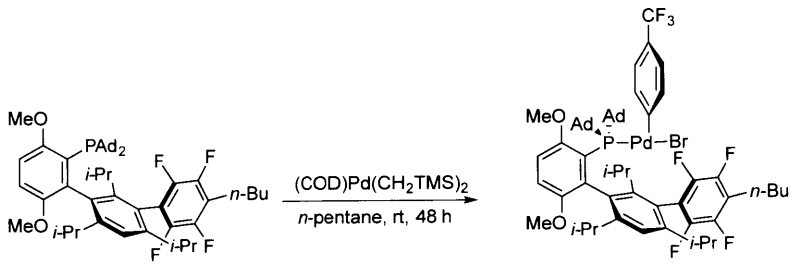

L2 **L2–Pd(Ar)Br** 42%

L2–Pd(Ar)Br was prepared following general procedure A. In a 36 mL reaction tube, a mixture of **L2** (100 mg, 0.118 mmol, 1.00 equiv), 4-bromobenzotrifloride (25 μL, 0.177 mmol, 1.50 equiv), and (COD)Pd($CH_2TMS)_2$ (50.6 mg, 0.130 mmol, 1.10 equiv) was stirred in pentane (10 mL) at rt for 48 h. The complex was filtered outside the glovebox to afford **L2–Pd(Ar)Br** as a light yellow-green solid (57 mg, 42%). **^{1}H NMR** (600 MHz, $CDCl_3$): δ 7.40 (d, J = 8.3 Hz, 2H), 7.32 (s, 1H), 7.06 (dd, J = 15.0, 8.3 Hz, 2H), 6.92 (d, J = 8.9 Hz, 1H), 6.84 (d, J = 8.8 Hz, 1H), 3.84 (s, 3H), 3.39 (s, 3H), 3.21 (h, J = 7.2 Hz, 1H), 2.80 (t, J = 7.8 Hz, 2H), 2.38 (m, 9H), 2.20 – 2.09 (m, 3H), 2.01 (m, 4H), 1.87 – 1.77 (m, 9H), 1.72 – 1.63 (m, 12H), 1.56 (d, J = 12.0 Hz, 5H), 1.41 (p, J = 7.5 Hz, 2H), 1.36 (d, J = 6.8 Hz, 3H), 1.28 (d, J = 7.1 Hz, 3H), 1.11 (d, J = 6.8 Hz, 3H), 0.97 (t, J = 7.4 Hz, 3H), 0.72 (d, J = 6.6 Hz, 3H), 0.67 (d, J = 7.0 Hz, 3H). **^{13}C NMR** (151 MHz, $CDCl_3$): δ 157.8, 155.4, 154.1, 153.5, 152.0 (d, J = 13.8 Hz), 146.30 – 145.33 (m), 145.1 (m), 144.6 – 144.2 (m), 144.2 – 143.8 (m), 143.5 (m), 142.1 (d, J = 7.5 Hz), 140.7 , 139.3 (d, J = 20.4 Hz), 138.4, 126.6, 126.4 (d, J = 14.2 Hz), 126.0, 125.3, 124.6 (q, J = 31.7 Hz), 124.2, 122.0, 121.6, 120.4 (t, J = 18.6 Hz), 119.5 (d, J = 3.8 Hz), 117.8 (t, J = 20.1 Hz), 113.2, 110.5 (d, J = 3.8 Hz), 54.3, 53.9, 47.9 (d, J = 10.1 Hz), 47.0 (d, J = 8.9 Hz), 42.5, 40.5, 36.4 (d, J = 42.9 Hz), 32.9, 31.6, 31.3 (d, J = 6.1 Hz), 29.7 (d, J = 9.6 Hz), 29.5 (d, J = 9.4 Hz), 26.4, 25.7, 24.7, 24.6, 24.5, 22.9, 22.5, 21.0, 13.9 (the observed complexity is due to C–P and C–F coupling). **^{19}F NMR** (565 MHz, $CDCl_3$) δ -61.7 (s), -130.5 (dd, J = 23.8, 12.5 Hz), -137.5 (dd, J = 24.2, 12.2 Hz), -145.0 (dd, J = 23.7, 12.2 Hz), -146.8 (dd, J = 24.1, 12.4 Hz). **^{31}P NMR** (162 MHz, $CDCl_3$): δ 67.5. IR (neat, cm^{-1}): 2957, 2905, 2849, 1583, 1476, 1457, 1420, 1324, 1261, 1156, 1115, 1067, 1005, 971, 814, 720. **HRMS** (ESI) m/z calcd for $C_{57}H_{67}BrF_7O_3PPd$ $[M–Br]^+$: 1095.4271; 1095.4290 found.

III. Experimental Procedures and Characterization Data for **L3** and its Corresponding Complex

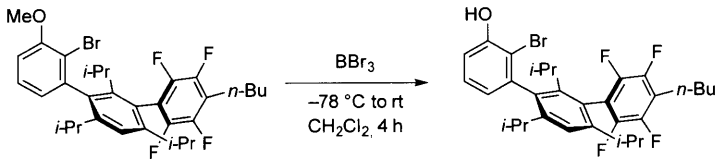

S1 **S2** 87%

A 50 mL oven-dried round-bottomed flask equipped with a magnetic stir bar was charged with **S1** (750 mg, 1.26 mmol, 1.00 equiv). The flask was sealed with a rubber septum and an inlet needle attached to a Schlenk line was inserted. The flask was evacuated and then backfilled with argon. This sequence was repeated two additional times. Then, anhydrous CH_2Cl_2 (18 mL) was added via syringe and the reaction mixture was allowed to begin stirring. The flask was then cooled to –78 °C using a dry ice/acetone bath. Once at this temperature, BBr_3 (150 μL, 1.58 mmol, 1.25 equiv) was added over the course of 2 min. The reaction mixture was stirred for five min at –78 °C before removing it from the cold bath and allowing it to warm to rt. It was then stirred for an additional 4 h. Once the reaction was complete, the excess BBr_3 was quenched by dropwise addition of MeOH. Then, the flask was opened to the air and the solvent removed with the aid of a rotary evaporator. The residue was purified by silica gel chromatography (10% EtOAc/hexanes) to afford **S2** as a white solid (637 mg, 87%). mp: 112–114 °C. **^{1}H NMR** (600 MHz, $CDCl_3$): (mixture of rotamers; major rotamer shift listed when not overlapping) δ 7.32 – 7.26 (m, 2H), 7.05 (dd, J = 8.1, 1.5 Hz, 1H), 6.84 (d, J = 7.5, 1H), 5.72 (s, 1H), 2.83 (t, J = 7.7 Hz, 2H), 2.73 (m, 1H), 2.42 (m, 2H), 1.70 (p, J = 7.7 Hz, 2H), 1.45 (sx, J = 7.4 Hz, 2H), 1.28 – 1.12 (m, 10H), 1.06 (dd, J = 6.9, 5.5 Hz, 3H), 1.00 (t, J = 7.4 Hz, 3H), 0.89 – 0.78 (m, 6H). **^{13}C NMR** (151 MHz, $CDCl_3$): (mixture of rotamers) δ 155.2, 152.6, 148.8, 148.6, 148.2, 147.9, 145.8, 145.0, 144.2, 142.9, 143.5, 142.9, 141.0, 137.2, 129.4, 128.2, 123.8, 123.0, 121.9, 120.8, 120.6, 120.3 (t, J = 18.8 Hz), 118.1 (t, J = 20.5 Hz), 114.4, 113.1, 32.3, 31.7, 30.9, 25.1, 24.9, 24.3, 24.2, 23.7, 23.6, 22.9, 22.6, 22.0, 21.7, 13.9 (the observed complexity is due to C–F coupling).**^{19}F NMR** (565 MHz, $CDCl_3$): (mixture of rotamers) δ -137.7 (br s), -145.6 (m). IR (neat, cm^{-1}): 3520, 3485, 2961, 2933, 2870, 1592, 1577, 1474, 1431, 1362, 1192, 1164, 971, 622.

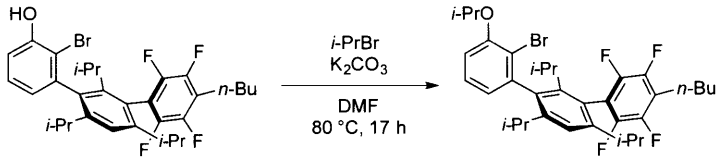

S2 **S3** 83%

A 25 mL oven-dried reaction tube equipped with a magnetic stir bar was charged with **S2** (95 mg, 0.16 mmol, 1.00 equiv) and K_2CO_3 (45 mg, 0.32 mmol, 2.00 equiv). The tube was sealed with a screw-cap fitted with a Teflon septum, and then an inlet needle attached to a Schlenk line was inserted. The tube was evacuated and then backfilled with argon. This sequence was repeated two additional times. Then, anhydrous DMF (0.70 mL) was added via syringe and the heterogeneous reaction mixture was allowed to begin stirring. Then, 2-bromopropane (50 μL, 0.53 mmol, 3.2 equiv) was added via syringe. The septum was then exchanged for one which had not been punctured, under a counterflow of argon, and the reaction mixture was allowed to stir in a pre-heated oil bath at 80 °C for 14 h. Once the reaction was complete, the tube was cooled to rt and then the cap removed. The reaction mixture was diluted with EtOAc (15 mL) and transferred to a separatory funnel. The organic layer was washed with DI water (5 x 15 mL), dried over magnesium sulfate, filtered, and concentrated with the aid of a rotary evaporator. The crude residue was purified via automated silica gel chromatography (Biotage KP-SIL 25 g column, eluting 0% to 10% EtOAc/hexanes) to afford **S3** as a white foam (85 mg, 83%). **^{1}H NMR** (600 MHz, C_6D_6): (mixture of rotamers; major rotamer shift listed when not overlapping) δ 7.50 (s, 1H), 6.99 (t, J = 7.9 Hz, 1H), 6.82 (d, J = 7.5 Hz, 1H), 6.52 (d, J = 8.3, 1H), 4.19 – 4.09 (m, J = 6.0 Hz, 1H), 3.10 (m, 1H), 2.68 (m, 2H), 2.57 (m, 2H), 1.43 (m, 2H), 1.32 (d, J = 6.9 Hz, 3H), 1.26 – 1.14 (m, 8H), 1.14 – 1.03 (m, 15H), 0.74 (t, J = 7.4 Hz, 3H). **^{13}C NMR** (151 MHz, C_6D_6): (mixture of rotamers) δ 157.4, 155.1, 148.5 (d, J = 15.1 Hz), 148.0, 146.0, 145.4, 144.4, 144.1, 144.0, 143.8, 143.7, 142.1, 138.6, 128.5, 123.5, 122.8, 121.9, 120.6, 120.5, 120.4, 120.3, 118.9 – 118.5 (m), 113.0, 111.3, 71.5, 71.4, 32.5, 31.3, 31.0, 24.8, 24.7, 24.1, 23.9, 23.8, 23.5, 23., 22.5, 22.2, 22.0, 21.7 (three overlapping signals), 21.6, 13.4 (the observed complexity is due to C–F coupling). **^{19}F NMR** (565 MHz, C_6D_6): (mixture of rotamers) -137.1 (br d, J = 305 Hz), -145.4. IR (neat, cm^{-1}): 2961, 2929, 2872, 1560, 1475, 1363, 1282, 1261, 1105, 976, 916, 784, 728.

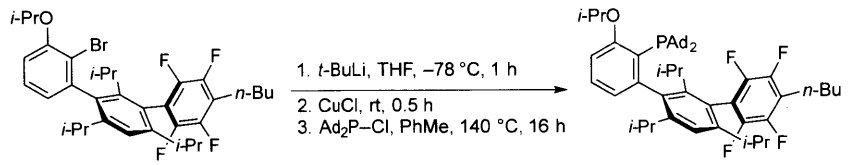

S3 **L3** 55%

L3 was prepared according to general procedure B. A mixture of **S3** (145 mg, 0.233 mmol, 1.00 equiv), *t*-BuLi (1.70 M in pentane; 0.29 mL, 0.49 mmol, 2.1 equiv), CuCl (40 mg, 0.40 mmol, 1.70 equiv), and Ad_2PCl (86 mg, 0.25, 1.1 equiv) was stirred at 140 °C for 16 h in a Schlenk tube behind a blast shield. Purified via trituration from MeOH to afford **L3** as a white solid (109 mg, 55%). mp: 228–230 °C. **^{1}H NMR** (600 MHz, $CDCl_3$): δ 7.24 (d, J = 7.8 Hz, 1H), 7.15 (s, 1H), 6.85 (d, J = 8.3 Hz, 1H), 6.0 (ddd, J = 7.5, 3.5, 1.0 Hz, 1H), 4.76 (h, J = 6.1 Hz, 1H), 2.78 (overlapping h and t (J = 7.7 Hz), 3H), 2.55 (h, J = 7.1 Hz, 1H), 2.39 – 2.29 (m, 1H), 2.02 – 1.81 (m, 19H), 1.72 – 1.57 (m, 15H), 1.54 (d, J = 6.0 Hz, 3H), 1.53 (d, J = 6.1 Hz, 3H), 1.42 (dq, J = 14.7, 7.3 Hz, 2H), 1.27 (d, J = 6.8 Hz, 3H), 1.14 (d, J = 3.4 Hz, 3H), 1.13 (d, J = 3.5 Hz, 3H) 0.98 (m, 6H), 0.87 (d, J = 7.0 Hz, 3H), 0.64 (d, J = 7.1 Hz, 3H). **^{13}C NMR** (151 MHz, $CDCl_3$): δ 160.9, 153.2, 152.9, 148.1, 147.3, 145.7, 145.0, 144.1, 144.0, 143.4, 140.3 (d = 7.0 Hz), 129.2, 128.5, 128.4, 125.5, 125.2 (d, J = 7.7 Hz), 123.5, 123.2, 120.4, 120.2, 119.7 (t, J = 18.7 Hz), 119.4, 119.3, 109.8, 69.7, 42.1 (d, J = 14.1 Hz), 38.7, 38.5, 38.3, 37.3, 37.2 (d, J = 7.7 Hz), 36.6, 32.2, 31.7, 31.4 (d, J = 3.0 Hz), 30.6, 29.4 (d, J = 8.9 Hz), 29.2 (d, J = 8.9 Hz), 28.4, 28.3, 26.6, 24.6, 24.4, 24.3, 24.1 (d, J = 3.2 Hz), 22.9, 22.8, 22.6, 22.5, 22.4, 21.7, 13.9 (the observed complexity is due to C–P and C–F coupling). **^{19}F NMR** (565 MHz, $CDCl_3$): δ -137.4 (dd, J = 24.1, 12.5 Hz), -138.0 (dd, J = 24.2, 12.4 Hz), -146.1 (dd, J = 24.1, 12.5 Hz), -146.5 (dd, J = 24.1, 12.4 Hz). **^{31}P NMR** (162 MHz, $CDCl_3$): δ 35.7. IR (neat, cm^{-1}): 2962, 2902, 2846, 1557, 1476, 1238, 1121, 1108, 975, 790, 739. **HRMS** (ESI) m/z calcd for $C_{54}H_{71}F_4OP$ $[M+H]^+$: 843.5257; 843.5253 found.

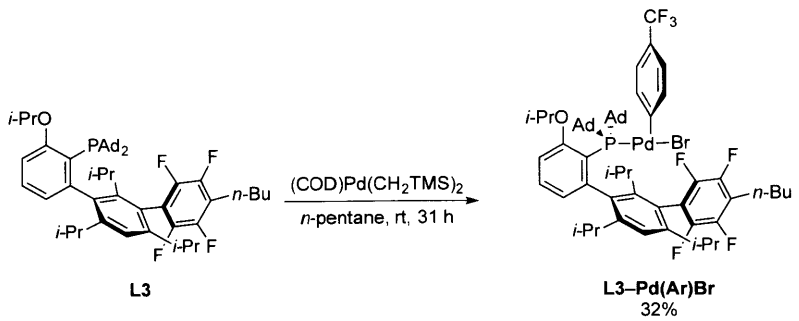

L3

L3–Pd(Ar)Br
32%

L3–Pd(Ar)Br was prepared following general procedure A. In a 25 mL reaction tube, a mixture of **L3** (147 mg, 0.175 mmol, 1.00 equiv), 4-bromobenzotrifloride (80 mg, 0.36 mmol, 2.0 equiv), and (COD)Pd($CH_2TMS)_2$ (69.5 mg, 0.179 mmol, 1.02 equiv) was stirred in pentane (13 mL) at rt for 31 h. The complex was filtered outside the glovebox to afford **L3–Pd(Ar)Br** as a light yellow-brown solid (65 mg, 32%). **^{1}H NMR** (400 MHz, $CDCl_3$): δ 7.41 (d, J = 8.2 Hz, 2H), 7.31 (m, 2H), 7.07 (t, J = 11.6 Hz, 2H), 6.91 (d, J = 8.5 Hz, 1H), 6.25 (d, J = 7.7 Hz, 1H), 4.90 (m, 1H), 3.21 (m, 1H), 2.81 (t, J = 7.8 Hz, 2H), 2.63 – 2.43 (m, 7H), 2.34 (m, 3H), 2.17 (m, 4H), 2.05 (s, 4H), 1.91 – 1.47 (m, 33H), 1.42 (m, 3H), 1.36 – 1.17 (m, 13H), 1.13 (d, J = 6.8 Hz, 3H), 1.07 – 0.61 (m, 16H). **^{13}C NMR** (126 MHz, $CDCl_3$): δ 159.9, 157.0, 152.9, 151.0 (d, J = 19.4 Hz), 150.5, 146.3 (m), 145.8 (m), 145.0 (m), 144.2 (m), 141.9 (d, J = 7.7 Hz), 140.8, 137.8, 131.3, 128.1 (d, J = 10.6 Hz), 127.0, 126.9 (d, J = 3.7 Hz), 126.1, 126.0, 124.6 (q, J = 31.7 Hz), 123.9, 123.4 (d, J = 12.6 Hz), 122.1, 121.8, 120.7 (t, J = 18.8 Hz), 117.4 (t, J = 20.2 Hz), 111.0, 71.0, 47.3 (d, J = 10.8 Hz), 46.6 (d, J = 9.3 Hz), 42.5, 40.6, 36.5, 36.2, 33.3, 31.6, 31.3 (d, J = 11.6 Hz), 29.6 (d, J = 9.5 Hz), 29.2 (d, J = 9.4 Hz), 26.7, 25.6, 25.1, 24.4, 24.0, 22.9, 22.5, 22.4, 22.1, 21.9, 13.9. (the observed complexity is due to C–P and C–F coupling). **^{19}F NMR** (376 MHz, $CDCl_3$): δ -61.8, -130.9 (dd, J = 23.7, 12.8 Hz), -137.1 (dd, J = 24.9, 12.2 Hz), -144.5 (dd, J = 23.7, 12.2 Hz), -146.2 (dd, J = 24.0, 12.7 Hz). **^{31}P NMR** (162 MHz, $CDCl_3$): δ 69.4. IR (neat, cm^{-1}): 2964, 2911, 2855, 1585, 1566, 1477, 1444, 1324, 1251, 1156, 1114, 1100, 1067, 1006, 970, 815. **HRMS** (ESI) m/z calcd for $C_{61}H_{75}BrF_7OPPd$ $[M–Br]^+$: 1093.4479; 1093.4496 found.

IV. Experimental Procedures and Characterization Data for **L4** and its Corresponding Complex

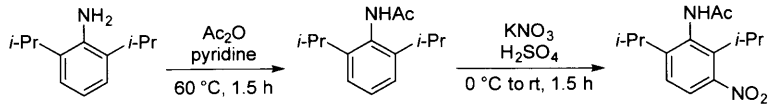

S4
84% over two steps

2,6-diisopropylaniline (50.0 g, 282 mmol, 1.00 equiv) was dissolved in pyridine (110 mL) in a 500 mL round-bottomed flask equipped with a magnetic stir bar and addition funnel. The reaction mixture was then allowed to begin stirring and cooled to 0 °C using an ice water bath. Then, acetic anhydride (32 mL, 339 mmol, 1.20 equiv) was added via addition funnel over the course of 5 min. After the addition was complete, the addition funnel was removed and a reflux condenser attached. The reaction mixture was then heated to 60 °C in a pre-heated oil bath for 1.5 h. At this time, the reaction mixture was cooled to rt and then poured into a 1 L Erlenmeyer flask containing a stirring solution of 2.0 M HCl (300 mL) at 0 °C (*Caution: exothermic!*). The resulting pink precipitate was filtered and washed with deionized water. This material was used in the next step without further purification.

A 500 mL Erlenmeyer flask equipped with a magnetic stir bar was charged with 2,6-diisopropylphenylacetamide (62.0 g, 283 mmol, 1.00 equiv; prepared above) and the vessel cooled to 0 °C in an ice water bath. Then, concentrated H_2SO_4 (95–98%; 300 mL) was added with vigorous stirring. KNO_3 (41.4 g, 409 mmol, 1.4 equiv) was added in portions over 2 h, and then the reaction mixture was allowed to stir at 0 °C for 2.5 h. At this time, the reaction mixture was quenched by pouring it into 1 L of deionized water (*Caution: exothermic!*). The resulting orange precipitate was filtered and then dissolved in CH_2Cl_2 (400 mL) and transferred to a separatory funnel. The organic phase was washed with brine (2 x 100 mL), dried over magnesium sulfate, filtered, and concentrated with the aid of a rotary evaporator to afford **S4** as a yellow-tan solid (62.4 g, 84% over two steps). mp: 198–200 °C. **^{1}H NMR** (600 MHz, $CDCl_3$): (mixture of rotamers; major rotamer shift listed) δ 7.47 (d, J = 27.9, 8.5 Hz, 1H), 7.28 (d, J = 8.5 Hz, 1H), 6.92 (s, 1H), 3.28 (h, J = 7.2 Hz, 1H), 3.04 (h, J = 6.9 Hz, 1H), 2.21 (s, 3H), 1.31 (d, J = 7.1 Hz, 6H; overlaps with minor rotamer), 1.18 (br m, 6H). **^{13}C NMR** (151 MHz, $CDCl_3$): (mixture of rotamers; major rotamer shift listed) δ 169.8, 152.3, 150.0, 138.4, 133.8, 124.9, 123.8, 29.2, 29.0, 24.7, 23.4, 21.0. IR (neat, cm^{-1}): 3247 (broad), 2966, 1658, 1519, 1464, 1364, 1352, 1284, 836.

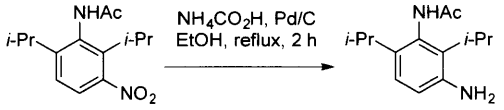

S4 **S5** 98%

A 200 mL round-bottomed flask equipped with a magnetic stir bar was charged sequentially with **S4** (5.02 g, 19.0 mmol, 1.00 equiv) and NH_4CO_2H (4.79 g, 76.0 mmol, 4.00 equiv). Ethanol (60 mL) was added and the reaction mixture allowed to begin stirring. Then, Pd/C (5 wt% Pd with 50% water content, 1.10 g) was added and the solution was heated to reflux in a pre-heated oil bath and stirred at this temperature for 2 h. At this time, the reaction mixture was cooled to rt, and then filtered through a pad of celite, eluting with EtOAc. The filtrate was concentrated with the aid of a rotary evaporator to afford **S5** as a red-pink solid (4.38 g, 98%). mp: 199–200 °C. **^{1}H NMR** (600 MHz, $CDCl_3$): (mixture of rotamers; major rotamer shift listed) δ 6.98 (d, J = 8.3 Hz, 1H), 6.71 (br s, 1H), 6.64 (d, J = 8.4 Hz, 1H), 3.69 (br s, 2H), 3.33 (h, J = 7.3 Hz, 1H), 2.93 (h, J = 6.9 Hz, 1H), 2.21 (s, 3H), 1.37 (d, J = 7.3 Hz, 3H), 1.30 (d, J = 7.3 Hz, 3H), 1.19 (d, J = 6.9 Hz, 3H), 1.09 (d, J = 6.8 Hz, 3H). **^{13}C NMR** (151 MHz, $CDCl_3$): (mixture of rotamers; major rotamer shift listed) δ 169.8, 143.3, 137.4, 132.3, 129.7, 124.2, 117.8, 28.6, 27.2, 24.8, 22.9, 20.2. IR (neat, cm^{-1}): 3475, 3353, 3226 (broad), 2963, 2929, 2870, 1629, 1538, 1483, 1304, 1285, 818.

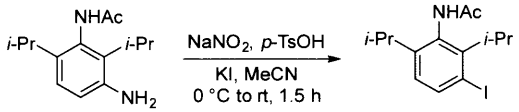

S5 **S6** 65%

A 100 mL round-bottomed flask equipped with a stir bar was charged with **S5** (2.14 g, 9.13 mmol, 1.00 equiv) and *p*-TsOH•H_2O (5.35 g, 28.1 mmol, 3.10 equiv). The flask was cooled to 10 °C, and then MeCN (47 mL) was added with vigorous stirring to give a heterogeneous solution. Separately, in a 20 mL scintillation vial, KI (3.86 g, 23.3 mmol, 2.55 equiv) and $NaNO_2$ (1.32 g, 19.1 mmol, 2.10 equiv) were dissolved in deionized water (6 mL). The aqueous KI/$NaNO_2$ solution was then added dropwise via syringe to the stirring heterogeneous solution of ammonium salt over 12 min, during which the reaction mixture took on a dark red/brown color and bubbles began forming. The temperature was maintained at 10 °C during the addition and for

10 min afterward. Then, the reaction mixture was allowed to warm to rt and stir for 20 min. At this time, the reaction mixture was poured into an Erlenmeyer flask containing aqueous sodium bicarbonate solution (200 mL) and aqueous saturated sodium thiosulfate solution (200 mL). A yellow precipitate formed, which was filtered, washed with deionized water (4 x 10 mL), and dried under high vacuum (1.55 g). The aqueous filtrate was then extracted with EtOAc (3 x 75 mL). The organic phase was washed with brine (1 x 200 mL), dried over magnesium sulfate, filtered, and concentrated with the aid of a rotary evaporator. This material was purified via automated silica gel chromatography (Biotage KP-SIL 50 g column, eluting 10% to 30% acetone/hexanes) to afford a second crop of **S5** as a yellow solid (0.494 g). Combined yield: 1.55 g + 0.49 g = 2.04 g (65%). mp: 194–196 °C. **^{1}H NMR** (400 MHz, $CDCl_3$): (mixture of rotamers; major rotamer shift listed) δ 7.82 (d, J = 8.4 Hz, 1H), 6.88 (m, 2H; overlapping Ar–H and N–H), 3.54 (h, J = 7.0 Hz, 1H), 2.95 (h, J = 6.7 Hz, 1H), 2.19 (s, 3H), 1.42 – 0.97 (m, 12H; overlapping –CH(**CH3**)$_2$ signals). **^{13}C NMR** (151 MHz, $CDCl_3$): (mixture of rotamers; major rotamer shift listed) δ 169.8, 149.5, 146.3, 140.1, 132.7, 126.2, 119.6, 40.5, 28.2, 24.8, 23.4, 20.5. IR (neat, cm^{-1}): 3253, 2960, 2927, 2869, 1651, 1520, 1441, 1362, 1285, 1283, 701, 630.

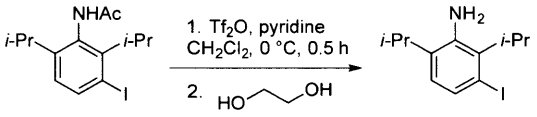

S6 **S7** 59%

A 500 mL Schlenk flask bearing a sidearm and equipped with a magnetic stir bar was charged with **S6** (10.0 g, 29.0 mmol, 1.00 equiv). The flask was sealed with a rubber septum, and the sidearm attached to a Schlenk line. The flask was then evacuated and backfilled with argon. This sequence was repeated two additional times. Anhydrous CH_2Cl_2 (140 mL) was added via syringe and the solution was allowed to begin stirring. The flask was then cooled to 0 °C in an ice water bath and anhydrous pyridine (7.00 mL, 86.9 mmol, 3.00 equiv) was added via syringe. Then, Tf_2O (6.32 mL, 37.7 mmol, 1.30 equiv) was added dropwise via syringe over the course of 10 min and the resulting dark red solution was allowed to stir for 30 min at 0 °C. At this time, anhydrous ethylene glycol (16.2 mL, 290 mmol, 10 equiv) was added via syringe and the reaction mixture allowed to slowly warm to rt over the course of 23 h. The flask was then opened to the air, and the reaction mixture diluted with CH_2Cl_2 (100 mL) and transferred to a separatory funnel. The organic phase was washed with deionized water (1 x 100 mL), dried over

magnesium sulfate, filtered, and concentrated with the aid of a rotary evaporator. The crude product was purified via flash column chromatography (silica gel, eluting 20% CH_2Cl_2/hexanes) to afford **S7** as an orange oil (5.21 g, 59%). **^{1}H NMR** (600 MHz, $CDCl_3$): δ 7.33 (d, J = 8.3 Hz, 1H), 6.70 (d, J = 8.2 Hz, 1H), 3.92 (s, 2H), 3.73 (h, J = 7.3 Hz, 1H), 2.86 (h, J = 6.8 Hz, 1H), 1.41 (d, J = 7.7 Hz, 6H), 1.27 (d, J = 7.0 Hz, 6H). **^{13}C NMR** (151 MHz, $CDCl_3$): δ 142.3, 133.9, 132.0, 129.8, 125.1, 100.9, 39.7, 27.5, 22.3, 19.5. IR (neat, cm^{-1}): 3509, 3418, 2959, 2870, 1616, 1443, 1411, 850, 794, 764.

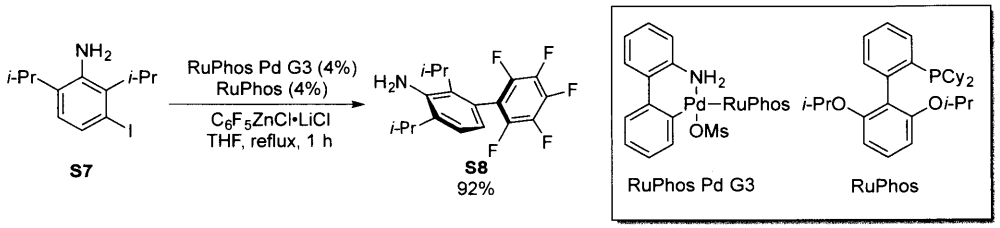

A 50 mL oven-dried round-bottomed flask equipped with a magnetic stir bar was sealed with a rubber septum. Then, an inlet needle attached to a Schlenk line was inserted through the septum. The flask was evacuated and then backfilled with argon. This sequence was repeated two additional times. Then, 1-bromo-2,3,4,5,6-pentafluorobenzene (2.73 g, 11.1 mmol, 1.00 equiv) was added via syringe and dissolved in anhydrous THF (12 mL) with the aid of stirring. The reaction vessel was cooled to –78 °C in a dry ice/acetone bath, followed by the addition of *i*-PrMgCl (1.55 M in THF; 7.15 mL, 11.1 mmol, 1.00 equiv) via syringe over the course of 5 min. The reaction mixture was allowed to stir at –78 °C for 30 min. At this time, a solution of $ZnCl_2$/LiCl was freshly prepared in a nitrogen-filled glovebox by dissolving $ZnCl_2$ (1.66 g, 12.2 mmol) and LiCl (528 mg, 12.5 mmol) in anhydrous THF (6.50 mL) in a 25 mL reaction tube. This solution was added via syringe to the ArMgCl solution at –78 °C. The flask was then removed from the cold bath and allowed to stir at rt for 30 min. Titration of this solution with iodine yields a titer of 0.357 M (theoretical titer = 0.43 M; 83% yield).[20]

Separately, a 50 mL round-bottomed flask equipped with a magnetic stir bar was charged sequentially with **S7** (2.10 g, 6.93 mmol, 1.00 equiv), RuPhos (163 mg, 0.350 mmol, 5.0 mol%), and RuPhos Pd G3 (301 mg, 0.360 mmol, 5.2 mol%). The flask was sealed with a rubber septum equipped with a balloon and an inlet needle attached to a Schlenk line. The flask was evacuated and then backfilled with argon. This sequence was repeated two additional times. Then, the

ArZnCl•LiCl solution (0.357 M in THF; 22.1 mL, 7.9 mmol, 1.20 equiv) was transferred into the flask via cannula. The reaction mixture was then allowed to stir in a pre-heated oil bath at 80 °C behind a blast shield for 1 h. At this time, the reaction mixture was cooled to rt and MeOH was added to quench any remaining ArZnCl•LiCl. The reaction mixture was diluted with EtOAc (50 mL) and then filtered through a plug of celite to remove Pd black. The filtrate was concentrated and then purified via silica gel chromatography (eluting 5% acetone/hexanes) to afford **S8** as an orange solid (2.18 g, 92%), which was approximately 88% pure by NMR spectroscopy. The two impurities present were 1,3-diisopropyl-2-amino-4-*n*-propylaniline and 1,3-diisopropyl-2-amino-4-*iso*-propylaniline, which likely result from C–C coupling with any *i*-PrZnCl•LiCl that may be present. mp: 66–69 °C. **^{1}H NMR** (600 MHz, $CDCl_3$): δ 7.12 (d, J = 7.9 Hz, 1H), 6.54 (d, J = 7.9 Hz, 1H), 3.94 (s, 2H), 2.97 (h, J = 6.9 Hz, 1H), 2.89 (h, J = 7.3 Hz, 1H), 1.33 (d, J = 7.0 Hz, 12H). **^{13}C NMR** (151 MHz, $CDCl_3$): δ 144.4 (d, J = 243.8 Hz), 142.7, 140.4 (dt, J = 253.1, 13.9 Hz), 137.6 (dt, J = 249.0, 14.5 Hz), 134.8, 130.1, 123.4, 123.3, 120.8, 117.4 (t, J = 20.6 Hz), 30.9, 27.8, 22.3, 19.9 (the observed complexity is due to C–F coupling). **^{19}F NMR** (565 MHz, $CDCl_3$): δ -139.8, -156.51 (m), -162.8 (m). IR (neat, cm^{-1}): 3480 (weak), 3402 (weak), 2961, 2931, 2872, 1620, 1521, 1489, 1422, 1059, 986, 819, 759.

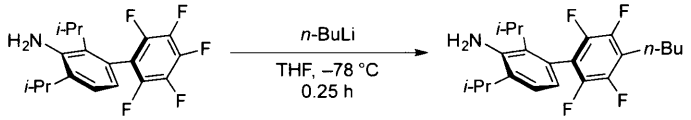

S8 **S9** 82%

A 50 mL oven-dried round-bottomed flask equipped with a magnetic stir bar was charged with **S8** (2.13 g, 6.29 mmol, 1.00 equiv). The flask was sealed with a rubber septum and an inlet needle attached to a Schlenk line was inserted. The vessel was then evacuated and backfilled with argon. This sequence was repeated two additional times. Anhydrous THF (32 mL) was added via syringe and the reaction mixture was allowed to begin stirring. Then, the flask was cooled to –78 °C in a dry ice/acetone bath, and *n*-BuLi (2.50 M in hexane; 5.00 mL, 12.5 mmol, 2.00 equiv) was added dropwise via syringe over the course of 10 min. The resulting bright orange solution was allowed to stir for 5 min at –78 °C, and then MeOH was added via syringe over the course of 1 min. Then, the flask was allowed to come to rt, at which time it was opened to the air and transferred to a separatory funnel containing Et_2O (200 mL) and deionized water (100 mL). The organic phase was dried over magnesium sulfate, filtered, and concentrated with

the aid of a rotary evaporator. The crude material was purified via automated silica gel chromatography (Biotage KP-SIL 50 g column, eluting 0% to 80% DCM/hexanes) to give **S9** as a colorless oil (1.96 g, 82%). **^{1}H NMR** (500 MHz, $CDCl_3$): δ 7.09 (d, J = 7.9 Hz, 1H), 6.56 (d, J = 7.9 Hz, 1H), 3.90 (s, 2H), 2.94 (m, 2H; overlapping –C**H**$(CH_3)_2$), 2.78 (t, J = 7.6 Hz, 2H), 1.66 (m, 2H), 1.44 (h, J = 7.3 Hz, 2H), 1.32 (d, J = 7.3 Hz, 6H), 1.31 (d, J = 6.8 Hz, 6H), 0.99 (t, J = 7.3 Hz, 3H). **^{13}C NMR** (151 MHz, $CDCl_3$): δ 146.0 – 143.8 (m), 144.8 – 142.9 (m), 142.5, 134.4, 130.2, 124.9, 123.2, 123.1, 121.0, 119.6 (t, J = 19.1 Hz), 31.6, 30.8, 27.9, 22.8, 22.6, 22.4, 20.1, 13.9 (the observed complexity is due to C–F coupling). **^{19}F NMR** (282 MHz, $CDCl_3$): δ -141.1 (m), -145.0 (dd, J = 23.7, 12.8 Hz). IR (neat, cm^{-1}): 3500, 3422, 2962, 2932, 2873, 1620, 1475, 1421, 970, 915, 814, 780, 734.

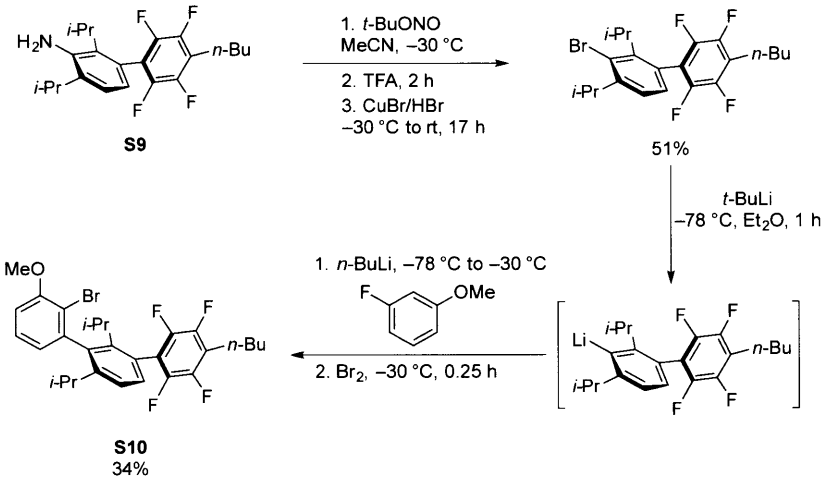

A 50 mL round-bottomed flask equipped with a magnetic stir bar was charged with **S9** (1.86 g, 4.88 mmol, 1.00 equiv). The flask was sealed with a rubber septum and an inlet needle attached to a Schlenk line was inserted. The flask was evacuated and backfilled with nitrogen atmosphere (*Note: the use of a nitrogen atmosphere is critical for this reaction!*). This sequence was repeated two additional times. Anhydrous MeCN (11 mL) was added via syringe and the reaction mixture was allowed to begin stirring. Then, the flask was cooled to –30 °C, and *t*-BuONO (0.770 mL, 6.47 mmol, 1.33 equiv) was added dropwise over the course of 2 min, followed by the addition of CF_3CO_2H (0.450 mL, 5.88 mmol, 1.21 equiv) via syringe over the course of 3 min. The resulting yellow solution was allowed to stir at –30 °C for 2 h. Separately, a 3-neck, 50 mL round-bottomed flask equipped with a magnetic stir bar was brought into a nitrogen-filled glovebox, charged with CuBr (1.36 g, 9.48 mmol, 1.94 equiv), and sealed with rubber septa. The

flask was removed from the glovebox, and a nitrogen inlet needle was inserted. Then, HBr (48%; 20 mL) was added under a counterflow of nitrogen. The resulting violet solution was allowed to stir at –40 °C before transferring it to the solution of the diazonium salt via cannula over the course of 2 min. The reaction mixture was then removed from the cold bath and allowed to warm to rt over 17 h; bubbles were noted to form as the solution warmed. At this time, the flask was opened to the air and the reaction mixture poured into a separatory funnel containing hexanes (100 mL) and aqueous saturated sodium thiosulfate solution (20 mL). The organic phase was washed with deionized water (2 x 100 mL), followed by brine (1 x 100 mL). The organic layer was then dried over magnesium sulfate, filtered, and concentrated with the aid of a rotary evaporator. The crude residue was purified via automated silica gel chromatography (Biotage KP-SIL 50 g column, eluting hexanes) to afford the product as a colorless oil (1.10 g, 51%), which was used directly in the next step.

A 50 mL oven-dried round-bottomed flask equipped with a magnetic stir bar was charged with the biaryl bromide (1.03 g, 2.31 mmol, 1.08 equiv) prepared above. The flask was sealed with a rubber septum and an inlet needle attached to a Schlenk line was inserted. The vessel was evacuated and backfilled with argon. This sequence was repeated two additional times. Anhydrous Et_2O (21 mL) was added via syringe and the reaction mixture was allowed to begin stirring. Then, the flask was cooled to –78 °C in a dry ice/acetone bath, and *t*-BuLi (1.70 M in pentane; 2.80 mL, 4.76 mmol, 2.22 equiv) was added dropwise via syringe over the course of 3 min. The solution was allowed to stir at –78 °C for 1 h. Separately, a 100 mL oven-dried round-bottomed flask equipped with a magnetic stir bar was sealed with a rubber septum and an inlet needle attached to a Schlenk line was inserted. The flask was evacuated and then backfilled with argon. This sequence was repeated two additional times. Then, 3-fluoroanisole (270 mg, 2.14 mmol, 1.00 equiv) was added via syringe, followed by anhydrous THF (11.5 mL), and the reaction mixture was allowed to begin stirring. The flask was then cooled to –78 °C in a dry ice/acetone bath, and *n*-BuLi (2.50 M in hexane; 0.900 mL, 2.23 mmol, 1.05 equiv) was added over the course of 2 min. The solution was allowed to stir for 1 h at –78 °C. At this time, the biaryl lithium reagent prepared above in Et_2O was transferred to the aryl lithium solution in THF via cannula. The resulting yellow-green reaction mixture was warmed to –30 °C and was allowed to stir at this temperature for 1 h, at which point the color had changed to orange. Then,

Br_2 (0.250 mL, 4.85 mmol, 2.30 equiv) was carefully added dropwise via syringe and the solution allowed to stir at –30 °C for 10 min before being allowed to warm to rt. At this time, the flask was opened to the air and aqueous saturated sodium thiosulfate solution was carefully added until the color of bromine disappeared. Then, the biphasic reaction mixture was transferred to a separatory funnel containing EtOAc (100 mL). The organic phase was washed with deionized water (1 x 100 mL), followed by brine (1 x 100 mL), and then dried over magnesium sulfate, filtered, and concentrated with the aid of a rotary evaporator. The crude residue was purified via automated silica gel chromatography (Biotage KP-SIL 100 g column, eluting 0% to 20% CH_2Cl_2/hexanes) to afford the **S10** as a white foam (405 mg, 34%). **^{1}H NMR** (600 MHz, $CDCl_3$): δ 7.33 (t, J = 7.9 Hz, 1H), 7.29 (d, J = 8.1 Hz, 1H), 7.07 (d, J = 8.0 Hz, 1H), 6.92 (d, J = 8.3 Hz, 1H), 6.86 (d, J = 7.6 Hz, 1H), 3.97 (s, 3H), 2.79 (t, J = 7.8 Hz, 2H), 2.72 (h, J = 7.2 Hz, 1H), 2.43 (h, J = 7.0 Hz, 1H), 1.66 (p, J = 7.5 Hz, 2H), 1.43 (sx, J = 7.5 Hz, 2H), 1.21 (d, J = 7.0 Hz, 3H), 1.04 (d, J = 6.9 Hz, 3H), 0.98 (t, J = 7.4 Hz, 3H), 0.91 (d, J = 7.3 Hz, 3H), 0.86 (d, J = 7.2 Hz, 3H). **^{13}C NMR** (151 MHz, $CDCl_3$): δ 156.3, 148.2, 144.9 (m), 144.4, 144.1 (dt, J = 231.0, 14.4 Hz), 143.5, 140.1, 131.8, 127.7, 123.7 (two overlapping signals), 123.3, 120.2 (t, J = 20.1 Hz; slight overlap), 120.0 (t, J = 18.7 Hz; slight overlap), 114.6, 110.4, 56.4, 32.1, 31.6, 30.8, 24.8, 23.6, 22.8, 22.5, 21.9, 13.9 (the observed complexity is due to C–F coupling). **^{19}F NMR** (565 MHz, $CDCl_3$): δ -138.7 (br s), -139.4 (br s), -145.8 (dd, J = 23.5, 12.5 Hz), -145.9 (dd, J = 23.7, 12.6 Hz). IR (neat, cm^{-1}): 2962, 2931, 2873, 1465, 1476, 1466, 1423, 1289, 1262, 1085, 1023, 971, 831, 778, 724.

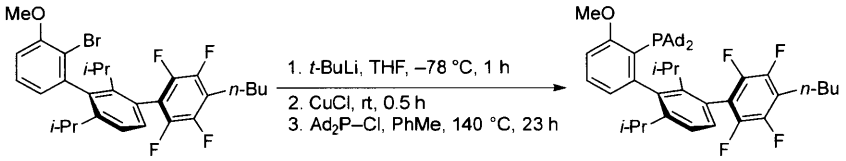

S10 **L4** 69%

L4 was prepared according to general procedure B. A mixture of **S10** (202 mg, 0.366 mmol, 1.00 equiv), *t*-BuLi (1.70 M in pentane; 0.490 mL, 0.833 mmol, 2.30 equiv), CuCl (57 mg, 0.576 mmol, 1.60 equiv), and Ad_2PCl (147 mg, 0.436 mmol, 1.20 equiv) were stirred at 140 °C for 23 h behind a blast shield. Purified via trituration from MeOH to afford **L4** as a white solid (194 mg, 69%). mp: 241–244 °C. **^{1}H NMR** (600 MHz, $CDCl_3$): δ 7.32 (t, J = 7.9 Hz, 1H), 7.20 (d, J = 8.0 Hz, 1H), 6.97 (d, J = 8.0 Hz, 1H), 6.90 (d, J = 8.1 Hz, 1H), 6.87 (dd, J = 7.6, 3.6 Hz, 1H),

3.87 (s, 3H), 2.77 (t, J = 7.7 Hz, 2H), 2.72 (h, J = 6.7 Hz, 1H), 2.63 (h, J = 6.9 Hz, 1H), 1.96 – 1.81 (m, 17H), 1.69 – 1.55 (m, 15H), 1.41 (sx, *J* = 7.4 Hz, 2H), 1.29 (d, J = 6.8 Hz, 3H), 0.97 (m, 6H; overlapping t and d; $-(CH_2)_3\mathbf{CH_3}$ and $-CH(\mathbf{CH_3})_2$), 0.91 (d, J = 6.9 Hz, 3H), 0.74 (d, J = 7.1 Hz, 3H). **^{13}C NMR** (151 MHz, $CDCl_3$): δ 162.1, 151.7 (d, J = 36.7 Hz), 148.1, 145.7 (m), 144.9, 144.0 (m), 142.2 (d, J = 6.0 Hz), 131.3, 128.8, 125.6 (d, J = 7.1 Hz), 123.5, 123.2, 122.8, 122.3, 121.3 (t, J = 20.3 Hz), 119.6 (t, J = 18.8 Hz), 108.7, 54.1, 42.0 (dd, J = 13.7, 11.3 Hz), 39.0 (d, J = 28.1 Hz), 38.7 (d, J = 29.7 Hz), 37.2 (d, J = 13.6 Hz), 31.9, 31.7, 31.3 (d, J = 3.3 Hz), 29.5 (d, J = 9.1 Hz), 29.3 (d, J = 9.1 Hz), 26.3, 24.3 (d, J = 3.0 Hz), 22.8, 22.8, 22.5, 21.5, 13.9 (the observed complexity is due to C–P and C–F coupling). **^{19}F NMR** (376 MHz, C_6D_6): δ -138.1 (dd, J = 23.9, 12.5 Hz), -138.8 (dd, J = 24.1, 12.5 Hz), -145.8 (dd, J = 24.2, 12.6 Hz), -145.9 (dd, J = 24.0, 12.4 Hz). **^{31}P NMR** (162 MHz, C_6D_6): δ 35.9. IR (neat, cm^{-1}): 2966, 2901, 2846, 1478, 1456, 1275, 1249, 1081, 974, 820, 805, 741. **HRMS** (ESI) m/z calcd for $C_{49}H_{61}F_4OP$ $[M+H]^+$: 773.4474; 773.4472 found.

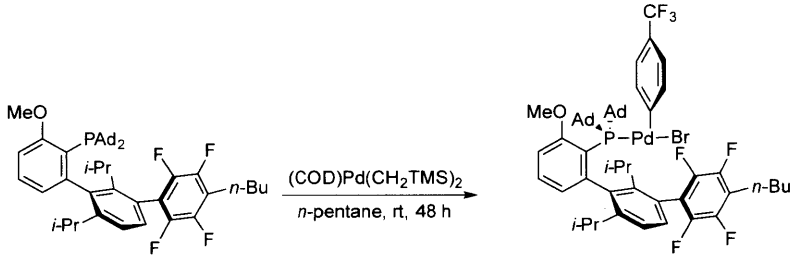

L4 **L4–Pd(Ar)Br** 69%

L4–Pd(Ar)Br was prepared following general procedure A. In a 25 mL reaction tube, a mixture of **L4** (162 mg, 0.210 mmol, 1.00 equiv), 4-bromobenzotrifloride (123 mg, 0.547 mmol, 2.61 equiv), and $(COD)Pd(CH_2TMS)_2$ (84 mg, 0.22 mmol, 1.0 equiv) was stirred in pentane (15 mL) at rt for 48 h. The complex was filtered outside the glovebox to afford **L4–Pd(Ar)Br** as a yellow solid (159 mg, 69%). **^{1}H NMR** (500 MHz, C_6D_6): δ 7.65 (t, J = 6.8 Hz, 2H), 7.57 (d, J = 8.2 Hz, 1H), 7.46 (d, J = 8.2 Hz, 1H), 7.36 (m, 1H), 6.99 (m, 2H), 6.85 (t, J = 7.7 Hz, 1H), 6.31 (m, 1H), 6.22 (d, J = 8.2 Hz, 1H), 3.35 (m, 1H), 3.14 (s, 1H), 3.10 (s, 3H), 2.65 – 2.37 (m, 14H), 2.31 (m, 1H), 2.11 (m, 4H), 2.00 (br s, 1H), 1.93 (br s, 5H), 1.82 – 1.58 (m, 23H), 1.57 – 1.34 (m, 10H), 1.30 – 1.13 (m, 5H), 1.10 (d, J = 6.9 Hz, 2H), 1.04 (d, J = 7.3 Hz, 2H), 0.97 – 0.86 (m, 2H), 0.80 (t, J = 7.4 Hz, 3H), 0.74 (m, 4H), 0.47 (m, 3H) (the observed complexity is due to a dearomative rearrangement). **^{13}C NMR** (126 MHz, $CDCl_3$): δ 161.5 (d, J = 2.3 Hz), 161.0 (d, J = 2.6 Hz),

151.8, 150.2 (d, J = 18.2 Hz), 149.7 (d, J = 18.1 Hz), 147.2, 145.9, 144.8, 144.3 – 143.2 (m), 141.8, 140.5, 137.0, 136.9, 133.1, 131.8, 131.7, 130.4, 129.7, 127.5 (d, J = 9.3 Hz), 126.6, 126.4 (t, J = 8.3 Hz), 126.0 , 125.3 – 125.2 (m), 125.1, 124.8, 122.7 (d, J = 13.8 Hz), 122.5, 122.0, 121.0, 120.8, 120.5, 119.5, 110.7 – 110.6 (m), 110.0 – 109.5 (m), 54.5, 54.1, 50.5, 47.9 (d, J = 10.5 Hz), 46.4 (d, J = 9.2 Hz), 44.6, 44.0 (d, J = 3.8 Hz), 43.7 (d, J = 7.8 Hz), 42.9, 42.0 (d, J = 2.4 Hz), 41.9, 39.9, 39.8, 36.7 (d, J = 3.7 Hz), 36.6, 36.3 (d, J = 18.4 Hz), 36.1, 33.1, 31.6, 31.3 – 31.1 (m), 30.9, 29.7 (d, J = 9.7 Hz), 29.6 (d, J = 5.7 Hz), 29.5 – 29.2 (m), 29.0, 25.4, 25.0, 23.8, 23.5 (d, J = 9.4 Hz), 23.1, 22.8, 22.5, 22.4, 20.2, 19.8, 13.9 (d, J = 2.2 Hz) (the observed complexity is due to a dearomative rearrangement as well as C–P and C–F coupling). **^{19}F NMR** (471 MHz, $CDCl_3$): δ -61.9, -62.4, -122.8 (br s), -132.1 (m), -137.44 (br s), -139.4 (dd, J = 23.5, 12.2 Hz), -143.6 (br s), -144.7 (dd, J = 23.4, 12.3 Hz), -145.9 (dd, J = 23.6, 12.5 Hz), -146.6 (br s). **^{31}P NMR** (202 MHz, $CDCl_3$): δ 97.9, 67.1. IR (neat, cm^{-1}): 2908, 2850, 1585, 1476, 1466, 1327, 1157, 1116, 1098, 1067, 1006, 978, 816, 805, 720. **HRMS** (ESI) m/z calcd for $C_{56}H_{65}BrF_7OPPd$ $[M–Br]^+$: 1023.3696; 1023.3705 found. *Note:* this complex appears to rearrange in solution, as judged by NMR spectroscopy. In addition, when a solution of this complex is treated with DBU and 4-bromobenzotrifluoride, ligand arylation is observed by LC/MS.

V. Experimental Procedures and Characterization Data for **L5** and its Corresponding Complex

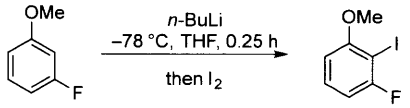

S11
74%

An oven-dried 200 mL Schlenk flask bearing a sidearm attached to a Schlenk line and equipped with a magnetic stir bar was sealed with a rubber septum. The flask was evacuated and then backfilled with argon. This sequence was repeated two additional times. Then, 3-fluoroanisole (3.76 g, 29.8 mmol, 1.00 equiv) was added via syringe, followed by anhydrous THF (100 mL) and the reaction mixture was allowed to begin stirring. The flask was then cooled to –78 °C in a dry ice/acetone bath, and *n*-BuLi (2.47 M in hexane; 13.0 mL, 32.1 mmol, 1.08 equiv) was added dropwise over the course of 13 min. The solution was allowed to stir at –78 °C for 20 min. Separately, a 100 mL oven-dried round-bottomed flask equipped with a magnetic stir bar was charged with I_2 (8.98 g, 35.4 mmol, 1.19 equiv). The flask was sealed with a rubber septum and

an inlet needle attached to a Schlenk line was inserted. The flask was evacuated and then backfilled with argon. This sequence was repeated two additional times. Anhydrous THF (60 mL) was added by syringe and the dark red solution was allowed to begin stirring. The iodine solution was transferred via cannula to the aryl lithium solution over the course of 1.5 h. After the addition was complete, the reaction mixture was allowed to stir at –78 °C for 30 min. At this time, the reaction vessel was allowed to warm to rt, the flask was unsealed, and aqueous saturated sodium thiosulfate solution was carefully added until the color of iodine dissipated. The biphasic mixture was then transferred to a separatory funnel containing Et_2O (200 mL). The organic phase was washed sequentially with aqueous saturated sodium thiosulfate solution (1 x 200 mL), deionized water (1 x 100 mL), and brine (1 x 100 mL). The organic layer was then dried over magnesium sulfate, filtered, and concentrated with the aid of a rotary evaporator. The crude residue was purified via automated silica gel chromatography (Biotage KP-SIL 100 g column, eluting 0% to 10% EtOAc/hexanes) to give **S11** as a slightly cloudy yellow oil (5.56 g, 74%). **^{1}H NMR** (600 MHz, C_6D_6): δ 6.70 (td, *J* = 8.2, 6.5 Hz, 1H), 6.39 (t, J = 7.9 Hz, 1H), 5.93 (d, J = 8.3 Hz, 1H), 3.12 (s, 3H). **^{13}C NMR** (151 MHz, C_6D_6): δ 163.4 (d, J = 243.7 Hz), 160.3 (d, J = 5.7 Hz), 130.2 (d, J = 9.8 Hz), 108.3 (d, J = 24.3 Hz), 106.5 (d, J = 2.9 Hz), 74.7 (d, J = 27.2 Hz), 56.1. **^{19}F NMR** (565 MHz, C_6D_6): δ -91.3. IR (neat, cm^{-1}): 2963, 2839, 1589, 1577, 1467, 1433, 1298, 1277, 1238, 1073, 1027, 987, 932, 765, 745, 697, 612. Spectral data were in accordance with those in the literature.[21]

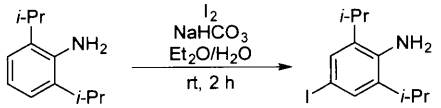

S12
97%

2,6-diisopropylaniline (10.7 g, 60.4 mmol, 1.00 equiv) was dissolved in Et_2O (60 mL) in a 500 mL round-bottomed flask equipped with a magnetic stir bar open to air. The solution was stirred and then I_2 (16.8 g, 66.2 mmol, 1.10 equiv) was added in one portion, followed by aqueous saturated sodium bicarbonate solution (160 mL). The biphasic reaction mixture was vigorously stirred for 2 h; bubbles were noted to form over the course of the reaction. At this time, the reaction mixture was diluted with Et_2O (240 mL) and transferred to a separatory funnel. The organic phase was washed with aqueous saturated sodium thiosulfate solution until the color of

iodine dissipated; deionized water (1 x 120 mL) was then added. The organic layer was separated and then dried over magnesium sulfate, filtered, and concentrated with the aid of a rotary evaporator to afford **S12** as a dark red, viscous oil (17.7 g, 97%). A portion of this material was used in the next step without any further purification. **^{1}H NMR** (400 MHz, $CDCl_3$): δ 7.30 (s, 2H), 3.75 (br s, 2H), 2.86 (h, J = 6.8 Hz, 2H), 1.26 (d, J = 6.9 Hz, 12H). **^{13}C NMR** (151 MHz, $CDCl_3$): δ 140.2, 135.1, 131.8, 81.2, 28.0, 22.4. IR (neat, cm^{-1}): 3486, 3402, 3253, 2959, 2870, 1616, 1459, 1437, 1363, 1348, 1249, 864, 831. Spectral data were in accordance with those in the literature.[22]

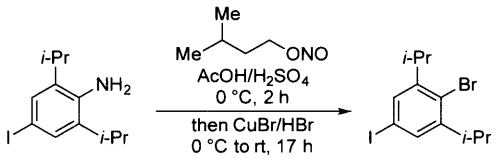

Open to air, **S12** (10.2 g, 33.7 mmol, 1.00 equiv) was dissolved in AcOH (78 mL) in a 200 mL round-bottomed flask equipped with a magnetic stir bar. The solution was vigorously stirred and the flask was cooled to 0 °C in an ice water bath. Then, concentrated H_2SO_4 (95–98%; 22 mL) was carefully added, followed by the addition of isopentyl nitrite (8.75 mL, 65.4 mmol, 1.94 equiv) via addition funnel over the course of 13 min. The solution was allowed to stir at 0 °C for 2 h (*Note: stirring for 2 h is critical ensure complete conversion of the aniline*). Separately, a 3-neck, 500 mL round-bottomed flask equipped with a magnetic stir bar was brought into a nitrogen-filled glovebox, charged with CuBr (6.61 g, 46.1 mmol, 1.37 equiv), and sealed with rubber septa. The flask was removed from the glovebox, and a nitrogen inlet needle was inserted. Then, HBr (48%; 121 mL) was added under a counterflow of nitrogen, and the reaction vessel cooled to 0 °C in an ice water bath. Once the diazonium solution had formed, it was poured into the CuBr/HBr solution under a counterflow nitrogen. A deflated balloon was attached to the reaction vessel to accommodate the nitrogen gas that evolved. The reaction mixture was allowed to warm to rt over the course of 17 h. At this time, the vessel was heated to 80 °C for 15 min, cooled back down to rt, and then the reaction solution was poured onto ice water. This was then transferred to a separatory funnel containing hexanes (250 mL), and the organic phase was washed with aqueous sodium sulfite solution (1 x 100 mL), followed by brine (1 x 100 mL). The organic layer was dried over magnesium sulfate, filtered, and concentrated with the aid of a

rotary evaporator. The crude material was purified via silica gel chromatography (eluting hexanes) to afford **S13** as a slightly yellow oil (7.78 g, 63%). **^{1}H NMR** (400 MHz, $CDCl_3$): δ 7.40 (s, 2H), 3.42 (h, J = 6.8 Hz, 2H), 1.22 (d, J = 6.8 Hz, 12H). **^{13}C NMR** (151 MHz, $CDCl_3$): δ 150.2, 133.5, 126.7, 93.8, 33.6, 23.0. IR (neat, cm^{-1}): 2961, 2926, 2868, 1549, 1461, 1422, 1383, 1068, 1011, 861, 785, 735. Spectral data were in accordance with those in the literature.[23]

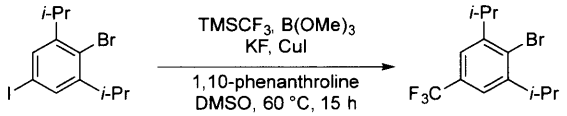

S13 **S14** 87%

A 100 mL oven-dried round-bottomed flask equipped with a magnetic stir bar was brought into a nitrogen-filled glovebox and sequentially charged with CuI (1.53 g, 8.03 mmol, 1.20 equiv), 1,10-phenanthroline (1.43 g, 7.94 mmol, 1.20 equiv), and KF (2.20 g, 38.0 mmol, 5.7 equiv). The flask was sealed with a rubber septum with a balloon inserted and removed from the glovebox. Then, anhydrous DMSO (23 mL) was added and the reaction mixture was allowed to begin stirring. To the resulting red-brown solution was added $B(OMe)_3$ (2.30 mL, 20.6 mmol, 3.10 equiv), **S13** (2.45 g, 6.67 mmol, 1.00 equiv), and $TMSCF_3$ (3.00 mL, 20.3 mmol, 3.04 equiv) via syringe. The reaction mixture was then allowed to stir in a pre-heated oil bath at 60 °C for 3 h. At this time, the reaction mixture was cooled to rt, and another portion of $TMSCF_3$ (3.00 mL, 20.3 mmol, 3.04 equiv) was added via syringe, and the flask was returned to the oil bath at 60 °C for 15 h. Then, the reaction mixture was allowed to cool to rt, the flask was opened to the air, and Et_2O (30 mL) was added. The reaction mixture was filtered through a plug of celite to remove insoluble material and the celite pad was washed with additional Et_2O (3 x 15 mL). The filtrate was transferred to a separatory funnel, and the organic phase was washed sequentially with deionized water (1 x 75 mL), ammonium hydroxide (28–30% NH_3 basis; 2 x 30 mL), and brine (1 x 50 mL). The organic layer was then dried over magnesium sulfate, filtered, and concentrated with the aid of a rotary evaporator. The crude residue was purified via silica gel chromatography (eluting hexanes) to afford **S14** as a colorless oil (1.90 g, 87%) with 95% purity (the impurity is the starting material, which has a similar polarity as the product). **^{1}H NMR** (400 MHz, $CDCl_3$): δ 7.35 (s, 2H), 3.54 (h, J = 6.9 Hz, 2H), 1.27 (d, J = 6.9 Hz, 12H). **^{13}C NMR** (151 MHz, $CDCl_3$): δ 149.1, 133.6, 130.3, 130.1 (q, J = 32.2 Hz), 121.1 (q, J = 3.7 Hz), 34.0, 23.0. **^{19}F**

NMR (565 MHz, $CDCl_3$): δ -62.5. IR (neat, cm^{-1}): 2966, 2875, 1355, 1226, 1160, 1123, 1017, 887. Spectral data were in accordance with those in the literature.[19]

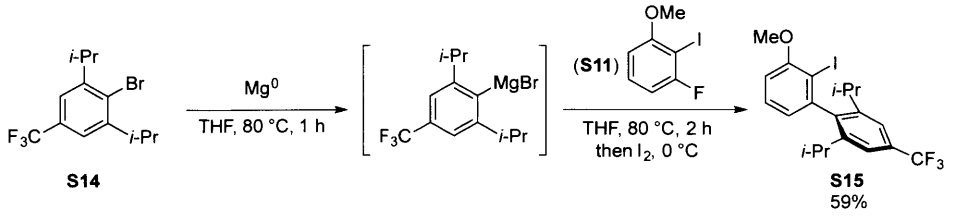

A 25 mL oven-dried reaction tube equipped with a magnetic stir bar was charged with Mg turnings (109 mg, 4.48 mmol, 1.53 equiv) and a single crystal of iodine. The tube was sealed with a screw-cap fitted with a Teflon septum, and an inlet needle attached to a Schlenk line was inserted. The tube was evacuated and backfilled with argon. This sequence was repeated two additional times. Anhydrous THF (3.00 mL) was added via syringe, followed by **S14** (982 mg, 3.18 mmol, 1.09 equiv) and the reaction mixture was allowed to begin stirring. The septum was then exchanged for one that had not been punctured, under a counterflow of argon, and the tube placed in a pre-heated oil bath at 80 °C for 1 h. At this time, the reaction mixture was cooled to rt, and **S11** (737 mg, 2.92 mmol, 1.00 equiv) was added via syringe. The septum was then exchanged for one that had not been punctured, under a counterflow of argon, and the tube placed back in the pre-heated oil bath at 80 °C for 2 h. At this time, the reaction mixture was cooled to 0 °C in an ice water bath, and I_2 was added dropwise via syringe as a solution in THF (2.5 mL; 1.08 g I_2, 4.26 mmol, 1.46 equiv). After the addition was complete, the tube was removed from the ice water bath. Once the reaction mixture had reached rt, the tube was uncapped and the contents poured into a separatory funnel containing EtOAc (75 mL) and aqueous saturated sodium thiosulfate solution (100 mL). The organic phase was washed with brine (1 x 25 mL), then dried over magnesium sulfate, filtered, and concentrated with the aid of a rotary evaporator. The crude residue was purified via automated silica gel chromatography (Biotage KP-SIL 50 g column, eluting 0% to 30% CH_2Cl_2/hexanes) to afford **S15** as a white solid (859 mg, 59%) with 95% purity (the impurity is dehalogenated product, which has a similar polarity as the product). mp: 169–171 °C. **^{1}H NMR** (600 MHz, $CDCl_3$): δ 7.47 (s, 2H), 7.39 (t, J = 7.8 Hz, 1H), 6.85 (dd, J = 8.3, 1.3 Hz, 1H), 6.78 (dd, J = 7.5, 1.3 Hz, 1H), 3.99 (s, 3H), 2.50 (h, J = 6.9 Hz, 2H), 1.25 (d, J = 6.9 Hz, 6H), 1.05 (d, J = 6.9 Hz, 6H). **^{13}C NMR** (151 MHz, $CDCl_3$): δ 158.6, 147.4, 146.4, 145.1, 130.7 (q, J = 30.2 Hz), 129.2, 122.6, 120.0 (q, J = 3.8 Hz), 109.4,

92.8, 56.6, 30.8, 24.9, 23.4 (Note: overlap of one aryl signal). **^{19}F NMR** (376 MHz, $CDCl_3$): δ -62.3. IR (neat, cm^{-1}): 2965, 2867, 1562, 1465, 1325, 1254, 1165, 1103, 1058, 887, 785, 780.

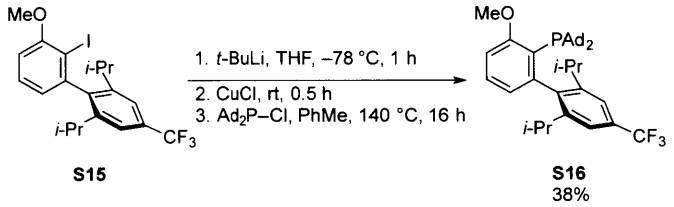

S15 **S16** 38%

S16 was prepared according to general procedure B. A mixture of **S15** (709 mg, 1.53 mmol, 1.00 equiv), *t*-BuLi (1.29 M in pentane; 2.50 mL, 3.23 mmol, 2.10 equiv), CuCl (175 mg, 1.76 mmol, 1.15 equiv), and Ad_2PCl (620 mg, 1.84 mmol, 1.20 equiv) was stirred in a Schlenk tube at 140 °C for 16 h behind a blast shield. Purified via trituration from MeOH, followed by crystallization from EtOAc/MeOH to afford **S16** as a white crystalline solid (371 mg, 38%). mp: 253–256 °C. **^{1}H NMR** (600 MHz, $CDCl_3$): δ 7.35 (s, 1H), 7.33 (t, J = 7.8 Hz, 2H), 6.93 (d, J = 8.2 Hz, 1H), 6.74 (dd, J = 7.6, 3.5 Hz, 1H), 3.88 (s, 3H), 2.65 (h, J = 6.6 Hz, 2H), 1.87 (q, J = 6.8, 5.0 Hz, 17H), 1.64 (s, 12H), 1.25 (d, J = 6.7 Hz, 6H), 0.96 (d, J = 6.6 Hz, 6H). **^{13}C NMR** (151 MHz, $CDCl_3$): δ 162.0, 150.3 (d, J = 36.4 Hz), 147.7, 144.1, 129.7 (q, J = 31.7 Hz), 129.2, 125.2 (d, J = 7.5 Hz), 123.4, 123.1, 119.4 (d, J = 3.8 Hz), 109.1, 54.1, 42.1 (d, J = 13.5 Hz), 39.0 (d, J = 28.0 Hz), 37.2, 31.1, 29.3 (d, J = 9.1 Hz), 26.5, 22.7 (the observed complexity is due to C–P and C–F coupling). **^{19}F NMR** (471 MHz, $CDCl_3$): δ -62.0. **^{31}P NMR** (203 MHz, $CDCl_3$): δ 35.6. IR (neat, cm^{-1}): 2901, 2884, 2845, 1456, 1309, 1246, 1147, 1117, 1101, 1090, 883, 791, 778, 736.

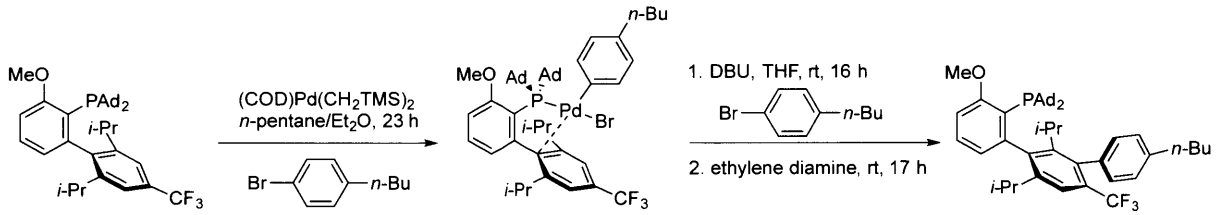

S16 65% **L5** 73%

In a nitrogen-filled glovebox, an oven-dried 25 mL screw-cap tube equipped with a magnetic stir bar was charged with **S16** (200 mg, 0.314 mmol, 1.00 equiv). Anhydrous Et_2O (10 mL) and anhydrous pentane (10 mL) were added and the reaction mixture stirred until all of the ligand had dissolved. Then, 1-bromo-4-*n*-butylbenzene (130 mg, 0.610 mmol, 1.94 equiv) was added via microliter pipette, followed by $(COD)Pd(CH_2TMS)_2$ (122 mg, 0.314 mmol, 1.00 equiv). The

solution turned yellow upon the addition of the Pd reagent, and a precipitate began to form. The reaction tube was sealed with a screw-cap fitted with a Teflon septum, removed from the glovebox, and vigorously stirred at rt for 24 h. At this time, the tube was uncapped and the precipitate was isolated using a sintered glass funnel. The filter cake was washed with pentane (3 x 3 mL) to afford the complex as a yellow solid (197 mg, 65%), which was used directly in the next step without further purification.

A 100 mL oven-dried round-bottomed flask equipped with a magnetic stir bar was charged with the complex (181 mg, 0.189 mmol, 1.00 equiv) formed in the previous step. The flask was sealed with a rubber septum and an inlet needle attached to a Schlenk line was inserted. The flask was evacuated and backfilled with argon. This sequence was repeated two additional times. Anhydrous THF (40 mL) and 1-bromo-4-*n*-butylbenzene (80 μL, 0.45 mmol, 2.4 equiv) were added sequentially via syringe, and the reaction mixture was allowed to begin stirring. Then, DBU (30 μL, 0.20 mmol, 1.10 equiv) was added via microliter syringe. The resulting yellow-brown solution was allowed to stir at rt for 16 h, at which time ethylene diamine (127 μL, 1.89 mmol, 10 equiv) was added and the reaction mixture was allowed to stir for another 17 h at rt. At this time, the reaction mixture was poured into a separatory funnel containing EtOAc (100 mL). The organic phase was washed with ammonium hydroxide (28–30% NH_3 basis)/brine solution (2:1; 5 x 40 mL), followed by brine (2 x 50 mL). The organic layer was then dried over magnesium sulfate, filtered, and concentrated with the aid of a rotary evaporator. The crude residue was purified via automated silica gel chromatography (Biotage KP-SIL 25 g column, eluting 0% to 100 DCM/EtOAc), which afforded **L5** as a yellow foam, which became a white solid after trituration from MeOH (106 mg, 73%). mp: 254–257 °C. **^{1}H NMR** (600 MHz, $CDCl_3$): δ 7.49 (s, 1H), 7.33 (t, J = 7.9 Hz, 1H), 7.21 (d, J = 8.6 Hz, 2H), 7.11 (t, J = 7.7 Hz, 2H), 6.90 (d, J = 8.2 Hz, 1H), 6.82 (dd, J = 7.6, 3.5 Hz, 1H), 3.87 (s, 3H), 2.83 (h, J = 6.7 Hz, 1H), 2.65 (t, J = 7.8 Hz, 2H), 2.56 (h, J = 6.2 Hz, 1H), 1.87 (m, 18H), 1.64 (m, 14H), 1.38 (h, J = 7.4 Hz, 2H), 1.27 (d, J = 6.8 Hz, 3H), 0.99 (d, J = 6.6 Hz, 3H), 0.94 (t, J = 7.3 Hz, 3H), 0.91 (d, J = 6.9 Hz, 3H), 0.44 (d, J = 7.1 Hz, 3H). **^{13}C NMR** (151 MHz, $CDCl_3$): δ 162.1, 151.6 (d, J = 36.5 Hz), 146.3, 145.6, 145.4 (d, J = 6.1 Hz), 141.9, 137.4, 135.4, 132.7, 131.3, 129.5 (q, J = 27.5 Hz), 129.0, 126.3 (d, J = 7.9 Hz), 125.7, 125.2 (d, J = 7.5 Hz), 123.0, 122.7, 120.1 (q, J = 5.3 Hz), 108.8, 54.1, 42.1 (d, J = 14.3 Hz), 42.0 (d, J = 14.3 Hz), 39.1 (d, J = 28.4 Hz), 38.9 (d, J =

28.4 Hz), 37.2 (d, J = 7.1 Hz), 35.6, 33.8, 32.9, 31.3, 29.4 (d, J = 3.8 Hz), 29.3 (d, J = 3.7 Hz), 26.5, 24.9, 23.4, 22.7, 22.5, 14.2 (the observed complexity is due to C–P and C–F coupling). **^{19}F NMR** (565 MHz, $CDCl_3$): δ -56.5. **^{31}P NMR** (162 MHz, $CDCl_3$): δ 36.0. IR (neat, cm^{-1}): 2901, 2847, 1562, 1458, 1309, 1255, 1143, 1119, 1060, 1028, 796, 702. **HRMS** (ESI) m/z calcd for $C_{50}H_{64}F_3OP$ $[M+H]^+$: 769.4725; 769.4716 found.

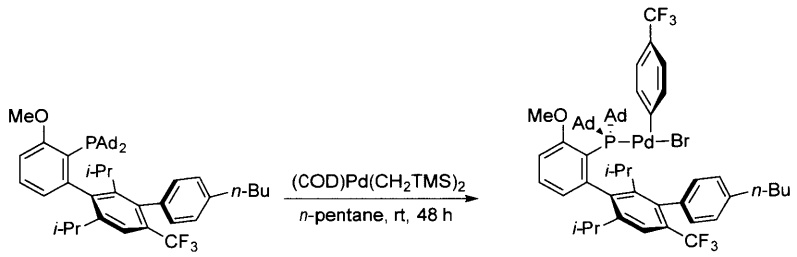

L5 **L5–Pd(Ar)Br** 84%

L5–Pd(Ar)Br was prepared following general procedure A. In a 25 mL reaction tube, a mixture of **L5** (80.5 mg, 0.105 mmol, 1.00 equiv), 4-bromobenzotrifloride (55.0 mg, 0.244 mmol, 2.34 equiv), and $(COD)Pd(CH_2TMS)_2$ (42 mg, 0.11 mmol, 1.0 equiv) was stirred in pentane (10 mL) at rt for 48 h. The complex was filtered outside the glovebox to afford **L5–Pd(Ar)Br** as a yellow solid (97 mg, 84%). **^{1}H NMR** (300 MHz, $CDCl_3$): δ 7.63 (m, 2H), 7.50 (d, J = 8.2 Hz, 1H), 7.38 (m, 3H), 7.09 (m, 4H), 6.94 (d, J = 8.3 Hz, 1H), 6.45 (d, J = 7.9 Hz, 1H), 3.92 (s, 3H), 3.12 (m, 1H), 2.65 (br t, J = 7.8 Hz, 3H), 2.37 (m, 7H), 2.05 (m, 7H), 1.86 – 1.48 (m, 27H), 1.34 (m, 4H), 1.06 – 0.74 (m, 5H). **^{13}C NMR** (126 MHz, $CDCl_3$): δ 161.1, 151.5, 149.3 (d, J = 18.4 Hz), 148.0, 142.5, 140.5 (m), 139.5, 139.2, 137.9 (m), 134.1, 134.0, 132.9, 132.2, 131.9, 131.2, 127.7 (d, J = 9.5 Hz), 127.0 (m), 126.5, 126.4 (d, J = 4.7 Hz), 126.0, 125.9, 122.7 (m), 122.2 (m), 109.8, 54.1, 47.8 (d, J = 10.0 Hz), 46.8 (d, J = 9.1 Hz), 42.5, 40.4, 36.3 (d, J = 39.6 Hz), 35.7, 34.0, 33.8, 31.1, 29.6 (d, J = 9.6 Hz), 29.4 (d, J = 9.6 Hz), 25.5, 25.0 (d, J = 22.1 Hz), 24.1, 22.5, 14.2 (the observed complexity is due to C–P and C–F coupling). **^{19}F NMR** (471MHz, $CDCl_3$): δ -56.6, -56.9, -61.9, -62.8. **^{31}P NMR** (121 MHz, C_6D_6): δ 66.0. IR (neat, cm^{-1}): 2907, 2850, 1584, 1564, 1324, 1267, 1160, 1131, 1115, 1104, 1067, 1005, 816, 800, 733. **HRMS** (ESI) m/z calcd for $C_{57}H_{68}BrF_6OPPd$ $[M–Br]^+$: 1019.3947; 1019.3957 found.

VI. Experimental Procedures and Characterization Data for **L6** and its Corresponding Complex

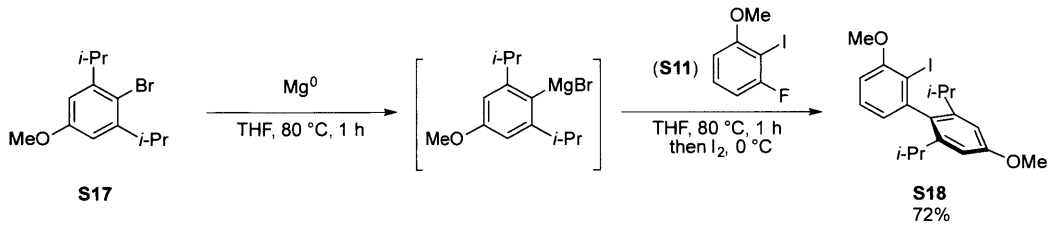

A 25 mL oven-dried reaction tube equipped with a magnetic stir bar was charged with Mg turnings (136 mg, 5.59 mmol, 1.87 equiv) and a single crystal of iodine. The tube was sealed with a screw-cap fitted with a Teflon septum, and an inlet needle attached to a Schlenk line was inserted. The tube was evacuated and backfilled with argon. This sequence was repeated two additional times. Anhydrous THF (3.00 mL) and **S17** (908 mg, 3.35 mmol, 1.12 equiv) were added sequentially via syringe, and the reaction mixture was allowed to begin stirring. The septum was then exchanged for one that had not been punctured, under a counterflow of argon, and the tube placed in a pre-heated oil bath at 80 °C for 1 h. At this time, the reaction mixture was cooled to rt, and **S11** (754 mg, 2.99 mmol, 1.00 equiv) was added via syringe. The septum was again exchanged for one that had not been punctured, under a counterflow of argon, and the tube placed back in the pre-heated oil bath at 80 °C for 1 h. At this time, the reaction mixture was cooled to 0 °C in an ice water bath, and I_2 was added dropwise via syringe as a solution in THF (2.0 mL; 1.14 g I_2, 4.49 mmol, 1.50 equiv). After the addition was complete, the tube was removed from the ice water bath. Once the reaction mixture had reached rt, the tube was uncapped and the contents poured into a separatory funnel containing EtOAc (100 mL) aqueous saturated sodium thiosulfate solution (100 mL). The organic phase was washed sequentially with deionized water (1 x 50 mL) and brine (1 x 50 mL). The organic layer was then dried over magnesium sulfate, filtered, and concentrated with the aid of a rotary evaporator. The crude residue was purified via automated silica gel chromatography (Biotage KP-SIL 50 g column, eluting 0% to 30% CH_2Cl_2/hexanes) to afford **S18** as a white solid (983 mg, 72%) with 93% purity (the impurity is dehalogenated product, which has a similar polarity as the product). mp: 141–143 °C. **^{1}H NMR** (600 MHz, $CDCl_3$): δ 7.32 (t, J = 7.8 Hz, 1H), 6.80 (ddd, J = 9.8, 7.8, 1.4 Hz, 2H), 6.76 (s, 1H), 3.95 (s, 3H), 3.88 (s, 3H), 2.43 (h, J = 6.9 Hz, 2H), 1.21 (d, J = 7.0 Hz, 6H), 1.02 (d, J = 6.9 Hz, 6H). **^{13}C NMR** (151 MHz, $CDCl_3$): δ 159.7, 147.8, 147.7, 135.0, 128.8,

123.6, 108.9, 108.4, 94.9, 56.5, 55.1, 30.9, 25.0, 23.5. IR (neat, cm^{-1}): 2958, 2864, 2835, 1601, 1460, 1334, 1278, 1260, 1195, 1113, 1018, 866, 846, 783, 770.

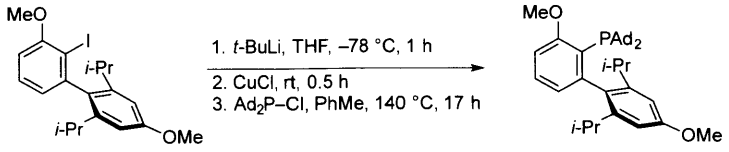

S18 **S19** 39%

S19 was prepared according to general procedure B. A mixture of **S18** (707 mg, 1.67 mmol, 1.00 equiv), *t*-BuLi (1.29 M in pentane; 2.70 mL, 3.48 mmol, 2.10 equiv), CuCl (213 mg, 2.15 mmol, 1.30 equiv), and Ad_2PCl (698 mg, 2.07 mmol, 1.24 equiv) was stirred at 140 °C in a Schlenk tube for 17 h behind a blast shield. Purified via automated silica gel chromatography (eluting 0% to 100% DCM/EtOAc) to afford **S19** as a white solid (387 mg, 39%). mp: 250–253 °C. **^{1}H NMR** (600 MHz, $CDCl_3$): δ 7.30 (t, J = 7.8 Hz, 1H), 6.89 (d, J = 8.1 Hz, 1H), 6.80 (ddd, J = 7.6, 3.8, 1.2 Hz, 1H), 6.68 (s, 2H), 3.87 (s, 3H), 3.86 (s, 3H), 2.60 (h, J = 6.7 Hz, 2H), 1.88 (m, 18H), 1.65 (m, 12H), 1.22 (d, J = 6.8 Hz, 6H), 0.96 (d, J = 6.6 Hz, 6H). **^{13}C NMR** (151 MHz, $CDCl_3$): δ 161.8 (d, J = 2.6 Hz), 159.0, 151.5 (d, J = 36.6 Hz), 148.2, 133.5 (d, J = 6.6 Hz), 128.8, 126.1 (d, J = 6.9 Hz), 124.0 (d, J = 45.9 Hz), 108.5, 107.7 , 55.0, 54.0 , 42.1 (d, J = 13.7 Hz), 38.8 (d, J = 28.7 Hz), 37.2, 31.1 (d, J = 2.2 Hz), 29.4 (d, J = 8.8 Hz), 26.5, 22.8 (the observed complexity is due to C–P coupling). **^{31}P NMR** (203 MHz, $CDCl_3$): δ 35.6. IR (neat, cm^{-1}): 2953, 2901, 2879, 2844, 1601, 1562, 1456, 1431, 1331, 1269, 1250, 1018, 843, 801, 771.

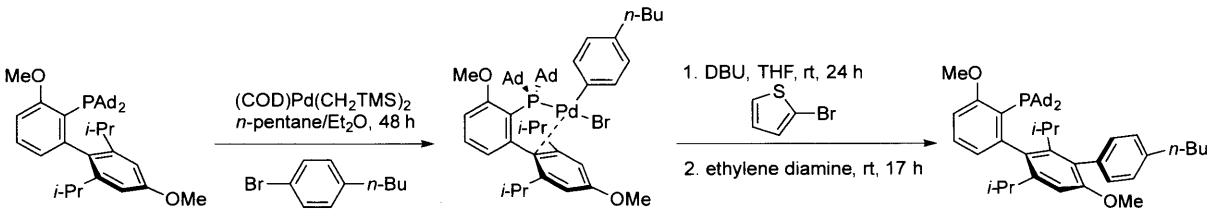

S19 77% **L6** 45%

In a nitrogen-filled glovebox, an oven-dried 25 mL screw-cap tube equipped with a magnetic stir bar was charged with **S19** (281 mg, 0.469 mmol, 1.00 equiv). Anhydrous Et_2O (15 mL) and anhydrous pentane (15 mL) were added and the reaction mixture stirred until all of the ligand had dissolved. Then, 1-bromo-4-*n*-butylbenzene (325 mg, 1.52 mmol, 3.25 equiv) was added via microliter pipette, followed by $(COD)Pd(CH_2TMS)_2$ (183 mg, 0.471 mmol, 1.01 equiv). The

solution turned yellow upon the addition of the Pd reagent, and a precipitate began to form. The reaction tube was sealed with a screw-cap fitted with a Teflon septum, removed from the glovebox, and vigorously stirred at rt for 48 h. At this time, the tube was opened to the air and the precipitate filtered using sintered glass funnel. The filter cake was washed with pentane (3 x 3 mL) to afford the complex as a red solid (332 mg, 77%), which was used directly in the next step without further purification.

A 100 mL oven-dried round-bottomed flask equipped with a magnetic stir bar was charged with the complex (332 mg, 0.362 mmol, 1.00 equiv) formed in the previous step. The flask was sealed with a rubber septum and an inlet needle attached to a Schlenk line was inserted. The flask was evacuated and backfilled with argon. This sequence was repeated two additional times. Anhydrous THF (30 mL) and 2-bromothiophene (60 μL, 0.62 mmol, 1.7 equiv) were added sequentially via syringe, and the reaction mixture was allowed to begin stirring. Then, DBU (56 μL, 0.37 mmol, 1.04 equiv) was added to the red solution via microliter syringe. The resulting orange solution was allowed to stir at rt for 24 h, at which time ethylene diamine (150 μL, 2.24 mmol, 6 equiv) was added and the reaction mixture allowed to stir for another 17 h at rt. At this time, the reaction mixture was poured into a separatory funnel containing EtOAc (100 mL). The organic phase was washed with ammonium hydroxide (28–30% NH_3 basis)/brine solution (2:1; 5 x 40 mL), followed by brine (2 x 50 mL). The organic layer was then dried over magnesium sulfate, filtered, and concentrated with the aid of a rotary evaporator. The crude residue was purified via crystallization from DCM/MeOH to afford **L6** as a light orange crystalline solid (120 mg, 45%). mp: 208–210 °C. **^{1}H NMR** (500 MHz, $CDCl_3$): δ 7.29 (t, J = 7.8 Hz, 1H), 7.15 (d, J = 5.3 Hz, 2H), 6.86 (dd, J = 7.8, 3.0 Hz, 2H), 6.72 (s, 1H), 3.86 (s, 3H), 3.69 (s, 3H), 2.71 (h, J = 7.0 Hz, 1H), 2.64 (dd, J = 8.9, 6.8 Hz, 2H), 2.56 (h, J = 6.6 Hz, 1H), 2.01 – 1.76 (m, 20 H), 1.73 – 1.55 (m, 15H), 1.39 (sx, J = 7.4 Hz, 2H), 1.26 (d, J = 6.7 Hz, 3H), 0.99 (d, J = 6.6 Hz, 3H), 0.96 – 0.90 (m, 6H; overlapping –$(CH_2)_3$**CH_3** and –$CH($**CH_3**$)_2$), 0.47 (d, J = 7.1 Hz, 3H). **^{13}C NMR** (126 MHz, $CDCl_3$): δ 161.9 (d, J = 2.5 Hz), 157.1, 152.8 (d, J = 36.6 Hz), 146.7, 144.9, 140.8, 136.6, 134.4 (d, J = 6.4 Hz), 132.2, 130.6, 128.6, 128.2, 127.2 (d, J = 5.3 Hz), 126.4 (d, J = 6.9 Hz), 123.9, 123.6, 108.3, 104.8, 55.9, 54.0, 42.1 (d, J = 11.3 Hz), 42.0 (d, J = 11.4 Hz), 39.0 (d, J = 11.7 Hz), 38.8 (d, J = 11.1 Hz), 37.3 (d, J = 8.9 Hz), 35.7, 33.8, 32.7, 31.5 (d, J = 2.3 Hz), 29.4 (d, J = 9.4 Hz), 29.3 (d, J = 9.4 Hz), 26.5, 25.1, 23.5, 23.0, 22.7, 14.2 (the observed

complexity is due to C–P coupling). **^{31}P NMR** (162 MHz, $CDCl_3$): δ 35.9. IR (neat, cm^{-1}): 2958, 2897, 2843, 1586, 1558, 1451, 1336, 1267, 1245, 1087, 794, 579. **HRMS** (ESI) m/z calcd for $C_{50}H_{67}O_2P$ $[M+H]^+$: 731.4957; 731.4955 found.

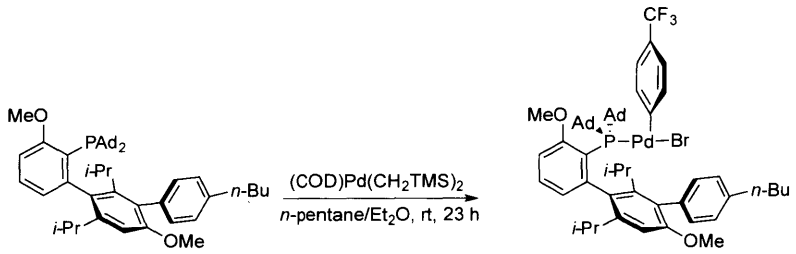

L6 **L6–Pd(Ar)Br** 36%

L6–Pd(Ar)Br was prepared following general procedure A. In a 25 mL reaction tube, a mixture of **L6** (107 mg, 0.146 mmol, 1.00 equiv), 4-bromobenzotrifloride (79 mg, 0.350 mmol, 2.4 equiv), and $(COD)Pd(CH_2TMS)_2$ (57.4 mg, 0.148 mmol, 1.01 equiv) was stirred in a mixture of pentane (10 mL) and Et_2O (11 mL) at rt for 23 h. The complex was filtered outside the glovebox to afford **L6–Pd(Ar)Br** as an orange solid (55.5 mg, 36%). **^{1}H NMR** (500 MHz, $CDCl_3$): δ 7.62 (d, J = 7.8 Hz, 1H), 7.42 (br s, 2H), 7.34 (br t, J = 7.9 Hz, 1H), 7.11 (m, 5H), 6.88 (d, J = 8.2 Hz, 1H), 6.73 (s, 1H), 6.42 (d, J = 7.7 Hz, 1H), 3.90 (s, 3H), 3.78 (s, 3H), 2.95 (br p, J = 7.1 Hz, 1H), 2.64 (br t, J = 7.8 Hz, 2H), 2.44 (br p, J = 6.7 Hz, 1H), 2.32 (s, 6H), 2.15 (d, J = 12.2 Hz, 3H), 2.03 – 1.88 (m, 7H), 1.89 – 1.52 (m, 20H), 1.38 (sx, J = 7.7 Hz, 2H), 1.04 (d, J = 7.0 Hz, 3H), 0.94 (br t, J = 7.4 Hz, 3H), 0.90 (d, J = 6.9 Hz, 3H), 0.86 (d, J = 6.6 Hz, 3H). **^{13}C NMR** (126 MHz, $CDCl_3$): δ 166.1, 160.8, 154.3, 153.6, 151.0 (d, J = 18.4 Hz), 141.3, 141.0, 140.5 (d, J = 8.1 Hz), 139.3, 134.9, 132.4, 131.5, 131.4, 130.8, 128.5 (d, J = 10.4 Hz), 127.5, 126.7, 126.1, 124.6 (q, J = 31.5 Hz), 124.2 (d, J = 15.5 Hz), 124.0, 121.7 (d, J = 25.6 Hz), 117.9 (d, J = 3.6 Hz), 109.3, 109.1, 56.9, 53.9, 47.4 (d, J = 10.3 Hz), 46.8 (d, J = 10.0 Hz), 42.2, 40.7, 36.4 (d, J = 28.7 Hz), 35.7, 33.8 (d, J = 7.4 Hz), 31.7, 29.6 (d, J = 9.5 Hz), 29.4 (d, J = 9.3 Hz), 25.3 (d, J = 6.5 Hz), 24.9, 23.8, 22.6, 14.2 (the observed complexity is due to C–P and C–F coupling). **^{19}F NMR** (376 MHz, $CDCl_3$): δ -61.7. **^{31}P NMR** (203 MHz, $CDCl_3$): δ 68.1. IR (neat, cm^{-1}): 2905, 2851, 1583, 1564, 1456, 1324, 1259, 1156, 1116, 1098, 1088, 1067, 1042, 1005, 818, 803, 721. **HRMS** (ESI) m/z calcd for $C_{57}H_{71}BrF_3O_2PPd$ $[M–Br]^+$: 981.4179; 981.4200 found.

VII. Experimental Procedure and Characterization Data for **L7**–Pd(Ar)Br

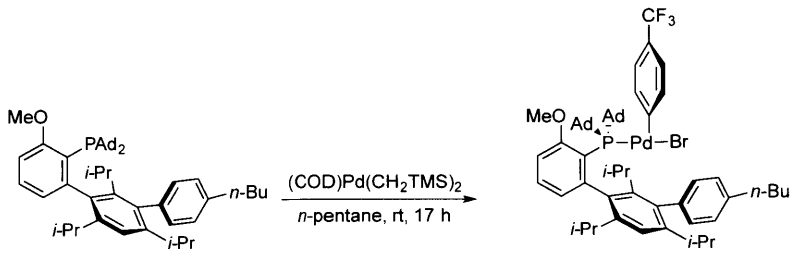

L7 **L7–Pd(Ar)Br** 48%

L7–Pd(Ar)Br was prepared following general procedure A. In a 50 mL round-bottomed flask a mixture of **L7** (70.0 mg, 98.2 μmol, 1.00 equiv), 4-bromobenzotrifloride (30 μL, 0.21 mmol, 2.3 equiv), and (COD)Pd($CH_2TMS)_2$ (40 mg, 0.104 mmol, 1.10 equiv) was stirred in pentane (8 mL) at rt for 17 h. The complex was filtered outside the glovebox to afford **L7–Pd(Ar)Br** as a yellow-green solid (49 mg, 48%). **^{1}H NMR** (600 MHz, $CDCl_3$): δ 7.69 (d, J = 7.8 Hz, 1H), 7.40 (d, J = 8.3 Hz, 2H), 7.33 (t, J = 7.9 Hz, 1H), 7.18 (s, 1H), 7.13 – 7.03 (m, 5H), 6.87 (d, J = 8.2 Hz, 1H), 6.39 (d, J = 7.3 Hz, 1H), 3.90 (s, 3H), 2.99 (h, J = 6.1 Hz, 1H), 2.64 (t, J = 7.8 Hz, 2H), 2.49 (m, 2H), 2.31 (m, 6H), 2.16 (m, 3H), 1.97 (m, 6H), 1.84 (s, 3H), 1.77 (m, 3H), 1.63 (m 17H), 1.38 (sx, J = 7.4 Hz, 2H), 1.25 (d, J = 6.8 Hz, 3H), 1.04 (d, J = 6.8 Hz, 3H), 1.01 (d, J = 7.1 Hz, 3H), 0.95 (t, J = 7.4 Hz, 3H), 0.87 (d, J = 6.6 Hz, 3H), 0.84 (d, J = 6.9 Hz, 3H). **^{13}C NMR** (151 MHz, $CDCl_3$): δ 160.7, 158.4, 152.2, 151.2, 151.1, 150.5 141.5, 141.4, 140.9, 140.1, 139.3, 137.6, 132.3, 131.9, 131.4, 131.0, 128.6 (d, J = 10.2 Hz), 127.3, 126.4, 124.8, 124.4 (q, J = 31.7 Hz; overlaps), 124.3, 123.7 (d, J = 15.1 Hz), 121.7 (d, J = 27.1 Hz), 109.0, 53.9, 47.4 (d, J = 10.2 Hz), 46.9 (d, J = 9.7 Hz), 42.0, 40.8, 36.4 (d, J = 28.0 Hz), 35.7, 33.9, 33.7, 31.5, 30.2, 29.6 (d, J = 9.5 Hz), 29.5 (d, J = 9.7 Hz), 26.1, 25.6, 25.4, 25.1 (d, J = 7.8 Hz), 23.6, 22.6, 14.2. **^{19}F NMR** (565 MHz, $CDCl_3$): δ -61.7. **^{31}P NMR** (162 MHz, $CDCl_3$): δ 67.4. IR (neat, cm^{-1}): 2905, 2848, 1584, 1565, 1456, 1325, 1156, 1114, 1104, 1068, 1005, 814, 798. **HRMS** (ESI) m/z calcd for $C_{59}H_{75}BrF_3OPPd$ $[M–Br]^+$: 993.4542; 993.4559 found.

VIII. Experimental Procedures and Characterization Data for **L8** and its Corresponding Complex

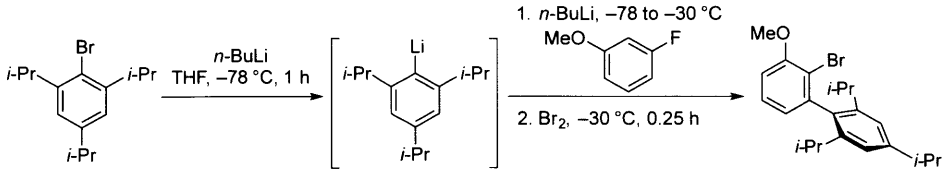

S20
53%

A 1 L oven-dried round-bottomed flask equipped with a magnetic stir bar was fitted with a rubber septum and an inlet needle attached to a Schlenk line was inserted. The flask was evacuated and backfilled with argon. This sequence was repeated two additional times. 2-bromo-1,3,5-triisopropylbenzene (17.4 g, 61.3 mmol, 2.00 equiv) was added via syringe, followed by anhydrous THF (250 mL), and the reaction mixture was allowed to begin stirring. The flask was cooled to –78 °C in a dry ice/acetone bath and then *n*-BuLi (2.50 M in hexane; 7.3 mL, 18.5 mmol + 1.35 M in hexane; 34 mL, 45.9 mmol = 64.4 mmol total, 2.05 equiv) was added dropwise via syringe over the course of 30 min. The resulting light yellow solution was allowed to stir at –78 °C for 1 h. Separately, a 1 L oven-dried round-bottomed flask equipped with a magnetic stir bar was fitted with a rubber septum and an inlet needle attached to a Schlenk line was inserted. The flask was evacuated and backfilled with argon. This sequence was repeated two additional times. 3-fluoroanisole (3.50 mL, 30.6 mmol, 1.00 equiv) was added via syringe, followed by anhydrous THF (150 mL), and the reaction mixture was allowed to begin stirring. The flask was cooled to –78 °C in a dry ice/acetone bath and then *n*-BuLi (1.35 M in hexane; 11 mL, 14.9 mmol + 2.06 M in hexane; 7.2 mL, 14.8 mmol = 29.7 mmol total, 1.00 equiv) was added dropwise via syringe over the course of 15 min. The resulting slightly cloudy solution was allowed to stir at –78 °C for 1 h. At this time, the solution of (2,4,6-triisopropylphenyl)lithium was transferred to the solution of (2-fluoro-6-methoxyphenyl)lithium via cannula over the course of 8 min. The reaction mixture was allowed to warm to –25 °C and the reaction mixture was stirred at this temperature for 1 h. At this time, Br_2 (4.0 mL, 78 mmol, 2.50 equiv) was carefully added dropwise via syringe over the course of 4 min. The resulting orange solution was allowed to warm to rt, at which time the flask was opened to the air and aqueous sodium thiosulfate solution (150 mL) was carefully added. The biphasic mixture was vigorously stirred for 5 min, and then deionized water (100 mL) and EtOAc (100 mL) were added, and the mixture

transferred to a separatory funnel. The separated organic phase was washed sequentially with aqueous saturated sodium thiosulfate solution (1 x 150 mL), deionized water (1 x 100 mL), and brine (1 x 150 mL). The organic layer was then dried over magnesium sulfate, filtered, and concentrated with the aid of a rotary evaporator. The crude yellow oil was purified by silica gel chromatography (eluting 0% to 4% EtOAc/hexanes), followed by crystallization from EtOAc/MeOH to afford **S20** as a white crystalline solid (6.29 g, 53%). mp: 117–119 °C. **^{1}H NMR** (500 MHz, $CDCl_3$): δ 7.29 (t, J = 7.9 Hz, 1H), 7.05 (s, 2H), 6.89 (d, J = 8.1 Hz, 1H), 6.81 (d, J = 7.5 Hz, 1H), 3.96 (s, 3H), 2.95 (h, J = 7.0 Hz, 1H), 2.44 (h, J = 6.9 Hz, 2H), 1.31 (d, J = 6.9 Hz, 6H), 1.16 (d, J = 6.9 Hz, 6H), 1.03 (d, J = 6.8 Hz, 6H). **^{13}C NMR** (126 MHz, $CDCl_3$): δ 156.2, 148.4, 146.1, 143.7, 135.9, 127.6, 123.9, 120.9, 114.7, 110.0, 56.4, 34.3, 30.8, 24.9, 24.2, 23.8. IR (neat, cm^{-1}): 2957, 2925, 2864, 1562, 1452, 1419, 1359, 1265, 1087, 1018, 783, 776, 719. Spectral data were in accordance with those in the literature.[19]

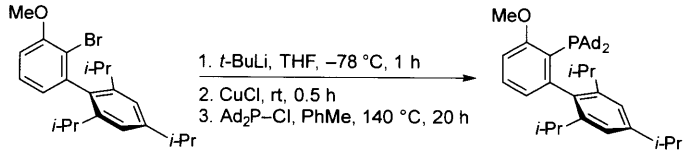

S20 **S21** 75%

S21 was prepared according to general procedure B. A mixture of **S20** (1.00 g, 2.57 mmol, 1.00 equiv), *t*-BuLi (1.4 M in pentane; 3.9 mL, 5.4 mmol, 2.1 equiv), CuCl (305 mg, 3.14 mmol, 1.22 equiv), Ad_2PCl (1.09 g, 3.24 mmol, 1.26 equiv) was stirred in a Schlenk tube at 140 °C for 20 h behind a blast shield. Purified via trituration from MeOH to afford **S21** as a white solid (1.17 g, 75%). mp: 220–222 °C. **^{1}H NMR** (400 MHz, $CDCl_3$): δ 7.27 (t, J = 9.4 Hz, 2H), 6.96 (s, 2H), 6.88 (d, J = 8.1 Hz, 1H), 6.80 (dd, J = 7.6, 3.6 Hz, 1H), 3.86 (s, 3H), 2.92 (h, J = 6.8 Hz, 1H), 2.58 (h, J = 7.2 Hz, 1H), 1.93 – 1.79 (m, 19H), 1.64 (m, 13H), 1.30 (d, J = 6.9 Hz, 6H), 1.22 (d, J = 6.7 Hz, 6H), 0.95 (d, J = 6.6 Hz, 6H). **^{13}C NMR** (126 MHz, $CDCl_3$): δ 161.6 (d, J = 2.6 Hz), 151.9 (d, J = 36.8 Hz), 147.2 , 145.9, 137.8 (d, J = 6.1 Hz), 128.6, 125.9 (d, J = 7.2 Hz), 123.5 (d, J = 46.4 Hz), 120.1, 108.2, 53.8, 41.9 (d, J = 13.6 Hz), 38.7 (d, J = 28.9 Hz), 37.1, 33.9, 30.8 (d, J = 2.4 Hz), 29.3 (d, J = 9.0 Hz), 26.5, 24.1, 22.9 (the observed complexity is due to C–P coupling). **^{31}P NMR** (203 MHz, $CDCl_3$): δ 35.7. IR (neat, cm^{-1}): 2958, 2898, 2847, 1563, 1450, 1427, 1245, 1009, 874, 794, 741.

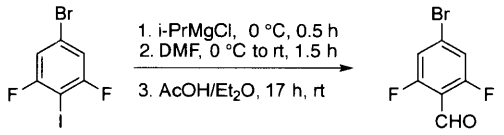

S22
76%

A 100 mL oven-dried round-bottomed flask equipped with a stir bar was charged with 5-bromo-1,3-difluoro-2-iodobenzene (2.30 g, 7.20 mmol, 1.00 equiv). The flask was sealed with a rubber septum and an inlet needle attached to a Schlenk line was inserted. The flask was evacuated and backfilled with argon. This sequence was repeated two additional times. Anhydrous THF (25 mL) was added via syringe and the reaction mixture was allowed to begin stirring. The vessel was cooled to 0 °C in an ice water bath and then *i*-PrMgCl (1.55 M in THF, 4.90 mL, 7.60 mmol, 1.05 equiv) was added dropwise via syringe over the course of 6 min. The solution was allowed to stir for 0.5 h, at which time anhydrous DMF (0.70 mL, 9.0 mmol, 1.3 equiv) was added via syringe. The reaction mixture was removed from the cold bath and allowed to stir for an additional 1.5 h. At this time, the flask was opened to air and a mixture of Et_2O/AcOH (1:1, v/v, 50 mL) was added (*Caution: exothermic*), and the solution allowed to stir for 17 h at rt. Then, the reaction mixture was diluted with ether (25 mL) and transferred to a separatory funnel. The organic phase was sequentially washed with aqueous saturated sodium bicarbonate solution (until pH = 8), deionized water (2 x 50 mL), and brine (1 x 50 mL). The organic layer was then dried over magnesium sulfate, filtered, and concentrated with the aid of a rotary evaporator to afford **S22** as a yellow solid (1.21 g, 76%) which was used without purification. mp: 76–78 °C. **^{1}H NMR** (600 MHz, $CDCl_3$): δ 10.25 (s, 1H), 7.19 (d, J = 8.5 Hz, 2H). **^{13}C NMR** (151 MHz, $CDCl_3$): δ 183.5 (t, J = 4.3 Hz), 162.9 (dd, J = 266.7, 6.9 Hz), 129.5 (t, J = 12.9 Hz), 116.7 (apparent dd, J = 30.6, 19.0 Hz), 113.3 (t, J = 10.9 Hz) (the observed complexity is due to C–F coupling). **^{19}F NMR** (565 MHz, $CDCl_3$): δ -113.2. IR (neat, cm^{-1}): 3081, 2894, 1694, 1609, 1562, 1424, 1195, 1037, 850. Spectral data were in accordance with those in the literature.[24]

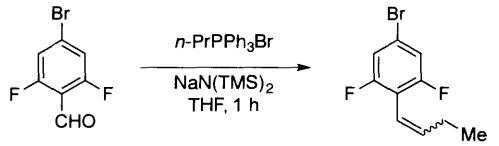

S22 **S23** 93%

A 25 mL oven-dried reaction tube equipped with magnetic stir bar was brought into a nitrogen-filled glovebox and charged with $NaN(TMS)_2$ (1.02 g, 5.56 mmol, 1.10 equiv). Anhydrous THF (7 mL) was added with stirring, and then the reaction tube was sealed with a screw-cap fitted with a Teflon septum and removed from the glovebox. A 50 mL oven-dried round-bottomed flask equipped with a magnetic stir bar was charged with *n*-$PrPPh_3Br$ (2.17 g, 5.63 mmol, 1.10 equiv). The flask was sealed with a rubber septum and an inlet needle attached to a Schlenk line was inserted. The flask was evacuated and backfilled with argon. This sequence was repeated two additional times. Anhydrous THF (25 mL) was added via syringe and the resulting suspension was allowed to begin stirring. Then, the $NaN(TMS)_2$ solution was added dropwise to the suspension via syringe over the course of 3 min. The resulting orange solution was allowed to stir at rt for 2.5 h. At this time, **S22** (1.12 g, 5.07 mmol, 1.00 equiv) was added as a solution in THF. The resulting yellow solution was allowed to stir for 1 h at rt. Then, MeOH was added via syringe to quench any remaining base. The flask was then opened to the air and the reaction mixture filtered through a pad of celite eluting with Et_2O. The filtrate was collected and transferred to a separatory funnel. The organic phase was washed sequentially with deionized water (3 x 50 mL) and brine (1 x 75 mL). The organic layer was then dried over magnesium sulfate, filtered, and concentrated with the aid of a rotary evaporator. The crude residue was suspended in pentane and filtered through a plug of silica gel, eluting with pentane (300 mL) to afford **S23** as a colorless oil (1.16 g, 93%; isolated as a 2.8 : 1 mixture of E/Z isomers as judged by GC). **^{1}H NMR** (500 MHz, $CDCl_3$): δ 7.06 (m, 2H), 6.57 (dt, J = 16.3, 6.5 Hz, 1H), 6.30 (dt, J = 16.3, 1.7 Hz, 1H), 6.01 (dt, J = 11.2, 1.4 Hz, 1H), 5.93 (dt, J = 11.2, 7.2 Hz, 1H), 2.34 – 2.20 (m, 2H), 2.07 – 1.95 (m, 2H), 1.10 (t, J = 7.5 Hz, 3H), 1.01 (t, J = 7.5 Hz, 3H). **^{13}C NMR** (126 MHz, $CDCl_3$): δ 160.6 (dd, J = 253.9, 9.4 Hz), 160.2 (dd, J = 251.7, 9.2 Hz), 141.0 (t, J = 7.4 Hz), 140.6, 120.3 (t, J = 12.6 Hz), 118.8 (t, J = 13.1 Hz), 115.5 (apparent dd; J = 29.0, 14.7 Hz), 115.3 (apparent dd, J = 29.4, 14.6 Hz), 114.8, 114.1 (t, J = 20.6 Hz), 113.5, 27.5, 23.4, 13.5. **^{19}F NMR** (471 MHz, $CDCl_3$): δ -109.4, -112.3. IR (neat, cm^{-1}): 3099, 2966, 2935, 2875, 1711, 1611, 1563, 1473, 1414, 1023, 859, 839.

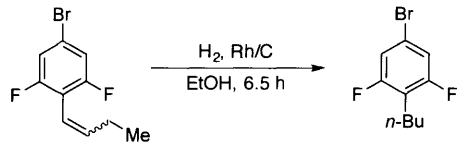

S23 **S24** 88%

A 50 mL round-bottomed flask equipped with a magnetic stir bar was charged sequentially with Rh/C (5 wt% Rh, 0.630 g), EtOH (24 mL), and **S23** (859 mg, 3.48 mmol, 1.00 equiv). The flask was fitted with a rubber septum and an inlet needle attached to a Schlenk line was inserted. The flask was rapidly evacuated and backfilled with argon. This sequence was repeated one additional time. The vessel was evacuated for a third time and then backfilled with hydrogen by using a hydrogen-filled balloon. The reaction mixture was allowed to stir at rt for 6.5 h. At this time, the flask was opened to the air to allow the hydrogen to escape, and then the reaction mixture was filtered through a pad of celite. The filtrate transferred to a separatory funnel containing pentane (50 mL) and deionized water (50 mL). The organic phase was then dried over sodium sulfate, filtered, and concentrated with the aid of a rotary evaporator to afford **S24** as a colorless oil (794 mg, 88%) with 96% purity as judged by ^{19}F NMR spectroscopy (the impurity is dehalogenated product, which has a similar polarity as the product). **^{1}H NMR** (600 MHz, $CDCl_3$): δ 7.02 (d, J = 6.5 Hz, 2H), 2.62 (t, J = 7.6 Hz, 2H), 1.54 (p, J = 7.6 Hz, 2H), 1.35 (sx, J = 7.4 Hz, 2H), 0.93 (t, J = 7.4 Hz, 3H). **^{13}C NMR** (151 MHz, $CDCl_3$): δ 161.6 (dd, J = 250.1, 10.5 Hz), 118.4 (t, J = 12.7 Hz), 117.8 (t, J = 20.6 Hz), 115.1 (apparent dd, J = 30.2 Hz, 16.4 Hz), 31.6, 22.5, 22.1, 13.9 (the observed complexity is due to C–F coupling). **^{19}F NMR** (565 MHz, $CDCl_3$): δ -114.1. IR (neat, cm^{-1}): 2960, 2931, 2873, 1617, 1575, 1475, 1413, 1113, 1007, 867, 839.

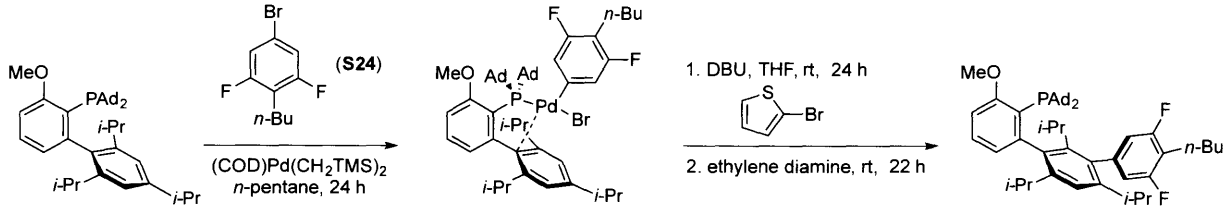

S21 67% **L8** 83%

In a nitrogen-filled glovebox, an oven-dried 50 mL round-bottomed flask equipped with a magnetic stir bar was charged with **S21** (306 mg, 0.501 mmol, 1.00 equiv). Anhydrous pentane (25 mL) was added and the reaction mixture stirred until all of the ligand dissolved. Then, **S24**

(185 mg, 0.744 mmol, 1.50 equiv) was added via microliter pipette, followed by (COD)Pd($CH_2TMS)_2$ (193 mg, 0.496 mmol, 1.00 equiv). The solution turned yellow upon the addition of the Pd reagent, and a precipitate began to form. The flask was sealed with a rubber septum, removed from the glovebox, and vigorously stirred at rt for 48 h. At this time, the flask was unsealed and the precipitate was collected using a sintered glass funnel. The filter cake was washed with pentane (3 x 3 mL) to afford the complex as a yellow solid (418 mg, 67%), which was used directly in the next step without further purification.

A 100 mL oven-dried round-bottomed flask equipped with a magnetic stir bar was charged with the complex (396 mg, 0.410 mmol, 1.00 equiv) prepared in the previous step. The flask was sealed with a rubber septum and an inlet needle attached to a Schlenk line was inserted. The flask was evacuated and backfilled with argon. This sequence was repeated two additional times. Anhydrous THF (50 mL) was added via syringe and the reaction mixture allowed to begin stirring. Then, 2-bromothiophene (42 μL, 0.434 mmol, 1.06 equiv) and DBU (64 μL, 0.428 mmol, 1.04 equiv) were added sequentially via microliter syringe. The resulting red-orange solution was allowed to stir at rt for 24 h, at which time ethylene diamine (0.150 mL, 2.24 mmol, 5.50 equiv) was added via syringe. The reaction mixture was allowed to stir at rt for an additional 22 h. At this time, the flask was opened to the air and the yellow solution transferred to a separatory funnel containing EtOAc (100 mL). The organic phase was washed with ammonium hydroxide (28–30% NH_3 basis)/brine solution (2:1; 4 x 50 mL) followed by brine (2 x 50 mL). The organic layer was dried over magnesium sulfate, filtered, and concentrated with the aid of a rotary evaporator. The crude residue was purified by trituration from MeOH to afford **L8** as an off-white solid (265 mg, 83%). mp: 208–211 °C. **^{1}H NMR** (600 MHz, $CDCl_3$): δ 7.29 (t, J = 7.9 Hz, 1H), 7.09 (s, 1H), 6.90 – 6.83 (m, 2H), 6.78 (dd, J = 9.8, 5.1 Hz, 2H), 3.86 (s, 3H), 2.84 (h, J = 7.0 Hz, 1H), 2.72 (t, J = 7.7 Hz, 2H), 2.49 – 2.40 (m, 2H), 1.94 – 1.76 (m, 18H), 1.64 (d, J = 9.3 Hz, 14H), 1.41 (sx, J = 7.4 Hz, 2H), 1.22 (d, J = 6.7 Hz, 3H), 1.13 (d, J = 6.9 Hz, 3H), 1.07 (d, J = 6.8 Hz, 3H), 1.00 – 0.94 (m, 6H; overlapping t and d; $-(CH_2)_3\mathbf{CH_3}$ and $-CH(\mathbf{CH_3})_2$), 0.91 (d, J = 7.0 Hz, 3H), 0.56 (d, J = 7.2 Hz, 3H). **^{13}C NMR** (151 MHz, $CDCl_3$): δ 161.9, 161.6 – 159.4 (m), 152.7 (d, J = 36.9 Hz), 146.8, 146.5, 142.1, 142.0 (t, J = 9.8 Hz), 139.1 (d, J = 5.6 Hz), 134.7, 128.7, 126.0 (d, J = 7.2 Hz), 123.4, 123.1, 119.2, 116.1 (t, J = 20.7 Hz), 114.8 (d, J = 21.8 Hz), 113.8 (d, J = 22.1 Hz), 108.3, 54.0, 42.1 (d, J = 13.7 Hz), 42.0 (d = J 13.7 Hz), 39.0 (d,

J = 28.7 Hz), 38.7 (d, J = 29.4 Hz), 37.2, 32.6 (d, J = 2.7 Hz), 32.1, 31.3, 29.6 – 29.0 (m; overlapping signals), 26.8, 24.9, 24.6 (d, J = 5.4 Hz), 23.8, 23.0, 22.6, 22.2, 14.1 (the observed complexity is due to C–P and C–F coupling). **^{19}F NMR** (282 MHz, $CDCl_3$): δ -117.4, -117.7. **^{31}P NMR** (121 MHz, $CDCl_3$): δ 36.6. IR (neat, cm^{-1}): 2958, 2901, 2846, 1631, 1588, 1456, 1414, 1245, 1090, 1040, 1004, 867, 893, 576. **Anal. Calcd. for $C_{52}H_{69}F_2OP$**: C, 80.17; H, 8.93, Found: C, 80.12; H, 9.09.

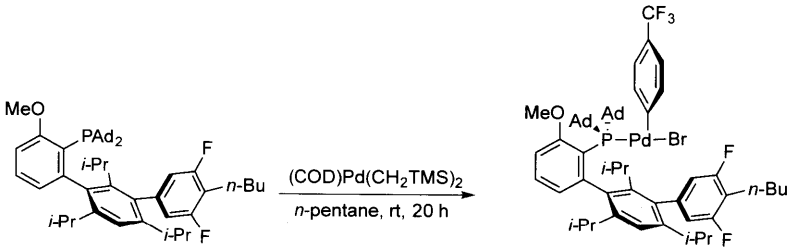

L8 **L8–Pd(Ar)Br** 66%

L8–Pd(Ar)Br was prepared following general procedure A. In a 25 mL reaction tube, a mixture of **L8** (148 mg, 0.191 mmol, 1.00 equiv), 4-bromobenzotrifloride (105 mg, 0.464 mmol, 2.44 equiv), and (COD)Pd($CH_2TMS)_2$ (71.0 mg, 0.183 mmol, 1.00 equiv) was stirred in pentane (10 mL) at rt for 20 h. The complex was filtered outside the glovebox to afford **L8–Pd(Ar)Br** as a yellow solid (139 mg, 66%). **^{1}H NMR** (500 MHz, $CDCl_3$): δ 7.44 (d, J = 10.0 Hz, 1H), 7.38 (d, J = 8.4 Hz, 2H), 7.35 (t, J = 7.8 Hz, 1H), 7.19 (s, 1H), 7.09 (d, J = 8.5 Hz, 1H), 7.07 (d, J = 8.4 Hz, 1H), 6.89 (d, J = 8.2 Hz, 1H), 6.74 (d, J = 9.7 Hz, 1H), 6.36 (d, J = 7.2 Hz, 1H), 3.90 (s, 3H), 2.99 (h, J = 7.1 Hz, 1H), 2.70 (t, J = 7.7 Hz, 2H), 2.50 (m (overlapping signals), 2H), 2.36 – 2.10 (m, 10H), 2.06 – 1.83 (m, 10H), 1.78 – 1.56 (m, 18H), 1.40 (sx, J = 7.4 Hz, 2H), 1.28 (d, J = 6.8 Hz, 3H), 1.08 (t, J = 6.9 Hz, 3H), 1.07 (d, J = 6.9 Hz, 3H), 0.95 (t, J = 7.4 Hz, 3H), 0.89 (d, J = 6.6 Hz, 3H), 0.85 (d, J = 6.9 Hz, 3H). **^{13}C NMR** (126 MHz, $CDCl_3$): δ 160.8 (d, J = 2.4 Hz), 160.7 (dd, J = 246.8, 9.8 Hz), 160.2 (dd, J = 244.9, 10.0 Hz), 159.5 (dd, J = 56.8, 9.9 Hz), 157.8, 153.3, 150.6 (d, J = 18.3 Hz), 150.1, 140.5, 140.2 (t, J = 10.2 Hz), 139.6, 137.7, 131.6, 128.5 (d, J = 10.2 Hz), 128.2, 126.1, 125.2 (d, J = 3.0 Hz), 124.8 (q, J = 31.7 Hz), 124.4, 123.9, 123.7 (d, J = 14.4 Hz), 121.8 (dd, J = 15.4, 2.5 Hz), 116.8 (t, J = 20.7 Hz), 115.1 (dd, J = 23.9, 2.5 Hz), 114.1 (dd, J = 22.7, 1.3 Hz), 109.2 (d, J = 1.3 Hz), 54.0, 47.4 (d, J = 10.1 Hz), 47.0 (d, J = 9.8 Hz), 41.8, 41.1, 36.4 (d, J = 16.8 Hz), 33.4, 32.0, 31.6, 30.2, 29.6 (d, J = 8.8 Hz), 29.5 (d, J = 8.8 Hz), 26.1, 25.6, 25.4, 25.2, 25.0, 23.7, 22.7, 22.3 (the observed complexity is due to C–P and C–

F coupling). **^{19}F NMR** (471 MHz, $CDCl_3$): δ -61.7, -116.5 (t, J = 8.9 Hz), -118.7 (t, J = 8.7 Hz). **^{31}P NMR** (203 MHz, $CDCl_3$): δ 68.1. IR (neat, cm^{-1}): 2905, 2850, 1584, 1565, 1454, 1414, 1325, 1157, 1104, 1068, 1005, 814, 796, 721. **HRMS** (ESI) m/z calcd for $C_{59}H_{73}BrF_5OPPd$ $[M–Br]^+$: 1029.4354; 1029.4368 found.

IX. Experimental Procedures and Characterization Data for **L9** and its Corresponding Complex

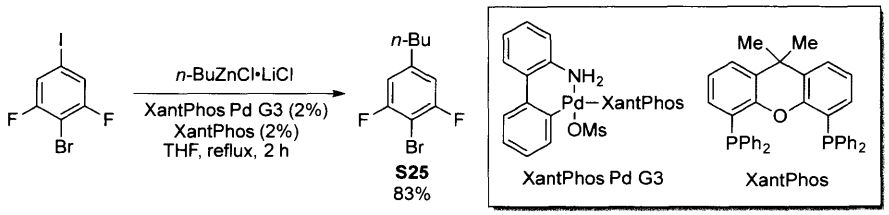

An oven-dried 100 mL 3-neck round-bottomed flask equipped with a magnetic stir bar was brought into a nitrogen-filled glovebox and charged with $ZnCl_2$ (1.66 g, 12.2 mmol, 1.20 equiv) and LiCl (508 mg, 12.0 mmol, 1.20 equiv). The flask was fitted with a reflux condenser, then sealed with rubber septa and removed from the glovebox. Anhydrous THF (20 mL) was added via syringe and the reaction mixture was allowed to begin stirring. The flask was cooled to 0 °C in an ice-water bath and *n*-BuLi (2.30 M in hexane; 4.80 mL, 11.0 mmol, 1.10 equiv) was added dropwise via syringe over the course of 4 min. The vessel was removed from the cold bath and the reaction mixture allowed to stir at rt for 0.5 h. Then, 2-bromo-1,3-difluoro-5-iodobenzene (3.20 g, 10.0 mmol, 1.00 equiv), XantPhos Pd G3 (188 mg, 0.198 mmol, 2 mol%), and XantPhos (123 mg, 0.213 mmol, 2 mol%) were added to the reaction solution under a counterflow of argon. The reaction was then heated to reflux in a pre-heated oil bath for 2 h. At this time, the reaction mixture was cooled to rt, the flask opened to the air, and the reaction mixture was diluted with Et_2O and transferred to a separatory funnel. The organic phase was washed with deionized water (3 x 50 mL), followed by brine (2 x 25 mL). The organic layer was then dried over magnesium sulfate, filtered, and concentrated with the aid of a rotary evaporator. The crude residue was purified by silica gel chromatography (eluting pentane) to afford **S25** as a colorless oil (2.07 g, 83%). **^{1}H NMR** (600 MHz, $CDCl_3$): δ 6.78 (d, J = 9.1 Hz, 2H), 2.58 (t, J = 7.6 Hz, 2H), 1.58 (p, J = 7.1, Hz, 2H), 1.34 (sx, J = 7.9, 7.4 Hz, 2H), 0.93 (dt, J = 8.7, 4.3 Hz, 3H). **^{13}C NMR** (151 MHz, $CDCl_3$): δ 159.9 (dd, J = 248.1, 4.8 Hz), 145.3 (t, J = 8.4 Hz), 112.0 (apparent

dd, J = 21.5, 3.5 Hz), 94.5 (t, J = 24.4 Hz), 35.3, 33.0, 22.3, 14.0. **^{19}F NMR** (565 MHz, $CDCl_3$): δ -106.7. IR (neat, cm^{-1}): 2958, 2932, 2862, 1618, 1585, 1477, 1434, 1214, 1021, 845.

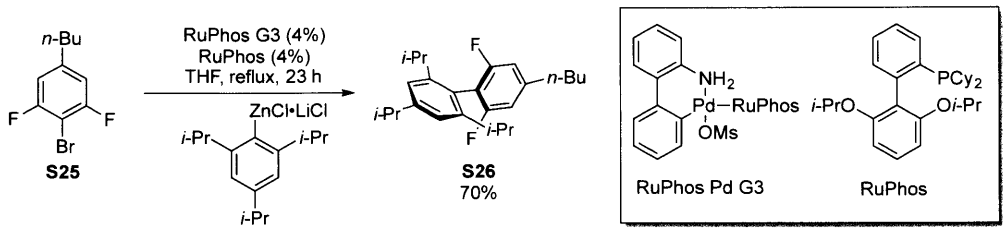

An oven-dried 50 mL round-bottomed flask equipped with a magnetic stir bar was charged with Mg turnings (363 mg, 14.9 mmol, 1.04 equiv) and a single crystal of iodine. The flask was sealed with a rubber septum and an inlet needle attached to a Schlenk line was inserted. The flask was evacuated and backfilled with argon. This sequence was repeated two additional times. Anhydrous THF (11 mL) was added and the suspension was allowed to begin stirring. Then, 2-bromo-1,3,5-triisopropylbenzene was added via syringe and the reaction was allowed to stir at 80 °C in a pre-heated oil bath for 1.5 h. At this time, the reaction mixture was cooled to rt, and then to 0 °C in an ice water bath. Then, a solution of $ZnCl_2$/LiCl was freshly prepared in a nitrogen-filled glovebox by dissolving $ZnCl_2$ (2.17 g, 15.9 mmol) and LiCl (677 mg, 16.0 mmol) in anhydrous THF (8 mL) in a 25 mL reaction tube. The $ZnCl_2$/LiCl solution was added via syringe to the ArMgBr solution at 0 °C. The flask containing ArZnCl•LiCl was then removed from the cold bath and allowed to stir at rt for 30 min. Titration of this solution with iodine yields a titer of 0.49 M (theoretical titer = 0.75 M; 65% yield). Then, **S25** (1.98 g, 7.95 mmol, 1.00 equiv), RuPhos Pd G3 (271 mg, 0.324 mmol, 4.1 mol%), and RuPhos (154 mg, 0.330 mmol, 4.2 mol%) were added rapidly as solids to the stirring solution of ArZnCl•LiCl. The septum was exchanged for a reflux condenser under a counterflow of argon, and then the reaction mixture heated to reflux for 23 h. At this time, the reaction mixture was cooled to rt and the flask opened to the air. EtOAc and deionized water were added, and the biphasic mixture transferred to a separatory funnel. The organic phase was washed with brine (2 x 50 mL), and then it was dried over magnesium sulfate, filtered, and concentrated with the aid of a rotary evaporator. The crude residue was purified by silica gel chromatography (eluting hexanes), followed by crystallization from MeOH to yield **S26** as a white crystalline solid. First crop: 1.75 g. Second crop: 0.310 g. Total yield: 70%. mp: 91–92 °C. **^{1}H NMR** (600 MHz, $CDCl_3$): δ 7.09 (s, 2H), 6.81 (d, J = 7.3 Hz, 2H), 2.96 (h, J = 6.7 Hz, 1H), 2.67 (t, J = 7.9 Hz, 2H), 2.55 (h, J = 6.2 Hz, 2H), 1.68 (p, J =

7.7 Hz, 2H), 1.43 (sx, J = 7.3 Hz, 2H), 1.32 (d, J = 7.0 Hz, 6H), 1.12 (d, J = 7.1 Hz, 12H), 0.99 (t, J = 7.4 Hz, 3H). **^{13}C NMR** (151 MHz, $CDCl_3$): δ 160.5 (dd, J = 244.7, 8.7 Hz), 149.2, 147.7, 145.1 (t, J = 9.0 Hz), 123.5, 121.0, 113.9 (t, J = 22.9 Hz), 111.1 (apparent dd, J = 26.1, 15.7 Hz), 35.5, 34.4, 33.0, 31.3, 24.2, 22.5, 14.1 (the observed complexity is due to C–F coupling). **^{19}F NMR** (565 MHz, $CDCl_3$): -111.7 (d, J = 7.2 Hz). IR (neat, cm^{-1}): 2957, 2930, 2869, 1636, 1570, 1461, 1429, 1365, 1022, 877, 857.

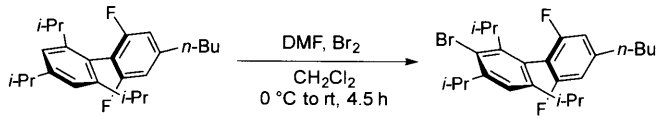

S26 **S27** 64%

Open to air, **S26** (1.50 g, 4.03 mmol, 1.00 equiv) was dissolved in CH_2Cl_2 (13.6 mL) in a 50 mL round-bottomed flask equipped with a magnetic stir bar. The flask was cooled to 0 °C in an ice water bath and the solution was allowed to begin stirring. In a separate reaction tube equipped with a magnetic stir bar and open to air, Br_2 (0.850 mL, 16.5 mmol, 4.10 equiv) was dissolved in DMF (4.0 mL). The tube was cooled to 0 °C in an ice water bath and the solution of bromine was allowed to stir for 10 min. At this time, the bromine solution was carefully added dropwise via syringe to the stirring solution of **S26** over the course of 10 min. The reaction mixture was then allowed to warm to rt and stir for 4.5 h. At this time, aqueous saturated sodium thiosulfate solution was carefully added and the biphasic mixture was transferred to a separatory funnel containing hexanes. The organic phase was washed with deionized water (5 x 20 mL), then dried over magnesium sulfate, filtered, and concentrated with the aid of a rotary evaporator. The crude material was purified via silica gel chromatography (eluting hexanes) to yield **S27** as a white solid (1.17 g, 64%). mp: 113–115 °C. **^{1}H NMR** (600 MHz, $CDCl_3$): δ 7.18 (s, 1H), 6.81 (br d, J = 7.3 Hz, 2H), 3.96 (s, 0.3H), 3.59 (m, 1H), 2.95 (br p, J = 7.6 Hz, 0.6H), 2.68 (t, J = 7.9 Hz, 2H), 2.44 (br sx, J = 6.8 Hz, 1H), 1.68 (p, J = 7.7 Hz, 2H), 1.41 (overlapping m and d, J = 7.4 Hz, 6H), 1.30 (d, J = 6.9 Hz, 6H), 1.09 (d, J = 7.0 Hz, 6H), 0.99 (t, J = 7.4 Hz, 3H), 0.94 (s, 2H) (broad and complex spectrum, likely due to hindered rotation). **^{13}C NMR** (151 MHz, $CDCl_3$): δ 160.7 (d, J = 245.2 Hz), 160.2 (d, J = 245.6 Hz), 149.2, 148.2 (d, J = 56.5 Hz), 147.4, 145.9 (m), 145.5 (m), 145.0 (m), 127.2, 122.7, 121.5, 114.4 (t, J = 22.9 Hz), 111.2 (d, J = 21.5 Hz), 35.5, 34.6, 33.3, 33.0, 31.5, 30.3, 24.0, 23.3, 22.5, 21.0, 20.1, 14.1 (broad and complex spectrum,

likely due to hindered rotation and C–F coupling). **^{19}F NMR** (565 MHz, $CDCl_3$): δ -108.9, -111.6. IR (neat, cm^{-1}): 2958, 2927, 2872, 1635, 1569, 1458, 1429, 1365, 1016, 886, 852.

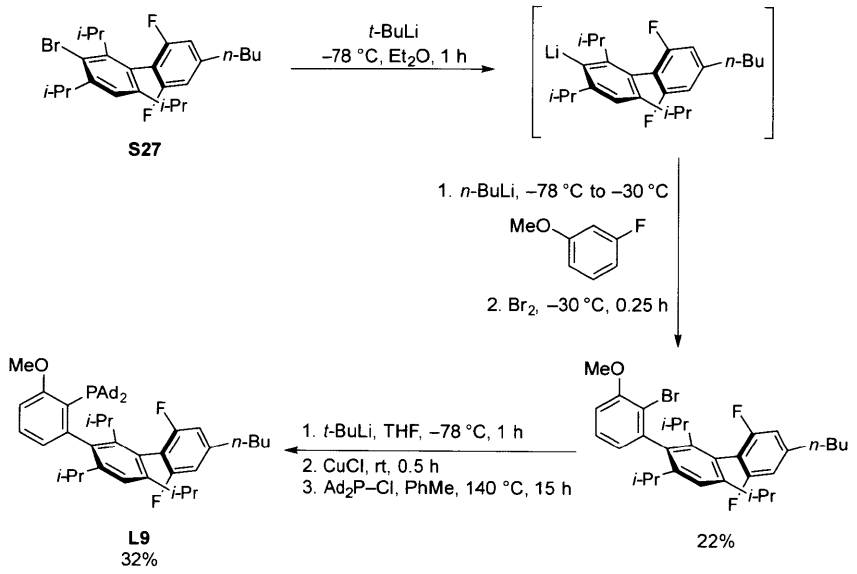

A 50 mL oven-dried round-bottomed flask equipped with a magnetic stir bar was charged with **S27** (1.10 g, 2.44 mmol, 1.06 equiv). The flask was sealed with a rubber septum and an inlet needle attached to a Schlenk line was inserted. The vessel was evacuated and backfilled with argon. This sequence was repeated two additional times. Anhydrous Et_2O (22 mL) was added via syringe and the reaction mixture was allowed to begin stirring. Then, the flask was cooled to –78 °C in a dry ice/acetone bath, and *t*-BuLi (2.30 M in heptane; 2.10 mL, 4.83 mmol, 2.10 equiv) was added dropwise via syringe over the course of 7 min. The solution was allowed to stir at –78 °C for 1 h. Separately, a 100 mL oven-dried round-bottomed flask equipped with a magnetic stir bar was sealed with a rubber septum and an inlet needle attached to a Schlenk line was inserted. The flask was evacuated and then backfilled with argon. This sequence was repeated two additional times. Then, 3-fluoroanisole (290 mg, 2.30 mmol, 1.00 equiv) and anhydrous THF (12 mL) were added sequentially via syringe, and the reaction mixture was allowed to begin stirring. The flask was then cooled to –78 °C in a dry ice/acetone bath, and *n*-BuLi (2.30 M in hexane; 1.00 mL, 2.30 mmol, 1.00 equiv) was added over the course of 4 min. The solution was allowed to stir for 1 h at –78 C. At this time, the biaryl lithium reagent prepared above in Et_2O was transferred to the aryl lithium solution in THF via cannula. The combined reaction mixture was warmed to –30 °C and was allowed to stir at this temperature for 1 h. Then, Br_2 (0.200 mL, 3.88

mmol, 1.70 equiv) was carefully added dropwise via syringe and the solution allowed to stir at –30 °C for 10 min. At this time, the flask was opened to the air, aqueous saturated sodium thiosulfate solution was carefully added until the color of bromine dissipated, and the reaction mixture was allowed to warm to rt. Then, the biphasic reaction mixture was transferred to a separatory funnel containing EtOAc (150 mL). The organic phase was washed with brine, dried over magnesium sulfate, filtered, and concentrated with the aid of a rotary evaporator. The crude residue was purified via automated silica gel chromatography (Biotage KP-SIL 100 g column, eluting 0% to 50% CH_2Cl_2/hexanes), followed by trituration from MeOH to afford the product as a white solid (276 mg, 22%).

L9 was prepared according to general procedure B, with the following modifications: a solution of CuCl•2LiCl was used in place of CuCl. A mixture of the triaryl bromide (190 mg, 0.341 mmol, 1.00 equiv) prepared above, *t*-BuLi (2.30 M in heptane, 0.300 mL, 0.71 mmol, 2.10 equiv), CuCl•2LiCl (1.00 M in THF; 0.400 mL, 0.40 mmol, 1.15 equiv), and Ad_2PCl (147 mg, 0.436 mmol, 1.30 equiv) was stirred at 140 °C in a Schlenk tube for 15 h behind a blast shield. Purified via trituration from MeOH to afford **S21** as a white solid (84 mg, 32%). mp: 227–230 °C. **^{1}H NMR** (600 MHz, $CDCl_3$): δ 7.28 (t, J = 8.0 Hz, 1H), 7.13 (s, 1H), 6.86 (m 2H), 6.76 (d, J = 9.3 Hz, 1H), 6.72 (d, J = 9.1 Hz, 1H), 3.86 (s, 3H), 2.73 (h, J = 6.6 Hz, 1H), 2.64 (t, J = 7.8 Hz, 2H), 2.57 (h, J = 6.7 Hz, 1H), 2.41 (h, J = 6.5 Hz, 1H), 1.97 – 1.79 (m, 18H), 1.70 – 1.54 (m, 15H), 1.40 (sx, J = 7.4 Hz, 2H), 1.28 (d, J = 6.7 Hz, 3H), 1.13 (d, J = 6.9 Hz, 3H), 1.11 (d, J = 6.8 Hz, 3H), 0.96 (t, J = 7.4 Hz, 3H), 0.95 (d, J = 6.6 Hz, 3H), 0.86 (d, J = 6.9 Hz, 3H), 0.63 (d, J = 7.1 Hz, 3H). **^{13}C NMR** (151 MHz, $CDCl_3$): δ 161.9, 161.5 (dd, J = 244.8, 8.5 Hz), 160.6 (dd, J = 242.5, 8.3 Hz), 152.8 (d, J = 36.9 Hz), 147.5, 147.1, 144.9 (t, J = 9.0 Hz), 144.0, 139.5 (d, J = 5.9 Hz), 128.6, 126.0 (d, J = 7.2 Hz), 123.6, 123.3, 122.9, 119.2, 116.3 (t, J = 22.4 Hz), 110.9 (t, J = 25.0 Hz), 108.2, 54.0, 42.1 (d, J = 13.9 Hz), 42.0 (d, J = 13.8 Hz), 38.9 (d, J = 28.6 Hz), 38.7 (d, J = 30.2 Hz), 37.3 (d, J = 12.4 Hz), 35.4, 33.1, 32.2, 31.3 (d, J = 3.2 Hz), 30.4, 29.5 (d, J = 9.0 Hz), 29.3 (d, J = 9.0 Hz), 26.4, 24.4, 24.3, 23.8 (d, J = 3.4 Hz), 23.0, 22.4, 21.6, 14.09 (the observed complexity is due to C–P and C–F coupling). **^{19}F NMR** (565 MHz, $CDCl_3$): δ -108.1 (d, J = 6.0 Hz), -108.9 (d, J = 6.6 Hz). **^{31}P NMR** (162 MHz, $CDCl_3$): δ 36.0. IR (neat, cm^{-1}): 2957, 2901, 2845, 1559, 1455, 1428, 1245, 1017, 846, 795, 763. **HRMS** (ESI) m/z calcd for $C_{52}H_{69}F_2OP$ $[M+H]^+$: 779.5132; 779.5130 found.

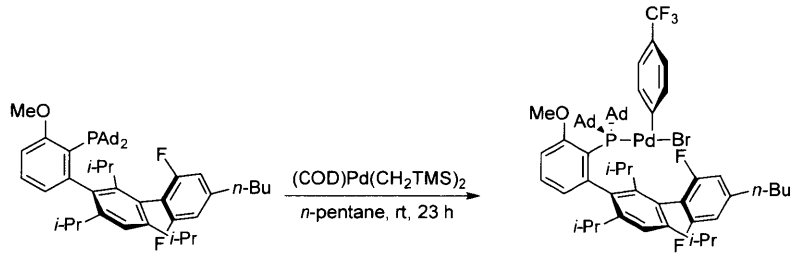

L9 **L9–Pd(Ar)Br** 56%

L9–Pd(Ar)Br was prepared following general procedure A. In a 25 mL reaction tube a mixture of **L9** (71 mg, 91 μmol, 1.00 equiv), 4-bromobenzotrifloride (53 mg, 0.24 mmol, 2.6 equiv), and (COD)Pd($CH_2TMS)_2$ (38 mg, 98 μmol, 1.1 equiv) was stirred in pentane (7 mL) at rt for 23 h. The complex was filtered outside the glovebox to afford **L9–Pd(Ar)Br** as a yellow solid (57 mg, 56%). **^{1}H NMR** (500 MHz, $CDCl_3$): δ 7.42 (m, 2H), 7.32 (m, 2H), 7.06 (m, 2H), 6.88 (d, J = 8.2 Hz, 1H), 6.76 (t, J = 8.8 Hz, 2H), 6.39 (d, J = 7.6 Hz, 1H), 3.90 (s, 3H), 3.18 (br h, J = 7.1 Hz, 1H), 2.66 (br t, J = 7.8 Hz, 2H), 2.52 – 2.36 (m, 7H), 2.25 (br h, J = 7.0 Hz, 2H), 2.07 (m, 6H), 1.86 – 1.49 (m, 22H), 1.39 (sx, J = 7.4 Hz, 2H), 1.30 (d, J = 6.9 Hz, 3H), 1.24 (d, J = 7.0 Hz, 3H), 1.12 (d, J = 6.8 Hz, 3H), 0.96 (t, J = 7.4 Hz, 3H), 0.86 (d, J = 6.9 Hz, 3H), 0.78 (d, J = 6.6 Hz, 3H). **^{13}C NMR** (126 MHz, $CDCl_3$): δ 162.8 (dd, J = 250.7, 7.6 Hz), 160.8, 160.6 (dd, J = 242.8, 7.7 Hz), 157.0, 152.1, 150.7 (d, J = 18.6 Hz), 149.1, 145.9 (t, J = 8.9 Hz), 141.7 (d, J = 7.0 Hz), 140.6, 137.5, 131.5, 128.4 (d, J = 10.0 Hz), 128.2, 127.4 (d, J = 2.5 Hz), 126.7, 126.1, 124.6 (q, J = 31.5 Hz), 123.4 (d, J = 13.5 Hz), 122.0 (m), 114.6 (t, J = 21.0 Hz), 111.5 (d, J = 22.0 Hz), 110.7 (d, J = 23.0 Hz), 109.2, 53.9, 47.7 (d, J = 10.7 Hz), 46.5 (d, J = 9.4 Hz), 42.7, 40.1, 36.6, 36.2, 35.4, 33.5, 33.1, 31.2 (d, J = 8.4 Hz), 29.7 (d, J = 9.5 Hz), 29.4 (d, J = 9.5 Hz), 26.5, 25.6, 25.1, 24.3, 23.8, 22.4, 22.2 (the observed complexity is due to C–P and C–F coupling). **^{19}F NMR** (471 MHz, $CDCl_3$): δ -61.8, -101.7, -108.4. **^{31}P NMR** (162 MHz, $CDCl_3$): δ 66.4. IR (neat, cm^{-1}): 2907, 2850, 1635, 1586, 1568, 1453, 1427, 1325, 1100, 1068, 1007. **HRMS** (ESI) m/z calcd for $C_{59}H_{73}BrF_5OPPd$ $[M–Br]^+$: 1029.4354; 1029.4366 found.

X. Experimental Procedures and Characterization Data for **L10**

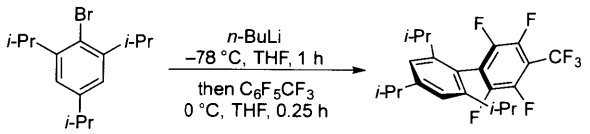

S28
75%

A 100 mL oven-dried round-bottomed flask equipped with a magnetic stir bar was fitted with a rubber septum and an inlet needle attached to a Schlenk line inserted. The flask was evacuated and backfilled with argon. This sequence was repeated two additional times. Then, 2-bromo-1,3,5-triisopropylbenzene (2.04 g, 7.20 mmol, 1.00 equiv) and anhydrous THF (30 mL) were added sequentially via syringe, and the solution was allowed to begin stirring. The flask was cooled to –78 °C in a dry ice/acetone bath, and then *n*-BuLi (2.47 M in hexane; 3.00 mL, 7.41 mmol, 1.03 equiv) was added dropwise via syringe over the course of 8 min. The solution was allowed to stir at –78 °C for 1 h. Separately, an oven-dried 100 mL round-bottomed flask was fitted with a rubber septum and an inlet needle attached to a Schlenk line was inserted. The flask was evacuated and backfilled with argon. This sequence was repeated two additional times. Then, perfluorotoluene (2.00 mL, 14.1 mmol, 2.00 equiv) and anhydrous THF (18 mL) were added sequentially via syringe, and the solution was allowed to begin stirring. The flask was cooled to 0 °C in an ice water bath. The ArLi solution was transferred via cannula to the solution of perfluorotoluene over the course of 3 min. The resulting dark red-brown solution was allowed to warm to rt over 15 min. At this time, the flask was opened to the air and the reaction mixture transferred to a separatory funnel containing hexanes (150 mL) and deionized water (150 mL). The organic phase was washed with deionized water (1 x 50 mL), followed by brine (2 x 50 mL), then dried over magnesium sulfate, filtered, and concentrated with the aid of a rotary evaporator. The crude residue was triturated from MeOH to afford **S28** as a white solid (1.69 g). The filtrate was concentrated and triturated from MeOH again to give a second crop of product (0.594 g). Total yield: 2.28 g (75%). mp: 105–106 °C. **^{1}H NMR** (600 MHz, $CDCl_3$): δ 7.13 (s, 2H), 2.96 (h, J = 6.8 Hz, 1H), 2.38 (h, J = 6.4 Hz, 2H), 1.31 (d, J = 7.0 Hz, 6H), 1.14 (d, J = 6.9 Hz, 12H). **^{13}C NMR** (151 MHz, $CDCl_3$): δ 151.0, 147.3, 144.8 (m), 144.2 (m), 124.7 (t, J = 20.7 Hz), 121.6, 119.8, 34.5, 31.8, 24.2, 24.1 (the observed complexity is due to C–F coupling). **^{19}F NMR** (565 MHz, $CDCl_3$): δ -56.1 (t, J = 21.6 Hz), -136.8 (td, J = 16.1, 6.1 Hz), -140.7 (tddd, J = 27.5,

21.7, 15.9, 8.4 Hz). IR (neat, cm^{-1}): 2965, 2871, 1655, 1493, 1478, 1333, 1189, 1131, 987, 850, 804, 715.

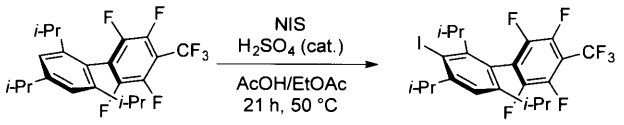

S28 **S29** 91%

Open to air, a 25 mL round-bottomed flask equipped with a magnetic stir bar was charged with **S28** (703 mg, 1.67 mmol, 1.00 equiv) and NIS (1.90 g, 8.44 mmol, 5.05 equiv). EtOAc (4 mL) and AcOH (4 mL) were added and the reaction mixture was allowed to begin stirring. Then, concentrated H_2SO_4 (95–98%; 0.40 mL, 5 vol%) was carefully added dropwise via syringe to give a peach-colored solution. The reaction mixture was stirred at 50 °C in a pre-heated oil bath for 21 h. At this time, the reaction mixture was cooled to rt and then transferred to a separatory funnel containing hexanes (20 mL) and deionized water (20 mL). The organic phase was washed sequentially with aqueous 2.0 M KOH solution (2 x 20 mL), aqueous saturated sodium thiosulfate solution (2 x 20 mL), and brine (1 x 20 mL). The organic layer was then dried over magnesium sulfate, filtered through a pad of silica gel to removed colored impurities, and then concentrated with the aid of a rotary evaporator to afford **S29** as an off-white solid (831 mg, 91%) with 97% purity (the impurity is starting material, which has a similar polarity as the product). mp: 125–127 °C. **^{1}H NMR** (600 MHz, $CDCl_3$): δ 7.19 (br d, J = 14.7 Hz, 1H), 3.89 (br h, J = 7.1 Hz, 0.6H), 3.53 (m, 1H), 2.82 (h, J = 7.4 Hz, 0.4H), 2.23 (m, 1H), 1.46 (d, J = 7.3 Hz, 3H), 1.30 (d, J = 6.9 Hz, 6H), 1.11 (d, J = 6.5 Hz, 6H), 0.95 (d, J = 7.3 Hz, 3H) (broad and complex spectrum, likely due to hindered rotation). **^{13}C NMR** (151 MHz, $CDCl_3$): δ 154.2, 153.8, 148.3, 147.8, 147.4, 146.9, 145.6, 145.4 – 144.7 (m), 144.0 (d, J = 14.1 Hz), 143.7 – 142.9 (m), 124.9 (q, J = 20.9 Hz), 123.8, 122.1, 121.9, 121.6, 120.4, 120.1, 110.5, 100.0, 42.0, 40.7, 39.3, 36.3, 31.9, 30.7, 29.9, 24.1, 24.1, 23.6, 23.5, 23.2, 21.4, 20.2 (complex spectrum, likely due to hindered rotation). **^{19}F NMR** (565 MHz, $CDCl_3$): δ -56.1 (m), -133.5 (m), -136.6 (m), -140.1 (m), -140.6 (m) (complex spectrum, likely due to hindered rotation). IR (neat, cm^{-1}): 2962, 2938, 1657, 1479, 1343, 1329, 1246, 1151, 986, 922, 852, 717.

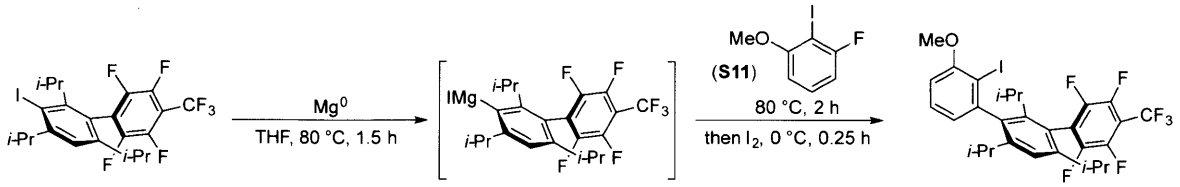

A 25 mL oven-dried reaction tube equipped with a magnetic stir bar was charged with Mg turnings (66 mg, 2.7 mmol, 1.4 equiv), **S29** (1.18 g, 2.16 mmol, 1.08 equiv) and a single crystal of iodine. The tube was sealed with a screw-cap fitted with a Teflon septum, and an inlet needle attached to a Schlenk line was inserted. The tube was evacuated and backfilled with argon. This sequence was repeated two additional times. Anhydrous THF (2.40 mL) was added via syringe and the reaction mixture was allowed to begin stirring. The septum was then exchanged for one that had not been punctured, under a counterflow of argon, and the tube placed in a pre-heated oil bath at 80 °C for 1.5 h. At this time, the reaction mixture was cooled to rt, and **S11** (504 mg, 2.00 mmol, 1.00 equiv) was added via syringe. The septum was again exchanged for one that had not been punctured, under a counterflow of argon, and the tube placed back in the pre-heated oil bath at 80 °C for 16 h. At this time, the reaction mixture was cooled to 0 °C in an ice water bath, and I_2 was added dropwise via syringe as a solution in THF (2.0 mL; 761 mg I_2, 3.00 mmol, 1.50 equiv) over the course of 2 min. After the addition was complete, the tube was removed from the ice water bath. Once the reaction mixture had reached rt, the tube was uncapped and the reaction mixture was diluted with EtOAc (3 mL) and aqueous saturated sodium thiosulfate solution (5 mL). The tube was capped and shaken until the red color of iodine had disappeared. Then, the tube was uncapped again and the contents poured into a separatory funnel containing EtOAc (100 mL) and aqueous saturated sodium thiosulfate solution (40 mL). The organic phase was washed with deionized water (1 x 50 mL), followed by brine (1 x 50 mL), then dried over magnesium sulfate, filtered, and concentrated with the aid of a rotary evaporator. The crude residue was purified via automated silica gel chromatography (Biotage KP-SIL 50 g column, eluting 0% to 20% DCM/hexanes) to afford **S30** as a white solid (850 mg, 65%). mp: 194–197 °C. **^{1}H NMR** (600 MHz, $CDCl_3$): δ 7.34 (t, J = 7.8 Hz, 1H), 7.30 (s, 1H), 6.86 (d, J = 7.2 Hz, 1H), 6.80 (d, J = 7.7 Hz, 1H), 3.95 (s, 3H), 2.70 (h, J = 5.8 Hz, 1H), 2.38 (h, J = 6.8 Hz, 1H), 2.29 (h, J = 6.6 Hz, 1H), 1.24 (d, J = 6.9 Hz, 3H), 1.19 (d, J = 6.8 Hz, 3H), 1.15 (d, J = 6.8 Hz, 3H), 1.03 (d, J = 6.9 Hz, 3H), 0.84 (d, J = 7.3 Hz, 3H), 0.80 (d, J = 7.2 Hz, 3H). **^{13}C NMR** (151

MHz, $CDCl_3$): δ 158.5, 148.8, 147.8, 147.7, 145.7 (m), 145.9 (m), 144.1 (m), 143.2 (m), 143.0, 141.6, 128.9, 126.1 (t, J = 20.5 Hz), 123.3, 122.0, 121.0, 120.1 (m), 109.1, 56.6, 31.1, 30.9, 25.0, 24.3, 23.5, 22.1 (the observed complexity is due to C–F coupling). **^{19}F NMR** (565 MHz, $CDCl_3$): δ -56.0 (t, J = 21.6 Hz), -133.5 (br d, J = 377.2 Hz), -141.3 (m). IR (neat, cm^{-1}): 2965, 2929, 2875, 1477, 1335, 1244, 1136, 986, 732, 714, 522.

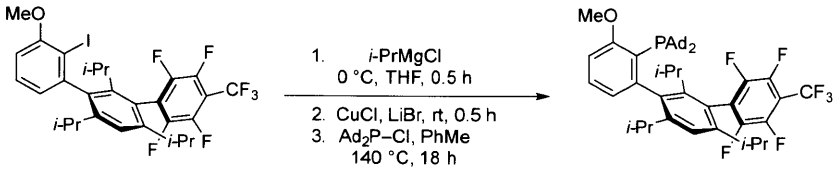

S30 **S31** 61%

A 25 mL oven-dried reaction tube equipped with a magnetic stir bar was charged with **S30** (800 mg, 1.15 mmol, 1.00 equiv). The tube was sealed with a screw-cap fitted with a Teflon septum and an inlet needle attached to a Schlenk line was inserted. The tube was evacuated and backfilled with argon. This sequence was repeated two additional times. Anhydrous THF (2.0 mL) was added via syringe and the reaction mixture allowed to begin stirring. The tube was cooled to 0 °C in an ice-water bath, and *i*-PrMgCl (1.60 M, 0.80 mL, 1.1 equiv) was added via syringe over the course of 1 min. The solution was allowed to stir at 0 °C for 0.5 h. Separately, an oven-dried 25 mL Schlenk tube bearing a side-arm and equipped with a magnetic stir bar was brought into a nitrogen-filled glovebox and charged with CuCl (139 mg, 1.40 mmol, 1.22 equiv) and LiBr (134 mg, 1.54 mmol, 1.54 equiv). The Schlenk tube was sealed with a Teflon stopcock, removed from the glovebox, attached to a Schlenk line, and placed under argon atmosphere. The Teflon stopcock was replaced by a rubber septum, and the ArMgX solution was transferred to the Schlenk tube at 0 °C via syringe. Then, the Schlenk tube was removed from the cold bath and the resulting black solution was allowed to stir at rt for 0.5 h. At this time, Ad_2PCl (433 mg, 1.29 mmol, 1.12 equiv) was added as a solid under a counterflow of argon. Then, toluene (3 mL) was added via syringe and the rubber septum was replaced with a Teflon stopcock. The reaction mixture was allowed to stir at 140 °C in a pre-heated oil bath **behind a blast shield** for 18 h. At this time, the reaction mixture was cooled to rt. Then, the tube was unsealed, diluted with EtOAc (25 mL) and transferred to a separatory funnel. The organic phase was washed with ammonium hydroxide (28–30% NH_3 basis)/brine solution (2:1; 5 x 50 mL) until the aqueous washings were no longer blue, followed by brine (1 x 30 mL). The organic layer was then dried over magnesium

sulfate, filtered, and concentrated with the aid of a rotary evaporator. The crude residue was triturated from MeOH to afford **S31** as a white solid (576 mg, 61%). mp: 252–255 °C. **^{1}H NMR** (600 MHz, $CDCl_3$): δ 7.33 (t, J = 7.8 Hz, 1H), 7.22 (s, 1H), 6.91 (d, J = 8.2 Hz, 1H), 6.87 (dd, J = 7.6, 3.5 Hz, 1H), 3.89 (s, 3H), 2.86 (h, J = 6.9 Hz, 1H), 2.59 (h, J = 6.7 Hz, 1H), 2.26 (h, J = 6.7 Hz, 1H), 1.89 (m, 18H), 1.66 (m, 12H), 1.30 (d, J = 6.8 Hz, 3H), 1.18 (d, J = 7.1 Hz, 3H), 1.16 (d, J = 7.1 Hz, 3H), 0.99 (d, J = 6.6 Hz, 3H), 0.89 (d, J = 7.0 Hz, 3H), 0.67 (d, J = 7.1 Hz, 3H). **^{13}C NMR** (151 MHz, $CDCl_3$): δ 162.1, 151.7 (d, J = 36.8 Hz), 149.1, 146.7, 146.3 (m), 145.5 (m), 145.1 (m), 144.7 (m), 144.0 (m), 143.6, 143.3 (m), 142.9 (m), 140.2 (d, J = 5.9 Hz), 128.9, 127.0 (t, J = 20.3 Hz), 125.7 (d, J = 7.1 Hz), 123.4 (d, J = 48.1 Hz), 119.9, 118.9, 108.7, 54.1, 42.1 (d, J = 13.9 Hz), 42.0 (d, J = 13.9 Hz), 38.9 (d, J = 13.8 Hz), 38.7 (d, J = 14.9 Hz), 37.2 (d, J = 11.4 Hz), 32.0, 31.4 (d, J = 3.0 Hz), 30.9, 29.4 (d, J = 9.1 Hz), 29.3 (d, J = 8.9 Hz), 26.5, 24.5, 24.3, 24.1 (d, J = 3.0 Hz), 22.9, 21.9 (the observed complexity is due to C–P and C–F coupling). **^{19}F NMR** (471 MHz, $CDCl_3$): δ -56.0 (t, J = 21.6 Hz), -133.2 (dd, J = 23.7, 12.4 Hz), -133.9 (dd, J = 23.6, 12.4 Hz), -141.3 (m), -141.8 (m). **^{31}P NMR** (203 MHz, $CDCl_3$): δ 36.3. IR (neat, cm^{-1}): 2960, 2902, 2847, 1558, 1475, 1333, 1324, 1245, 1144, 1050, 985, 740, 714.

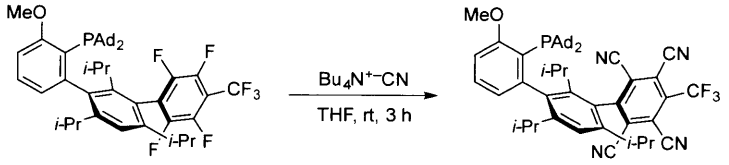

S31 **L10** 13%

WARNING: Tetrabutylammonium cyanide is extremely toxic. Use caution.

An 8 mL oven-dried reaction tube equipped with a magnetic stir was brought into a nitrogen-filled glovebox and charged with **S31** (202 mg, 0.244 mmol, 1.00 equiv). Anhydrous THF (1.50 mL) was added and the solution was allowed to begin stirring. Tetrabutylammonium cyanide (269 mg, 1.00 mmol, 4.10 equiv) was added in one portion. Then, the tube was sealed with a screw-cap fitted with a Teflon septum and removed from the glovebox. The deep violet solution was allowed to stir at rt for 3 h. At this time, the tube was uncapped and diluted with EtOAc (3 mL) and carefully transferred to a separatory funnel containing EtOAc (50 mL) and aqueous saturated sodium bicarbonate solution (20 mL). The organic phase was washed sequentially with deionized water (5 x 30 mL) and brine (1 x 30 mL). The aqueous washings containing excess cyanide were carefully transferred to an empty plastic container clearly and appropriated labeled

as cyanide waste. This container was immediately transported to the main waste accumulation area in a secondary container. The organic layer was then dried over magnesium sulfate, filtered, and concentrated with the aid of a rotary evaporator. The crude brown residue was purified via automated silica gel chromatography (Biotage KP-SIL 50 g column) by first equilibrating the column with a solution of 1% NEt_3 in hexanes. The product was then purified by using a gradient of 0% to 20% [1% NEt_3/hexanes]/EtOAc. Isolated **L10** as an orange solid (28 mg, 13%). mp: 230 °C (slow decomposition). **^{1}H NMR** (400 MHz, $CDCl_3$): δ 7.37 (t, J = 7.9 Hz, 1H), 7.33 (s, 1H), 6.94 (d, J = 8.2 Hz, 1H), 6.89 (dd, J = 7.6, 3.6 Hz, 1H), 3.90 (s, 3H), 3.14 (h, J = 7.0 Hz, 1H), 2.50 (h, J = 7.2, 6.6 Hz, 1H), 1.91 – 1.81 (m, 18H), 1.65 (m, 13H), 1.28 (d, J = 6.7 Hz, 9H), 1.04 (d, J = 6.6 Hz, 3H), 0.99 (d, J = 7.1 Hz, 3H). **^{13}C NMR** (151 MHz, $CDCl_3$): δ 162.3, 157.5, 152.3, 150.5 (d, J = 36.6 Hz), 145.5, 142.6, 141.0, 135.6 (q, J = 34.5 Hz), 129.2, 127.3, 125.5 (d, J = 7.0 Hz), 125.4, 125.3, 123.3, 123.0, 121.4, 120.9, 119.1, 117.9 (d, J = 12.4 Hz), 112.4, 111.9, 111.0, 109.2, 54.2, 43.6, 41.9 (d, J = 13.8 Hz), 39.1 (d, J = 28.1 Hz), 38.7 (d, J = 29.6 Hz), 37.2 (d, J = 5.9 Hz), 32.7 (d, J = 5.0 Hz), 31.6 (d, J = 15.3 Hz), 29.3 (d, J = 9.2 Hz), 29.3 (d, J = 9.2 Hz), 26.8, 25.8, 25.1, 24.8, 23.9, 22.5. **^{19}F NMR** (376 MHz, $CDCl_3$): δ -58.1. **^{31}P NMR** (162 MHz, $CDCl_3$): δ 36.6. IR (neat, cm^{-1}): 2963, 2901, 2847, 2157, 1972, 1728, 1560, 1457, 1319, 1246, 1158, 1044, 732. **HRMS** (ESI): m/z calcd for $C_{53}H_{58}F_3N_4OP$ $[M+H]^+$: 855.4379; 855.4376 found.

XI. Experimental Procedures and Characterization Data for **L11**

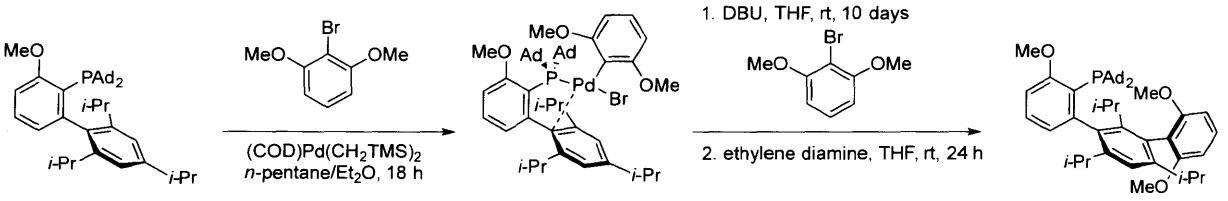

In a nitrogen-filled glovebox, an oven-dried 100 mL round-bottomed flask equipped with a magnetic stir bar was charged with **S21** (401 mg, 0.656 mmol, 1.00 equiv). Anhydrous pentane (50 mL) and anhydrous Et_2O (25 mL) were added and the reaction mixture stirred until all of the ligand had dissolved. Then, 2-bromo-1,3-dimethoxybenzene (265 mg, 1.22 mmol, 1.86 equiv) was added, followed by the addition of $(COD)Pd(CH_2TMS)_2$ (274 mg, 0.704 mmol, 1.07 equiv).

The solution turned yellow, then orange in color, upon the addition of the Pd reagent, and a precipitate began to form. The flask was sealed with a rubber septum, removed from the glovebox, and vigorously stirred at rt for 18 h. At this time, the flask was unsealed and the precipitate was collected by filtration over a sintered glass funnel. The filter cake was washed with pentane (3 x 3 mL) to afford the complex as a crimson red solid (505 mg, 82%), which was used directly in the next step without further purification.

A 50 mL oven-dried round-bottomed flask equipped with a magnetic stir bar was charged with the complex (301 mg, 0.322 mmol, 1.00 equiv) prepared in the previous step and 2-bromo-1,3-dimethoxybenzene (207 mg, 0.954 mmol, 3.00 equiv). The flask was sealed with a rubber septum and an inlet needle attached to a Schlenk line was inserted. The flask was evacuated and backfilled with argon. This sequence was repeated two additional times. Anhydrous THF (25 mL) was added via syringe and the reaction mixture allowed to begin stirring. Then, DBU (100 μL, 0.663 mmol, 2.06 equiv) was added via microliter syringe. The resulting dark red solution was allowed to stir at rt for 10 days, at which time ethylene diamine (0.215 mL, 3.22 mmol, 10 equiv) was added via syringe. (*Note:* although the reaction was allowed to stir for 10 days, prior experiments indicate that the first arylation is complete in 24 h. The prolonged reaction time was used in an effort to prepare the bis(arylated) compound, which was unsuccessful.) The reaction mixture was allowed to stir at rt for an additional 24 h. At this time, the flask was opened to the air and the solution transferred to a separatory funnel containing EtOAc (100 mL). The organic phase was washed with ammonium hydroxide (28–30% NH_3 basis)/brine solution (2:1; 3 x 50 mL), followed by brine (2 x 50 mL). The organic layer was then dried over magnesium sulfate, filtered, and concentrated with the aid of a rotary evaporator. The crude residue was purified by automated silica gel chromatography (Biotage KP-SIL 25 g column, eluting 0% to 100% CH_2Cl_2/EtOAc) to afford **L11** as a slightly orange solid. (152 mg, 63%). mp: 233–235 °C. **^{1}H NMR** (600 MHz, $CDCl_3$): δ 7.26 (t, J = 8.1 Hz, 2H), 7.09 (s, 1H), 6.89 (dd, J = 7.3, 3.3 Hz, 1H), 6.84 (d, J = 8.0 Hz, 1H), 6.59 (d, J = 8.4 Hz, 1H), 6.50 (d, J = 8.2 Hz, 1H), 3.86 (s, 3H), 3.70 (s, 3H), 3.65 (s, 3H), 2.60 (m; two overlapping h, J = 6.6 Hz, 2H), 2.38 (h, J = 6.8 Hz, 1H), 2.00 – 1.78 (m, 18H), 1.72 – 1.57 (m, 12H), 1.30 (d, J = 6.8 Hz, 3H), 1.06 (d, J = 6.7 Hz, 3H), 1.05 (d, J = 6.7 Hz, 3H), 0.96 (d, J = 6.7 Hz, 3H), 0.81 (d, J = 6.9 Hz, 3H), 0.49 (d, J = 7.0 Hz, 3H). **^{13}C NMR** (151 MHz, $CDCl_3$): δ 161.8 (d, J = 2.4 Hz), 159.4, 158.2, 153.7 (d, J = 36.8 Hz), 146.9,

145.0, 142.9, 138.9 (d, J = 5.8 Hz), 128.3, 128.1, 126.3 (d, J = 7.2 Hz), 123.5, 123.1, 120.1, 118.9, 107.9, 103.3, 103.0, 54.9, 54.8, 53.9, 42.1 (d, J = 14.1 Hz), 41.9 (d, J = 13.6 Hz), 39.0 (d, J = 28.0 Hz), 38.6 (d, J = 30.5 Hz), 37.3 (d, J = 16.9 Hz), 32.6, 31.2 (d, J = 3.6 Hz), 30.1, 29.6 (d, J = 8.9 Hz), 29.3 (d, J = 8.9 Hz), 26.3, 24.5, 24.3, 23.9, 23.3, 21.1 (the observed complexity is due to C–P coupling). **^{31}P NMR** (162 MHz, $CDCl_3$): δ 35.5. IR (neat, cm^{-1}): 2960, 2902, 2887, 2848, 1587, 1556, 1470, 1452, 1430, 1244, 1105, 1031, 799, 744, 735. **HRMS** (ESI): m/z calcd for $C_{50}H_{67}O_3P$ $[M+H]^+$: 747.4906; 747.4907 found.

XII. Experimental Procedures for Collection of the Initial Rate Data

Preparation of stock solutions for Initial Rate Data. All stock solutions were prepared in a nitrogen-filled glovebox. A 0.40 M stock solution of **1** was prepared by dissolving **1** (135 mg, 0.400 mmol) in anhydrous MTBE (1.00 mL) in a 3 mL vial. A 0.50 M stock solution of 1,5-cyclooctadiene (COD) was prepared by dissolving COD (108 mg, 1.00 mmol) in anhydrous MTBE (2.00 mL) in a 3 mL vial. A stock solution of the appropriate oxidative addition complex (or ligand) was formed by dissolving it in anhydrous THF (the molarity of the stock solution was between 0.03 and 0.06 M, depending on the complex (or ligand) used). A 250 µL syringe was used to dispense stock solutions of **1**, oxidative addition complexes, and ligands. A 100 µL syringe was used to dispense the stock solution of COD.

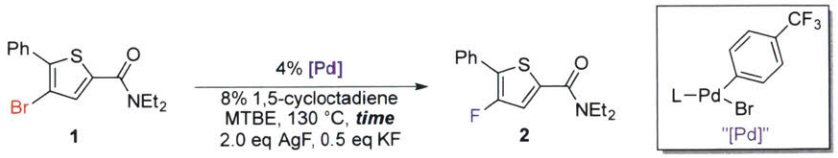

General Procedure C–Collection of the Initial Rate Data using Oxidative Addition Complexes: Four 16 mL oven-dried reaction tubes (Fisher Scientific 16 x 125 mm, Cat No. 14-959-35A) each equipped with a small magnetic stir bar (see image below) were brought into a nitrogen-filled glovebox. Each tube was charged with KF (3 mg, 0.050 mmol, 0.5 equiv) and AgF (25 mg, 0.50 mmol, 2.00 equiv). Then, the tubes were each sequentially charged with **1** (250 µL of a 0.400 M stock solution in MTBE, 0.100 mmol, 1.00 equiv), 1,5-cyclooctadiene (16 µL of a 0.50 M stock solution in MTBE, 8.0 µmol, 8 mol%), and the appropriate oxidative

addition complex (as a stock solution in THF, 4.0 μmol, 4 mol% Pd). Then, the reaction mixture was diluted with MTBE to bring the concentration to 0.10 M with respect to **1**. The tubes were sealed tightly with screw-caps (Kimble-Chase, Open Top S/T Closure, Part No. 73804-15425) fitted with thick Teflon septa (Thermo Scientific, PTFE/Silicone, Part No. NS-B799515; see image below), removed from the glovebox, and heated to 130 °C in a pre-heated oil bath **behind a blast shield**. At the appropriate timepoint (1 h, 3 h, or 5 h), the reaction tube was removed from the oil bath and allowed to cool to rt. The tube was uncapped and 1-fluoronaphthalene (15 μL, 0.116 mmol) was added via microliter syringe as an internal standard. The tube was capped, shaken vigorously, and then uncapped again. The reaction mixture transferred to an NMR tube via glass pipette, and analyzed directly by ^{19}F NMR spectroscopy, changing the following parameters: d1 = 1.50 and p1 = 6.00.

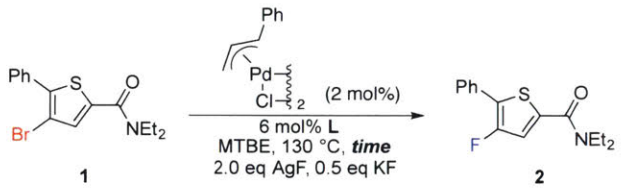

General Procedure D–Collection of the Initial Rate Data using [Pd(cinnamyl)Cl]$_2$: Four 15 mL oven-dried reaction tubes each equipped with a small magnetic stir bar (see image below) were brought into a nitrogen-filled glovebox and each charged with KF (3 mg, 0.050 mmol, 0.5 equiv), AgF (25 mg, 0.50 mmol, 2.00 equiv), and [Pd(cinnamyl)Cl]$_2$ (1.0 mg, 2.0 μmol, 4 mol% Pd). Then, the tubes were each sequentially charged with **1** (250 μL of a 0.400 M stock solution in MTBE, 0.100 mmol, 1.00 equiv), and the appropriate ligand (as a stock solution in THF, 6.0 μmol, 6 mol%). Then, the reaction mixture was diluted with MTBE to bring the concentration to 0.10 M with respect to **1**. The tubes were sealed tightly with screw-caps (Kimble-Chase, Open Top S/T Closure, Part No. 73804-15425) fitted with thick Teflon septa (Thermo Scientific, PTFE/Silicone, Part No. NS-B799515; see image below), removed from the glovebox, and heated to 130 °C in a pre-heated oil bath **behind a blast shield**. At the appropriate timepoint (1 h, 3 h, or 5 h), the reaction tube was removed from the oil bath and allowed to cool to rt. The tube was uncapped and 1-fluoronaphthalene (15 μL, 0.116 mmol) was added via microliter syringe as an internal standard. The tube was capped, shaken vigorously, and then uncapped

again. The reaction mixture transferred to an NMR tube via glass pipette, and analyzed directly by ^{19}F NMR spectroscopy, changing the following parameters: d1 = 1.50 and p1 = 6.00.

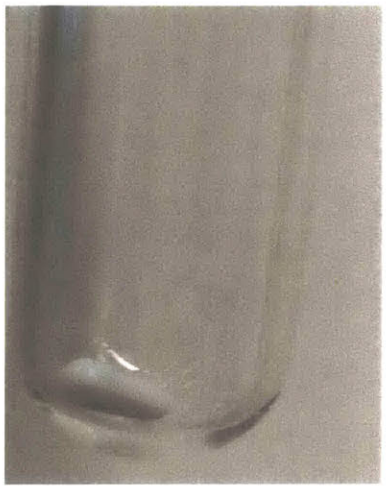

small magnetic stir bar

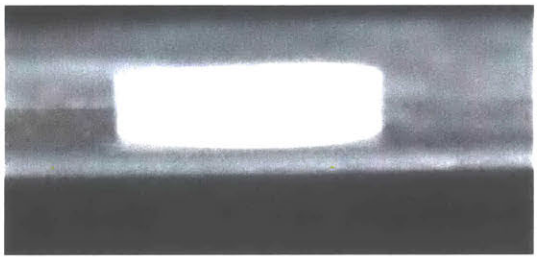

thick Teflon septum

3.5. References and Notes

1. Vitaku, E.; Smith, D. T.; Njardarson, J. T. Analysis of the Structural Diversity, Substitution Patterns, and Frequency of Nitrogen Heterocycles among U.S. FDA Approved Pharmaceuticals. *J. Med. Chem.* **2014**, *57*, 10257–10274.

2. Milner, P. J.; Yang, Y.; Buchwald, S. L. In-Depth Assessment of the Palladium-Catalyzed Fluorination of Five-Membered Heteroaryl Bromides. *Organometallics,* **2015**, *34*, 4775–4780.

3. Yamada, S.; Gavryushin, A.; Knochel, P. Convenient Electrophilic Fluorination of Functionalized Aryl and Heteroaryl Magnesium Reagents. *Angew. Chem. Int. Ed.* **2010**, *49*, 2215–2218.

4. Hutchinson, J.; Sandford, G. Elemental Fluorine in Organic Chemistry; Springer, Berlin, Heidelberg, 1997; pp 1–43.

5. Chambers, R. D.; Fox, M. A.; Sandford, G.; Trmcic, J.; Goeta, A. Elemental Fluorine: Part 20. Direct Fluorination of Deactivated Aromatic Systems Using Microreactor Techniques. *J. Fluor. Chem.* **2007**, *128*, 29–33.

6. Düfert, M. A.; Billingsley, K. L.; Buchwald, S. L. Suzuki-Miyaura Cross-Coupling of Unprotected, Nitrogen-Rich Heterocycles: Substrate Scope and Mechanistic Investigation. *J. Am. Chem. Soc.* **2013**, *135*, 12877–12885.

7. Hooper, M.W.; Hartwig, J. F. Understanding the Coupling of Heteroaromatic Substrates: Synthesis, Structures, and Reductive Eliminations of Heteroarylpalladium Amido Complexes. *Organometallics*, **2003,** *22*, 3394–3403..

8. Su, M.; Buchwald, S. L. A Bulky Biaryl Phosphine Ligand Allows for Palladium-Catalyzed Amidation of Five-Membered Heterocycles as Electrophiles. *Angew. Chem. Int. Ed.* **2012**, *51*, 4710–4713.

9. Hooper, M.W.; Utsunomiya, M.; Hartwig, J.F. Scope and Mechanism of Palladium-Catalyzed Amination of Five-Membered Heterocyclic Halides. *J. Org. Chem.* **2003**, *68*, 2861.

10. Sather, A. C.; Lee, H. G.; De La Rosa, V. Y.; Yang, Y.; Müller, P.; Buchwald, S. L. A Fluorinated Ligand Enables Room-Temperature and Regioselective Pd-Catalyzed Fluorination of Aryl Triflates and Bromides. *J. Am. Chem. Soc.* **2015**, *137*, 13433–13438.

11. Though the initial rate of fluorination obtained with **L3**–Pd(Ar)Br is similar to that of **L1**–Pd(Ar)Br, the reaction did not reach full conversion overnight. This may indicate decomposition of the catalyst; futher analysis is required.

12. Hirsch, J.A. *Topics in Stereochemistry,* **1967**, *1*, 199–222.

13. Milner, P.J.; Maimone, T.J.; Su, M.; Chen, J.; Müller, P.; Buchwald, S. L. Investigating the Dearomative Rearrangement of Biaryl Phosphine-Ligated Pd(II) Complexes. *J. Am. Chem. Soc.* **2012**, *134*, 19922–19934.

14. When [Pd(cinnamyl)Cl]$_2$ is used as the palladium source, the corresponding HetArCl can be detected by GC. Furthermore, the reactions do not always reach full conversion, though the initial rates appears similar to what is obtained with an oxidative addition complex is used.

15. Köllhofer, A.; Plenio, H. Homogeneous Catalysts Supported on Soluble Polymers: Biphasic Sonogashira Coupling of Aryl Halides and Acetylenes Using MeOPEG-Bound Phosphine–Palladium Catalysts for Efficient Catalyst Recycling. *Chem. - A Eur. J.* **2003**, *9*, 1416–1425.

16. Lee, H. G.; Milner, P. J.; Buchwald, S. L. An Improved Catalyst System for the Pd-Catalyzed Fluorination of (Hetero)Aryl Triflates. *Org. Lett.* **2013**, *15*, 5602–5605.

17. Glick, G.; Ghosh, S.; Roush, W.R. Compounds and Compositions for Treating Conditions Associated with NLRP Activity. U.S. Patent WO2017184624, October 26, 2017.

18. Bruno, N.C.; Tudge, M.T.; Buchwald, S.L. Design and Preparation of New Palladium Precatalysts for C–C and C–N Cross-Coupling Reactions. *Chem. Sci.* **2013**, *4* 916–920.

19. Olsen, E. P. K.; Arrechea, P. L.; Buchwald, S. L. Mechanistic Insight Leads to a Ligand Which Facilitates the Palladium-Catalyzed Formation of 2-(Hetero)Arylaminooxazoles and 4-(Hetero)Arylaminothiazoles. *Angew. Chem. Int. Ed.* **2017**, *56*, 10569–10572.

20. Yang, Y.; Oldenhuis, N.J.; Buchwald, S.L. Mild and General Conditions for Negishi Cross-Coupling Enabled by the Use of Palladacycle Precatalysts. *Angew. Chem. Int. Ed.* **2013**, *52*, 615–619.

21. Yoshida, S.; Nagai, A.; Uchida, K.; Hosoya, T. Enhancing the Synthetic Utility of 3-Haloaryne Intermediates by Their Efficient Generation from Readily Synthesizable *ortho*-Iodoaryl Triflate-type Precursors. *Chem. Lett.* **2017**, *46*, 733–736.

22. Hospital, A.; Gibard, C.; Gaulier, C.; Nauton, L.; Théry, V.; El-Ghozzi, M.; Avignant, D.; Cisnetti, F.; Gautier, A. Access to functionalised silver(I) and gold(I) *N*-heterocyclic carbenes by [2 + 3] dipolar cycloadditions. *Dalton Trans.* **2012**, *41*, 6803–6812.

23. Sasaki, S.; Murakami, F.; Murakami, M.; Watanabe, M.; Kato, K.; Sutoh, K.; Yoshifuji, M. Synthesis of crowded triarylphosphines carrying functional sites. *J. Organomet. Chem.* **2005**, *690*, 2664–2672.

24. Czub, M.; Durka, K.; Luliński, S. Łosiewicz, J.; Serwatowski, J.; Urban, M.; Woźniak, K. Synthesis and Transformations of Functionalized Benzosiloxaboroles. *Eur. J. Org. Chem.* **2017**, 818–826.

3.6. NMR Spectra

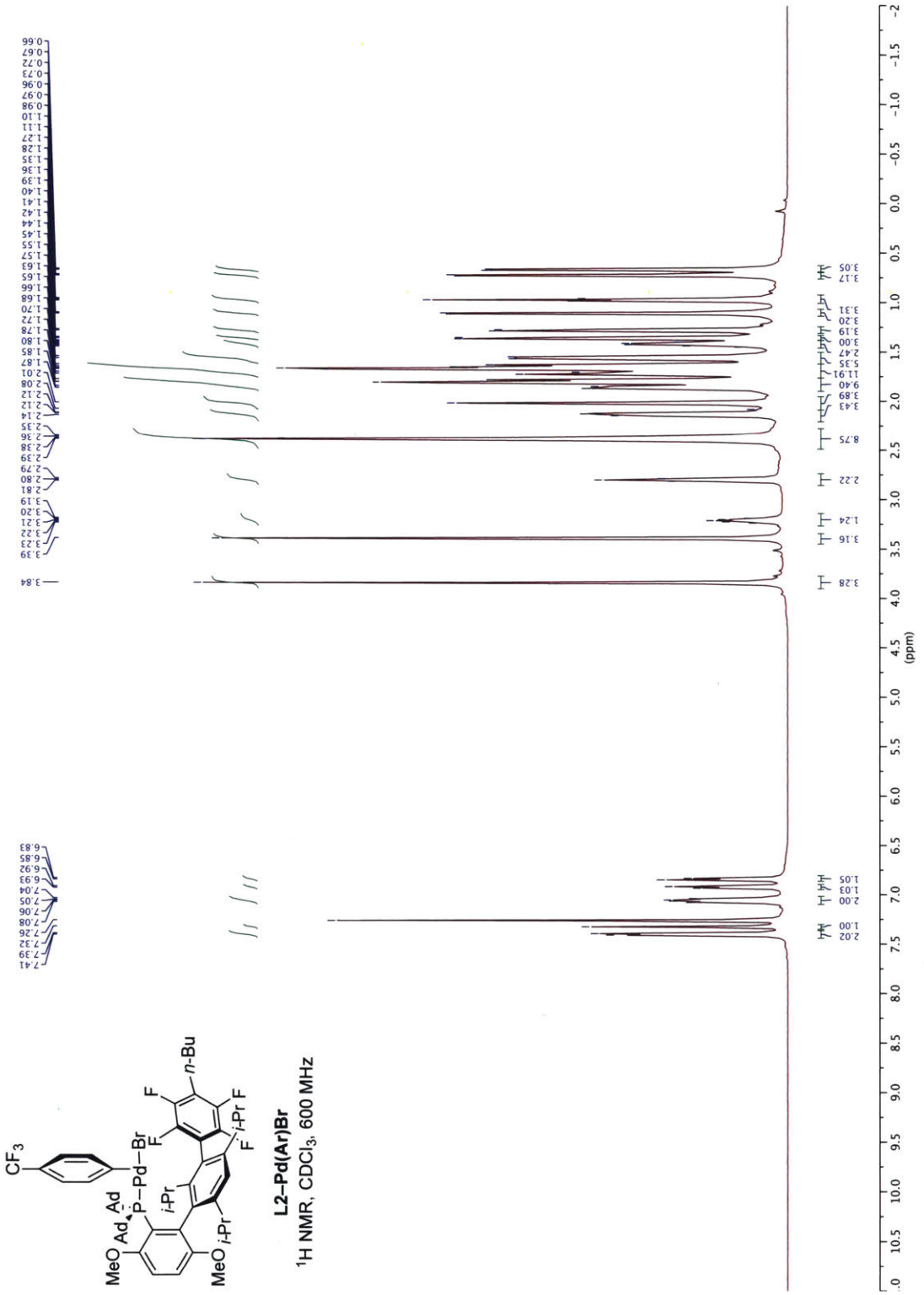

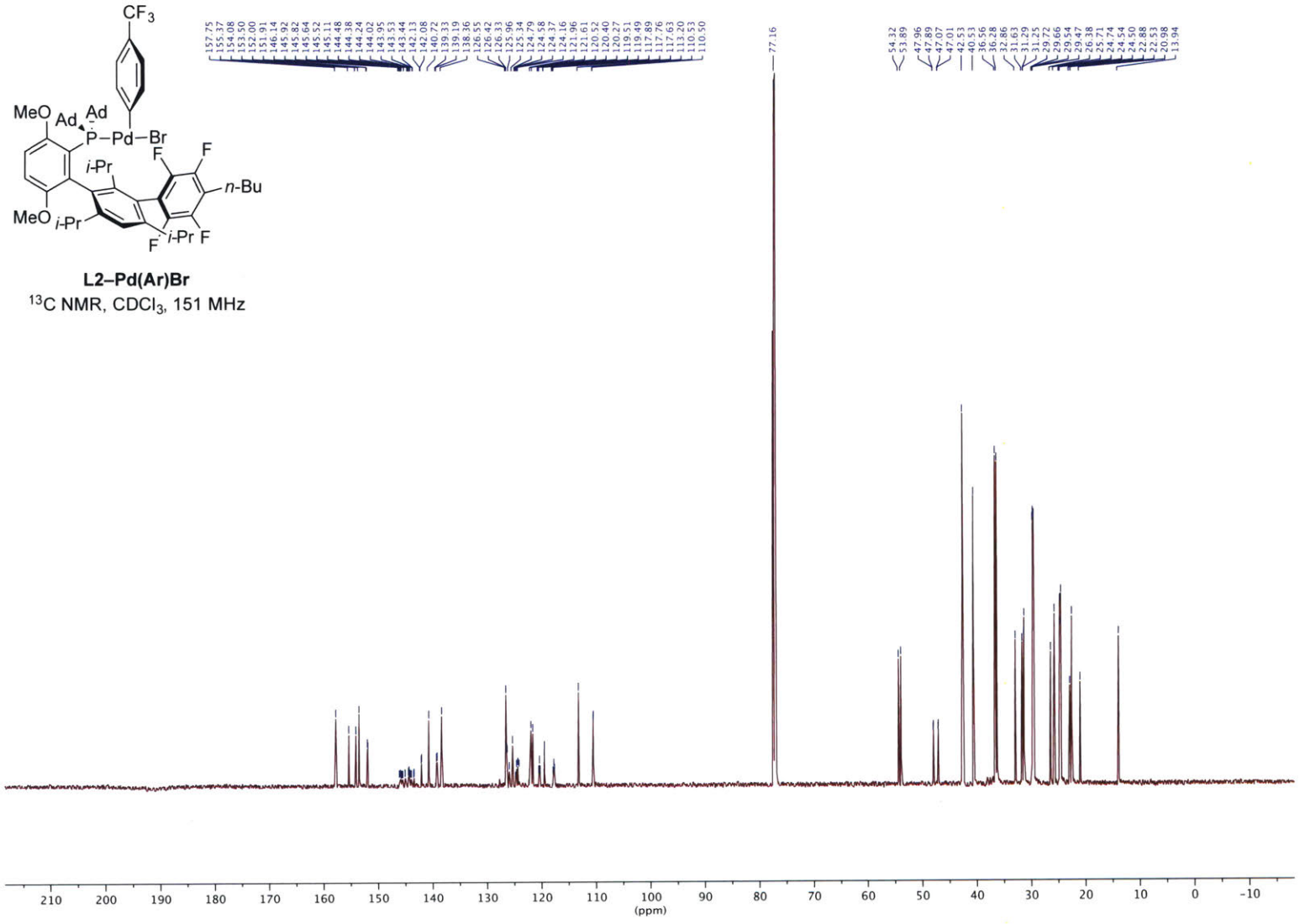

L2–Pd(Ar)Br

^{13}C NMR, $CDCl_3$, 151 MHz

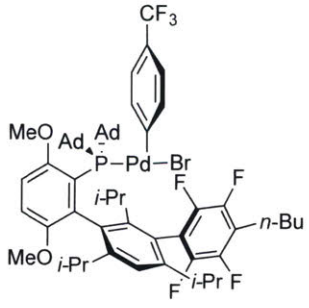

L2–Pd(Ar)Br

^{19}F NMR, $CDCl_3$, 565 MHz

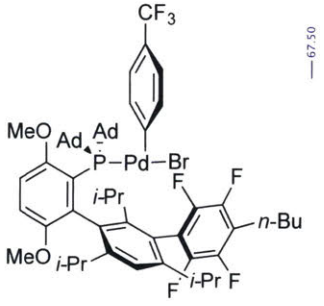

L2–Pd(Ar)Br

^{31}P NMR, $CDCl_3$, 162 MHz

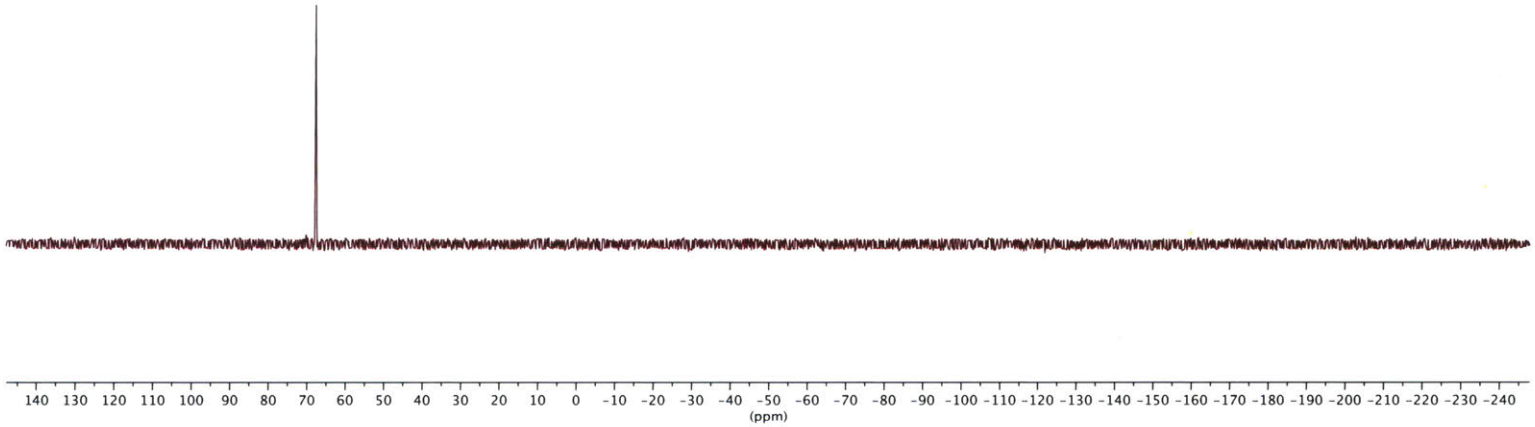

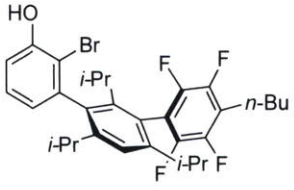

S2

^{1}H NMR, 600 MHz, $CDCl_3$

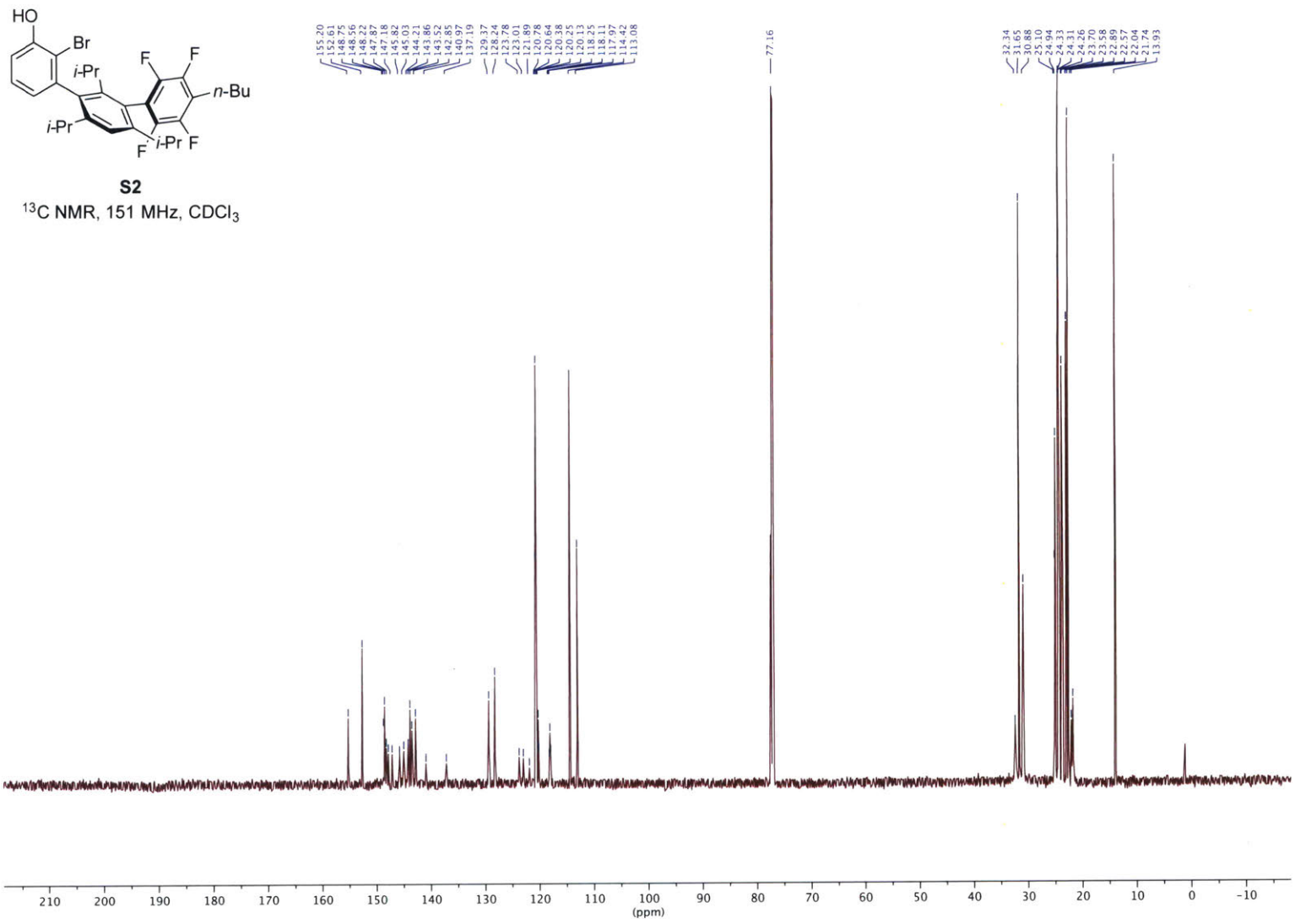

S2

^{13}C NMR, 151 MHz, $CDCl_3$

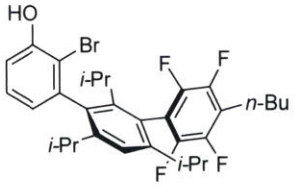

S2

^{19}F NMR, 565 MHz, $CDCl_3$

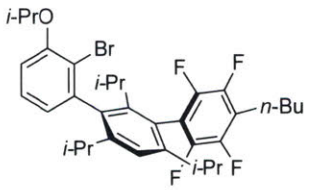

S3

^{1}H NMR, 600 MHz, C_6D_6

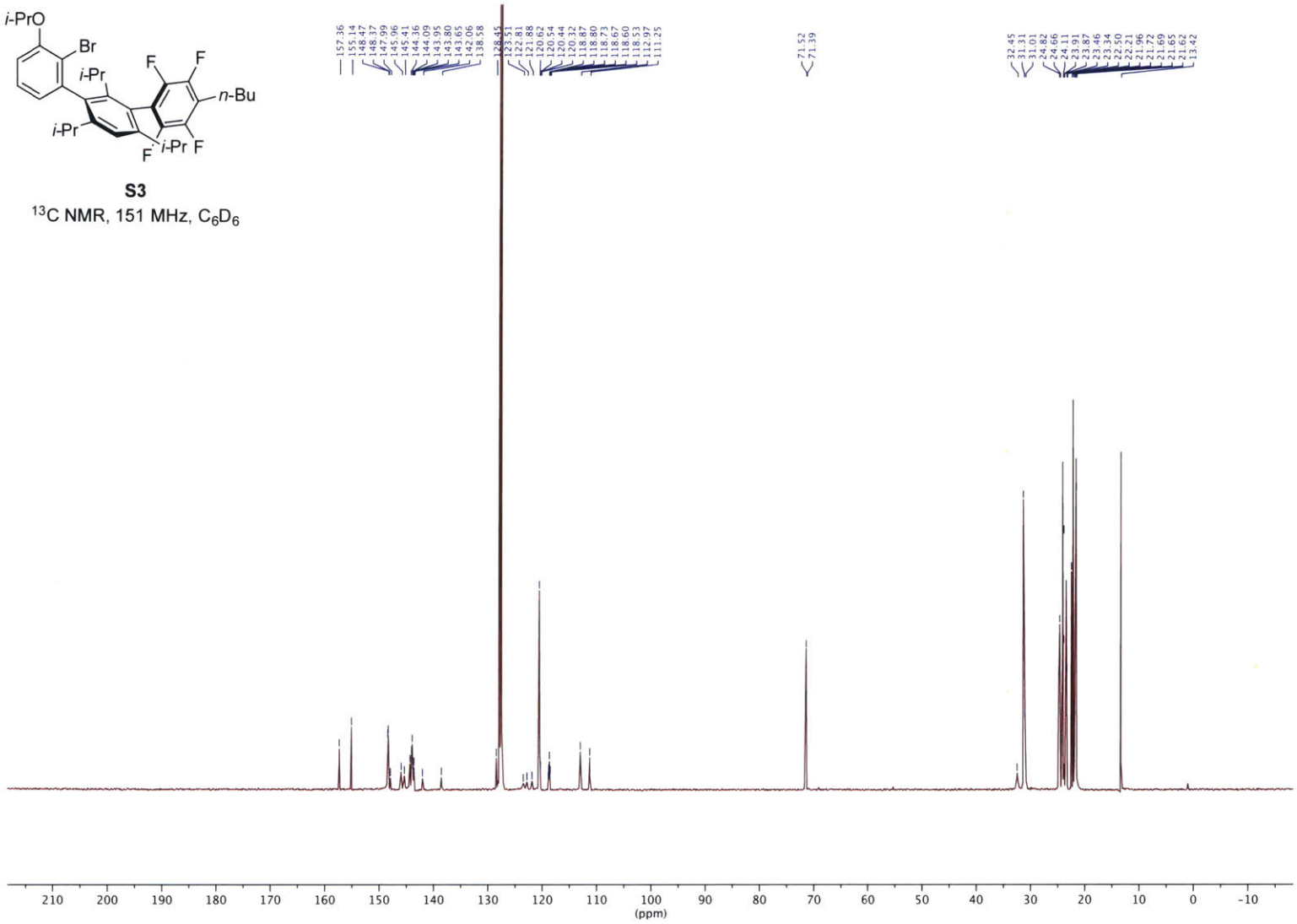

S3

^{13}C NMR, 151 MHz, C_6D_6

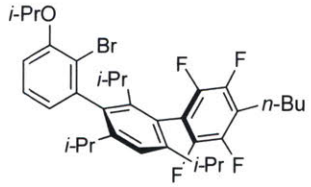

S3

^{19}F NMR, 565 MHz, C_6D_6

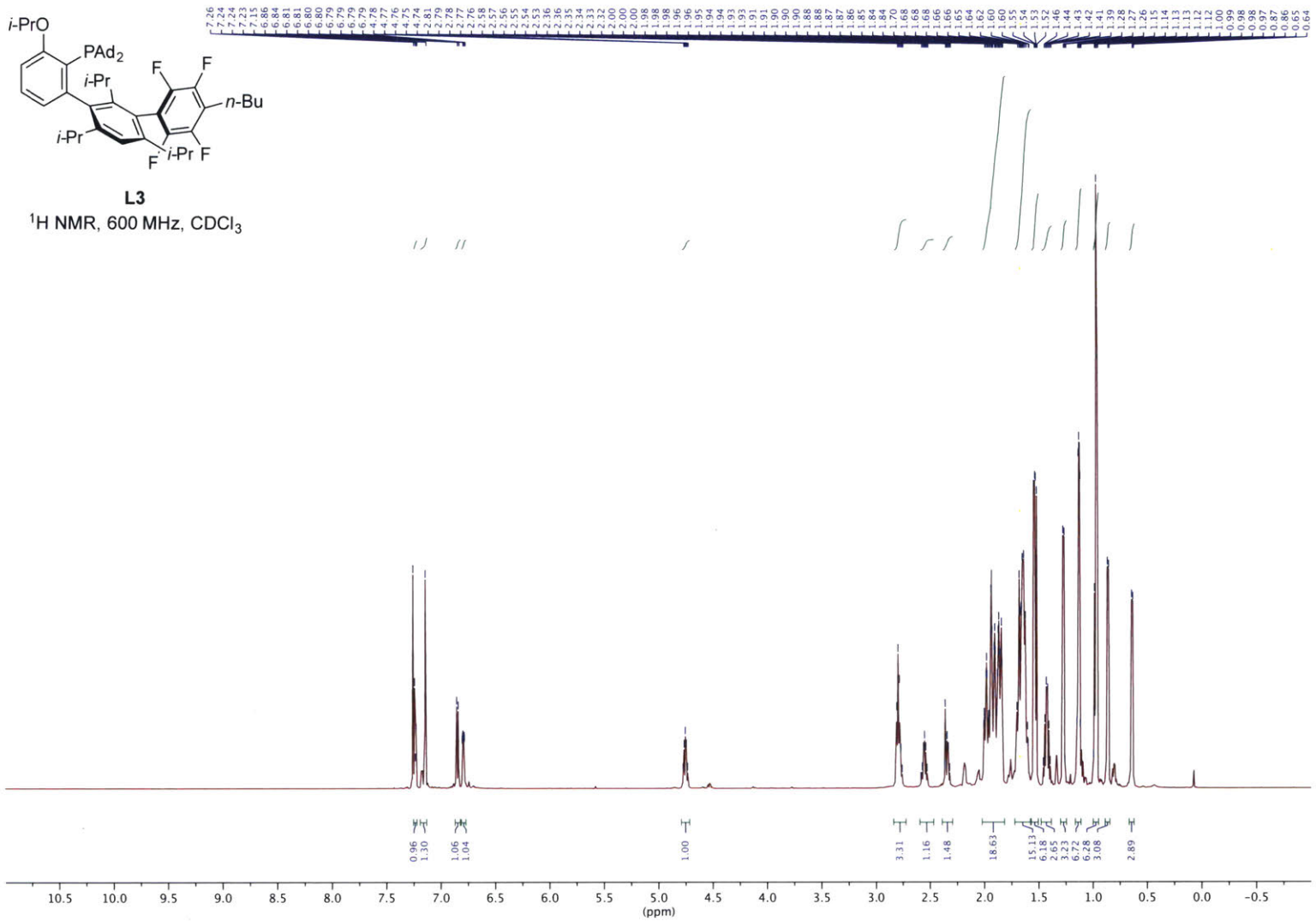
i-PrO
PAd2
i-Pr
i-Pr
F
F
n-Bu
F
i-Pr
F
L3
1H NMR, 600 MHz, CDCl3
(ppm)

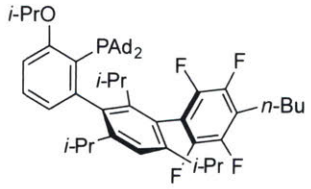

L3

^{13}C NMR, 151 MHz, $CDCl_3$

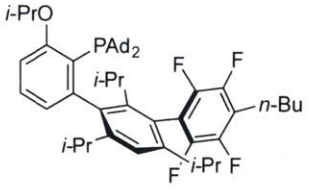

L3

^{19}F NMR, 565 MHz, $CDCl_3$

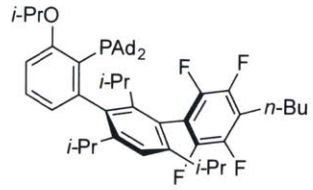

L3

^{31}P NMR, 162 MHz, $CDCl_3$

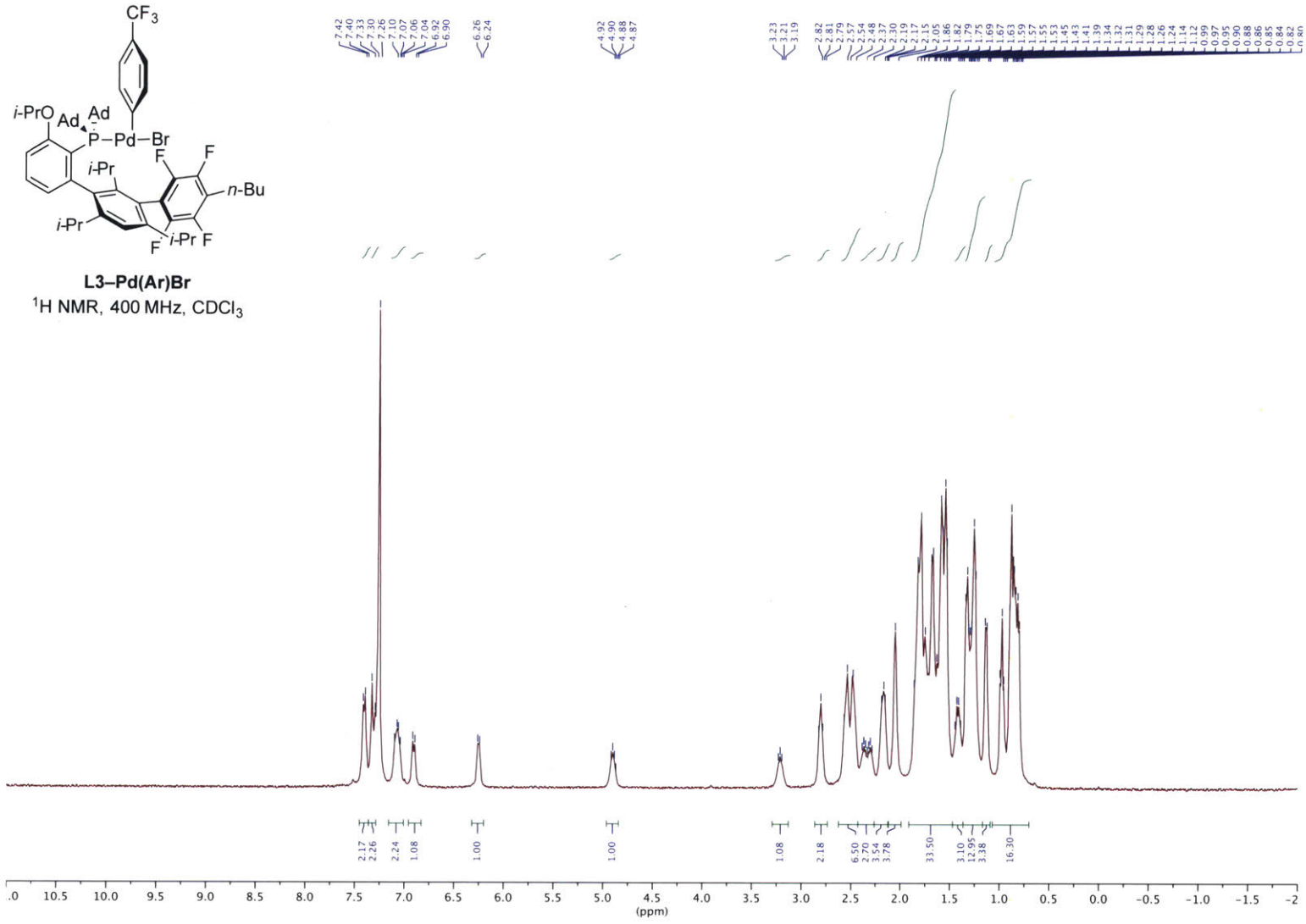
CF3
i-PrO
Ad
Ad
P–Pd–Br
F
F
i-Pr
n-Bu
i-Pr
F
i-Pr
F
L3–Pd(Ar)Br
1H NMR, 400 MHz, CDCl3
(ppm)

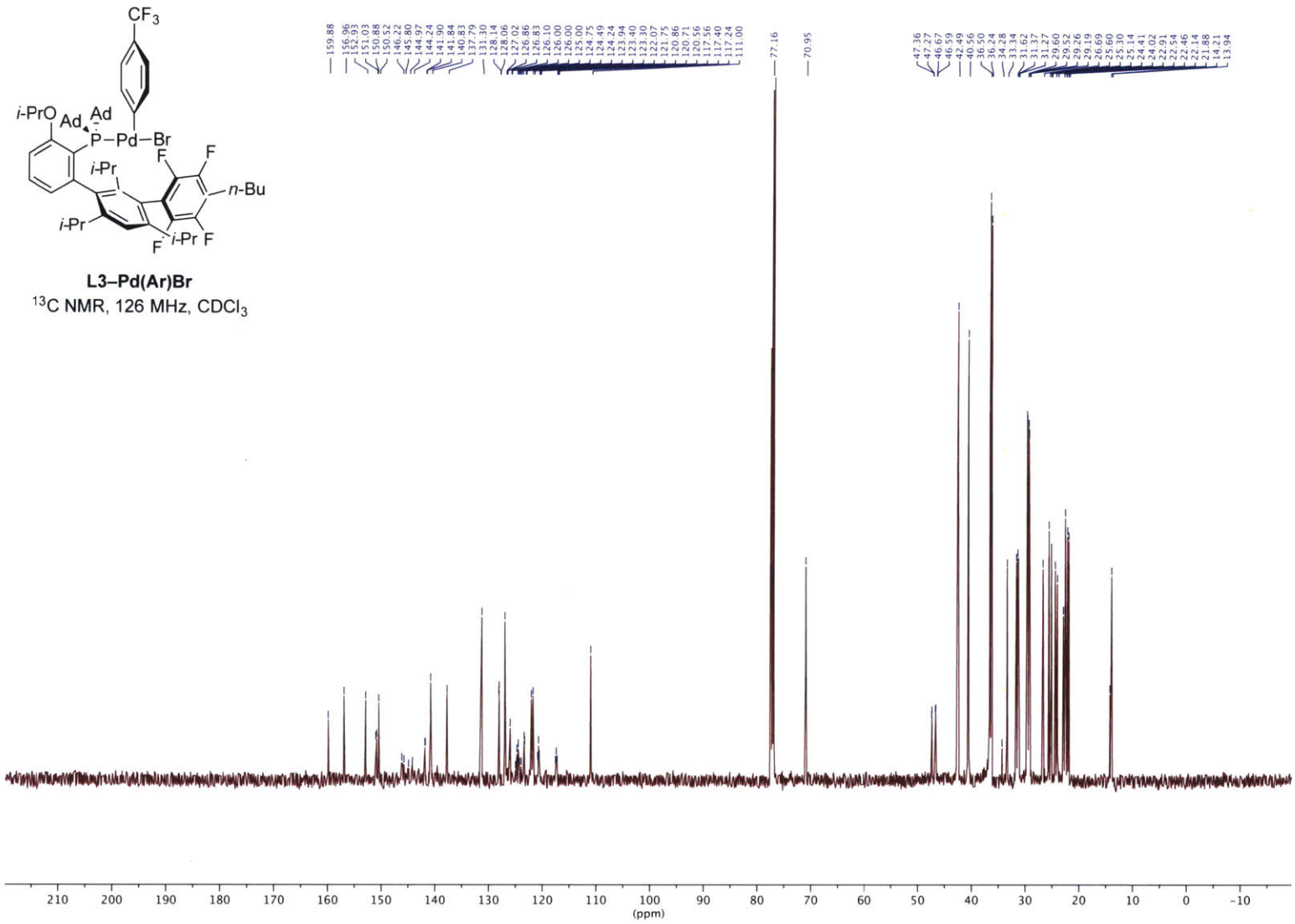

L3–Pd(Ar)Br

^{13}C NMR, 126 MHz, $CDCl_3$

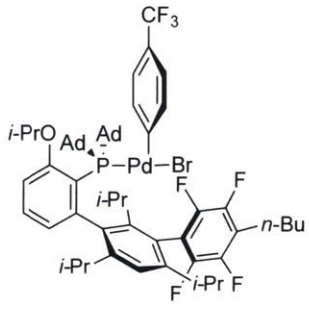

L3–Pd(Ar)Br

^{19}F NMR, 376 MHz, $CDCl_3$

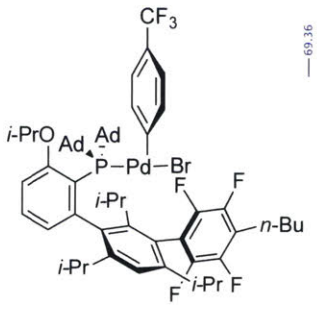

L3–Pd(Ar)Br

^{31}P NMR, 162 MHz, $CDCl_3$

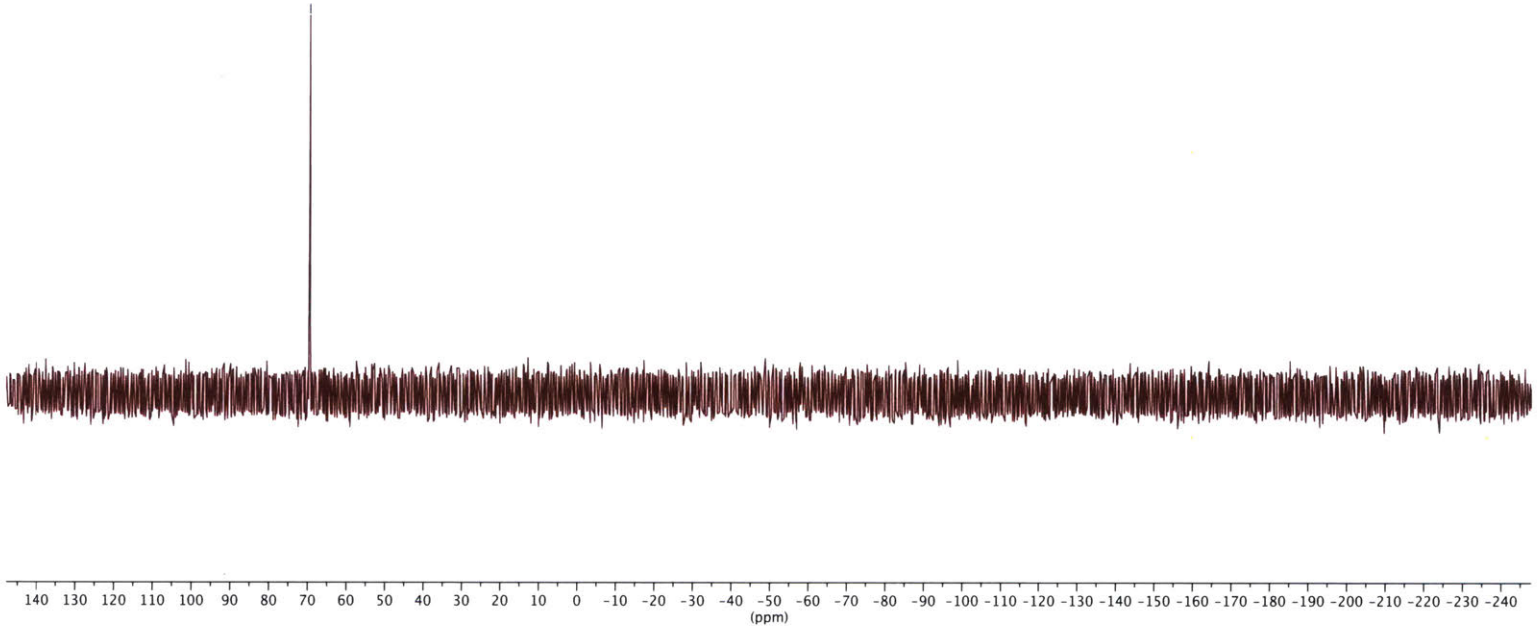

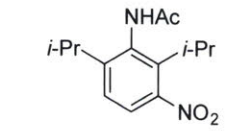

S4

^{1}H NMR, 600 MHz, $CDCl_3$

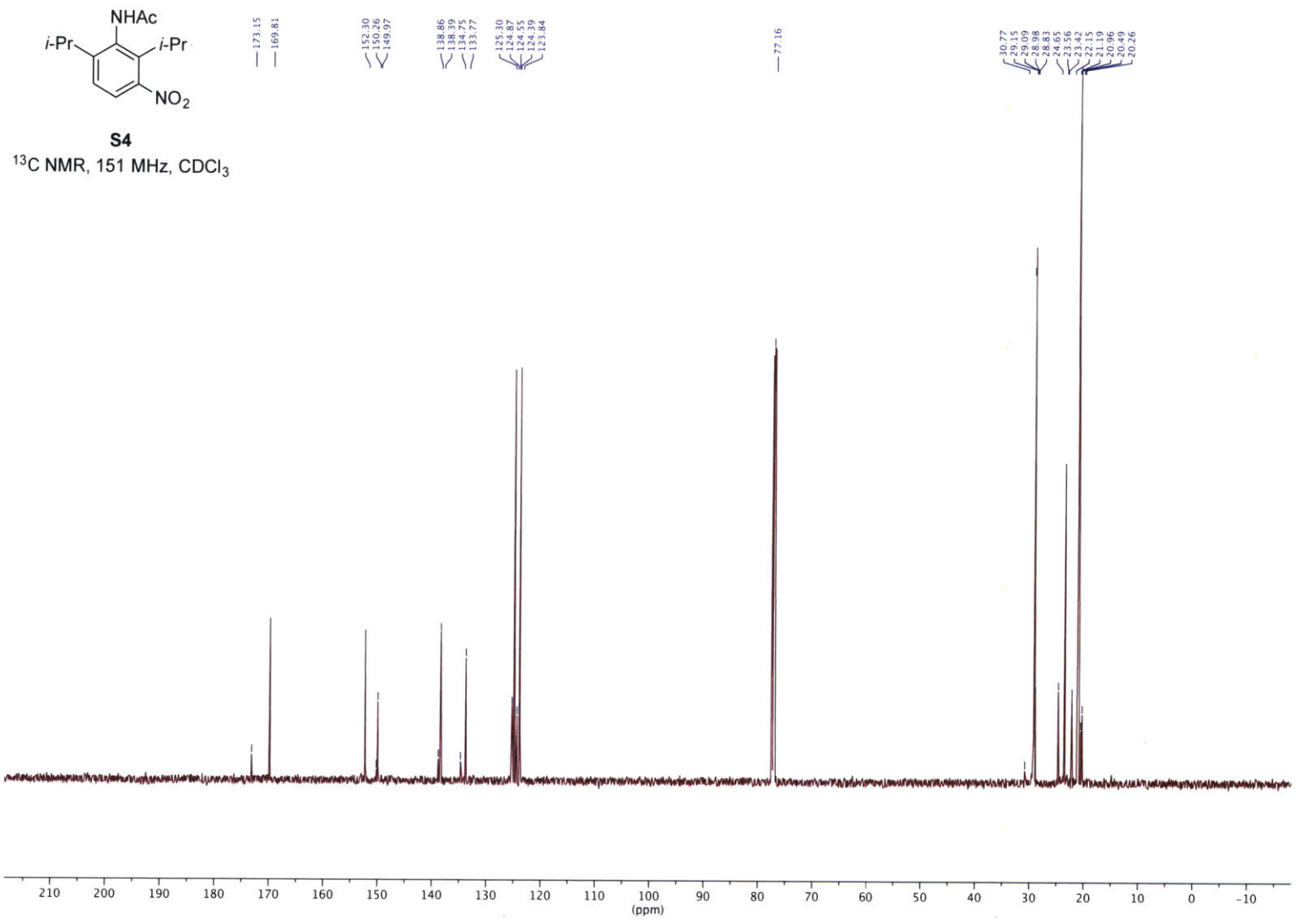

S4

^{13}C NMR, 151 MHz, $CDCl_3$

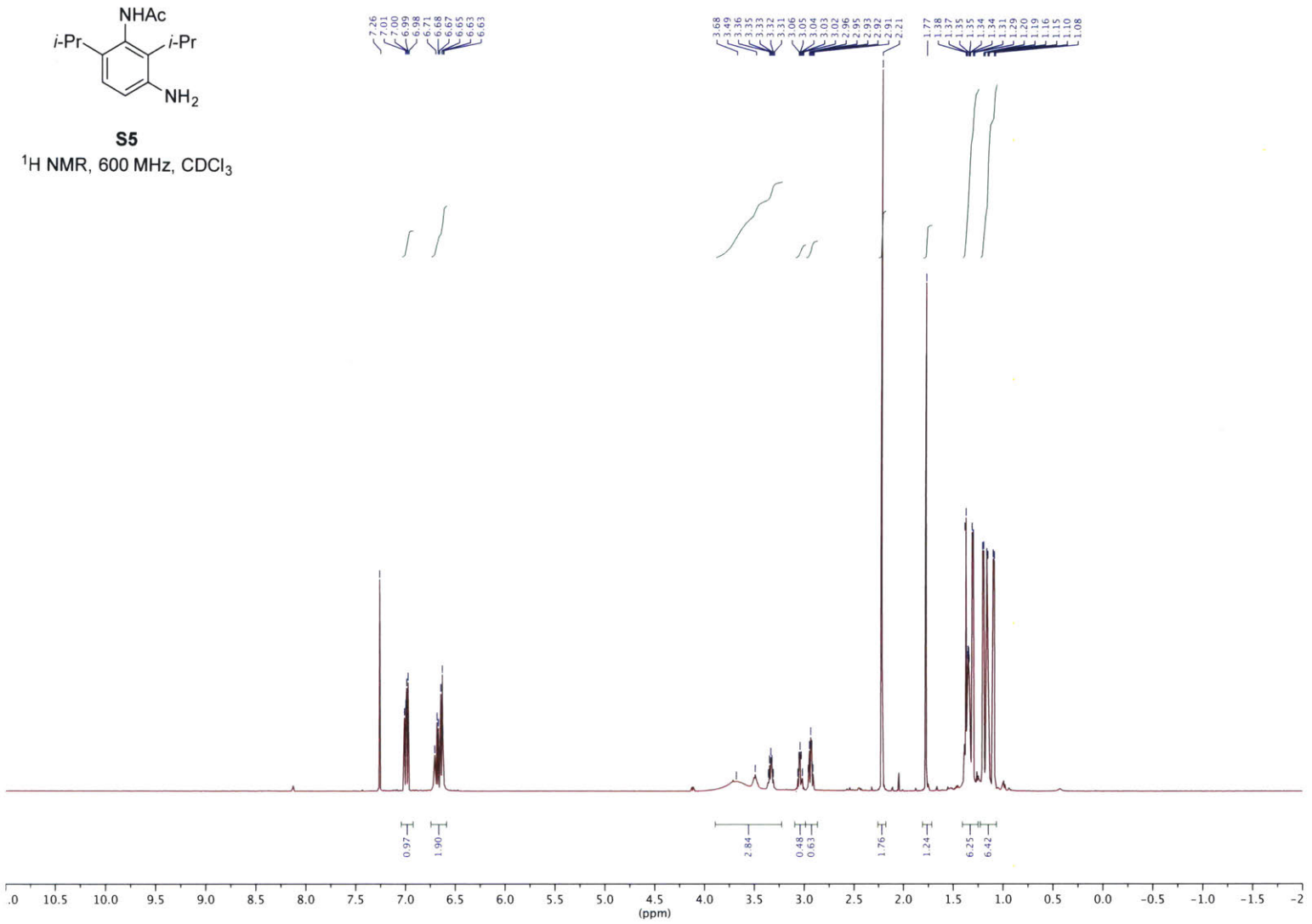
NHAc
i-Pr
i-Pr
NH2
S5
1H NMR, 600 MHz, CDCl3
7.26
7.01
7.00
6.99
6.98
6.71
6.68
6.67
6.65
6.63
6.63
3.68
3.49
3.36
3.35
3.33
3.32
3.31
3.06
3.05
3.04
3.03
3.02
2.96
2.95
2.93
2.92
2.91
2.21
1.77
1.38
1.37
1.35
1.35
1.34
1.34
1.31
1.29
1.20
1.19
1.16
1.15
1.10
1.08
0.97
1.90
2.84
0.48
0.63
1.76
1.24
6.25
6.42
(ppm)

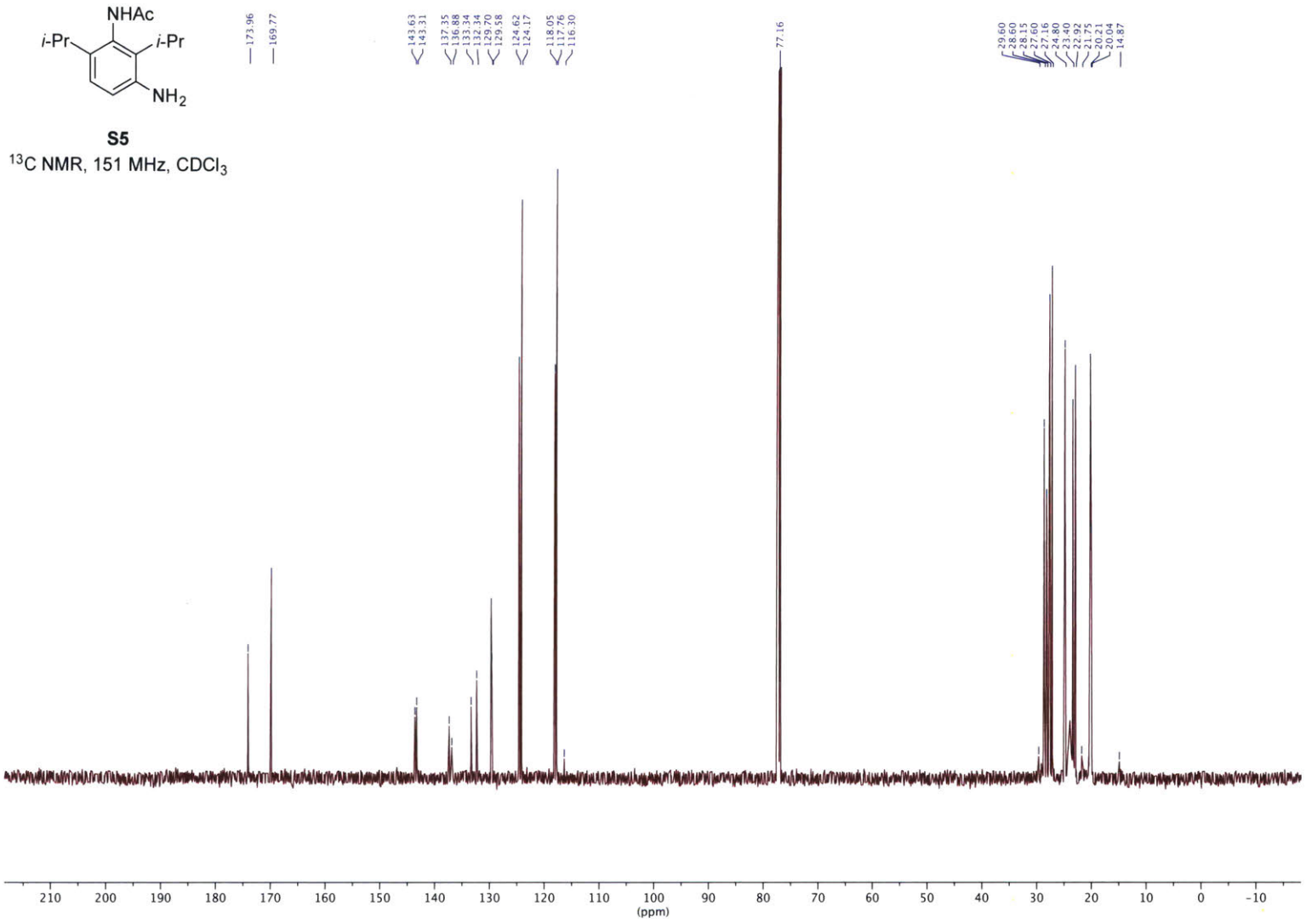

S5

^{13}C NMR, 151 MHz, $CDCl_3$

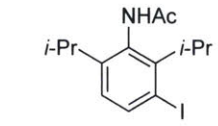

S6

^{1}H NMR, 600 MHz, $CDCl_3$

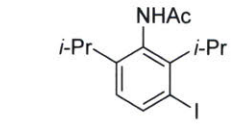

S6

^{13}C NMR, 151 MHz, $CDCl_3$

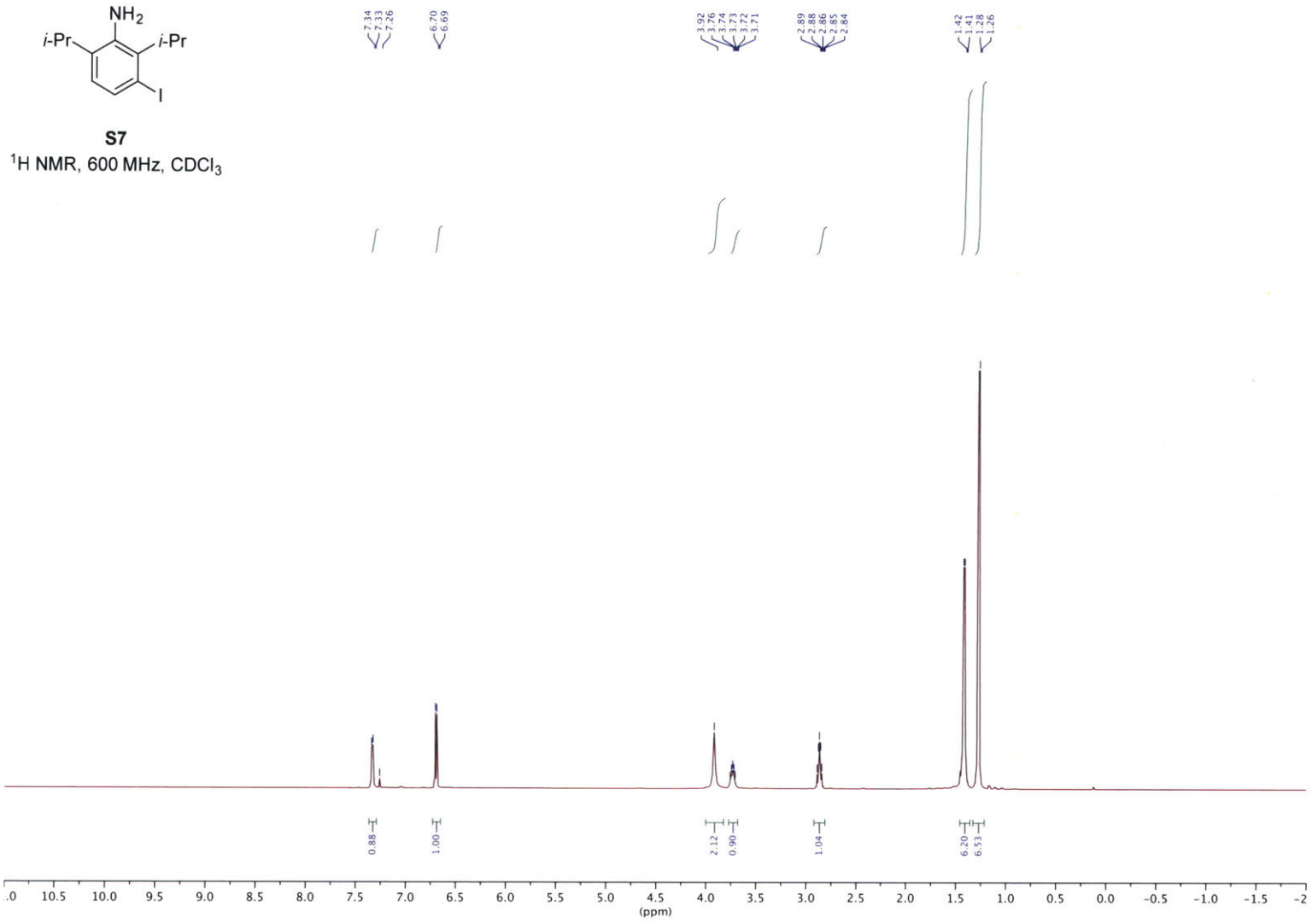
NH2
i-Pr
i-Pr
I
S7
1H NMR, 600 MHz, CDCl3
7.34
7.33
7.26
6.70
6.69
3.92
3.76
3.74
3.73
3.72
3.71
2.89
2.88
2.86
2.85
2.84
1.42
1.41
1.28
1.26
0.88
1.00
2.12
0.90
1.04
6.20
6.53
(ppm)

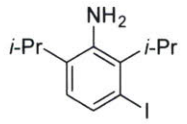

S7

^{13}C NMR, 151 MHz, $CDCl_3$

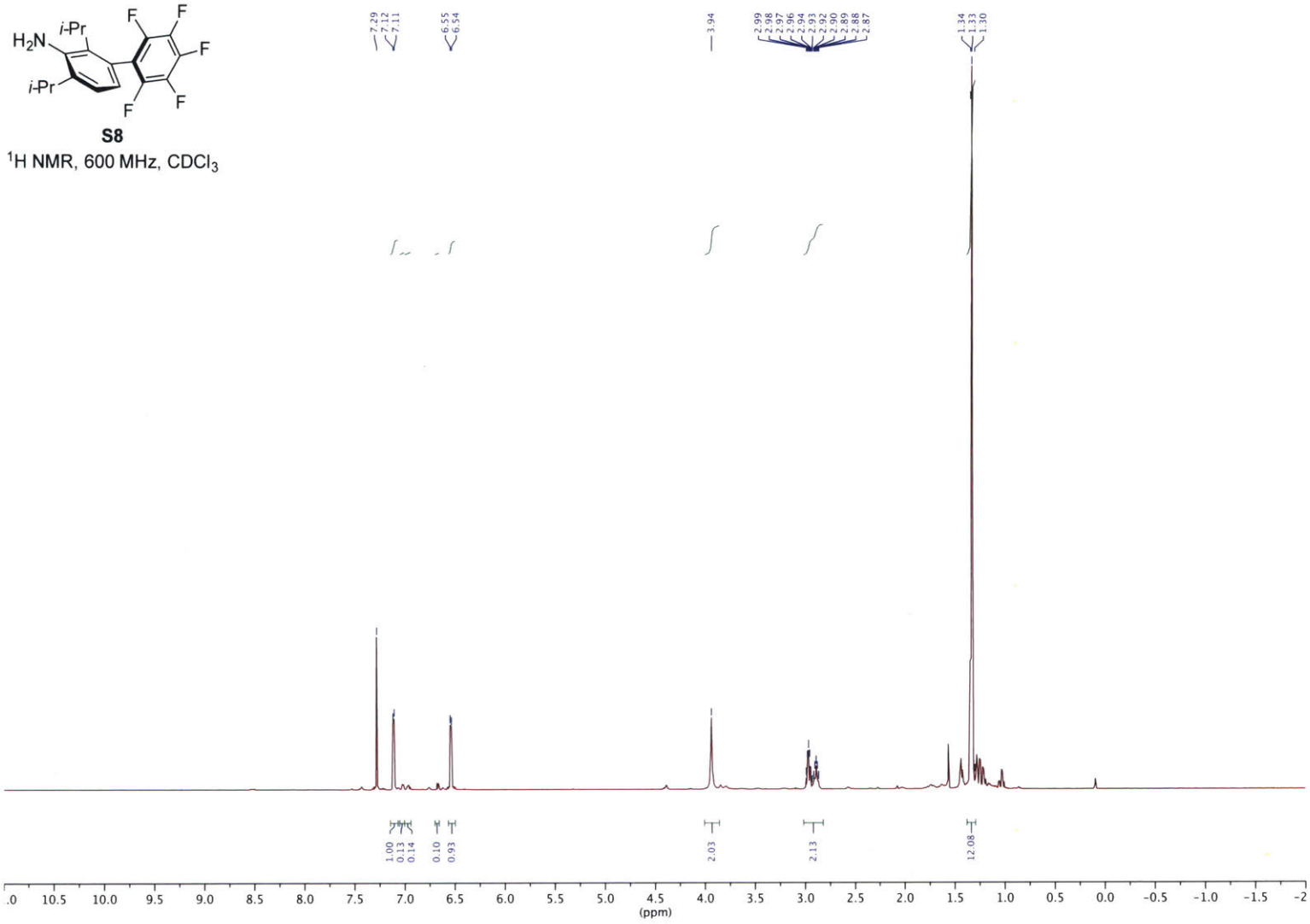
H2N
i-Pr
i-Pr
F
F
F
F
F
S8
1H NMR, 600 MHz, CDCl3
7.29
7.12
7.11
6.55
6.54
3.94
2.99
2.98
2.97
2.96
2.94
2.93
2.92
2.90
2.89
2.88
2.87
1.34
1.33
1.30
1.00
0.13
0.14
0.10
0.93
2.03
2.13
12.08
(ppm)

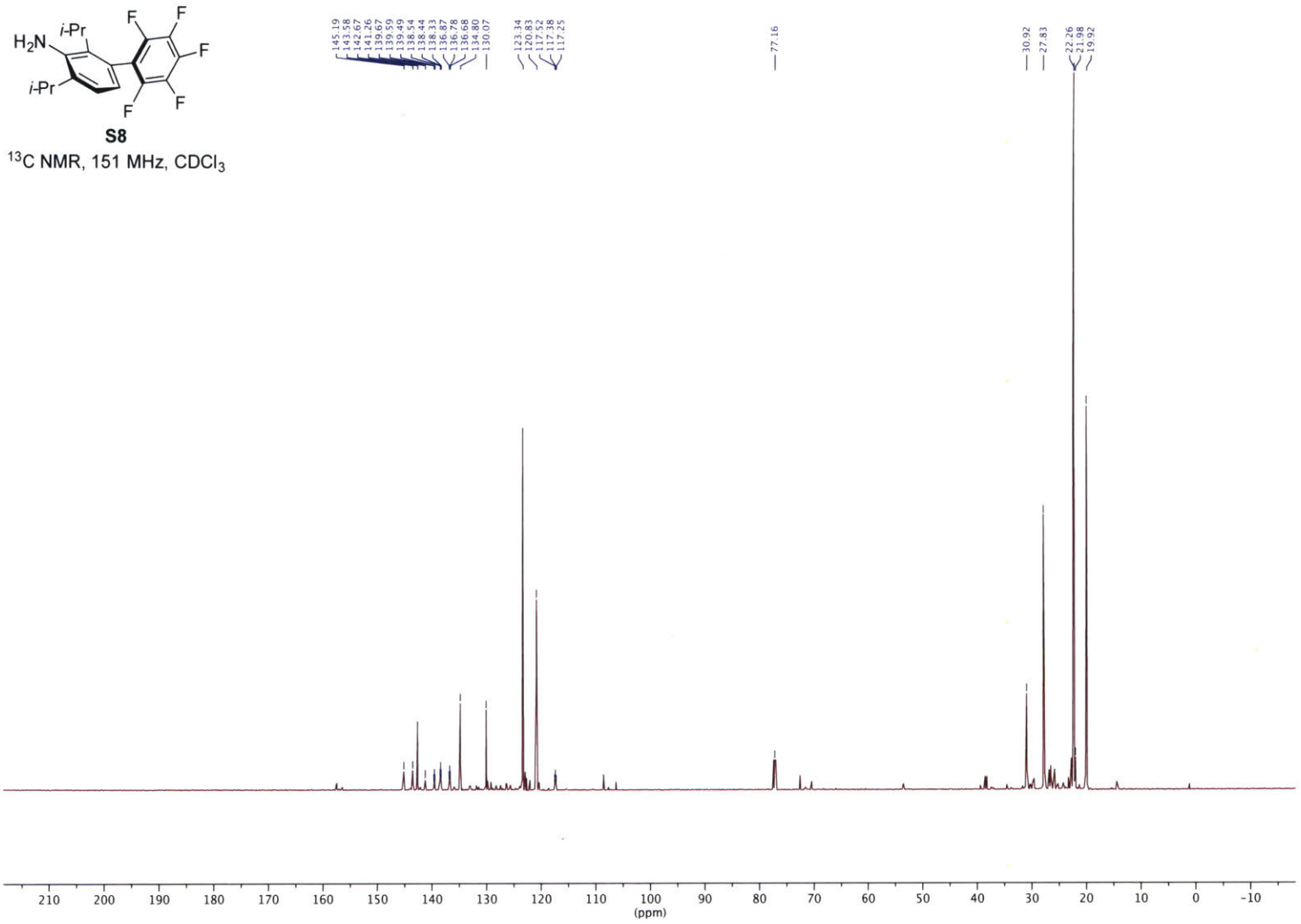

S8

^{13}C NMR, 151 MHz, $CDCl_3$

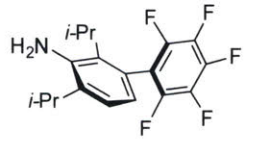

S8

^{19}F NMR, 565 MHz, $CDCl_3$

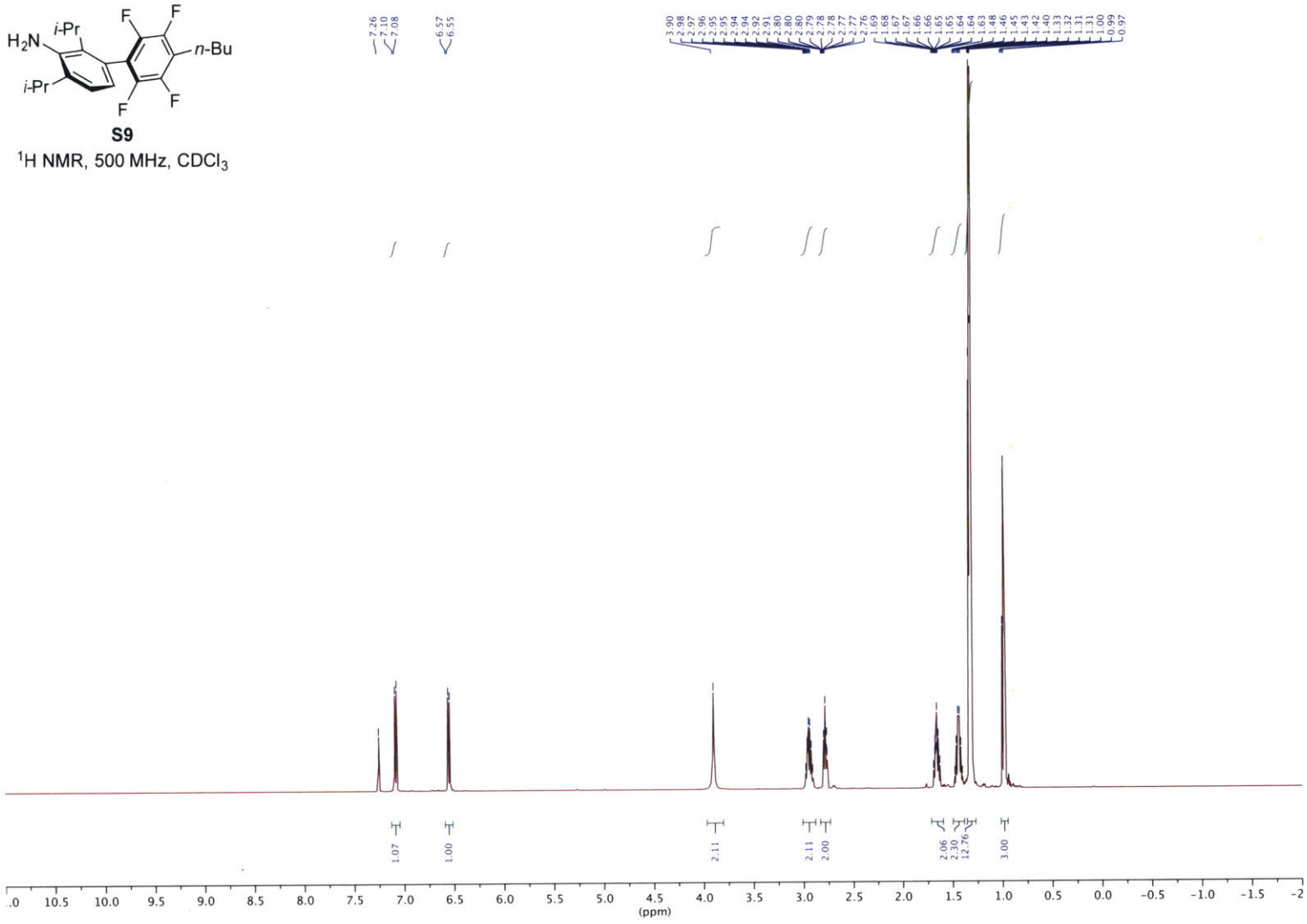
H2N
i-Pr
i-Pr
F
F
F
F
n-Bu
S9
1H NMR, 500 MHz, CDCl3
7.26
7.10
7.08
6.57
6.55
1.07
1.00
2.11
2.11
2.00
2.06
2.30
12.76
3.00
(ppm)

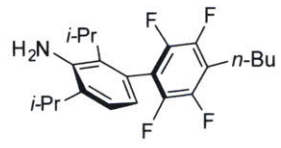

S9

^{13}C NMR, 151 MHz, $CDCl_3$

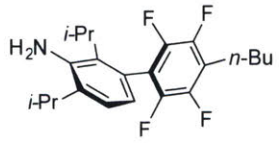

S9

^{19}F NMR, 282 MHz, $CDCl_3$

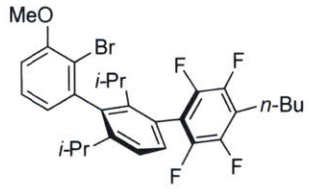

S10

^{1}H NMR, 600 MHz, $CDCl_3$

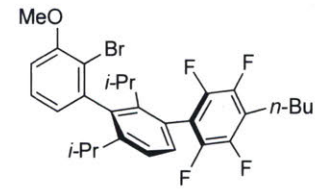

S10

^{13}C NMR, 151 MHz, $CDCl_3$

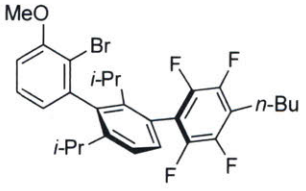

S10

^{19}F NMR, 565 MHz, $CDCl_3$

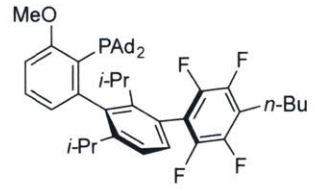

L4

^{1}H NMR, 600 MHz, $CDCl_3$

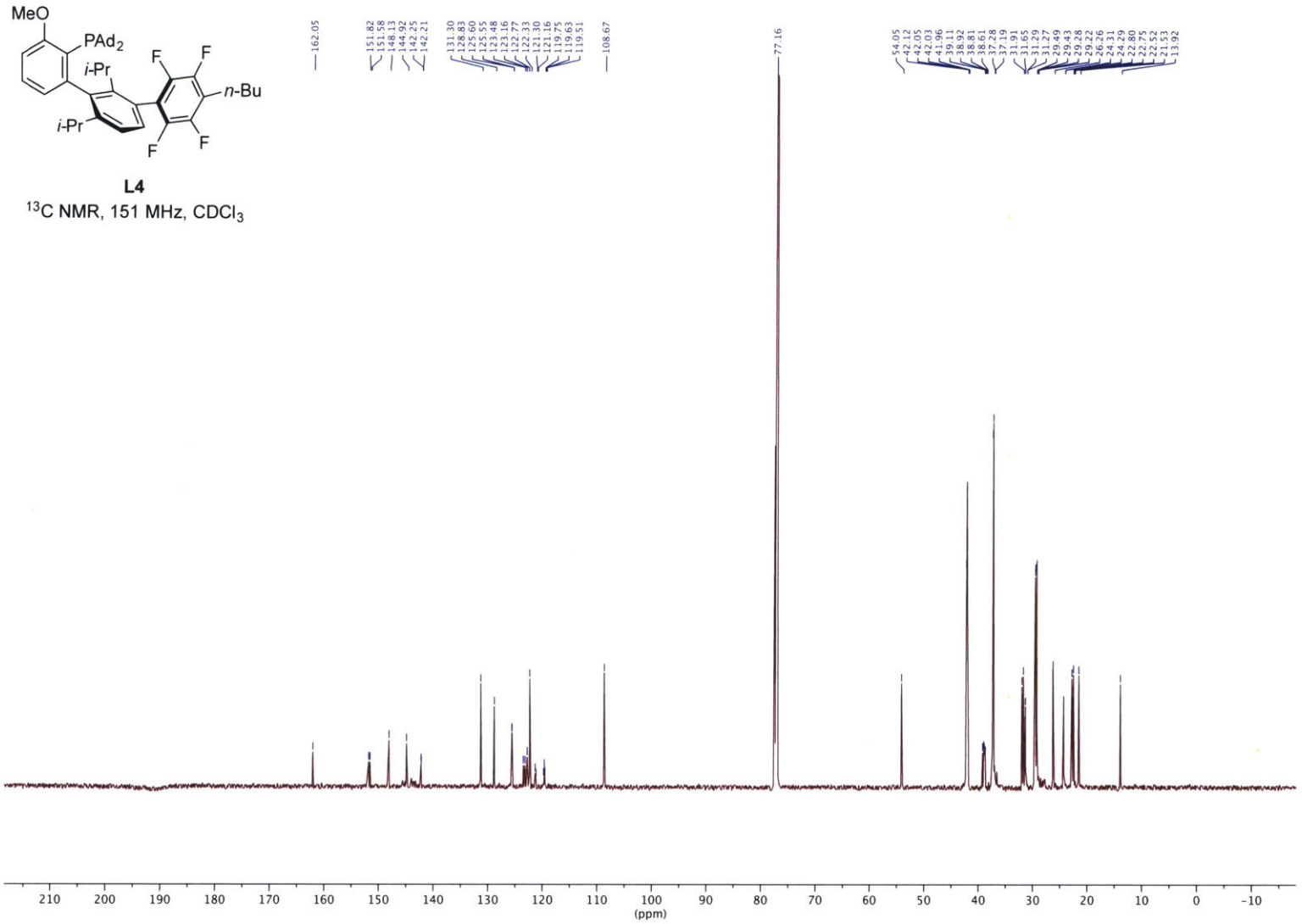
MeO
PAd2
i-Pr
i-Pr
F
F
F
F
n-Bu
L4
13C NMR, 151 MHz, CDCl3
162.05
151.82
151.58
148.13
144.92
142.25
142.21
131.30
128.83
125.60
125.55
123.48
123.16
122.77
122.33
121.30
121.16
119.75
119.63
119.51
108.67
77.16
54.05
42.12
42.05
42.03
41.96
39.11
38.92
38.81
38.61
37.28
37.19
31.91
31.85
31.29
31.27
29.49
29.43
29.28
29.22
26.26
24.31
24.29
22.80
22.75
22.52
21.53
13.92
210
200
190
180
170
160
150
140
130
120
110
100
90
80
70
60
50
40
30
20
10
0
-10
(ppm)

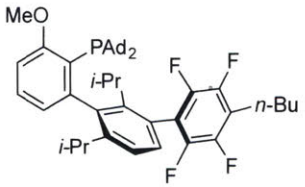

L4

^{19}F NMR, 376 MHz, C_6D_6

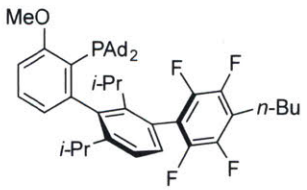

L4

^{31}P NMR, 162 MHz, C_6D_6

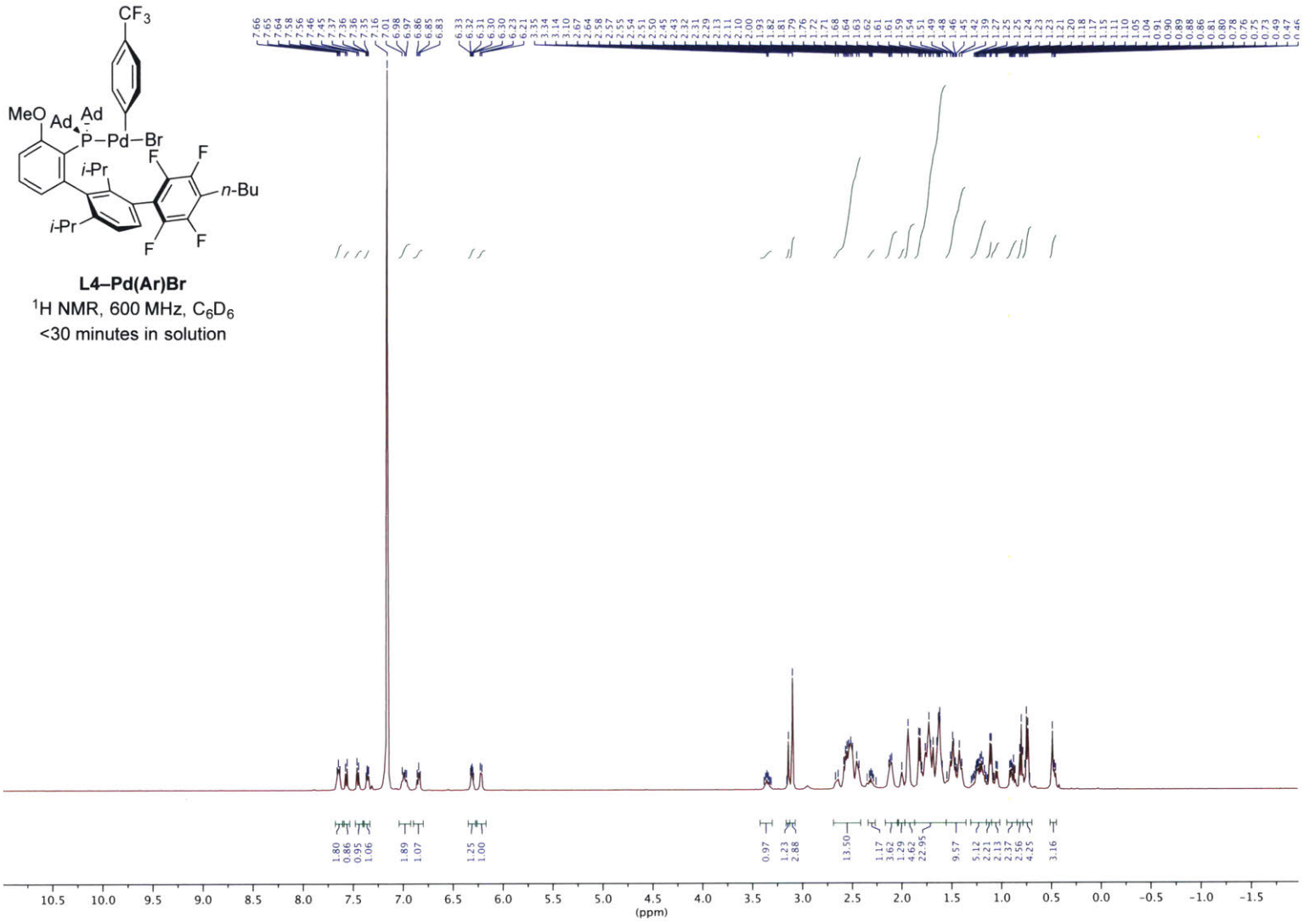
CF3
MeO
Ad
Ad
P–Pd–Br
i-Pr
i-Pr
F
F
F
F
n-Bu
L4–Pd(Ar)Br
1H NMR, 600 MHz, C6D6
<30 minutes in solution
(ppm)

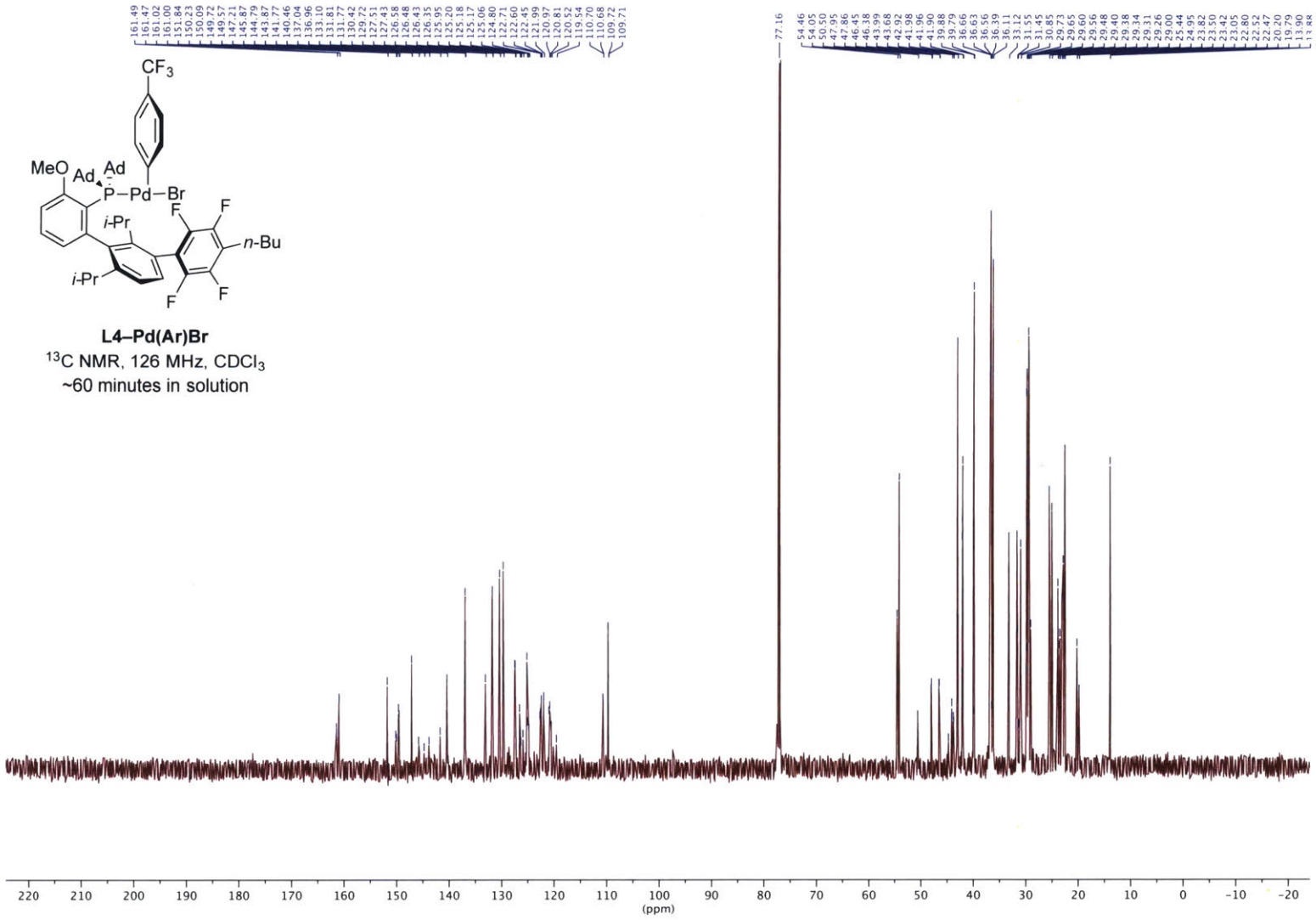
CF3
MeO
Ad
Ad
P–Pd–Br
F
F
i-Pr
n-Bu
i-Pr
F
F
L4–Pd(Ar)Br
13C NMR, 126 MHz, CDCl3
~60 minutes in solution
77.16
(ppm)

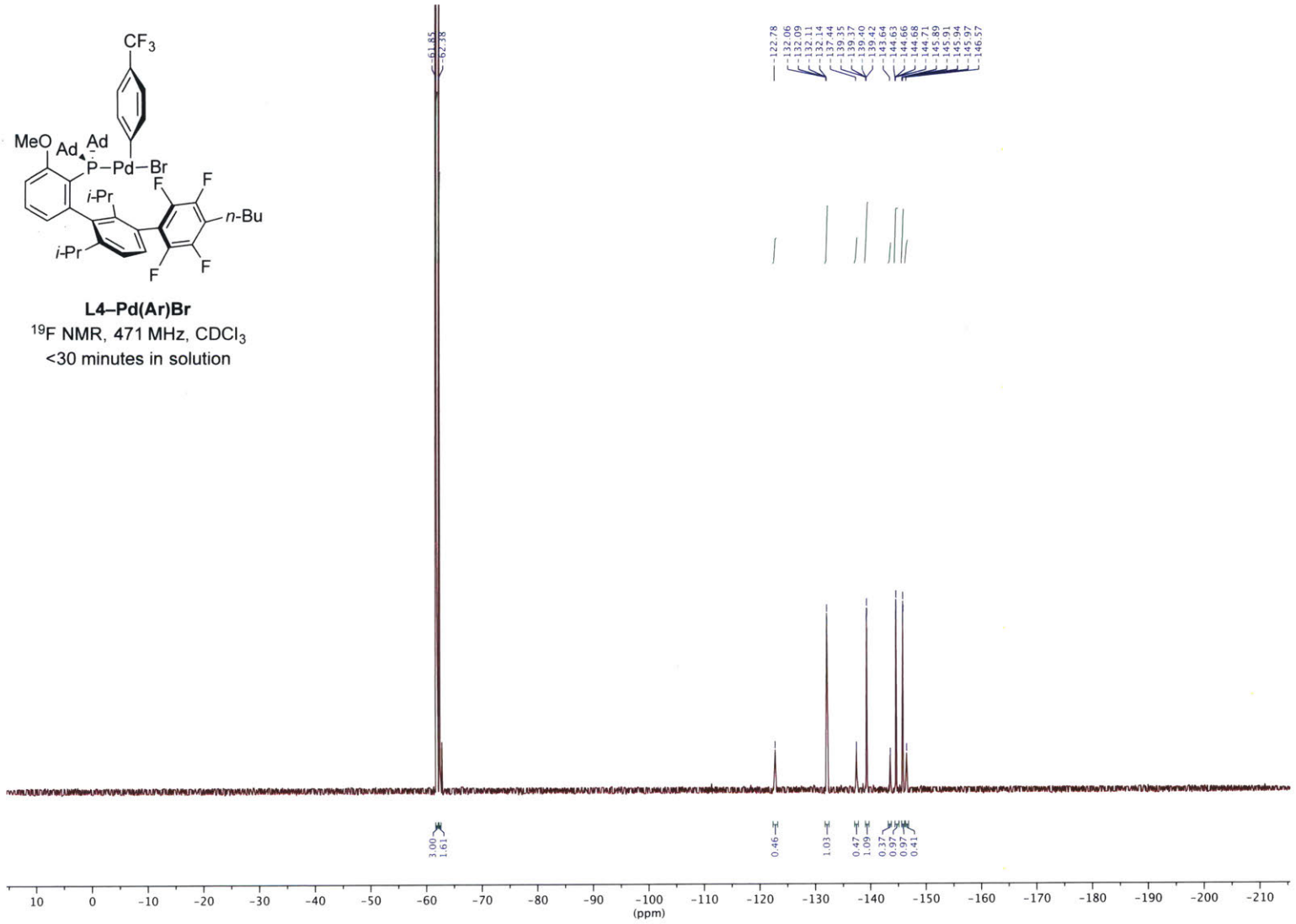

L4–Pd(Ar)Br

^{19}F NMR, 471 MHz, $CDCl_3$

<30 minutes in solution

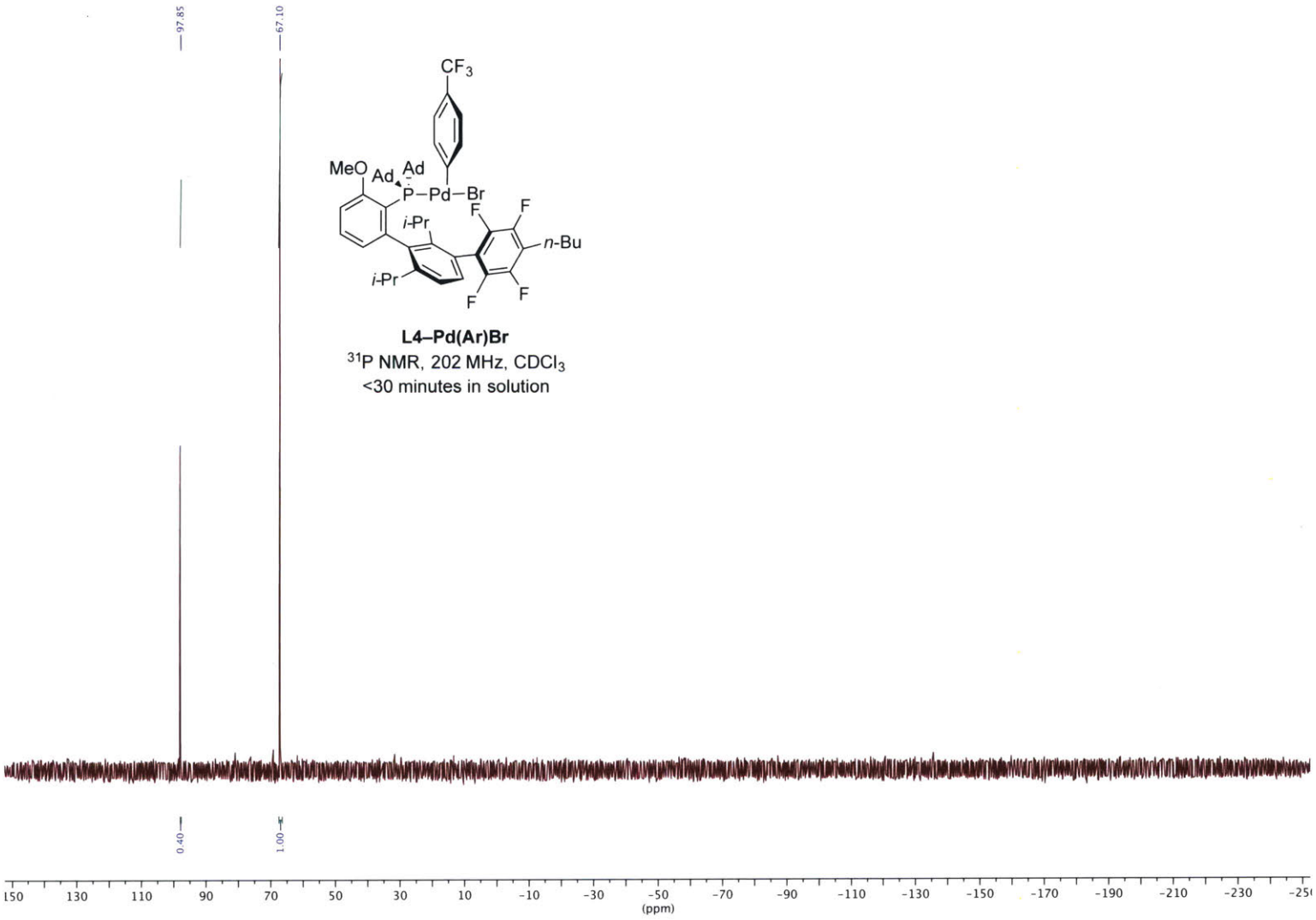

L4–Pd(Ar)Br

^{31}P NMR, 202 MHz, $CDCl_3$

<30 minutes in solution

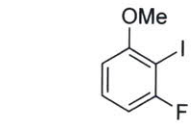

S11

^{1}H NMR, 600 MHz, C_6D_6

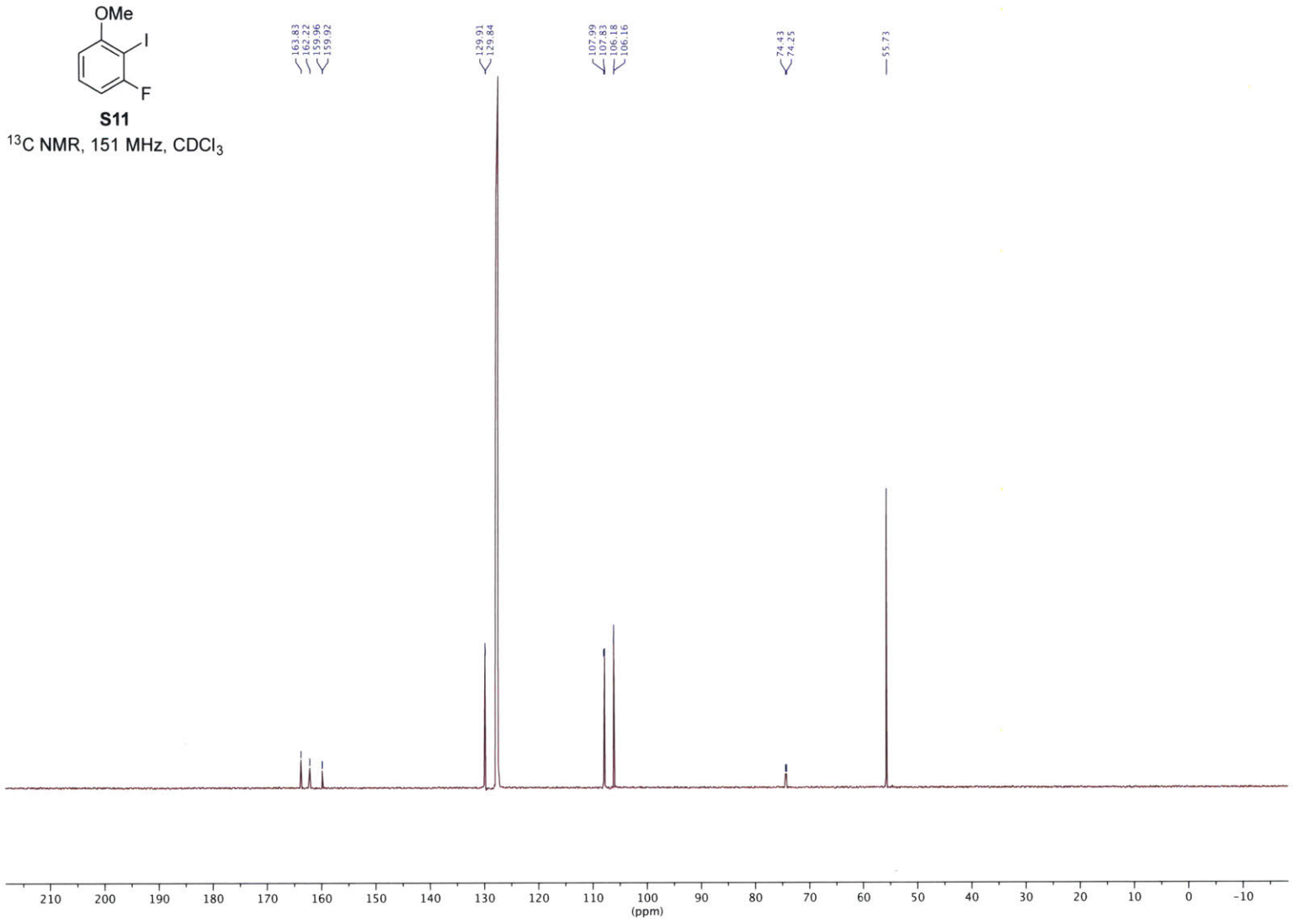
OMe
I
F
S11
^{13}C NMR, 151 MHz, $CDCl_3$
163.83
162.22
159.96
159.92
129.91
129.84
107.99
107.83
106.18
106.16
74.43
74.25
55.73
210 200 190 180 170 160 150 140 130 120 110 100 90 80 70 60 50 40 30 20 10 0 -10
(ppm)

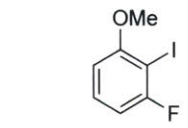

S11

^{19}F NMR, 565 MHz, $CDCl_3$

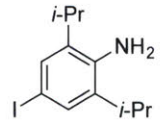

S12

^{1}H NMR, 400 MHz, $CDCl_3$

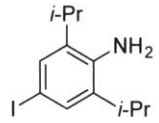

S12

^{13}C NMR, 151 MHz, $CDCl_3$

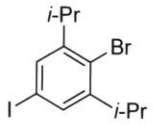

S13

^{1}H NMR, 400 MHz, $CDCl_3$

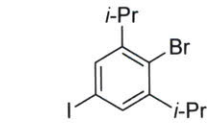

S13

^{13}C NMR, 151MHz, $CDCl_3$

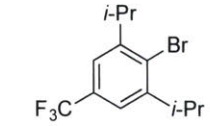

S14

^{1}H NMR, 400 MHz, $CDCl_3$

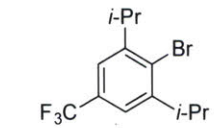

S14

^{13}C NMR, 151 MHz, $CDCl_3$

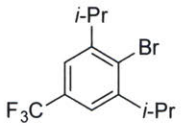

S14

^{19}F NMR, 565 MHz, $CDCl_3$

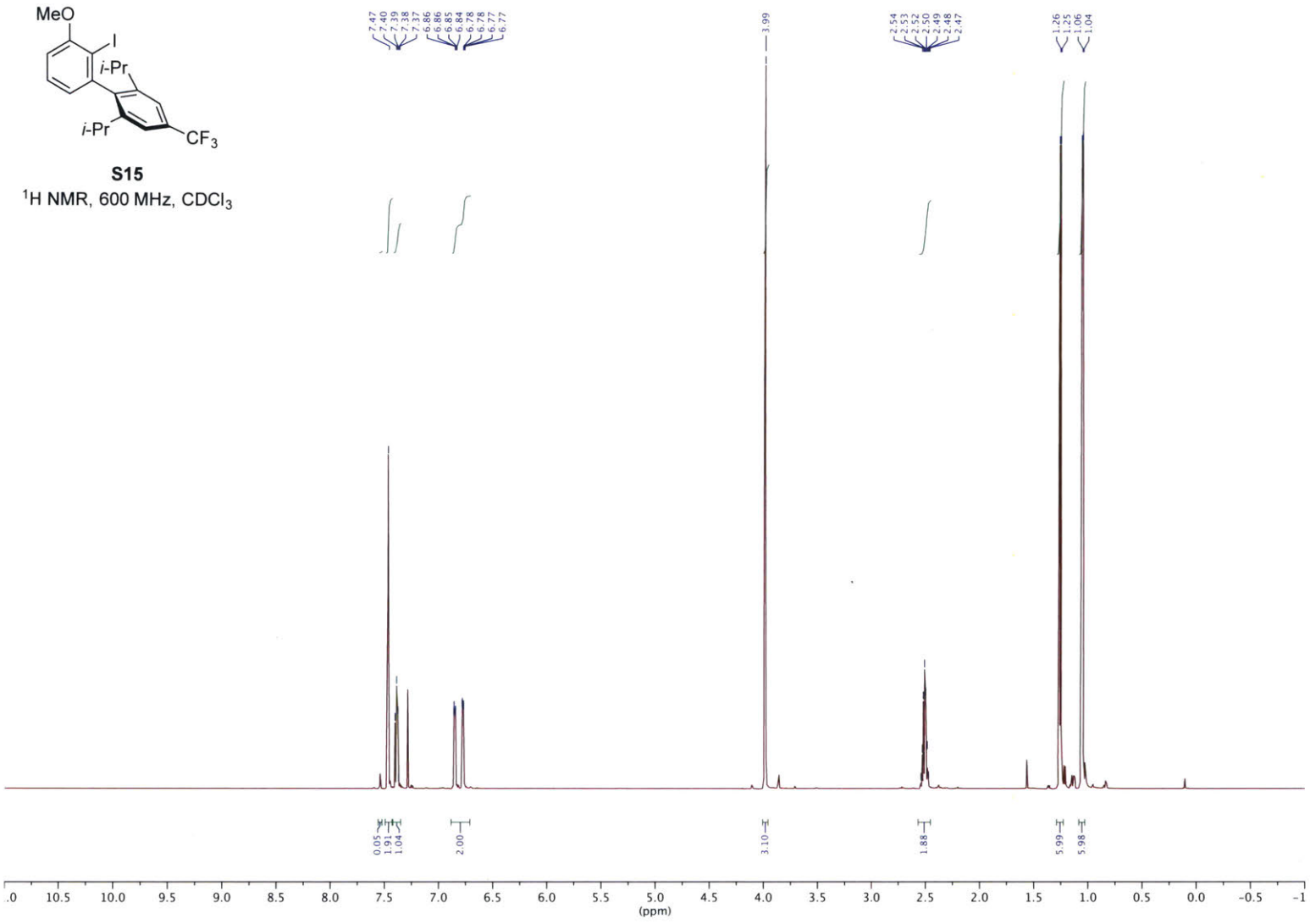
MeO
I
i-Pr
i-Pr
CF3
S15
1H NMR, 600 MHz, CDCl3
7.47
7.40
7.39
7.38
7.37
6.86
6.86
6.85
6.84
6.78
6.78
6.77
6.77
6.77
3.99
2.54
2.53
2.52
2.50
2.49
2.48
2.47
1.26
1.25
1.06
1.04
0.05
1.91
1.04
2.00
3.10
1.88
5.99
5.98
(ppm)

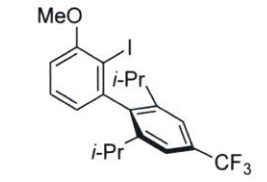

S15

^{13}C NMR, 151 MHz, $CDCl_3$

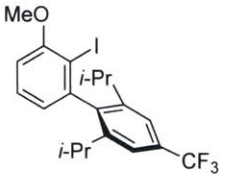

S15

^{19}F NMR, 376 MHz, $CDCl_3$

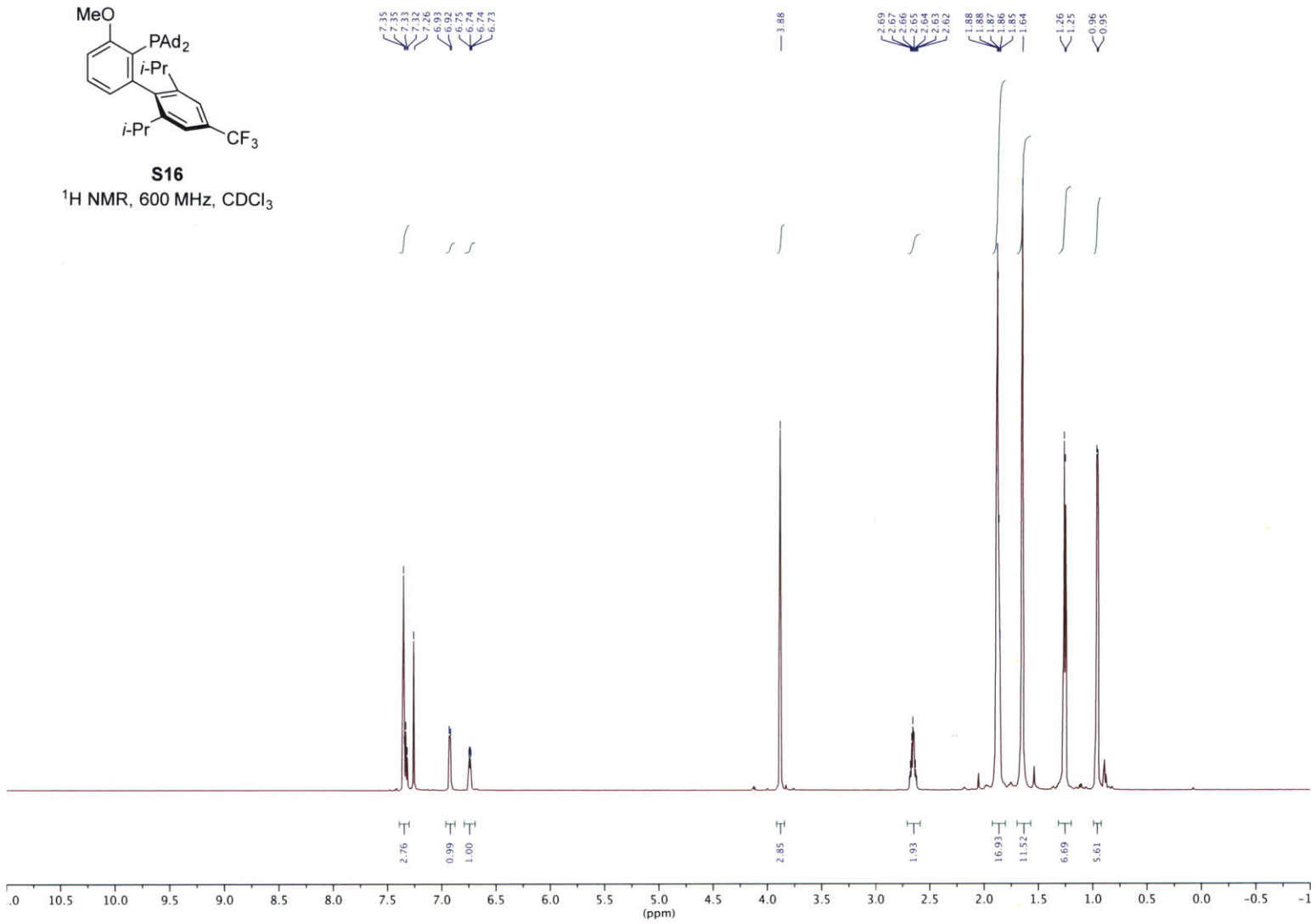
MeO
PAd2
i-Pr
i-Pr
CF3
S16
1H NMR, 600 MHz, CDCl3
7.35
7.35
7.33
7.32
7.26
6.93
6.92
6.75
6.74
6.74
6.73
3.88
2.69
2.67
2.66
2.65
2.64
2.63
2.62
1.88
1.88
1.87
1.86
1.85
1.64
1.26
1.25
0.96
0.95
2.76
0.99
1.00
2.85
1.93
16.93
11.52
6.69
5.61
(ppm)

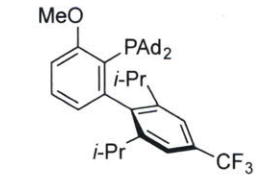

S16

^{13}C NMR, 151 MHz, $CDCl_3$

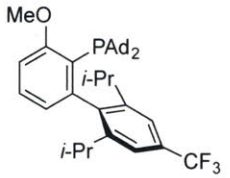

S16

^{19}F NMR, 471 MHz, $CDCl_3$

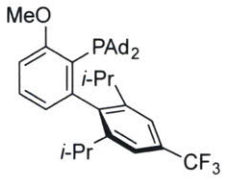

S16

^{31}P NMR, 203 MHz, $CDCl_3$

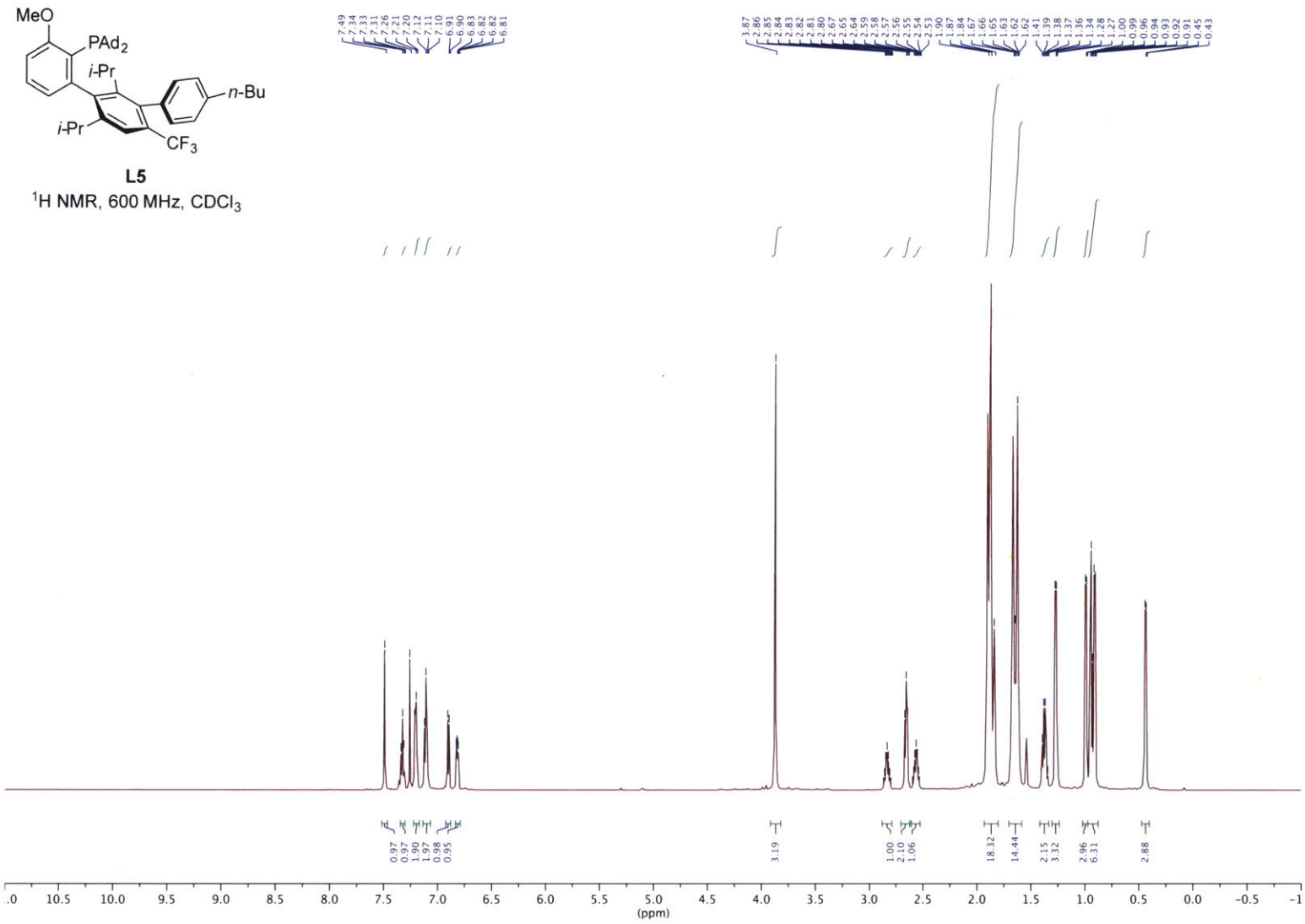
MeO
PAd2
i-Pr
i-Pr
n-Bu
CF3
L5
1H NMR, 600 MHz, CDCl3
(ppm)

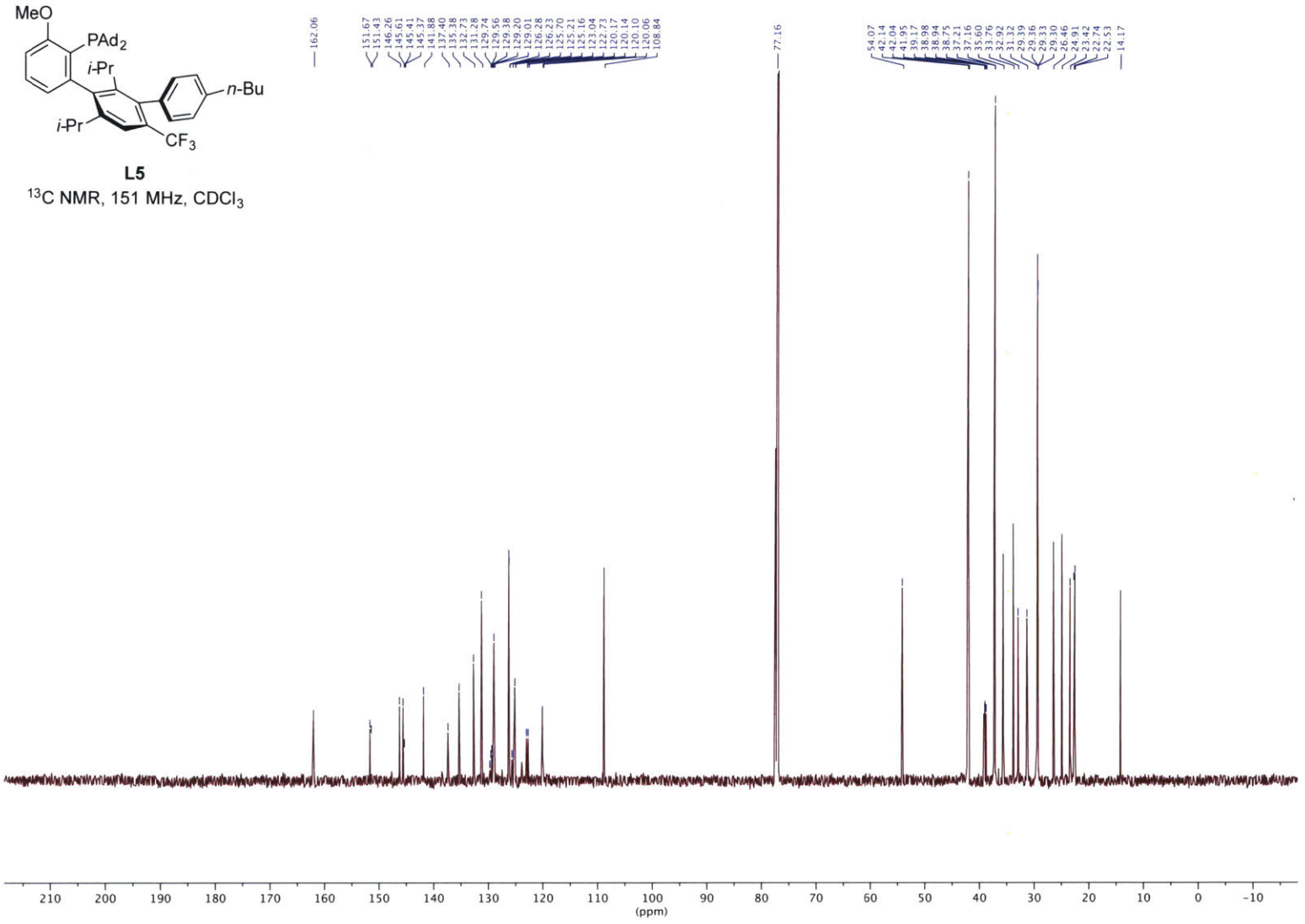
MeO
PAd2
i-Pr
i-Pr
n-Bu
CF3
L5
13C NMR, 151 MHz, CDCl3
162.06
151.67
151.43
146.26
145.61
144.41
143.37
141.88
137.40
135.38
132.73
131.28
129.74
129.56
129.38
129.20
129.01
126.28
126.23
125.70
125.21
125.16
123.04
122.73
120.17
120.14
120.10
120.06
108.84
77.16
54.07
42.14
42.04
41.95
39.17
38.98
38.94
38.75
37.21
37.16
35.60
33.76
33.52
31.32
29.39
29.36
29.33
29.30
26.46
24.91
23.42
22.74
22.53
14.17
210
200
190
180
170
160
150
140
130
120
110
100
90
80
70
60
50
40
30
20
10
0
-10
(ppm)

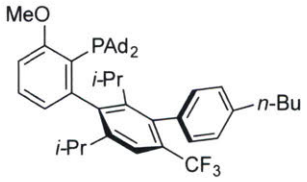

L5

^{19}F NMR, 565 MHz, $CDCl_3$

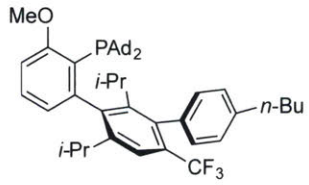

L5

^{31}P NMR, 162 MHz, $CDCl_3$

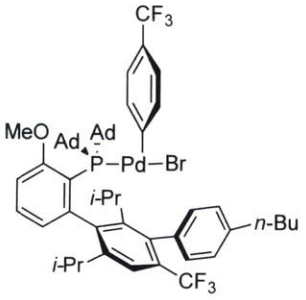

L5–Pd(Ar)Br

^{1}H NMR, 300 MHz, $CDCl_3$

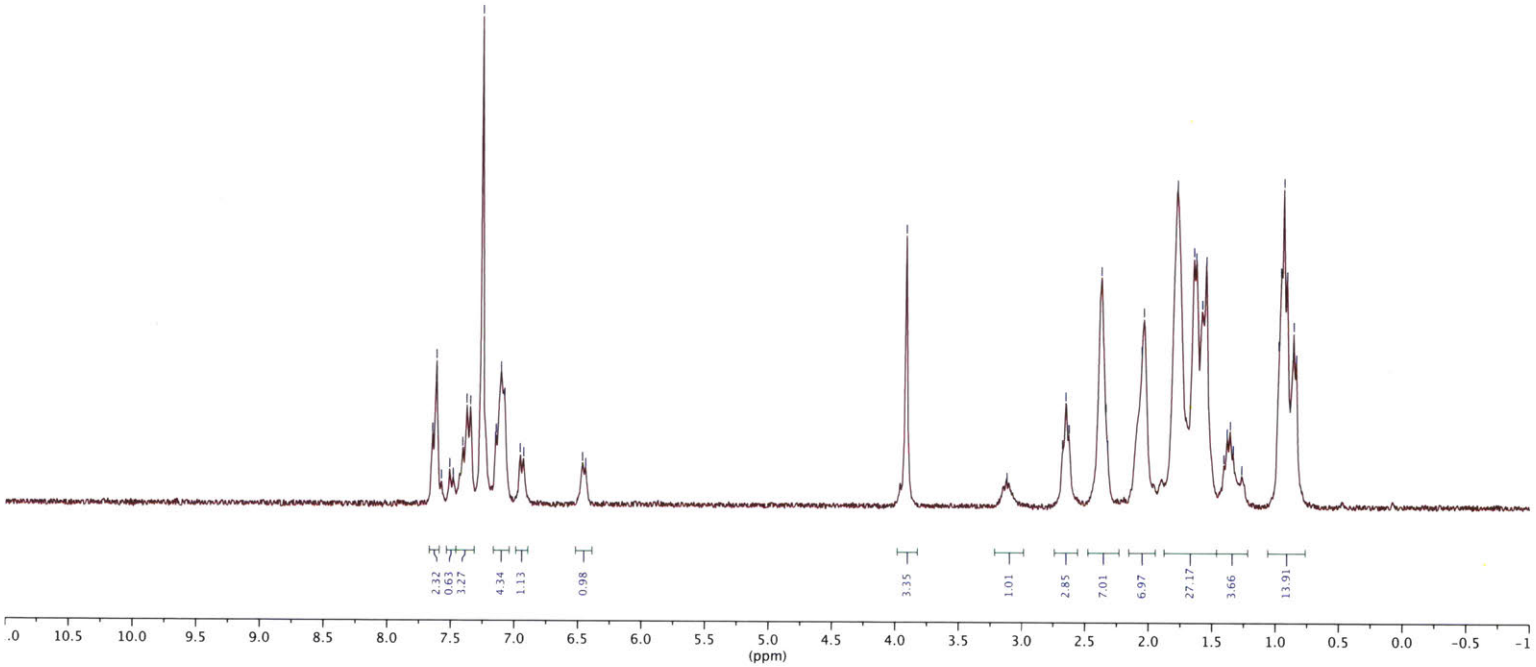

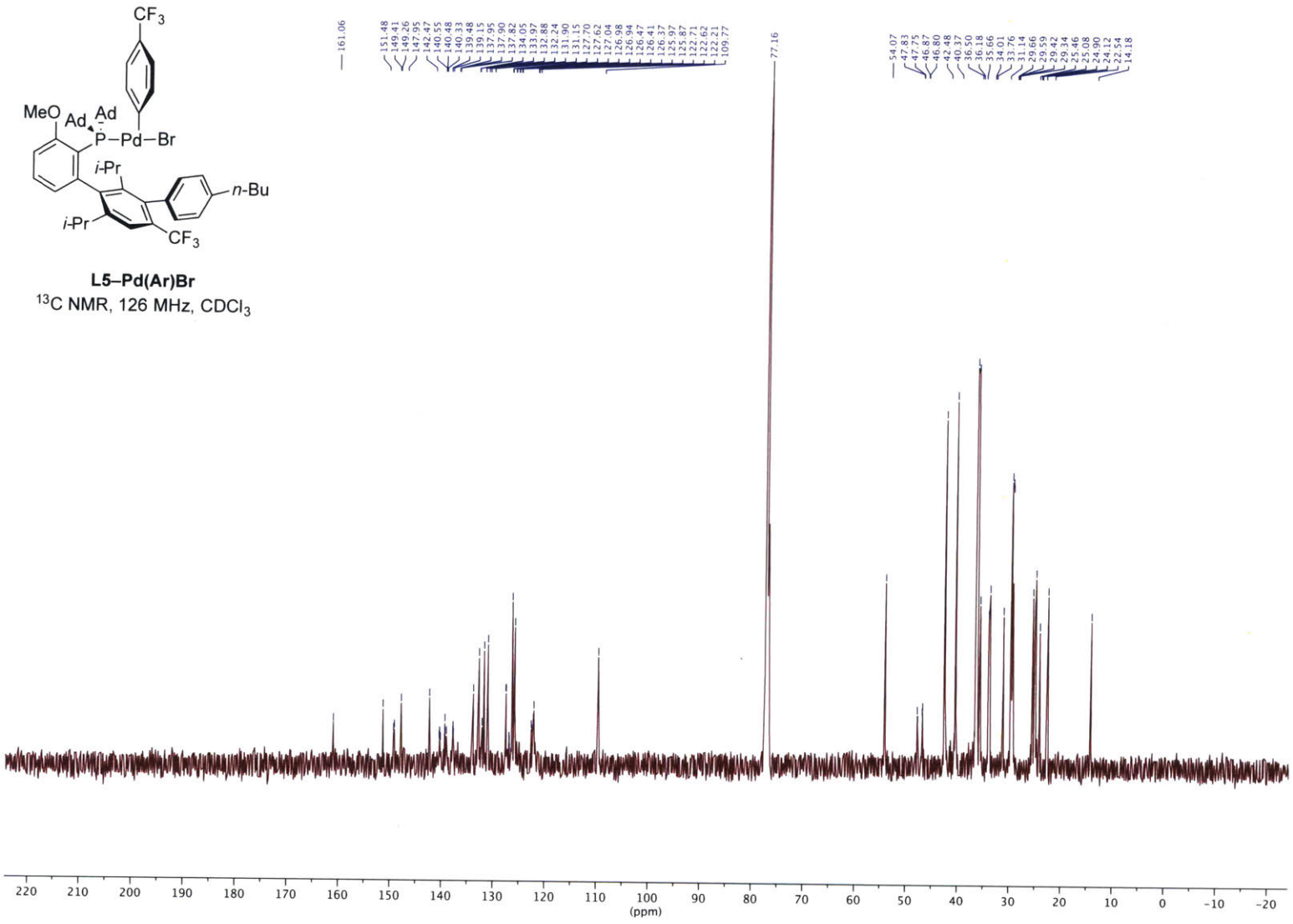

L5–Pd(Ar)Br

^{13}C NMR, 126 MHz, $CDCl_3$

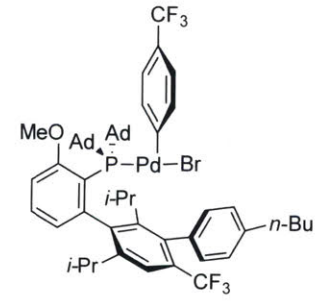

L5–Pd(Ar)Br

^{19}F NMR, 471 MHz, $CDCl_3$

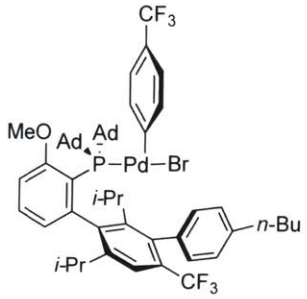

L5–Pd(Ar)Br

^{31}P NMR, 162 MHz, C_6D_6

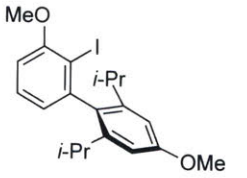

S18

^{1}H NMR, 600 MHz, $CDCl_3$

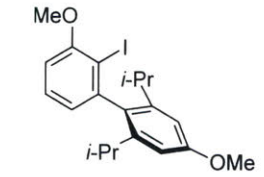

S18

^{13}C NMR, 151 MHz, $CDCl_3$

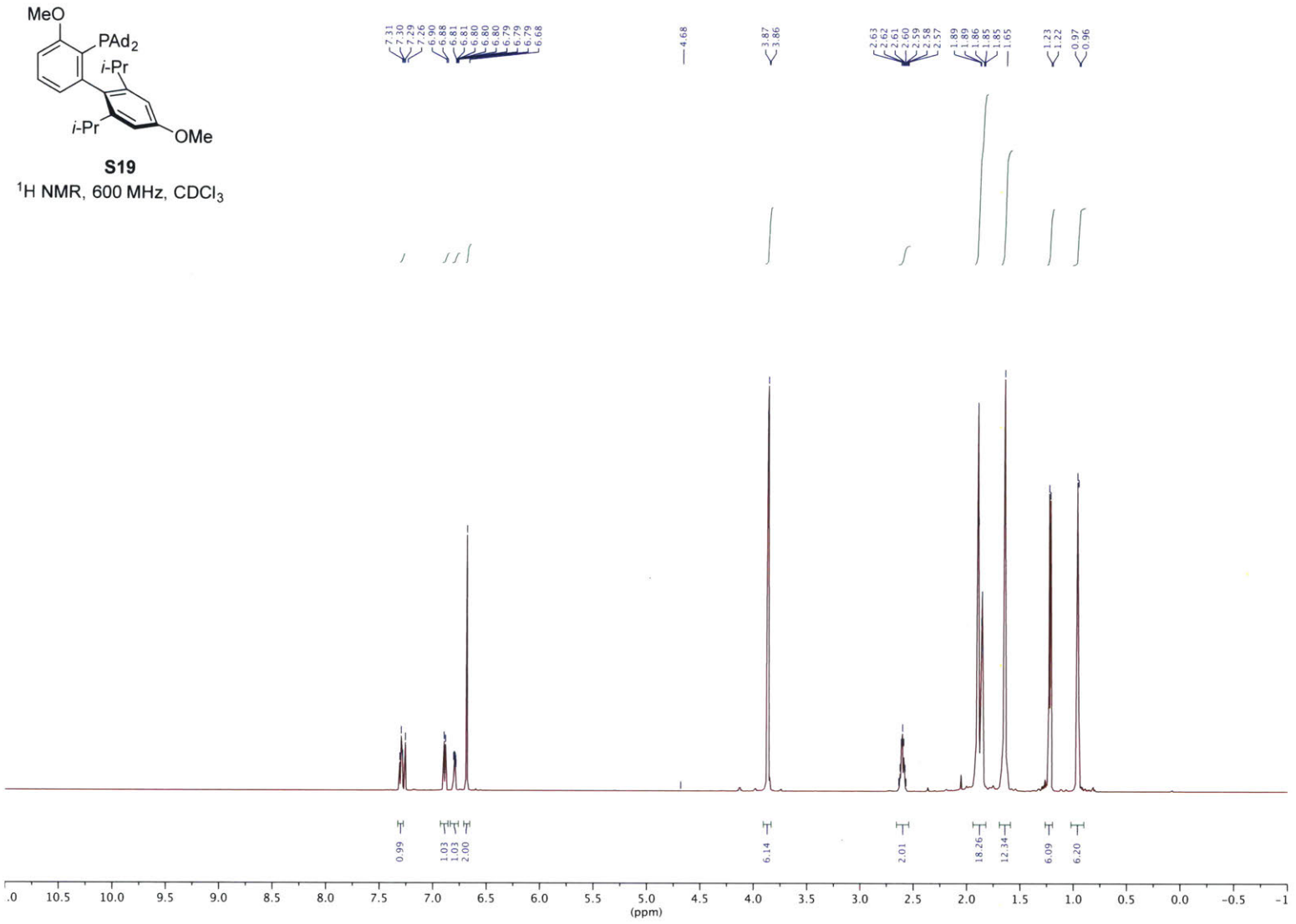

S19

^{1}H NMR, 600 MHz, $CDCl_3$

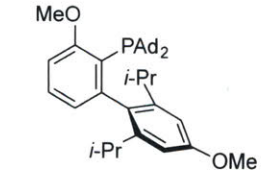

S19

^{13}C NMR, 151 MHz, $CDCl_3$

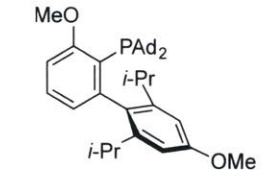

S19

^{31}P NMR, 203 MHz, $CDCl_3$

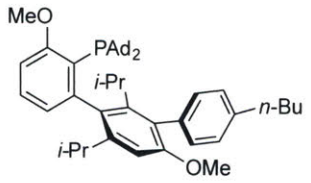

L6

^{1}H NMR, 500 MHz, $CDCl_3$

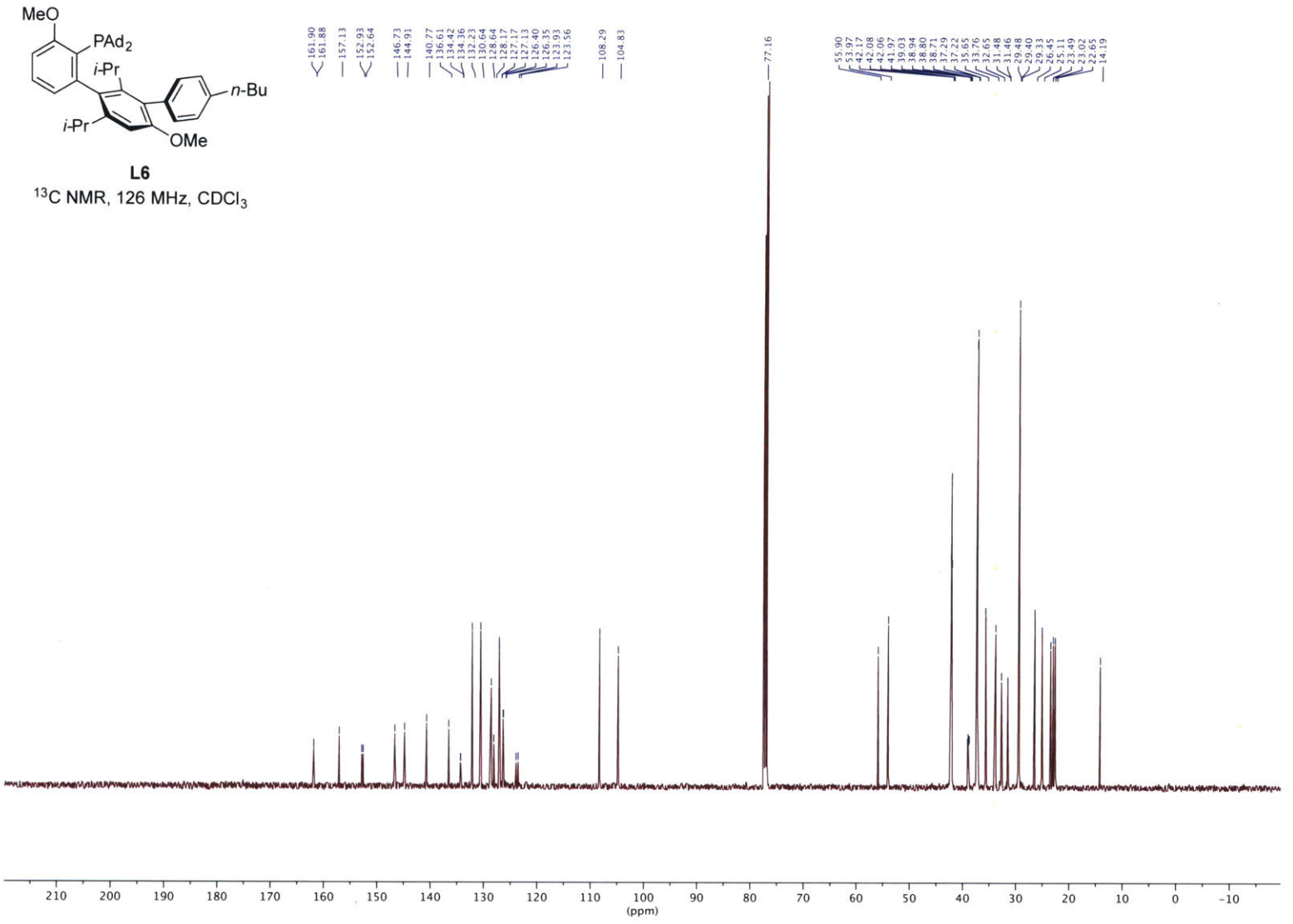

L6

^{13}C NMR, 126 MHz, $CDCl_3$

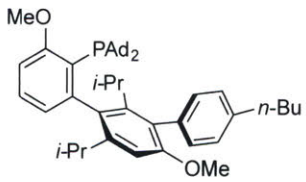

L6

^{31}P NMR, 162 MHz, $CDCl_3$

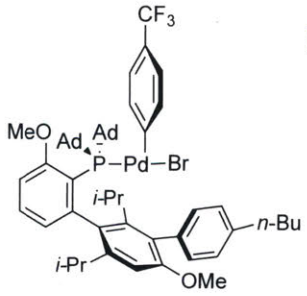

L6–Pd(Ar)Br

^{1}H NMR, 500 MHz, $CDCl_3$

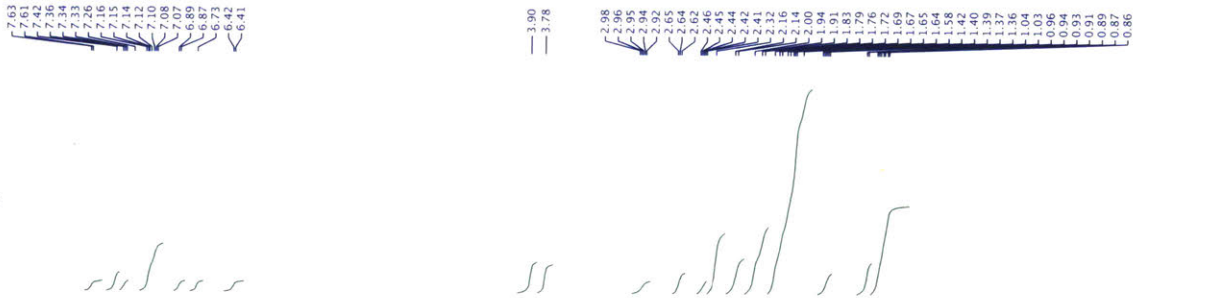

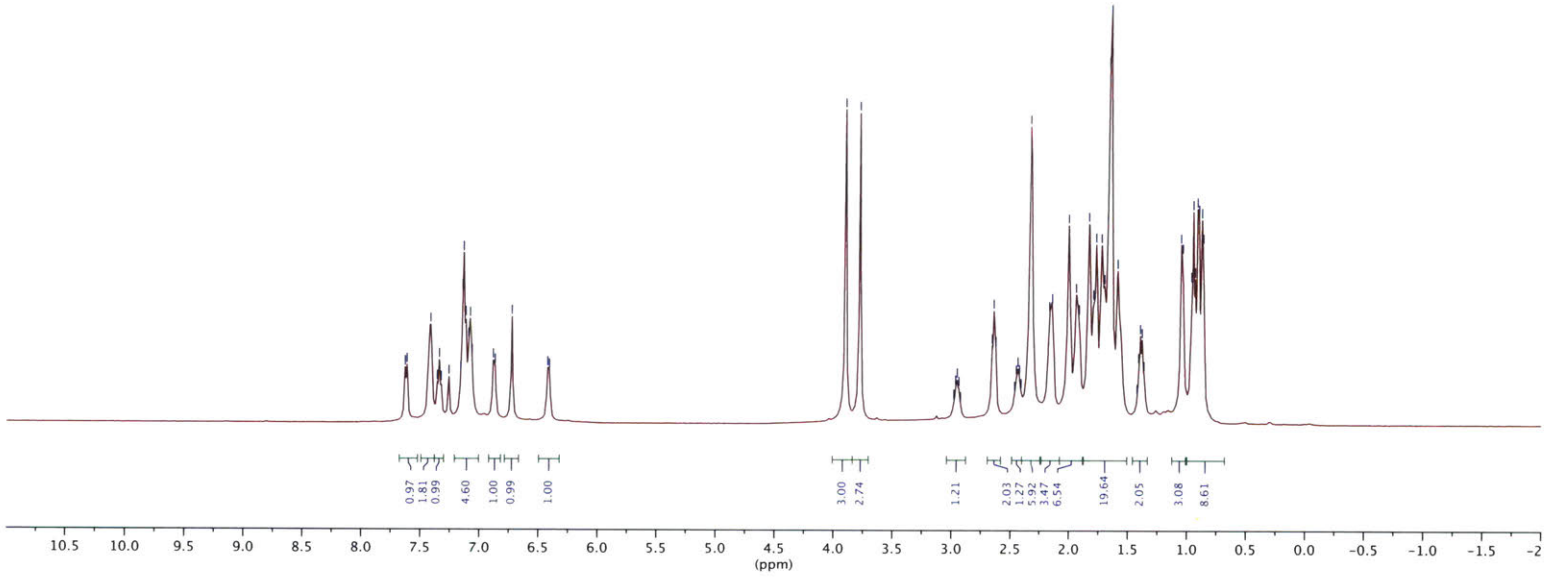

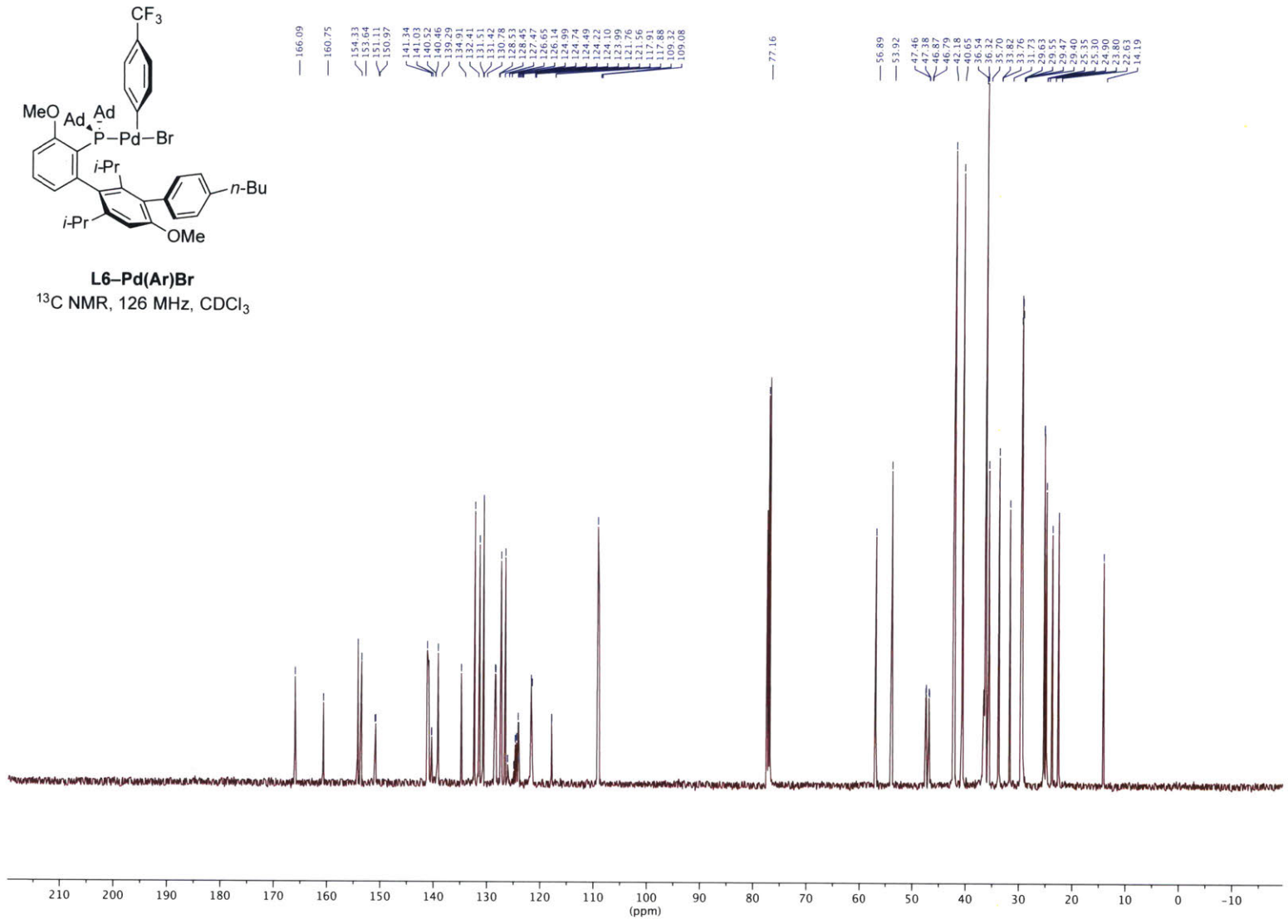

L6–Pd(Ar)Br

^{13}C NMR, 126 MHz, $CDCl_3$

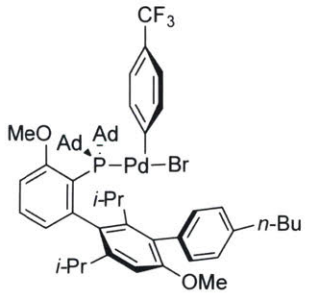

L6–Pd(Ar)Br

^{19}F NMR, 376 MHz, $CDCl_3$

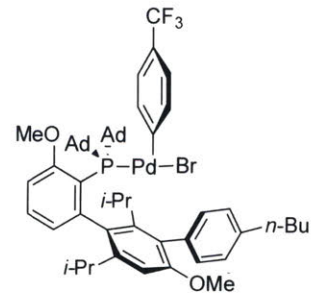

L6–Pd(Ar)Br

^{31}P NMR, 203 MHz, C_6D_6

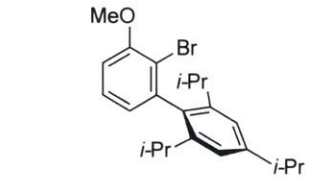

S20

^{1}H NMR, 500 MHz, $CDCl_3$

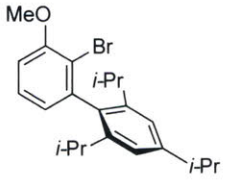

S20

^{13}C NMR, 126 MHz, $CDCl_3$

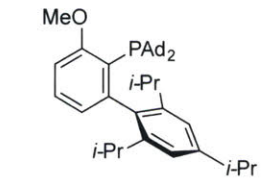

S21

^{1}H NMR, 400 MHz, $CDCl_3$

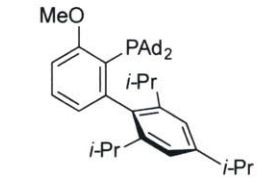

S21

^{13}C NMR, 126 MHz, $CDCl_3$

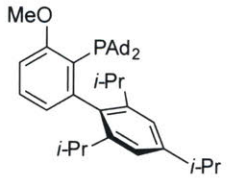

S21

^{31}P NMR, 203 MHz, $CDCl_3$

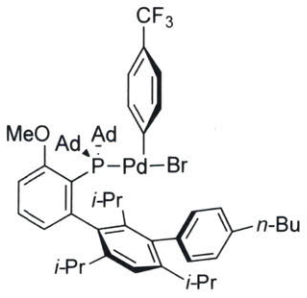

L7–Pd(Ar)Br

^{1}H NMR, 500 MHz, $CDCl_3$

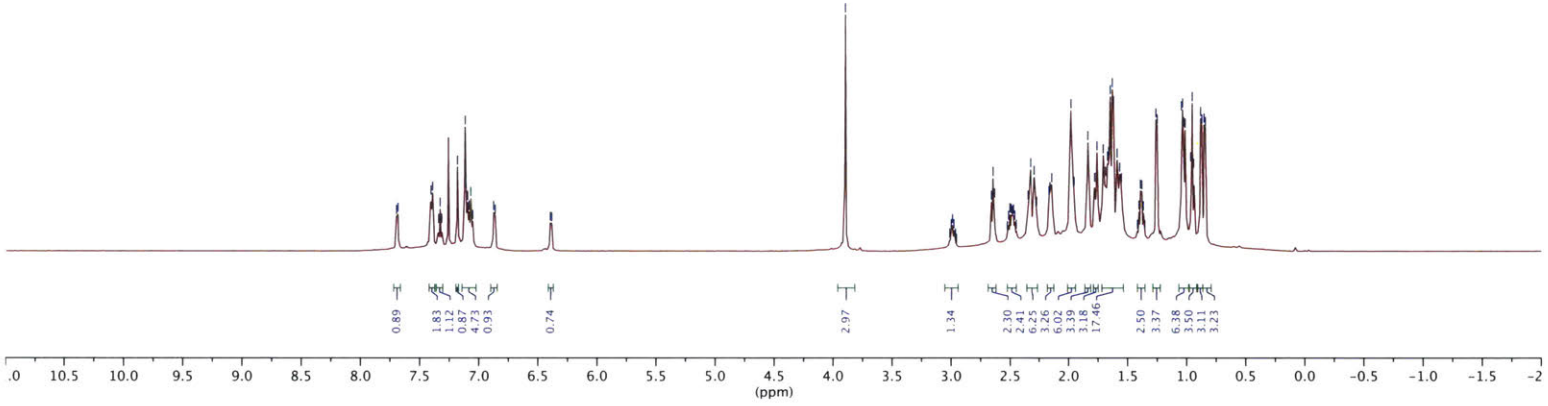

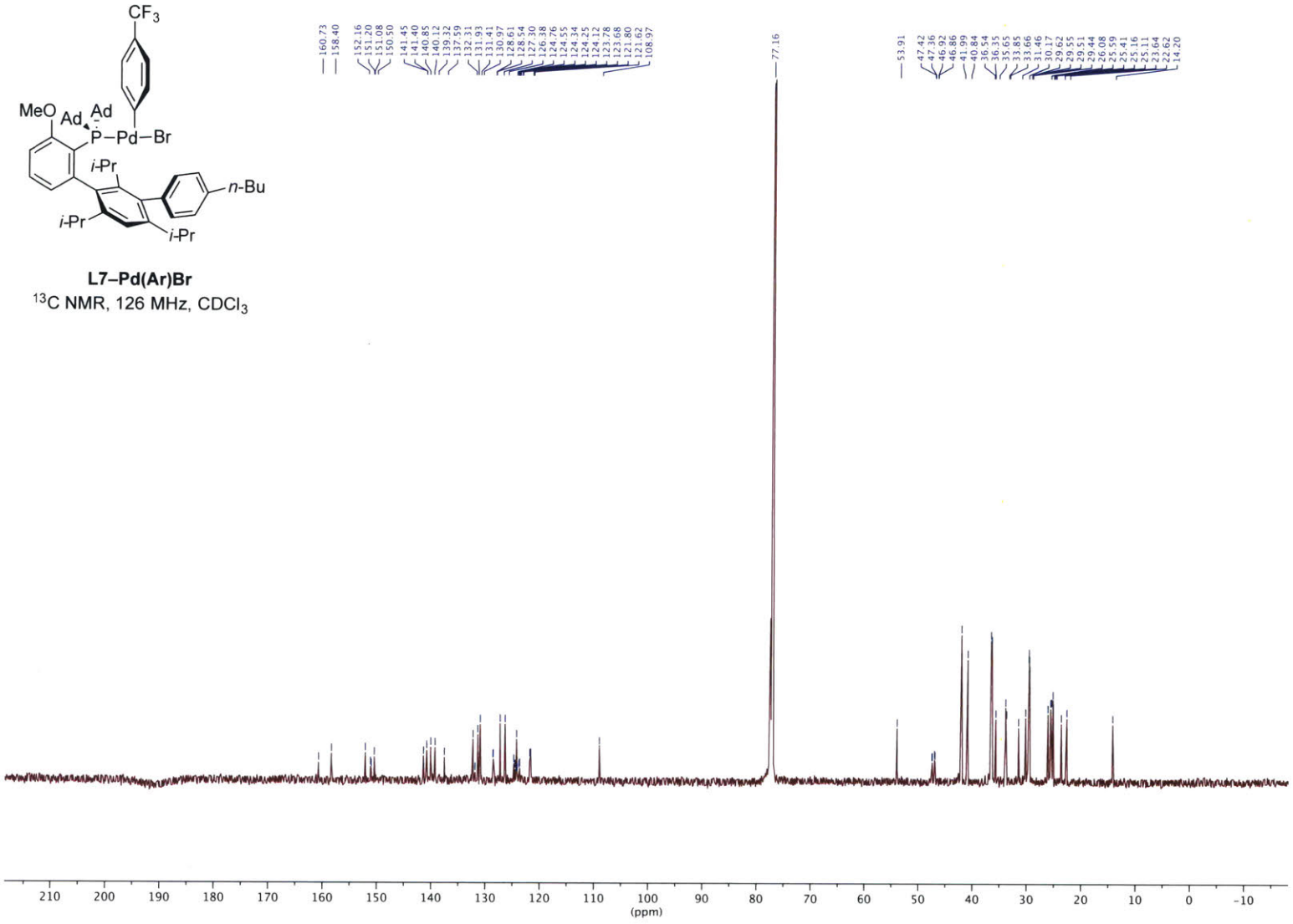

L7–Pd(Ar)Br

^{13}C NMR, 126 MHz, $CDCl_3$

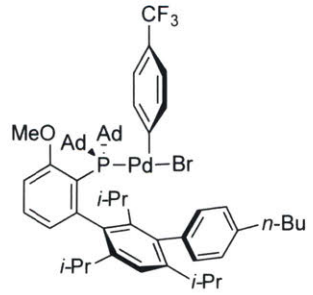

L7–Pd(Ar)Br

^{19}F NMR, 565 MHz, $CDCl_3$

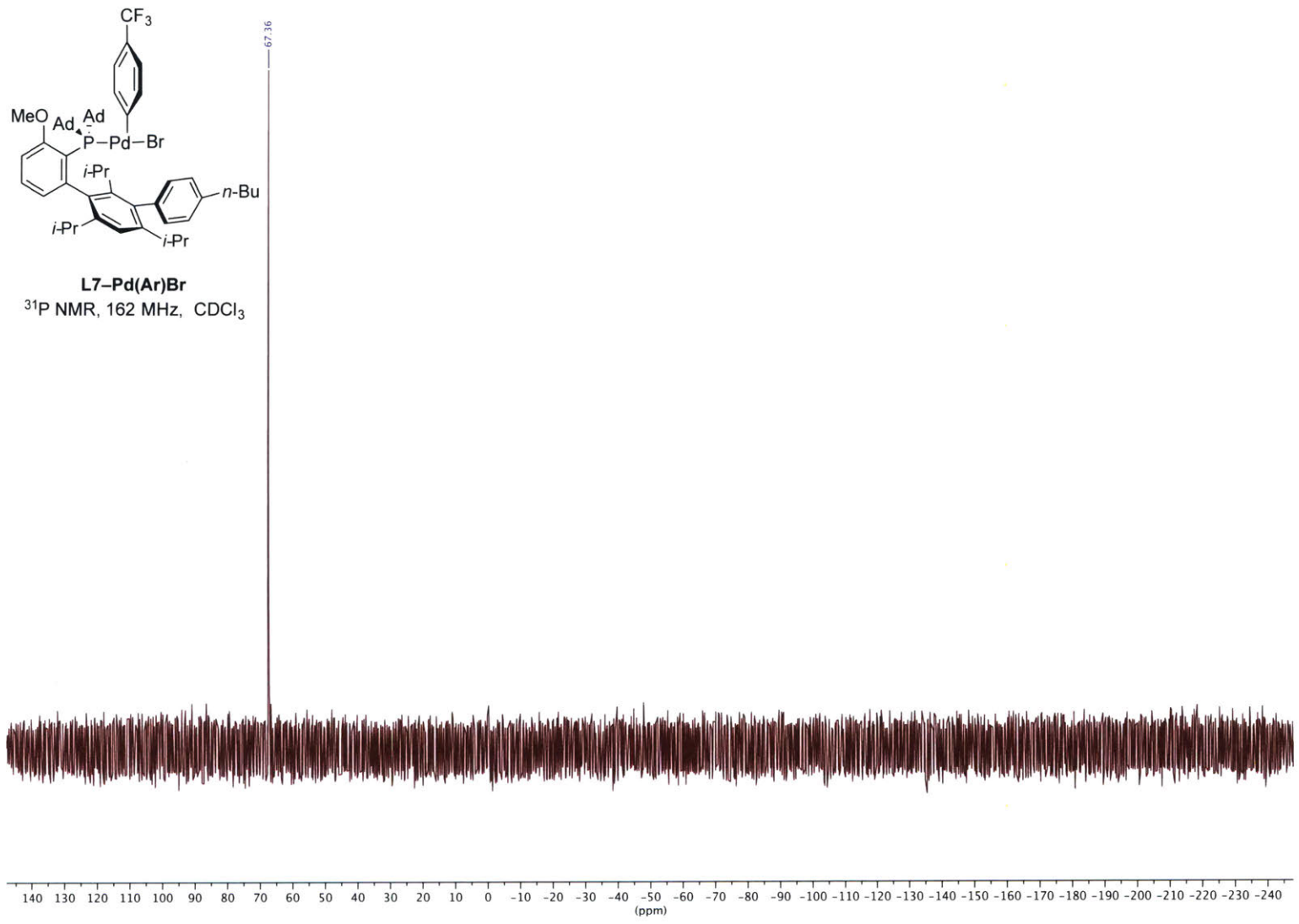

L7–Pd(Ar)Br

^{31}P NMR, 162 MHz, $CDCl_3$

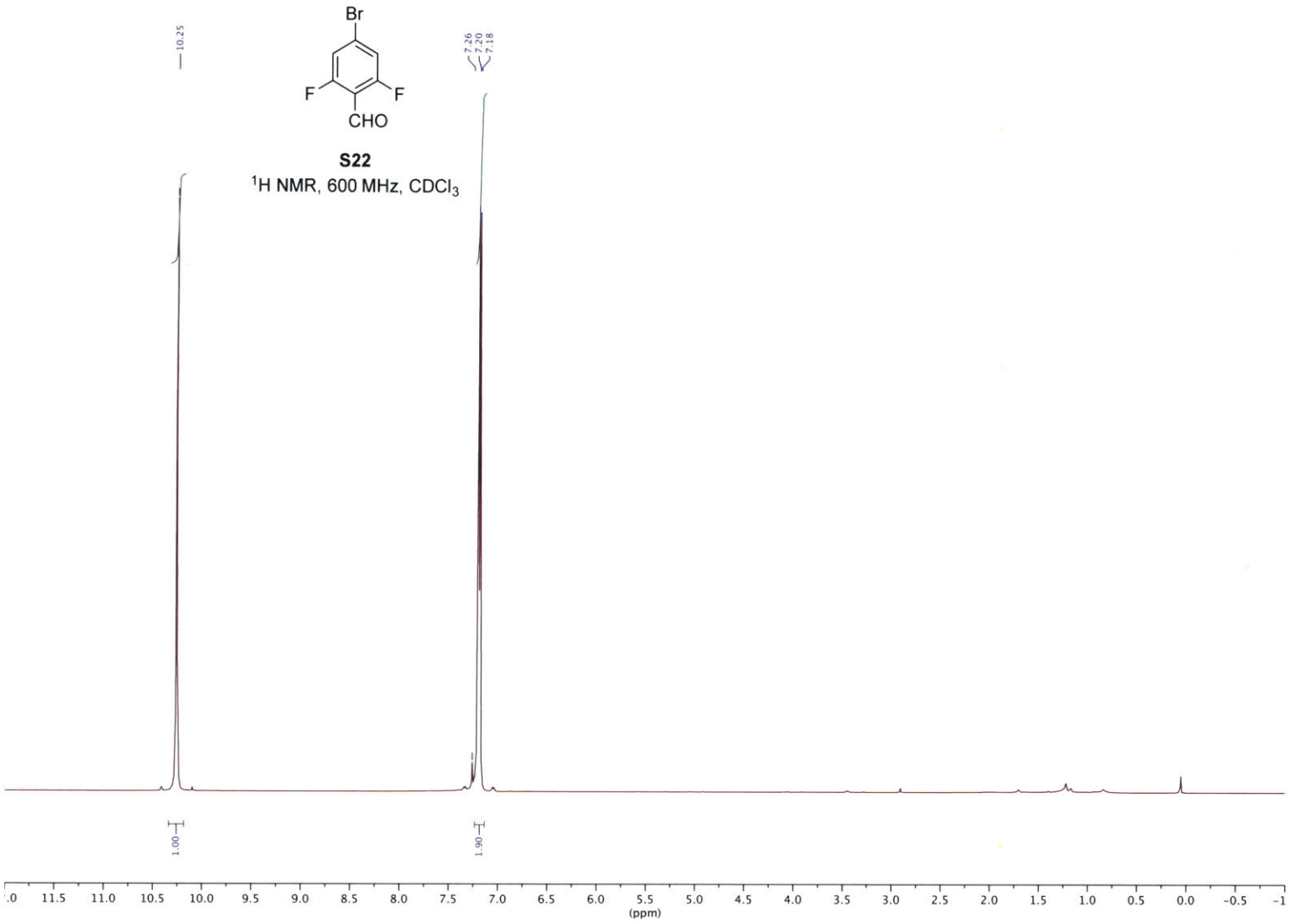

S22

^{1}H NMR, 600 MHz, $CDCl_3$

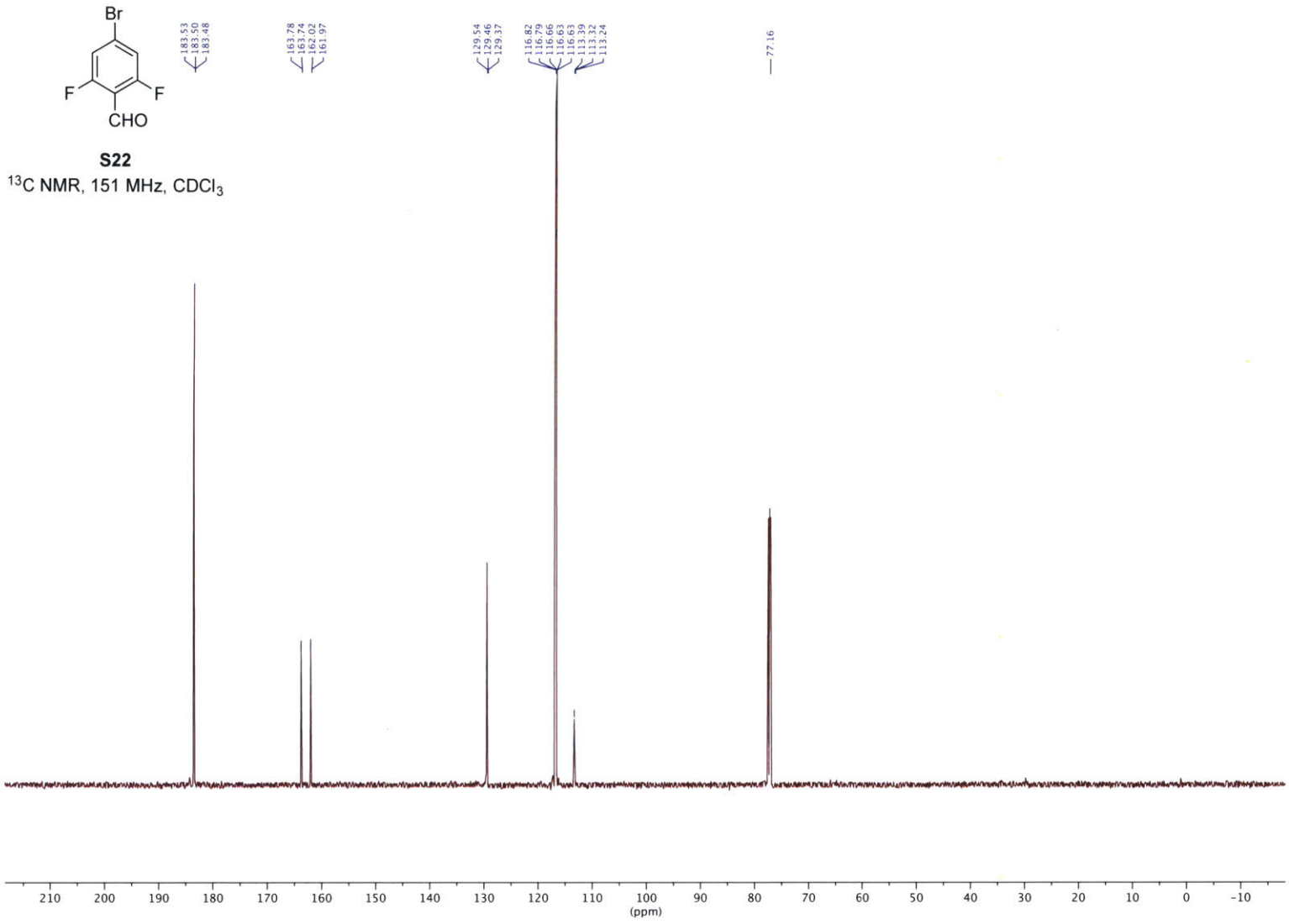

S22

^{13}C NMR, 151 MHz, $CDCl_3$

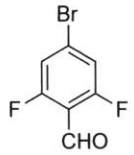

S22

^{19}F NMR, 565 MHz, $CDCl_3$

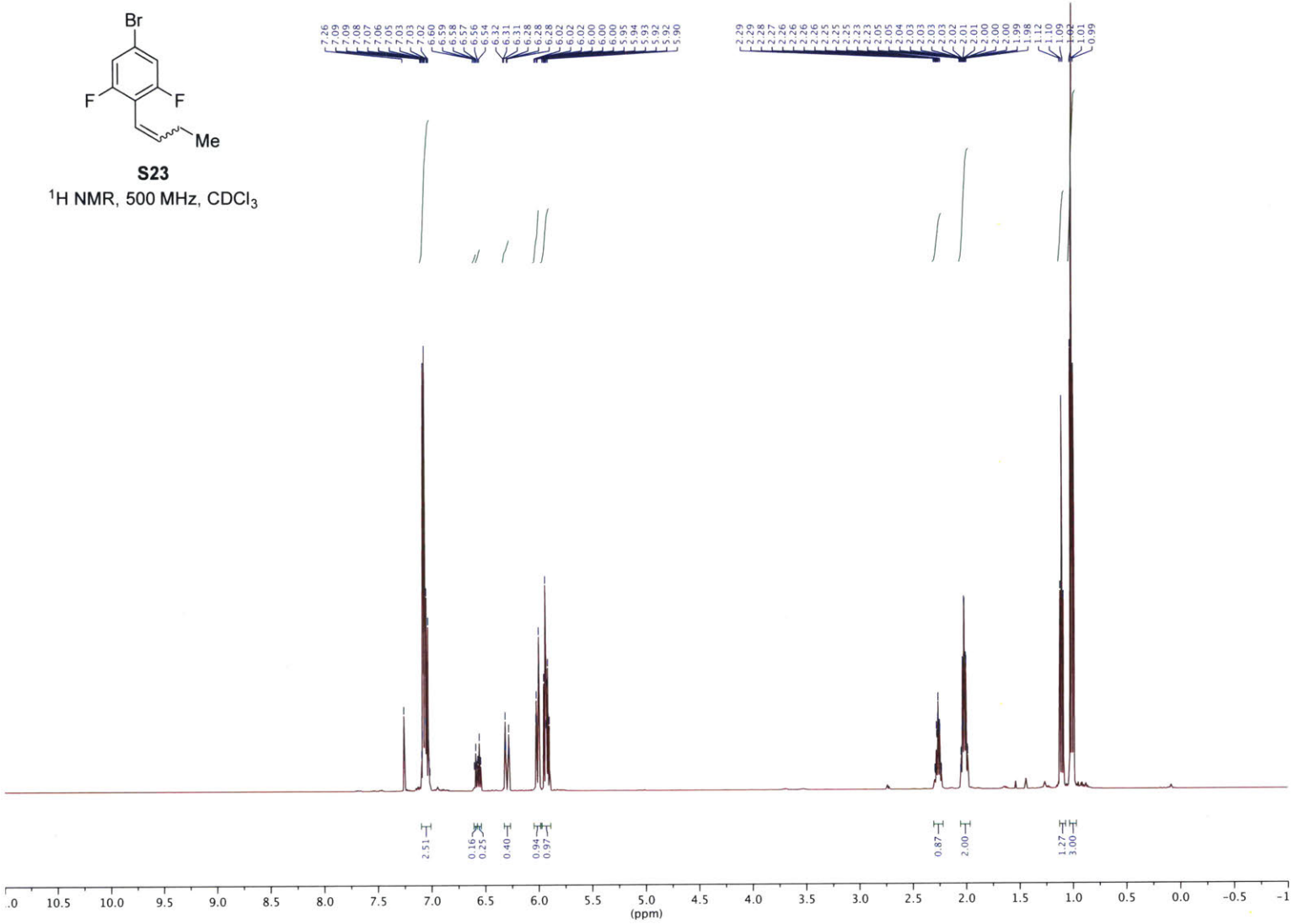
Br
F
F
Me
S23
1H NMR, 500 MHz, CDCl3
(ppm)

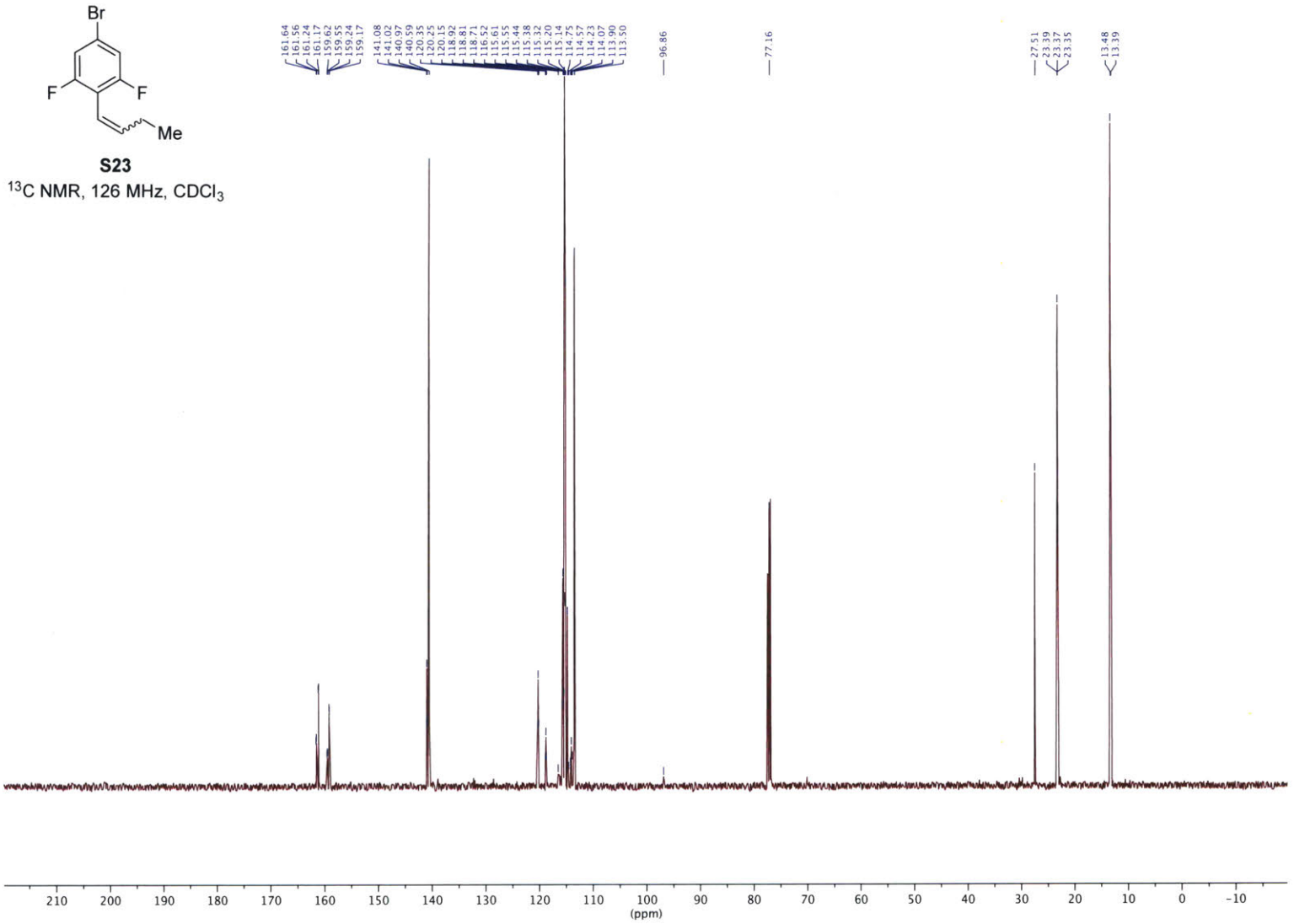
Br
F
F
Me
S23
^{13}C NMR, 126 MHz, $CDCl_3$
161.64
161.56
161.24
161.17
159.62
159.55
159.24
159.17
141.08
141.02
140.97
140.59
120.35
120.25
120.15
118.82
118.81
118.71
116.52
115.61
115.55
115.44
115.38
115.32
115.20
115.14
114.75
114.57
114.23
114.07
113.90
113.50
96.86
77.16
27.51
23.39
23.37
23.35
13.48
13.39
210 200 190 180 170 160 150 140 130 120 110 100 90 80 70 60 50 40 30 20 10 0 -10
(ppm)

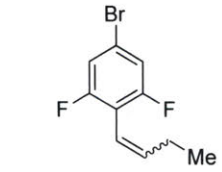

S23

^{19}F NMR, 471 MHz, $CDCl_3$

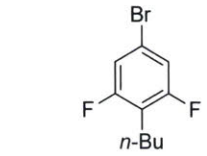

S24

^{1}H NMR, 600 MHz, $CDCl_3$

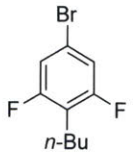

S24

^{13}C NMR, 151 MHz, $CDCl_3$

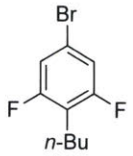

S24

^{19}F NMR, 565 MHz, $CDCl_3$

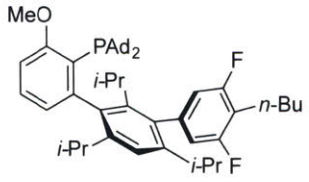

L8

^{1}H NMR, 600 MHz, $CDCl_3$

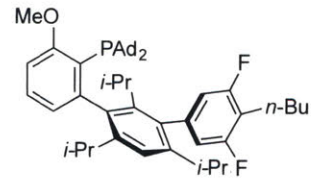

L8

^{13}C NMR, 151 MHz, $CDCl_3$

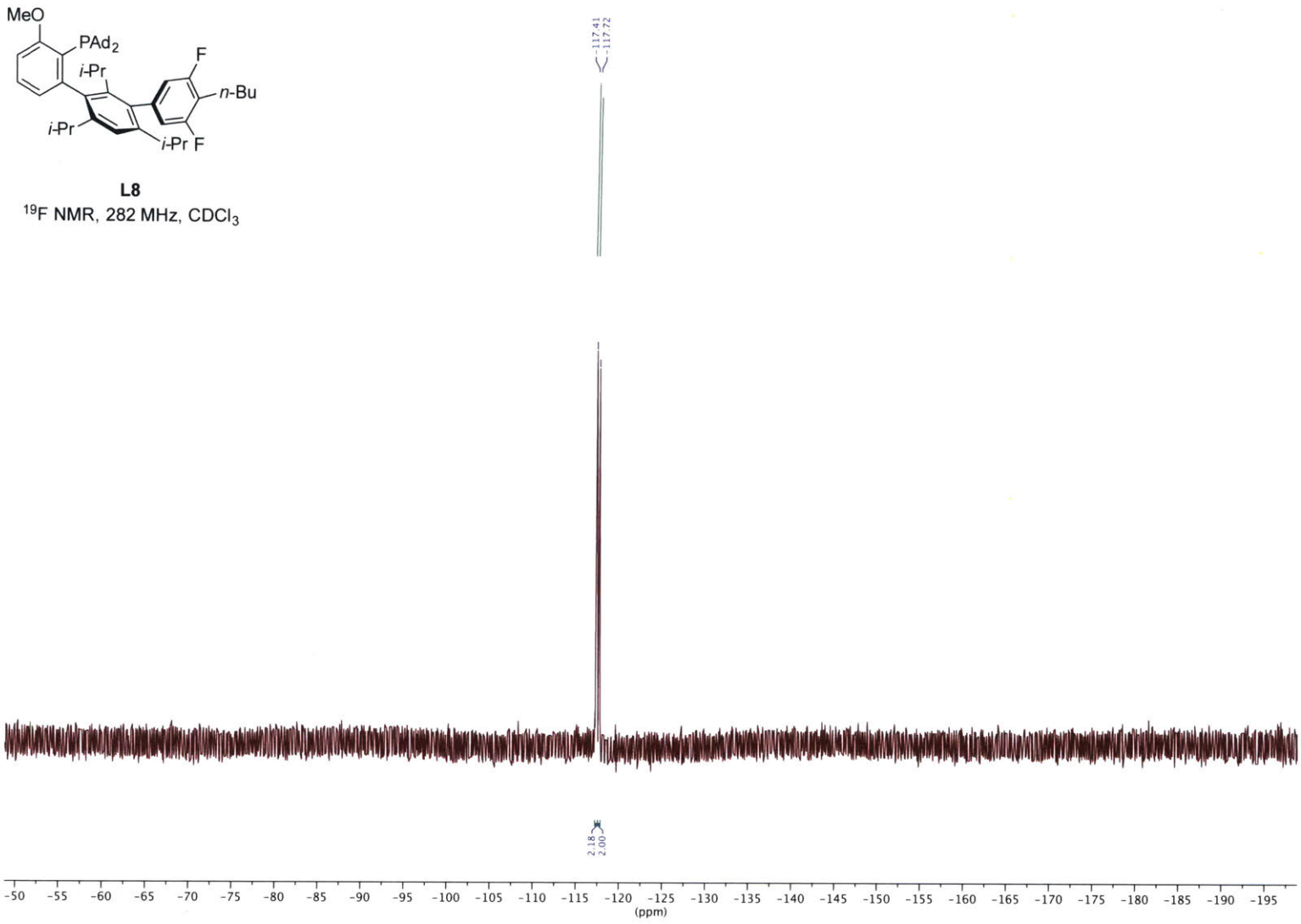
MeO
PAd2
i-Pr
F
n-Bu
i-Pr
i-Pr F
L8
19F NMR, 282 MHz, CDCl3
-117.41
-117.72
2.18
2.00
-50 -55 -60 -65 -70 -75 -80 -85 -90 -95 -100 -105 -110 -115 -120 -125 -130 -135 -140 -145 -150 -155 -160 -165 -170 -175 -180 -185 -190 -195
(ppm)

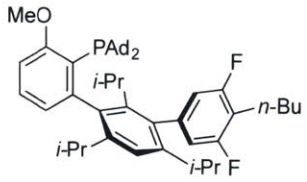

L8

^{31}P NMR, 121 MHz, $CDCl_3$

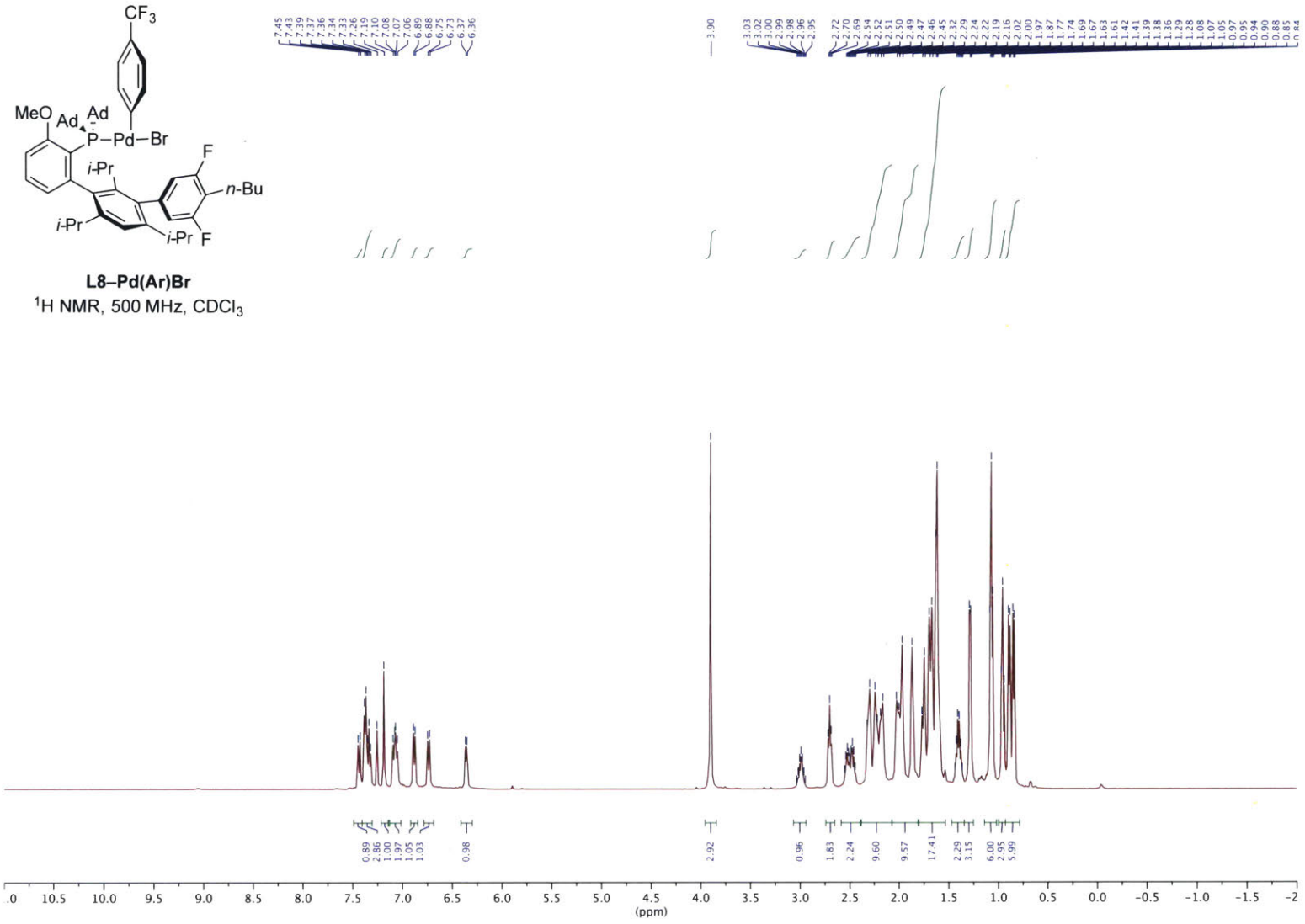

L8–Pd(Ar)Br

^{1}H NMR, 500 MHz, $CDCl_3$

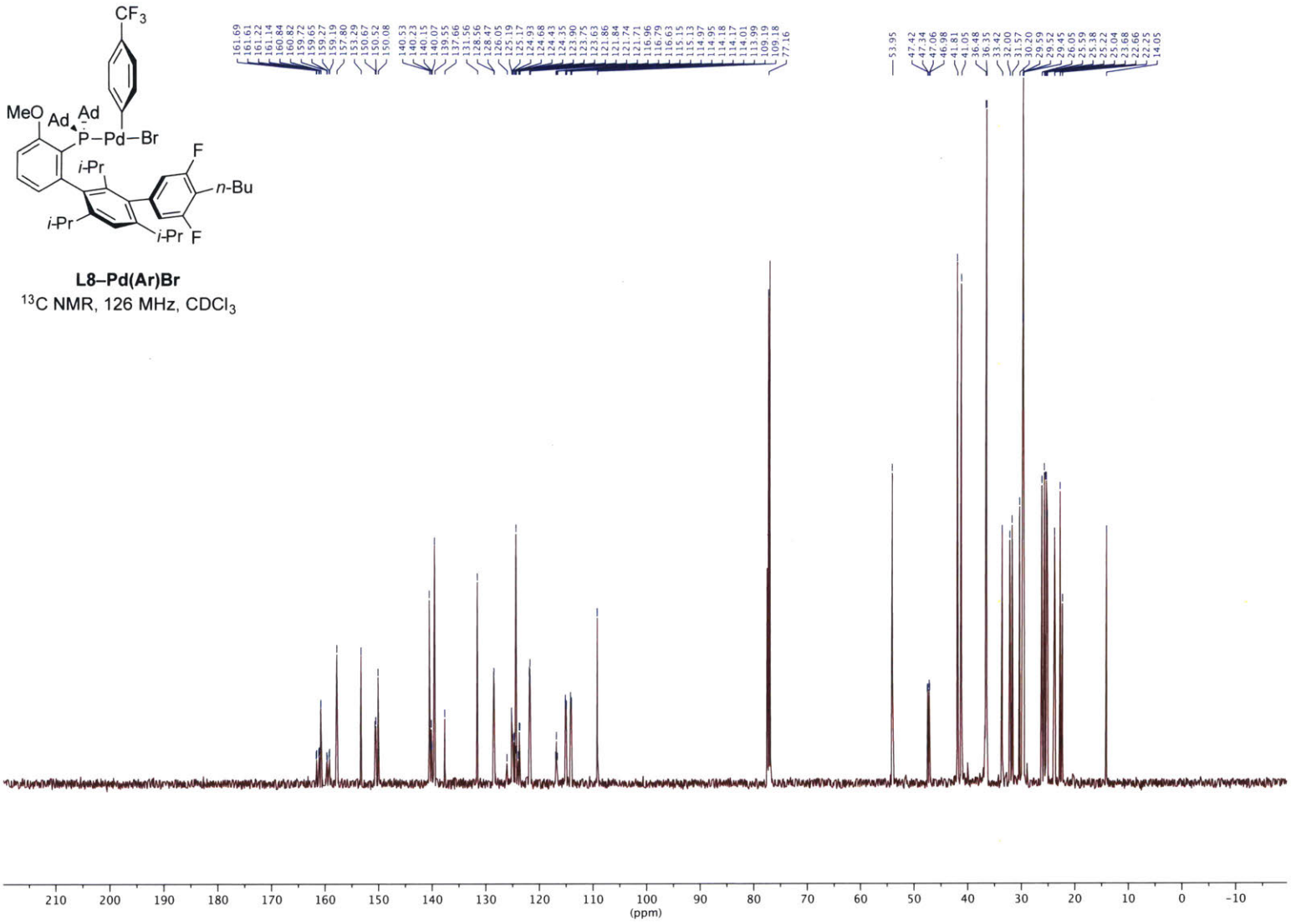
CF3
MeO
Ad
Ad
P–Pd–Br
i-Pr
i-Pr
i-Pr
F
F
n-Bu
L8–Pd(Ar)Br
13C NMR, 126 MHz, CDCl3
161.69
161.61
161.22
161.14
160.84
160.82
159.72
159.65
159.27
159.19
157.80
153.29
150.67
150.52
150.08
140.53
140.23
140.15
140.07
139.55
137.66
131.56
128.56
128.47
126.05
125.19
125.17
124.93
124.68
124.43
124.35
123.90
123.75
123.63
121.86
121.84
121.74
121.71
116.96
116.79
116.63
115.15
115.13
114.97
114.95
114.18
114.17
114.01
113.99
109.19
109.18
77.16
53.95
47.42
47.34
47.06
46.98
41.81
41.05
36.48
36.35
33.42
32.00
31.57
30.20
29.59
29.52
29.45
26.05
25.59
25.38
25.22
25.04
23.68
22.66
22.25
14.05
210
200
190
180
170
160
150
140
130
120
110
100
90
80
70
60
50
40
30
20
10
0
-10
(ppm)

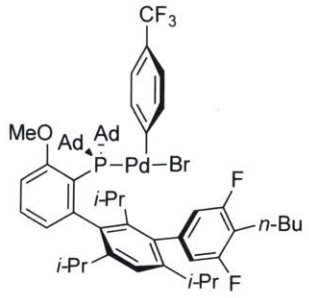

L8–Pd(Ar)Br

^{19}F NMR, 471 MHz, $CDCl_3$

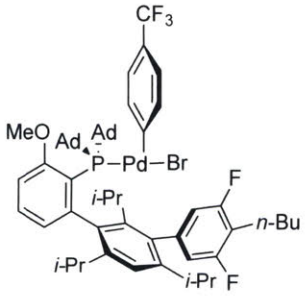

L8–Pd(Ar)Br
^{31}P NMR, 203 MHz, $CDCl_3$

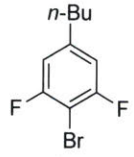

S25

^{1}H NMR, 600 MHz, $CDCl_3$

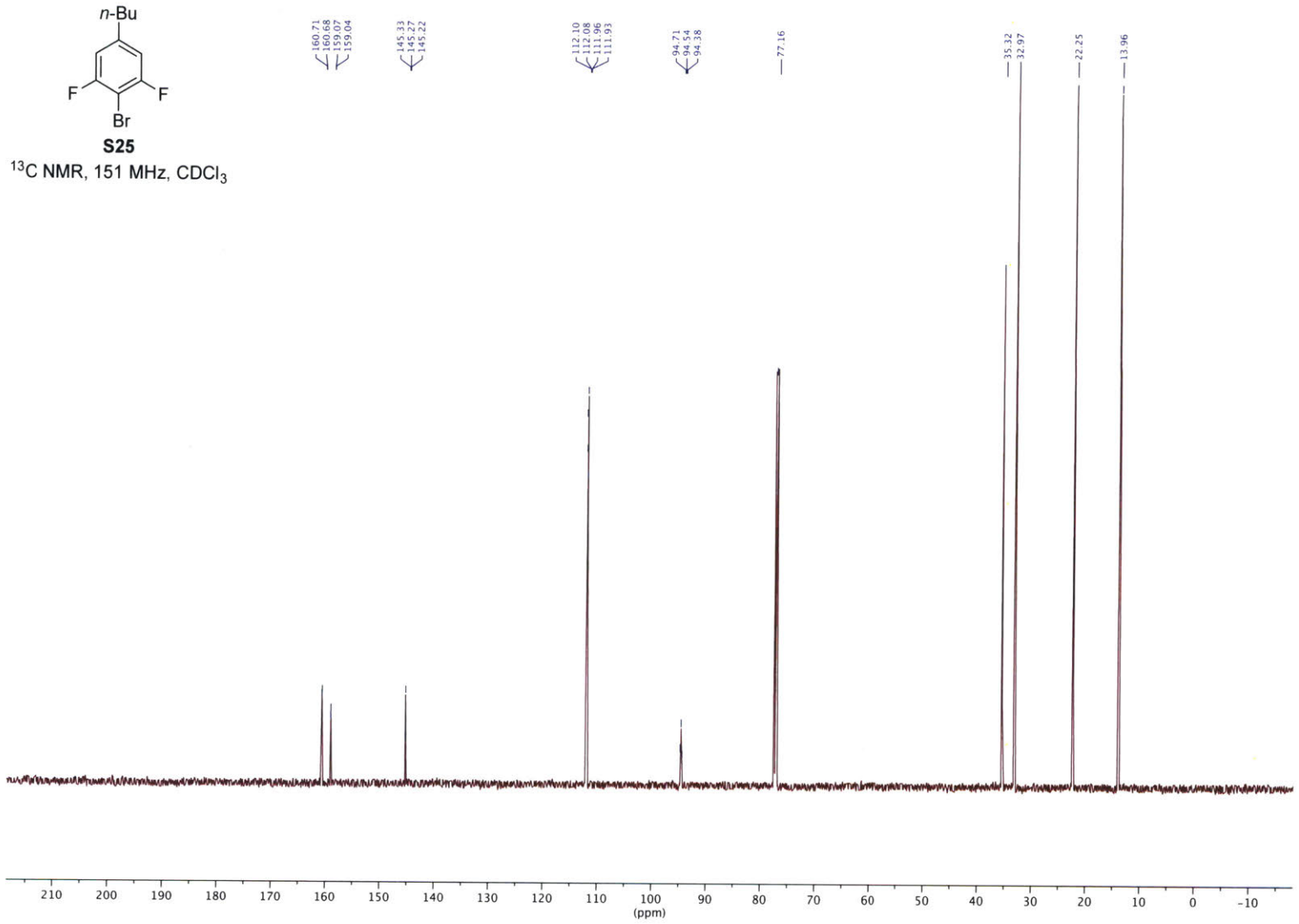
n-Bu
F
F
Br
S25
13C NMR, 151 MHz, CDCl3
160.71
160.68
159.07
159.04
145.33
145.27
145.22
112.10
112.08
111.96
111.93
94.71
94.54
94.38
77.16
35.32
32.97
22.25
13.96
210
200
190
180
170
160
150
140
130
120
110
100
90
80
70
60
50
40
30
20
10
0
-10
(ppm)

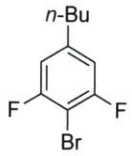

S25

^{19}F NMR, 565 MHz, $CDCl_3$

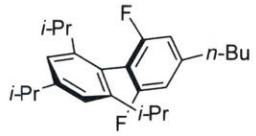

S26

^{1}H NMR, 600 MHz, $CDCl_3$

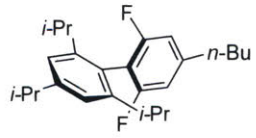

S26

^{13}C NMR, 151 MHz, $CDCl_3$

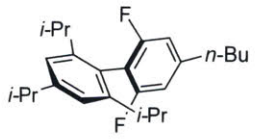

S26

^{19}F NMR, 565 MHz, $CDCl_3$

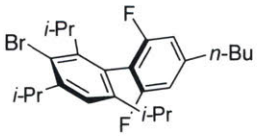

S27

^{1}H NMR, 600 MHz, $CDCl_3$

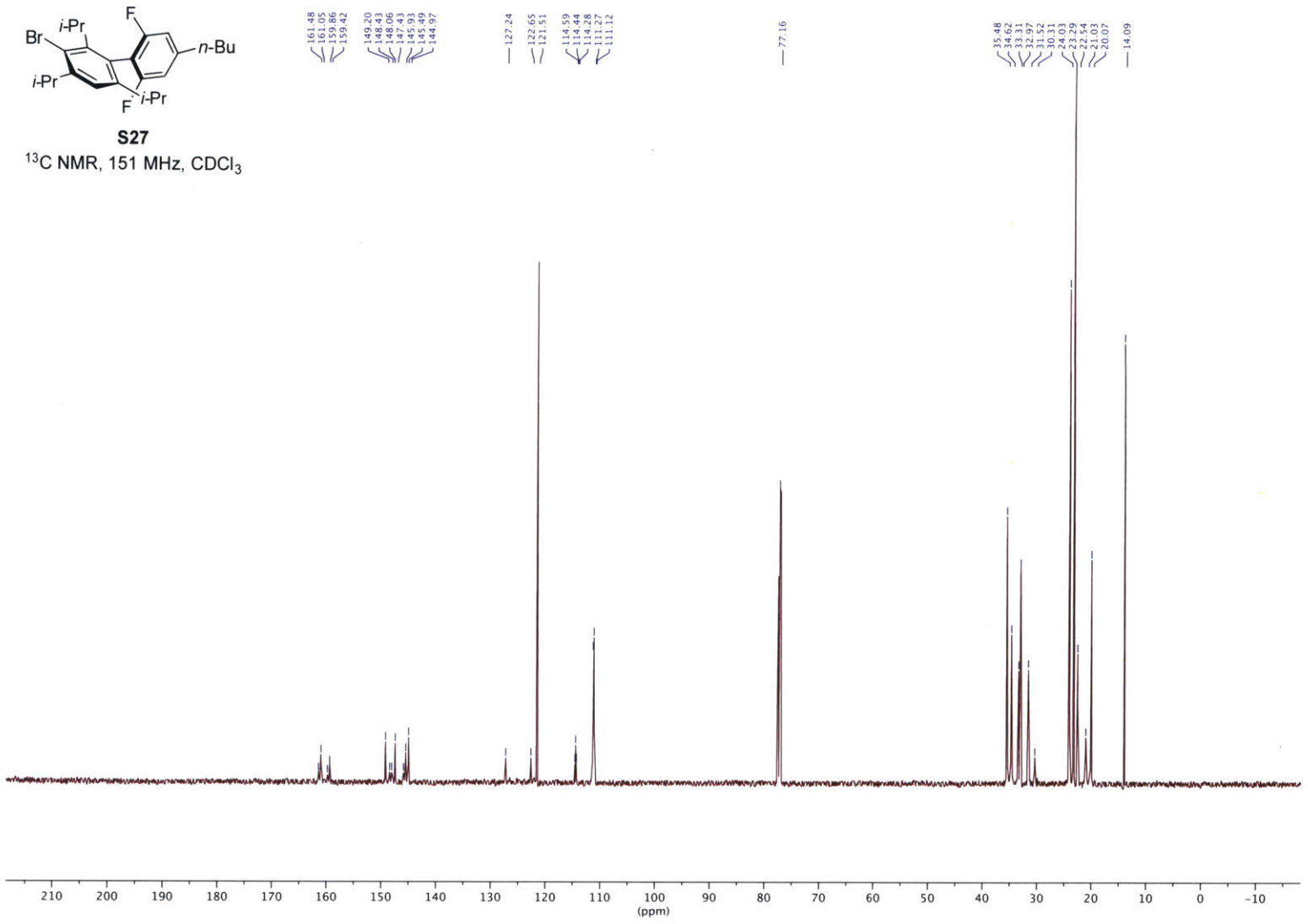

S27

^{13}C NMR, 151 MHz, $CDCl_3$

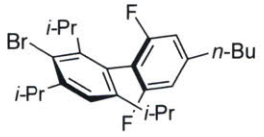

S27

^{19}F NMR, 565 MHz, $CDCl_3$

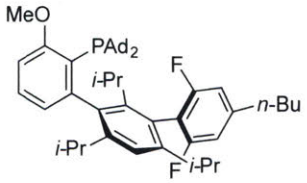

L9

^{1}H NMR, 600 MHz, $CDCl_3$

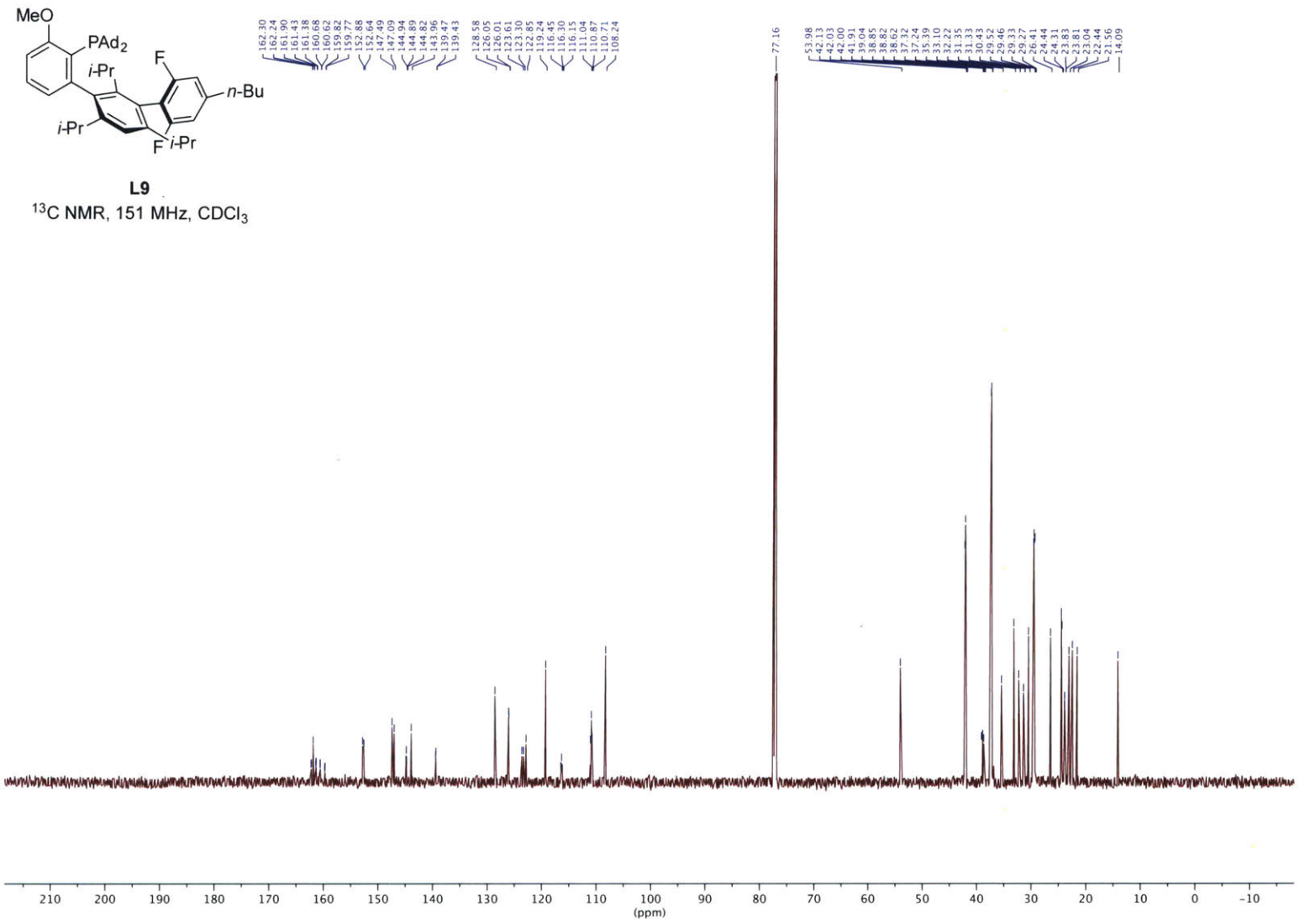
MeO
PAd2
i-Pr
F
n-Bu
i-Pr
F
i-Pr
L9
13C NMR, 151 MHz, CDCl3
77.16
(ppm)

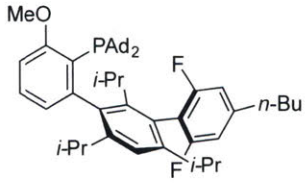

L9

^{19}F NMR, 565 MHz, $CDCl_3$

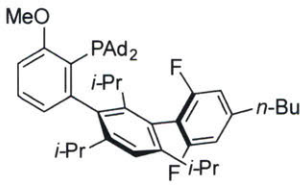

L9

^{31}P NMR, 162 MHz, $CDCl_3$

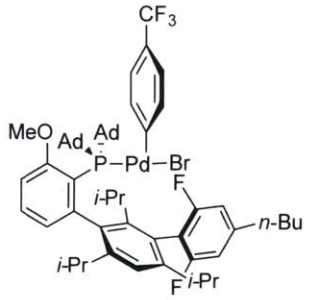

L9–Pd(Ar)Br

^{1}H NMR, 500 MHz, $CDCl_3$

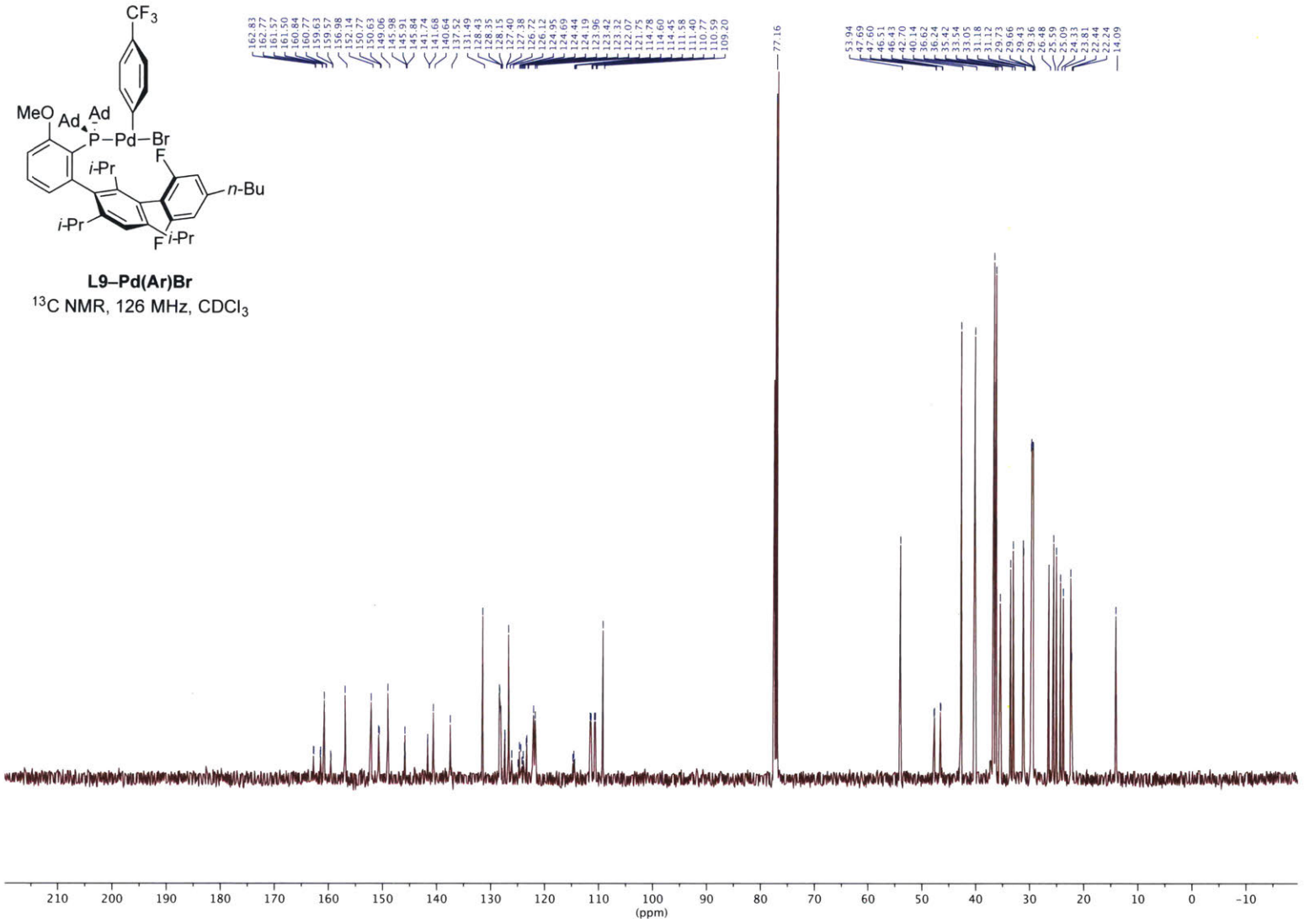
CF3
MeO
Ad
Ad
P–Pd–Br
F
i-Pr
n-Bu
i-Pr
F
i-Pr
L9–Pd(Ar)Br
13C NMR, 126 MHz, CDCl3
77.16
210
200
190
180
170
160
150
140
130
120
110
100
90
80
70
60
50
40
30
20
10
0
-10
(ppm)

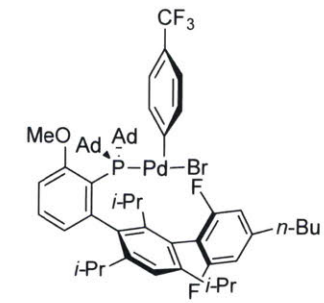

L9–Pd(Ar)Br

^{19}F NMR, 471 MHz, $CDCl_3$

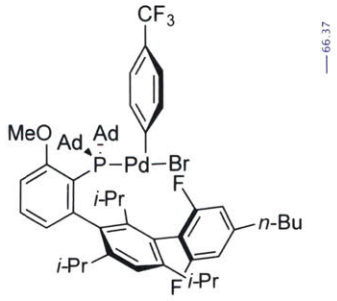

L9–Pd(Ar)Br

^{31}P NMR, 162 MHz, $CDCl_3$

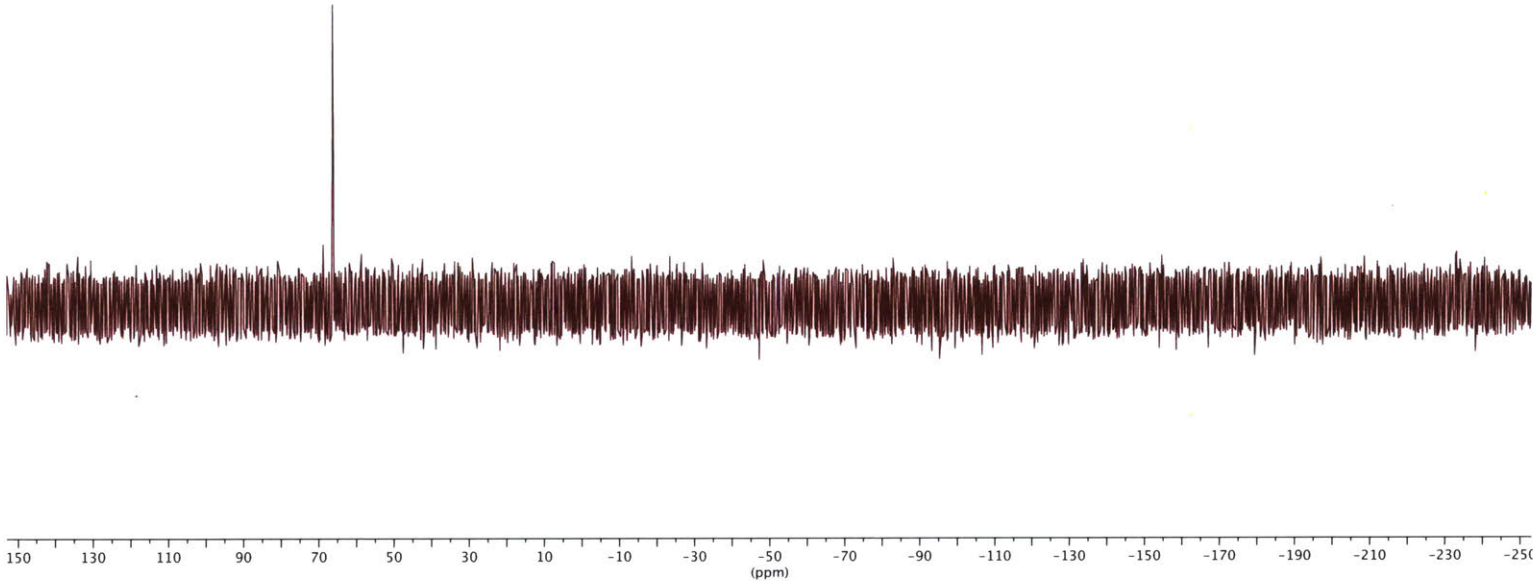

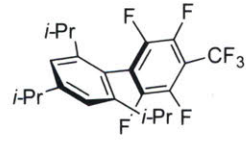

S28

^{1}H NMR, 600 MHz, $CDCl_3$

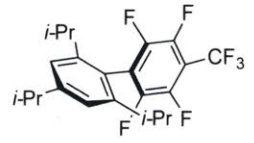

S28

^{13}C NMR, 151 MHz, $CDCl_3$

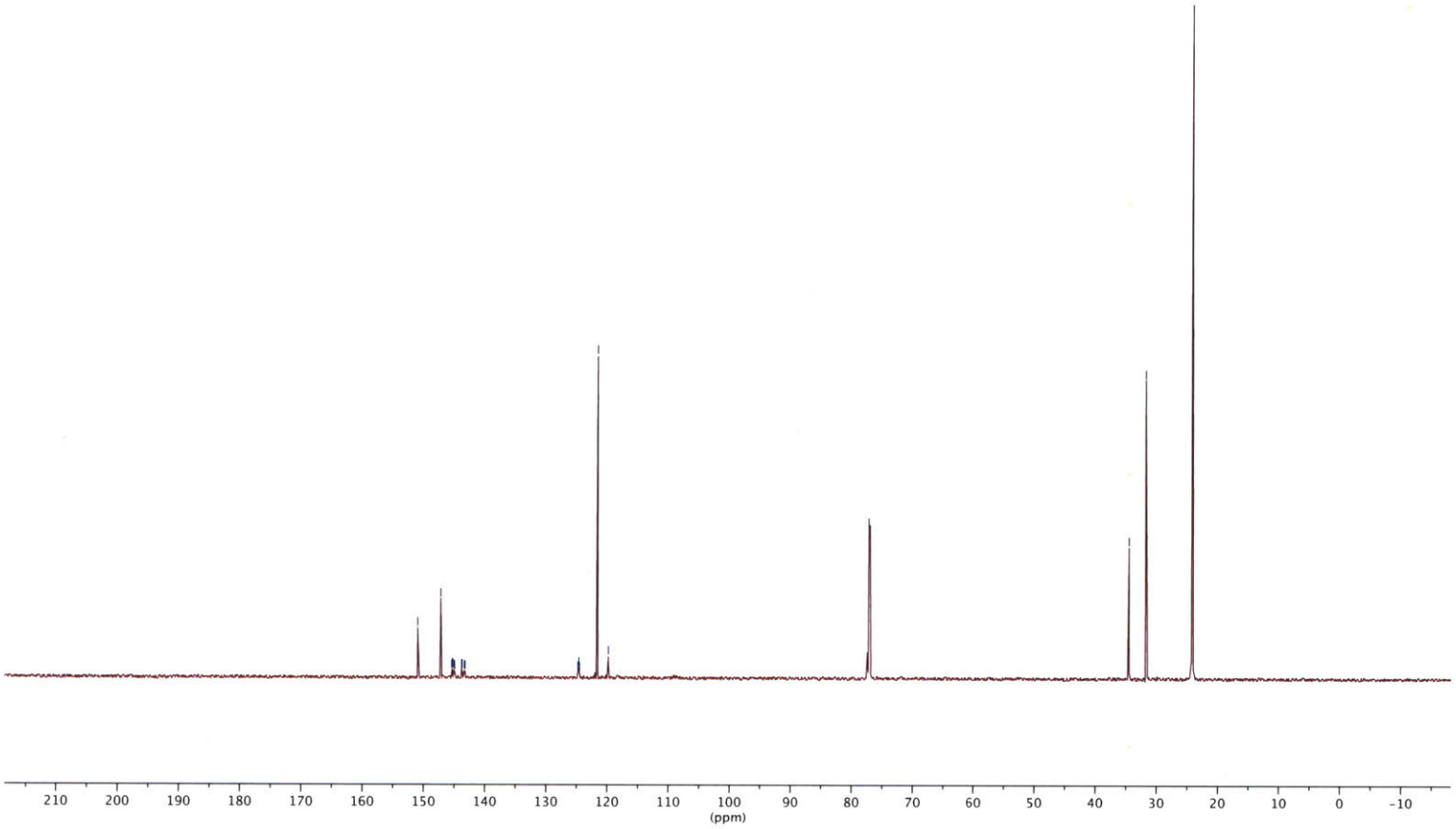

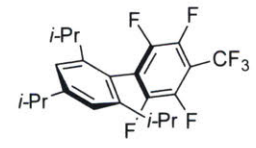

S28

^{19}F NMR, 565 MHz, $CDCl_3$

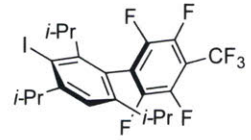

S29

^{1}H NMR, 600 MHz, $CDCl_3$

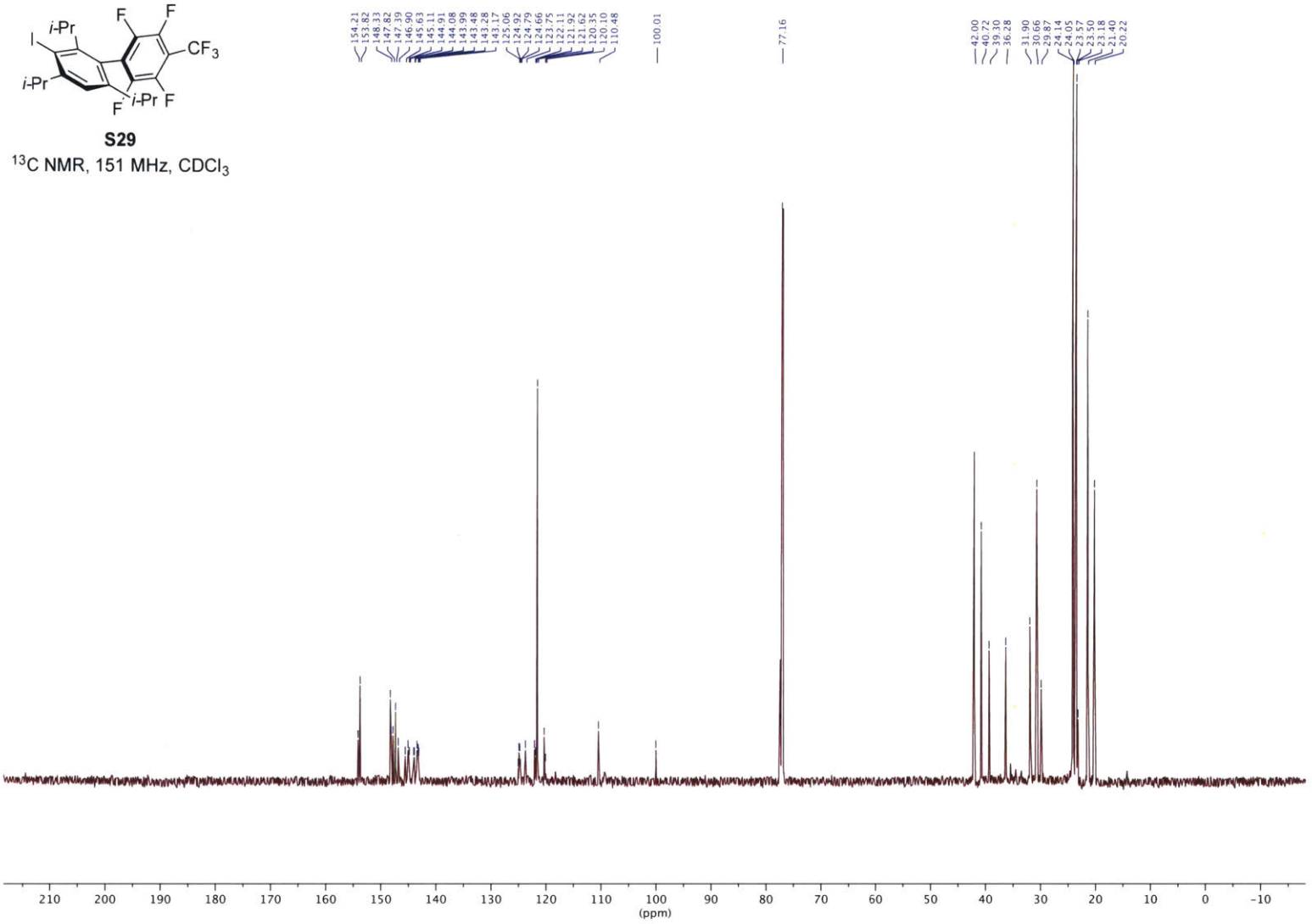

S29

^{13}C NMR, 151 MHz, $CDCl_3$

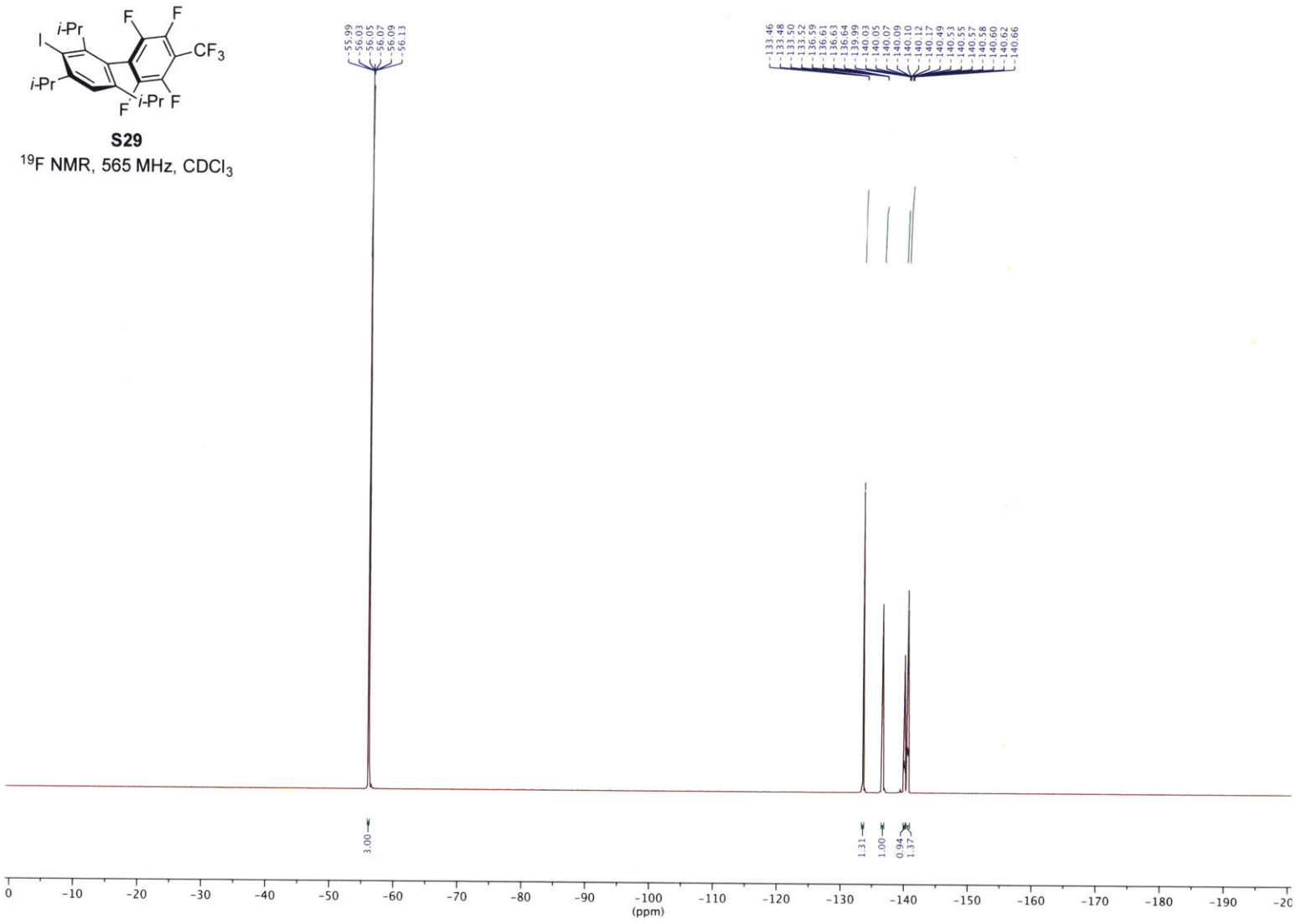
i-Pr
F
F
I
CF3
i-Pr
F
i-Pr F
S29
19F NMR, 565 MHz, CDCl3
-55.99
-56.03
-56.05
-56.07
-56.09
-56.13
-133.46
-133.48
-133.50
-133.52
-136.59
-136.61
-136.63
-136.64
-139.99
-140.03
-140.05
-140.07
-140.09
-140.10
-140.12
-140.17
-140.49
-140.53
-140.55
-140.57
-140.58
-140.60
-140.62
-140.66
3.00
1.31
1.00
0.94
1.37
0
-10
-20
-30
-40
-50
-60
-70
-80
-90
-100
-110
-120
-130
-140
-150
-160
-170
-180
-190
(ppm)

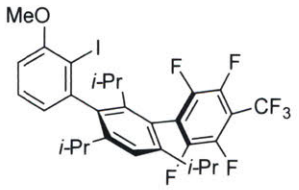

S30

^{1}H NMR, 600 MHz, $CDCl_3$

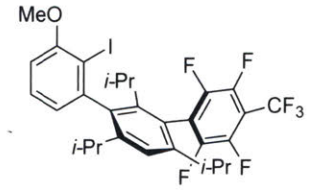

S30

^{13}C NMR, 151 MHz, $CDCl_3$

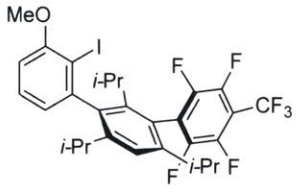

S30

^{19}F NMR, 565 MHz, $CDCl_3$

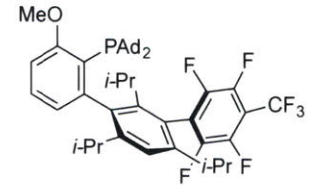

S31

^{1}H NMR, 600 MHz, $CDCl_3$

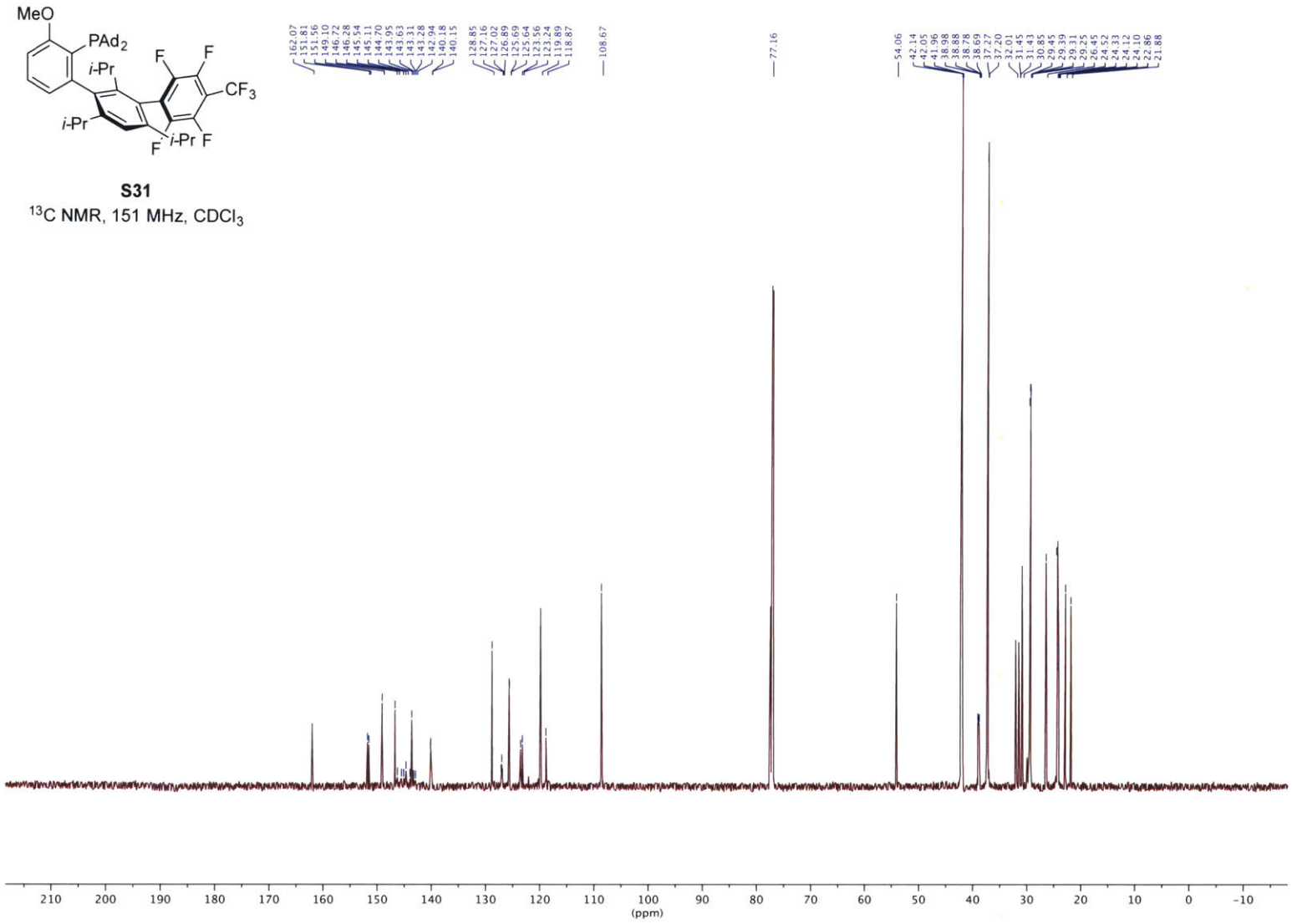

S31

^{13}C NMR, 151 MHz, $CDCl_3$

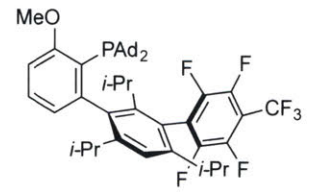

S31

^{19}F NMR, 471 MHz, $CDCl_3$

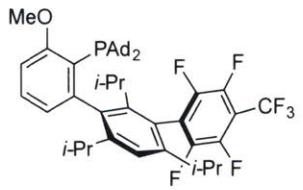

S31

^{31}P NMR, 203 MHz, $CDCl_3$

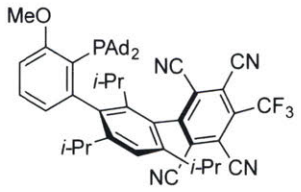

L10

^{1}H NMR, 400 MHz, $CDCl_3$

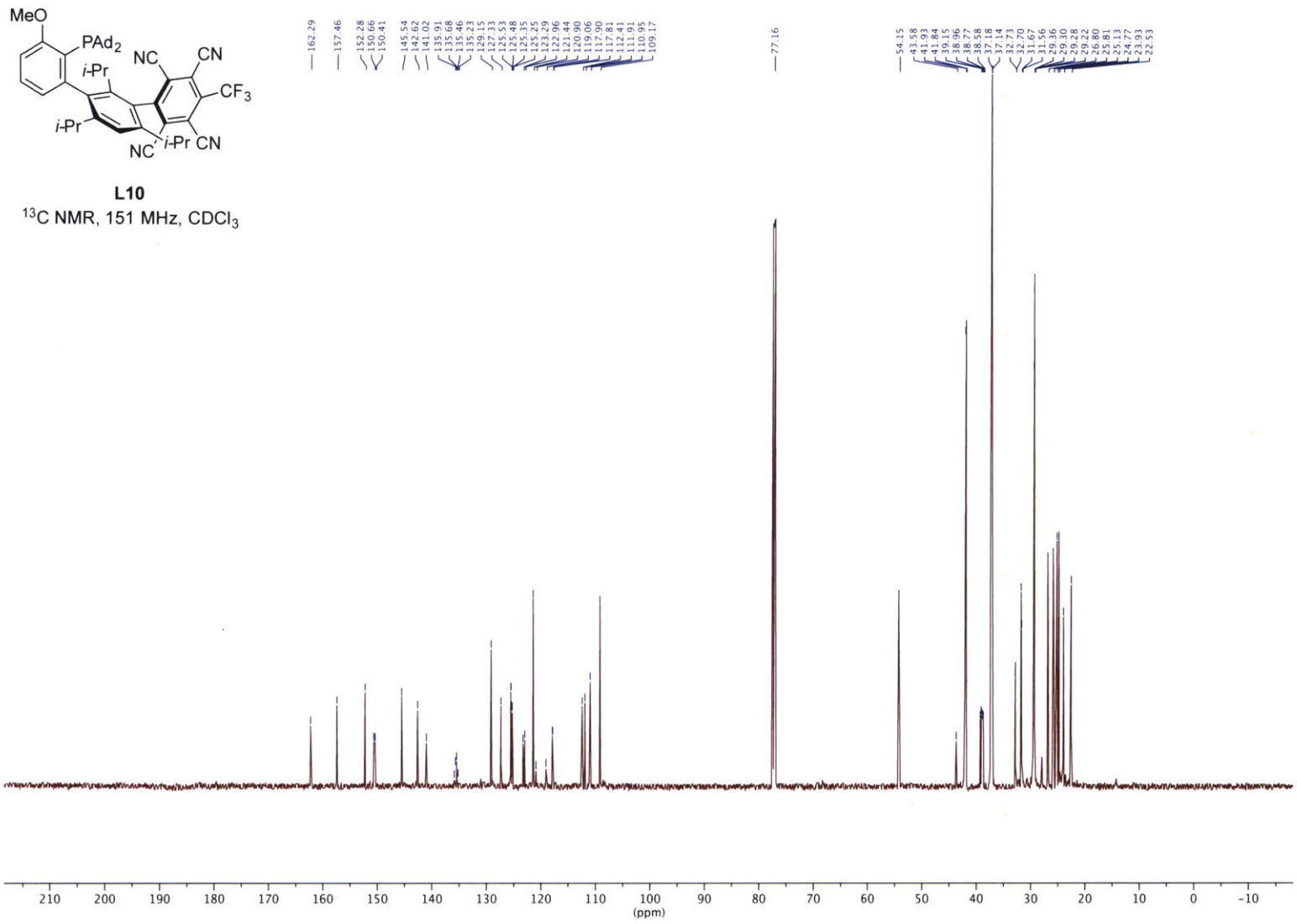
MeO
PAd2
i-Pr
NC
CN
CF3
i-Pr
NC
i-Pr
CN
L10
13C NMR, 151 MHz, CDCl3
162.29
157.46
152.28
150.66
150.41
145.54
142.62
141.02
135.91
135.68
135.46
135.23
129.15
127.33
125.53
125.48
125.35
125.25
123.29
122.96
121.44
120.90
119.06
117.90
117.81
112.41
111.91
110.95
109.17
77.16
54.15
43.58
41.93
41.84
39.15
38.96
38.77
38.58
37.18
37.14
32.73
32.70
31.67
31.56
29.36
29.30
29.28
29.22
26.80
25.81
25.13
24.77
23.93
22.53
210
200
190
180
170
160
150
140
130
120
110
100
90
80
70
60
50
40
30
20
10
0
-10
(ppm)

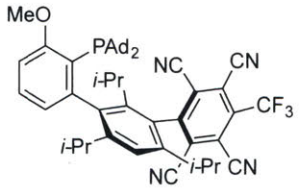

L10

^{19}F NMR, 376 MHz, $CDCl_3$

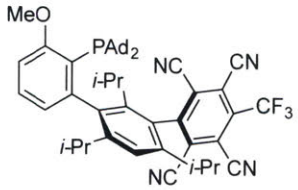

L10

^{31}P NMR, 162 MHz, $CDCl_3$

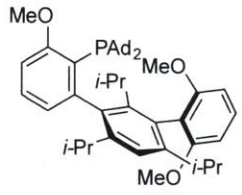

L11

^{1}H NMR, 600 MHz, $CDCl_3$

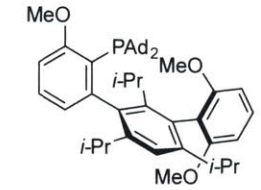

L11

^{13}C NMR, 151 MHz, $CDCl_3$

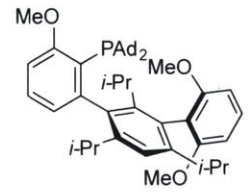

L11

^{31}P NMR, 162 MHz, $CDCl_3$

Chapter 4. Discovery of a Sterically Encumbered Hexasubstituted Arene through the Pd-mediated Dearomative Rearrangement of Biaryl Monophosphine Ligands

4.1. Introduction

It is known that certain metal complexes of biaryl monophosphines bearing extremely large groups on phosphorus (i.e., *tert*-Bu or 1-adamantyl) groups can undergo a dearomative rearrangement.[1–4] This reaction with L–Pd(Ar)X (X = I, Br, Cl) complexes (Figure 1) has had important implications for ligand design in the context of C–F bond formation.[5]

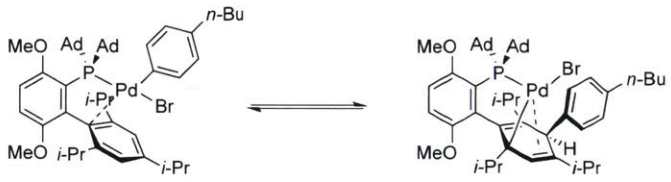

Figure 1. Dearomative rearrangement of AdBrettPhos-based complexes.

As shown in Chapter 3, this transformation can be leveraged to expediently modify the 3′ position of the ligand backbone. Herein we describe the formation of an unexpected, structurally unique hexasubstituted arene using this dearomative rearrangement.

4.2. Results and Discussion

Triaryl phosphine **L1** was an initial ligand of interest for systematically studying the impact of ligand architecture on C–F cross-coupling (Chapter 3). Attempts to synthesize **L1** through the Pd-mediated dearomative rearrangement resulted in approximately a 1:1 mixture of two phosphorus-containing products with similar polarities, as judged by TLC (Figure 2, top).

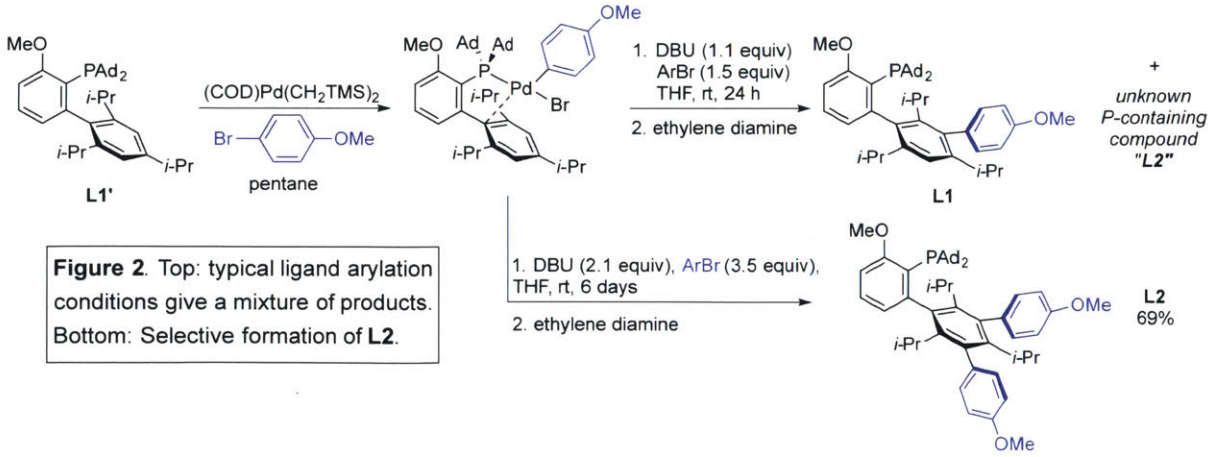

Figure 2. Top: typical ligand arylation conditions give a mixture of products. Bottom: Selective formation of **L2**.

By prolonging the reaction time, increasing the amount of DBU to two equivalents, and using excess aryl halide (3.5 equiv), a single product, **L2**, could be isolated cleanly in moderate yield (Figure 2, bottom). The structure of **L2** was elucidated through NMR spectroscopy, as well as X-ray diffraction (Figure 3). Crystallographic analysis shows substantial deviation from planarity around the central ring: the dihedral angles of C1′–C2′ and C2′–C3′ are 6.5° and 12.4° off from zero, respectively (Figure 3b, 3c).

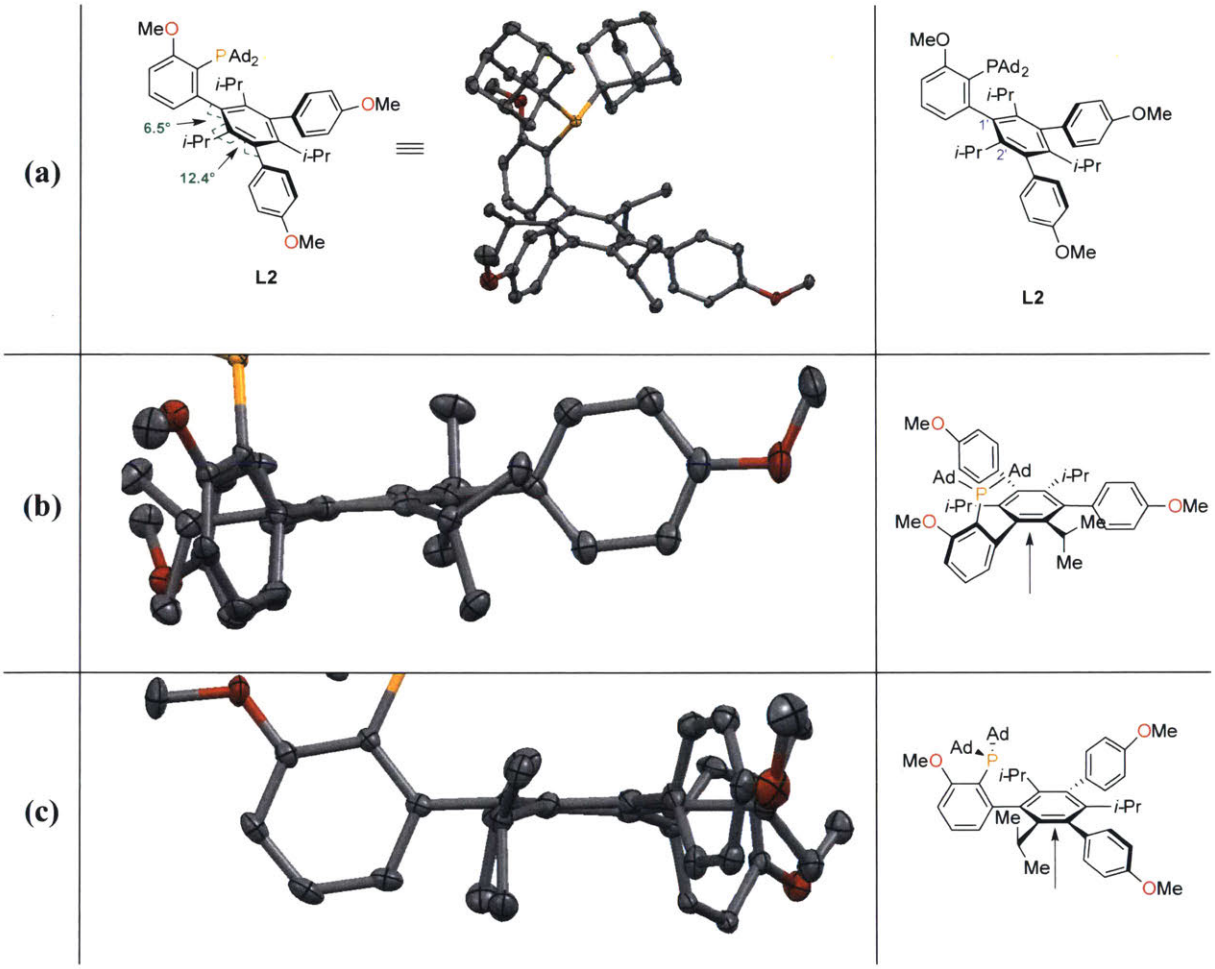

Figure 3. **(a)** Left: X-Ray Structure of **L2**. Thermal ellipsoid plot shown at 50% probability. Hydrogen atoms are omitted for clarity. Right: numbering system of **L2**. **(b)** Visualization along C1′–C2′. **(c)** Visualization along C2′–C3′.

To the best of our knowledge, this compound represents the first example of a hexasubstituted arene bearing three isopropyl groups and three aryl groups. This type of scaffold is challenging

to prepare despite advances in metal-catalyzed cross-coupling,[6,7] cycloaddition chemistry,[8] and [2+2+2] alkyne trimerization,[9,10] all of which have been used to prepare such structures. We have also demonstrated that two different aryl groups may be installed onto the central ring system using this strategy (**L3**, Figure 4).

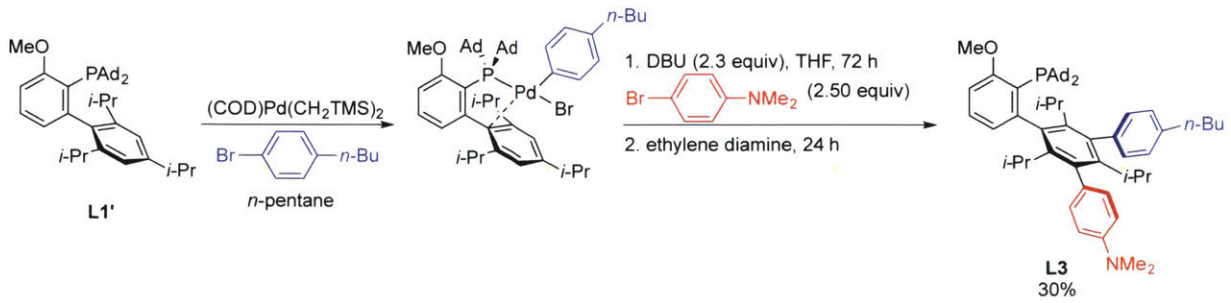

Figure 4. Synthesis of a hexasubstituted arene with two different aryl groups.

First, an oxidative addition complex is formed and isolated with the first aryl group to be added (e.g., 1-bromo-4-*n*-butylbenzene). In the presence of base, the central ring rearomatizes, resulting in a net arylation of the ligand along with concomitant formation of Pd(0). By trapping the Pd(0) complex with a second sufficiently electron-rich aryl halide (e.g., *N*,*N*-dimethylaniline), a second, distinct aryl group can be installed in a single pot.

The reactions of aryl bromides with *ortho* substitutions, such as such as 2-bromo-1,3-dimethoxybenzene, were also explored. However, oxidative addition complexes with this aryl group only undergo a single arylation (see section **3.4.XI.**), even with prolonged reaction times, suggesting that steric hindrance has a strong influence on subsequent arylations. This also implies that doubly *ortho* substituted aryl halides would be suitable Pd(0) traps to selectively access to structures like **L1**, although we contemporaneously discovered that 2-bromothiophene could serve the same purpose (see sections **3.4.VI.** and **3.4.VIII.**). Thus, by choosing an appropriate aryl halide, selective monoarylation of ligands can also be realized.

4.3. Conclusion

The Pd-mediated dearomative rearrangement provides a convenient, rapid way to modify biaryl phosphines at the 3′ position. Though single dearomative rearrangements have previously been studied, current efforts in ligand synthesis have demonstrated that, with appropriate

stoichiometry, electron-rich aryl halides undergo a second arylation reaction to form sterically encumbered hexasubstituted aromatic systems. Future work in this area could involve modifications to the central ring to form unsymmetrical, heavily substituted arenes.

4.4. Experimental

I. General Information

A) General Reagent Information: Commercial solvents and reagents were purchased from Aldrich Chemical Company, Alfa Aesar, and Chem-Impex and used as received, with the following exceptions. Tetrahydrofuran (THF) was purchased from J.T. Baker in CYCLE-TAINER® solvent-delivery kegs and vigorously purged with argon for 2 h, followed by passing it under argon pressure through two packed columns of neutral alumina. Medium reaction tubes (25 mL capacity, 20 x 125 mm, Part No. 14-959-37A), medium screw-caps (Kimble-Chase, Open Top S/T Closure, Part No. 73804-18400), and medium septa (Thermo Scientific PTFE/silicon, Cat No. B7995-18), were purchased from Fischer Scientific. Compounds were purified using a Biotage® Isolera system, employing polypropylene cartridges preloaded with silica gel (Silicycle SilaFlash® F60 silica gel) or with new Biotage® SNAP cartridges, unless otherwise noted. Samples were eluted using a flow rate of 50–100 mL/min, with detection by UV (254 nm). Analytical thin-layered chromatography (TLC) was performed using glass plates pre-coated with silica gel (0.25 mm, 60 Å pore size) impregnated with a fluorescent indicator (254 nm). TLC plates were visualized by exposure to ultraviolet light (UV). **L1′** was prepared as described in Chapter 3 (Section **3.4.VIII**).

B) General Analytical Information: Compounds were analyzed by ^{1}H, ^{13}C, ^{19}F, and ^{31}P nuclear magnetic resonance (NMR) spectroscopy where appropriate. NMR spectra were recorded on a Bruker Avance Neo-400 MHz spectrometer, a Bruker Avance Neo-500 MHz spectrometer, and a Bruker Avance Neo-600 MHZ spectrometer. ^{1}H and ^{13}C spectra were calibrated using residual solvent as an internal reference ($CDCl_3$: δ 7.26 ppm and δ 77.16 ppm, respectively; CD_2Cl_2: δ 5.32 ppm and 53.84 ppm, respectively). Elemental analyses were performed by Atlantic Microlabs Inc., Norcross, GA, USA. High-resolution mass spectra were recorded on an Agilent Technologies 6545 Q-TOF LC/MS system. The following abbreviations were used to explain multiplicities: s = singlet, bs = broad singlet, d = doublet, t = triplet, q = quartet, p = pentet, sx = sextet, h = heptet, m = multiplet. Melting points were obtained using a Stanford Research Systems EZ-Melt melting point apparatus. Attenuated total reflectance Fourier transform infrared spectra (ATR-FTIR) were obtained using a Thermo Scientific Nicolet iS5 FT-IR

spectrometer (iD5 ATR, diamond) referenced to a polystyrene standard and data reported as frequency of absorption (cm^{-1}).

II. Experimental Procedures and Characterization of **L2** and **L3**

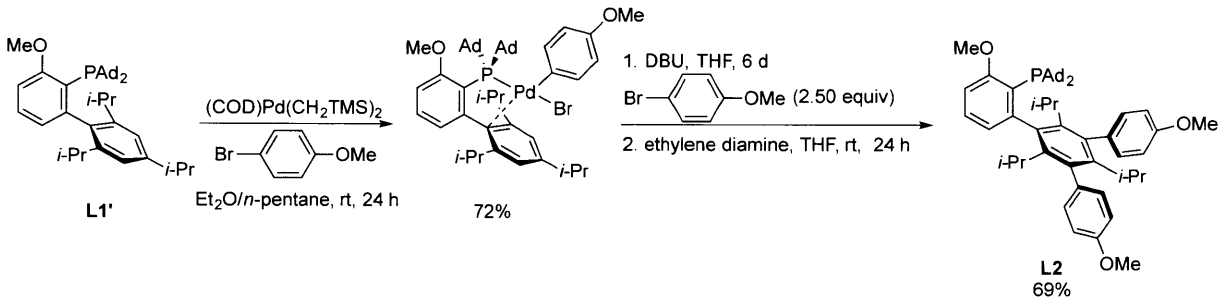

An oven-dried 100 mL round-bottomed flask equipped with a magnetic stir bar was brought into a nitrogen-filled glovebox and charged with **L1′** (400 mg, 0.655 mmol, 1.00 equiv) and subsequently dissolved in a mixture of anhydrous Et_2O (10 mL) and pentane (52 mL). Then, 4-bromoanisole (306 mg, 1.64 mmol, 2.50 equiv) was added via microliter pipette, followed by (COD)Pd(CH2TMS)$_2$ (280 mg, 0.720 mmol, 1.10 equiv). The flask was sealed with a rubber septum, removed from the glovebox, and allowed to stir at rt for 24 h. At this time, the resulting red precipitate was collected using a sintered glass funnel. The filter cake was washed with pentane (3 x 3 mL) to afford the oxidative addition complex, which was used directly in the next step without further purification (426 mg, 72%).

An oven-dried 100 mL round-bottomed flask equipped with a magnetic stir bar was charged with the oxidative complex prepared above (426 mg, 0.472 mmol, 1.00 equiv). The flask was sealed with a rubber septum and an inlet needle attached to a Schlenk line inserted. The vessel was evacuated and backfilled with argon. This sequence was repeated two additional times. Anhydrous THF (50 mL) was added via syringe and the reaction mixture was allowed to begin stirring. Then, 4-bromoanisole (240 μL, 1.90 mmol, 4.0 equiv) and DBU (175 μL, 1.16 mmol, 2.45 equiv) were sequentially added via syringe. The reaction mixture was then allowed to stir at 40 °C in a pre-heated oil bath for 6 days. At this time, the reaction mixture was cooled to rt. Then, ethylene diamine (0.185 mL, 2.76 mmol, 5.85 equiv) was added via syringe and the reaction mixture allowed to stir at rt for 24 h. Then, the flask was opened to the air and

transferred to a separatory funnel containing EtOAc (50 mL). The organic phase was washed ammonium hydroxide (28–30% NH_3 basis)/brine (2:1; 2 x 50 mL), followed by brine (1 x 50 mL). The organic layer was then dried over magnesium sulfate, filtered, and concentrated with the aid of a rotary evaporator. The crude residue was triturated from MeOH, followed by crystallization from CH_2Cl_2/MeOH to afford **L2** as light pink crystals suitable for X-ray diffraction (crop 1: 257 mg, crop 2: 57 mg; total yield: 313 mg (69%)). mp: 214–215 °C. **^{1}H NMR** (400 MHz, CD_2Cl_2): δ 7.24 (m, 4H), 7.14 – 7.08 (d, J = 6.8 Hz, 1H), 6.89 – 6.76 (m, 6H), 3.83 (s, 3H), 3.81 (s, 6H), 2.87 (h, J = 7.2 Hz, 1H), 2.72 (h, J = 6.9 Hz, 2H), 1.92 – 1.84 (m, 18H), 1.72 – 1.58 (m, 12H), 0.85 (d, J = 6.9 Hz, 6H), 0.76 (d, J = 7.3 Hz, 3H), 0.54 (d, J = 7.2 Hz, 3H), 0.41 (d, J = 7.0 Hz, 3H), 0.39 (d, J = 7.0 Hz, 3H). **^{13}C NMR** (126 MHz, $CDCl_3$): δ 162.0 (d, J = 2.6 Hz), 158.6, 158.2, 154.7 (d, J = 36.2 Hz), 144.9, 144.0, 142.9, 140.2, 138.2 (d, J = 5.8 Hz), 136.0, 135.7, 134.1, 134.0, 133.6, 133.4, 131.3, 128.4, 125.7 (d, J = 7.0 Hz), 123.0, 122.6, 112.6, 112.2, 111.1 (d, J = 22.0 Hz), 107.9, 55.3, 54.0, 42.0 (d, J = 14.0 Hz), 38.8, 38.6, 37.3, 33.1, 32.9, 30.7, 29.4 (d, J = 9.0 Hz), 25.1 (d, J = 10.0 Hz), 23.9, 23.7, 23.0 (the observed complexity is due to C–P coupling). **^{31}P NMR** (203 MHz, $CDCl_3$): δ 37.0. IR (neat, cm^{-1}): 2991, 2901, 2845, 1506, 1455, 1281, 1236, 1173, 1041, 1029, 802, 792, 737. **HRMS** (ESI): m/z calcd for $C_{56}H_{71}O_3P$ $[M+H]^+$: 823.5219; 823.5204 found.

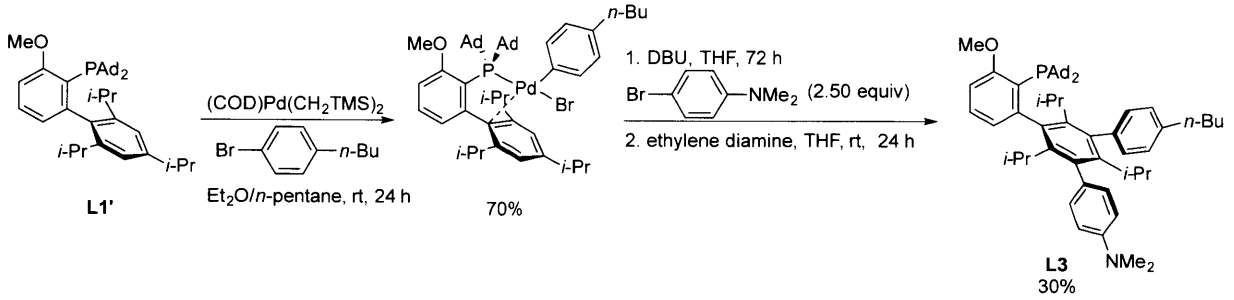

An oven-dried 100 mL round-bottomed flask equipped with a magnetic stir bar was brought into a nitrogen-filled glovebox and charged with **L1′** (400 mg, 0.655 mmol, 1.00 equiv) and subsequently dissolved in a mixture of anhydrous Et_2O (10 mL) and pentane (52 mL). Then, 1-bromo-4-*n*-butylbenzene (209 mg, 0.982 mmol, 1.50 equiv) was added via microliter pipette, followed by (COD)Pd(CH2TMS)$_2$ (280 mg, 0.720 mmol, 1.10 equiv). The flask was sealed with a rubber septum, removed from the glovebox, and the red heterogeneous solution allowed to stir at rt for 24 h. At this time, the resulting yellow precipitate was collected using a sintered glass

funnel. The filter cake was washed with pentane (5 x 3 mL) to afford the oxidative addition complex, a portion of which was used directly in the next step without further purification (424 mg, 70%).

An oven-dried 25 mL reaction tube equipped with a magnetic stir bar was charged with the oxidative complex prepared above (106 mg, 0.114 mmol, 1.00 equiv) and 4-bromo-*N,N*-dimethylaniline (57.0 mg, 0.285 mmol, 2.50 equiv). The tube was sealed with a screw-cap fitted with a Teflon septum and an inlet needle attached to a Schlenk line was inserted. The vessel was evacuated and backfilled with argon. This sequence was repeated two additional times. Anhydrous THF (7 mL) was added via syringe and the reaction mixture was allowed to begin stirring. Then, DBU (40 μL, 0.27 mmol, 2.3 equiv) was added via microliter syringe and the septum exchanged for one that had not been punctured, under a counterflow of argon. The reaction mixture was then allowed to stir at rt for 3 days. At this time, ethylene diamine (0.100 mL, 1.50 mmol, 13.0 equiv) was added via syringe and the reaction mixture was allowed to stir at rt for 24 h. Then, the tube was opened to the air, and transferred to a separatory funnel containing EtOAc (50 mL). The organic phase was washed ammonium hydroxide (28–30% NH_3 basis)/brine (2:1; 3 x 50 mL), followed by brine (1 x 50 mL). The organic layer was then dried over magnesium sulfate, filtered, and concentrated with the aid of a rotary evaporator. The crude residue was purified via automated silica gel chromatography (Biotage KP-SIL 25 g column, eluting 0% to 100% CH_2Cl_2/EtOAc), followed by crystallization from CH_2Cl_2/MeOH to afford **L3** as a white solid (29.4 mg, 30%). Contains approximately 5% (as judged by LC/MS spectroscopy) of **L1′**. mp: 239–241 °C. **^{1}H NMR** (600 MHz, $CDCl_3$): δ 7.25 – 7.22 (m, 1H), 7.18 (d, J = 8.2 Hz, 1H), 7.16 – 7.02 (m, 5H), 6.97 (dd, J = 7.7, 3.5 Hz, 1H), 6.81 (d, J = 8.1 Hz, 1H), 6.69 (d, J = 8.3 Hz, 1H), 6.64 (m, 1H), 3.84 (s, 3H), 2.96 (d, J = 5.3 Hz, 6H), 2.84 (m, 1H), 2.67 (m, 2H), 2.63 (t, J = 7.9 Hz, 2H), 1.87 (m, 18H), 1.64 (m, 14H), 1.37 (h, J = 6.9 Hz, 2H), 0.92 (m, 9H), 0.75 (dd, J = 21.5, 7.2 Hz, 3H), 0.57 (dd, J = 32.3, 7.3 Hz, 3H), 0.43 (dd, J = 15.3, 7.1 Hz, 3H), 0.34 (dd, J = 13.1, 6.8 Hz, 3H) (complex spectrum, see section 4.6). **^{13}C NMR** (151 MHz, $CDCl_3$): δ 162.0, 154.9 (d, J = 36.5 Hz), 149.5, 149.1, 144.9, 144.2, 143.3, 143.1, 141.2, 140.7 (d, J = 14.8 Hz), 140.0, 138.8, 138.5 (d, J = 13.1 Hz), 135.6, 134.9, 133.7, 133.1, 132.4, 131.6, 131.0, 130.3, 129.6, 128.3, 126.9 (d, J = 7.0 Hz), 125.9 (d, J = 7.4 Hz), 125.6 (d, J = 4.7 Hz), 123.0, 122.6, 111.5, 111.2, 110.0 (d, J = 22.1 Hz), 107.8, 54.0, 42.0 (d, J = 14.0 Hz), 40.9,

38.8, 38.6, 37.3, 35.6, 33.9 (d, J = 20.4 Hz), 33.2 (d, J = 16.7 Hz), 32.9 (d, J = 19.1 Hz), 30.8, 30.6, 29.4 (d, J = 9.0 Hz), 25.1 (d, J = 11.0 Hz), 24.0, 23.8, 23.0, 22.6 (d, J = 16.8 Hz), 14.2 (complex spectrum, in part due to C–P coupling; see section 4.6). **^{31}P NMR** (203 MHz, $CDCl_3$): δ 36.9. IR (neat, cm^{-1}): 2901, 2846, 1613, 1516, 1456, 1350, 1264, 1028, 822, 797. **HRMS** (ESI) m/z calcd for $C_{60}H_{80}NOP$ $[M+H]^+$: 862.6056; 862.6051 found.

III. X-Ray Structure Details

Low-temperature diffraction data (*Φ*-and *ω*-scans) were collected on a Bruker-AXS X8 Kappa Duo diffractometer coupled to a Smart APEX2 CCD detector with Mo Kα radiation (λ = 0.71073 Å) from an IμS micro-source for the structure of compound **L2**. Absorption and other corrections were applied using SADABS.[11] All structures were solved by direct methods using SHELXT[12] and refined against F^2 on all data by full-matrix least squares with SHELXL-2017[13]using established refinement approaches.[14] All hydrogen atoms were included into the model at geometrically calculated positions and refined using a riding model. The isotropic displacement parameters of all hydrogen atoms were fixed to 1.2 times the U_{eq} value of the atoms they are linked to (1.5 times for methyl groups). Details about crystal properties, diffraction data, and crystal structures can be found in the tables below.

Compound **L2** crystallizes in the monoclinic space group $P2_1/n$. SQUEEZE[15] as implemented in PLATON[16] was used to account for highly disordered solvent.

Crystal data structure refinement for **L2**

Identification code	X8_18049	
Empirical formula	$C_{56}H_{71}O_3P$	
Formula weight	823.152	
Temperature	–173.0 °C	
Wavelength	0.71073 Å	
Crystal system	Monoclinic	
Space group	$P2_1/n$	
Unit cell dimensions	a = 12.5922(9) Å b = 28.656(2) Å c = 13.3383(10) Å	α = 90.00° β = 100.726(2)° γ = 90.00°
Volume	4728.68 $Å^3$	
Z	4	
Density (calculated)	1.156 g/cm^3	

Absorption coefficient	0.101 mm^{-1}	
F(000)	1784	
Crystal size	0.210 x 0.160 x 0.120 mm^3	
Theta range for data collection	1.421 to 32.032°	
Reflections collected	365858	
Independent reflections	16449	
Absorption correction	T_{max} = 0.7464; T_{min} = 0.7268	
Refinement method	Full-matrix least-squares on F^2	
Goodness-of-fit on F^2	1.067	

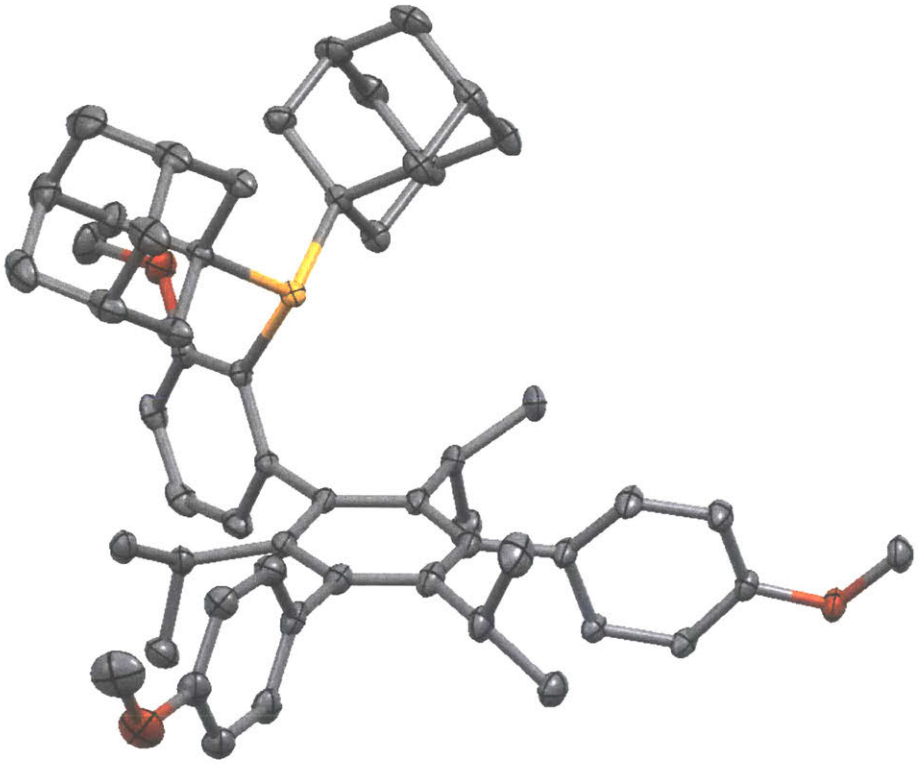

X-ray crystal structure of **L2**. Hydrogen atoms omitted for clarity.

4.5. References and Notes

1. Maimone, T. J.; Milner, P. J.; Kinzel, T.; Zhang, Y.; Takase, M. K.; Buchwald, S. L. Evidence for in Situ Catalyst Modification during the Pd-Catalyzed Conversion of Aryl Triflates to Aryl Fluorides. *J. Am. Chem. Soc.* **2011**, *133*, 18106–18109.

2. Milner, P. J.; Maimone, T. J.; Su, M.; Chen, J.; Müller, P.; Buchwald, S. L. Investigating the Dearomative Rearrangement of Biaryl Phosphine-Ligated Pd(II) Complexes. *J. Am. Chem. Soc.* **2012**, *134*, 19922–19934.

3. Allgeier, A. M.; Shaw, B. J.; Hwang, T. L.; Milne, J. E.; Tedrow, J. S.; Wilde, C. N. Characterization of Two Stable Degradants of Palladium ^{t}BuXPhos Catalyst and a Unique Dearomatization Reaction. *Organometallics,* **2012**, *31*, 519–522.

4. Nielsen, D. K.; Doyle, A. G. Nickel-Catalyzed Cross-Coupling of Styrenyl Epoxides with Boronic Acids. *Angew. Chem. Int. Ed.* **2011**, *50*, 6056–6059.

5. Lee, H. G.; Milner, P. J.; Buchwald, S. L. Pd-Catalyzed Nucleophilic Fluorination of Aryl Bromides. *J. Am. Chem. Soc.* **2014**, *136*, 3792–3795.

6. Li, C.; Chen, T.; Li, B.; Xiao, G.; Tang, W. Efficient Synthesis of Sterically Hindered Arenes Bearing Acyclic Secondary Alkyl Groups by Suzuki-Miyaura Cross-Couplings. *Angew. Chem. Int. Ed.* **2015**, *54*, 3792–3796.

7. Zhao, Q.; Li, C.; Senanayake, C. H.; Tang, W. An Efficient Method for Sterically Demanding Suzuki-Miyaura Coupling Reactions. *Chem. - A Eur. J.* **2013**, *19*, 2261–2265.

8. Janvier, P.; Bienaymé, H.; Zhu, J. A Five-Component Synthesis of Hexasubstituted Benzene. *Angew. Chem. Int. Ed.* **2002**, *41*, 4291–4294.

9. Siegel, J.; Gutierrez, A.; Schweizer, W. B.; Ermer, O.; Mislow, K. Static and Dynamic Stereochemistry of Hexaisopropylbenzene: A Gear-Meshed Hydrocarbon of Exceptional Rigidity. *J. Am. Chem. Soc.* **1986**, *108*, 1569–1575.

10. Jhingan, A. K.; Maier, W. F. Homogeneous Catalysis with a Heterogeneous Palladium Catalyst. An Effective Method for the Cyclotrimerization of Alkynes. *J. Org. Chem.* **1987**, *52*, 1161–1165.

11. Krause, L.; Herbst-Irmer, R.; Sheldrick, G. M.; Stalke, D. Comparison of Silver and Molybdenum Microfocus X-Ray Sources for Single-Crystal Structure Determination. *J. Appl. Crystallogr.* **2015**, *48*, 3–10.

12. Sheldrick, G. M. *SHELXT* – Integrated Space-Group and Crystal-Structure Determination. *Acta Cryst.* **2015**, *A71*, 3–8.

13. Sheldrick, G. M. Crystal Structure Refinement with *SHELXL*. *Acta Cryst.* **2015**, *C71*, 3–8.

14. Müller, P. Practical Suggestions for Better Crystal Structures. *Crystallography Reviews,* **2009**, *15*, 57–83.

15. Van der Sluis, P.; Spek, A. L. BYPASS: An effective method for the refinement of crystal structures containing disordered solvent regions. *Acta Cryst.* **1990**, *A46*, 194–201.

16. Spek, A. L. Structure validation in chemical crystallography. *Acta Cryst.* **2009**, *D65*, 148–155.

4.6. NMR Spectra

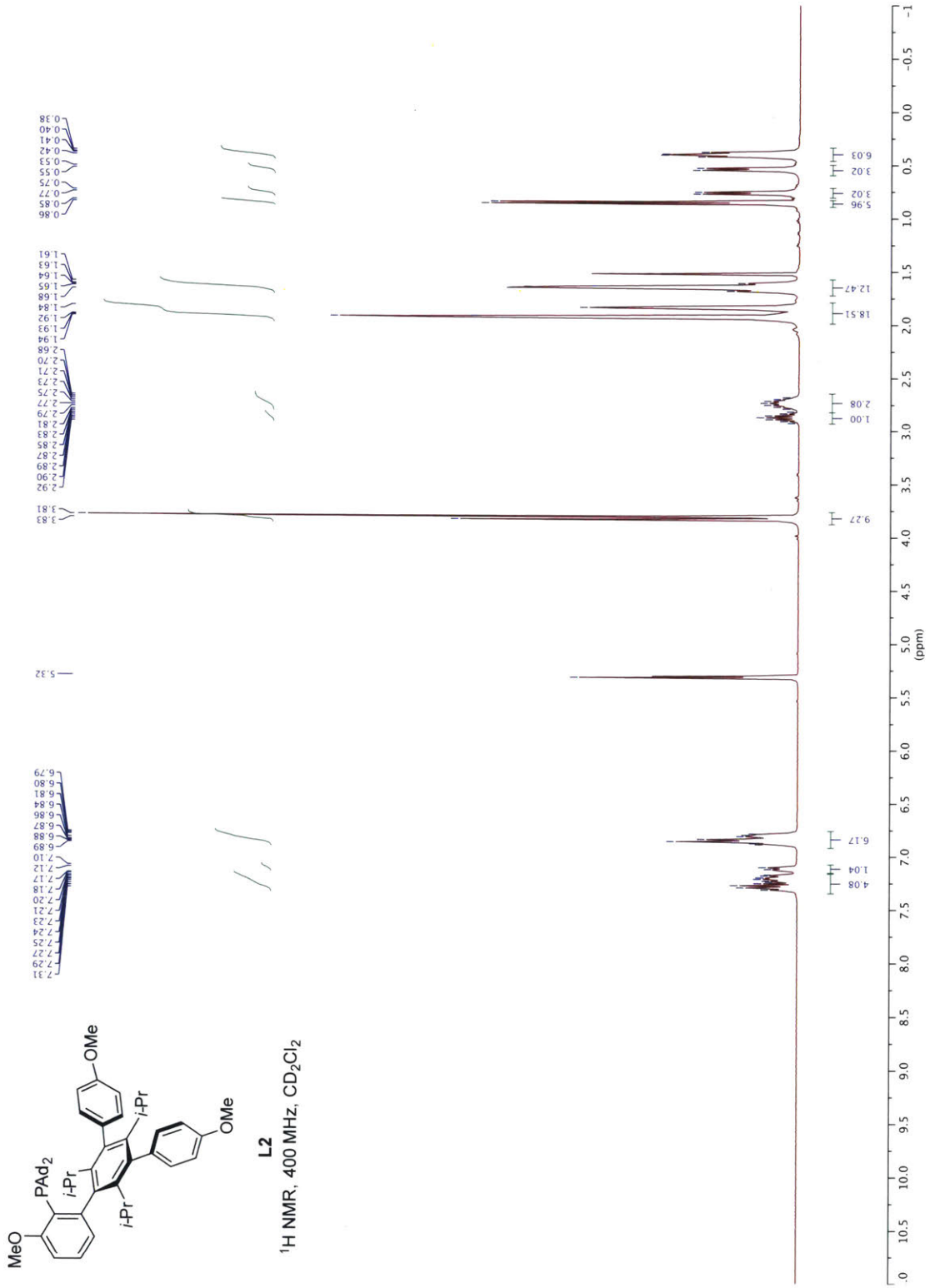

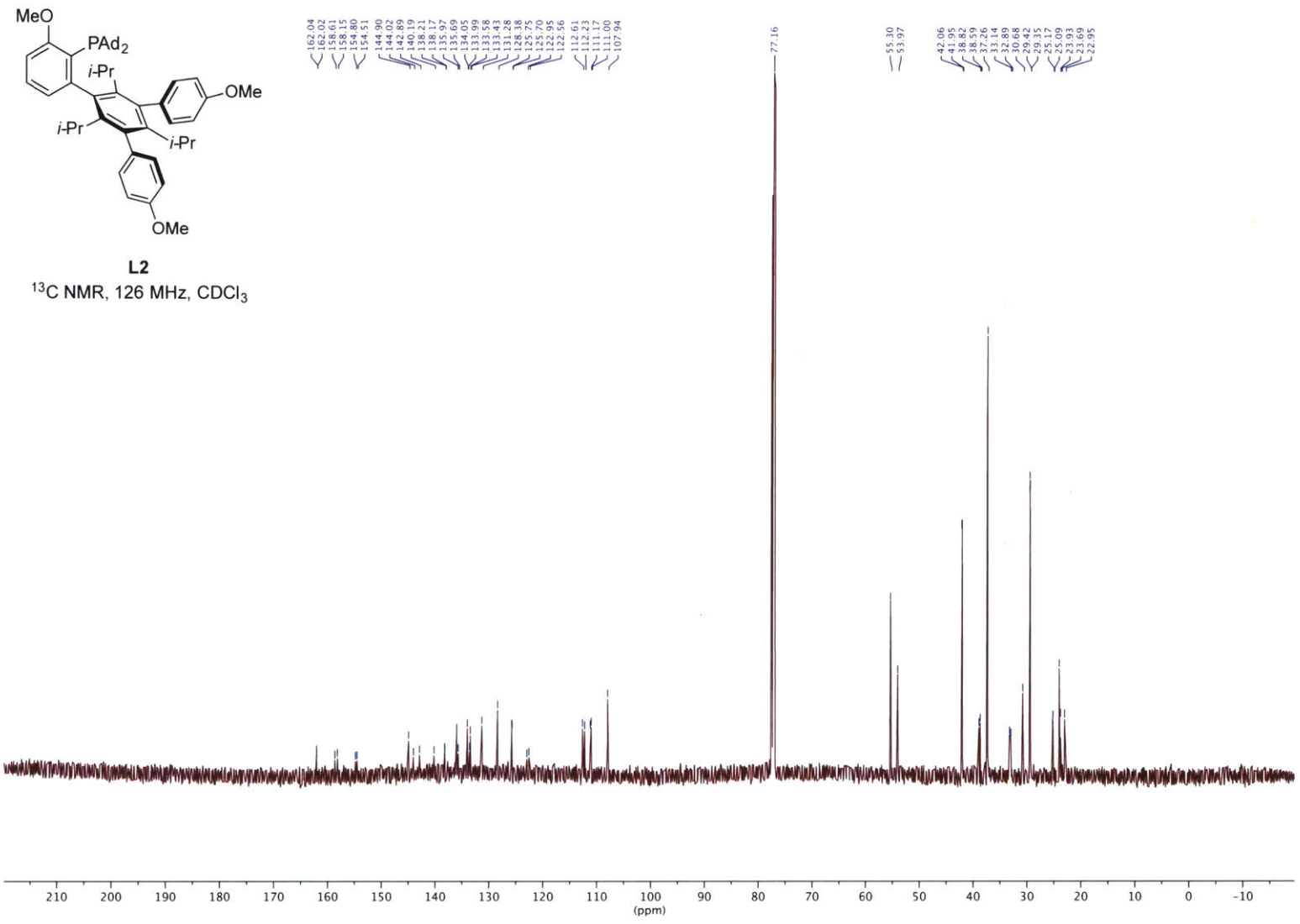

L2

^{13}C NMR, 126 MHz, $CDCl_3$

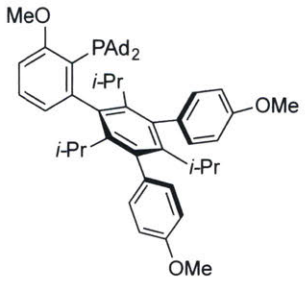

L2

^{31}P NMR, 203 MHz, $CDCl_3$

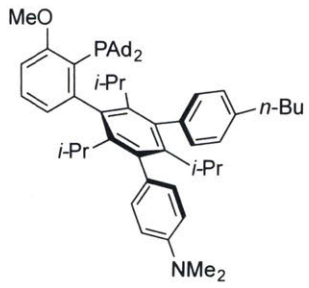

L3

^{1}H NMR, 600 MHz, $CDCl_3$

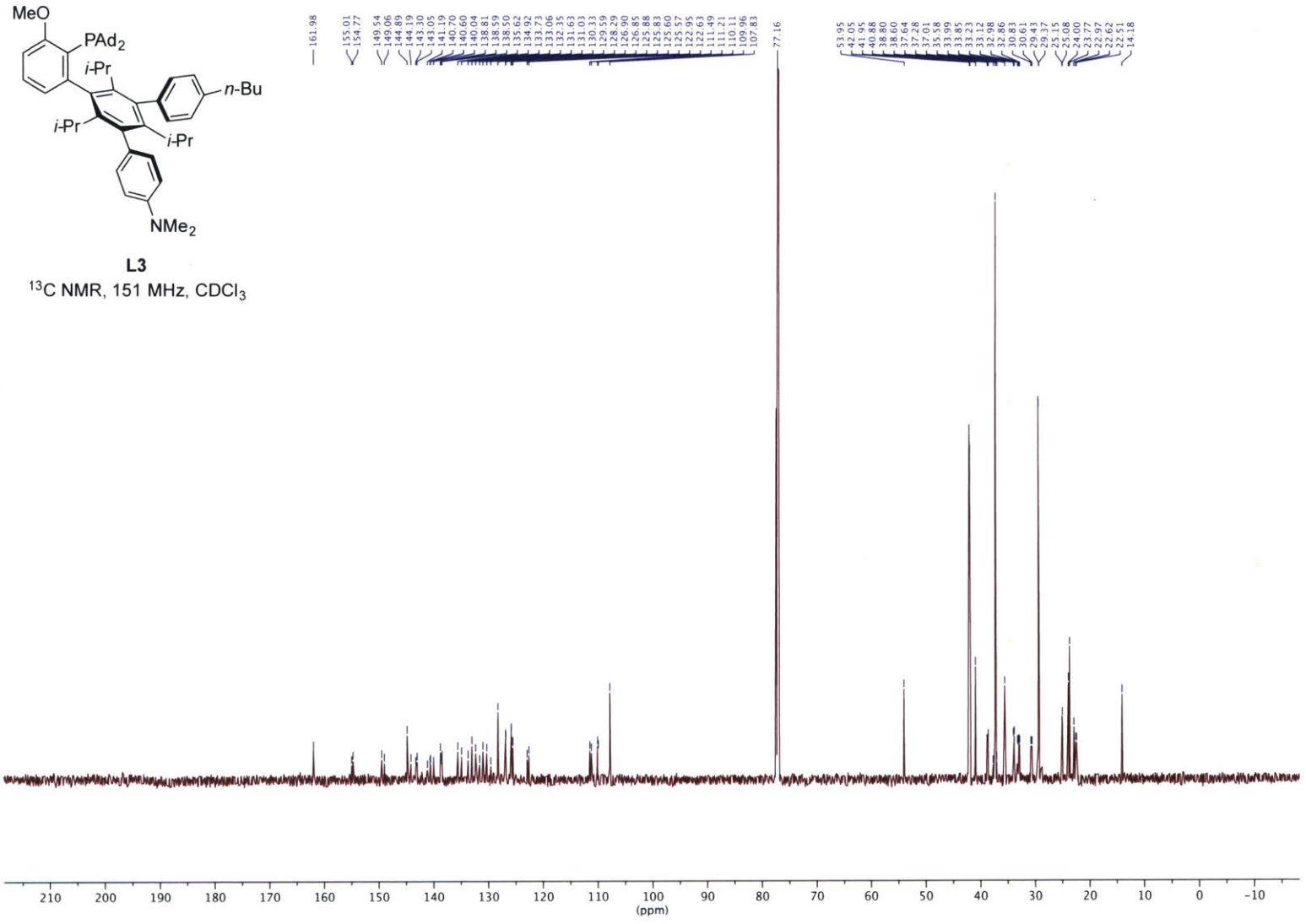

L3

^{13}C NMR, 151 MHz, $CDCl_3$

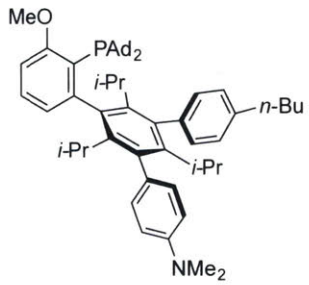

L3

^{31}P NMR, 203 MHz, $CDCl_3$